



UNIVERSITY OF
LEICESTER

THE PREVALANCE OF PROTOZOA
DURING CANINE PERIODONTAL
DISEASE

Thesis submitted for the degree of
Doctor of Philosophy
at the University of Leicester

by

Niran Patel BSc (Leicester)

Department of Infection, Inflammation and Immunity

University of Leicester

DECEMBER 2018

Abstract

The Prevalence of Protozoa during Canine Periodontal Disease Niran Patel

Canine periodontal disease is a widespread oral disorder of dogs and has a population prevalence estimated to range from 44-64% of all individuals. For several decades researchers have focused on examining the bacterial communities present in plaque, the aetiological agent of periodontal disease. Other microorganisms, such as protozoa, are also known to exist in plaque, however, the role they play in contributing to periodontal disease is less well understood.

Molecular biology protocols were developed that enabled the rapid, multiplexed identification of protozoa in mixed-microorganism canine plaque samples collected from dogs with diverse oral health states. Protozoa from the genera *Trichomonas* and *Entamoeba* were detected with overall prevalence in the total sample population being 56.52 % (52/92) and 4.34 % (4/92) respectively. To address primer bias weaknesses inherent in PCR-based methods, a protozoa identification techniques not based on the use of pre-existing sequence information and PCR was also devised. These methods were based on the sequencing of ribosomal RNA extracted from plaque samples using state-of-the-art sequencing technologies. Quantitative molecular assays (qPCR) were also developed to enable the detection and quantification of the organisms localised to teeth. The method revealed the abundance of both protozoa to be correlated with more diseased samples and to specific tooth types (molars and premolars) within the mouth. Finally, investigations were conducted, to assess the potential of these organisms to contribute to canine periodontal disease.

The research outcomes of this thesis provide the first conclusive evidence that oral protozoa are present in canine mouths, are associated with periodontal disease samples and are capable of contributing to the disease process. Researchers of periodontal disease and those attempting to reduce the diseases burden in dogs and humans should focus more attention to both Entamoebae and Trichomonad presence in the mouth and investigate their biology and function further.

Acknowledgments

I'd like to express my sincerest gratitude to Professor Peter Andrew, Dr Lucy Holcombe and Dr Steve Harris, for providing me with excellent advice, supervision and encouragement during the course of my research and thesis write up. Their enthusiasm, helpfulness, insights and critical analyses have kept me focussed and dedicated, and have been invaluable during the course of my studies.

Much of my work has been conducted at the Waltham Centre for Pet Nutrition, from which I would like to acknowledge all the associates I have encountered over the last seven years. I thank the statistical analysis team based at the Waltham Centre for Pet Nutrition, especially Alison Colyer, Ruth Staunton and Richard Haydock. Many of the complex analyses undertaken in this thesis were devised with, and conducted under the guidance of the WCPN statistical analysis team who provided me with their expertise, knowledge and skills, striving to help me understand principles that I find complex and challenging.

Numerous other individuals and teams at the Waltham Centre for Pet Nutrition also deserve praise for the production of this work. The Laboratory, Oral Health and Digestive Health teams have all witnessed me labouring away in various WCPN laboratories. Their help and encouragement have been much appreciated. I also thank the WCPN animal carers and veterinarians who have collected canine plaque and faeces and blood for this work on many occasions, helpfully and diligently. And finally at WCPN, I must thank the magnificent dogs who have provided the material and study groups for me to analyse!

My work has also required the collection, processing and analyses of samples external to the Waltham Centre for Pet Nutrition. I would like to express my gratitude to Natalie Allcock and Anna Straatman-Iwanowska from the University of Leicester Electron Microscopy Facility. Their helpfulness with the scanning and transmission electron microscopy processing work in this thesis was invaluable, teaching and guiding me to conduct the imaging on these equipment. I would especially like to thank Natalie for her patience and perseverance whilst helping me to find a successful protocol to image the protozoa. Also, I thank Professor Graham Clark from the London School of Hygiene & Tropical Medicine who so kindly provided me with a living stain of *Entamoeba invadens* and genetic materials from a range of other protozoa, all crucial to my work. In addition, I would like to show my appreciation to Dr Ivan Čepička from the Charles University, Prague, who provided to me the elusive, “working”, Protargol staining protocol for trichomonads.

Penultimately, I thank the Waltham Centre for Pet Nutrition, Mars Petcare UK, Mars Inc and the University of Leicester for providing the funding, support, and further education processes that have allowed this work and thesis to take place.

And finally...I must acknowledge my wife Sheetal, and children Shivam and Tulsi. Over that last seven years they have endured my absence, and preoccupation with the work required for this thesis. Conducting this thesis part-time, whilst also working full-time, has required me to use weekend and evening time, which should have been dedicated to them. Thankfully, they understood and accepted my commitment, without complaint, and graciously sacrificed to allow me to work, write and complete this thesis in time.

Table of contents

Abstract.....	2
Acknowledgments	3
Table of contents.....	4
List of Tables	11
List of Figures.....	14
List of Abbreviations	17
CHAPTER 1: INTRODUCTION AND LITERATURE REVIEW	19
Introduction.....	19
1.1. Canine periodontal disease.....	19
1.1.1. Human oral plaque bacteria	20
1.1.2. Canine oral plaque bacteria	20
1.2. Protozoa.....	22
1.2.1. Oral protozoa	22
1.3. <i>Entamoeba gingivalis</i>	23
1.3.1. <i>E. gingivalis</i> and periodontal disease	23
1.3.2. <i>E. gingivalis</i> in canine oral health	25
1.3.3. <i>E. gingivalis</i> and pathogenesis	25
1.4. <i>Trichomonas tenax</i>	26
1.4.1. <i>T. tenax</i> and periodontal disease.....	26
1.4.2. <i>T. tenax</i> and a pathogenic role	27
1.4.3. <i>T. tenax</i> in canine oral health.....	28
1.5. Other protozoa of the oral cavity	29
1.6. Aims and objectives	29
CHAPTER 2: MATERIALS AND METHODS	33
2.1. Screening tools for identification of protists in biological samples	33
2.1.1. Sequence alignment and 18S rRNA PCR primer design.	33

2.1.2.	Ribosomal 18S rDNA gene PCR amplification and optimisation.	33
2.1.3.	Bacterial 16S PCR amplification.....	35
2.1.4.	18S- <i>Giardia gdh</i> duplex PCR	36
2.1.5.	Gel electrophoresis	37
2.1.6.	Bacterial cultures	37
2.1.7.	Protozoan cultures – type strains	37
2.1.8.	Protozoan cultures – environmental isolates	38
2.1.9.	Yeast and fungal cultures	38
2.1.10.	Protozoa and control organism genomic DNA samples and extraction	38
2.1.11.	DNA quantification	39
2.1.12.	Genomic DNA limits of detection PCRs.....	39
2.1.13.	Limit of cellular detection	39
2.1.14.	Mixed 18S rRNA PCR	41
2.1.15.	Canine faecal sample collection and storage	41
2.1.16.	Faecal sample DNA extraction and 18S- <i>Giardia gdh</i> duplex PCR protocol.....	42
2.1.17.	Spiking of Faeces with protozoa.	43
2.1.18.	18S- <i>Giardia gdh</i> duplex PCR protocol test with canine plaque samples.	44
2.1.19.	18S PCR screen of periodontal health state samples.....	44
2.1.20.	Statistical analysis 18S PCR screen.	48
2.1.21.	Next Generation Sequencing of pooled canine plaque samples.....	48
2.1.22.	Analysis of Roche 454™ GS FLX+ sequencing data.	49
2.1.23.	Statistical Analysis of 454™ GS FLX+ sequencing data.....	50
2.2.	Quantification of <i>Trichomonas</i> and <i>Entamoeba</i> and levels during the progression of canine periodontal disease	51

2.2.1.	Generation of amplification targets for the development of quantitative real-time polymerase chain (qPCR) reaction protocols.....	51
2.2.2.	Real-time assay primer design.....	52
2.2.3.	Real-time PCR assay conditions.....	52
2.2.4.	Real-time assay standard curves, assay efficiencies, limits of detection and copy number calculations.	53
2.2.5.	Real-time assay cross reactivity examination.....	54
2.2.6.	Real-time quantification of <i>E. gingivalis</i> and <i>Trichomonas</i> spp. In canine plaque	55
2.2.7.	Restriction digest of Real-time qPCR assay amplicons for the species level identification of <i>Trichomonas</i> spp.	56
2.2.8.	Real-time quantification of canine plaque – data manipulation	57
2.2.9.	Real-time quantification of canine plaque – statistical analysis.....	57
2.3.	Primer independent screen of canine plaque for the detection of protists ..	60
2.3.1.	Canine plaque collection – Health samples	60
2.3.2.	Canine plaque collection – Disease samples	61
2.3.3.	Re-precipitation of Total RNA samples	63
2.3.4.	Visualisation and analysis of RNA samples.....	64
2.3.5.	Bacterial 16S and 23S rRNA depletion from total RNA samples.....	64
2.3.6.	2D cDNA sequencing of Health and Disease samples using the MinION™ device	65
2.3.7.	Direct RNA sequencing of Health and Disease samples using the MinION™ device	67
2.3.8.	RNA sequence taxonomic assignment	69
2.3.9.	Statistical analysis of MinION cDNA and direct RNA sequencing sequence proportions	70
2.4.	Functional activity of <i>Trichomonas canistomae</i>	71
2.4.1.	Modified TYI-S-33 medium for the culture of canine oral Trichomonads (Gannon and Linke, 1991).....	71

2.4.2.	Canine filtered saliva	71
2.4.3.	Isolation and culture of canine oral trichomonads.....	72
2.4.4.	Cryopreservation and resurrection of canine oral trichomonads.....	73
2.4.5.	Genomic DNA extraction from cultured canine oral Trichmonads	73
2.4.6.	18S PCR of cultured canine oral Trichmonads	74
2.4.7.	18S full length PCR of cultured canine oral Trichmonads using Dimasuay and Rivera (2013) primers.....	74
2.4.8.	ITS1-5.8S-ITS2 full length PCR of cultured canine oral Trichmonads using Felleisen, (1997) primers	75
2.4.9.	Amplicon Sanger sequencing and identification	75
2.4.10.	Phylogenetic analysis of <i>Trichomonas</i> genetic sequences	76
2.4.11.	Culture and identification of bacteria in co-culture with <i>T. canistomae</i> (CLEO strain)	77
2.4.12.	β -tubulin staining of the <i>Trichomonas</i> flagella	78
2.4.13.	Protargol (Silver Proteinate) synthesis	79
2.4.14.	Protargol staining of trichomonads.....	80
2.4.15.	Scanning electron microscopy.....	82
2.4.16.	Transmission electron microscopy	83
2.4.17.	Enzyme detection using API® ZYM®	84
2.4.18.	General protease detection assay	85
2.4.19.	BAPNA assay for Trypsin activity.....	86
2.4.20.	Haemolysis assay.....	87
2.4.21.	Elastase activity assay	89
2.4.22.	Culture of immortalised canine gingival fibroblasts	90
2.4.23.	Co-culture of <i>T. canistomae</i> (CLEO strain) and gingival fibroblasts...	90

CHAPTER 3: IDENTIFICATION OF <i>TRICHOMONAS</i> AND <i>ENTAMOEBA</i> IN CANINE PLAQUE AND THEIR ASSOCIATION WITH PERIODONTAL DISEASE	94
Introduction.....	94
Results and discussion	96
3.1. Development of an 18S rRNA gene PCR targeting protist organisms.	96
3.2. Specificity of 18S rRNA gene universal PCR	97
3.3. Detection limits of the 18S rRNA gene PCR.....	101
3.4. 18S duplex PCR for the additional detection of <i>Giardia</i> spp.	104
3.5. Detection of protozoa in canine plaque and their association to periodontal disease	115
CHAPTER 4: IDENTIFICATION AND QUANTIFICATION OF <i>TRICHOMONAS</i> AND <i>ENTAMOEBA</i> IN LONGITUDINALLY COLLECTED PLAQUE SAMPLES USING TWO NOVEL REAL-TIME QUANTITATIVE POLYMERASE CHAIN REACTIONS	123
Introduction.....	123
Results and discussion	124
4.1. qPCR reaction assay primer design and assay conditions.	124
4.2. qPCR reaction assay efficiency and detection limits.	125
4.3. qPCR reaction assays EG1 and TC2 cross reactivity.....	127
4.4. qPCR assay TC2 amplicon digestion with BcnI.	128
4.5. ..EG1 and TC2 assay qPCR screen of longitudinally collected canine plaque samples	130
4.5.1. Primary analyses of data set – protozoa abundance and progression of periodontal disease.	133
4.5.2. Secondary analysis of data set – probability of detecting of protozoa.	136
4.5.3. Additional analysis of data – <i>Trichomonas</i> species identification	140
4.5.4. Covariate analysis of data – exploration of sample metadata	144

CHAPTER 5: IDENTIFICATION OF ORAL PROTISTS IN CANINE TOTAL RNA ISOLATED FROM PLAQUE	156
Introduction.....	156
Results and discussion	158
5.1. Canine plaque collection from WALTHAM (Health) and client owned (Disease) dogs and total RNA extractions	158
5.2. Bacterial ribosomal RNA depletion	158
5.3. MinION™ sequencing of 16S/23S depleted total rRNA using barcoded 2D cDNA sequencing	160
5.4. Direct MinION™ sequencing of total RNA extracted from canine plaque for the identification of protozoa.....	166
5.5. Comparison of total RNA sequencing techniques	173
CHAPTER 6: FUNCTIONAL AND POTENTIAL VIRULENCE ATTRIBUTES OF <i>TRICHOMONAS CANISTOMAE BRIXI</i> AND CONTRIBUTION TO PERIODONTAL DISEASE	176
Introduction.....	176
6.1. Isolation and molecular identification of a novel canine oral <i>Trichomonas</i> . ..	177
6.2. Culture, structure and morphology of <i>Trichomonas bixi</i>	183
6.2.1. Culture and propagation of canine oral Trichomonads.	183
6.2.2. <i>T. bixi</i> structure	183
6.3. Functional activity of <i>T. bixi</i> and its potential contribution to canine periodontal disease	194
6.3.1. API® ZYM® semi-quantitative enzymatic activity strips.....	195
6.3.2. Non-specific protease detection.....	197
6.3.3. Serine protease activity of <i>T. bixi</i>	199
6.3.4. Haemolytic activity of <i>T. bixi</i>	202
6.3.5. Elastase activity of <i>T. bixi</i>	206
6.3.6. <i>T. bixi</i> cytopathic effect on canine gingival fibroblasts	207

CHAPTER 7: GENERAL CONCLUSIONS AND DISCUSSION	213
7.1. Detection of protozoa	213
7.2. Temporal dynamics	216
7.3. Primer independent tools.....	219
7.4. Virulence	222
7.5. Final conclusions.....	225
Bibliography	227
Appendices.....	242
Supplemental Tables.....	243
Supplemental Figures	304

List of Tables

Table 1. NCBI GenBank (Coordinators, 2017) protozoan sequences chosen for sequence alignment during 18S rDNA PCR primer design.	34
Table 2. 18S rRNA gene amplicon sizes produced from protozoa and other eukaryotic organisms using the 18S PCR developed in this study.	36
Table 3. Source of protozoan, bacterial, yeast and fungal cultures and genomic DNA used in this study.	40
Table 4. Faecal samples collected at the WALTHAM centre for Pet Nutrition	43
Table 5. Metadata associated with canine subgingival plaque collected from animals presenting with severe periodontal disease (stages 3-4), periodontal disease stage 1, gingivitis, or from healthy animals.	45
Table 6. Sequences and locations of primers used in real-time quantification of <i>E. gingivalis</i> and an unidentified <i>Trichomonas</i> in canine plaque	52
Table 7. Dogs used in the study with good oral health	62
Table 8. Dogs used in the study with poor oral health.	63
Table 9. Details of dogs from which canine oral trichomonads were isolated from.	73
Table 10. Universal PCR primers designed in this study to amplify variable regions 4 to 8 of the 18S rRNA gene of protozoa.	97
Table 11. PCR limit of detection values for protozoan genomic DNA templates using 18S rRNA primers.	102
Table 12. The cellular limit of detection values for protozoa tested using the 18S rRNA protozoan PCR.	102
Table 13. Faecal samples collected from animals exhibiting poor quality faeces.	114
Table 14. Two-sample binomial tests on proportions of trichomonads and Entamoebae positive plaque samples.	118
Table 15. Total number of 454 reads obtained from trichomonad and entamoebae.	119
Table 16. Probability scores for trichomonad and Entamoebae 454 sequence reads	121
Table 17. Summary of standard curve data calculations for protozoa-targeted qPCR assays.	126
Table 18. Abundance (gene copy number) of the canine oral <i>Trichomonas</i> sp. and <i>E. gingivalis</i> using qPCR at the indicated time points of the study.	134

Table 19. Abundance (gene copy number) fold changes of <i>Trichomonas</i> sp. and <i>E. gingivalis</i> at the indicated time points of the study..	135
Table 20. Estimated probability of detection of the isolated canine oral <i>Trichomonas</i> sp. and <i>E. gingivalis</i> using qPCR.....	137
Table 21. Odds ratios for the detection of the isolated canine <i>Trichomonas</i> sp. and <i>E. gingivalis</i>	139
Table 22. Estimated probability of the presence of the isolated canine oral <i>Trichomonas</i> sp. and <i>T. tenax</i> in progressing (PD_PRESENT) and non-progressing (NO_PD) periodontitis tooth groups.....	141
Table 23. Odds ratios for the probability of the detection of the isolated canine <i>Trichomonas</i> sp. and <i>T. tenax</i>	143
Table 24. Estimated abundance (gene copy number) fold changes for the canine oral <i>Trichomonas</i> sp. (assay TC2) and <i>E. gingivalis</i> (assay EG1) using qPCR in sample groups that progress (PD_PRESENT) or do not progress (NO_PD) to early stage periodontal disease.....	146
Table 25. Estimated abundance (gene copy number) fold changes for the canine oral <i>Trichomonas</i> sp. (assay TC2) and <i>E. gingivalis</i> (assay EG1) using qPCR in sample groups that progress (PD_PRESENT) or do not progress (NO_PD) to early stage periodontal disease.....	147
Table 26. Estimated abundance (gene copy number) fold changes for the canine oral <i>Trichomonas</i> sp. (assay TC2) and <i>E. gingivalis</i> (assay EG1) using qPCR in sample groups that progress (PD_PRESENT) or do not progress (NO_PD) to early stage periodontal disease.....	149
Table 27. Estimated abundance (gene copy number) fold changes for the canine oral <i>Trichomonas</i> sp. (assay TC2) and <i>E. gingivalis</i> (assay EG1) using qPCR in sample groups that progress (PD_PRESENT) or do not progress (NO_PD) to early stage periodontal disease.....	150
Table 28. Estimated abundance (gene copy number) fold changes for the canine oral <i>Trichomonas</i> sp. (assay TC2) and <i>E. gingivalis</i> (assay EG1) using qPCR in a sample group that did not progress (NO_PD) to early stage periodontal disease.....	152
Table 29. Estimated abundance (gene copy number) fold changes for the canine oral <i>Trichomonas</i> sp. (assay TC2) and <i>E. gingivalis</i> (assay EG1) using qPCR in a sample group that progressed (PD_SEEN) to early stage periodontal disease.....	155

Table 30. Statistics for MinION™ cDNA sequencing run (1D reads) of 16S/23S depleted total rRNA samples..	162
Table 31. Statistics for MinION™ cDNA sequencing run (2D reads) of 16S/23S depleted total rRNA samples..	163
Table 32. Total numbers of MinION cDNA sequencing reads and percentages for <i>Trichomonas</i> sp. and <i>Entamoeba</i> sp.	164
Table 33. Total sequences proportions and odds ratios with confidence intervals (C.I) for <i>Trichomonas</i> sp. and <i>Entamoeba</i> sp. sequences found in pooled Health or Disease 16S/23S depleted RNA samples.....	165
Table 34. Summary statistics of sequences obtained from Direct MinION™ RNA sequencing of total RNA obtained from a canine Health pooled plaque sample. ...	167
Table 35. Summary statistics of sequences obtained from Direct MinION™ RNA sequencing of total RNA obtained from a canine Disease pooled plaque sample. .	169
Table 36. Total numbers of Direct MinION™ RNA sequencing reads and percentages for <i>Trichomonas</i> sp. and <i>Entamoeba</i> sp.....	171
Table 37. Total sequences proportions and odds ratios with confidence intervals (C.I) for <i>Trichomonas</i> sp. and <i>Entamoeba</i> sp. sequences found in pooled Health or Disease total RNA samples.....	172
Table 38. API® ZYM® semi-quantitative enzymatic activity strip results for <i>T. brixii</i>	196
Table 39. Non-specific protease detection..	198
Table 40. Mean trypsin levels (n=6) for <i>T. brixii</i> cell pellets and supernatants, <i>T. brixii</i> /canine gingival fibroblast co-culture cell pellets and supernatants and <i>P. gulae II</i> cell pellets and supernatants.....	201

List of Figures

Figure 1. Gel electrophoresis of 18S rRNA PCR amplicons formed from representative protozoa and other tested organisms.	98
Figure 2. Protozoan 18S rRNA gene PCR with a range of canine oral bacterial isolates.	100
Figure 3. Gel electrophoresis of PCR products amplified from mixed DNA template pools.....	103
Figure 4. Gel electrophoresis of PCR products amplified using an 18S- <i>Giardia</i> duplex PCR protocol (section 2.1.4) designed to amplify a broad range of protozoa including <i>G. intestinalis</i>	105
Figure 5. Gel electrophoresis of PCR products amplified from <i>G. intestinalis</i> DNA.	106
Figure 6. Gel electrophoresis of PCR products amplified from <i>G. intestinalis</i> genomic DNA.	107
Figure 7. Gel electrophoresis of PCR products amplified using the 18S- <i>Giardia gdh</i> duplex PCR protocol and <i>T. tenax</i> and <i>E. invadens gDNA</i>	108
Figure 8. Gel electrophoresis of PCR products amplified using the 18S- <i>Giardia gdh</i> duplex PCR protocol and <i>T. tenax</i> and <i>E. invadens gDNA</i>	109
Figure 9. 18S- <i>Giardia gdh</i> PCR on protozoan “spiked” faecal samples.....	111
Figure 10. (A) 18S rRNA and (B) duplex 18S- <i>Giardia gdh</i> PCRs of canine plaque samples known to contain protozoal DNA.....	112
Figure 11. Percentage of trichomonad- and Entamoebae-positive canine plaque samples detected in categorised groups by 18S PCR (n=92)..	117
Figure 12. Cumulative percentage of trichomonad and Entamoebae 18S sequences (detected through Roche 454 TM sequencing) in categorised pooled canine plaque samples.....	120
Figure 13. Agilent Bioanalyzer electropherogram of qPCR TC2 assay amplicons, digested with BcnI enzyme.....	130
Figure 14. Study design for samples collected from the individual dogs over a sixty week period.....	132
Figure 15. Plotted data for the estimated probability of the presence of an isolated canine oral <i>Trichomonas</i> sp. and <i>T. tenax</i> in canine plaque samples collected prior to early stage periodontal disease..	142

Figure 16. Total RNA extracted from 15-dog pooled canine plaque samples from animals with a good oral health state, and animals with moderate to severe periodontal disease (> PD2).....	159
Figure 17. Bioanalyser electropherograms showing the depletion of bacterial 16S and 23S RNA.	161
Figure 18. Proportion of <i>Trichomonas</i> sp. and <i>Entamoeba</i> sp. sequences found in pooled Health or Disease, 16S/23S depleted, RNA samples using a MinION cDNA sequencing protocol and BLAST+ assignment of sequence taxonomy against the SILVA 128 SSURef database.	165
Figure 19. Dot plots of Pre- and Post-NanoFilt software processed Direct MinION™ RNA sequencing reads obtained from total RNA of a canine Health pooled plaque sample.	168
Figure 20. Dot plots of Pre- and Post-NanoFilt software (Decoster, 2018) processed Direct MinION™ RNA sequencing reads obtained from total RNA of a canine Disease pooled plaque sample.	170
Figure 21. Proportion of <i>Trichomonas</i> sp. and <i>Entamoeba</i> sp. sequences found in pooled Health or Disease total RNA samples using a Direct MinION™ RNA sequencing protocol and BLAST+ assignment of sequence taxonomy against the SILVA 132 SSURef database.	172
Figure 22. Phylogenetic relationships between 10 unidentified canine oral <i>Trichomonas</i> isolates and the trichomonad genus group based on the full length eukaryotic ribosomal 18S gene.	179
Figure 23. Phylogenetic relationships between 10 unidentified canine oral <i>Trichomonas</i> isolates and the trichomonad genus group based on the ITS1–5.8SrRNA-ITS2 gene.	181
Figure 24. <i>Trichomonas bixi</i> cells fixed in Bouin’s solution and stained with anti-β-tubulin antibody to reveal flagella.	184
Figure 25. Scanning electron micrographs of <i>T. bixi</i> cells fixed with 2.5 % (v/v) glutaraldehyde and post stained with 0.5 % (v/v) Osmium Tetroxide.	186
Figure 26. High magnification scanning electron micrographs of <i>T. bixi</i> cells fixed with 2.5 % (v/v) glutaraldehyde and post stained with 0.5 % (v/v) Osmium tetroxide.	187
Figure 27. Transmission electron micrograph of <i>T. bixi</i> cells fixed with 2.5 % (v/v) glutaraldehyde and post stained with 1 % (v/v) Osmium Tetroxide.	189

Figure 28. Transmission electron micrograph of <i>T. brixii</i> cells fixed with 2.5 % (v/v) glutaraldehyde and post stained with 1 % (v/v) Osmium Tetroxide, displaying details of the anterior flagella.....	190
Figure 29. Transmission electron micrograph of <i>T. brixii</i> cells fixed with 2.5 % (v/v) glutaraldehyde and post stained with 1 % (v/v) Osmium Tetroxide.	190
Figure 30. Transmission electron micrograph of <i>T. brixii</i> cells fixed with 2.5 % (v/v) glutaraldehyde and post stained with 1 % (v/v) Osmium Tetroxide, displaying the pelta and axostyle microtubules, and the basal body complexes.....	193
Figure 31. Mean trypsin detected in <i>T. brixii</i> cell pellets (n=6) and supernatants, and <i>T. brixii</i> /canine gingival fibroblast co-culture cell pellet and supernatants..	200
Figure 32. Mean percentage haemolysis values (n=6) of canine red blood cells and equine blood cells, exhibited by <i>T. brixii</i> cell pellets and supernatants, and <i>T. brixii</i> /canine gingival fibroblast co-culture supernatant.	203
Figure 33. Mean percentage haemolysis values (n=6) of canine red blood cells and equine blood cells, exhibited by canine gingival fibroblast (CGFIB) cell pellets and cell supernatant.	205
Figure 34. Elastase enzyme activity of <i>T. brixii</i> cell pellets and supernatants (n=6), <i>T. brixii</i> /canine gingival fibroblast co-culture cell pellet and supernatants (n=6), and <i>P. gulae II</i> cell pellets and supernatants (n=6)..	207
Figure 35. Mean values (n=6) of cellular activity from canine gingival fibroblasts co-cultured with, and without, the canine oral trichomonad, <i>T. brixii</i>	209
Figure 36. Mean values for cell numbers of canine gingival fibroblasts co-cultured with, and without, the canine oral trichomonad, <i>T. brixii</i>	210

List of Abbreviations

ATCC	American Type Culture Collection
BLAST	Basic local alignment search tool
bp	base pair
°C	degrees Celsius
CCAP	Culture Collection of Algae and Protozoa
CFU	colony forming unit
DNA	deoxyribonucleic acid
DPBS	Dulbecco's phosphate buffered saline
dNTP s	deoxynucleotide triphosphates
dH ₂ O	distilled water
EDTA	ethylenediaminetetracetic acid
g	Gravity
M	molar
mM	millimolar
Ng	nannograms
OD	optical density
OTU	operational taxonomic units
PCR	polymerase chain reaction
RNA	ribonucleic acid
rRNA	ribosomal RNA
SDS	sodium dodecyl sulphate
SEM	scanning electron microscopy
SSU	small subunit
TAE	tris-acetate EDTA
TE	Tris-EDTA
TEM	transmission electron microscopy
T _m	melting temperature
μL	microlitre
μM	micromolar
WCPN	WALTHAM® Centre for Pet Nutrition

Introduction and Literature Review

CHAPTER 1: INTRODUCTION AND LITERATURE REVIEW

Introduction

1.1. Canine periodontal disease

Oral disorders are considered the most prevalent cause of concern in dog health currently. Of these disorders, periodontal disease is seen to be the most widespread (Kyllar and Witter, 2005), with estimates ranging from 44-64% of all individuals (V. Butković et al., 2001, Hamp et al., 1984). Periodontal disease results when inflammatory responses occur in the oral periodontium (soft tissues around the tooth root) following exposure to plaque (Page and Schroeder, 1976, Socransky and Haffajee, 1992). Periodontal disease is comprised of two distinct stages. Plaque build-up initially results in the gingivitis stage – a mild inflammatory response where the gingiva reddens, becomes swollen and tender (Wiggs and Lobprise, 1997). Gingivitis can be treated and reversed to a healthy state using professional dental treatment (descale and polish) and consistent homecare, such as tooth brushing (Niemić, 2008). However, if left uncontrolled, gingivitis may progress to inflammation of deeper regions of the tooth supporting structures leading to tissue destruction (Page and Schroeder, 1976). This continued damage results in gingival recession and periodontal pocket formation. Although small periodontal pockets may be treatable, if left, they can deteriorate to result in periodontal ligament destruction, alveolar bone loss, and eventual loss of teeth (severe periodontitis) (Page and Schroeder, 1976). The bone loss caused by this second stage of the disease is not reversible (Cochran, 2008, Grossi et al., 1995, Page and Schroeder, 1976, Ramfjord et al., 1973).

Dental plaque is associated with periodontal disease and comprises a complex biofilm including a variable population of microorganisms that secrete proteins and glycoproteins. These bacterial products can contribute directly to tissue destruction (Socransky and Haffajee, 1992) but can also initiate a host immune response. This is particularly true for host matrix metalloproteinases that in turn help bring about the tissue destruction and inflammation observed in periodontal disease (Genco and Slots, 1984). Although bacterial invasion and proteolytic enzymes may contribute to the disease (Socransky and Haffajee, 1992, Popova et al., 2013), the host

response produced as a result of the bacterial presence is thought to result in the more harmful outcome (Tatakis and Kumar, 2005).

Understanding and effectively treating periodontal disease at all stages of its progression still requires extensive research. In particular little is known currently about the full causes of, and aetiology of, canine periodontal disease.

1.1.1. Human oral plaque bacteria

The bacteria currently thought to be involved in human dental plaque formation have been described (Kolenbrander and London, 1993). Bacteria identified from oral plaque have been grouped into complexes that illustrate their association with disease (Socransky et al., 1998). The red complex, *Porphyromonas gingivalis*, *Treponema denticola* and *Tannerella forsythensis* (renamed from *Bacteroides forsythus* (Sakamoto et al., 2002), is most strongly associated with clinical signs such as increased pocket depth and bleeding on probing. Organisms of the orange complex, which include members of the *Fusobacterium nucleatum/periodonticum* subspecies, *Prevotella intermedia*, *Prevotella nigrescens*, *Peptostreptococcus micros*, *Eubacterium nodatum*, *Campylobacter rectus*, *Campylobacter showae*, *Streptococcus constellatus* and *Campylobacter gracilis* were found to precede the red complex organisms in colonisation of the periodontal pocket. Three other complexes of organisms have been also identified but are less well described. Other bacteria associated specifically with human periodontal disease are a mainly gram-negative group of anaerobes that include *Aggregatibacter actinomycetemcomitans*, *P. gingivalis*, *P. intermedia*, *T. forsythensis*, *C. rectus*, *E. nodatum*, *P. micros*, *Staphylococcus intermedius* and *Treponema* sp. (Lovegrove, 2004).

Although many species are present in plaque, key species from the red complex are thought to disrupt the complex communities, inducing inflammation and interfering with the host response during periodontal disease (Hajishengallis et al., 2011, Darveau, 2010).

1.1.2. Canine oral plaque bacteria

In contrast to the human field, the microorganisms and contributory agents associated with canine biofilm formation and periodontal disease have not been described in the same detail. However, there are studies indicating major

differences between human and canine plaque bacteria. Initial work by (Elliott et al., 2005) identified 84 canine plaque phylotypes from 37 genera. Approximately half of these 84 phylotypes were identified to species level and of these only 28% were identified as also being found in human plaque. The remaining 50% of phylotypes were identified as candidate new species. The predominant genera of bacteria seen in canine plaque were *Porphyromonas*, *Actinomyces* and *Neisseria*. Other bacteria associated with canine periodontal disease, are *Synergistes* spp., *Odoribacter denticanis*, *Peptostreptococcus* spp. *Eubacterium nodatum*, *Porphyromonas* spp. and novel undescribed species from the taxa *Clostridiales*, *Selenomonas* and *Bacteroidetes* (Marshall-Jones; et al., 2007). Individual species identified that also showed an association to periodontal disease were *T. denticola*; *Desulfomicrobium orale*, *Bacteroides denticanoris* and *Filifactor villosus* (Marshall-Jones; et al., 2007).

More recently, the increased sensitivity of molecular sequencing techniques has revealed many more species of bacteria present in canine plaque than were previously identified via traditional culture-based techniques (Davis et al., 2013). In a study of 223 canine plaque samples, 274 taxonomically different bacteria were discovered and those from the genus *Porphyromonas*, *Moraxella* and *Bergeyella* found to be more associated with clinically healthy samples, while *Peptostreptococcus*, *Actinomyces*, and *Peptostreptococcaceae* were the most abundant genera in samples from periodontal disease (Davis et al., 2013). Bacteria colonise the tooth surface in microbial succession. The early colonising species present in the dog mouth have been identified using in vitro biofilm models and molecular analyses of canine teeth following descale and polish of teeth (Holcombe et al., 2014). The bacteria found to have the highest relative abundance after early colonisation (post descale and polish) were *Bergeyella zoohelcum*, *Neisseria shayeganii* and a *Moraxella* spp. Interestingly, Streptococcal species that are found to be the most abundant species in early human plaque formation (Rickard et al., 2003, Li et al., 2004), are found at relatively low levels in canine early biofilms (Holcombe et al., 2014). Through longitudinal studies it has been shown that early health associated bacteria reduce over time and this abundance change is linked to the progression of teeth towards periodontal disease (Wallis et al., 2015).

Although a considerable amount of research has been undertaken towards the discovery of the bacterial species present in canine plaque and those associated with

oral health and disease, many other microorganisms could be present in canine plaque and involved in this complex pathogenesis.

1.2. Protozoa

Protozoa are eukaryotic, unicellular organisms that are highly abundant in the environment (Taylor, 2000). They may occupy many environments, habitats and niches and play a vital role in maintaining the balance of bacterial and other microbial life. There are approximately 65,000 described protozoa and, by comparison, only about 4,500 bacteria have been described (Taylor, 2000). Most protozoa exist as free-living or harmless commensal organisms, but several are linked with some of the most important global diseases of both man and animals. Many play critical roles in human and animal pathogenesis. These include *Plasmodium falciparum* - which causes malaria, *Entamoeba histolytica* - which causes amoebic dysentery and *Trichomonas vaginalis* - which causes trichomoniasis. A fourth protozoan, *Leishmania* spp. is an important organism in canine health. It not only affects dogs by causing cutaneous lesions, amongst other symptoms, but dogs also act as a zoonotic reservoir for the protozoan which can infect human hosts (Baneth et al., 2008).

1.2.1. Oral protozoa

Several protozoans are found in the human oral cavity. Compared to investigations of bacteria in oral health, a relatively small number of studies have focused on the role of oral protozoa in human periodontal diseases. The two most reported protozoa in the field of human periodontal health are *Entamoeba gingivalis* and *Trichomonas tenax*. Several studies (discussed in further sections of this chapter) have shown that these organisms may be of significance in the pathogenicity of periodontal disease (Athari et al., 2007, Bonner et al., 2014, Dao et al., 1983, Decarneri and Giannone, 1964, Ghabanchi et al., 2010, Gottlieb and Miller, 1971, Kurnatowska et al., 2004, Linke et al., 1989, Marty et al., 2017a, Ribeiro et al., 2015, Trim et al., 2011, Yazar et al., 2016). Although reports have indicated the presence and links to disease of both *Entamoeba* (Bonner et al., 2014, Dao et al., 1983, Decarneri and Giannone, 1964, Ghabanchi et al., 2010, Gottlieb and Miller, 1971, Linke et al., 1989, Trim et al., 2011, Yazar et al., 2016) and *Trichomonas*

(Athari et al., 2007, Decarneri and Giannone, 1964, Ghabanchi et al., 2010, Kurnatowska et al., 2004, Marty et al., 2017a, Ribeiro et al., 2015, Trim et al., 2011, Yazar et al., 2016) in the human mouth, there are no reported studies of oral protozoa and their association with periodontal disease in dogs (or other animals). The lack of knowledge in this area may detrimentally influence our understanding of the causes and persistence of periodontal disease in dogs.

1.3. *Entamoeba gingivalis*

E. gingivalis was first described by Gros in 1849 who found the organism in dental tartar scrapings. It was in fact the first parasitic protozoan to be described in humans. This microorganism is commonly found in the gingiva and periodontal pockets of humans, and is occasionally found in saliva and on the tonsils (Brumpt, 1913, Gros, 1849). *E. gingivalis* is also part of the same genus as the lumen dwelling pathogen *E. histolytica*, which has infected an estimated 50 million people worldwide and causes approximately 100,000 deaths per year (W.H.O., 1997). The two species are morphologically very similar. *E. gingivalis* trophozoites are 10-30 µm in length, with cytoplasm containing a zone of clear ectoplasm and an endoplasm containing food vacuoles. They feed predominantly on leucocytes, epithelial cells, red blood cells and bacteria (Brumpt, 1913, Gros, 1849). To date, there is no evidence of *E. gingivalis* having a cyst stage, and this seems to be the only major structural or cellular difference when compared to *E. histolytica*. However, some authors have noted *E. gingivalis* as having a resistant or putative cyst-like form (Wantland and Wantland, 1960, Lyons and Stanfield, 1989), but this is not seen by all researches and the evidence for a cyst stage is sparse. There are also recent reports indicating the presence of two *E. gingivalis* subtypes in the human mouth (Garcia et al., 2018b) however their individual roles in periodontal disease are unclear (Garcia et al., 2018a).

1.3.1. *E. gingivalis* and periodontal disease

Since Gros's discovery in 1849, there have been several reports describing the association between *E. gingivalis* and periodontal disease. Studies conducted in the 1960s isolated *E. gingivalis* from 39% of 700 dental patients examined (Wantland and Wantland, 1960). From the 700 patients surveyed, 26.4% of individuals with

healthy mouths were positive for *E. gingivalis*. Of those individuals showing signs of early periodontitis, 65% were positive for *E. gingivalis* and in individuals exhibiting advanced periodontitis, 100% were positive for the protozoan (Wantland and Wantland, 1960). Decarneri and Giannone (1964) showed 138 cases (37.6%) of oral *E. gingivalis* infection on examination of 367 women (aged 14-75) from an Italian hospital. The women were randomly chosen for the study; however no mention of the patient's oral health state is mentioned in the report.

In a later study, Lyons et al. (1983) examined 200 dental patients at a practice in Canada. Of these, 62.5% were found to possess *E. gingivalis* in their plaque. On reassessment of all 200 patients, all those with destructive periodontal lesions were found to have oral protozoan infections. Lyons also noted that if *E. gingivalis* was found in individuals with an apparently good state of oral health, in subsequent examinations a deterioration of periodontal health was observed (unless the *E. gingivalis* infection had been treated in the meantime using Metronizadole – a common and effective amoebacide). In the same year, a similar study documented *E. gingivalis* in 59% of 113 dental patients with poor oral hygiene, but also in 32% of 96 individuals that were considered to have a good standard of oral health (Dao et al., 1983). Of the dental patients found to be positive for *E. gingivalis*, 51% were found in those patients with dental caries and 17% were found in patients with periodontal disease. The remainder were found in patients with oral deformities or tooth extractions.

Linke et al. (1989) also found a correlation between *E. gingivalis* and severe periodontal disease. *E. gingivalis* was present in all 10 dental patients' surveyed (ages 20-68 years), however up to 10 sampling points were required to rule out any false negatives due to low detection levels. Most studies involve the screening of dental patients with good or poor oral health, for the presence or absence of oral protozoa using microscopic techniques and identification through morphology. Microscopic analysis of plaque samples has proved a useful, quick and cheap method of identification, but may have resulted in a large number of false negatives due to the relatively low numbers of protozoa found in each sample. A more accurate detection method may be the use of culture enrichment or polymerase chain reaction (PCR) techniques, which are capable of detecting smaller numbers of organisms in the original sample.

1.3.2. *E. gingivalis* in canine oral health

Very few studies have been conducted to assess oral protozoa in companion animals. Only two peer reviewed articles have been published in the last 80 years. (Simitch, 1938) examined 165 dogs using microscopy and detected an *Entamoeba* in three samples that did not resemble *E. gingivalis*. This was designated as *Entamoeba canibuccalis* however has not been reported since. Rousset et al. (1970) conducted a study in Parisian dogs from 1 year old to greater than 10 years old and found oral protozoa in 19 out of the 100 dogs examined. *E. gingivalis* was observed in 4 of the 19 positive dogs. The samples in which protozoa were identified were from older dogs (>5 years), which may suggest that the age of a dog plays a role in susceptibility to or colonisation by oral protozoa. Age is a significant risk factor for the onset of periodontal disease and its severity (Grossi et al., 1995, Grossi et al., 1994, Genco, 1994).

1.3.3. *E. gingivalis* and pathogenesis

As there have been very few studies investigating the role of *E. gingivalis* may in periodontal disease. In one study, an *E. gingivalis* oral isolate has been shown to cause inflammation of the gingiva in healthy rats and also induce periodontal abscesses and necrosis in rats which were immunocompromised (Al-Saeed, 2003). The morphologically and genetically related *E. histolytica* has been shown to play a key role in pathogenesis of amoebic dysentery. *E. histolytica* expresses multiple virulence factors at high levels that are involved in tissue destruction (Tillack et al., 2007). The organism also has the ability to evade the host immune defences using a variety of mechanisms (Que and Reed, 1997, Ghosh et al., 1995, Wang and Chadee, 1995). Being genetically and phenotypically similar, it is possible that *E. gingivalis* may possess similar pathogenic capabilities.

The findings in publications highlighted above, suggest that *E. gingivalis* may be an opportunistic pathogen, able to cause a pathogenic effect when the host's immune system is weakened or disabled. Many of the published reports find high numbers of protozoa, not only in diseased mouths but also in normal and healthy mouths. Lucht et al. (1998) found, that in 45 HIV-1 infected individuals examined, 29% had periodontal disease. Of those with periodontal disease, 77% showed the presence of *E. gingivalis* but the protozoan was not found in patients who showed

no signs of periodontal disease. This was the first time that *E. gingivalis* was shown to be present in HIV-1 infected individuals with periodontal disease. *E. gingivalis* was subsequently found in the pulmonary abscess of a 60-year old man (Jian et al., 2008). The patient was a heavy consumer of alcohol and tobacco, both of which suppress the human immune system (Szabo et al., 1999, McAllister-Sistilli et al., 1998). This further supports the hypothesis that *E. gingivalis* may be an opportunistic pathogen.

1.4. *Trichomonas tenax*

Trichomonas tenax is an anaerobic flagellate protozoan found in the oral cavity. It has been considered for some time to be an anaerobic commensal of the human oral cavity. However recent investigations have suggested a far greater role for this flagellate in periodontal disease and other oral disorders. *T. tenax* was the first *Trichomonas* species discovered and was found in dental plaque in the late 1700's (O. F Muller, 1773). It is commonly found in interdental spaces and pockets and in and around lesions of the oral mucosa (Dudko and Kurnatowska, 2007). *T. tenax* has two closely related species within the human host; the intestinal tract-dwelling *Trichomonas hominis*, and the urinary tract-dwelling *Trichomonas vaginalis* - a well-studied human pathogen. *T. tenax* is a pear or oval shaped organism that is highly motile with oscillating flagella that provide locomotor functionality (Ohira and Noguchi, 1917). It has a mean length of between 10 and 15µm and has four unequal flagella (14-16 µm in length) at the anterior end that radiate out from a basal granule in front of the nucleus.

1.4.1. *T. tenax* and periodontal disease.

As with *E. gingivalis*, the aetiological and pathogenic role of *T. tenax* is unclear and more work is needed to elucidate this. There have been various studies that report links or associations between *T. tenax*, periodontal disease and poor oral health, reviewed by (Marty et al., 2017b). In one study, Gharavi M. J. et al. (2006) found *T. tenax* in only 9.2% of 240 dental samples examined and found no correlation to the age or oral health of the patient. Similarly, Vrablic et al. (1991) found *T. tenax* in only 2 out of 176 children and adolescents examined and Cuevas et al. (2008) found *T. tenax* in only 12.7% of 150 children and adolescents sampled in their

study. These results imply little or no link between the presence of *T. tenax* and periodontal disease.

However, other studies have shown a stronger association between the organism and periodontal disease. In one example, Kurnatowska et al. (2004) found *T. tenax* in the mouths of 37% of the 91 individuals (aged between 23-79, including 52 women and 39 men) studied. The study also showed a correlation between the periodontal status/oral hygiene of the individual and the occurrence of *T. tenax*. An earlier study found *T. tenax* in 23% of the 700 patients examined (Jaskoski, 1963). Of the patients with healthy mouths, 11.2% were found to be positive for *T. tenax*. Of the patients with early periodontitis, 48.2% were found to be positive for *T. tenax* and of those patients with advanced periodontitis, 80% were found to be positive for *T. tenax* (Wantland and Wantland, 1960). Dudko and Kurnatowska (2007) also published a repeat of their 2004 study (highlighted above). This time they examined 189 patients (aged 23-80) and found 58 (31%) of the patients were positive for *T. tenax*. They also found a statistical correlation with the occurrence of *T. tenax* and deep periodontal pockets and loose teeth. Also in another study, 160 patients with periodontal disease were examined over a 1-year period using a specific and sensitive PCR method (Athari et al. (2007). 33 (20.6%) of the 160 patients with periodontal disease were PCR positive for *T. tenax*. In comparison only 2 (1.9%) of the 160 control patients (those considered to have good oral health) tested positive for this protozoan. The various studies carried out to assess the prevalence of *T. tenax* in the diseased and healthy mouth show considerably different outcomes. One reason for this may be the relative difficulty in identification due to low numbers leading to false negative results. The more sensitive PCR-based method undertaken by (Athari et al., 2007) may present a more realistic picture due to the enhanced accuracy of modern PCR methodologies.

1.4.2. *T. tenax* and a pathogenic role

Genetically, *T. tenax* has a very similar gene expression profile to that of *T. vaginalis*, and could be a genetic variant of this well-studied vaginal pathogen (Kucknoor et al., 2009). In a similar manner to *T. vaginalis* (Crouch and Alderete, 1999), *T. tenax* may also begin the breakdown of periodontal tissues by binding to gingival epithelial cells, using fibronectin-like adhesion cell surface ligands

(Ribaux et al., 1983). As with many of the bacteria associated with periodontal disease, *T. tenax* are also capable of expressing a range of enzymes that may play a role in any pathogenic effect it may have. It has been found to produce a series of cell-associated and extracellular proteolytic enzymes, resembling cysteine proteases and matrix metalloproteinases (Bozner and Demes, 1991a). Furthermore, *T. tenax* has been shown to produce at least 19 protease-like molecules, many of which are likely to be cysteine proteases (El Sibaei et al., 2012). These cysteine-proteases have been shown to be most likely cathepsin B-like enzymes and play important roles in pathogenesis, facilitating host tissue invasion, digestion of host proteins and host immune system evasion (Yamamoto et al., 2000).

A key marker of periodontal disease is the hydrolysis of connective tissue and collagen surrounding the tooth, eventually leading to tooth loss. Human collagenases have been implicated in this process (Reynolds et al., 1994) and it has also been shown that *T. tenax* can release extracellular enzymes that can degrade collagen types I, III, IV and V (Bozner and Demes, 1991b).

In addition, *T. tenax* exhibits and secretes at least two haemolytic enzymes, one protein-like (extracellular) and the other lipid-like (cell associated) (Nagao et al., 2000). Haemolytic enzymes represent another virulence factor of many oral pathogens currently implicated in human and canine periodontal disease. (Hillman et al., 1993).

1.4.3. *T. tenax* in canine oral health

As with *E. gingivalis*, there is a distinct lack of studies to assess the presence of oral trichomonads in the canine population. It is unclear as to whether a separate species of *Trichomonas* affects the oral cavity of dogs, or indeed cats. trichomonads found in canine and feline mouths have been described as having slight morphological differences when compared to the human species (Hegner and Ratcliffe, 1927). However, the human oral trichomonad, *T. tenax*, also survives and proliferates in the dog and cat mouth (Cielecka et al., 2000). Identifying the specific species of trichomonad in the dog and cat mouth requires further molecular and morphological analysis.

1.5. Other protozoa of the oral cavity

If the human host provides a model for animals, *E. gingivalis* and *T. tenax* are the most likely protozoans to be found within the dog and cat oral cavity. However a number of reports suggest the presence of other, potentially pathogenic, protozoa (such as free-living amoebas) in the human mouth (Bergquist, 2009, Rivera et al., 1986, Rivera et al., 1984). Studies conducted by Rivera et al. (1984 & 1986) looked at protozoa cultured from the nasal and oral regions of 30 randomly selected patients (male and female) visiting a Mexican dental clinic. Two of the most frequently identified oral isolates were *Naegleria fowleri* and *Acanthamoeba* spp. Both, if able to infect the brain can cause serious forms of meningoencephalitis (Visvesvara et al., 2007). *Acanthamoeba* spp. also plays an important role in protecting bacteria from antimicrobials by enclosing them within their highly resistant cyst, and has been shown to act as a reservoir for periodontopathogenic bacteria such as *Porphyromonas gingivalis* and *Prevotella intermedia* (Wagner et al., 2006).

1.6. Aims and objectives

The overall aims of this thesis are to identify the protozoa present in canine plaque and to investigate any potential role they play in canine periodontal disease. This thesis consists of four distinct sections:

1. The first section aim is: To identify the protozoa found in canine plaque and to assess any associations they may have with canine periodontal disease. It had the following objectives to achieve the aim:
 - Develop a targeted, molecular based method for the identification of protozoa in complex, microbial samples.
 - Identify the protozoa present in present in the canine mouth.
 - Use the developed method to screen for the presence of protozoa in a cohort of canine plaque samples collected from dogs with various stages of periodontal disease. Assign any associations which may be present between the protozoa identified and periodontal health or disease.

2. The second section aim is: To quantify the temporal abundance of protozoa in canine plaque during the progression of periodontal disease, and to assess any associations of the protozoa with the progression of disease. It had the following objectives to achieve the aim:
 - Develop quantitative polymerase chain reaction-based protocols to quantify individual protozoa abundance in samples containing low numbers of protozoa.
 - Using the methods developed, quantify the levels of protozoa in longitudinally collected plaque samples, from individual teeth that progress into early stage periodontal disease, and to assign any associations that may be present.
3. The third section aim is: To develop a primer-independent method using cutting edge third generation-based sequencing technologies to identify the protozoa present in canine plaque samples. It had the following objectives to achieve the aim:
 - Use of MinION™ sequencing technology to develop a method to sequence the ribosomal RNA of canine plaque samples
 - Identify the presence of protozoa present in periodontally healthy or diseased plaque samples using the developed methods and to assign any associations that may be present.
4. The fourth section aim is: To isolate and culture canine oral protozoa, describe their classification and morphology and to assess their potential to contribute to canine periodontal disease. It had the following objectives to achieve the aim:
 - Isolate, culture and identify the molecular phylogeny of canine oral protozoa.
 - Describe the structure and morphology of isolates.
 - Assess the putative functional activities of the isolates by examining cell associated or secreted factors that have potential to contribute to canine periodontal disease.

- Investigate the host cell destruction caused by the isolated canine oral protozoa.

Materials and Methods

CHAPTER 2: MATERIALS AND METHODS

2.1. Screening tools for identification of protists in biological samples

2.1.1. Sequence alignment and 18S rRNA PCR primer design.

Protist ribosomal 18S rDNA sequences (Table 1) were obtained from the National Institutes of Health genetic sequence database, GenBank (Benson et al., 2015). Protist sequences for alignment were chosen based on literature indicating pathogenic potential or ability to inhabit humans or animals. All sequences chosen for alignment were greater than 1000 base pairs and represented the most complete 18S rDNA gene for that particular organism at the time of design (circa 2014). Sequences were aligned using the VectorNTI software (ThermoFisher Scientific, UK), with the default alignment settings. A consensus sequence was calculated and a conserved region for PCR primer design chosen manually, the goal being to encompass as wide a region of the gene as possible, and to cover as many organisms as possible within the alignment. The degenerate PCR primers identified through this process were np-SSU-570-fwd-5'(tgccagcagcYgcggaattc) and np-SSU-1633-rev-5'(gtgtaNcaaagggcagggacgt) and were synthesised by Eurofins Genomics, Ebersberg, Germany. These primers allow the identification of protists present in the sample, based on their PCR product size (Table 2 and Supplemental Table 1).

2.1.2. Ribosomal 18S rDNA gene PCR amplification and optimisation.

Amplification of the 18S rDNA gene was performed via a touchdown PCR protocol using Platinum® Pfx DNA Polymerase kit (ThermoFisher Scientific, Life Technologies, Warrington, UK), a high fidelity enzyme preparation with proofreading (3' to 5' exonuclease) activity. After optimisation of the PCR conditions, the following PCR reaction mix was used: 5 µl Pfx amplification buffer, 5 µl PCRx Enhancer Solution, 1.5 µl deoxynucleotide triphosphates 10 mM (dNTPs – Promega Ltd, Southampton, UK), 1.5 µl of each primer (10 µM), 1.0 µl magnesium sulphate (50 mM), and 1 unit Platinum® Pfx DNA Polymerase.

Table 1. NCBI GenBank (Coordinators, 2017) protozoan sequences chosen for sequence alignment during 18S rDNA PCR primer design.

GenBank sequence name and description	Sequence length (base pairs)	GenBank Accession number	GenBank GI
<i>Acanthamoeba polyphaga</i> JAC/S2 ATCC 50372 18S rRNA gene	2,276	U07415	507411
<i>Acanthamoeba polyphaga</i> 18S ribosomal RNA gene, partial sequence	2,233	AF132135	7110083
<i>Babesia bovis</i> isolate BRC01 18S ribosomal RNA gene, partial sequence	1,612	FJ426364	237860001
<i>Balamuthia mandrillaris</i> 18S ribosomal RNA gene, partial sequence	1,972	AF019071	2979671
<i>Balamuthia mandrillaris</i> isolate V451 small subunit ribosomal RNA gene, partial sequence	1,972	AF477022	28194488
<i>Isospora felis</i> 18S ribosomal RNA gene, partial sequence	1,755	L76471	46560453
<i>Encephalitozoon cuniculi</i> small ribosomal RNA gene, complete	1,299	L17072	305102
<i>Encephalitozoon hellem</i> small ribosomal RNA gene sequence	1,314	L19070	305103
<i>Entamoeba coli</i> gene for 18S ribosomal RNA, complete sequence	2,106	AB444953	238767589
<i>Entamoeba dispar</i> genes for 18S rRNA, ITS1, 5.8S rRNA, ITS2, complete sequence	2,426	AB282661	145698417
<i>Entamoeba gingivalis</i> SrRNA gene	1,918	D28490	728491
<i>E.histolytica</i> extrachromosomal 18S rRNA gene (partial)	2,211	X75434	577006
<i>E.histolytica</i> DNA for 18S ribosomal RNA gene (partial)	1,162	X89636	908848
<i>Entamoeba histolytica</i> genes for 18S rRNA, ITS1, 5.8S rRNA, ITS2, complete sequence, strain: HK-9	2,411	AB282658	145698414
<i>Entamoeba histolytica</i> genes for 18S rRNA, ITS1, 5.8S rRNA, ITS2, complete sequence, strain: Rahman	2,411	AB282659	145698415
<i>Entamoeba histolytica</i> genes for 18S rRNA, ITS1, 5.8S rRNA, ITS2, complete sequence, strain: NOT-12	2,411	AB282660	145698416
<i>Entamoeba invadens</i> 18S ribosomal RNA gene, complete sequence	1,958	AY769863	53988537
<i>Entamoeba muris</i> gene for 18S ribosomal RNA, complete sequence	2,146	AB445018	238767590
<i>Entamoeba nuttalli</i> genes for 18S rRNA, ITS1, 5.8S rRNA, ITS2, complete sequence	2,407	AB282657	145698413
<i>Euglypha filifera</i> 18S rRNA gene, strain Costa Rica	1,815	AJ418785	18075908
<i>Euglypha rotunda</i> 18S rRNA gene, strain La Gomera	1,790	AJ418783	18075906
<i>Hartmannella</i> sp. T5-5 18S ribosomal RNA (rrn) gene, partial sequence	1,146	EF378675	125710734
<i>Isospora</i> sp. Harbin/01/08 18S ribosomal RNA gene, partial sequence	1,768	FJ357797	209865619
<i>Leishmania donovani</i> clone NE78 18S ribosomal RNA gene, partial sequence	1,450	L38572	703124
<i>Naegleria fowleri</i> 18S ribosomal RNA gene, partial sequence	1,982	U80059	2351571
<i>Naegleria fowleri</i> 18S ribosomal RNA gene, partial sequence	1,988	AF338423	13398505
<i>Balantidium coli</i> isolate BC34706 18S ribosomal RNA gene, partial sequence	1,314	EU680309	195969704
<i>Balantidium coli</i> 18S rRNA gene, isolated from ostrich	1,634	AM982723	206721408
<i>Plasmodium vivax</i> 18S ribosomal RNA gene, partial sequence	1,582	DQ660817	110084549
<i>Tetrahymena pyriformis</i> strain MDL4u 18S small subunit ribosomal RNA gene, partial sequence	1,635	EF070255	126142782
<i>Tetrahymena tropicalis</i> strain Lahorensis 18S ribosomal RNA gene, partial sequence	1,752	EF428128	148362050
<i>Tetramitus</i> sp. BD1-5 18S ribosomal RNA (rrn) gene, partial sequence	1,331	EF378693	125710752
<i>Tetramitus thermacidophilus</i> 18S rRNA gene, isolate CU8	2,065	AJ621575	46019917
<i>Toxoplasma gondii</i> 18S ribosomal RNA gene, complete sequence	1,738	L37415	642127
<i>Trichomonas gallinae</i> isolate 3 18S ribosomal RNA gene, partial sequence	1,466	EU215372	167515069
<i>Trichomonas gallinae</i> isolate 4 18S ribosomal RNA gene, partial sequence	1,508	EU215373	167515070
<i>Trichomonas gallinae</i> isolate 5 18S ribosomal RNA gene, partial sequence	1,459	EU215374	167515071
<i>Trichomonas gallinae</i> isolate 6 18S ribosomal RNA gene, partial sequence	1,007	EU215375	167515072
<i>Trichomonas</i> sp. RWG-2007-1 18S ribosomal RNA gene, partial sequence	1,160	EU215371	167515068
<i>Trichomonas</i> sp. RWG-2007-2 18S ribosomal RNA gene, partial sequence	1,451	EU215370	167515067
<i>Trichomonas tenax</i> 16S-like ribosomal RNA, complete sequence	1,580	U37711	1033186

<i>Trichomonas tenax</i> gene for SrRNA	1,552	D49495	1132484
<i>Vahlkampfia</i> 18S ribosomal RNA gene, complete sequence	2,045	AY394431	37624757
<i>Vannella epipetala</i> clone 1 18S ribosomal RNA gene, partial sequence	1,953	DQ913094	117626942
<i>Hartmannella vermiformis</i> strain CRIB-19 18S ribosomal RNA gene, complete sequence	2,813	EU137741	157688561
<i>Vexillifera armata</i> small subunit ribosomal RNA gene, complete sequence	1,977	AY183891	34485581
<i>Vexillifera minutissima</i> small subunit ribosomal RNA gene, partial sequence	1,960	AY294149	33946342

To the reaction mix, 10-50 ng of genomic DNA template was added. The final volume was brought to 50 µl using nuclease-free water (Qiagen Ltd, UK). A GeneAmp PCR 9700 thermal cycler (Thermofisher Scientific, Applied Biosystems, Warrington, UK) was used to amplify the 18S rDNA gene using the following touchdown cycle conditions: 94 °C for 2 minutes, followed by 15 cycles of 94 °C for 45 seconds, 63 °C for 45 seconds (decreasing by 0.5 °C per cycle), and 68 °C for 2.5 minutes. This was followed by 20 cycles of 94 °C for 45 seconds, 53 °C for 45 seconds, and 68 °C for 2.5 minutes and a final extension step of 68 °C for 10 minutes. The reaction was then stopped by holding at 4 °C.

2.1.3. Bacterial 16S PCR amplification

Amplification of the bacterial 16S rRNA gene in samples was performed via previously described PCR protocol (Dewhirst et al., 2012). In brief, the following PCR reaction mix was used per DNA sample: 5 µl Pfx amplification buffer, 5 µl PCRx Enhancer Solution, 1.5 µl deoxynucleotide triphosphates 10 mM (dNTPs – Promega Ltd, Southampton, UK), 1.5 µl of each 16S forward (5' - aga gtt tga tcc tgg ctc ag - 3') and reverse primer (5' - acg gct acc ttg tta cga ctt- 3') (10 mM), 1.0 µl magnesium sulphate (50 mM), and 1 unit Platinum® Pfx DNA Polymerase. To the reaction mix, 1-50 ng of genomic DNA template was added. The final volume was brought to 50 µl using nuclease-free water (Qiagen, UK). A GeneAmp PCR 9700 thermal cycler (Thermofisher Scientific, UK) was used to amplify the 16S rRNA gene using the following touchdown cycle conditions: 94 °C for 2 minutes followed by 10 cycles of 94 °C for 45 seconds, 68 °C for 45 seconds (decreasing by 0.8 °C per cycle), and 68 °C for 1.5 minutes. This was followed by 25 cycles of 94 °C for 45 seconds, 58 °C for 45 seconds, and 68 °C for 1.5 minutes and a final extension step of 68 °C for 15 minutes. The reaction was then stopped by holding at 4 °C.

Table 2. 18S rRNA gene amplicon sizes produced from protozoa and other eukaryotic organisms using the 18S PCR developed in this study.

Organism	Approximate 18S PCR amplicon size (base pairs)
<i>Plasmodium falciparum</i> (isolate 3D7)	1400
<i>Leishmania donovani</i> (MHOM/IN/80/DD8)	1500
<i>Trypanosoma b. brucei</i> (strain 427)	1450
<i>Toxoplasma gondii</i> (ATCC 50174D)	1050
<i>Hartmannella</i> sp.(environmental isolate)	1150
<i>Acanthamoeba polyphaga</i> (CCAP 1501/3G)	1500
<i>Entamoeba moshkovskii</i> (Laredo strain)	1250
<i>Trichomonas tenax</i> (ATCC 30207)	950
<i>Vahlkampfia</i> sp. (environmental isolate)	1400
<i>Tetramitus</i> sp. (environmental isolate)	1450
<i>Naegleria</i> sp. (environmental isolate)	1300
<i>Saccharomyces cerevisiae</i> gDNA	1100
<i>E.coli</i> DH5 α (ATCC 53868)	0

2.1.4. 18S-*Giardia* *gdh* duplex PCR

Amplification of the *Giardia* spp. glutamate dehydrogenase (*gdh*) gene in parallel with other protist 18S rDNA sequences was performed via a touchdown PCR protocol similar to that described above. The following PCR reaction mix was used per DNA sample: 5 μ l Pfx amplification buffer, 5 μ l PCRx Enhancer Solution, 1.5 μ l deoxynucleotide triphosphates 10 mM (dNTPs – Promega Ltd, UK), 1.5 μ l of each 18S rRNA degenerate PCR primer (np-SSU-570-fwd-5'(tgccagcagcYgcggttaattc) and np-SSU-1633-rev-5'(gtgtaNcaaagggcagggacgt) (10 mM), 1.5 μ l of each *Giardia* *gdh* gene primer (Babaei et al., 2011, Read et al., 2004); forward (5' - tcaacgtcaaccgcggcttcgt - 3') and reverse (5' - gttgtccttgcatctcc - 3') (10 mM), 1.0 μ l magnesium sulphate (50 mM), and 1 unit Platinum® Pfx DNA Polymerase. To the reaction mix, 1-50 ng of genomic DNA template was added. The final volume was brought to 50 μ l using nuclease-free water (Qiagen Ltd, UK). A GeneAmp PCR 9700 thermal cycler (Thermofisher Scientific, UK) was used to amplify the 18S rRNA genes using the following touchdown cycle conditions: 94 °C for 2 minutes followed by 15 cycles of 94 °C for 45 seconds, 63 °C for 45 seconds (decreasing by 0.5 °C per cycle), and 68 °C for 2.5 minutes. This was followed by 20 cycles of 94 °C for 45 seconds, 53 °C for 45

seconds, and 68 °C for 2.5 minutes and a final extension step of 68 °C for 10 minutes. The reaction was then stopped by holding at 4 °C.

2.1.5. Gel electrophoresis

PCR amplicons were separated in 0.5 X TAE (Tris-acetate-EDTA) buffer by gel electrophoresis either in standard 1 % (w/v) agarose gels pre-stained with 1 X GelRed (Biotium Inc., USA) and viewed on a UVP Gel Doc-it imaging system (UVP LLC, UK) or using the FlashGel system (Lonza, UK) following the manufacturer's instructions.

Longer run gels were obtained by using standard 1 % (w/v) agarose gels and undergoing electrophoresis in sodium boric acid buffer (Brody and Kern, 2004).

2.1.6. Bacterial cultures

Escherichia coli DH5 α (ATCC 53868), *Porphyromonas gulae* (OH3471), *Actinomyces canis* (OH770), and *Neisseria zoodegmatis* (OH4191) were cultured on Columbia blood agar plates (Oxoid, UK) at 38 °C. *E. coli* DH5 α was purchased from the American Type Culture Collection, USA. *P. gulae* (OH3471), *A. canis* (OH770), and *N. zoodegmatis* (OH4191) were previously isolated from canine plaque samples using Columbia blood agar plates as part of studies conducted at the WALTHAM Centre for Pet Nutrition (Davis et al., 2013, Dewhirst et al., 2012). Aerobically grown cultures were incubated for 1-2 days before subculture and anaerobically grown cultures were incubated for 7-10 days in an anaerobic workstation (Don Whitley Scientific, UK) before subculture.

2.1.7. Protozoan cultures – type strains

Trichomonas tenax (Muller) Dobell, ATCC 30207, was purchased from the American Type Culture Collection (ATCC). *T. tenax* was cultured in Modified LYI Entamoeba Medium - ATCC medium 2692 (ATCC, USA) at 35 °C and passaged every 3-5 days. *Giardia intestinalis* Alexeieff (ATCC 50581) was purchased from the ATCC and cultured in ATCC medium: 2155 LYI Giardia medium (ATCC, USA). The cultures were grown at 35 °C and subcultured every 7 days. *Entamoeba invadens* Rodhain IP-1 (ATCC 30994) was kindly provided by Dr Graham Clark (London School of Hygiene and Tropical Medicine) and was cultured in ATCC

medium: 2154 LYI Entamoeba medium (ATCC, USA) at 25 °C and subcultured every 7-10 days. *Acanthamoeba polyphaga* (CCAP 1501/3G) was kindly provided by Dr Simon Kilvington from the University of Leicester and cultured in ATCC medium: 712 PYG (ATCC, USA). It was cultured at 32 °C for 5-7 days before subculture.

2.1.8. Protozoan cultures – environmental isolates

Hartmanella sp., *Tetramitus* sp., *Vahlkampfia* sp., and *Naegleria* sp. cultures were isolated and propagated from randomly surveyed soil samples taken at the Waltham Centre for Pet Nutrition, Leicestershire, England. The strains were isolated on non-nutrient agar (Lab-M, UK) seeded with a lawn of *E. coli* DH5α (ATCC 53868). The cultures were passaged onto several non-nutrient agar plates until there were sufficient amoebae for genomic DNA extraction. The identity of each culture was confirmed through sequencing of the 18S rDNA amplicon using the above PCR protocol (data not shown).

2.1.9. Yeast and fungal cultures

Aspergillus niger (DSM 737) was obtained from the Deutsche Sammlung von Mikroorganismen und Zellkulturen GmbH, Germany. The culture was propagated on Potato Dextrose agar (Oxoid, UK) for 10-14 days at room temperature. *Fusarium solani* (ATCC 36031) was kindly provided by Dr Simon Kilvington from the University of Leicester and propagated on Potato Dextrose agar (Oxoid, UK) for 10-14 days at room temperature. For DNA extraction, both *Aspergillus* and *Fusarium* conidia were isolated by filtering a culture suspension through glass wool to remove the hyphae. The resultant filtrates containing the conidia were stored at -20°C until ready for genomic DNA extraction.

2.1.10. Protozoa and control organism genomic DNA samples and extraction

Genomic DNA samples of *Plasmodium falciparum* (3D7), *Leishmania donovani* (MHOM/IN/80/DD8) and *Trypanosoma b. brucei* (strain 427) were kindly provided by Professor Graham Clarke of the London School of Hygiene and Tropical Medicine for use in validating this protocol (Table 2). *Toxoplasma gondii*

(ATCC 50174D) genomic DNA was purchased from the ATCC. High molecular weight Canine and *Saccharomyces cerevisiae* genomic DNA, were purchased from Novagen (Merck Millipore, UK),

Laboratory cultured organisms were subjected to genomic DNA extraction by one of the following methods. The total genomic DNA from *T. tenax*, *G. intestinalis*, and *A. polyphaga* were extracted using the Qiagen DNeasy Blood and Tissue DNA extraction Kit (Qiagen, UK) using the manufacturer's animal cell protocol. Total genomic DNA from *Hartmanella* sp., *Vahlkampfia* sp., *Naegleria* sp., *A. niger*, and *F. solani* and the bacterial cultures were extracted using a previously published Chelex extraction resin method (Iovieno et al., 2011).

2.1.11. DNA quantification

Genomic DNA and PCR amplicons were quantified using the Qubit® dsDNA Assay Kit (Life Technologies, UK) and a Qubit fluorometer. Depending on the estimated sample concentration, either the Qubit broad range or the high sensitivity assay was used according to the manufacturer's standard protocols.

2.1.12. Genomic DNA limits of detection PCRs

PCRs were carried out using the 18S rRNA gene amplification protocol ([section 2.1.3](#)) or the 18S-*Giardia* *gdh* duplex protocol ([section 2.1.16](#)), on serially diluted genomic DNA preparations from protozoan organisms listed in Table 3. Genomic DNA obtained from either cultured organisms or genomic DNA samples acquired from external sources were diluted to 10 ng per µl and serially diluted 1 part DNA sample to 5 parts nuclease free water. PCRs were carried out for each organism at 10 ng, 2 ng, 0.4 ng, and 0.08 ng of DNA per PCR reaction. If the PCR was successful at the lowest concentration (0.08 ng) then that genomic DNA was additionally diluted to give 0.016 ng, 0.0032 ng, 0.00064 ng, and 0.000128 ng per PCR reaction and the PCR amplification process was repeated with these lower dilutions.

2.1.13. Limit of cellular detection

Protozoa listed as 'cultured' in Table 3, were propagated using the appropriate growth conditions for each (see culture methods). Each organism was washed twice

using ¼ Ringer's Solution (Sigma-Aldrich, UK) and enumerated using a Modified Fuchs Rosenthal Counting Chamber (Hawksley, UK).

Table 3. Source of protozoan, bacterial, yeast and fungal cultures and genomic DNA used in this study.

Organism/DNA sample	Sample type	Sample Source
<i>Plasmodium falciparum</i> (isolate 3D7)	Genomic DNA	LSHTM
<i>Leishmania donovani</i> (MHOM/IN/80/DD8)	Genomic DNA	LSHTM
<i>Trypanosoma b. brucei</i> (strain 427)	Genomic DNA	LSHTM
<i>Toxoplasma gondii</i> (ATCC 50174D)	Genomic DNA	ATCC
<i>Hartmannella</i> sp.(environmental isolate)	Cultured	LEICS
<i>Acanthamoeba polyphaga</i> (CCAP 1501/3G)	Cultured	UofL
<i>Giardia intestinalis</i> (ATCC 50581)	Cultured	ATCC
<i>Entamoeba moshkovskii</i> (Laredo strain)	Genomic DNA	LSHTM
<i>Entamoeba invadens</i> (Rodhain IP-1: ATCC 30994)	Cultured	LSHTM
<i>Trichomonas tenax</i> (ATCC 30207)	Cultured	ATCC
<i>Vahlkampfia</i> sp. (environmental isolate)	Cultured	LEICS
<i>Tetramitus</i> sp. (environmental isolate)	Cultured	LEICS
<i>Naegleria</i> sp. (environmental isolate)	Cultured	LEICS
<i>Saccharomyces cerevisiae</i> gDNA	Genomic DNA	Novagen
Canine gDNA	Genomic DNA	Novagen
<i>Fusarium solani</i> (ATCC 36031)	Cultured	UofL
<i>Aspergillus niger</i> (DSM 737)	Cultured	DSM
<i>E.coli</i> DH5α (ATCC 53868)	Cultured	ATCC
<i>Porphyromonas gulae</i> (OH3471)	Cultured	WCPN
<i>Actinomyces canis</i> (OH770)	Cultured	WCPN
<i>Neisseria zoodegmatis</i> (OH4191)	Cultured	WCPN

Samples were kindly donated by Dr Graham Clarke - London School of Hygiene and Tropical Medicine (LSHTM) and Dr Simon Kilvington - University of Leicester (UofL), or cultured at the Waltham Centre for Pet nutrition (WCPN), or cultured from environmental samples collected in the Leicestershire area of England (LEICS), or purchased from the American Type Culture Collection (ATCC), Novagen - Merck Millipore International (Novagen) or the Deutsche Sammlung von Mikroorganismen und Zellkulturen GmbH, Germany (DSM).

The organisms were adjusted to 10000 cells in 200 µL of Tris(10 mM)-EDTA(1mM) buffer pH 8.0 (Sigma-Aldrich, UK) and then underwent genomic DNA extraction using the Qiagen DNeasy Blood and Tissue DNA extraction Kit (Qiagen Ltd, UK), following the manufacturer's animal cell protocol. The final

genomic DNA extraction for each sample was eluted into 50 µL of Qiagen elution buffer AE (supplied with the extraction kit). This equates to the genomic DNA extracted from 200 cells per µL of extraction.

18S rRNA or 18S-Giardia gdh duplex protocol PCRs were performed using 10 µL of template from 1 in 10, 1 in 100, 1 in 1000 and 1 in 10000 dilutions of the 200 cells per µL genomic DNA extractions.

2.1.14. Mixed 18S rRNA PCR

To assess any PCR bias towards particular DNA templates, 1 µL of extracted genomic DNA from *Hartmannella* sp., *Acanthamoeba polyphaga* (CCAP 1501/3G), *Entamoeba invadens* (Rodhain IP-1: ATCC 30994), and *Trichomonas tenax* (ATCC 30207), equating to the genomic DNA from 200 cells, was pooled to provide a 7 µL DNA template for the 18S rRNA PCR. For the PCR, the pooled sample was serially diluted two-fold to produce a neat, 1 in 2, 1 in 4, 1 in 8, 1 in 16, and 1 in 32 dilution of original template. 7 µL of each dilution was then used as PCR template for the 18S rRNA protozoan PCR (as above).

2.1.15. Canine faecal sample collection and storage

Canine faecal samples were collected from the WALTHAM® Centre for Pet Nutrition from dogs suffering from poor faeces quality. Poor faeces quality is defined according to the Waltham faecal scoring system. Faeces scoring 3.75 or above was considered poor and is described as most or all of the form is lost, consistency is viscous ('cow dung appearance'), no real shape, and retains water within stool. Samples were collected over a 3 day period into a single sterile 50 mL tubes and stored at 4 °C during the collection procedure. Where the identified dog was housed in shared pens the faeces of the pen mate was also collected. As per the WALTHAM® Centre for Pet Nutrition policy, a portion of the 3 day sample was sent for independent microbiological analysis (IDEXX Laboratories, Inc, UK) using standard industry practises. The analysis results are used by the on-site veterinarian to devise a treatment schedule if necessary. Faeces from animals undergoing existing antibiotic treatment were not included in the study. An additional historical control faecal sample collected and stored several years previous was also available during the experiments. All faeces were immediately

stored at -80 °C to preserve DNA integrity until ready for DNA extraction (see below). Sample identities and collection dates for each samples are detailed in Table 4.

2.1.16. Faecal sample DNA extraction and 18S-*Giardia* *gdh* duplex PCR protocol

Faecal DNA was extracted from samples using the QIAamp DNA Stool Mini Kit (Qiagen Ltd, UK), following a modified version of the manufacturer's protocol. In brief, the modified protocol was as follows. 1 g of faecal material was added to 10 mL of Buffer ASL and thoroughly homogenised. 2 mL of the homogenised solution was heated for 10 minutes at 99 °C. The sample was vortexed for 15 seconds and centrifuged at maximum speed (16000 \times g) for 1 minute. 1 X InhibitEX tablet was added to 1.2 mL of supernatant and vortexed continuously until the tablet was completely re-suspended. After a further 5 minutes incubation at room temperature the sample was centrifuged at 16000 \times g for 3 minutes to pellet the inhibitor bound InhibitEX matrix. 1.5 mL of supernatant was transferred to a clean microcentrifuge tube and centrifuged at 16000 \times g for 3 minutes. 30 μ L of proteinase K and 400 μ L of Buffer AL was added to 400 μ L of supernatant and vortexed for 15 seconds. The extraction mixture was then incubated for 10 minutes at 70 °C, after which 400 μ L of ice cold 100% ethanol (Sigma-Aldrich, UK) was added. The lysate was mixed by vortexing and passed through a QIAamp spin column through centrifugation (16000 \times g for 1 minute) to bind the precipitated DNA to the column matrix. The columns were washed with 500 μ L of Buffer AW1 and AW2, and the DNA was eluted from the column by adding 50 μ L of pre-warmed (70 °C) Buffer AE directly to the column surface and centrifuging at 16000 \times g for 1 minute. The eluted DNA was stored at -20 °C.

The 18S/*Giardia* *gdh* genes from each extracted DNA sample was amplified using the 18S-*Giardia* *gdh* duplex PCR protocol described in [section 2.1.4](#). Bovine serum albumin was also added to the reaction mix (Farell and Alexandre, 2012), to reduce PCR inhibition, at a final concentration of 0.5 μ g/ μ L of PCR mix. The PCR products were visualised using the gel electrophoresis methods detailed in [section 2.1.5](#).

Table 4. Faecal samples collected at the WALTHAM centre for Pet Nutrition. Samples were collected and a portion was sent to IDEXX laboratories for standard the standard microbiological analyses indicated.

Sample collection date	Sample number	Animal name	IDEXX test result date	IDEXX test
15/08/2016	1	Esther	22/08/2016	Faecal screen - Bacteria & Giardia
15/08/2016	1	Henry	22/08/2016	Faecal screen - Bacteria & Giardia
11/08/2016	2	Willoughby	17/08/2016	Faecal screen - Bacteria & Giardia
11/08/2016	2	Ophelia	17/08/2016	Faecal screen - Bacteria & Giardia
29/07/2016	3	Rodger	03/08/2016	BASIC FAECAL SCREEN
29/07/2016	3	Rabbit	03/08/2016	BASIC FAECAL SCREEN
29/07/2016	3	Elsa	03/08/2016	BASIC FAECAL SCREEN
10/08/2016	4	Opal	12/08/2016	Faecal screen - Bacteria & Giardia
10/08/2016	4	Ivy	12/08/2016	Faecal screen - Bacteria & Giardia
10/08/2016	5	Diesel	09/08/2016	Faecal screen - Bacteria & Giardia
14/08/2016	6	Roy	22/08/2016	Faecal screen - Bacteria & Giardia
14/08/2016	6	Lois	22/08/2016	Faecal screen - Bacteria & Giardia
23/06/2016	7	Shelby	25/06/2016	BASIC FAECAL SCREEN
28/06/2016	8	Ophelia	17/08/2016	Faecal screen - Bacteria & Giardia
01/06/2009	9	Nancy	Collected from animal with good faeces previously	

2.1.17. Spiking of Faeces with protozoa.

Faeces collected as sample “Rodger, Rabbit and Elsa” (see Table 4) was identified as PCR negative when amplified with the 18S-*Giardia gdh* duplex PCR protocol (see results section). To test the 18S-*Giardia gdh* duplex PCR protocol for sensitivity these faeces samples were chosen as a protozoa negative matrix for protozoa spiking experiments. Four samples were prepared using 200 mg of faeces each spiked with either 2000 cells of *Trichomonas canistomae* (CLEO strain), 2000 cells *E. invadens*, 20000 cells of *G. intestinalis*, or all three organisms at these cell numbers respectively. The DNA from each sample was extracted from each 200 mg sample using the faecal DNA extraction method detailed above. This resulted in 4 samples containing *T. canistomae* and *E. invadens* at 40 cells per uL of DNA extraction and *G. intestinalis* at 400 cells per uL of DNA extraction, respectively. The fourth sample contained *T. canistomae* and *E. invadens* at 40 cells and *G. intestinalis* at 400 cells per uL of DNA extraction.

These four samples, containing two-times the limit of detection for each organism (see results), were amplified for their 18S/*Giardia gdh* genes using the 18S-*Giardia gdh* duplex PCR protocol described in [section 2.1.4](#). The PCR products from each sample were visualised using the gel electrophoresis methods detailed in [section 2.1.5](#).

2.1.18. 18S-*Giardia gdh* duplex PCR protocol test with canine plaque samples

Samples, 1P, 4P, 5P, 8P, 9P, 10P, 11P, and 14P were identified as protozoa positive from canine plaque samples taken from dogs with severe periodontal disease stages 3 to 4 ([section 3.5](#)). To test the 18S-*Giardia gdh* duplex PCR protocol on other sample types, these canine plaque DNA samples were amplified with the 18S-*Giardia gdh* duplex PCR protocol described above. The PCR products from each sample were visualised using the gel electrophoresis methods detailed previously.

2.1.19. 18S PCR screen of periodontal health state samples.

Individual animal subgingival plaque samples were collected from client-owned dogs recruited in 2008/2009 from a veterinary dental referral practice (Wey Referrals, Surrey, UK) as part of other research projects undertaken at the WALTHAM® Centre for Pet Nutrition. The study was approved by the WALTHAM® Centre for Pet Nutrition ethical review committee and owner consent was obtained. Table 5 lists a total of 92 samples taken from periodontally healthy animals and from dogs presenting with various stages of periodontal disease; healthy gingiva (n=20, average age 4.64 years), gingivitis (n=28, average age 4.91), periodontal disease stage 1 (n=26, average age 7.94 years) and severe periodontal disease stages 3 to 4 (n=18, average age 10.00 years). Animals were sampled during treatment for other non-related veterinary procedures requiring anaesthesia, including extractions of fractured teeth and orthopaedic treatments or during the course of their normal treatment for early periodontal disease.

Table 5. Metadata associated with canine subgingival plaque collected from animals presenting with severe periodontal disease (stages 3-4), periodontal disease stage 1, gingivitis, or from healthy animals.

‘Health’ Samples (n=20)

Sample number	Breed	Age	PD score
1H	German Shepherd	4	Health
2H	Staffordshire Bull Terrier	4	Health
3H	Collie cross	5	Health
4H	Daschund	4	Health
5H	Border Collie	13	Health
6H	Border Collie	6	Health
7H	Daschund	2.5	Health
8H	American Bull dog	3	Health
9H	Chinese Crested	2	Health
10H	Labrador Retriever cross	4	Health
11H	Golden Retriever	3	Health
12H	Belgian Shepherd	3	Health
13H	Weimaraner	5	Health
14H	Staffordshire Bull Terrier	4	Health
15H	Labrador Retriever cross	6	Health
16H	Schnauzer	3	Health
17H	Labrador Retriever	7	Health
18H	Labrador Retriever	5	Health
19H	Data not collected	Data not collected	Health
20H	Data not collected	Data not collected	Health
Average age: 4.64			

‘Gingivitis’ Samples (n=28)

Sample number	Breed	Age	PD score
G1	Labrador Retriever	8	Gingivitis
G2	Staffordshire Bull Terrier	4	Gingivitis
G4	Labrador Retriever	4	Gingivitis
G5	Bouvier des Flandres	4	Gingivitis
G6	Border Collie	3	Gingivitis
G7	Flat Coated Retriever	3	Gingivitis
G8	Jack Russel Terrier	11	Gingivitis
G9	Cocker spaniel	Data not collected	Gingivitis
G10	Staffordshire Bull Terrier	6	Gingivitis
G11	Border Collie	3	Gingivitis
G12	Border Collie	5	Gingivitis
G13	Unknown	Data not collected	Gingivitis
G14	Labrador Retriever	Data not collected	Gingivitis
G15	Yorkshire Terrier	2	Gingivitis
G16	Border Collie	8	Gingivitis

G17	Weimaraner	3	Gingivitis
G18	Jack Russel Terrier	9	Gingivitis
G19	Data not collected	Data not collected	Gingivitis
G22	Labrador Retriever	4	Gingivitis
G23	Shetland Sheepdog	2	Gingivitis
G25	Labrador Retriever	3	Gingivitis
G26	Border Collie	9	Gingivitis
G27	German Shepherd	8	Gingivitis
G28	Leonberger	5	Gingivitis
G31	Boxer	4	Gingivitis
G32	Staffordshire Bull Terrier	4	Gingivitis
G35	Staffordshire Bull Terrier	3	Gingivitis
G37	Golden Retriever	3	Gingivitis
Average age: 4.91			

'PD1' Samples (n=26)

Sample number	Breed	Age	PD score
Pd1	Bichon Frise	3	PD1
Pd3	Miniature Schnauzer	10	PD1
Pd4	Rottweiler	3	PD1
Pd5	Unknown Cross breed	10	PD1
Pd8	Greyhound	Data not collected	PD1
Pd10	Greyhound	Data not collected	PD1
Pd11	Greyhound	Data not collected	PD1
Pd12	Greyhound	Data not collected	PD1
Pd13	Greyhound	Data not collected	PD1
Pd14	Border terrier	3	PD1
Pd15	Unknown Cross breed	Data not collected	PD1
Pd16	Bichon Frise	14	PD1
Pd17	Staffordshire Bull Terrier	9	PD1
Pd18	German Shepherd	4	PD1
Pd20	Cocker spaniel	5	PD1
Pd21	Doberman	11	PD1
Pd22	Toy poodle	8	PD1
Pd24	Cocker spaniel	5	PD1
Pd25	Doberman	8	PD1
Pd26	Golden Retriever	12	PD1
Pd29	Cavalier King Charles Spaniel	8	PD1
Pd30	Maltese	5	PD1
Pd31	Irish Terrier	Data not collected	PD1
Pd32	Border Terrier	11	PD1
Pd35	Golden retriever	11	PD1
Pd36	Standard poodle	11	PD1
Average age: 7.94			

‘Severe Disease’ Samples (n=18)

Sample number	Breed	Age	PD score
1 Perio	Labrador Retriever	8	4
2 Perio	Greyhound	11	4
3 Perio	King Charles cocker spaniel	6	4
4 Perio	Greyhound	10	3
5 Perio	West highland white terrier	16	3
6 Perio	Old English sheep dog	15	4
7 Perio	Border collie	10	3.5
8 Perio	Cavalier King Charles Spaniel	8	3
9 Perio	Yorkshire terrier	13	4
10 Perio	Data not collected	Data not collected	3.5
11 Perio	Miniature poodle	15	4
12 Perio	Dobermann	13	3.5
13 Perio	Greyhound	5	3
14 Perio	Dachshund	14	4
15 Perio	Wheaten Terrier	8	3
16 Perio	Weimaraner	8	4
17 Perio	Weimaraner	9	4
18 Perio	Yorkshire terrier	5	4
19 Perio	Yorkshire terrier	8	4
20 Perio	Tibetan Terrier	8	3
Average age: 10.00			

* Where fields specify ‘data not collected’, this indicates the animal information was unknown or unavailable during the sampling procedure.

For inclusion into the healthy group (Health), clinically healthy gingiva were required with no or only low levels of localised gingivitis. Where such gingivitis was present, this was at locations away from the sampling sites. Gingivitis group samples (Gingivitis) were collected from animals displaying localised gingivitis but no attachment loss (disease stage 1). For inclusion into periodontal disease group 1 (PD1), samples were collected from animals displaying periodontal disease of at least stage 2; equivalent to less than 25% attachment loss. Severe disease group plaque samples (Severe Disease) were required to have a minimum of four sites displaying periodontal disease of at least stage 3; equivalent to between 25% and 50% or greater attachment loss. Animals below the age of two were not sampled in order to avoid exaggerating any age bias between healthy and diseased groups.

Samples were collected into 350ul of 50mM Tris (pH 7.6), 1mM EDTA, and 0.5% (v/v) Tween 20 and stored immediately at -20°C prior to DNA extraction. Genomic DNA from each sample was extracted using the Qiagen DNeasy Blood and Tissue DNA extraction Kit (Qiagen Ltd, UK) following the manufacturers standard protocol.

The 18S gene of organisms present in each sample was amplified using the 18S gene PCR protocol described in [section 2.1.2](#). The resultant amplicons produced from samples were separated through electrophoresis on standard 1.5% (w/v) agarose gels, stained with 3X GelRed (Biotium Inc., California, USA) and visualised using a Kodak IS200R gel documentation system (Kodak UK, UK). Protozoan identities were determined on the basis of amplicon size according to Supplemental Table 1. Where no PCR amplicon was seen in a sample, the sample was PCR amplified using bacterial 16S primers (see [section 2.1.3](#)) to rule out false negatives.

2.1.20. Statistical analysis 18S PCR screen.

Analyses were carried out using GenStat v18.1 (VSN International Ltd, UK). For 18S PCR screen results, the proportion of samples identified with each protist were compared between the ‘Health’ and each subsequent group (‘Gingivitis’, ‘PD1’ and ‘Severe disease’), using two-sample binomial tests with a normal approximation. The percentage of positive samples in each health state and the difference from ‘Health’ were calculated with 95% confidence intervals. A Bonferroni significance level of $p < 0.025$ was used to adjust for two protozoa being tested.

2.1.21. Next Generation Sequencing of pooled canine plaque samples.

Four DNA pools were created from subgingival plaque DNA, one pool representing each health state (‘Health’, ‘Gingivitis’, ‘PD1’, and ‘Severe disease’), see Table 5. From each individual sample 1 μl of extracted genomic DNA was included in the pool. Amplification of the eukaryotic 18S genes present in each of the pools was performed using the 18S gene PCR protocol described above. Products from each reaction were purified using the QIAquick PCR Purification Kit (Qiagen Ltd, UK), following the manufacturer’s standard protocol and 1500 ng of DNA from each was used for sequencing using the Roche 454™ GS FLX+ platform. Library preparation

and sequencing of the samples for 454TM sequencing was undertaken by Source BioScience, UK. The amplicons were fragmented using Covaris Adaptive Focused AcousticsTM technology (Covaris Inc., Massachusetts, USA), a sonication based method to shear the PCR products to sizes compatible for 454TM sequencing. The sheared samples were analysed on a 2100 Bioanalyzer instrument (Agilent Technologies, UK) to assess sample integrity and provide sample quantification. Sheared PCR products of 400 to 700 base pairs in size were purified for library preparation from each sample using a Pippin Prep Targeted Size Selection System (Sage Science Inc., Massachusetts, USA). For 454TM library preparation, each sample was processed using a NEBNext[®] DNA Library Prep Master Mix Set for 454TM (New England Biolabs, UK). Each library was then pooled and sequenced to target 250000 total reads on a quarter of a plate on the Roche 454TM GS FLX+ platform.

2.1.22. Analysis of Roche 454TM GS FLX+ sequencing data.

Sequences were processed for quality and analysed using Qiime (Quantitative Insights Into Microbial Ecology) software (Caporaso et al., 2010), a pipeline for performing microbial community analysis. The analysis was carried out according to the 18S sequence identification methodology outlined in QIIME tutorials (Caporaso et al., 2010) and modified as follows.

To reduce the amount of erroneous OTUs and to increase the accuracy of the pipeline, the returned raw sequences were denoised in Qiime using the `denoise_wrapper.py` script with default parameters. Chimeric sequences were removed from the analysis using the Qiime `identify_chimeric_seqs.py` script and employing ChimeraSlayer as the method of chimeric sequence identification. Operational Taxonomic Units (OTUs) were picked by clustering the sequences with `uclust` using the `pick_otus.py` script and default settings (97% sequence similarity and no reverse strand matching). A representative sequence for each OTU, the most abundant sequence in each, was chosen using the `pick_rep_set.py` script. Each representative sequence was assigned taxonomy using the `assign_taxonomy.py` script using the RDP classifier (to genus level, 97% sequence identity) employing the Silva 104 taxonomic map and reference sequences (Quast et al., 2013) <http://www.arb-silva.de/download/archive/qiime/>.

2.1.23. Statistical Analysis of 454™ GS FLX+ sequencing data.

For each protozoan, the proportion of sequences identified within the ‘Health’ pool sample was compared to those found in ‘Gingivitis’, ‘PD1’ and ‘Severe Disease’ pool samples using two-sample binomial tests with a normal approximation. The proportion of positive samples for each protist identified for each health state and the difference in proportions from ‘Health’ to each disease group, along with 95% confidence intervals were calculated. A Bonferroni significance level of $p < 0.025$ was used to adjust for two protozoa being tested.

2.2. Quantification of *Trichomonas* and *Entamoeba* and levels during the progression of canine periodontal disease

2.2.1. Generation of amplification targets for the development of quantitative real-time polymerase chain (qPCR) reaction protocols.

PCR amplicons for two canine oral protozoa discovered in the plaque sample screens (see results) were produced to allow the development of qPCR assays for both organisms. The unidentified oral trichomonad was cultured in defined medium (see below for method of culture) and DNA was extracted using a Qiagen DNA extraction kit (protocol described above). A 350bp product from the ITS1-5.8S-ITS2 gene region was amplified using a previously published primer set (TRF1 and TRF2) and PCR methodology (Felleisen, 1997).

The second oral protozoan identified from the molecular screens was *E. gingivalis* (see results section). It was not possible to culture this organism so to obtain a purified target amplicon for qPCR development the 18S gene PCR protocol described in the above sections was employed. Sample 10P was previously identified as *Entamoeba* positive from canine plaque samples collected from dogs with severe periodontal disease stages 3 to 4 (see 18S PCR screen of periodontal health state samples in methods and results). A 1257bp amplicon from the *E. gingivalis* 18S rRNA gene was amplified from sample 10P genomic DNA using the 18S PCR protocol. The PCR product was separated from other non-related PCR amplicons though gel electrophoresis (2 % agarose gel) and the 1257bp amplicon was excised using a sterile scalpel blade. The sample was gel-purified using a QIAquick Gel Extraction Kit (Qiagen, UK), following the manufacturers protocol. This purified sample was used as template in a fresh 18S PCR to produce the final amplicon for use as a qPCR development target.

Both *Trichomonas* ITS1-5.8S-ITS2 gene amplicon (350bp) and *Entamoeba* 18S gene amplicon (1257bp) samples were purified using a Diffinity RapidTip®2 PCR purification system (Sigma-aldrich, UK) and quantified using the previously mentioned Qubit assay (see above). A sample from each purified amplicon was sent for Sanger sequencing (Sanger and Coulson, 1975, Smith et al., 1986) (Beckman Coulter Genomics, UK) using both forward and reverse primers to confirm their identities.

2.2.2. Real-time assay primer design.

For qPCR primer design the *Trichomonas* 350 bp sequence from the ITS1-5.8S-ITS2 gene identified above and an *E. gingivalis* 18S full length sequence (D28490) obtained from the SILVA rRNA database project (Quast et al., 2013, Yilmaz et al., 2014) were used. Primer3 software (<http://bioinfo.ut.ee/primer3-0.4.0/>) (Koressaar and Remm, 2007, Untergasser et al., 2012) was used to identify suitable priming sites using the default settings. Suitability criteria for the chosen primers were: 18-25 nucleotides in length, a GC content between 40-60% and no more than 4 G or C base runs. The Primer3 identified primers were then checked using the PCR Primer Stats tool of the Sequence Manipulation Suite webpage (Stothard, 2000) to confirm no unacceptable primer dimer or hairpin secondary structure formation. Each primer set was also analysed using Primer-Blast (Ye et al., 2012) to check for primer non-specific binding to other organisms.

Two primer sets per organism were chosen (TC1 and TC2; EG1 and EG2) from the above criteria for further development. The primer sequences and priming locations are detailed in Table 6.

Table 6. Sequences and locations of primers used in real-time quantification of *E. gingivalis* and an unidentified *Trichomonas* in canine plaque

Primer	Target gene	Primer sequence and gene location
TC1 Forward	<i>Trichomonas</i> ITS1-5.8S-ITS2 gene	(210)CGTGTGAGGAGCCAAGACAT(229)
TC1 Reverse	<i>Trichomonas</i> ITS1-5.8S-ITS2 gene	(348)CCTGCCGTTGGATCAGTTCT(329)
TC2 Forward	<i>Trichomonas</i> ITS1-5.8S-ITS2 gene	(94)ACTGTTACACGCATGCTCCT(113)
TC2 Reverse	<i>Trichomonas</i> ITS1-5.8S-ITS2 gene	(229)ATGTCTTGGCTCCTCACACG(210)
EG1 Forward	<i>E. gingivalis</i> 18S gene	(735)GCATGGGACAATAAGAAGGAGA(756)
EG1 Reverse	<i>E. gingivalis</i> 18S gene	(932)CGACGGTATCTGATCGTCTTTGT(910)
EG2 Forward	<i>E. gingivalis</i> 18S gene	(890)CAAGAACGAAAGTTAGGGGAACA(912)
EG2 Reverse	<i>E. gingivalis</i> 18S gene	(1086)CCCCTGAAGTTCATACACTCAAGA(1063)

2.2.3. Real-time PCR assay conditions.

Real-time PCRs were undertaken on a 7900HT Fast Real-Time PCR System (Applied Biosystems, UK). Assays were conducted using the QuantiNova SYBR Green PCR Kit (Qiagen, UK) to detect real-time amplicon formation. Each 10 µL

qPCR reaction mix was comprised of: 5 μ L of 2x SYBR Green PCR Master Mix, 1 μ L of QN ROX Reference Dye, 0.5 μ L of each forward and reverse primer (10 μ M) and 1 μ L of DNA template. The final volume was brought to 10 μ L using nuclease-free water (Qiagen, UK). The assay cycle conditions were as follows: one cycle of 95°C for 2 minutes for initial denaturation, and 40 cycles of 95°C for 5 seconds and 60°C for 10 seconds for primer annealing and product elongation. All samples were run as three technical replicates and analysed using the default thermocycler settings with automatic cycle threshold (C_t) and baseline calculations. Calculated C_t values for each sample were observed and recorded using the cycler software, SDS V2.4. Outlier C_t recording within each technical replicate were discarded if they were more than 0.25 C_t units apart. At the end of each denaturation and elongation the fluorescence was detected by the thermocycler. Amplicon specificity was determined for each sample by performing a dissociation curve analysis (rate of 1°C every 30 seconds from 60 to 95°C) of the formed PCR amplicons.

2.2.4. Real-time assay standard curves, assay efficiencies, limits of detection and copy number calculations.

To assess the assay properties, suitability and robustness, the template amplicons produced for each organism (see above) were adjusted to 0.1 ng/ μ L of template to allow for the production of standard curves for each assay. Template DNA was diluted serially 10-fold (or further two-fold dilutions near to the limit of detection point to produce dilutions ranging from 100 pico grams to 0.3125 atto grams of DNA per μ L. These dilutions were also used as the basis for standard curves. Each standard sample was amplified and monitored in real-time using the above described real-time assays reagents and conditions. The Applied Biosystems SDS V2.4 software was used to record, plot and calculate the standard curve assay slopes, Y-intercept, R^2 values, and assay efficiencies.

Standard curve sample molecule copy numbers were calculated using an online tool (Staroscik, 2004). This system calculates sample copy number using the following method:

“The calculation is based on the assumption that the average weight of a base pair is 650 Daltons, meaning one mole of a base pair weighs 650 grams, and that

the molecular weight of any double stranded DNA template can be estimated by taking the product of its length (in base pairs) and multiplying by 650. The inverse of the molecular weight is the number of moles of template present in one gram of material. Using Avogadro's number, 6.022×10^{23} molecules/mole, the number of molecules of the template per gram can be calculated as such:

$$\text{mol/g} * \text{molecules/mol} = \text{molecules/g}$$

The number of molecules or number of copies of template in the sample can be estimated by multiplying by 1×10^9 to convert to ng and then multiplying by the amount of template (in ng)

The formula used is:

$$\text{number of copies} = (\text{amount} * 6.022 \times 10^{23}) / (\text{length} * 1 \times 10^9 * 650)$$

$$\text{number} = (\text{ng} * \text{number/mole}) / (\text{bp} * \text{ng/g} * \text{g/mole of bp})''$$

The limit of detection for each assay was defined as the final standard curve dilution in which at least valid two replicates were observed once removing all outliers (>0.25 C_t units difference from the triplicate median).

2.2.5. Real-time assay cross reactivity examination

Real-time qPCR assays EG1, TC1 and TC2 were tested against a range of protozoa (*G. intestinalis*, *A. polyphaga*, *E. invadens*, *T. tenax*, and *T. canistomae* (CLEO strain), mammalian (Human and Canine), fungal (*S. cerevisiae*) and bacterial (*E. coli*) DNA samples for evidence of cross-reactivity. DNA samples were obtained from either in-house extractions carried out on laboratory grown cultures (see sections [2.1.6](#), [2.1.7](#), [2.1.8](#) and [2.1.9](#)) or from externally acquired or purchased DNA samples (see [section 2.1.10](#)). Additionally, a canine oral bacterial mock-community sample containing bacterial 16S DNA clone sequences (Davis et al., 2013) and previously collected canine plaque DNA extractions (see [section 2.1.19](#)) known to contain protozoa, bacterial and yeast DNA were also tested. DNA from each test sample was adjusted to 1 ng/μL and added in triplicate to the real-time assay detailed in [section 2.2.3](#) using EG1, TC1 and TC2 primers in separate reactions. C_t values for each sample were calculated and recorded using

the cycler software, SDS V2.4. Replicates were discarded if they were more than 0.25 C_t units apart. Cross-reactivity was determined for each sample by examining amplification plots and performing a dissociation curve analysis (rate of 1°C every 30 seconds from 60 to 95°C) of any formed PCR amplicons.

2.2.6. Real-time quantification of *E. gingivalis* and *Trichomonas* spp. In canine plaque

Canine subgingival plaque was collected over a sixty week period as part of another study undertaken at the WALTHAM Centre for Pet Nutrition (Marshall et al., 2014, Wallis et al., 2015) from fifty two miniature schnauzers aged between 1 and 7 years. Plaque was collected from individual teeth using sterile dental probes inserted below the gingival margin. Sample collections took place every six weeks during pre-planned dental examinations where the teeth were scored for health. For ethical reasons, teeth were only allowed to progress to early periodontal disease (<25% attachment loss). At this stage the tooth was scaled and polished to prevent progression into the later stages of periodontitis and then was no longer included in the study. If 12 or more teeth from an individual dog developed into early stage periodontitis, the animal received a full mouth scale and polish and was removed from the study.

Samples were collected into TE buffer pH 8.0, and the DNA extracted from each using Lysozyme (Epicentre, UK) and a Nucleospin® 96 Tissue DNA extraction kit (Macherey-Nagel, UK) – see Wallis et al., 2015 for further details. For analysis, a subset of samples were chosen based on their disease progression profile. 444 samples from 30 dogs were chosen, which resulting in 47 teeth that progressed to mild periodontitis (<25 % attachment loss), designated as “Progressing” and 47 teeth that remained healthy or did not progress further than mild gingivitis during the 60 week study, designated as “Non Progressing”. For balanced analysis, the samples were paired within groups, firstly through tooth number, e.g. 108 and 208 or 308 and 408. If this was not possible the teeth were paired by tooth type within a dog, e.g. premolar to premolar. If neither of the above was possible then the teeth were matched by tooth number but from different dogs of comparable age.

1 μL of DNA from each of the 444 samples were quantified using the Qubit® High sensitivity dsDNA Assay Kit (Life Technologies, UK) and a Qubit fluorometer according to the manufacturer's standard protocols. DNA concentrations were recorded and used to normalise the resultant qPCR data (see below). 1 μL of DNA, in triplicate from each sample, was then tested for the presence of oral protozoa using the real-time assay developed using the EG1 and TC2 primers in separate reactions ([section 2.2.3](#)). In addition, standard curves of 10-fold dilutions were also prepared from 1 ng/ μL DNA samples of *E. gingivalis* 18S gene and *T. canistomae* (CLEO strain) ITS1-5.8S-ITS2 gene amplicons. All standard curve samples were also analysed using the real-time qPCR protocol during the same run as the test samples. C_t values for each sample were calculated and recorded using the cycler software, SDS V2.4. Replicates were discarded if they were more than 0.25 C_t units apart. Amplicon specificity was determined for each sample by performing a dissociation curve analysis (rate of 1°C every 30 seconds from 60 to 95°C) of the formed PCR amplicons.

2.2.7. Restriction digest of Real-time qPCR assay amplicons for the species level identification of *Trichomonas* spp.

Samples identified as *Trichomonas* positive (amplicon melting temperature between 79-81 °C) from the real-time qPCR assay (TC2 primers) were further processed to identify the species present in each sample. The amplicons produced during each qPCR were digested using the restriction enzyme BcnI (ThermoFisher Scientific, UK). A digestion mix for each sample was prepared on ice containing 2 μL of 10X Tango buffer, 1 μL of BcnI enzyme (10 U/ μL), 23 μL of nuclease-free dH₂O, and 5 μL of qPCR reaction amplicon. The digestion mix was then incubated for 1 hour at 37 °C to allow full digestion of the amplicons. 1 μL of each digested sample was visualised through electrophoresis using a 2100 Bioanalyser and DNA chip (Agilent Technologies, UK) following the manufacturer's standard protocol. A single digestion product of approximately 130 bp indicates the presence of *T. tenax* only. Two digestion products, approximately 104 and 32 bp in size, indicated the presence of *T. canistomae* only. Three digestion products, approximately 130, 104 and 32 bp in size indicates the presence of both *T. tenax* and *T. canistomae* in the sample.

The bioanalyser composite gels and electropherograms were analysed for the digestion products produced and noted for each sample.

2.2.8. Real-time quantification of canine plaque – data manipulation

As teeth or dogs were removed from trial when they were identified as having early stage PD1, often there were more time points for the non-progressing teeth than progressing. As a result, time points were re-parameterised to be ‘time point relative to periodontal disease’, and only data from time points -5 (Health) to 0 (Periodontal disease) were used. Cycle threshold data for each sample obtained from the thermocycler software and the recorded DNA concentrations were transferred to GenEx software (MultiD Analyses AB, Sweden) for transformation and manipulation. Normalisation of the data set was undertaken using the in-built normalisation to sample amounts analysis module of GenEx. The module converts data using the equation $CT_{conc=1} = CT_{conc} + \log_2(conc)$. Absolute copy numbers for each samples were next calculated using the normalised C_t values and the reverse calibration module of GenEx. Each sample triplicate value was reverse calibrated to absolute copy numbers using the standard curve and their previously calculated copy numbers, see [section 2.2.4](#).

2.2.9. Real-time quantification of canine plaque – statistical analysis

For each organism, a linear mixed effects model was fitted, modelling the copy number against PD group, time relative to PD and their interaction with gender and age at the start of trial as covariates. The random structure was animal with pairing nested in animal. Visual inspection of the residuals indicated that a transformation of the copy number was necessary so a \log_{10} transformation was implemented for both models. Likelihood ratio tests were used to assess the necessity of the random structure and the covariates. Abundance with 97.5% confidence intervals was estimated for all combinations of PD group and time relative to PD. Within each time relative to PD, the PD groups were compared to each other and within each PD group, and all time points were compared to 0. The fold-changes with 97.5% confidence intervals were extracted, along with p -values. Due to the two models, a Bonferonni corrected significance level of 2.5% was used.

Additionally, two generalised linear mixed models were fit for each organism modelling the binary variables ‘detected’ and ‘quantifiable’ against PD group, time relative to PD and their interaction with gender and age at the start of trial as covariates. The random structure was animal with pairing nested in animal. As before, likelihood ratio tests were used to assess the necessity of the random structure and the covariates. Probabilities of detection or quantification with 95% confidence intervals were estimated for all combinations of PD group and time relative to PD. Within each time relative to PD, the PD groups were compared to each other and within each PD group, and all time points were compared to 0. The odds ratios with 95% confidence intervals, were extracted, along with p -values. This was a secondary analysis, so no correction for multiplicity was applied.

Two further analyses were also conducted after the production of the data set. Firstly, within the TC2 data set, the presence/absence of the canine oral trichomonads or *T. tenax* was recorded in a binary format for each sample. These results were analysed using a binomial generalised linear mixed models as described above. The probability of presence of each species, with 95% confidence intervals were calculated for all combinations of PD group and time relative to PD. Within each time relative to PD, the PD groups were compared to each other and within each PD group. All time points were compared to time point 0 (PD). The odds ratios with 95% confidence intervals were extracted along with p -values.

Secondly, five metadata variables for each animal samples were investigated within each organism. The five variables, age at the start of trial (in weeks), sex, tooth type, tooth side (mouth) and tooth area (mouth), were investigated to assess their relationship with the abundance of either protozoan. For each organism, a linear mixed effects model was fit for each variable, modelling the organism gene copy number against PD group, time relative to PD, the variable of interest and their interaction as fixed effects. The random structure was animal with pairing nested in animal. Visual inspection of the residuals indicated that a transformation of the copy number was necessary so a \log_{10} transformation was implemented for all models. Likelihood ratio tests were used to assess the necessity of the random structure.

From each model, abundance with 95% confidence intervals were calculated for all combinations of PD group, time relative to PD and the variable of interest (at yearly intervals for the continuous variable age). Within each time relative to PD by PD

group combination, the levels of the variable of interest were compared to each other. The fold changes with 95% confidence intervals were calculated along with *p*-values.

All analyses were performed in R version 3.2.0 -2015-04-16 (The R Foundation for Statistical Computing, US). Packages used for the computations were lme4 (Bates et al., 2015), multcomp (Hothorn et al., 2008) and ggplot2 (Wickham, 2009).

2.3. Primer independent screen of canine plaque for the detection of protists

2.3.1. Canine plaque collection – Health samples

Canine whole mouth plaque from trained conscious animals was collected at the WALTHAM Centre for Pet Nutrition. All available dogs were assessed for their suitability prior to the start of the trial. Animals that had demonstrated good behaviour during previous trials involving mouth handling were chosen. All animals were of good oral health, as assessed through regular dental screening. Details of the dogs are recorded in Table 7.

26 dogs consisting of two breeds, Labrador Retrievers and Miniature Schnauzers, were sampled first thing in the morning before any tooth brushing or feeding, once a week for four consecutive weeks. Supra-gingival plaque was collected by rubbing 1 μ L loops along the gingival margin of the teeth and gathering the loop tips with plaque into 1 mL of RNeasy Lysis Solution (Qiagen, UK). Multiple loops were used, if required, until the maximum possible amount of plaque from each dog was collected. Once collection was complete the samples were snap-frozen in liquid nitrogen and stored at -80 °C until required for RNA extraction.

Total RNA from 15 samples were extracted using the Qiagen RNeasy Mini Kit (Qiagen, UK) using a modified version of the manufacturer's protocol. 15 plaque samples from the second week's collections (Table 7, highlighted samples) were chosen for total RNA extraction. Each sample was gently thawed on ice and vortexed vigorously to remove all plaque from the loops. Loops were then removed from the tubes and the samples were pooled in a single tube. The pooled sample was centrifuged at 10000 x g for 5 minutes to pellet all cellular material and then re-suspended into 200 μ L of DPBS. Cells were disrupted by the addition of 600 μ L of Qiagen Buffer RLT Plus (containing 10 μ L β -mercaptoethanol per 1 mL Buffer RLT Plus).

To homogenise the lysate, each sample was directly added to the centre of a QASHredder spin column (Qiagen, UK) placed in a 2 mL collection tube, and centrifuged for 2 minutes at maximum speed. The homogenised lysate was transferred to a gDNA Eliminator spin column placed in a 2 mL collection tube and centrifuged for 30 seconds at ≥ 8000 x g. To the flow-through, 1 volume (600 μ L) of

freshly prepared 70% (v/v) ethanol was added and mixed well by pipetting. The sample, including any precipitate that may have formed, was transferred to RNeasy spin columns placed in a 2 mL collection tube and centrifuged for 15 seconds at $\geq 8000 \times g$. 700 μ l Buffer RW1 was added to each RNeasy spin column and centrifuged for 15 seconds at $\geq 8000 \times g$ to wash the spin column membrane. 500 μ l Buffer RPE was then added to the RNeasy spin column and centrifuged for 15 seconds at $\geq 8000 \times g$ to wash the spin column membrane. 500 μ l Buffer RPE was again added to the RNeasy spin column and centrifuged for 2 minutes at $\geq 8000 \times g$ to wash and dry the spin column membrane. The RNeasy spin column was placed in a new nuclease free 1.5 mL collection tube. 40 μ l of RNase-free water was added directly to the spin column membrane and centrifuges for 1 minute at $\geq 8000 \times g$ to elute the RNA.

2.3.2. Canine plaque collection – Disease samples

15 total mouth supra-gingival plaque samples were collected by external veterinary practitioners (Rachel Perry BSc, BVM&S, MANZCVS - Small Animal Dentistry & Oral Surgery, and Gerhard Putter MRCVS) from indiscriminate animals visiting veterinary practices for a variety of procedures. Animals were excluded from plaque collection if they had received significant veterinary oral care, systemic or oral antibiotic treatment or evidence of any extra-oral bacterial infections in the preceding three months. Also, animals suffering from oral carcinomas were excluded. Only animals with a health state of PD2 or above (severe periodontal disease) were included in the sampling process (Marshall et al., 2014). Owner consent was obtained and an owner survey was completed, to obtain animal history and metadata, prior to sampling. The animal data and sample details are displayed in the Table 8. Supra-gingival plaque was collected by rubbing 1 μ L loops along the gingival margin of the teeth and gathering the loop tips with plaque into 1 mL of RNAlater™ Stabilisation solution (ThermoFisher Scientific, UK). Multiple loops were used, if required, until the maximum possible amount of plaque was collected from each dog. Once collection was complete the samples were transferred to -20 °C and then to -80 °C upon return to the laboratory. For pooling, each sample was gently thawed on ice and vortexed vigorously to remove all plaque from the loops.

Table 7. Dogs used in the study with good oral health. Supra-gingival plaque was collected from each animal over a four consecutive weeks.

Dog ID number	Dog name	Sex	Breed	Age
LR04880	Branston	M	Labrador	6.6
LR05299	JoJo	F	Labrador	3.1
LR05315	Lois	F	Labrador	3
MS04643	Faith	F	Miniature Schnauzer	8.9
MS05115	Yoyo	F	Miniature Schnauzer	5.1
MS05269	Hobo	M	Miniature Schnauzer	3.2
MS05273	Hobbit	M	Miniature Schnauzer	3.2
MS04651	Madison	F	Miniature Schnauzer	8.9
MS04707	Ethel	F	Miniature Schnauzer	7.9
MS04715	Edna	F	Miniature Schnauzer	7.9
MS04935	Oxo	F	Miniature Schnauzer	6.3
MS05113	Wanda	F	Miniature Schnauzer	5.1
MS05114	Yasmine	F	Miniature Schnauzer	5.1
MS05119	Yoda	M	Miniature Schnauzer	5.1
LR04991	Romany	F	Labrador	5.8
LR05124	Arnold	M	Labrador	5
LR05198	Eliza	F	Labrador	4.2
LR05202	Esme	F	Labrador	4.2
LR05203	Evie	F	Labrador	4.2
LR05260	Flick	F	Labrador	3.5
MS05158	Connie	F	Miniature Schnauzer	4.5
MS05163	Chesney	M	Miniature Schnauzer	4.5
LR04640	Autumn	F	Labrador	9
LR05406	Merlin	M	Labrador	2.7
LR05411	Minnie	F	Labrador	2.7
MS05268	Hutch	M	Miniature Schnauzer	3.2

*Animals highlighted were used for the 15 dog pooled health sample.

Loops were then removed from the tubes and the samples were pooled in a single tube. The pooled sample was centrifuged at 10000 x g for 5 minutes to pellet all cellular material and then re-suspended into 200 µL of DPBS.

Total RNA from the 15-dog pool was extracted using the Qiagen RNeasy Mini Kit (Qiagen, UK) using a modified version of the manufacturer's protocol described in [section 2.3.1](#).

Table 8. Dogs used in the study with poor oral health. Supra-gingival plaque was collected from each animal. Those highlighted were pooled to produce a 15-dog disease plaque pool.

Sample ID	Name of dog	Breed	Weight (KGS)	Date of collection	Health score
GP1	Jack	Labrador Retriever	36.4	23/11/2015	>PD 2
GP2	Bobby	Collie Cross	17.4	24/11/2015	>PD 2
GP3	Peppy	Greyhound	25.3	25/11/2015	>PD 2
GP4	Dorothy	Miniature 'Long Haired' Dachshund	6.7	10/12/2015	>PD 2
GP5	Douglas	Jack Russel Terrier	5.7	13/01/2016	>PD 2
GP6	Stanley	Cavalier King Charles Spaniel	10	13/01/2016	>PD 2
GP7	Millie	West Highland Terrier	8.7	19/01/2016	>PD 2
GP8	Che	Labrador Retriever	32	28/01/2016	>PD 2
GP9	Blue	Lurcher	11.7	28/01/2016	>PD 2
RP01	Timmy	Bichon	7.7	27/02/2015	>PD 2
RP02	Lucy	Cavalier King Charles Spaniel	8.8	24/03/2015	>PD 2
RP03	Betsy	Miniature Poodle	4.9	07/04/2015	>PD 2
RP04	Lulu	Cavalier King Charles Spaniel	11.5	09/06/2015	>PD 2
RP05	Daisy	Yorkshire Terrier	2.5	24/07/2015	>PD 2
RP06	Stanley	Greyhound	32	04/08/2015	>PD 2
RP07	Sammy	Basset Hound	27.5	25/08/2015	>PD 2
RP08	Pepi	Yorkshire Terrier	3	15/09/2015	>PD 2
RP09	Daisy	Bishon Frise	9.4	04/12/2015	>PD 2
RP10	Molly	Bishon Frise	9.4	04/12/2015	>PD 2
RP11	Ben	Not Recorded	10.5	08/12/2015	>PD 2
RP12	Wilf	Border Collie Cross	16	11/12/2015	>PD 2
RP13	Louis	Yorkshire Terrier	6.8	18/12/2015	>PD 2

*Animals highlighted were used for the 15 dog pooled disease sample.

2.3.3. Re-precipitation of Total RNA samples

In an attempt to remove any contaminating substances from the samples, each was re-precipitated. To each 40 μ L RNA sample 4 μ L of 3M sodium acetate (Sigma Aldrich, UK), 5 μ g of glycogen (ThermoFisher Scientific, UK), and 120 μ L of 100% ice cold Ethanol (Sigma Aldrich, UK) was added. The samples were mixed well and incubated at -80 °C for 60 minutes. The RNA in each was recovered by centrifugation at 12000 x g for 30 minutes at 4 °C. The supernatant was gently removed and the pellet was washed by gently adding 1 mL of freshly prepared 70 % (v/v) Ethanol. The RNA was pelleted by centrifugation at 12000 x g for 10 minutes at 4 °C and washed a further two times with 70 % (v/v) Ethanol. The final

pellet was re-suspended in 20 μ L of Tris(10 mM)-EDTA(1mM) buffer solution pH 8.0 (Sigma-Aldrich, UK).

2.3.4. Visualisation and analysis of RNA samples

1.5 μ L samples of RNA were analysed for purity and quantified using a NanoDrop™ 1000 Spectrophotometer (ThermoFisher Scientific, UK) using the manufacturer's RNA protocol. For RNA species visualisation 1 μ L of each RNA sample was run out on an Agilent 2100 Bioanalyzer Instrument (Agilent Technologies, UK) using the manufacturer's standard eukaryotic RNA nano protocol and an Agilent RNA 6000 nano chip and reagents.

2.3.5. Bacterial 16S and 23S rRNA depletion from total RNA samples

10 μ g of total RNA pooled plaque sample, Health and Disease, was depleted of bacterial small and large subunit rRNA using the MICROBExpress™ Bacterial mRNA Enrichment Kit (ThermoFisher Scientific, UK). A modified version of the manufacturer's protocol was employed. 10 μ g of total RNA was added to 200 μ L of binding buffer and mixed gently. 4 μ L of capture oligonucleotides were added to the mix and mixed gently. The sample was incubated for 10 minutes at 70 °C to denature the RNA and then incubated for 1 hour at 37 °C to hybridise bacterial RNA to the capture oligonucleotides. 50 μ L of pre-prepared Oligo MagBeads were added to the RNA/capture oligonucleotide mix to bind the MagBeads to the complex. The MagBead/RNA/capture oligonucleotide complex mix was captured by placing the tube on a magnetic rack for 3 minutes. The supernatant containing Eukaryotic rRNA and other non-ribosomal RNA species was aspirated away to a clean tube. Any remaining eukaryotic rRNA in the MagBead /RNA/capture oligonucleotide complex was recovered by adding 100 μ L of pre-warmed (37 °C) washing solution to the captured oligo MagBeads. The tubes were removed from the magnetic stand and the beads resuspended and returned to the magnetic stand to recapture the beads. The supernatant was carefully removed and pooled with the previously recovered Eukaryotic RNA. To purify the recovered rRNA samples, they were re-precipitated according to the method detailed in [section 2.3.3](#). The final rRNA pellet was resuspended in 25 μ L of Tris (10 mM)-EDTA(1mM) buffer solution pH 8.0 (Sigma-Aldrich, UK).

2.3.6. 2D cDNA sequencing of Health and Disease samples using the MinION™ device

Each RNA sample prepared in [section 2.3.5](#) above was processed using modified versions of the Oxford Nanopore Technologies 2D cDNA sequencing protocol for the SQK-NSK007 reagent kit and barcoding EXP-NDB002 protocol. For first strand cDNA synthesis, 250 ng of 16S/23S depleted RNA ([section 2.3.5](#)) was added to 0.5 µL of 250 µM random hexanucleotide primers (New England Biolabs Inc, USA), 1 µL of 10 mM dNTP's (ThermoFisher Scientific, UK). The total volume of the reaction was brought to 13 µL using nuclease-free water (Qiagen Ltd, UK). After a gentle mix, the tube was incubated at 65 °C for 5 minutes to denature the RNA and the snap cooled on ice for 10 minutes. To begin the first strand synthesis, from the SuperScript™ II Reverse Transcription kit (ThermoFisher Scientific, UK), 4 µL of First Strand buffer and 2 µL of 100 mM DTT were added to each reaction tube. The tubes were gently vortexed and incubated at 25 °C for 2 minutes to allow priming of the random hexanucleotide primers, after which 1 µL of SuperScript™ II Reverse Transcriptase (200 U/µL) was added to each. The tubes were incubated at 25 °C for 20 minutes to begin the reverse transcription reaction. The reaction was terminated by incubating the tubes at 70 °C for 15 minutes and immediately storing the tubes at 4 °C. Second strand synthesis was conducted using a NEBNext mRNA Second Strand Synthesis module (New England Biolabs Inc, USA). In brief, to each completed first strand reaction tube, 48 µL of nuclease-free water (Qiagen Ltd, UK), 8 µL of 10 X Second Strand Synthesis Reaction Buffer, and 4 µL of Second Strand Synthesis Enzyme mix, was added. The reactions in each tube were mixed by gently pipetting up and down and second strand synthesis was initiated by incubating the tubes at 16 °C for 2.5 hours, after which the tubes were held at 4 °C. To purify the newly formed double stranded cDNA products, each sample was transferred to a fresh tube and 288 µL of AMPure XP beads (Beckman Coulter Inc., USA) was added to each at room temperature. Each tube was incubated for 5 minutes on a tube rotator, pelleted using a magnetic base, and washed twice with 400 µL of freshly prepared 70 % Ethanol. The final pellet was resuspended in 52 µL of nuclease-free water (Qiagen Ltd, UK) and incubated at room temperature for 2 minutes, to release the purified RNA from the AMPure beads. The AMPure beads were pelleted using a magnetic base, and the cDNA containing eluate was transferred to a clean PCR tube for the next steps.

To repair sequence ends and to add dA-tails the NEBNext Ultra II End-Repair/dA-tailing module (New England Biolabs Inc, USA) was used. To 51 µL of each cDNA preparation, 7 µL of Ultra II End-Prep buffer and 3 µL of Ultra II End-Prep enzyme mix was added. The samples were mixed through inversion and incubated at 20 °C for 8 minutes, then 65 °C for 30 minutes, followed by holding at 4°C. The end-prepared sequences were purified using 110 µL of AMPure beads per sample using the magnetic separation and wash steps outline above. The final purified sequences were resuspended into 23.5 µL of nuclease-free water (Qiagen Ltd, UK).

Each sample, Health and Disease, were barcoded using the Oxford Nanopore Technologies Native Barcoding kit (EXP-NDB002). Barcode ligation reactions were undertaken by adding 22.5 µL of end-prepped cDNA to 2.5 µL of a barcode mix (NB01 for the Health sample and NB03 for the disease sample), and 25 µL of Blunt/TA Ligase Master Mix (New England Biolabs Inc, USA). The tubes were mixed through inversion and incubated at 25 °C for 15 minutes to ligate the barcode. Each sample was purified using 50 µL of AMPure beads using the magnetic separation and wash steps outline above. The final purified sequences were resuspended into 16 µL of nuclease-free water (Qiagen Ltd, UK).

To prepare the cDNA for sequencing adaptors, equimolar amounts of each sample (Health and Disease) was mixed together and to produce a final sequencing sample and brought to 58 µL with nuclease free water. To this 58 µL sample, 10 µL of BAM adaptor reagent (EXP-NDB002), and 2 µL of BHP adaptor reagent (EXP-NDB002) were added, as was 20 µL of 5 X NEBNext Quick Ligation Reaction Buffer (New England Biolabs Inc, USA) and 10 µL of Quick T4 DNA ligase (New England Biolabs Inc, USA). The sequencing sample was mixed through gentle inversion and incubated at room temperature for 10 minutes to ligate on the adaptors. To this reaction mix, 1 µL of reagent HPT adaptor reagent (EXP-NDB002) was added and the sample was mixed through gentle inversion and incubated at room temperature for 10 minutes. To purify the adapted cDNA sample, 100 µL of pre-washed Dynabeads™ MyOne™ Streptavidin C1 beads (ThermoFisher Scientific, UK) was added to the mixture at room temperature. The tube was incubated for 5 minutes on a tube rotator, pelleted using a magnetic base, and washed twice with 150 µL of BBB reagent (EXP-NDB002). The final pellet was resuspended in 25 µL of ELB reagent (EXP-NDB002) and incubated at 37 °C for 10 minutes to release the adapted library from the beads. The MyOne™

Streptavidin C1 beads were pelleted using a magnetic base, and the adapted library containing eluate was transferred to a clean tube for sequencing.

To sequence the sample the MinION™ device was prepared and loaded using the standard method described in the SQK007 protocol. In brief, a Platform QC was run on the unloaded flow cell to detect the number of active pore and to check the flow cell validity. The flow cell (FLO-MIN105) was primed using a priming mix containing 500 µL of RBF1 reagent (SQK007) and 500 µL of nuclease-free water (Qiagen Ltd, UK). The library was prepared by adding 6 µL of adapted, tethered library to 37.5 µL of RBF1 reagent (SQK007) and 31.5 µL of nuclease free water to produce a 75 µL final library to load onto the MinION™ device. This 75 µL sample was loaded, drop by drop, into the SpotON port of the flow cell and the sequencing was initiated by running the

MAP_48H_Sequencing_Run_SQK_MAP104.py sequencing script. 3 additional 75 µL volumes of library were also prepared and loaded into the MinION™ device, as described above, at 4.5, 21, and 28.5 hours post initiation of the sequencing.

Sequence analysis and base calling was undertaken in real time using the Metrichor Desktop Agent software and the 2D Basecalling plus Barcoding for FLO-MIN105 250bps work flow (123683), Rev 1.125.

2.3.7. Direct RNA sequencing of Health and Disease samples using the MinION™ device

Each RNA sample prepared in [section 2.3.5](#) above was processed for direct RNA sequencing using the Oxford Nanopore Technologies Direct RNA Sequencing Protocol using reagent kit SQK-RNA001. For preparation of the total RNA for the MinION™ device sequencing processing, 3' poly (A) tailing of sequences was undertaken using an *E. coli* Poly(A) Polymerase tailing kit (New England Biolabs Inc, USA). 1 µg of total RNA from each pooled plaque total RNA sample (Health and Disease), in 15 µL of nuclease free water was added to 2 µL of 10X *E. coli* Poly(A) Polymerase Reaction Buffer, 2 µL of 10 mM ATP, and 1 µL of *E. coli* Poly(A) Polymerase from the Poly(A) tailing kit. The reactions were incubated at 37 °C for 30 minutes to add 3' Poly(A) tails to the RNA sequences. Each sample was then purified of enzymes by precipitation using the method detailed in [section 2.3.3](#). For first strand cDNA synthesis, 750 ng of Poly(A) tailed RNA, in 9 µL, was

added to 0.5 μ L of RNA calibration strand (RCS) and 1 μ L of RT adapter (RTA) from the MinION SQK-RNA001 sequencing kit reagents. To this mix, 3 μ L of NEBNext Quick Ligation Reaction Buffer (New England Biolabs Inc, USA) and 1.5 μ L of T4 DNA Ligase (New England Biolabs Inc, USA) was added. Each reaction was mixed through gentle pipetting and then incubated at room temperature for 10 minutes to ligate the reverse transcription adapters to the RNA sequences. To each adapter ligation reaction, a reverse transcription master mix consisting of 9 μ L of nuclease-free water (Qiagen Ltd, UK), 2 μ L of 10 mM dNTP's (ThermoFisher Scientific, UK), 8 μ L of First Strand buffer from the SuperScript™ III Reverse Transcription kit (ThermoFisher Scientific, UK), and 4 μ L of 0.1 mM DTT, were added and gently mixed. The tubes were incubated at 50 °C for 50 minutes to begin the reverse transcription reaction. The reaction was terminated by incubating the tubes at 70 °C for 15 minutes and immediately storing the tubes at 4 °C. To purify the newly formed cDNA, each sample was transferred to a fresh tube and 72 μ L of RNAClean XP beads (Beckman Coulter Inc., USA) was added to each at room temperature. Each tube was incubated for 5 minutes on a tube rotator, pelleted using a magnetic base, and washed once with 150 μ L of freshly prepared 70 % Ethanol. The final pellet was resuspended in 20 μ L of nuclease-free water (Qiagen Ltd, UK) and incubated at room temperature for 5 minutes, to release the purified cDNA from the RNAClean XP beads. The beads were again pelleted using a magnetic base, and the RNA containing eluate was transferred to a clean PCR tube for the next steps.

To add RNA sequencing adapters, 8 μ L of NEBNext Quick Ligation Reaction Buffer (New England Biolabs Inc, USA), 6 μ L of RNA adapter (RMX) from the MinION SQK-RNA001 sequencing kit, 3 μ L of nuclease-free water (Qiagen Ltd, UK), and 3 μ L of T4 DNA Ligase (New England Biolabs Inc, USA) was added to 20 μ L of each reverse-transcribed RNA sample. . Each reaction was mixed through gentle pipetting and then incubated at room temperature for 10 minutes to ligate on the sequencing adapters. To purify the sample, 40 μ L of RNAClean XP beads (Beckman Coulter Inc., USA) was added at room temperature. Each tube was incubated for 5 minutes on a tube rotator, pelleted using a magnetic base, and washed twice with 150 μ L of reagent WSB from the MinION SQK-RNA001 sequencing kit. The final pellet was resuspended in 21 μ L of reagent ELB from the MinION SQK-RNA001 sequencing kit and incubated at room temperature for 5

minutes, to release the purified RNA from the RNAClean XP beads. The beads were again pelleted using a magnetic base, and the adapter-ligated RNA containing eluate was transferred to a clean tube.

To sequence the RNA sample the MinION™ device was prepared and loaded using the standard method described in the Direct RNA sequencing protocol (DRS_9026_v1_revM. In brief, a Platform QC was run on the unloaded flow cell (FLO-MIN106, R9.4 version) to detect the number of active pores and to check the flow cell validity. The flow cell was primed using a priming mix containing 600 µL of RRB reagent (SQK-RNA001) and 600 µL of nuclease-free water (Qiagen Ltd, UK). The library was prepared by adding 20 µL of adapter-ligated RNA to 17.5 µL of µL of nuclease free water and 37.5 µL of RRB reagent to produce a 75 µL final library to load onto the MinION™ device. This 75 µL sample was loaded, drop by drop, into the SpotON port of the flow cell and the sequencing was initiated by running the NC_48H_Sequencing_Run_FLO-MIN106_SQK-RNA001 sequencing script. Base calling of RNA sequences was undertaken locally in real time using the Metrichor EPI2ME software and the local RNA base calling script.

FastQ format RNA sequence reads produced by the MinION™ sequencer were initially merged into a single file and sequences greater than 2500 bp were removed using the awk script (Aho et al., 1978):

```
awk '{y= i++ % 4 ; L[y]=$0; if(y==3 && length(L[1])<=2500)
{printf("%s\n%s\n%s\n%s\n",L[0],L[1],L[2],L[3]);}}'
```

The reads were next filtered to concentrate high quality reads using NanoFilt software (Decoster, 2018) using the arguments -q 4 and -l 400, which removed all sequences with a quality score of less than 4 and a read length of less than 400 bases. NanoPlot software (Decoster, 2018), was used to produce summary statistics and graphs for the sequences pre and post processing, using the script arguments -t 4 --fastq reads.fastq -p -o / -f png. Each sequencing FastQ file was then converted to Fasta file format, for further taxonomic processing, using the linux sed command: sed -n '1~4s/^@/>/p;2~4p' INFILE.fastq > OUTFILE.fasta .

2.3.8. RNA sequence taxonomic assignment

Sequences produced by the MinION sequencer were analysed using BLAST+ command line tools package (Altschul et al., 1990). The BLAST+ package was

installed onto the University of Leicester's High Performance Computing (HPC) service, SPECTRE, for use. A BLAST nucleotide database was prepared from the SILVA 128 (for cDNA sequencing) or the 132 (for direct RNA sequencing) SSURef sequence files of all curated SSU sequences (Quast et al., 2013). The makeblastdb script was used to create BLAST nucleotide databases from the SILVA files and sequence were compared against the databases, using the blastn script and the following parameters: blastn -task blastn -evalue 0.0001 -dust no -max_target_seqs 5 -num_threads 4 -outfmt 6. The top hit match for each sequence was recorded from the output. Any sequence with a bitscore of less than 400 and less than a 97% similarity (genus level) to the query sequence (pident) were discarded. All bacterial, archaeal, fungal and non-protozoan sequences were discarded. The sequences identified taxonomically as protozoan were collated and recorded with Excel.

2.3.9. Statistical analysis of MinION cDNA and direct RNA sequencing sequence proportions

For each protozoan species, the proportion of sequences identified within the Health sample was compared to those found in Disease sample using two-sample binomial tests, with the health state as the fixed effect and a normal approximation. Mean proportions for each health state were estimated and the odds ratio difference between health state proportions was calculated and tested for significance. 95% confidence intervals were calculated with p value of <0.05 considered significant to determine relationships between the sequence proportions. All analyses were performed using R version 3.3.3 using the multcomp library.

2.4. Functional activity of *Trichomonas canistomae*

2.4.1. Modified TYI-S-33 medium for the culture of canine oral

Tichomonads (Gannon and Linke, 1991)

Modified TYI-S-33 is based on an established culture medium for intestinal protozoa (Clark and Diamond, 2002) and modified by (Gannon and Linke, 1991). The medium was prepared by adding the following ingredients to 348 mL of distilled water; 1 g of Trypticase peptone (211929 BD, UK), 0.5 g Yeast extract (211929 BD, UK), 0.4 g Dextran I 100000-200000 MW (Sigma Aldrich, UK), 0.8 g Sodium chloride, 0.08 g L-Ascorbic acid (Sigma Aldrich, UK), 0.4 g Potassium phosphate dibasic (Sigma Aldrich, UK), 0.4 g Potassium phosphate monobasic basic (Sigma Aldrich, UK), and 0.08 g Ferric ammonium citrate (Sigma Aldrich, UK). The constituents were completely dissolved and the pH of the solution was adjusted to pH 8.5 using 1M NaOH. The solution was aliquoted into 4 bottles (approximately 87 mL per bottle) and autoclaved for 15 minutes at 121 °C. For long term storage this autoclaved basal medium was stored at -20 °C.

For use, 1 X 87 mL aliquot of medium was thawed to room temperature and 10 mL of bovine serum (26170035 ThermoFisher Scientific/Invitrogen, UK), and 2.5 mL of 40X strength Diamond's vitamin tween solution (Sigma Aldrich, UK) was aseptically added. The completed medium was aliquoted into 10 mL volumes and stored at -20 °C for up to 6 months.

2.4.2. Canine filtered saliva

Canine filtered saliva was collected and prepared from dog's resident at the WALTHAM Centre for Pet Nutrition. Trained Labrador retrievers were presented with sterile cotton pads and encouraged to lick them, allowing the canine saliva to be absorbed into the pad. Saliva soaked pads were placed into salivette tubes (Starstedt, UK) and centrifuged within 15 mL centrifuge tubes at 2000 x g for 5 minutes to collect the saliva at the bottom of the tubes. The saliva from individual animals was pooled to a single samples and filtered through a 0.2 µM filter to produce sterile canine saliva. The saliva was placed at -20 °C for long term storage.

2.4.3. Isolation and culture of canine oral trichomonads

Canine oral strains of *Trichomonas* were cultured from plaque samples obtained from Labrador retriever, Miniature schnauzer, or Cocker spaniel dog's resident at the WALTHAMH Centre for Pet Nutrition. During unrelated procedures requiring anaesthesia, supra gingival plaque samples were obtained from ten separate animals (Table 9) by rubbing 1 μ L loops along the gingival margin of the teeth and gathering the loop tips with plaque into 1 mL of modified TYI-S-33 medium (see above). Multiple loops were used if required until the maximum amount of plaque from each dog was collected. The 1 mL plaque samples were vortexed vigorously to remove plaque material from the loops and then transferred (without loops) into 10 mL of pre-warmed 50 % (v/v) Modified TYI-S-33 medium/50 % (v/v) sterile filtered canine pooled saliva, in a sterile flat bottomed Nunc™ Cell Culture Tube (156758 ThermoFisher Scientific, UK). The tube was centrifuged at 800 X g for 30 seconds to bring the plaque mass down to the bottom of the tube to concentrate the protozoa to the bottom of the tube. If the plaque/bacterial load in the tube seemed high, 100 μ L of penicillin-Streptomycin solution (10,000 units penicillin and 10 mg streptomycin/mL) (Sigma Aldrich, UK) was added to the tube. The tubes were then incubated at 35°C for 3-5 days at a 15° angle. The cultures were examined daily using an inverted microscope (Nikon TMS inverted equipped with phase contrast, Nikon, UK) for the presence of free swimming viable trichomonads.

If the organisms survived the initial isolation from plaque, they were passaged on to further tubes. Tubes were placed on ice for 5 mins to detach any trichomonads attached to the surfaces, gently vortexed and centrifuged at 800 x g for 5 minutes to pellet the cells. The supernatant was discarded and the pellet was divided across 3 X fresh pre-warmed 50 % (v/v) Modified TYI-S-33 medium/50 % (v/v) sterile filtered canine pooled saliva tubes. The tubes were incubated at 35°C for 3-5 days at a 15° angle. Successful cultures were passaged by transferring 0.1 mL to 0.5 mL aliquots from 80% confluent culture tubes to 10 mL volumes of fresh sterile 100% Modified TYI-S-33 medium containing 100 μ L of penicillin-Streptomycin solution (10,000 units penicillin and 10 mg streptomycin/mL) (Sigma Aldrich, UK) and incubating at 35°C for 3-5 days at a 15° angle.

Table 9. Details of dogs from which canine oral trichomonads were isolated from.

Animal ID	Dog name	Breed	Sex
MS05114	Yasmine	Miniature Schnauzer	Female
LR05412	Macy	Labrador Retriever	Female
CS04357	Cleo	Cocker Spaniel	Female
LR05202	Esme	Labrador Retriever	Female
LR05445	Oasis	Labrador Retriever	Female
LR05009	Tigger	Labrador Retriever	Male
LR05446	Orla	Labrador Retriever	Female
MS05156	Brock	Miniature Schnauzer	Male
LR05830	Wiggle	Labrador Retriever	Male
MS05118	Yoshi	Miniature Schnauzer	Male

2.4.4. Cryopreservation and resurrection of canine oral trichomonads

trichomonad cells were harvested at 80% or more confluency by centrifugation at $800 \times g$ for 5 minutes. Cells were adjusted to 1×10^6 to 1×10^7 per mL in fresh Modified TYI-S-33 medium containing 5% dimethyl sulfoxide (DMSO Sigma Aldrich, UK). The cells, plus cryopreservant solution were incubated at 35 °C for 15 minutes and then split into 1 mL cryovials (0.5 mL per vial). The vials were placed into a CoolCell freezing container (Sigma Aldrich, UK) and frozen at -80 °C for 24 hours. After 24 hours, all vials were removed from the CoolCell vessel and transferred to a cryobox for long term storage at -80 °C.

For use, a frozen vial was removed from -80 °C and placed into a 35 °C water bath for 3 to 5 minutes until the vial has completely defrosted. Immediately after thawing, the contents of the vial was gently transferred to a flat bottomed Nunc™ Cell Culture Tube (156758 ThermoFisher Scientific, UK) containing 10 mL of pre-warmed Modified TYI-S-33 medium and 100 µL of penicillin-Streptomycin solution (10,000 units penicillin and 10 mg streptomycin/mL) (Sigma Aldrich, UK). The tube was incubated at 35°C for 3-5 days at a 15° angle.

2.4.5. Genomic DNA extraction from cultured canine oral Trichomonads

Genomic DNA from the canine oral trichomonad isolates listed in Table 9 was extracted using the Qiagen DNeasy Blood and Tissue DNA extraction Kit (Qiagen, UK) using the manufacturer's animal cell protocol. A confluent 10 mL culture tube was placed on ice for 5 minutes to remove adherent cells, then gently vortexed and

centrifuged at 800 x g for 5 minutes to pellet the cells. The supernatant was discarded and the pellet washed three times with DPBS and centrifugation. The final pellet was resuspended in 200 µL of DPBS and then processed using the Qiagen extraction kit. Genomic DNA samples were quantified using the Qubit® dsDNA Assay Kit (Life Technologies, UK) using the High Sensitivity kit and a Qubit fluorometer.

2.4.6. 18S PCR of cultured canine oral Trichomonads

Amplification of an approximately 950bp region of the 18S rRNA gene was performed via the touchdown PCR protocol listed in section [2.1.2](#) using a Platinum® Pfx DNA Polymerase kit. The amplification product for each sample was assessed using electrophoresis (see above methods), purified of PCR polymerases and other PCR impurities using a Diffinity RapidTip®2 PCR purification system (Sigma-Aldrich, UK), and quantified using the previously mentioned Qubit assay (see above). To confirm their identities, a sample from each purified amplicon was sent to Beckman Coulter Genomics, UK, for Sanger sequencing (Sanger and Coulson, 1975, Smith et al., 1986) using forward and reverse primers detailed in section [2.1.1](#)

2.4.7. 18S full length PCR of cultured canine oral Trichomonads using Dimasuay and Rivera (2013) primers

Amplification of the full length 18S rRNA gene of each trichomonad isolate was performed using a modified version of a previously published PCR protocol (Dimasuay and Rivera, 2013) and using a Platinum® Pfx DNA Polymerase kit. The following PCR reaction mix was prepared per sample: 5 µl Pfx amplification buffer, 1.5 µl deoxynucleotide triphosphates 10 mM (dNTPs – Promega Ltd, UK), 1.5 µl of each primer (10 µM), 1.0 µl magnesium sulphate (50 mM), and 1 unit Platinum® Pfx DNA Polymerase. To the reaction mix, 10-50 ng of genomic DNA template was added. The final volume was brought to 50 µl using nuclease-free water (Qiagen Ltd, Manchester, UK). A GeneAmp PCR 9700 thermal cycler (ThermoFisher Scientific, Applied Biosystems, UK) was used to amplify the first and second halves of the full length 18S rRNA gene using primer sets T18SF/T18Sri and T18SFi/T18SR (Dimasuay and Rivera, 2013). The following

cycle conditions were used for the PCR: 94 °C for 5 minutes followed by 35 cycles of 94 °C for 60 seconds, 55 °C for 60 seconds, and 68 °C for 2 minutes. This was followed by a final extension step of 68 °C for 10 minutes. The reaction was then stopped by holding at 4 °C.

2.4.8. ITS1-5.8S-ITS2 full length PCR of cultured canine oral Trichomonads using Felleisen, (1997) primers

Amplification of the full length ITS1-5.8S-ITS2 genome region of each trichomonad isolate was performed using a modified version of a previously published PCR protocol (Felleisen, 1997) and using a Platinum® Pfx DNA Polymerase kit. The following PCR reaction mix was prepared per sample: 5 µl Pfx amplification buffer, 1.5 µl deoxynucleotide triphosphates 10 mM (dNTPs – Promega Ltd, Southampton, UK), 1.5 µl of each primer (10 µM), 1.0 µl magnesium sulphate (50 mM), and 1 unit Platinum® Pfx DNA Polymerase. To the reaction mix, 10-50 ng of genomic DNA template was added. The final volume was brought to 50 µl using nuclease-free water (Qiagen, UK). A GeneAmp PCR 9700 thermal cycler (ThermoFisher Scientific, Applied Biosystems, UK) was used to amplify the full length ITS-1-5.8S-ITS2 genome region using primer set TRF1/TRF2 (Felleisen, 1997). The following cycle conditions were used for the PCR: 94 °C for 5 minutes followed by 40 cycles of 94 °C for 60 seconds, 60 °C for 60 seconds, and 68 °C for 2 minutes. This was followed by a final extension step of 68 °C for 10 minutes. The reaction was then stopped by holding at 4 °C.

2.4.9. Amplicon Sanger sequencing and identification

PCR amplicons were purified of PCR polymerases and other PCR impurities using a Diffinity RapidTip®2 PCR purification system (Sigma Aldrich, UK) and quantified using the previously mentioned Qubit assay (see above). A sample from each purified amplicon was sent for Sanger sequencing (Smith et al., 1986, Sanger and Coulson, 1975) to Beckman Coulter Genomics, UK, and sequencing via the forward and reverse primer of each reaction. Raw sequences returned from the sequencing service provider were manually checked by examining the sequence chromatograms and automatically based called in Sequencher 5.2 (Gene coded Corporation, USA) using the default parameters. Primer flare sequence and low

quality flanking sequences were removed using the software's inbuilt modules and default settings. Forward and reverse high quality amplicon sequences were aligned in Sequencher using software default parameters to provide full length sequences for each sequencing sample and project.

Each full length sequence was analysed through the Basic Local Alignment Search Tool (BLAST) developed by the National Centre for Biotechnology information (NCBI) in the United States (Coordinators, 2017, Altschul et al., 1990). Sequences were submitted to the BLAST website and analysed against the NCBI nucleotide database using the default search parameters. The top 10 sequence matches and associated sequence information were recorded for each sequence search.

2.4.10. Phylogenetic analysis of *Trichomonas* genetic sequences

Full length 18S ribosomal RNA and ITS1-5.8S-ITS2 region DNA sequences representing all species found in the taxonomic genus *Trichomonas* were obtained from the Silva rRNA database project (Quast et al., 2013) (for 18S sequences) and the NCBI nucleotide database (Coordinators, 2017) (for ITS1-5.8S-ITS2 region sequences). The sequences were downloaded as FASTA files and imported into MEGA 6.06 phylogenetic analysis software (Tamura et al., 2013). For phylogenetic analysis all sequence manipulation and analyses were carried out in MEGA. The full length 18S and ITS-5.8S-ITS2 sequences obtained through Sanger sequencing of the unknown canine oral trichomonad isolates were aligned using the default parameters with these trichomonad representative sequences using the align DNA and ClustalW (Thompson et al., 2002) method function of MEGA. Alignments were manually checked for accuracy and adjusted manually if required. The “find best DNA model” function of MEGA was next used to find the appropriate substitution models to use to construct phylogenetic trees. For the 18S sequences the evolutionary distances were computed using the Kimura 2-parameter method (Kimura, 1980) and rate variation among sites was modelled with a gamma distribution (shape parameter = 1). For the ITS1-5.8S-ITS2 sequences the evolutionary distances were computed using the Tamura 3-parameter method (Tamura, 1992) and rate variation among sites was modelled with a gamma distribution (shape parameter = 1). For each alignment neighbour joining, maximum likelihood, minimum evolution and UPGMA trees were all computed

using the pre-selected models. Tree node reliability was estimated using the bootstrap method (Felsenstein, 1985) and 1000 bootstrap replicates per test.

2.4.11. Culture and identification of bacteria in co-culture with *T. canistomae* (CLEO strain)

Bacteria that were present with the *T. canistomae* CLEO strain were cultured by inserting sterile 10 µL plastic loops into a tube of containing a 3 day culture of *T. canistomae* CLEO strain and the accompanying bacteria. The loops were removed and streaked out using standard microbiological methods onto 2 X Columbia blood agar plates (Oxoid, UK). The first plate was incubated at 35 °C under microaerobic conditions for 3-5 days and the second plate was incubated at 38 °C under anaerobic conditions for 7 days. Bacterial colonies observed were picked out using 1 µL sterile loops and re-streaked onto Columbia blood agar plates and incubated under the same conditions that the colonies were isolated with.

The DNA from individually isolated bacterial colonies was extracted using the Chelex extraction resin method (Iovieno et al., 2011) of DNA extraction. In brief, a single colony of the culture was transferred and resuspended into a microcentrifuge tube containing 1 mL of 5 % (w/v) chelex resin solution (Sigma Aldrich, UK). The tube was vortexed vigorously for 30 seconds and 200 µL aliquots were transferred into 0.2 mL PCR tubes. The PCR tubes containing bacterial suspensions and chelex were heated using a PCR block to 95 °C for 10 minutes to lyse the cells and then centrifuged at 16000 x g for 5 minutes to pellet the cell debris. 100 µL of the DNA containing supernatant was pooled in a fresh DNA/RNA free microcentrifuge tube. 1 in 10 dilutions of the chelex DNA preparations from each bacterial isolate were used as template in a 16S PCR reaction according to the method described in section [2.1.3](#). The 16S PCR amplicons from each sample were purified of PCR polymerases and other PCR impurities using a Diffinity RapidTip®2 PCR purification system (Sigma-Aldrich, UK) and quantified using the previously mentioned Qubit assay (see above). A sample from each purified amplicon was sent for Sanger sequencing (Smith et al., 1986, Sanger and Coulson, 1975) (Beckman Coulter Genomics, UK) using both forward and reverse 16S primers to confirm their identities. The returned raw reads from the sequencing

were processed in Sequencher software and identified through BLAST analysis as describes above in section [2.4.9](#).

2.4.12. β -tubulin staining of the *Trichomonas* flagella

A near confluent tube of *T. canistomae* (CLEO strain) was cultured in Modified TYI-S-33 medium according to the methods described in section [2.4.1](#) and [2.4.3](#). The cells were harvested through centrifugation at 800 x g for 5 minutes and washed three times using DPBS and centrifugation. The final cell pellet was resuspended in 1 mL of DPBS and gently added to 2 mL of Bouin's solution (Sigma Aldrich, UK) to fix the cells for 5 minutes. The cells were pelleted through centrifugation (800 x g for 5 minutes) and rapidly washed three times with DPBS and centrifugation. The final pellet, free of traces of Bouin's solution, was resuspended in 2 mL of DPBS.

For immunostaining, 10 μ L of fixed organism was pipetted into the wells of a 10-well Thermo Scientific epoxy diagnostic microscope slide (ThermoScientific, UK) and air dried in a fume hood for 1 hour. The air dried cells were made permeable by incubating each well with 10 μ L of 0.5 % (v/v) Triton X-100 (Sigma Aldrich, UK) in DPBS for 10 minutes. The Triton X-100 was removed and the cells were washed with 10 μ L of DPBS three times to remove traces of Triton X-100. The cells in each well were blocked by incubating with 10 μ L of 1 % (v/v) Bovine Serum Albumin (BSA) (Sigma Aldrich, UK) and 22.52 mg per mL of Glycine (Sigma Aldrich, UK) in DPBS with 0.1 % (v/v) Tween 20 (Sigma Aldrich, UK) (DPBST) for 30 minutes at room temperature. For antibody binding, the blocking solution was removed and replaced with 10 μ L per well of a 1 in 100 dilution of Rabbit polyclonal anti- β -tubulin antibody (ab6046, Abcam, UK) in 1 % (v/v) BSA, for 1 hour, in the dark at room temperature. Then the primary antibody was aspirated away and the cells were washed with 10 μ L of DPBS, three times, to remove traces of unbound antibody. The wells were next incubated with 10 μ L of a 1 in 200 dilution of secondary antibody, Goat Anti-Rabbit IgG H&L (Alexa Fluor® 488) (ab150077, Abcam, UK) in 1% (v/v) BSA, for 1 hour in the dark at room temperature. The secondary antibody was next aspirated and the cells were washed with 10 μ L of DPBS, three times, to remove traces of unbound antibody. 10 μ L of 0.1 mg per mL DAPI (Sigma Aldrich, UK) was added each well for 1

minute in the dark at room temperature, to counterstain the cell nuclei. The DAPI stain was decanted and the cells were washed with 10 μ L of DPBS, three times, to remove traces of extracellular DAPI.

The well slides were mounted with 50 μ L of DPX Mountant for histology (Sigma Aldrich, UK) and visualised on a Nikon E400 upright microscope equipped with a DAPI and FITC filter set and 100 X objective, images were acquired using an Andor CCD camera system (Oxford Instruments, UK) in conjunction with the microscope set up.

2.4.13. Protargol (Silver Proteinate) synthesis

Protargol was synthesised in-house based on a protocol published by (Pan et al., 2013). 50 g of peptone from gelatin (Sigma Aldrich, UK) was added to a 500 mL beaker and 50 mL of distilled water was added, while stirring the mixture. The brown gummy precipitate was allowed to settle and the cloudy supernatant was gently poured away leaving only the precipitate. The residual fluid was allowed to evaporate from the precipitate for 5 mins. The precipitate was re-dissolved in 40 mL of distilled water whilst heating on a warming plate at 50 °C for 20 minutes. When completely dissolved, 120 mL of absolute ethanol (Sigma Aldrich, UK) was added, whilst constantly stirring, to precipitate the mixture. The milky mixture was covered with foil and cooled using running water for 30 minutes to allow complete precipitation. The supernatant was carefully poured off to leave a gummy precipitate. This was allowed to stand for 10 minutes and re-dissolved by adding 40 mL of distilled water whilst gently swirling the beaker. Half of this purified peptone was poured into a fresh 500 mL beaker and the other half was poured into a 100 mL beaker. The beakers were transferred to a fume hood where 2 mL of 29 % (v/v) ammonium hydroxide (Sigma Aldrich, UK) was added to the purified peptone in the 500 mL beaker. The solution was mixed well and a solution of silver nitrate (20 g in 60 mL of distilled water) (Sigma Aldrich, UK) was added. The light brown precipitate that formed was allowed to settle to the bottom of the beaker. Both beakers (500 and 100mL) were sealed with parafilm and left for 18 hours in the dark at 13 to 18 °C. The supernatant from the larger 500 mL beaker was poured away leaving the brown precipitate. 100 mL of distilled water was carefully added to the beaker and incubated with the precipitate, with no stirring, for 10 minutes at

room temperature. The water was discarded and the process was repeated. The purified peptone from the smaller 100 mL beaker was added to the washed precipitate in the 500 mL beaker and dissolved by gently mixing on a warming plate set to 50 °C. Once dissolved, the solution was allowed to cool to room temperature. The pH of the solution was taken and adjusted to pH 8.0 to 9.0 by adding concentrated drops of ammonium hydroxide (Sigma Aldrich, UK). To this 100 mL of acetone (Sigma Aldrich, UK) was added whilst slowly stirring with a glass rod. It was allowed to stand for 5 minutes and the milky supernatant was carefully poured off and discarded leaving the precipitate. The precipitate was left to stand for 10 minutes and another 100 mL of acetone was added whilst slowly stirring with a glass rod. It was allowed to stand for 5 minutes and the milky supernatant was carefully poured off and discarded, leaving the precipitate. This process was repeated until the acetone supernatant remained clear and not milky in appearance. The precipitate, now adhered to the glass sides, was scraped off using a glass rod and transferred to a mortar containing 30 mL of acetone to cover the precipitate. The precipitate was pulverised under acetone using a pestle for 30 minutes to 1 hour. Once very fine particles begin to cloud the acetone the suspension was transferred to a glass funnel lined with a grade 2 Whatman filter paper (Sigma Aldrich, UK). Another 30 mL of acetone was added to the mortar and the process was repeated approximately 10 times until all of the precipitate was pulverised and transferred to the filter paper. The filter paper was allowed to stand for 30 minutes at room temperature and was then transferred to a glass petri dish. The precipitate was scrapped constantly across the glass dish surface using a glass microscope slide until the acetone was completely evaporated and a dry, very fine, light brown powder remained. The powder was transferred to a glass brown bottle and stored under nitrogen.

2.4.14. Protargol staining of trichomonads

For staining of cells with in-house synthesised Protargol, the following method was used, adapted from (Nie, 1950). A confluent tube of *T. canistomae* (CLEO strain) was cultured in Modified TYI-S-33 medium according to the methods described in section [2.4.1](#) and [2.4.3](#). The cells were harvested through centrifugation at 800 x g for 5 minutes, washed three times using DPBS and

centrifugation and the final pellet resuspended into 1 mL of DPBS. 50 μ L of cell suspension was pipetted onto standard glass microscope slides. The culture was spread across the lower half of the slide using the flat side of a coverslip and allowed to air dry for 5 minutes at room temperature. Slides were then immersed into Bouin's solution (Sigma Aldrich, UK) for 5 minutes to fix the cells. Preparations were passed through 50 %, 60 %, 70 %, 70 % and 70 % Ethanol (Sigma Aldrich, UK) for 3 minutes each to wash out the fixative. Fixed organisms stored in 70 % Ethanol were passed through 50 % Ethanol for 5 minutes and then stored in distilled water prior to the staining procedure. To stain, the slides were immersed into a jars containing 0.5 % potassium permanganate solution (Sigma Aldrich, UK) for 5 minutes and then rinsed 5 times for 30 seconds each, in distilled water. Preparations were then immersed for 5 minutes in 5 % oxalic acid (Sigma Aldrich, UK) and immediately rinsed 5 times for 30 seconds each, in distilled water. The slides were next immersed into a 1 % solution of pre-warmed Protargol. The solution was prepared by dispersing the powder onto the surface of distilled water and left to dissolve spontaneously. 15 cm thin copper wires (stripped and cut from electrical cable) were also immersed vertically into the Protargol solution along the edge of the slides. The slides in 1% Protargol solution, were incubated at 37 °C for 48 hours after which they were rinsed twice for 30 seconds each, in distilled water. The slides were then placed in freshly prepared reducing solution (1 % hydroquinone and 5 % Na₂SO₃, Sigma Aldrich, UK) for 10 minutes. Slides were then rinsed 5 times for 30 seconds each in distilled water and subsequently immersed for 5 minutes in 0.5 % AuCl₃ (Sigma Aldrich, UK) and then rinsed for 5 seconds in distilled water. Then, they were immersed for 5 minutes in 2 % oxalic acid solution. After washing the slides 5 times for 30 seconds each in distilled water, they were immersed for 10 minutes in a 5 % solution of Na₂SO₃ (Sigma Aldrich, UK) to stop the staining reaction. The stained slides were washed for 20 minutes under gentle running tap water and transferred through a series of Ethanol dehydration jars (50 %, 70 %, 80 %, 96 %, and 100 %) for 3 minutes each. Finally the slides were immersed into xylene (Sigma Aldrich, UK) twice, for 3 minutes each. The finished slides were mounted with 50 μ L of DPX Mountant for histology (Sigma Aldrich, UK) and visualised with a Nikon E400 upright microscope (Nikon Instruments, UK) equipped with a

100 X objective. Images were acquired using a Nikon D500 SLR colour camera (Nikon Instruments, UK) in conjunction with the microscope set up.

Images taken from 100 separate cells were stored to a hard drive. Cellular measurements were undertaken in ImageJ version 1.51n, using a calibrated image of a graticule for micrometre calibration. Cell body and width, axostyle projection, undulating membrane length, and nucleus length and width, were measured and recorded. Mean values for all measurements along with standard deviation of the means were calculated using Microsoft Excel 2013.

2.4.15. Scanning electron microscopy

For high resolution images, the scanning electron microscopy (Reichelt, 2007) technique was employed. A confluent tube of *T. canistomae* (CLEO strain) was cultured in Modified TYI-S-33 medium according to the methods described in section [2.4.1](#) and [2.4.3](#). The cells were harvested through centrifugation at 800 x g for 5 minutes and washed three times using DPBS and centrifugation and the final pellet resuspended into 1 mL of DPBS. 1 mL of electron microscopy grade Glutaraldehyde solution (Sigma Aldrich, UK) was added to the cells to give a final concentration of 2.5 % and incubated at room temperature for 2 hours. Post glutaraldehyde fixation the cells were harvested through centrifugation at 800 x g for 5 minutes and washed three times using DPBS and centrifugation and the final pellet was resuspended into 1 mL of DPBS.

20 µL aliquots of the cells were pipetted onto poly-L-lysine (ThermoFisher Scientific, UK) coated glass coverslips and allowed to adhere for 30 minutes. Excess liquid was removed and the coverslips were washed with DPBS. The cells on coverslips were post-fixed in 0.5 % (v/v) Osmium tetroxide (ThermoFisher Scientific, UK), for 60 minutes at room temperature and washed in distilled deionised water 3 times for 5 minutes to remove any traces of Osmium. Coverslips were next dehydrated through a 30, 50, 70, 90 and 100 % Ethanol series for 30 minutes each and two final 100 % analytical grade Ethanol (ThermoFisher Scientific, UK) dehydration steps. Following dehydration the cells were dried using three 30 minute incubations with a 2:1, 1:1 and 2:1 ratio of ethanol:Hexamethyldisilazane (HMDS) (ThermoFisher Scientific, UK) cell drying mix and two final 100% HMDS incubations for 30 minutes. Excess HMDS was

removed and the coverslips were dried in a fume hood until dry. Coverslips were mounted onto 33mm aluminium stubs using carbon sticky tabs and Gold sputter coated using a VG Microtech SC7640 Sputter Coater (Quorum Technologies Ltd, UK) and viewed on a Hitachi S3000H Scanning Electron Microscope (Hitachi High-Technologies Group, UK) with an accelerating voltage of 10kV.

2.4.16. Transmission electron microscopy

For high resolution cross-sectional imaging the transmission electron microscopy (Williams and Carter, 2009) technique was employed. A confluent tube of *T. canistomae* (CLEO strain) was cultured in Modified TYI-S-33 medium according to the methods described in section [2.4.1](#) and [2.4.3](#). The cells were harvested through centrifugation at 800 x g for 5 minutes, washed three times using DPBS and centrifugation and the final pellet resuspended into 1 mL of DPBS. 1 mL of fixation solution was prepared and added to the cells to give a final concentration of 2.5 % (v/v) glutaraldehyde solution (Sigma Aldrich, UK), and 5 mM calcium chloride (Sigma Aldrich, UK) in 0.1 M cacodylate buffer (pH 7.2) (Sigma Aldrich, UK). The cells were incubated in the fixation solution at room temperature for 2 hours. After initial fixation, the cells were harvested through centrifugation at 800 x g for 5 minutes and washed three times using DPBS and centrifugation. The cells were post-fixed in 1 % (v/v) osmium tetroxide (ThermoFisher Scientific, UK), 0.8 % (v/v) potassium ferricyanide (Sigma Aldrich, UK) and 5 mM CaCl₂ in 0.1 M cacodylate buffer for 15 minutes at 4 °C. The cells were harvested through centrifugation at 800 x g for 5 minutes and washed three times using DPBS and centrifugation to remove any traces of Osmium, and the final pellet was resuspended into 1 mL of DPBS.

Fixed cells were embedded into 3 % agar gel (Agar scientific, UK) and cooled to enable cutting up of the sample into smaller pieces. The agar sections were washed in DPBS and dehydrated in an Acetone (ThermoFisher Scientific, UK) series, 10% (v/v) for 30 minutes, 30% (v/v) for 25 minutes, and 50% (v/v) for 20 minutes. The sections were stored in 70 % (v/v) acetone overnight after which the acetone dehydration series was continued; 90% (v/v) for 30 minutes and 100% for 1 x 25 minutes, 1 x 20 minutes and 1 x 25 minutes. For resin infiltration of the sample, a 5:1 ratio of Acetone to Spurr resin (Sigma Aldrich, UK) was added at room

temperature for 60 minutes, followed by a 3:1 ratio for 75 minutes, a 1:1 ratio for 90 minutes, a 1:3 ratio for 90 minutes, a 1:5 ratio for 75 minutes respectively, and finally 100 % Spurr resin overnight. Fresh 100 % Spurr resin was replaced for 3 hours the next day and then another fresh Spurr resin for 4 hours. The samples were then embedded into BEEM capsules (ThermoFisher Scientific, UK) and polymerised at 60 °C for 16 hours. The polymerised samples were collected onto copper mesh grids, submerged briefly into Methanol (ThermoFisher Scientific, UK), and stained with 2 % (v/v) aqueous uranyl acetate (ThermoFisher Scientific, UK) for 30 minutes followed by 5 minutes in lead citrate (ThermoFisher Scientific, UK). The stained samples were sectioned and viewed on a JEOL JEM-1400 transmission electron microscope (Jeol USA, Inc) with an accelerating voltage of 100kV. Digital images were collected with a Megaview III digital camera (EMSIS GmbH, Germany) and iTEM software package.

2.4.17. Enzyme detection using API® ZYM®

API® ZYM® semi-quantitative enzymatic activity strips were obtained from Biomerieux, USA. A confluent tube of *T. canistomae* (CLEO strain) was cultured in Modified TYI-S-33 medium according to the methods described in section [2.4.1](#) and [2.4.3](#). The cells were harvested through centrifugation at 800 x g for 5 minutes, washed three times using DPBS and centrifugation and the final pellet resuspended into 2 mL of Modified TYI-S-33 medium. 5 mL of distilled water was distributed into the incubation box of an API® ZYM® strip, and the strip was placed into the top of the box. 65 µL of the *Trichomonas* suspension was added to each of the api ZYM capsules. The lid of the incubation box was fitted and the chamber and strip were incubated at 38 °C under humidified anaerobic conditions for 4 hours. Post incubation the API® ZYM® strip was removed from the incubator and 1 drop of ZYM A reagent and then 1 drop of ZYM B reagent was added to each cupule. The enzymatic colour change in each capule was allowed to develop by incubating at room temperature for 5 minutes after which the degree of colour change was recorded by assigning a value from 0 to 5, 0 corresponding to a negative reaction and 5 being a maximum intensity reaction (see API® ZYM® manual for further detail).

2.4.18. General protease detection assay

The detection of general protease production by trichomonads was undertaken using milk agar medium and zones of clearance observations. Milk peptone agar was prepared by adding the following ingredients to 483.5 mL of distilled water; 7.5 g of Agar (Oxoid, UK), 2.5 g of Bacto Peptone (BD 211677), 1.5 g of Yeast Extract (212750 – BD, UK), and 5 g of instant dried skimmed milk (Tesco, UK). The constituents were completely dissolved and autoclaved for 15 minutes at 121°C. Post-autoclaving, the medium was cooled to 50 °C and aseptically poured as 5-7 mm thick plates in plastic petri dishes. The agar plates were allowed to solidify and then stored at 4 °C until use.

Milk agar was prepared by adding the following ingredients to 487.5 mL of distilled water; 7.5 g of Agar (Oxoid, UK), and 5 g of Instant dried skimmed milk (Tesco, UK). The constituents were completely dissolved autoclaved for 15 minutes at 121°C. Post autoclaving the media was cooled to 50 °C and aseptically poured as 5-7 mm thick plates in plastic petri dishes. The agar plates were allowed to solidify and then stored at 4 °C until use.

5 mm holes were bored into the agar plates using an ethanol-sterilised hole boring tool. A confluent tube of *T. canistomae* (CLEO strain) was cultured in Modified TYI-S-33 medium according to the methods described in section [2.4.1](#) and [2.4.3](#). The cells were harvested through centrifugation at 800 x g for 5 minutes, washed three times using DPBS and centrifugation and the final pellet resuspended into 2 mL of antibiotic-free Dulbecco's Modified Eagle's Medium (DMEM) - low glucose (Sigma Aldrich, UK). 100 µL of the resuspended culture was pipetted in duplicate into the 5 mm bored holes in each agar plate type. As a positive control, a single colony of *Bacillus subtilis* (ATCC 6051) was incubated in antibiotic-free low glucose DMEM at 38°C for 18 hours. The bacterial cells were harvested through centrifugation at 4000 x g for 10 minutes, washed three times using DPBS and centrifugation and the final pellet resuspended into 2 mL of antibiotic-free low glucose DMEM. 100 µL of the resuspended bacterial culture was also pipetted in duplicate into the 5 mm bored holes in each agar plate type.

All plates were incubated overnight (18 hours) under humidified conditions in anaerobic or 5 % (v/v) CO₂ conditions at 38 °C. Zones of clearance in the medium were measured using a SYNBIOISIS ProtoCOL automated colony counter (Don

Whitley Scientific, UK) using the Inhibition zones detection module and default settings.

2.4.19. BAPNA assay for Trypsin activity

A confluent tube of *T. canistomae* (CLEO strain) was cultured in canine gingival fibroblast (CGFIB) medium (see [section 2.4.22](#) for recipe) with the addition of the antibiotics kanamycin sulphate (100 µg/mL), meropenem (5 µg/mL) and penicillin/streptomycin (200 U/200 µg/mL). The cells were harvested through centrifugation at 800 x g for 5 minutes, washed three times using DPBS and centrifugation and the final pellet resuspended into low glucose DMEM (31885-023, ThermoFisher Scientific, UK) medium (no antibiotics) at a concentration of 1×10^7 cells per mL. The initial cell culture supernatant of the *T. canistomae* (CLEO strain) was kept for use in the experiment, as was the cell supernatant and cellular pellet collected from a canine gingival cell/ *T. canistomae* (CLEO strain) co-culture experiment that was undertaken separately (see [section 2.4.22](#)). Both supernatants were centrifuged at 4000 x g for 10 minutes to remove any bacterial/cell contaminants. For a positive microorganism control in the experiment, an overnight culture of *P. gulae* II (Davis et al., 2013) grown in antibiotic-free low glucose DMEM medium was harvested and washed using DPBS three times through centrifugation at 4000 x g for 10 minutes each time. The initial bacterial cell culture supernatant was removed and saved for use in the assay. The final pellet was resuspended into antibiotic-free low glucose DMEM medium, at an absorbance of approximately O.D. 0.2 at 600nm, which has previously been determined to be approximately 1×10^7 cells per mL (data not shown).

700 µL of *T. canistomae* (CLEO strain) cell pellet solution, cell supernatant solution, canine gingival cell/ *T. canistomae* (CLEO strain) co-culture experiment pellet and supernatant, and *P. gulae* II cell pellet and supernatant solutions were added to separate aliquots of 700 µL of 0.1M Trizma® hydrochloride solution pH 8.0 (Sigma Aldrich, UK). As a negative control, 700 µL of antibiotic-free low glucose DMEM medium was also added to 700 µL Trizma® hydrochloride solution. 6 X 180 µL aliquots from each solution was pipetted into the wells of a sterile Nunc™ 96-Well Polystyrene flat bottom microwell plate (ThermoFisher Scientific, UK). Also, in triplicate, a trypsin standard curve was prepared on the microplate by

serially diluting a trypsin stock solution, between 0.1 mg/mL and 1×10^{-12} mg/mL trypsin from bovine pancreas (Sigma Aldrich, UK), across the plate to give 180 μ L of each standard in each well. Then to each well 20 μ L of assay substrate, 12mM *N* α -Benzoyl-DL-arginine 4-nitroanilide hydrochloride (Sigma Aldrich, UK - BAPNA), was added. The plate was incubated at room temperature for 10 minutes, after which the plate was centrifuged at 2500 x g to remove any cell debris. 150 μ L of supernatant from each well was transferred to a clean sterile flat-bottomed microwell plate and the absorbance of each sample was measured using a FLUOstar Omega microplate reader (BMG LABTECH, UK) at 410 nm. The raw data obtained from the plate reader was analysed using Prism (GraphPad Prism software, USA). The standard curve was plotted using a non-linear fit Allosteric sigmoidal model. Test sample data was plotted as a bar graph and the values for each were interpolated using the standard curve and the equation $Y = \text{Bottom} + (\text{Top} - \text{Bottom}) / (1 + 10^{-(\text{LogEC}_{50} - X) * \text{HillSlope}})$ in Prism. A multiple comparison (Dunnett's) of each sample mean verses the DMEM control was carried out in Prism using Ordinary one-way ANOVA analysis.

2.4.20. Haemolysis assay

A *Trichomonas* haemolysis assay was adapted from (Dailey et al., 1990). 0.5 mL of canine blood was collected from a single dog when sampling was undertaken for other non-related trials at the WALTHAM centre for pet nutrition. The blood was collected into blood tubes containing EDTA (Sarstedt AG & Co, Germany) to prevent coagulation of the sample. This and 0.5 mL of defibrinated horse blood (Oxoid, UK) was added to two separate 9.5 mL tubes of DPBS and inverted gently several times. Both blood tubes were centrifuged at 4 °C at 1000 x g for 10 minutes to pellet the cells. The supernatant was gently removed and the cells were resuspended in 9.5 mL of fresh DPBS. This was repeated two further times and the final pellet was resuspended in 9.5 mL of fresh DPBS and stored on ice. 100 μ L each blood sample was pipetted into 42 wells of two separate Nunc™ 96-Well polystyrene round bottom microwell plates (ThermoFisher Scientific, UK). The plates were stored on ice until ready for use.

A confluent tube of *T. canistomae* (CLEO strain), approximately 1.0×10^7 cells, was cultured in CGFIB medium (see [section 2.4.1](#) for method) with the addition of

the antibiotics kanamycin sulphate (100 µg/mL), meropenem (5 µg/mL) and penicillin/streptomycin (200 U/200 µg/mL). The cells were harvested through centrifugation at 800 x g for 5 minutes, washed three times using DPBS and centrifugation and the final pellet resuspended into low glucose DMEM (31885-023, ThermoFisher Scientific, UK) media (no antibiotics) at a concentration of 1×10^7 cells per mL. The initial cell culture supernatant of the *T. canistomae* (CLEO strain) was kept for use in the experiment, as was also a cell supernatant collected from a canine gingival cell/ *T. canistomae* (CLEO strain) co-culture experiment that was undertaken separately (see [section 2.4.22](#)). Both of these supernatants were centrifuged at 4000 x g for 10 minutes to remove any bacterial/cell contaminants. For a positive microorganism control, an overnight culture of *P. gulae* II (Davis et al., 2013) grown in antibiotic-free low glucose DMEM medium was harvested and washed three times through centrifugation at 4000 x g for 10 minutes each time. The final pellet was resuspended into antibiotic-free low glucose DMEM medium, at an absorbance of approximately O.D. 0.2 at 600 nm, which has previously been determined to be approximately 1×10^7 cells per mL (data not shown).

100 µL of *T. canistomae* (CLEO strain) cell pellet solution, cell supernatant solution, canine gingival cell/ *T. canistomae* (CLEO strain) co-culture experiment supernatant, and *P. gulae* II cell pellet solution were pipetted into 6 wells of the canine blood and horse blood in 96-well round bottomed plates prepared earlier. As 100 % lysis controls, 100 µL of 1 % (v/v) Triton X-100 (Sigma Aldrich, UK) and distilled water were pipetted into another 6 wells of the canine blood and horse blood 96-well round bottomed plates. As a negative control 100 µL of antibiotic-free low glucose DMEM medium was pipetted into another 6 wells of the canine blood and horse blood 96-well round bottomed plates. Both plates were incubated in 5 % (v/v) CO₂ at 38 °C for 18 hours in humidified conditions. Post incubation the plates were centrifuged at 2000 x g for 10 minutes to pellet any cell debris. 150 µL of supernatant from each well was transferred to the wells of a clean Nunc™ 96-Well Polystyrene flat bottom microwell plate (ThermoFisher Scientific, UK). The absorbance of each sample was measured using a FLUOstar Omega microplate reader (BMG LABTECH, UK) at 405 nm and the percentage haemolysis exhibited was calculated by dividing the optical density reading by the average of the 405nm readings of the 100 % lysis control replicates (Triton X-100) and expressed as a percentage. Statistical comparisons of samples were computed in

Prism (GraphPad Prism software, USA). A multiple comparison (Dunnet's) of each sample mean verses the DMEM control was carried out in using Ordinary one-way ANOVA analysis.

2.4.21. Elastase activity assay

An assay to measure elastase activity was adapted from the Worthington Enzyme Manual (Worthington Biochemical Corporation, USA). The assay is based on previously published elastase assays (Bieth et al., 1974, Feinstein et al., 1973).

A confluent tube of *T. canistomae* (CLEO strain) was cultured in CGFIB medium with the addition of the antibiotics kanamycin sulphate (100 µg/mL), meropenem (5 µg/mL) and penicillin/streptomycin (200 U/200 µg/mL). The cells were harvested through centrifugation at 800 x g for 5 minutes, washed three times using DPBS and centrifugation and the final pellet resuspended into low-glucose DMEM (31885-023, ThermoFisher Scientific, UK) media (no antibiotics) at a concentration of 1×10^7 cells per mL. The initial cell culture supernatant of the *T. canistomae* (CLEO strain) was kept for use in the experiment, as was the cell supernatant that was collected from a canine gingival cell/ *T. canistomae* (CLEO strain) co-culture experiment that's was undertaken separately (see [section 2.4.22](#)). Both of these supernatants were centrifuged at 4000 x g for 10 minutes to remove any bacterial/cell contaminants. 180 µL of Trizma® base buffer pH 8.0 (Sigma Aldrich, UK) was pipetted into the wells of a sterile Nunc™ 96-Well Polystyrene flat bottom microwell plate (ThermoFisher Scientific, UK). To each well 13.3 µL of assay substrate, 4.4 mM N-Succinyl-Ala-Ala-Ala-p-nitroanilide (Sigma Aldrich, UK) was added. Each well was mixed through gentle pipetting and the plate was allowed to equilibrate to room temperature. 6 X 6.6 µL of *T. canistomae* (CLEO strain) cell pellet solution, cell supernatant solution, canine gingival cell/ *T. canistomae* (CLEO strain) co-culture experiment pellet and supernatant, and *P. gulae* II cell pellet and supernatant solutions were added to individual substrate/buffer wells. As a positive and negative controls respectively, 6 X 6.6 µL of 0.4 U/mL Elastase from Porcine pancreas (Sigma Aldrich, UK) and 6 X 6.6 µL of antibiotic free low glucose DMEM media were added to a further 6 wells each. The plate was incubated at 25 °C for 5 mins after which the increase in absorbance of each sample/well was continuously measured and recorded for 30 minutes using a FLUOstar Omega microplate reader

(BMG LABTECH, UK) at 410 nm. All raw data were imported into Prism (GraphPad Prism software, USA) and plotted as a line graphs.

2.4.22. Culture of immortalised canine gingival fibroblasts

A previously immortalised canine gingival fibroblast cell line (CGFIB145H) was cultured. The cell line was initially isolated as a primary cell line from a 6 year old Great Dane using post mortem tissue. The cell line was immortalised using established methods (Kamata et al., 2004, Kedjarune et al., 2001) at the University of Brighton, as part of other studies and subsequently cultured in canine gingival fibroblast (CGFIB) medium. The CGFIB medium was prepared as follows: To 435 mL of low glucose DMEM (31885-023, ThermoFisher Scientific, UK), 50 mL of Foetal bovine serum GOLD (PAA laboratories, UK), 5 mL of penicillin-Streptomycin solution (10,000 units penicillin and 10 mg streptomycin/mL) (Sigma Aldrich, UK), 5 mL of Non Essential Amino Acids (Sigma Aldrich, UK) and 5 mL of L-Glutamine (ThermoFisher Scientific, UK) were aseptically added. To resurrect the frozen immortalised cell line a vial was removed from the liquid nitrogen storage vessel and thawed rapidly in a 37 °C water bath. The contents of the thawed vial were gently transferred to 9 mL of pre-warmed CGFIB medium and swirled gently to disperse the cells. The cells were gently pelleted by centrifugation at 200 x g for 5 minutes. The supernatant was discarded and the cell pellet was resuspended in 10 mL of fresh pre-warmed CGFIB medium. Approximately 1 million cells were seeded into T75 sized flask for culture. The cells were incubated at 37 °C, 5 % (v/v) CO₂. The culture medium was replaced every 2 days and the cells were passaged when the cell monolayer achieved 80 to 90 % confluency.

2.4.23. Co-culture of *T. canistomae* (CLEO strain) and gingival fibroblasts

Canine gingival fibroblasts (CGFIB145H – see [section 2.4.22](#)) were seeded into 12 wells of 5 X 24-well tissue culture plates. The cells were cultured in CGFIB medium with the addition of the antibiotics, kanamycin sulphate (100 µg/mL), meropenem (5 µg/mL) and penicillin/streptomycin (200 U/200 µg/mL) to suppress the growth of bacteria. The plates were incubated at 37 °C under 5 % (v/v) CO₂ conditions until the cell monolayer achieved 80 to 90 % confluency, at approximately 10000 cells per well. 5 confluent tubes of *T. canistomae* (CLEO strain) that were cultured in

CGFIB medium (see above) with the addition of the antibiotics kanamycin sulphate (100 µg/mL), meropenem (5 µg/mL) and penicillin/streptomycin (200 U/200 µg/mL). The cells were pooled and harvested through centrifugation at 800 x g for 5 minutes, washed three times using DPBS and centrifugation and the final pellet resuspended into 30 mL of CGFIB medium (see above) with the addition of the antibiotics kanamycin sulphate, meropenem and penicillin/streptomycin at a concentration of 50000 trichomonad cells per mL. The medium was aspirated from all wells of the 5 X CGFIB 24-well plates. For each plate, 1 mL of *Trichomonas* suspension (at 5000 cells per mL) was added to 6 of the wells (the co-culture wells) and 1 mL of CGFIB medium with the addition of the antibiotics kanamycin sulphate, meropenem and penicillin/streptomycin was added to the remaining 6 CGFIB wells. In addition, to 6 empty wells (containing no CGFIB cells), 1 mL of CGFIB medium with the addition of the antibiotics kanamycin sulphate, meropenem and penicillin/streptomycin was added (media control wells).

All plates were incubated at 37 °C under 5 % (v/v) CO₂ conditions. At 2, 4, 6, 24 and 48 hours post-incubation, each 24-well plate was removed from incubation and processed in the following way. At the appropriate time point the media from all wells was gently aspirated away and the wells were washed, gently twice, with 1 mL of pre-warmed DPBS to remove any remaining trichomonad cells. 0.5 mL of 10% (v/v) alamarBlue® cell viability reagent (ThermoFisher Scientific, UK) diluted in low glucose DMEM, 1 % (v/v) FBS GOLD, kanamycin sulphate (100 µg/mL), meropenem (5 µg/mL) and penicillin/streptomycin (200 U/200 µg/mL), was added. Each plate was incubated at 37 °C in 5 % (v/v) CO₂ for 18 hours. After 18 hours of incubation 150 µL of the alamarBlue® medium was removed and placed into the wells of a 96-well black walled plate. The fluorescence from each was measured at excitation 584 nm and 620-10nm emission using a FLUOstar Omega microplate reader (BMG LABTECH, UK).

The remaining alamarBlue® medium was gently aspirated from the 24-well plates and the wells were washed gently twice with 1 mL of pre-warmed DPBS. The remaining CGFIB cells in each well were fixed using 1 mL of 2 % (w/v) paraformaldehyde (PFA) (Sigma Aldrich, UK) and incubation for 20 minutes at room temperature, after which the PFA was gently aspirated and wells washed gently, twice, with 1 mL of DPBS. To stain the nuclei of the remaining cells 1 mL of DPBS containing 1 µg/mL of DAPI was added to the wells and incubated for 30

minutes. The cells were washed of excess DAPI by washing gently, twice, with 1 mL of DPBS.

The cells (nuclei) in each well were quantified using an ImageXpress Micro XLS Widefield High-Content Analysis System and MetaXpress software V5.3 (Molecular Devices, UK). A 10X objective was used to image six randomly chosen fields of view per well, combined with a DAPI filter set. Images were acquired using the DAPI channel with an exposure time of 185ms, auto focusing per well, laser offset of -3.16uM, and targeting a maximum intensity of 30000 units. The six images of each adjacent field of view were stitched together using the imaging software to produce a single composite image per well. The individual cells (nuclei) per image were identified and quantified per well using a custom built module created using the MetaXpress® Custom Module Editor. The custom module was designed to segment using the "Find Round Objects" module using a minimum width of 10uM, a maximum width of 30uM, and an intensity above local background of 1000. This enabled the identification and counting of the canine gingival cell nuclei but not include any remaining trichomonad cells present. Cell counts per well were recorded and exported to excel files for data analysis.

Statistical comparisons of sample means were computed in Prism (GraphPad Prism software, USA). Each time point mean value for canine gingival cell only wells were compared to co-culture wells using a repeated measure two-way ANOVA analysis and Sidak's multiple comparison test. *P* values of 0.05 or less were considered significant.

Results and Discussions

CHAPTER 3: IDENTIFICATION OF *TRICHOMONAS* AND *ENTAMOEB*A IN CANINE PLAQUE AND THEIR ASSOCIATION WITH PERIODONTAL DISEASE

Introduction

Oral disorders are important causes of concern in dog health and, of these, periodontal (gum) disease is the most common (Kyllar and Witter, 2005). Periodontal disease results from localised inflammatory responses in the oral periodontium (soft tissues around the tooth root) upon exposure to plaque. Plaque is composed primarily of bacterial communities; but, evidence from the human field suggests that protist organisms, such as *Entamoeba gingivalis* and *Trichomonas tenax*, are also present and are more prevalent in people with periodontal disease (Athari et al., 2007, Dao et al., 1983, Decarneri and Giannone, 1964, Dudko and Kurnatowska, 2007, Linke et al., 1989, Kurnatowska et al., 2004). At present it is unclear what role they play, if any, in the aetiology of periodontal disease or do they have no effect and opportunistically take advantage of the reduced health state of the mouth and consequent enhanced nutrient availability. Are they a cause of periodontal disease or just the effect? In canine periodontal disease a considerable amount of research has been undertaken towards the discovery of the bacterial species interactions associated with oral health and disease (Davis et al., 2013, Dewhirst et al., 2012, Holcombe et al., 2014) however, many other microorganisms may be involved in this complex pathogenesis.

Protozoa infections can be important and in some cases the resultant illness may be fatal without effective treatment. Illnesses such as amoebic dysentery and malaria, are caused by *Entamoeba histolytica* and *Plasmodium falciparum* respectively, and causes hundreds of thousands deaths each year (Collaborators, 2015). The clinical indicators presented with protozoan, bacterial and viral infections can be very similar and therefore can lead to difficulty in diagnosing the cause of illness. The timely identification of the infectious agent is helpful for the application of a targeted and effective treatment regime. Classic diagnostic methods to identify protozoan infections rely on species specific modes of identification which employ time and labour intensive microscopy protocols (CDC_protocol, 2013, Bogoch et al., 2006, Gonzalez-Ruiz et al., 1994, Utzinger et al., 2010) or use costly antigen

detection systems (Badaro et al., 1986, Davison et al., 1999, Kehl et al., 1995, Moody, 2002, Ota-Sullivan and Blecker-Shelly, 2013, Singh et al., 2009, Zimmerman and Needham, 1995). More recently, molecular based methods of detection have been developed that have proven to be highly sensitive but are inclined to be species specific in their detection (Becker et al., 2004, Bharti et al., 2007, Birkenheuer et al., 2003, Huston et al., 1999, Madico et al., 1998, Qvarnstrom et al., 2006, Verweij, 2014, Verweij and Stensvold, 2014) or require multiplex PCR techniques to identify a limited group of organisms within samples (Bruijnesteijn van Coppenraet et al., 2009, Maas et al., 2014, Orlandi and Lampel, 2000, Verweij et al., 2004). Broad spectrum ‘universal’ primers that may enable protozoan identification via amplification and sequencing of the eukaryotic 18S gene, are available; but they either also amplify non-protozoan eukaryotic sequences within samples (Hadziavdic et al., 2014, Machida and Knowlton, 2012, Valster et al., 2009) or are designed and validated to amplify from limited groups of protozoa, for example, ciliates only (Shin et al., 2004, Leng et al., 2011, Ishaq and Wright, 2014). In clinical or research situations where the presence of multiple organisms is the norm, for example the mouth, skin or intestines, a fast and efficient technique, capable of identifying a broad spectrum of protozoa in a single test is desirable. There are currently no published sets of primers that are designed to target or validated to amplify DNA from a broad range of protozoan organisms.

The objectives of this chapter is to develop molecular protocols, based on PCR and next generation sequencing, that enable the rapid, multiplexed identification of protozoa in multi-species clinical samples. The developed tools will then be used to identify the protozoa that may be present in the canine mouth and analyse any associations they may have with canine periodontal disease.

Results and discussion

3.1. Development of an 18S rRNA gene PCR targeting protist organisms.

18S rRNA gene DNA sequences from environmental protozoa and protozoa known to inhabit or cause diseases in animals were chosen to develop a set of 18S PCR primers. The eukaryotic 18S rDNA gene sequence consists of 9 variable regions interspersed with conserved sequence (Van de Peer and De Wachter, 1997). These variable regions contain sequence substitutions and/or sequence insertions/deletions that vary by organism (Van de Peer and De Wachter, 1997). Forty seven 18S rRNA gene sequences (>1000 base pairs in length, Table 1) obtained from the NCBI Genbank database (Benson et al., 2015) were aligned to each other, and a consensus sequence was determined. From this consensus, regions of homology were manually chosen that would be suitable for PCR primer design, regions that contain both variable and non-variable sequence. The degenerate PCR primer sequences identified through the sequence alignment process are shown in Table 10. The primers enable the amplification of an approximately 900 to 1500bp amplicon (depending on the organism) of the eukaryotic 18S rRNA gene containing variable regions 4 to 8 (Van de Peer and De Wachter, 1997). These 18S primer sequences were selected because they were predicted to give the longest amplification product from all sequences. The longest possible region of the gene was selected for amplification as this would reduce the chance of false positive identifications from gene sequencing and also allow identification of the organisms based on their PCR product size.

Table 10. Universal PCR primers designed in this study to amplify variable regions 4 to 8 of the 18S rRNA gene of protozoa.

Primer	Position ^a	Orientation	Sequence (5' - 3')
NP_fwd	570-590	Forward	tgccagcagcYgcggtaatc
NP_rev	1633-1653	Reverse	gtgtaNcaaagggcagggacgt

^a Position relative to *S. cerevisiae* SSU rRNA sequence (Van de Peer and De Wachter, 1997)

3.2. Specificity of 18S rRNA gene universal PCR

Genomic DNA samples extracted from cultures listed in Table 2 were used to amplify 18S rRNA genes from across the protozoan classification groups (Adl et al., 2005, Adl et al., 2012). Successful amplification of 18S rRNA PCR products from these protozoan DNA, with the exception of *G. intestinalis*, was achieved (Figure 1, lanes 1 to 12). Figure 1 shows the amplicons produced by each tested organism, and the size of PCR product, approximated by comparison with the accompanying molecular marker lanes. A summary of the amplicon sizes are detailed in Table 2. For those PCRs that produced more than 1 band, the brightest PCR product between 900 and 1500 base pairs was used for size comparison. These PCR results show that the specific size of the 18S rRNA products varied according to the genus being tested (Van de Peer and De Wachter, 1997). These PCR amplicon size differences result from sequence differences in their respective rRNA 18S genes. One of the tested protozoa, *G. intestinalis*, failed to produce a visible PCR product in testing (Figure 1, lane 8). *In silico* analysis of the *G. intestinalis* 18S rRNA gene suggests that the PCR primers developed here should enable the amplification of a *Giardia* specific PCR product. Consequently, it is not clear why a *Giardia* amplicon is not produced. One possibility is that the 18S gene sequence of the *Giardia* isolate tested does not match the sequence used for the alignment. The PCR primers developed here were designed with clinical and research samples in mind.

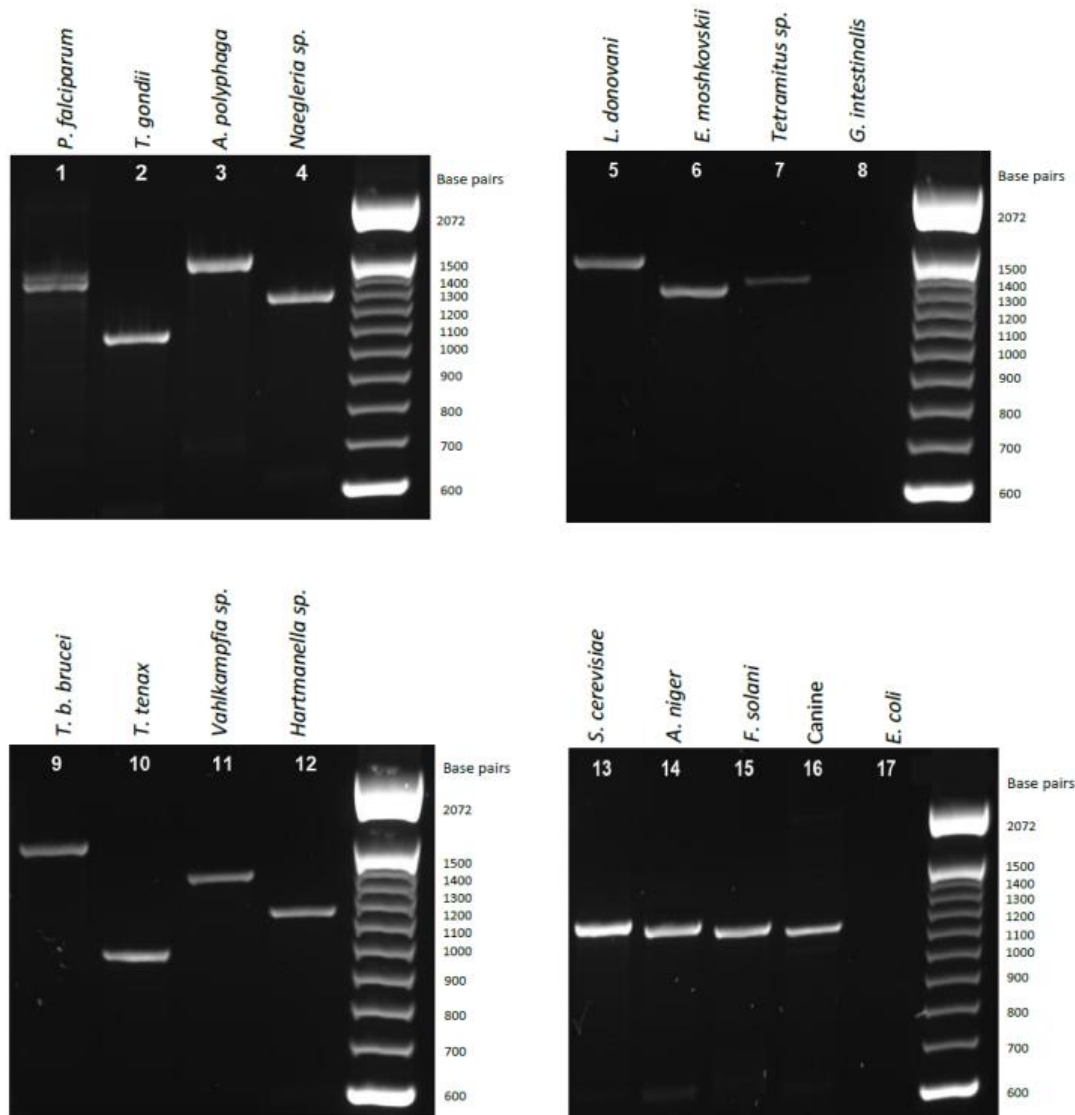


Figure 1. Gel electrophoresis of 18S rRNA PCR amplicons formed from representative protozoa and other tested organisms. Each protozoan tested produced a specific sized rDNA 18S gene amplicon (Lanes 1-12) and sized using the accompanying molecular markers. Non-protozoan samples tested all produced the same sized, 1100bp, amplicon (Lanes 13-16).

(Lane 1 *Plasmodium falciparum*, Lane 2 *Toxoplasma gondii*, Lane 3 *Acanthamoeba polyphaga*, Lane 4 *Naegleria sp.*, Lane 5 *Leishmania donovani*, Lane 6 *Entamoeba moshkovskii*, Lane 7 *Tetramitus sp.*, Lane 8 *Giardia intestinalis*, Lane 9 *Trypanosoma b. brucei*, Lane 10 *Trichomonas tenax*, Lane 11 *Vahlkampfia sp.*, Lane 12 *Hartmannella sp.*, Lane 13 *Saccharomyces cerevisiae*, Lane 14 *Aspergillus niger*, Lane 15 *Fusarium solani*, Lane 16 Canine gDNA, Lane 20 *Escherichia coli*. Molecular marker lanes are 100bp ladder (Invitrogen, UK). rRNA 18S gene PCR products for each organism were sized and recorded in Table 2.

Clinical samples may contain a complex community of microorganisms that comprise not only protozoa, but also bacterial, yeast, fungal, and higher eukaryotic DNA (Jakubovics and Palmer Jr., 2013). Non-target molecules could interfere with the identification of protozoa within the sample if they are co-amplified. The PCR did not amplify any bacterial DNA from a group of Gram positive and Gram negative species tested. Figure 2 displays the amplicons produced for PCRs carried out on representative Gram negative and Gram positive bacterial genomic DNA samples (undiluted and 1:10 dilutions) with the 18S rRNA gene primers. The results confirm that no bacterial ribosomal 18S or other non-targeted genomic bacterial PCR products were formed using the primers tested (Figure 2, lanes 1-4 and 6-9). A 1:10 dilution of each bacterial template was performed to confirm that PCR inhibitors were not present in the undiluted genomic DNA samples (data not shown). In addition, a 16S PCR amplification (Dewhirst et al., 2012) using universal 16S PCR primers was performed to confirm the presence of viable DNA in the samples (see [section 2.1.3](#)). Each sample produced a strong 16S PCR product (data not shown) confirming the presence of amplifiable bacterial DNA.

Mammalian and fungal genomic DNA are also likely to be present in many clinical or research samples. The aim of the project was to develop a primer set that would amplify only from protozoa 18S targets and not from other non-target sequences such as mammalian or fungal DNA. This objective, however, was found not to be possible. The chosen primer set was found to generate an 1100bp amplicon from yeast, fungal and mammalian (canine) DNA (Figure 1, lanes 13 to 16). However, all these non-protozoan organisms gave rise to the same sized PCR product (approximately 1100bp) allowing them to be distinguished from the vast majority of protozoa tested in these experiments. Two of the protozoa tested did, however, produce PCR products that were of similar size (*T. gondii* – 1050bp, and *Hartmannella* sp. – 1150bp) to the higher eukaryotic amplicon (Table 2). This makes identification of these organisms still possible, but more difficult in a mixed population sample based on PCR product size alone. The use of longer electrophoresis times or high resolution gels could help to alleviate this problem. If this did not allow clear identification then further amplicon cloning and sequencing could be employed for a definitive answer. The 18S rRNA PCR amplicon size formed from each organism tested is listed in Table 2.

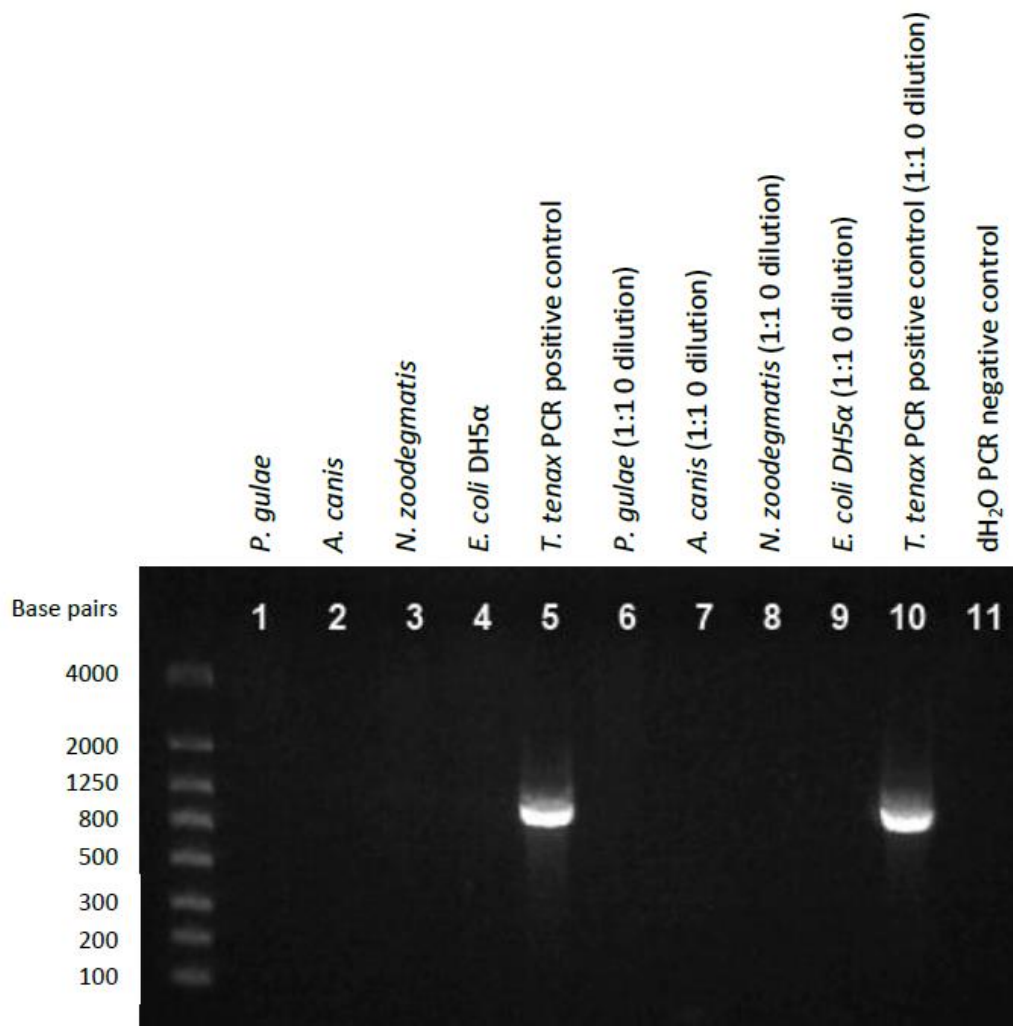


Figure 2. Protozoan 18S rRNA gene PCR with a range of canine oral bacterial isolates. No bacterial DNA was amplified using the described PCR protocol (section 2.1.2). None of the bacterial DNA samples tested resulted in a PCR product, confirming that the protozoan 18S PCR primers do not amplify bacterial genomic DNA. Lane's 1-5 neat DNA templates, Lane's 6-10 1 in 10 dilution DNA templates. (Lane 1 *Porphyromonas gulae*, Lane 2 *Actinomyces canis*, Lane 3 *Neisseria zoodegmatidis*, Lane 4 *Escherichia coli* DH5α, Lane 5 *Trichomonas tenax* PCR positive control, Lane 6 *Porphyromonas gulae*, Lane 7 *Actinomyces canis*, Lane 8 *Neisseria zoodegmatidis*, Lane 9 *Escherichia coli* DH5α, Lane 10 *Trichomonas tenax* PCR positive control, Lane 11 dH₂O PCR negative control. Marker is 100 bp to 4Kb Lonza FlashGel ladder).

3.3. Detection limits of the 18S rRNA gene PCR

The genomic PCR limits of detection for each of the protozoan DNA samples tested are summarised in Table 11. Each genomic DNA dilution was subjected to the 18S rRNA PCR amplification and the products formed were separated and analysed by gel electrophoresis. A visible PCR product of expected size was considered a positive result for the dilution. The PCR was seen to be highly sensitive with detection limits as low as 3.2 picograms of protozoan DNA. All organisms were detected at 10 ng of DNA per PCR reaction with the lowest level of detection found with *A. polyphaga*, for which there was a visible PCR product when using 3.2 picograms of genomic DNA template per PCR (Table 11).

These genomic DNA detection values do not take into consideration differences in gene copy number or differences in extraction efficiencies that may exist between different organisms. Therefore the performance of the primers under ‘real world’ conditions was assessed using DNA extracted from known numbers of target organisms. The cellular limit of detection for each of the protozoa tested is detailed in Table 12. Genomic DNA was diluted to 200, 20, 2 and 0.2 protozoan cell equivalents per PCR reaction and subjected to the PCR amplification. The products formed were separated and analysed via gel electrophoresis. A visible PCR product was considered a positive detection result for the dilution. All organisms were detected at 200 cells per PCR reaction and *T. tenax* and *E. invadens* were also detectable at 20 cells per PCR reaction. No organisms were detected at the lower levels tested: 2 and 0.2 cells per PCR reaction.

To assess the use of the primers on a mixed population of protozoa, a selection of laboratory cultivable organisms (see [section 2.1.14](#)) was pooled in equal proportions and then diluted to 200, 100, 50, 25, 12.5, and 6.25 cells per organism per reaction and subjected to PCR (Figure 3). PCR products were observed for each sample apart from the 6.25 cells per PCR reaction (Figure 3, lane 6). Multiple PCR products are observed from the reactions with 200, 100, 50, and 25 cells (Figure 3, Lanes 1 to 4), whereas only two or possibly three products are seen in reactions with 12.5 cells (Figure 3, Lane 5). The PCR products formed were approximately 950, 1150, 1250, and 1500 base pairs in size, equating to the amplicons produced by each organism present in the sample (Table 2). At the higher cell concentrations, 200, 100, and 50 cells per organism per PCR, all organisms present were detected, as assessed by the PCR amplicons formed (Figure 3, lanes 1-3).

Table 11. PCR limit of detection values for protozoan genomic DNA templates using 18S rRNA primers. The limit of detection data for each organism tested is stated in nanograms of total DNA per PCR.

Genomic DNA sample	Limit of detection (nanograms of total DNA per PCR)
<i>Plasmodium falciparum</i> (isolate 3D7)	0.016
<i>Leishmania donovani</i> (MHOM/IN/80/DD8)	10
<i>Trypanosoma b. brucei</i> (strain 427)	10
<i>Toxoplasma gondii</i> (ATCC 50174D)	10
<i>Hartmannella</i> sp.(environmental isolate)	0.4
<i>Acanthamoeba polyphaga</i> (CCAP 1501/3G)	0.0032
<i>Giardia intestinalis</i> (ATCC 50581)	ND
<i>Entamoeba moshkovskii</i> (Laredo strain)	0.08
<i>Entamoeba invadens</i> (IP-1)	0.016
<i>Trichomonas tenax</i> (ATCC 30207)	0.08
<i>Vahlkampfia</i> spp. (environmental isolate)	2
<i>Tetramitus</i> spp. (environmental isolate)	2
<i>Naegleria</i> spp. (environmental isolate)	0.4

Table 12. The cellular limit of detection values for protozoa tested using the 18S rRNA protozoan PCR. Each detection value represents the lowest tested number of cells with which a visible PCR product was formed in the PCR.

Organism	Cellular limit of detection (numbers of protozoan cells per PCR)
<i>Acanthamoeba polyphaga</i> (CCAP 1501/3G)	200
<i>Entamoeba invadens</i> (IP-1)	20
<i>Trichomonas tenax</i> (ATCC 30207)	20
<i>Hartmannella</i> spp.(environmental isolate)	200
<i>Vahlkampfia</i> spp. (environmental isolate)	200
<i>Tetramitus</i> spp. (environmental isolate)	200
<i>Naegleria</i> spp. (environmental isolate)	200

However at 25 and 12.5 cells per organism per PCR, fewer products are observed, due to the higher cellular limits of detection of *Hartmannella* sp., and *Acanthamoeba polyphaga* (Table 12). At these lower concentrations only the *Trichomonas* sp. (approx. 950bp) and *Entamoeba* sp. (approx. 1250bp), amplicons

are clearly visible as these two species are detectable at the lower cell concentrations (Figure 3, lanes 4 and 5). These results again confirm that multiple species are detectable in the same sample, different cellular limits of detection between the organisms are evident, perhaps equating to differing 18S rRNA gene copy numbers for each organism or differing DNA extraction efficiencies of each.

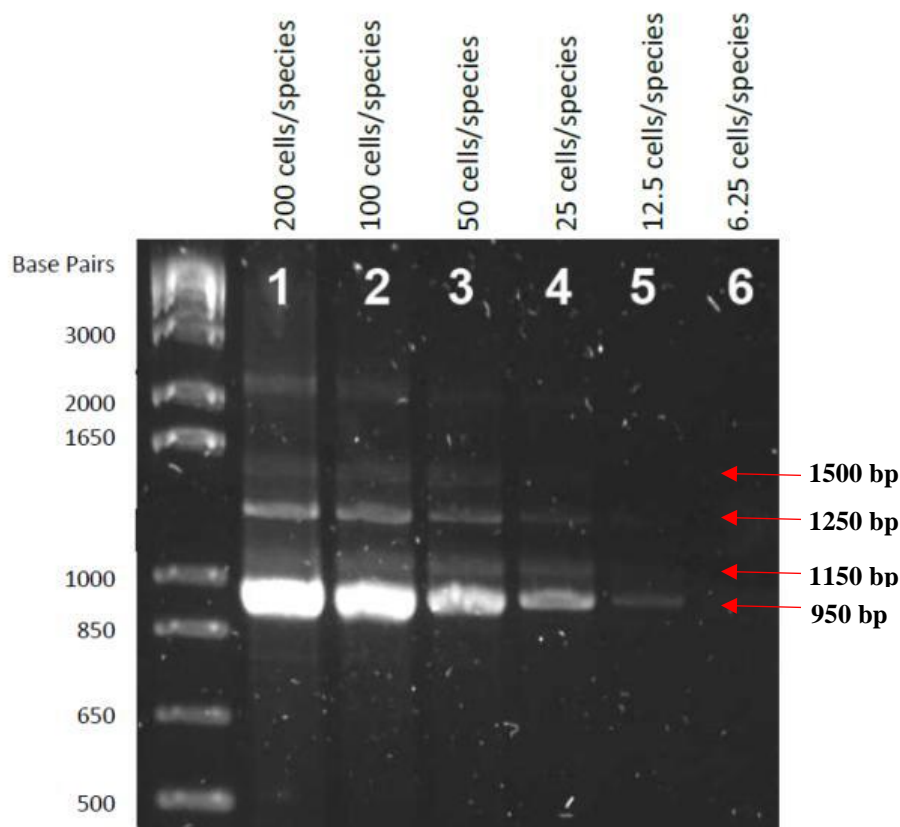


Figure 3. Gel electrophoresis of PCR products amplified from mixed DNA template pools (*Hartmannella* sp. 1150 bp, *Acanthamoeba polyphaga* (CCAP 1501/3G) 1500 bp, *Entamoeba invadens* (Rodhain IP-1: ATCC 30994) 1250 bp, *Trichomonas tenax* (ATCC 30207) 950 bp). Lane 1: 200, Lane 2: 100, Lane 3: 50, Lane 4: 25, Lane 5: 12.5, Lane 6: 6.25 cells per organism per PCR reaction. Lane marker is 1Kb+ ladder (Invitrogen, UK).

To conclude, a successful, targeted and sensitive PCR protocol to screen for the presence of protozoa has been developed. The methodology employs a single targeted PCR screening tool capable of identifying multiple genera of protozoa from genomic DNA samples, from as few as 20 protist cells per PCR. This single

PCR may be employed in clinical and research settings where the identity of protozoa present within samples is unclear or unknown. It also has the added benefit of more rapid detection and sensitivity in comparison to more traditional methods such as antigen detection or microscopy (CDC_protocol, 2013, Bogoch et al., 2006, Singh et al., 2009). The procedure provides a viable alternative to current microscopy or antigen based techniques which rely on single species methods of identification for protozoa and use slow, expensive and technically challenging methodologies. It also delivers a more targeted molecular method of identification of protozoan species, in contrast to the broad spectrum eukaryotic primers or ciliate only primers which are currently published (Bharti et al., 2007, Bruijnesteijn van Coppenraet et al., 2009, Maas et al., 2014, Verweij et al., 2004, Verweij and Stensvold, 2014).

3.4. 18S duplex PCR for the additional detection of *Giardia* spp.

The 18S PCR, described in sections [2.1.2](#) and [3.1](#), has been shown to exhibit broad spectrum amplification of the 18S gene DNA from protozoa representing all the protozoan classification groups (except the Fornicata group, e.g. *G. intestinalis*). Although *in silico*, the PCR is predicted to amplify DNA from organisms representing the classification group Fornicata ([section 2.1.1](#)), it is evident that an amplicon was not produced from *G. intestinalis* (Figure 1, lane 8). *Giardia* spp. are anaerobic flagellates that are present and parasitise the intestinal tract of a variety of mammals, birds and reptiles (Ortega and Adam, 1997). In humans, infective giardiasis results in an assortment of unpleasant and debilitating gastrointestinal symptoms; therefore the early detection of *Giardia* spp. infection is paramount for an effective treatment regime. As the 18S PCR developed in this thesis, is directed at identifying prominent protists species within clinical samples, the lack of *Giardia* spp. detection and other members of the Fornicata family is a noteworthy deficiency of the protocol.

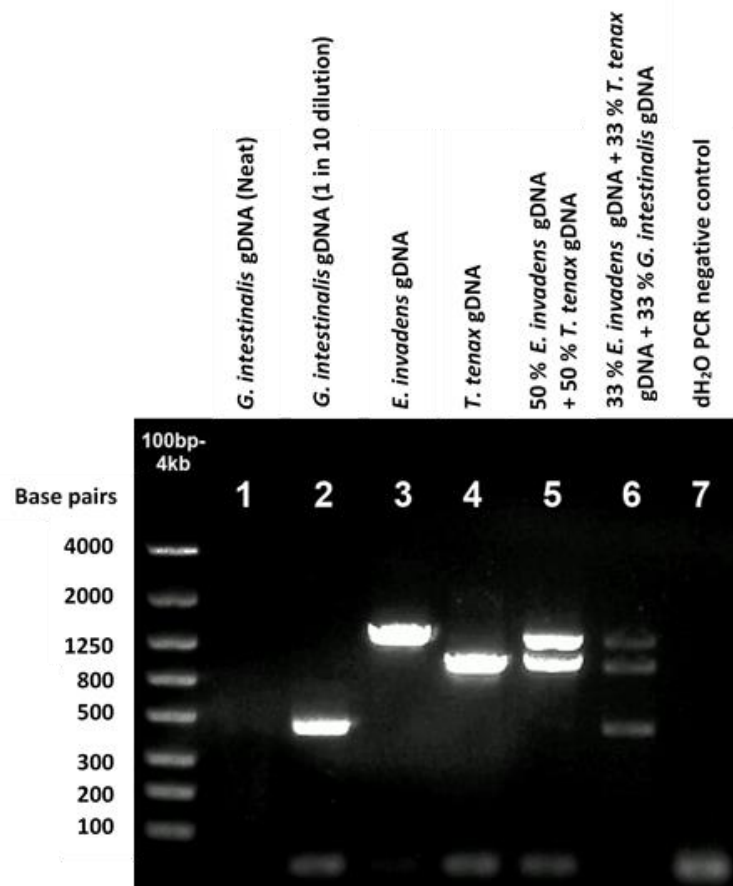


Figure 4. Gel electrophoresis of PCR products amplified using an 18S-*Giardia* duplex PCR protocol ([section 2.1.4](#)) designed to amplify a broad range of protozoa including *G. intestinalis*. The PCR was tested against genomic DNA samples to assess the effectiveness of the protocol. Lanes 1 and 2, *G. intestinalis*, Lane 3 *E. invadens*, and Lane 4 *T. tenax*. Pool of all three organism DNA (1μL each) were also tested (Lane 5: neat sample, Lane 6: 1 in 10 dilution). Lane marker is 100bp to 4Kb+ ladder (Lonza, UK).

To alleviate this problem, in samples where *Giardia* spp. presence is suspected (in addition to other protozoa), a duplex PCR was established which utilises the broad spectrum detection of protozoa using the 18S PCR developed in [section 2.1.2](#), and also adds *Giardia* spp. specific detection. The 18S primers were paired in a duplex PCR with a previously published primer set (Babaei et al., 2011, Read et al., 2004) (see [section 2.1.4](#) for primer sequence) which enables the detection of *Giardia* spp. This duplex PCR protocol was tested against genomic DNA samples obtained from *G. intestinalis*, *T. tenax* and *E. invadens*. The PCR enables the amplification of a

458 base pair amplicon from *Giardia* (Figure 4, lanes 2 and 6) and also the expected sized amplicons from the other protozoal species, *T. tenax* and *E. invadens* (Figure 4, lanes 3, 4, 5 and 6). No other non-specific amplicons were observed. This duplex 18S-*giardia gdh* PCR, in parallel to the 18S-only PCR, exhibits excellent detection levels. Figures 5 and 6 reveal the genomic and cellular detection levels exhibited by the PCR protocol. The expected 458 base pair *Giardia* PCR product is detectable from as little as 200 *Giardia* cells (Figure 5 , lane 1) and 0.4 ng of genomic DNA (Figure 6, lane 3). Both values are within the detection range observed with other protozoal species tested and detected by the standalone 18S PCR, described in [section 2.1.2.](#)

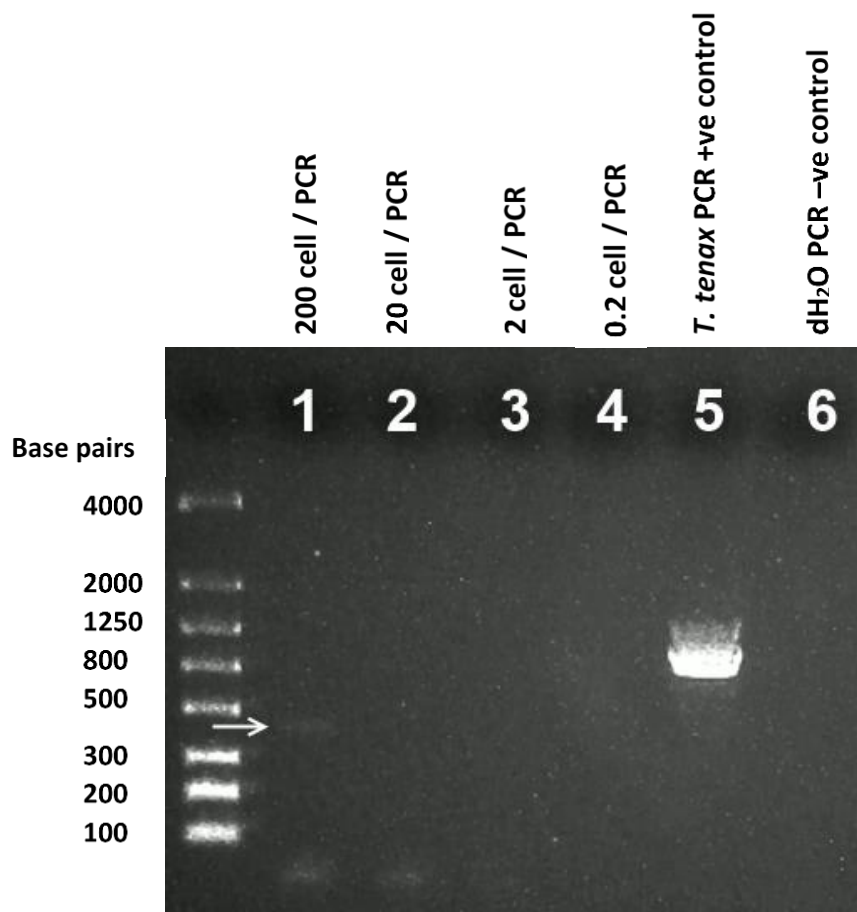


Figure 5. Gel electrophoresis of PCR products amplified from *G. intestinalis* DNA. *G. intestinalis* is shown to be detectable from as least 200 cell per PCR. A 458 bp amplicon is indicated with a white arrow. DNA in each PCR was to Lane 1: 200, Lane 2: 20, Lane 3: 2, and Lane 4: 0.2, *Giardia* cells per PCR reaction. Lane 5, *T. tenax* PCR positive control. Lane 6: dH₂O PCR negative control. Lane marker is 100bp-Kb ladder (Lonza, UK).

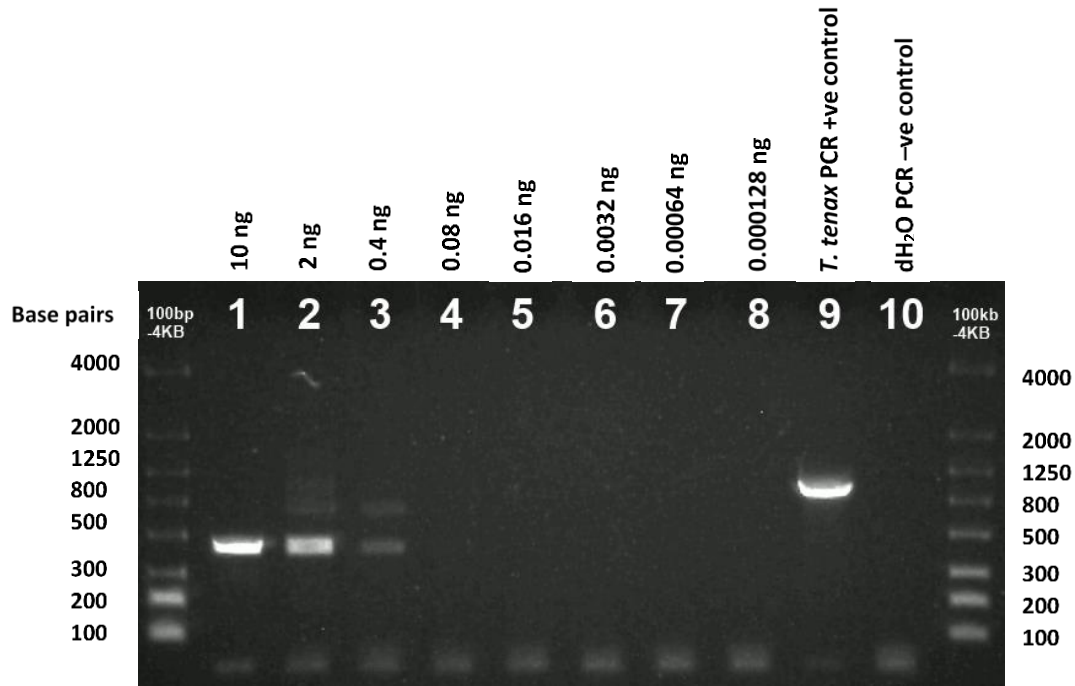


Figure 6. Gel electrophoresis of PCR products amplified from *G. intestinalis* genomic DNA. *G. intestinalis* is detectable from at least 0.4 ng of genomic DNA (Lane 3). DNA of each PCR was, Lane 1: 10, Lane 2: 2, Lane 3: 0.4, Lane 4: 0.08, Lane 5: 0.016, Lane 6: 0.0032, Lane 7: 0.00064 and Lane 8 0.000128 ng of *G. intestinalis* genomic DNA per PCR. Lane 9: *T. tenax* PCR positive control. Lane 10: dH₂O PCR negative control. Lane marker is 100bp-4Kb ladder (Lonza, UK).

To test if the values seen with the standalone 18S PCR are significantly affected by the addition of the *Giardia* specific primers, the cellular detection limits and genomic DNA detection limits for both *T. tenax* and *E. invadens* were tested with the full 18S-*Giardia gdh* duplex PCR protocol (Figure 7 and 8). Both the cellular limits of detection and genomic limits of detection, were seen to be exactly the same or highly similar to the 18S standalone PCR. The cellular limits of detection for *T. tenax* and *E. invadens* with the duplex PCR, were both 20 protozoan cell equivalents per PCR reaction (Figure 7 lanes 2 and 6), exactly the same as seen with the standalone 18S PCR protocol (Table 12). The DNA limits of detection for *T. tenax* and *E. invadens* with the duplex PCR, were calculated as 0.08 ng and 0.4 ng of genomic DNA per PCR (Figure 8A, lane 4 and Figure 8B, lane 12), respectively. The *T. tenax* detection value is exactly what we see with the standalone 18S PCR

however, the *E. invadens* detection value is a little different, 0.4 ng as opposed to the 0.016 ng seen previously (Table 12).

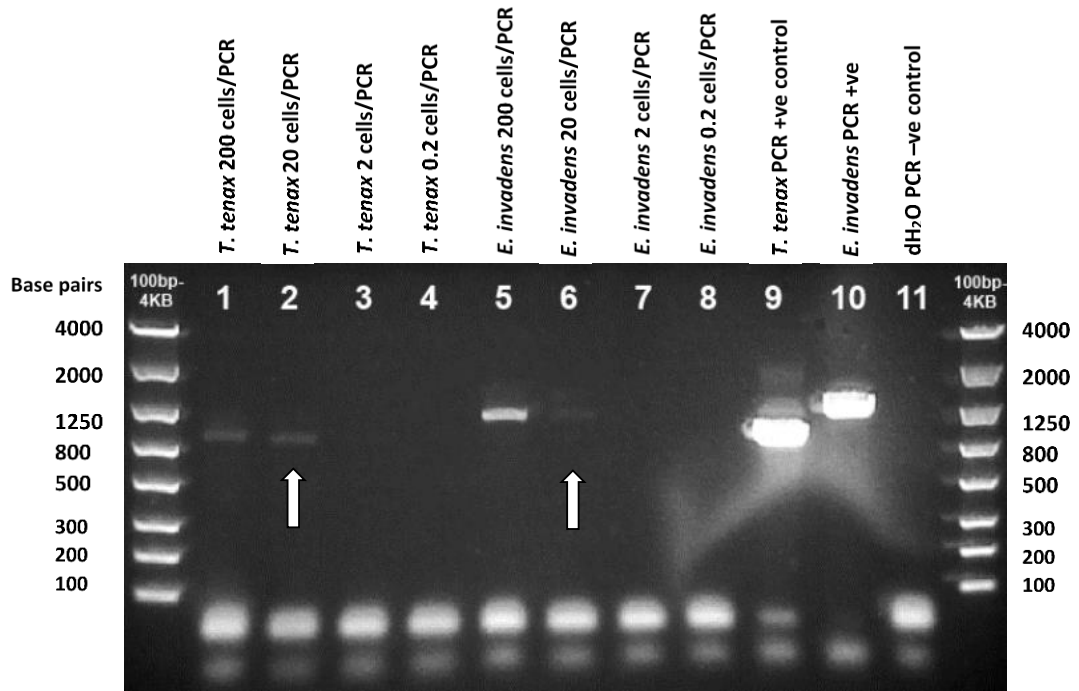


Figure 7. Gel electrophoresis of PCR products amplified using the 18S-*Giardia* *gdh* duplex PCR protocol ([section 2.1.4](#)) and *T. tenax* and *E. invadens* gDNA. PCRs were carried out on cell extracts of known numbers of between 200 to 0.2 cells per PCR reaction. Both *T. tenax* and *E. invadens* are detectable at 20 cells per PCR reaction (indicated by white arrows). Lane 1 & 5: 200 cells, Lane 2 & 6: 20 cells, Lane 3 & 7: 2 cells, Lane 4 & 8: 0.2 cell equivalents per PCR. Lane 9: *T. tenax* PCR positive control. Lane 10: *E. invadens* PCR positive control. Lane 11: dH₂O PCR negative control. Lane marker is 100bp-4Kb ladder (Lonza, UK).

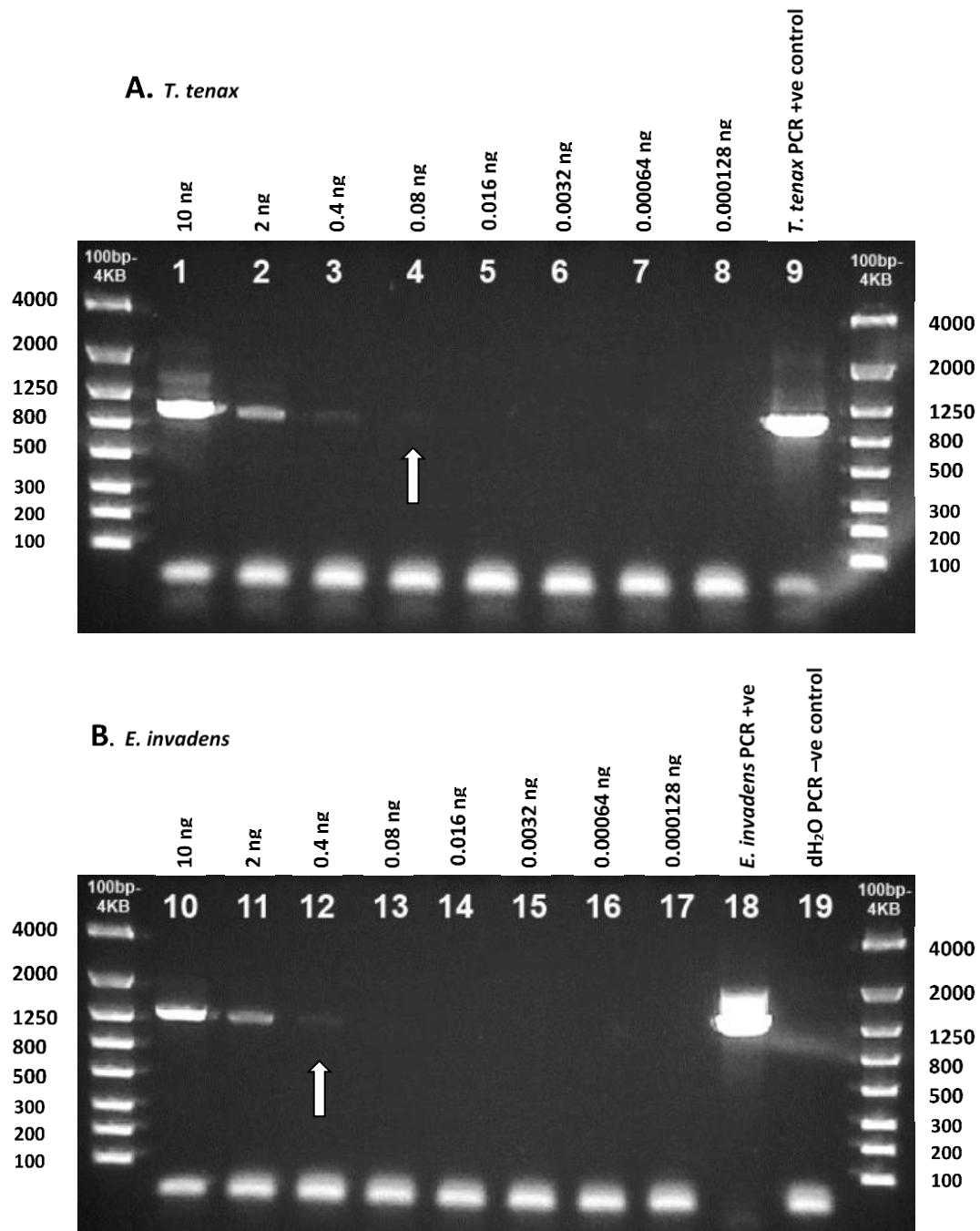


Figure 8. Gel electrophoresis of PCR products amplified using the 18S-*Giardia* *gdh* duplex PCR protocol and (A) *T. tenax* and (B) *E. invadens* gDNA. PCRs were carried out on genomic DNA dilutions from 10 to 0.000128 ng of DNA per PCR reaction. *T. tenax* was detected at 0.08 ng per PCR and *E. invadens* was detectable at 0.4 ng of DNA per PCR reaction (indicated by white arrows). Lanes 1-8 and 10-17: genomic DNA dilutions between 10 ng to 0.00128 ng per PCR. Lane 9: *T. tenax* PCR positive control. Lane 18: *E. invadens* PCR positive control. Lane 19: dH₂O PCR negative control. Lane marker is 100bp-4Kb ladder (Lonza, UK).

The above results conclude that the 18S-*Giardia gdh* PCR is proficient at the detection of *Giardia* spp. and other target protozoan species under laboratory conditions. This was tested using purified laboratory cell and genomic DNA samples. As stated previously, these PCR protocols were designed for use with clinical, as well as, research samples. Clinical samples tend to be a more challenging sample type as they may contain a plethora of contaminating agents that may inhibit or disrupt the detection mechanism (Schrader et al., 2012, Zhang et al., 2010). To evaluate if the developed duplex 18S-*Giardia gdh* PCR is suitable for the detection of protozoa in clinical samples, the duplex PCR was tested with both canine faecal DNA (Figure 9) and canine dental plaque DNA (Figure 10). To assess clinical faecal samples, a protozoan negative faecal sample (tested previously with the same PCR) was used as a sample base matrix, in which, three different protists were “spiked” (see section [2.1.17](#) for detailed methods) at two-times their cellular limit of detection. From these spiked faecal samples we found that all organism were detected successfully using the duplex PCR. A PCR product of expected size was seen for samples spiked with *G. intestinalis* (Figure 9, lane 1), *T. tenax* (Figure 9, lane 2), and *E. invadens* (Figure 9, lane 3). When all three organisms were spiked together in the faeces matrix at two-times their limit of detection, we see all three are detected by the PCR (Figure 9, lane 4).

The second sample type tested with this PCR was canine oral dental plaque. It has been recently been reported that at least two protists are present in canine plaque (Patel et al., 2017). Eight canine plaque samples from a sample set previously utilised in this report (see [section 2.1.19](#)), were used to test the two PCR protocols for effectiveness with clinical sample DNA extractions. All eight samples were found to be protozoa positive with the standalone 18S PCR (Figure 10.A, lanes 1-8), and the same results were observed with the duplex 18S-*Giardia gdh* PCR protocol (Figure 10.B, lanes 1-8). Six of the samples produced an approximate 950 bp amplicon only (Figures 10.A and B, Lanes 1, 3, 4, 7 and 8), concluding the presence of *Trichomonas* sp. only in these samples. One sample produced an approximate 1250 bp amplicon only (Figures 10.A and B, Lane 2), concluding the presence of *Entamoeba* sp. only in this sample and one sample produced two amplicons, approximately 950 and 1250 bp in size (Figures 10.A and B, Lane 6), concluding the presence of both *Trichomonas* sp. and *Entamoeba* sp. this sample.

These “real world” experiments tested both the PCR protocols against clinical samples and showed that both the standalone and duplex PCR protocols are proficient at the accurate and sensitive detection of protozoal species in a variety of sample types.

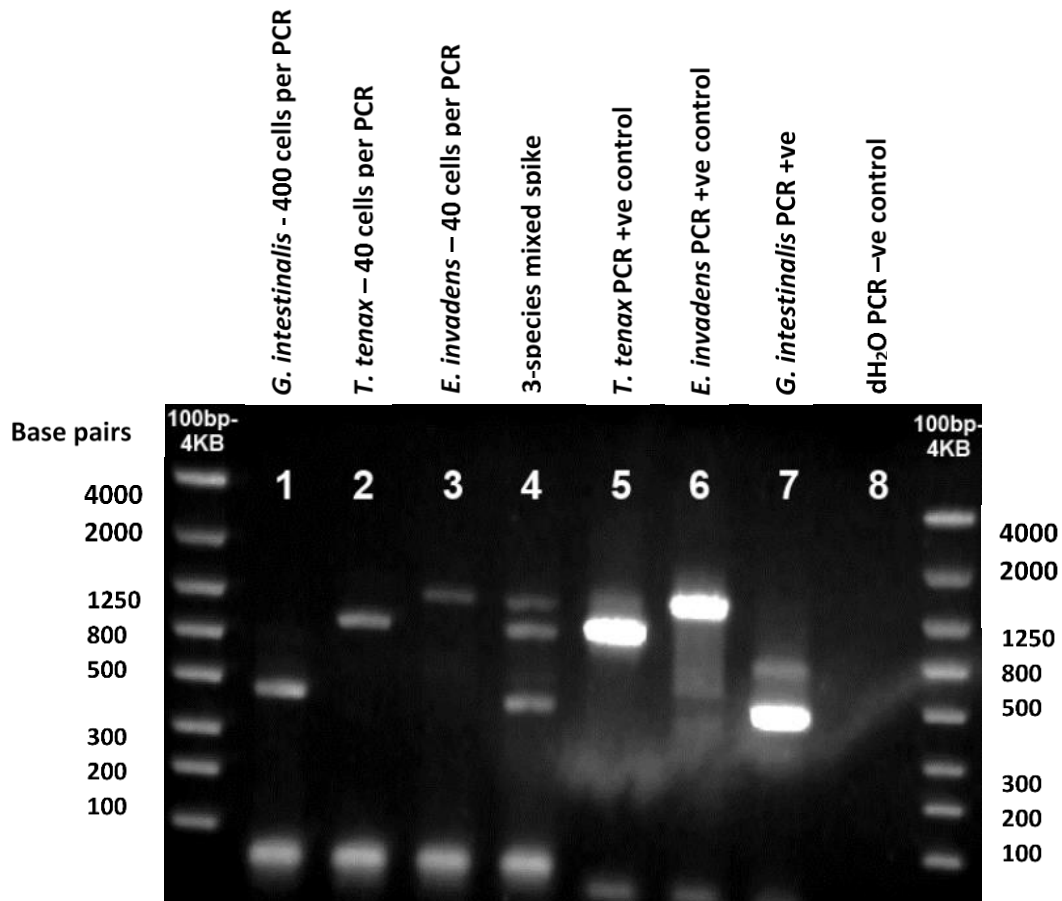


Figure 9. 18S-*Giardia* *gdh* PCR on protozoan “spiked” faecal samples. *G. intestinalis*, *T. tenax*, and *E. invadens* were inoculated individually or as a 3-species mix into PCR negative faecal material at two-times the limit of detection for PCR. Lane 1: *G. intestinalis* 400 cells, Lane 2: *T. tenax* 40 cells, Lane 3: *E. invadens* 40 cells, Lane 4: 3-species mix, Lane 5: *T. tenax* positive PCR control, Lane 6: *E. invadens* positive PCR control, Lane 7: *G. intestinalis* positive PCR control, Lane 8 dH₂O negative PCR control. Lane marker is 100bp-4Kb ladder (Lonza, UK).

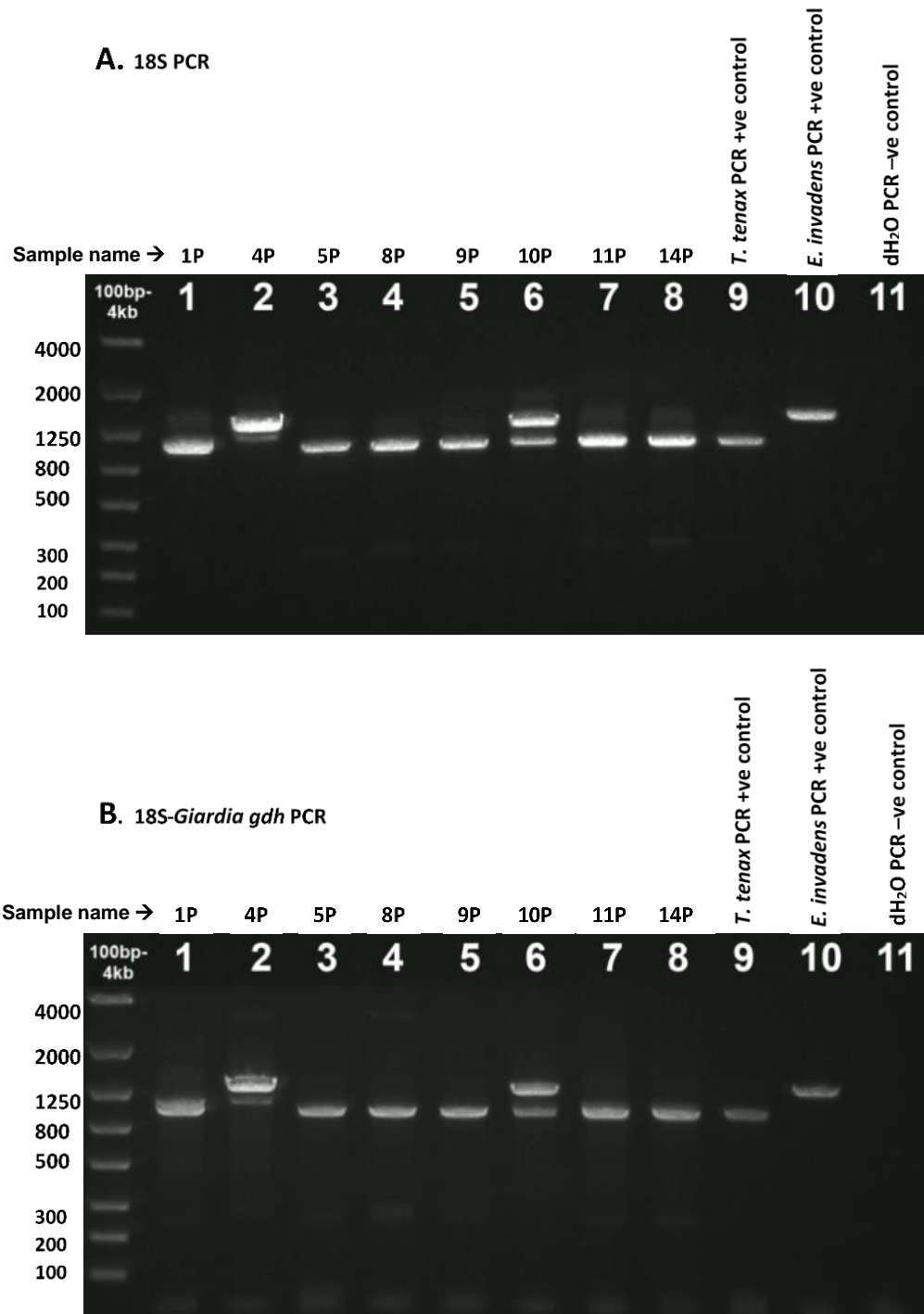


Figure 10. (A) 18S rRNA and (B) duplex 18S-*Giardia* *gdh* PCRs of canine plaque samples known to contain protozoal DNA. Both PCR protocols produce exactly the same sized amplicons, indicating no unintentional effects from the additional primers in the duplex 18S-*Giardia* *gdh* PCR (B). Figure A and B: Lanes 1-8: Canine plaque samples previously seen to be PCR positive for protozoa ([section 2.1.19](#)). Lane 9: *T. tenax* positive PCR control, Lane 10: *E. invadens* positive PCR control, Lane 11 dH₂O negative PCR control. Lane marker is 100bp-4Kb ladder (Lonza, UK).

There are a variety of diagnostic methods available to researchers and healthcare professionals that enable the identification of microorganisms in clinical samples (CDC_protocol, 2013, Bogoch et al., 2006, Singh et al., 2009, Bharti et al., 2007, Bruijnesteijn van Coppenraet et al., 2009, Maas et al., 2014, Verweij et al., 2004, Verweij and Stensvold, 2014), helping to provide information for effective treatment regimes. In veterinary practice, microscopy is widely utilised to identify protozoa from clinical samples from faecal samples. When individual animals or closely-housed animals are taken ill, faecal samples are taken and sent, usually, to independent commercial testing facilities for analysis. For protozoal identification, wet-mount microscopy and antigen detection are the “gold-standard” methods used (CDC_protocol, 2013). Transport of samples and waiting for the results can take up to a week, by which time the disease signs may become more acute or transfer to other animals. Therefore, the prompt and accurate identification of protozoa in clinical samples is paramount. We tested the duplex 18S-*giardia gdh* PCR protocol during a diarrheal outbreak at the WALTHAM Centre for Pet Nutrition, comparing the PCR method to the widely used commercial techniques of identification. At the WALTHAM centre for pet nutrition, dogs are housed in mixed, shared and open pens. It is not uncommon for diarrheal illness to emerge within an individual or small group of animals in the unit facilities and then spread rapidly to other animals with the same unit. In one situation, nine samples were collected from animals that were suffering from diarrhoea (see section [2.1.15](#)). The resident veterinarian suspected a giardial outbreak (personal oral communication) within the units and requested samples to be sent externally for bacterial and protozoal analysis. Samples collected over a 3-day period were sent for independent microbiological analysis using standard industry practises (IDEXX Laboratories, Inc, UK). In addition, a sample of each faeces was processed using the duplex 18S-*giardia gdh* PCR protocol (see [section 2.1.18](#)). IDEXX laboratories reported their results from each sample (Table 13). Through wet-mount microscopy and *Giardia* antigen detection, IDEXX laboratory identified 3 out of the 8 samples (37.5 %, Table 13, samples 1, 2 and 6) as positive for protozoa, more specifically, positive for *Giardia* spp.

Table 13. Faecal samples collected from animals exhibiting poor quality faeces. Each sample was tested for the presence of protozoa using standard industry practices by an independent laboratory and also using the 18S-*Giardia gdh* PCR developed here. The table summarises the microbes detected by each method used. The 18S-*Giardia gdh* PCR protocol exhibits increased detection sensitivity and enables the detection of multiple protozoa in a single step.

Sample date	Sample number	Animal name	IDEXX test result date	IDEXX test requested	Microscopy - faecal	<i>Salmonella</i> spp.	<i>Campylobacter</i> spp.	<i>Giardia</i> antigen test	18S- <i>giardia gdh</i> PCR detected protists
15/08/2016	1	Esther	22/08/2016	Faecal screen - Bacteria & Giardia	Not Detected	Not Detected	Not Detected	Positive	<i>Entamoeba</i> spp. & <i>Giardia</i> spp.
5/08/2016	1	Henry	22/08/2016	Faecal screen - Bacteria & Giardia	Not Detected	Not Detected	Not Detected	Positive	
11/08/2016	2	Willoughby	17/08/2016	Faecal screen - Bacteria & Giardia	Not Detected	Not Detected	Not Detected	Positive	<i>Entamoeba</i> spp. & <i>Giardia</i> spp.
11/08/2016	2	Ophelia	17/08/2016	Faecal screen - Bacteria & Giardia	Not Detected	Not Detected	Not Detected	Positive	
29/07/2016	3	Rodger	03/08/2016	BASIC FAECAL SCREEN	Not Detected	Not Detected	Positive	Not Tested	Negative
29/07/2016	3	Rabbit	03/08/2016	BASIC FAECAL SCREEN	Not Detected	Not Detected	Positive	Not Tested	
29/07/2016	3	Elsa	03/08/2016	BASIC FAECAL SCREEN	Not Detected	Not Detected	Positive	Not Tested	
10/08/2016	4	Opal	12/08/2016	Faecal screen - Bacteria & Giardia	Not Detected	Not Detected	Not Detected	Negative	Negative
10/08/2016	4	Ivy	12/08/2016	Faecal screen - Bacteria & Giardia	Not Detected	Not Detected	Not Detected	Negative	
10/08/2016	5	Diesel	09/08/2016	Faecal screen - Bacteria & Giardia	Not Detected	Not Detected	Not Detected	Negative	<i>Trichomonas</i> spp & <i>Giardia</i> spp.
14/08/2016	6	Roy	22/08/2016	Faecal screen - Bacteria & Giardia	Giardia Cysts Present	Not Detected	Positive	Negative	<i>Entamoeba</i> spp. & <i>Giardia</i> spp.
14/08/2016	6	Lois	22/08/2016	Faecal screen - Bacteria & Giardia	Giardia Cysts Present	Not Detected	Positive	Negative	
23/06/2016	7	Shelby	25/06/2016	BASIC FAECAL SCREEN	Not Detected	Not Detected	Not Detected	Not Tested	Negative
28/06/2016	8	Ophelia	17/08/2016	Faecal screen - Bacteria & Giardia	Not Detected	Not Detected	Not Detected	Negative	<i>Entamoeba</i> spp. & <i>Giardia</i> spp.
01/06/2009	9	Nancy	Faeces collected from animal with normal faecal score						Negative

In comparison, the 18S-*Giardia gdh* PCR protocol identified 5 out of the 8 samples sent (62.5 %, Table 13, samples 1, 2 5, 6, and 8) as protozoa positive. In addition to identifying more positive samples, the PCR protocol was also able to identify multiple species of protozoa in contrast to the commercial protocols. The *Giardia* spp. identified by IDEXX tests were confirmed by the PCR but in addition, *Entamoeba* spp. and *Trichomonas* spp. was also found to be present in the samples (Table 13, samples 1, 2 5, 6, and 8).

The additional detection of protozoal species by the 18S-*Giardia gdh* PCR display the sensitivity and accuracy of the method. In comparison to the commercial wet-mount microscopy and antigen detection method, the 18S-*giardia gdh* PCR protocol identified more positive samples and more protozoan species present in the samples. This exhibits a marked improvement in protozoa detection in clinical (faecal) samples and provides a more effective tool for researchers, clinicians and healthcare professionals.

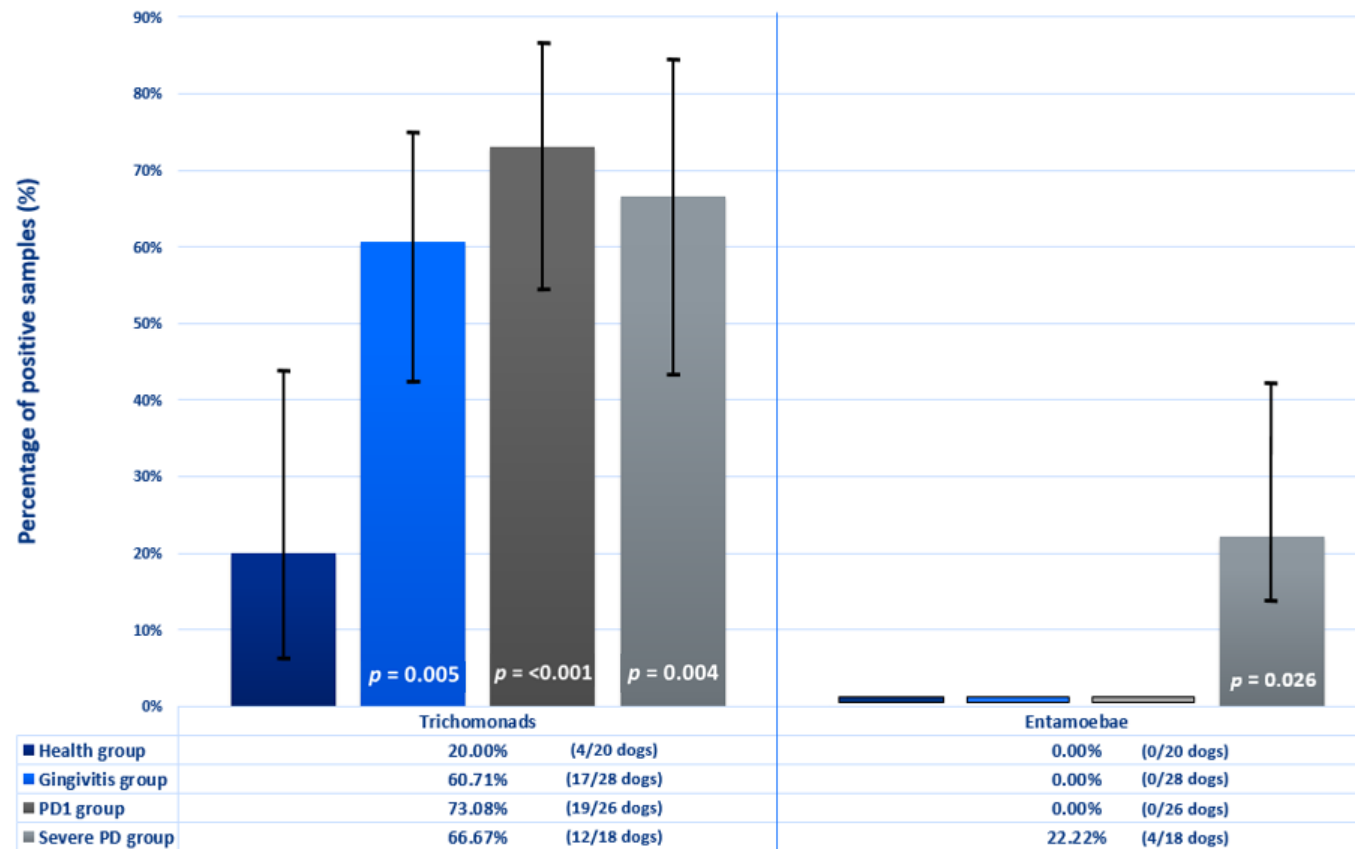
3.5. Detection of protozoa in canine plaque and their association to periodontal disease

In the human mouth, protists are commonly observed and there is a growing body of evidence indicating their association and potential contribution to periodontal disease (Athari et al., 2007, Decarneri and Giannone, 1964, Dudko and Kurnatowska, 2007, Linke et al., 1989, Marty et al., 2017a, Ribeiro et al., 2015). To investigate the presence of protists in canine dental plaque and to determine any associations with canine periodontal disease, the new, broad spectrum 18S PCR (see section [3.1-3.3](#)) was used to characterise the protist content of canine subgingival plaque. Based on the 18S PCR protocol, two distinct protists were identified as being present in a collection of canine plaque, consisting of 92 samples. An amplicon of approximately 950 bp was identified as representing *Trichomonas* sp. and was observed in 20% of healthy dogs, 61% of dogs with gingivitis, 73% of dogs with periodontal disease stage 1, and 67% of dogs with severe periodontal disease (Figure 11). *Entamoeba* sp. gave rise to an 18S PCR amplicon of approximately 1250 bp and this was identified in 22% of severe disease samples but was not seen in any of the other sample types (Figure 11). The overall prevalence of trichomonads and Entamoebae detected in the total sample

population was 56.52 % (52/92) and 4.34 % (4/92) respectively. To rule out false negative samples, in samples where no amplicon was seen, a 16S bacterial PCR was carried out to confirm the presence of amplifiable DNA in the sample. All negative samples produced a strong bacterial 16S PCR amplicon indicating the presence of amplifiable DNA in the samples (data not shown).

Two sample binomial tests for *Trichomonas* sp. showed statistically significant differences ($p < 0.025$) between the 'Health' and 'Gingivitis' groups ($p = 0.005$), the 'Health' and 'PD1' groups ($p < 0.001$) and the 'Health' and 'Severe Disease' groups ($p = 0.004$) (Figure 11 and Table 14). Entamoebae comparisons (Figure 11 and Table 14) were calculated for each 'Health' verses disease state group and showed a difference between the 'Health' group and the 'Severe Disease' group, but this was non-significant after Bonferroni adjustment ($p = 0.026$). No significant differences were found between any of the other groups and 'Health'.

Four DNA pools were created from these subgingival plaque DNA, one pool representing each health state ('Health', 'Gingivitis', 'PD1', and 'Severe disease'), see Table 5 for sample details. The four pooled plaque samples were processed and sequenced (see section [2.1.21](#)) using the Roche 454™ GS FLX+ sequencing platform. A total of 34207 reads were obtained for analysis after denoising and chimeric sequence removal. The number of reads per sample ranged from 7265 to 11574, with a median number of reads of 7941 bases across all four samples (Table 15). OTU sequence numbers identified by the Qiime pipeline as protozoan in origin, and their abundance within each sample type, are shown in Figure 12. Unassignable, non-relevant (i.e. canine, yeast or fungal) and ambiguous sequences were excluded.



p values of 0.025 or less were considered statistically significant. Pairwise statistical significance (white text) was calculated by comparing to the 'Health' group. 95% upper and lower confidence intervals are indicated in black.

Figure 11. Percentage of trichomonad- and Entamoebae-positive canine plaque samples detected in categorised groups by 18S PCR (n=92). trichomonads are detected across all health states with positive sample numbers increasing as the disease stage progresses. Entamoebae-positive samples are only seen in the 'Severe Disease' samples. Trichomonads are statistically associated with 'Gingivitis', 'PD1' and 'Severe Disease' group samples. Entamoebae are statistically associated with 'Severe Disease' group samples only.

Table 14. Two-sample binomial tests on proportions of trichomonads and Entamoebae positive plaque samples. Statistically significant difference are observed between health/disease groups for both organism, indicated with asterisks.

A. Comparison of proportions of trichomonads.

Comparison groups	Sample size	Successes	Proportion	Approximate s.e. of difference	Probability	Lower 95% CI for Diff	Upper 95% CI for Diff
Severe PD group	18	12	0.667	0.143	* 0.004	0.1871	0.7462
Health group	20	4	0.2				
Comparison groups	Sample size	Successes	Proportion	Approximate s.e. of difference	Probability	Lower 95% CI for Diff	Upper 95% CI for Diff
PD1 group	26	19	0.731	0.125	* <0.001	0.2862	0.7753
Health group	20	4	0.2				
Comparison groups	Sample size	Successes	Proportion	Approximate s.e. of difference	Probability	Lower 95% CI for Diff	Upper 95% CI for Diff
Gingivitis group	28	17	0.607	0.129	* 0.005	0.1552	0.659
Health group	20	4	0.2				

A. Comparison of proportions of Entamoebae.

Comparison groups	Sample size	Successes	Proportion	Approximate s.e. of difference	Probability	Lower 95% CI for Diff	Upper 95% CI for Diff
Severe PD group	18	4	0.222	0.026	* 0.026	0.03016	0.4143
Health group	20	0	0				
Comparison groups	Sample size	Successes	Proportion	Approximate s.e. of difference	Probability	Lower 95% CI for Diff	Upper 95% CI for Diff
PD1 group	26	0	0	0	1	0	0
Health group	20	0	0				
Comparison groups	Sample size	Successes	Proportion	Approximate s.e. of difference	Probability	Lower 95% CI for Diff	Upper 95% CI for Diff
Gingivitis group	28	0	0	0	1	0	0
Health group	20	0	0				

Two distinct protist genera were identified in the canine pooled samples. 18S protozoan sequences belonging to the genus *Entamoeba* made up 0.013 % of the ‘Health’ pool sample, 0.014 % of the ‘Gingivitis’ pool sample, 0.80 % of the ‘PD1’ pool and 7.914 % of the ‘Severe Disease’ pool sample (Figure 12). 18S protozoan sequences belonging to the genus *Trichomonas* were 3.51 % of the ‘Health’ pool sample, 2.84 % of the ‘Gingivitis’ pool sample, 6.07 % of the ‘PD1’ pool and 35.04 % of the ‘Severe Disease’ pool (Figure 12). Statistical analysis of the 454 sequences (see section [2.1.22](#)) showed a significant difference between the proportion of sequences identified as *Trichomonas* sp. when comparing the ‘Health’ pool to the ‘PD1’ and ‘Severe Disease’ pool samples (Table 16). No statistical difference was seen between the ‘Health’ sample and the ‘Gingivitis’ sample. A significant difference was also observed when comparing the proportion of sequences identified as *Entamoeba* sp. in the ‘Health’ group to those in the ‘PD1’ and ‘Severe Disease’ groups (Table 16). No statistically significant difference in *Entamoeba* sp. sequences was seen between the ‘Health’ sample and the ‘Gingivitis’ sample.

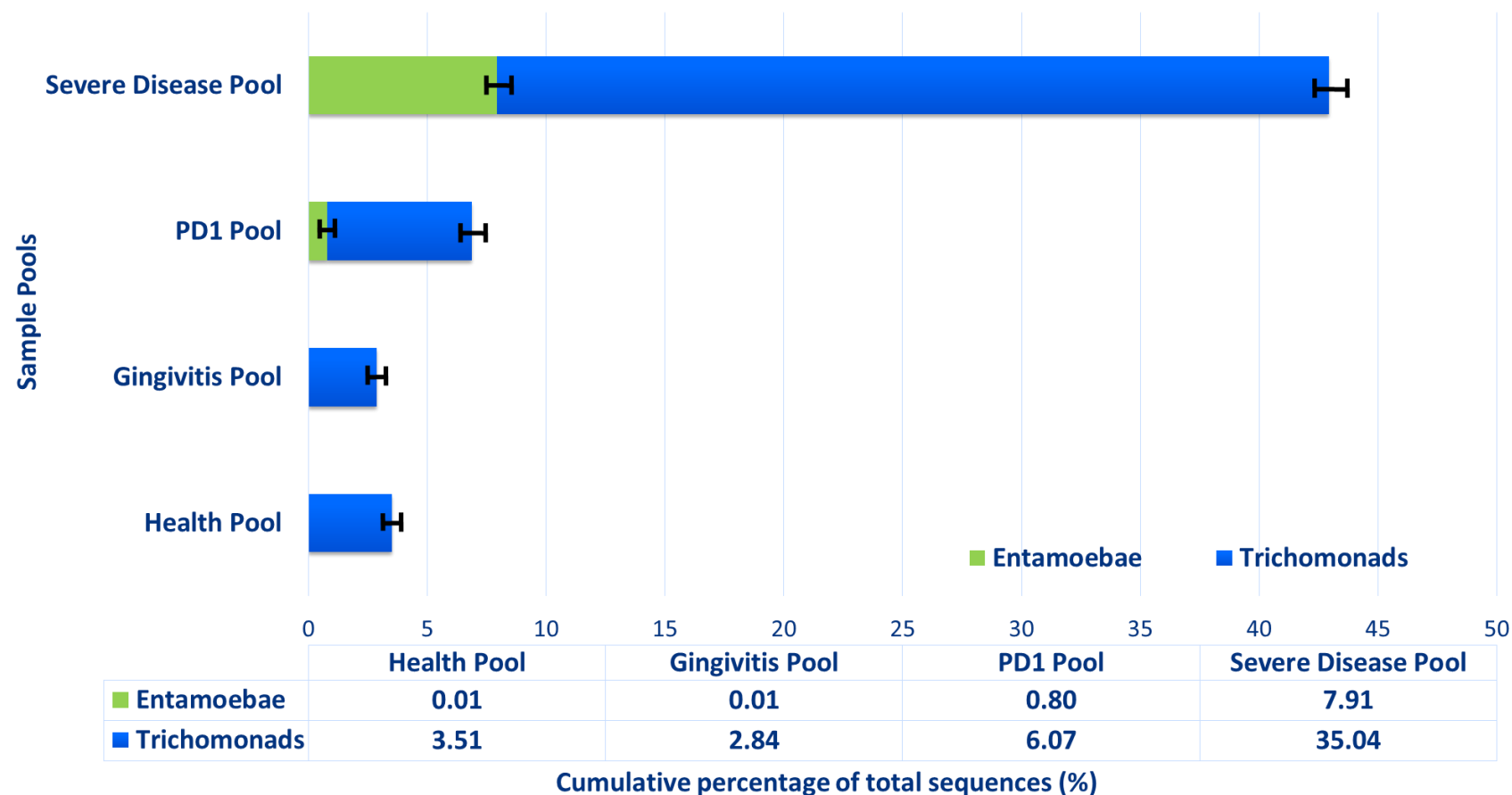
Table 15. Total number of 454 reads and percentage trichomonad (a) and Entamoebae (b) 454 sequence reads, with 95% confidence interval values, in each categorised pool sample.

a. trichomonad 454 reads

	Total number of 454 reads	trichomonad reads	95% Confidence intervals	
	(n)	(%)	Lower (%)	Upper (%)
‘Health’ pool	7265	3.51	3.09	3.95
‘Gingivitis’ pool	6750	2.84	2.46	3.26
‘PD1’ pool	8618	6.07	5.57	6.59
‘Severe Disease’ pool	11574	35.04	34.17	35.91

b. Entamoebae 454 reads

	Total number of 454 reads	Entamoebae reads	95% Confidence intervals	
	(n)	(%)	Lower (%)	Upper (%)
‘Health’ pool	7265	0.013	0.000	0.077
‘Gingivitis’ pool	6750	0.014	0.000	0.083
‘PD1’ pool	8618	0.800	0.624	1.012
‘Severe Disease’ pool	11574	7.914	7.429	8.421



* 95 % upper and lower confidence intervals are indicated by the black bars.

Figure 12. Cumulative percentage of trichomonad and Entamoebae 18S sequences (detected through Roche 454™ sequencing) in categorised pooled canine plaque samples. Trichomonad sequences are ubiquitous in all pooled samples but increased proportions are detected in the non-reversible stages of the disease - early and severe periodontal disease. Entamoebae are also more prevalent in the later stages of the disease and most abundant in the severe disease pool sample.

Table 16. Probability scores for (a) trichomonad and (b) Entamoebae 454 sequence reads in each pool sample. Binomial statistical analysis was conducted to analyse the proportion of trichomonads and Entamoebae ‘Health’ sequences compared to the proportion of sequences found in each of the disease states. *p* values were calculated for each pair of groups using the test.

a. trichomonad reads

Comparator	<i>Proportion of ‘Health’ reads</i>	<i>Proportion of Comparator reads</i>	<i>Approximate s.e. of difference</i>	<i>p value</i>
‘Gingivitis’	0.031	0.028	0.0029	0.379
‘PD1’	0.031	0.061	0.0033	< 0.001
‘Severe disease’	0.031	0.350	0.0049	< 0.001

b. Entamoebae reads

Comparator	<i>Proportion of ‘Health’ reads</i>	<i>Proportion of Comparator reads</i>	<i>Approximate s.e. of difference</i>	<i>p value</i>
‘Gingivitis’	0.00014	0.0001	0.00020	0.959
‘PD1’	0.00014	0.0080	0.00097	< 0.001
‘Severe disease’	0.00014	0.0791	0.00251	< 0.001

Both techniques reveal for the first time the presence of trichomonads and Entamoebae in the dental plaque of dogs. The overall prevalence of each genus in canine plaque was 56.52 % (52/92) and 4.34 % (4/92) respectively. Binomial statistical analysis of the PCR detections and next generation sequencing data revealed that both genera were more likely to be associated with later stage periodontal disease samples (gingivitis and above). The data show that trichomonads were found to be frequently present in canine dental plaque. trichomonads were detected in all sample groups, with their prevalence increasing as the disease severity increased. Further investigations such as longitudinal studies or the elucidation of functional attributes which may contribute to the disease process are required, to discover if they are important to disease progression or simply proliferate in numbers due to a change to more favourable conditions. In the human mouth, trichomonads are commonly detected with positive detection rates varying between 12.7 % and 37 %, and statistically associated to samples from people with periodontal disease (Athari et al., 2007, Cuevas et al., 2008, Dudko and Kurnatowska, 2007). Their presence and potential impact on human periodontal disease has been discussed. Several recent studies have confirmed the parasitic

potential of oral trichomonads, and question their prior description as commensal organisms. The human oral species, *T. tenax* has been shown to produce secretory molecules capable of contributing to the disease process and they also damage host cells through direct cellular contact, hastening cytopathic effect (El Sibaei et al., 2012, Ribeiro et al., 2015, Yamamoto et al., 2000).

In this study, Entamoebae PCR positive samples and 18S rRNA sequences were found principally in the later stages of disease – ‘PD1’ and ‘Severe Disease’. These findings may point to association between Entamoebae and the progression of the mouth from a healthy to more diseased state, however more investigation is required to separate cause and effect. Do Entamoebae actively contribute through cellular and cytopathic processes, to advance a healthy mouth to a disease mouth, or do they merely take advantage of a changed oral environment, where increased nutrient availability and a reduced host immune state allows proliferation? In humans the contribution of oral Entamoebae is equally unclear. Entamoebae prevalence in human plaque varies between 37.6% and 81% (Bonner et al., 2014, Decarneri and Giannone, 1964, Trim et al., 2011), and their presence is reported to be confined to gingival pockets, directly at sites where disease is more prevalent. As seen with the human oral protist, *T. tenax*, the role and contribution of *E. gingivalis* to periodontal disease is poorly understood. More research is required to elucidate the role of *E. gingivalis* in periodontal disease.

The findings of these studies provide the first conclusive evidence for the ubiquitous presence of protozoa in the dog mouth and give an initial indication of a role for canine oral protists in the periodontal disease process. Over recent decades, researchers have predominantly investigated the presence and functions of bacterial communities in both human and other mammalian mouths along with their contribution to periodontal disease. It is thought that the disease results as a consequence of the complex interaction between bacterial species and the host immune system (Genco and Slots, 1984), however these findings indicate that protists may also be involved in this process and require greater consideration.

CHAPTER 4: IDENTIFICATION AND QUANTIFICATION OF *TRICHOMONAS* AND *ENTAMOEB*A IN LONGITUDINALLY COLLECTED PLAQUE SAMPLES USING TWO NOVEL REAL-TIME QUANTITATIVE POLYMERASE CHAIN REACTIONS

Introduction

Two canine oral protists have been discovered in plaque using PCR and next generation sequencing methods ([Chapter 3](#)). Both methods required the use of whole mouth plaque samples. To identify and quantify protozoa that are found in samples collected at the individual tooth level, samples that contain very little target sequence, methods such as real-time quantitative polymerase chain reactions (qPCR) can be employed. To develop these qPCR assays, the primary steps of assay development are to produce suitable amplification products from each target species. These amplicons allow the *in silico* design of qPCR assay primers to specifically detect the organisms of interest. It was not possible to culture *E. gingivalis*, so to obtain a purified target amplicon of sufficient length for qPCR assay development and testing, the 18S rRNA gene PCR protocol, developed above ([section 2.12](#) and [section 3.1](#)), was used to produce an 18S gene amplicon. 18S full length gene sequences for *E. gingivalis* (accession number D28490) are available from the SILVA rRNA database project database (Quast et al., 2013, Yilmaz et al., 2014), however the physical DNA was also required for assay testing and further development.

This chapter describes the development of two qPCR assays, targeting the two canine oral protozoa identified in chapter 3, *E. gingivalis* and a canine *Trichomonas* sp. The optimised qPCR assays would be used to survey an exceptional set of samples collected from the individual teeth of 30 dogs over a period of 60 weeks. These assays would enable the identification and quantification of the two species, localised to teeth, within a longitudinal data set, giving further insights into their associations with periodontal disease.

Results and discussion

4.1. qPCR reaction assay primer design and assay conditions.

The 18S gene PCR was used to amplify a 1257 bp fragment from the *E. gingivalis* 18S rRNA gene from a canine plaque sample shown previously to contain the protist ([section 2.1.19](#) and [section 3.5](#)). This amplicon was gel extracted and was subjected to a second round of PCR ([section 2.1.2](#)) to produce a final 18S gene amplicon from *E. gingivalis*. This purified amplicon was sent to Beckman Coulter Genomics, UK, for Sanger sequencing (Sanger and Coulson, 1975, Smith et al., 1986) using both forward and reverse 18S primers to confirm the source of the amplicon. The returned sequence was found to be a 99.8% match to a sequence (accession no. D28490.1) in the NCBI Genbank database (Benson et al., 2015), annotated as the *Entamoeba gingivalis* SrRNA gene, with no other closely related sequences found. This confirmed the amplicons' purity and identity.

A similar approach was used to develop qPCR assays to identify and quantify the uncharacterised canine oral *Trichomonas* sp., in clinical samples. The assays were initially developed to target the 18S gene of trichomonads, as for *E. gingivalis*, however it was soon apparent that the DNA sequence in this region is less variable in trichomonads, and therefore, unsuitable for qPCR assay development (data not shown). To overcome this problem, a 350bp product from the ITS1-5.8S-ITS2 gene region of trichomonads was amplified ([section 2.2.3](#)) using a previously published primer set (TRF1 and TRF2) and PCR methodology (Felleisen, 1997). This region was found to be more suitable and enabled the discovery of appropriate qPCR primer sites. The purified amplicon was sent to Beckman Coulter Genomics, UK, for Sanger sequencing (Sanger and Coulson, 1975, Smith et al., 1986) and confirmed the amplicon purity and identity (data not shown).

From each purified target amplicon, two sets of qPCR primers were identified (Table 6), using established primer design software and techniques ([section 2.2.2](#)). The suggested primers were analysed using the PCR Primer Stats tool of the Sequence Manipulation Suite webpage (Stothard, 2000), which showed no unacceptable primer dimer or hairpin secondary structure were likely to occur with the primer sets (data not shown), confirming their suitability for qPCR. Each primer set was also analysed using Primer-Blast (Ye et al., 2012) to check for primer

binding to other non-specific targets. No priming sites were found in bacterial or protozoan species, other than the intended organism with the *E. gingivalis* qPCR primer pairs (data not shown). The canine oral *Trichomonas* sp. primers did show some *in silico* cross reactivity (against *Trichomonas gallinae*, and to unspecified *Trichomonas* sp.), but not in closely related or oral trichomonad species. The primers were therefore deemed suitable and further tested as below.

4.2. qPCR reaction assay efficiency and detection limits.

The sensitivity and robustness of each primer pair, in assay, were evaluated by preparing standard curve dilutions from the purified target amplicons ([section 2.2.4](#)). Each template amplicon was diluted serially, 10-fold, from 100 pico grams to 100 atto grams per μL , and each dilution was amplified using the qPCR assay conditions described in [section 2.2.3](#), and monitored in real-time. The recorded raw cycle data for each assay standard curve is detailed in Supplemental Tables 2 to 5.

All four assays displayed excellent reaction efficiencies, well within the accepted range of 90-105% efficiency, and R^2 values greater than 0.980 (Bustin et al., 2009). The *E. gingivalis* assay EG1, exhibited an assay efficiency of 94.44 % and an R^2 value of 0.998 (Supplemental Figures 1 to 3 and Table 17), and assay EG2 exhibited an assay efficiency of 91.02 % and an R^2 value of 0.999 (Supplemental Figures 4 to 6 and Table 17). The unidentified *Trichomonas* targeted TC1 qPCR assay exhibited an assay efficiency of 96.48 % and an R^2 value of 0.999 (Supplemental Figures 7-9 and Table 17) and assay TC2 exhibited an assay efficiency of 97.01 % and an R^2 value of 0.997 (Supplemental Figures 10-12 and Table 17). In terms of suitability for qPCR, all four assays are deemed acceptable by their assay efficiencies and R^2 values (Bustin et al., 2009).

Each assay was also tested to ascertain its limit of detection. Template DNA was diluted serially 10-fold from 10 nano grams to 0.31 atto grams of DNA per μL to produce samples to be tested. It was possible to detect DNA, using both EG and TC assays, at approximately the 10^{-9} and 10^{-10} dilutions (Table 17). This gave limits of detection of 30.63 C_t units (467 gene copies) and 30.13 C_t units (933 gene copies) for the EG1 and EG2 assays respectively (Table 17). The TC assays were calculated

to have a detection limit of 28.43 C_t units (26600 gene copies) and 31.16 C_t units (666 gene copies) for the TC1 and TC2 assays, respectively (Table 17).

Each of the four assays were found to be suitable as a robust and sensitive qPCR assay. However, it was decided to take forward assays EG1 and TC2 for further assay suitability testing (see below) because they exhibited the highest levels of efficiency for each species.

Table 17. Summary of standard curve data calculations for protozoa-targeted qPCR assays. The values for assay slope, Y-intercept, R² value, and assay efficiency for qPCR assays EG1, EG2, TC1 and TC2 are shown. Data were recorded by 7900HT Fast Real-Time PCR System (Applied Biosystems, UK) and analysed with the Applied Biosystems SDS V2.4 software. Assay limit of detections (LOD) were defined as the lowest standard curve dilution at which at least two valid replicates were observed at less than 0.25 C_t units difference from the median value. LOD values were converted to sequence copy number (Staroscik, 2004) and assigned as the limit of quantification. Two assays, EG1 and TC2, were taken forward for further analyses (indicated with grey shading).

Primer set	Slope (cycles/log decade)	Y-Intercept	R ²	Assay efficiency	Limit of detection (dilution)	Limit of detection (Average Ct)	Limit of quantification (no. of target sequences)
EG1	-3.46	-0.57	0.998	94.44%	6.25e -10	30.63	467 (18S)
EG2	-3.55	0.35	0.999	91.02%	2.5E -9	30.13	933 (18S)
TC1	-3.40	-2.04	0.999	96.48%	1E -9	28.43	26600 (ITS1-5.8S-ITS2)
TC2	-3.39	-1.01	0.997	97.01%	2.5E -10	31.16	666 (ITS1-5.8S-ITS2)

4.3. qPCR reaction assays EG1 and TC2 cross reactivity.

The cross-reactivity of assays EG1 and TC2 to microorganisms that may be present in samples was assessed by testing the assays against a range of protozoa (*G. intestinalis*, *A. polyphaga*, *E. invadens*, *T. tenax*, and the isolated canine oral *Trichomonas* sp.). Mammalian (Human and Canine), fungal (*S. cerevisiae*) and bacterial (*E. coli*) DNA samples also were included (see sections [2.1.6](#), [2.1.7](#), [2.1.8](#) and [2.1.9](#)). Additionally, a canine oral bacterial mock-community sample containing bacterial small sub unit (16S) DNA clone sequences (Davis et al., 2013) and previously collected canine plaque DNA extractions (see [section 2.1.19](#)), known to contain protozoa, bacterial and yeast DNA, were tested. 1 ng/μL, triplicate samples, were tested using both assays ([section 2.2.3](#)). The recorded raw cycle data, assay amplification plot, and dissociation analysis curve for assay EG1 are displayed in Supplemental Table 6, and Supplemental Figures 13 and 14.

The Assay EG1 did not show cross-reactivity with any of the microorganisms tested (Supplemental Table 6, and Supplemental Figure 13). A positive reaction was seen only with the *E. gingivalis* 18S amplicon sample and the two clinical plaque DNA extractions, sample 18P and SD pool (Supplemental Figure 13), which were previously shown to contain *Entamoeba* DNA ([section 3.5](#)).

The dissociation curve analysis for these samples also indicates that the assay is specific for *E. gingivalis* (Supplemental Figure 14). A single qPCR product was seen across all three qPCR positive samples (Supplemental Figure 14), with an average melt temperature of 76.3°C (+/- 0.3) (Supplemental Table 6), confirming the production of the same product in each positive sample and the specificity of the assay.

The Assay TC2 showed cross-reactivity with only one of the microorganisms tested (Supplemental Table 7, and Supplemental Figure 15). A positive reaction was seen with the isolated *Trichomonas* sp. ITS1-5.8S-ITS2 amplicon sample and the isolated *Trichomonas* sp. (CLEO) genomic DNA sample (Supplemental Table 7, and Supplemental Figures 15 and 16), but a strong, unexpected positive reaction, was also found with the *T. tenax* genomic DNA sample (Supplemental Table 7, and Supplemental Figures 15 and 16). A qPCR amplicon was also detected with the two clinical plaque DNA samples, 18P and SD pool (data not shown), however their C_t values were outside the calculated detection limits for the assay (Table 17) and were

therefore not considered as positive, and thus they are not included in the Tables or Figures. Increasing the template concentration could make these organisms detectable, however higher template concentration samples were not available to test this. No other positive reactions were seen for the other samples tested.

The *T. tenax* positive sample was surprising, as during the *in silico* qPCR primer design stage, *T. tenax* and other non-related trichomonads were calculated to not bind to the primers tested ([see section 4.1](#)). The dissociation curves for this assay and samples, also indicate that the assay exhibits cross reactivity with *T. tenax* (Supplemental Figure 16). A qPCR amplicon with an average melt temperature of 80.8°C was seen with the isolated *Trichomonas* sp. ITS1-5.8S-ITS2 and the isolated *Trichomonas* sp. (CLEO) genomic DNA samples. The *T. tenax* genomic DNA sample produces an amplicon with an average melt temperature of 80.0°C (+/- 0.3) (Supplemental Figure 16), separate and distinct from the canine *Trichomonas* amplicons. This suggests either a slightly smaller qPCR amplicon is formed, or a gene sequence difference is present in the *T. tenax* target sequence and amplicon, giving rise to an altered melt dissociation point. This poses a problem for the TC2 assay because it would not be possible to easily distinguish between the two *Trichomonas* species using this assay alone. Even though the species produce different qPCR amplicons, shown through the dissociation curves (Supplemental Figure 16), if the two species are present in a mixed sample, a single merged melt curve peak is produced (Supplemental Figure 17) due to the similarity of the amplicon sizes and composition, removing the ability to differentiate the species using a dissociation melt curve alone. The TC2 assay, therefore, does not offer the same level of specificity as assay EG1. However, currently it is the only qPCR assay that offers a quantifiable, sensitive qPCR method of detection of canine oral *Trichomonas* sp.

4.4. qPCR assay TC2 amplicon digestion with BcnI.

The qPCR assay TC2 developed in this project provides a quantifiable method for the identification of canine oral trichomonads, but also exhibits cross-reactivity with *T. tenax*, a human oral trichomonad. To discover the identity of the trichomonad(s) in each tested sample, whether the isolated canine *Trichomonas* sp.,

T. tenax, or a mixture of the two, a method was developed, using the restriction enzyme BcnI.

The use of restriction digestion in this situation relies on the differential digestion of the qPCR product based on the amplicon length and composition ([section 2.2.7](#)). The resultant size of digestion products categorically identifies the trichomonad species present in the sample, as the isolated canine *Trichomonas* sp., *T. tenax*, or a mixture of the two.

Several restriction enzymes were considered for this differential digestion, with *in silico* analyses used to find suitable enzyme candidates (data not shown). BcnI was found, *in silico*, to give digestion products with suitably distinct digestion product sizes to enable the differentiation of the two species. The digestion products of the TC2 assay qPCR amplicons from the isolated canine *Trichomonas* sp. and *T. tenax* were analysed using a 2100 Bioanalyzer (Agilent Genomics, USA), with a DNA chip (Figure 13). In the presence of *T. tenax* only, digestion of TC2 assay amplicons with BcnI resulted in a single product of approximately 130 bp (Figure 13, Lane 5). Whereas observation of two digestion products, approximately 104 and 32 bp in size, indicated the presence of the isolated canine *Trichomonas* sp. only (Figure 13 Lane 4). In turn, three digestion products, approximately 130, 104 and 32 bp in size indicated the presence of a mixture of *T. tenax* and the isolated canine *Trichomonas* sp. (Figure 13, Lanes 1-3). The digestion results were not affected by altering the proportions of qPCR amplicons in samples, replicating how differing levels of each species may be found in plaque samples. (Figure 13, Lanes 1-3).

If a single species is present in samples then the TC2 qPCR assay can be used without modification. However, recent publications have indicated the possibility of several *Trichomonas* species being present in canine mouths (Kellerova and Tachezy, 2017, Kutisova et al., 2005). In this mixed sample type, the TC2 assay should offer a more efficient method of oral *Trichomonas* identification and quantification due to the duplex identification technique. Without this method a separate, species-specific, assay for each trichomonad present in the samples would need to be designed, validated and conducted for all samples, adding significant cost and time.

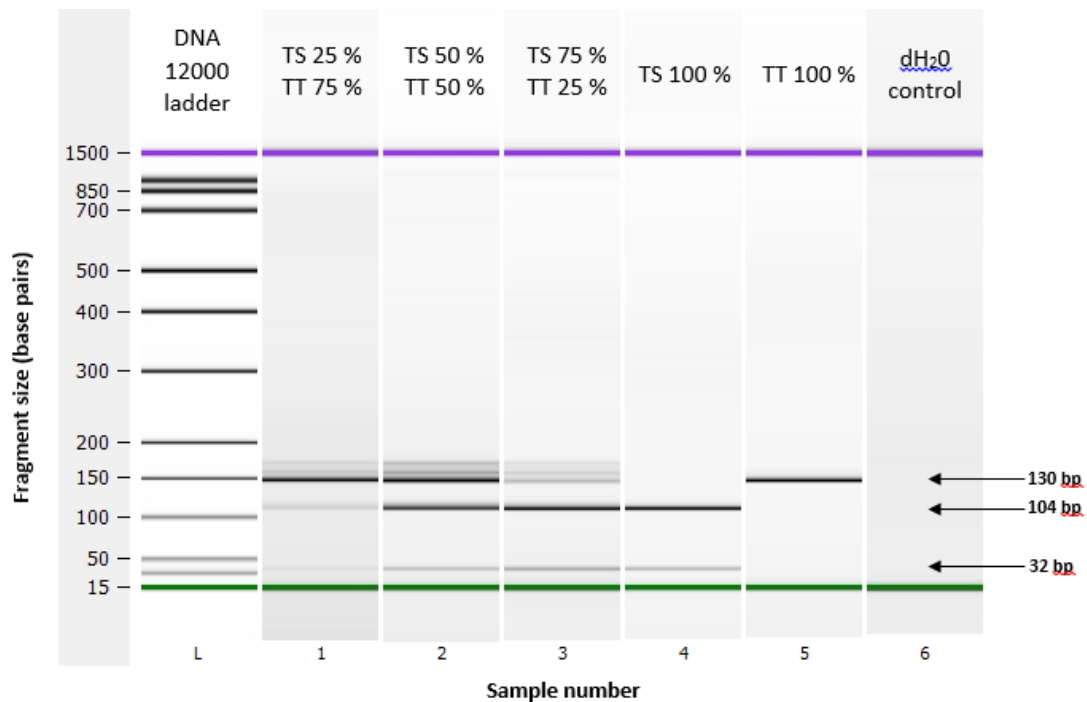


Figure 13. Agilent Bioanalyzer electropherogram of qPCR TC2 assay amplicons, digested with BcnI enzyme. The digestion products formed indicate the presence of either the canine oral *Trichomonas* sp. (TS), *T. tenax* (TT), or a mixture of the two species within the digest sample. Digestion with BcnI resulting in a single digestion product of approximately 130 bp, indicates the presence of *T. tenax* only (Lane 5). Two digestion products, approximately 104 and 32 bp in size, indicate the presence of the isolated canine *Trichomonas* sp. only (Lane 4). Three digestion products, approximately 130, 104 and 32 bp indicates the presence of both *T. tenax* and the isolated canine *Trichomonas* sp. in the sample. Lanes 1-3 show the digestion products produced with varying proportions of the TC2 qPCR amplicons.

4.5. EG1 and TC2 assay qPCR screen of longitudinally collected canine plaque samples

The canine oral *Trichomonas* sp. and *E. gingivalis* discovered by PCR and next generation sequencing have been shown to be more likely associated with plaque samples taken from animals suffering from gingivitis and late stage canine periodontal disease (Patel et al., 2017) (and [section 3.5](#)). These data provide the first evidence for the presence of protozoa in canine oral plaque and indicates a potential role in the periodontal disease process. Unfortunately, the data do not indicate if the protozoa present in canine plaque are a cause of the disease progression. It is uncertain if they opportunistically make use of favourable environmental conditions

or play a more direct role in the transition of a healthy mouth to the changed conditions (a more diseased state).

To investigate if these organisms are involved in this health state change, canine plaque samples were collected from the individual animals over a period of time ([section 2.2.6](#)) after cessation of tooth brushing whilst monitoring their oral health. Canine subgingival plaque was collected from individual teeth over a sixty week period from fifty two miniature schnauzers aged between 1 and 7 years ([section 2.2.6](#)). Sample collections took place every six weeks and the health state of teeth was monitored and only allowed to progress until early stage periodontal disease (<25% attachment loss).

A subset of samples, 444 from 30 dogs were identified for analysis using both the qPCR EG1 and TC2 assays (Supplemental Tables 8 and 9). The sample set consisted of 47 teeth that progressed to early periodontitis (<25% attachment loss), designated as “Progressing” and a separate set of 47 teeth that did not progress beyond mild gingivitis during the 60 week study, designated as “Non Progressing” (Figure 14). For balanced analysis, the samples were paired within groups, firstly through tooth number, e.g. 108 and 208 or 308 and 408. If this was not possible the teeth were paired by tooth type within a dog, e.g. premolar to premolar. If neither of the above was possible, the teeth were matched by tooth number but from different dogs of comparable age.

DNA from each sample time point were tested, in triplicate, for the presence and abundance of the two oral protozoa, using the real-time assays EG1 and TC2 ([section 2.2.3](#)). All cycle threshold data were collected, tabulated (Supplemental Table 10), normalised to the sample concentration and the absolute gene copy numbers calculated, using the in-run standards samples ([section 2.2.8](#)).

With nearly 3000 data points, the data set obtained for this project was extensive and with the associated metadata supplied with each sample (Supplemental Table 10) it was possible to conduct a variety of analyses ([section 2.2.9](#)). For each analysis, a linear mixed effects model was fitted, modelling the gene copy number of each organism against the groups (progressing and non-progressing to PD), time during the study, and their interaction with gender and age at the start of the trial (weeks) as covariants.

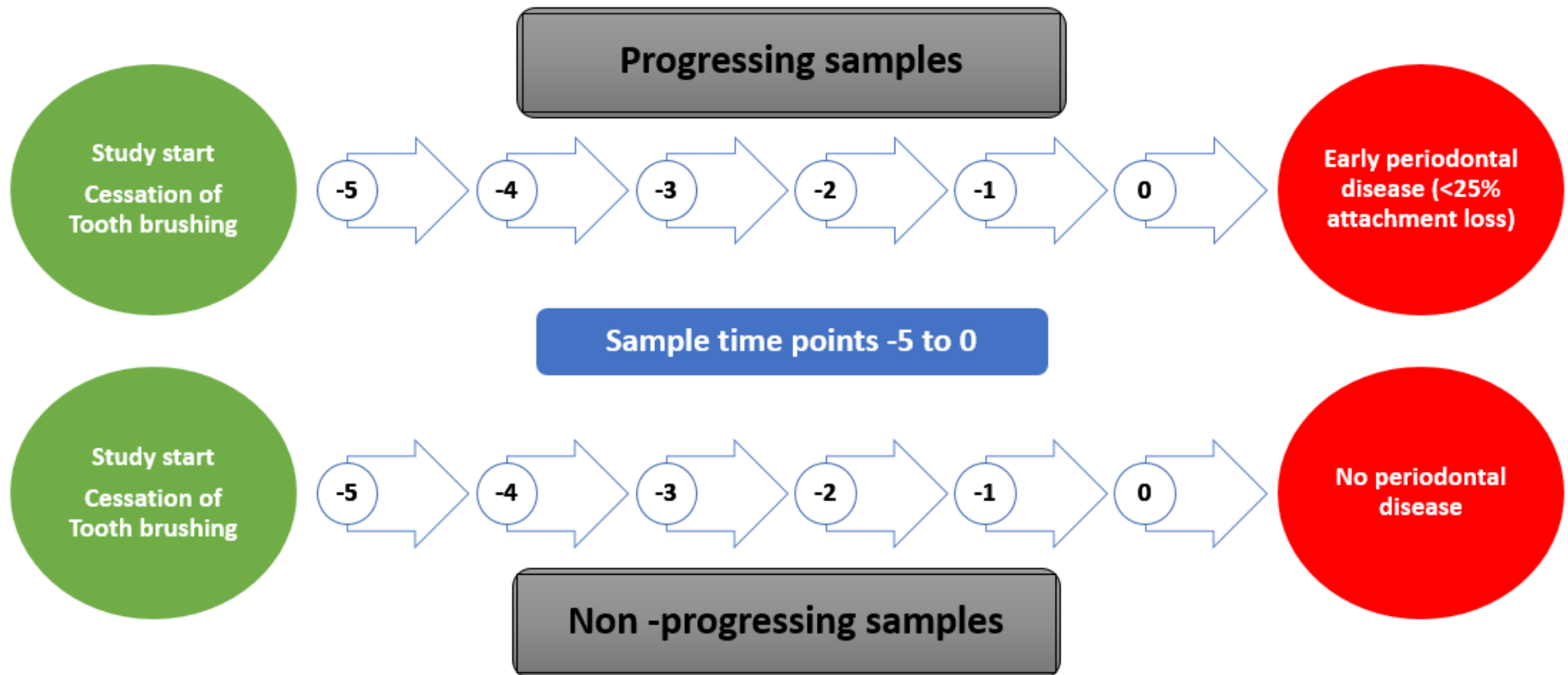


Figure 14. Study design for samples collected from the individual dogs over a sixty week period. Sub gingival plaque samples from fifty two miniature schnauzers aged between 1 and 7 years were collected every six weeks and the health state of teeth was monitored and only allowed to progress until early stage periodontal disease (<25% attachment loss). A sample set of 47 teeth that progressed to early periodontitis (<25% attachment loss), designated as “Progressing” and a separate matched set of 47 teeth that did not progress beyond mild gingivitis during the study, designated as “Non Progressing”. For balanced analysis, the samples were paired within groups, firstly through tooth number, e.g. 108 and 208 or 308 and 408. If this was not possible the teeth were paired by tooth type within a dog, e.g. premolar to premolar. If neither of the above was possible then the teeth were matched by tooth number but from different dogs of comparable age.

4.5.1. Primary analyses of data set – protozoa abundance and progression of periodontal disease.

The primary analysis of the qPCR data compared the abundance of each protozoan in each tooth subset group, progressing (PD_PRESENT) or non-progressing (NO_PD), over the course of the study.

The estimated collective abundance (estimated by gene copy number) of each organism at each time point during the study (-5 to 0) is displayed in Table 18. The estimated protozoa abundances (gene copy numbers) at each of these time points were compared to each other and also against the same time point in the opposing tooth group, i.e. progressing vs non-progressing (Table 19 a&b). The fold-changes with 97.5% confidence intervals for each comparison were determined, together with *p*-values. No significant differences in abundance of the canine oral *Trichomonas* sp. or *E. gingivalis* were seen when comparing teeth that progress into early periodontal disease or teeth that did not progress (Table 19a). Over the time points there was 0.90 to 1.60-fold change in *E. gingivalis*, and 0.80 to 1.12-fold change in the canine trichomonad abundance (Table 19a), but none are statistically significant changes.

The abundance of each organism was also analysed at each time point during the study, within each tooth group, progressing or non-progressing, comparing the organism abundances at each time point to time point 0, the final time point in the study (Table 19b). In this comparison, statistically significant increases in organism abundance were observed when comparing the earliest time points to the latest (time point 0), for both protozoa (Table 19b). For *E. gingivalis*, significant increases in protozoa numbers are seen in the 0 to -5 (2.93-fold increase, *p* value= 0.0001), and 0 to -4 (2.22-fold increase, *p* value= 0.0047) time point comparisons for the non-progressing group, and in the 0 to -5 (2.75-fold increase, *p* value= 0.0009) time point comparison for teeth that do progress to PD (PD_PRESENT) (Table 19b).

Similar significant increases in abundance were also seen with the canine *Trichomonas* sp. across both teeth groups. Significant fold changes are seen in the 0 to -4 (2.43-fold increase, *p* value= 0.0061), and 0 to -2 (2.71-fold increase, *p* value= 0.0002) comparisons for teeth in the non-progressing group (No_PD), and in the 0 to -4 (3.06-fold increase, *p* value= 0.0001), and 0 to -2 (3.06-fold increase, *p* value= 0.0001) comparisons for teeth that do progress to PD (PD_PRESENT) (Table 19b).

Table 18. Abundance (gene copy number) of the canine oral *Trichomonas* sp. and *E. gingivalis* using qPCR at the indicated time points of the study. Samples were collected over 6 times points (-5 to 0), and the organism abundance at each time point was estimated by qPCR.

qPCR assay	Tooth group	Time point during study	Estimated Gene Copy Number	97.5% CI
EG1	NO_PD	-5	3.64	(1.2, 11.04)
EG1	NO_PD	-4	4.81	(1.65, 14.03)
EG1	NO_PD	-3	6.35	(2.23, 18.09)
EG1	NO_PD	-2	6.88	(2.42, 19.54)
EG1	NO_PD	-1	6.11	(2.13, 17.57)
EG1	NO_PD	0	10.67	(3.76, 30.27)
EG1	PD_PRESENT	-5	3.50	(1.14, 10.75)
EG1	PD_PRESENT	-4	5.61	(1.94, 16.17)
EG1	PD_PRESENT	-3	9.54	(3.36, 27.08)
EG1	PD_PRESENT	-2	8.74	(3.04, 25.13)
EG1	PD_PRESENT	-1	9.79	(3.44, 27.85)
EG1	PD_PRESENT	0	9.62	(3.38, 27.37)
TC2	NO_PD	-5	14.36	(6.15, 33.54)
TC2	NO_PD	-4	13.37	(6.16, 29.02)
TC2	NO_PD	-3	15.67	(7.6, 32.27)
TC2	NO_PD	-2	11.99	(5.87, 24.47)
TC2	NO_PD	-1	16.82	(8, 35.35)
TC2	NO_PD	0	32.45	(15.89, 66.25)
TC2	PD_PRESENT	-5	14.50	(6.06, 34.71)
TC2	PD_PRESENT	-4	10.64	(5.03, 22.51)
TC2	PD_PRESENT	-3	17.49	(8.57, 35.7)
TC2	PD_PRESENT	-2	10.63	(5.06, 22.36)
TC2	PD_PRESENT	-1	19.93	(9.72, 40.88)
TC2	PD_PRESENT	0	32.51	(15.86, 66.64)

EG1= qPCR assay targeting *E. gingivalis*. TC2= qPCR assay targeting canine oral *Trichomonas* sp.
Tooth groups: NO_PD= non-progressing teeth, PD_PRESENT= teeth progressing to early periodontal disease.
Study time points: -5, -4, -3, -2, -1, and 0 – Chronologically progressing in the study where samples were collected from subjects.

Both tooth groups also show apparent abundance increases at the other time point comparisons, with both organisms, but none were statistically significantly ($p > 0.025$) (Table 19b).

In conclusion, the primary analyses of the data set suggests that the abundance of *E. gingivalis* and the canine oral *Trichomonas* sp. is not associated with the progression of canine teeth into early stage periodontal disease (Table 19a). However, statistically significant increases in both protozoa numbers (abundance) were seen as time progressed through the study, in both groups of teeth.

Table 19. Abundance (gene copy number) fold changes of *Trichomonas* sp. and *E. gingivalis* at the indicated time points of the study. **(a)** Comparisons were undertaken in samples that progress (PD_PRESENT) compared to those that did not progress (NO_PD) to early stage periodontal disease. **(b)** Abundances were compared within each tooth group, progressing and non-progressing, comparing each time point to the final time point, 0. 97.5% confidence intervals for all comparisons are displayed, with significant *p* values (<0.025) for each comparison highlighted with pink shading.

a.

qPCR assay	Tooth group comparison	Time point during study	Estimated fold change of abundance	97.5% confidence intervals (lower and upper)	<i>p</i> value
EG1	PD_PRESENT vs NO_PD	-5	0.96	(0.41, 2.28)	1.00
EG1	PD_PRESENT vs NO_PD	-4	1.17	(0.57, 2.38)	0.99
EG1	PD_PRESENT vs NO_PD	-3	1.50	(0.79, 2.85)	0.43
EG1	PD_PRESENT vs NO_PD	-2	1.27	(0.66, 2.46)	0.95
EG1	PD_PRESENT vs NO_PD	-1	1.60	(0.82, 3.11)	0.28
EG1	PD_PRESENT vs NO_PD	0	0.90	(0.48, 1.71)	1.00
TC2	PD_PRESENT vs NO_PD	-5	1.01	(0.38, 2.71)	1.00
TC2	PD_PRESENT vs NO_PD	-4	0.80	(0.35, 1.8)	0.99
TC2	PD_PRESENT vs NO_PD	-3	1.12	(0.54, 2.32)	1.00
TC2	PD_PRESENT vs NO_PD	-2	0.89	(0.42, 1.89)	1.00
TC2	PD_PRESENT vs NO_PD	-1	1.19	(0.56, 2.53)	0.99
TC2	PD_PRESENT vs NO_PD	0	1.00	(0.48, 2.07)	1.00

b.

qPCR assay	Tooth group	Time point comparison	Estimated fold change of abundance	97.5% confidence intervals (lower and upper)	<i>p</i> value
EG1	NO_PD	0 vs 5	2.93	(1.37, 6.25)	0.0001
EG1	NO_PD	0 vs 4	2.22	(1.11, 4.42)	0.004
EG1	NO_PD	0 vs 3	1.68	(0.89, 3.19)	0.13
EG1	NO_PD	0 vs 2	1.55	(0.82, 2.92)	0.31
EG1	NO_PD	0 vs 1	1.75	(0.9, 3.37)	0.10
EG1	PD_PRESENT	0 vs 5	2.75	(1.26, 6)	0.0009
EG1	PD_PRESENT	0 vs 4	1.72	(0.88, 3.36)	0.14
EG1	PD_PRESENT	0 vs 3	1.01	(0.53, 1.91)	1.00
EG1	PD_PRESENT	0 vs 2	1.10	(0.57, 2.14)	1.00
EG1	PD_PRESENT	0 vs 1	0.98	(0.52, 1.86)	1.00
TC2	NO_PD	0 vs 5	2.26	(0.95, 5.36)	0.04
TC2	NO_PD	0 vs 4	2.43	(1.11, 5.32)	0.006
TC2	NO_PD	0 vs 3	2.07	(1, 4.3)	0.02
TC2	NO_PD	0 vs 2	2.71	(1.32, 5.57)	0.0002
TC2	NO_PD	0 vs 1	1.93	(0.91, 4.09)	0.08
TC2	PD_PRESENT	0 vs 5	2.24	(0.92, 5.47)	0.06
TC2	PD_PRESENT	0 vs 4	3.06	(1.42, 6.57)	0.0001
TC2	PD_PRESENT	0 vs 3	1.86	(0.9, 3.84)	0.09
TC2	PD_PRESENT	0 vs 2	3.06	(1.43, 6.53)	0.0001
TC2	PD_PRESENT	0 vs 1	1.63	(0.79, 3.38)	0.36

EG1= qPCR assay targeting *E. gingivalis*. TC2= qPCR assay targeting canine oral *Trichomonas* sp.
Tooth groups: NO_PD= non-progressing teeth, PD_PRESENT= teeth progressing to early periodontal disease.

Study time points: -5, -4, -3, -2, -1, and 0 – Chronologically progressing in the study where samples were collected from subjects.

The disease data set was comprised only of teeth that progressed to early stage periodontal disease (<25 % attachment loss). At this early stage, the disease is still reversible. The data set is therefore not a set that progresses to the final stages of periodontal disease. The animal's oral state can still be returned to a healthy situation through dental treatment (Harvey, 1998, Socransky and Haffajee, 1992). It was seen that both protozoan numbers increased as the samples progressed towards early periodontal disease (Table 19b), indicating the potential that these two organisms may be important in the progression of the disease from the reversible early stages of the disease to the more advanced disease stages, periodontal disease stages 2 and above. However, it is still unclear if either organism are contributors to the disease or merely taking advantage of the more favourable conditions. More studies are required with sample types that progress further into the more advanced stages of the disease, to test this hypothesis.

4.5.2. Secondary analysis of data set – probability of detecting of protozoa.

For a secondary analysis of the abundance data, a generalised linear mixed model was fitted for each organism, modelling the binary variable 'detected', which describes the probability of detecting each protozoan using the qPCR assays described in [section 2.2.5](#), across the various time points of the study. Using the C_t detection limit of each assay ([section 4.2](#)), and average melting points determined for each amplicon ([section 4.3](#)), each test sample was assigned a value as 'detected' or 'not detected' based on whether or not it met the detection limits and melt curve criteria. Supplemental Table 10 displays the binary (1: Yes or 0: No) values assigned to each sample. For analyses, a linear mixed effects model was fitted, modelling the protozoan abundance (gene copy number determined by the qPCR assay) against tooth progression group, at each time point in the study. The estimated probabilities of detecting each protozoan in each tooth progression groups and at each study time point, were calculated, along with 95% confidence intervals (Table 20). The probability of each species being detected in a sample group is expressed as a value between 0 and 1.0. The closer this value is to 1.0, the more likely the protozoan will be detected, in the sample group.

Table 20. Estimated probability of detection of the isolated canine oral *Trichomonas* sp. and *E. gingivalis* using qPCR, in progressing (PD_PRESENT) and non-progressing (NO_PD) periodontitis teeth and at time points during the study. Data includes 95% confidence intervals for all detection probabilities.

qPCR assay	Tooth group	Time point during study	Estimated Probability of detection	95% confidence intervals (lower and upper)
EG1	NO_PD	-5	0.759	(0.53, 0.9)
EG1	NO_PD	-4	0.761	(0.55, 0.89)
EG1	NO_PD	-3	0.802	(0.62, 0.91)
EG1	NO_PD	-2	0.731	(0.52, 0.87)
EG1	NO_PD	-1	0.816	(0.63, 0.92)
EG1	NO_PD	0	0.815	(0.64, 0.92)
EG1	PD_PRESENT	-5	0.817	(0.6, 0.93)
EG1	PD_PRESENT	-4	0.740	(0.53, 0.88)
EG1	PD_PRESENT	-3	0.799	(0.61, 0.91)
EG1	PD_PRESENT	-2	0.793	(0.6, 0.91)
EG1	PD_PRESENT	-1	0.775	(0.58, 0.9)
EG1	PD_PRESENT	0	0.809	(0.63, 0.91)
TC2	NO_PD	-5	0.912	(0.76, 0.97)
TC2	NO_PD	-4	0.917	(0.79, 0.97)
TC2	NO_PD	-3	0.920	(0.82, 0.97)
TC2	NO_PD	-2	0.919	(0.82, 0.97)
TC2	NO_PD	-1	0.953	(0.85, 0.99)
TC2	NO_PD	0	0.947	(0.86, 0.98)
TC2	PD_PRESENT	-5	0.887	(0.71, 0.96)
TC2	PD_PRESENT	-4	0.906	(0.79, 0.96)
TC2	PD_PRESENT	-3	0.925	(0.83, 0.97)
TC2	PD_PRESENT	-2	0.887	(0.76, 0.95)
TC2	PD_PRESENT	-1	0.908	(0.8, 0.96)
TC2	PD_PRESENT	0	0.951	(0.86, 0.98)

EG1= qPCR assay targeting *E. gingivalis*. TC2= qPCR assay targeting canine oral *Trichomonas* sp. Tooth groups: NO_PD= non-progressing teeth, PD_PRESENT= teeth progressing to early periodontal disease.

Study time points: -5, -4, -3, -2, -1, and 0 – Chronologically progressing in the study where samples were collected from subjects.

Estimated probability of detection expressed as a value between 0 and 1.0. The closer this value is to 1.0, the more likely the detection of the protozoan is, in the sample group.

At each time point of the study (-5 to 0), each tooth group (progressing or non-progressing) detection probabilities were compared against each other (Table 21a). Each time point was also compared, within each tooth group, to time point 0, the final time point in the study, to understand if the probability of detection increases as the study time progressed (Table 21b). Odds ratios for each comparison, with 95% confidence intervals were extracted, along with *p* values for each of the comparisons. Odds ratios are defined as the probability that the event will occur

divided by the probability that the event will not occur, and are calculated as $Y/(1-Y)$. They are expressed as a value between 0 and infinity; the higher the ratio the more likely the event. No significant differences in odds ratios were seen for the probability of detection for either protozoan using their respective qPCR detection probabilities. (Table 21). In conclusion, the probability of detecting either *E. gingivalis* or the isolated canine oral *Trichomonas* sp. does not increase in either progressing or non-progressing groups or at any of the study time points when compared to the final study time point, time point 0. Through molecular sequencing ([section 3.5](#)), it can be seen that both *E. gingivalis* and the isolated canine oral *Trichomonas* sp. have a greater association with samples from later stage periodontal disease, although the samples tested with the qPCR here did not progress past early periodontal disease, < 25% attachment loss.

Table 21. Odds ratios for the detection of the isolated canine *Trichomonas* sp. and *E. gingivalis*, along with 95% confidence intervals for all comparisons. Significant *p* values (<0.05) for comparison are displayed with pink shading. **(a)** Detection probabilities were compared in groups of teeth which progress (PD_PRESENT) or do not progress (NO_PD) to early stage periodontal disease. **(b)** Detection probabilities were compared within each tooth group, at each time point against the final time point of the study (time point 0).

a.

qPCR assay	Tooth group comparison	Time point during study	Odds ratio of detection	95% confidence intervals (upper and lower)	<i>p</i> value
EG1	PD_PRESENT vs NO_PD	-5	1.41	(0.45, 4.4)	0.99
EG1	PD_PRESENT vs NO_PD	-4	0.89	(0.34, 2.31)	1.00
EG1	PD_PRESENT vs NO_PD	-3	0.98	(0.41, 2.37)	1.00
EG1	PD_PRESENT vs NO_PD	-2	1.42	(0.58, 3.48)	0.96
EG1	PD_PRESENT vs NO_PD	-1	0.78	(0.31, 1.95)	0.99
EG1	PD_PRESENT vs NO_PD	0	0.96	(0.4, 2.31)	1.00
TC2	PD_PRESENT vs NO_PD	-5	0.75	(0.15, 3.73)	0.99
TC2	PD_PRESENT vs NO_PD	-4	0.87	(0.22, 3.38)	1.00
TC2	PD_PRESENT vs NO_PD	-3	1.06	(0.29, 3.9)	1.00
TC2	PD_PRESENT vs NO_PD	-2	0.70	(0.21, 2.37)	0.99
TC2	PD_PRESENT vs NO_PD	-1	0.49	(0.11, 2.16)	0.84
TC2	PD_PRESENT vs NO_PD	0	1.09	(0.23, 5.11)	1.00

b.

qPCR assay	Tooth group	Time point comparison	Odds ratio of detection	95% confidence intervals (upper and lower)	<i>p</i> value
EG1	NO_PD	0 vs 5	1.40	(0.51, 3.83)	0.98
EG1	NO_PD	0 vs 4	1.38	(0.54, 3.52)	0.98
EG1	NO_PD	0 vs 3	1.09	(0.45, 2.62)	1.00
EG1	NO_PD	0 vs 2	1.63	(0.69, 3.82)	0.68
EG1	NO_PD	0 vs1	1.00	(0.4, 2.48)	1.00
EG1	PD_SEEN	0 vs 5	0.95	(0.33, 2.69)	1.00
EG1	PD_SEEN	0 vs 4	1.49	(0.6, 3.69)	0.91
EG1	PD_SEEN	0 vs 3	1.07	(0.44, 2.57)	1.00
EG1	PD_SEEN	0 vs 2	1.10	(0.44, 2.78)	1.00
EG1	PD_SEEN	0 vs1	1.22	(0.51, 2.95)	0.99
TC2	NO_PD	0 vs 5	1.72	(0.36, 8.36)	0.97
TC2	NO_PD	0 vs 4	1.62	(0.37, 7.06)	0.98
TC2	NO_PD	0 vs 3	1.55	(0.38, 6.31)	0.99
TC2	NO_PD	0 vs 2	1.59	(0.4, 6.3)	0.98
TC2	NO_PD	0 vs1	0.89	(0.18, 4.44)	1.00
TC2	PD_SEEN	0 vs 5	2.50	(0.51, 12.24)	0.66
TC2	PD_SEEN	0 vs 4	2.03	(0.48, 8.59)	0.82
TC2	PD_SEEN	0 vs 3	1.59	(0.37, 6.79)	0.98
TC2	PD_SEEN	0 vs 2	2.49	(0.61, 10.17)	0.50
TC2	PD_SEEN	0 vs1	1.99	(0.48, 8.16)	0.83

EG1= qPCR assay targeting *E. gingivalis*. TC2= qPCR assay targeting canine oral *Trichomonas* sp. Tooth groups: NO_PD= non-progressing teeth, PD_PRESENT= teeth progressing to early periodontal disease.

Study time points: -5, -4, -3, -2, -1, and 0 – Chronologically progressing in the study where samples were collected from subjects.

4.5.3. Additional analysis of data – *Trichomonas* species identification

Supplemental Table 11 displays the identity of the species of trichomonad, isolated canine oral *Trichomonas* sp. or *T. tenax*, detected using the novel restriction digest protocol ([section 2.27](#)) for the qPCR amplicon formed from each tested sample. The data are recorded in binary format for each sample, namely presence or absence of each species (Supplemental Table 11). From a total of 444 qPCR samples, 262 were identified as *Trichomonas*-positive using the TC2 qPCR assay. They were considered positive if the assay detected an amplicon of the expected melt temperature (79-81°C). Of the 262 *Trichomonas*-positive samples, the restriction analysis identified 179 as containing the isolated canine oral *Trichomonas* sp., and 213 containing *T. tenax* (Supplemental Table 11).

As with previous analyses, the data were tested using a binomial generalised linear mixed model as described before ([section 2.2.9](#)). The estimated probability of the presence of either species, with 95% confidence intervals, were calculated for each time point during the study (Table 22 and Figure 15). At each time point of the study (-5 to 0), each tooth group (progressing or non-progressing) detection probabilities for each species, were compared against each other (Table 23a). Each time point was also compared, within each tooth group, to time point 0, the final time point in the study, to understand if the probability of each species being present increased as the study progressed (Table 23b). The odds ratios, with 95% confidence intervals, were extracted for all analyses, along with p-values for the comparisons.

As discussed previously, odds ratios are defined as the probability that the event will occur divided by the probability that the event will not occur, and are calculated as $Y/(1-Y)$. They are expressed as a value between 0 and infinity, the higher the ratio the more likely the detected event is to occur. The estimated probability of each species being present, using the two qPCR assays, remained similar at each time point. The estimated probability for the presence of the isolated canine *Trichomonas* sp. ranged between 0.234 and 0.535 (Table 22 and Figure 15), and between 0.319 and 0.654 for the probability of presence of *T. tenax* (Table 22 and Figure 15), across both tooth progression groups. Although a small increase in the probability of occurrence is evident for both species tested as the sample collection times approach early canine periodontal disease, at time point 0 (Figure 15), no differences in the probability odds ratios were calculated (Table 23).

Table 22. Estimated probability of the presence of the isolated canine oral *Trichomonas* sp. and *T. tenax* in progressing (PD_PRESENT) and non-progressing (NO_PD) periodontitis tooth groups, and at time points during the study. Data displays 95% confidence intervals for all detection probabilities.

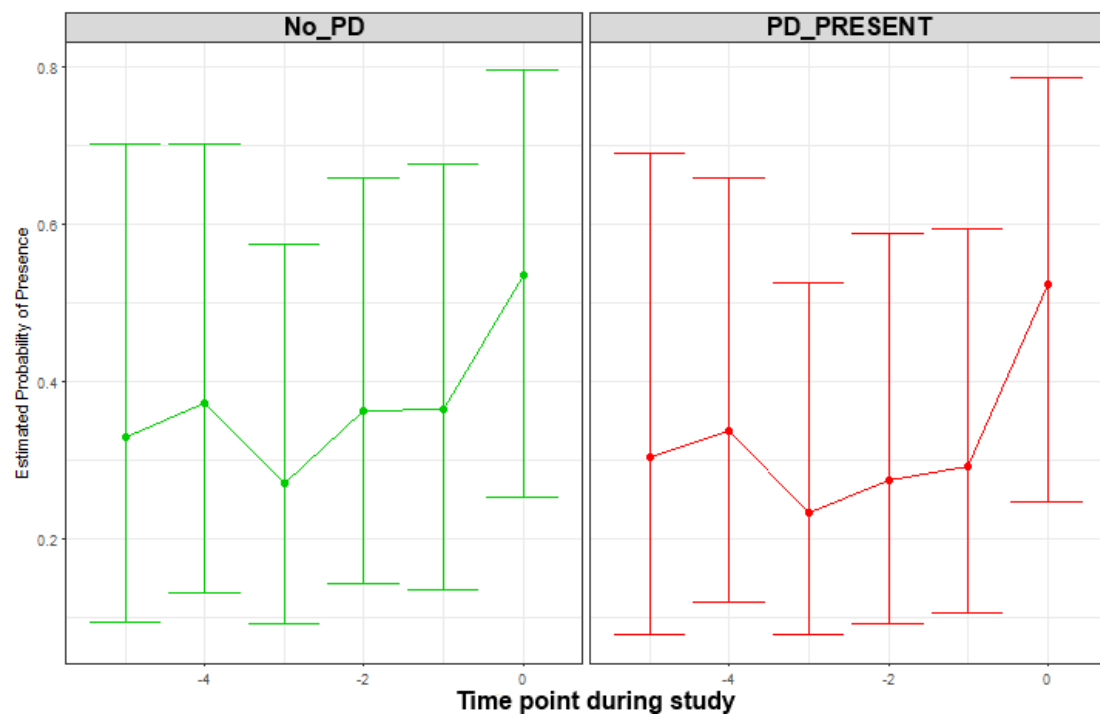
<i>Trichomonas</i> species detected	Tooth group	Time point during study	Estimated Probability of Presence	95% confidence intervals (lower and upper)
<i>Trichomonas</i> sp.	NO_PD	-5	0.330	(0.09, 0.7)
<i>Trichomonas</i> sp.	NO_PD	-4	0.373	(0.13, 0.7)
<i>Trichomonas</i> sp.	NO_PD	-3	0.271	(0.09, 0.57)
<i>Trichomonas</i> sp.	NO_PD	-2	0.362	(0.14, 0.66)
<i>Trichomonas</i> sp.	NO_PD	-1	0.364	(0.14, 0.68)
<i>Trichomonas</i> sp.	NO_PD	0	0.535	(0.25, 0.8)
<i>Trichomonas</i> sp.	PD_PRESENT	-5	0.304	(0.08, 0.69)
<i>Trichomonas</i> sp.	PD_PRESENT	-4	0.338	(0.12, 0.66)
<i>Trichomonas</i> sp.	PD_PRESENT	-3	0.234	(0.08, 0.53)
<i>Trichomonas</i> sp.	PD_PRESENT	-2	0.275	(0.09, 0.59)
<i>Trichomonas</i> sp.	PD_PRESENT	-1	0.293	(0.11, 0.59)
<i>Trichomonas</i> sp.	PD_PRESENT	0	0.523	(0.25, 0.79)
<i>T. tenax</i>	NO_PD	-5	0.483	(0.18, 0.79)
<i>T. tenax</i>	NO_PD	-4	0.403	(0.16, 0.7)
<i>T. tenax</i>	NO_PD	-3	0.491	(0.24, 0.75)
<i>T. tenax</i>	NO_PD	-2	0.440	(0.21, 0.7)
<i>T. tenax</i>	NO_PD	-1	0.354	(0.14, 0.64)
<i>T. tenax</i>	NO_PD	0	0.587	(0.32, 0.81)
<i>T. tenax</i>	PD_PRESENT	-5	0.401	(0.13, 0.74)
<i>T. tenax</i>	PD_PRESENT	-4	0.319	(0.12, 0.62)
<i>T. tenax</i>	PD_PRESENT	-3	0.555	(0.29, 0.79)
<i>T. tenax</i>	PD_PRESENT	-2	0.447	(0.2, 0.73)
<i>T. tenax</i>	PD_PRESENT	-1	0.440	(0.21, 0.7)
<i>T. tenax</i>	PD_PRESENT	0	0.654	(0.38, 0.85)

Tooth groups: NO_PD= non-progressing teeth, PD_PRESENT= teeth progressing to early periodontal disease.

Study time points: -5, -4, -3, -2, -1, and 0 – Chronologically progressing in the study where samples were collected from subjects.

Estimated probability of the presence expressed as a value between 0 and 1.0. The closer this value is to 1.0, the more likely the presence of the species is, in the sample group.

a. Canine *Trichomonas* sp.



b. *T. tenax*

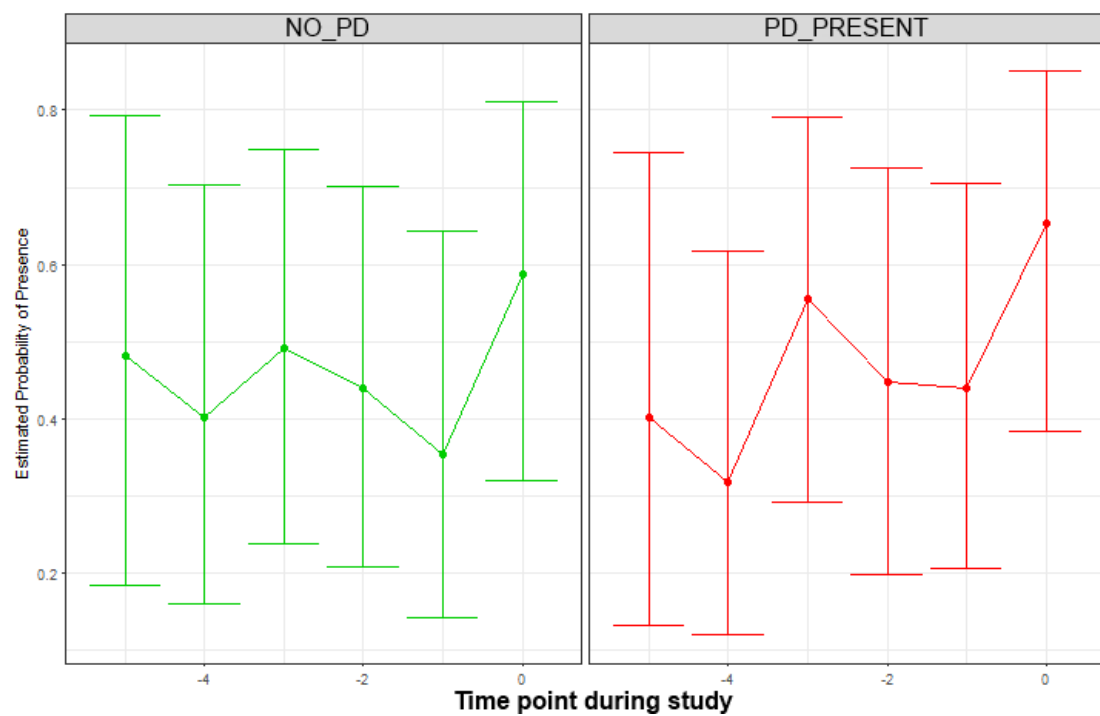


Figure 15. Plotted data for the estimated probability of the presence of **(a)** an isolated canine oral *Trichomonas* sp. and **(b)** *T. tenax* in canine plaque samples collected prior to early stage periodontal disease, Error bars display the 95% confidence intervals calculated for each estimated probability at each time point during the study.

Table 23. Odds ratios for the probability of the detection of the isolated canine *Trichomonas* sp. and *T. tenax*, along with 95% confidence intervals for all comparisons. Any significant *p* values (<0.05) for comparison are displayed with pink shading. **(a)** Presence probabilities were compared in groups of teeth which progress (PD_PRESENT) or do not progress (NO_PD) to early stage periodontal disease. **(b)** Detection probabilities were compared within each tooth group, at each time point against the final time point of the study (time point 0).

a.

Species detected	Tooth group comparison	Time point during study	Odds ratio for probability of presence	95% confidence intervals (lower and upper)	<i>p</i> value
<i>Trichomonas</i> sp	PD_SEEN vs NO_PD	-5	0.89	(0.12, 6.81)	1.0000
<i>Trichomonas</i> sp	PD_SEEN vs NO_PD	-4	0.86	(0.16, 4.57)	1.0000
<i>Trichomonas</i> sp	PD_SEEN vs NO_PD	-3	0.82	(0.17, 3.89)	1.0000
<i>Trichomonas</i> sp	PD_SEEN vs NO_PD	-2	0.67	(0.14, 3.15)	0.9983
<i>Trichomonas</i> sp	PD_SEEN vs NO_PD	-1	0.72	(0.15, 3.4)	0.9998
<i>Trichomonas</i> sp	PD_SEEN vs NO_PD	0	0.95	(0.22, 4.08)	1.0000
<i>T. tenax</i>	PD_SEEN vs NO_PD	-5	0.72	(0.11, 4.9)	1.0000
<i>T. tenax</i>	PD_SEEN vs NO_PD	-4	0.69	(0.13, 3.58)	0.9996
<i>T. tenax</i>	PD_SEEN vs NO_PD	-3	1.29	(0.3, 5.5)	1.0000
<i>T. tenax</i>	PD_SEEN vs NO_PD	-2	1.03	(0.23, 4.58)	1.0000
<i>T. tenax</i>	PD_SEEN vs NO_PD	-1	1.44	(0.32, 6.47)	0.9991
<i>T. tenax</i>	PD_SEEN vs NO_PD	0	1.33	(0.32, 5.59)	0.9998

b.

Species detected	Tooth group	Time point during study	Odds ratio for probability of presence	95% confidence intervals (lower and upper)	<i>p</i> value
<i>Trichomonas</i> sp	NO_PD	0 - -5	2.34	(0.4, 13.75)	0.8629
<i>Trichomonas</i> sp	NO_PD	0 - -4	1.94	(0.39, 9.61)	0.9423
<i>Trichomonas</i> sp	NO_PD	0 - -3	3.10	(0.68, 14.23)	0.3239
<i>Trichomonas</i> sp	NO_PD	0 - -2	2.03	(0.47, 8.84)	0.8603
<i>Trichomonas</i> sp	NO_PD	0 - -1	2.01	(0.43, 9.3)	0.8957
<i>Trichomonas</i> sp	PD_SEEN	0 - -5	2.51	(0.41, 15.47)	0.8207
<i>Trichomonas</i> sp	PD_SEEN	0 - -4	2.15	(0.45, 10.14)	0.8429
<i>Trichomonas</i> sp	PD_SEEN	0 - -3	3.58	(0.79, 16.19)	0.1698
<i>Trichomonas</i> sp	PD_SEEN	0 - -2	2.89	(0.61, 13.66)	0.4413
<i>Trichomonas</i> sp	PD_SEEN	0 - -1	2.65	(0.6, 11.69)	0.5041
<i>T. tenax</i>	NO_PD	0 - -5	1.52	(0.28, 8.26)	0.9988
<i>T. tenax</i>	NO_PD	0 - -4	2.10	(0.44, 10.02)	0.8650
<i>T. tenax</i>	NO_PD	0 - -3	1.47	(0.34, 6.26)	0.9979
<i>T. tenax</i>	NO_PD	0 - -2	1.81	(0.43, 7.54)	0.9402
<i>T. tenax</i>	NO_PD	0 - -1	2.59	(0.57, 11.71)	0.5520
<i>T. tenax</i>	PD_SEEN	0 - -5	2.82	(0.49, 16.18)	0.6363
<i>T. tenax</i>	PD_SEEN	0 - -4	4.03	(0.86, 18.93)	0.1120
<i>T. tenax</i>	PD_SEEN	0 - -3	1.52	(0.36, 6.4)	0.9957
<i>T. tenax</i>	PD_SEEN	0 - -2	2.33	(0.52, 10.53)	0.7061
<i>T. tenax</i>	PD_SEEN	0 - -1	2.41	(0.57, 10.17)	0.6048

Tooth groups: NO_PD= non-progressing teeth, PD_PRESENT= teeth progressing to early periodontal disease. Study time points: -5, -4, -3, -2, -1, and 0 – Chronologically progressing in the study where samples were collected from subjects.

Small increases in overall *Trichomonas* abundance were seen in previous analyses ([section 4.5.1](#)) when comparing teeth that progress into early periodontal disease with teeth that did not progress (Table 19a). Statistically significant increases in *Trichomonas* abundances were observed when comparing the sample collection time points to the latest time point, time point 0 (Table 19b). However, the analysis here analysing individual *Trichomonas* species show no statistically significant differences in the probability of the detection of either. As with previous samples, this may be due to an overall low number of protozoal cells being present in these single tooth samples, which come from teeth prior to the onset of early stage periodontal disease. Analysis of samples that progress to the later stages of periodontal disease may give a better indication as to whether the canine oral *Trichomonas* sp., or *T. tenax*, or both have an influence on the progression of canine periodontal disease.

4.5.4. Covariate analysis of data – exploration of sample metadata

The data set was analysed further to identify if any of the data covariates, age at the start of trial (in weeks), sex, tooth type, tooth location (side of the mouth) and tooth area (of the mouth), have a relationship with the abundance of either organism. This large data set has the information for all of these variables for each animal, making it an excellent data set for an analysis of this type.

These five variables were investigated to assess their relationship with the abundance of either protozoan, in each tooth progression group. Using a linear mixed effects model fitted for each variable, the organism abundance (gene copy number) was modelled against each tooth progression group (progressing or non-progressing teeth), time points during the study (-5 to 0), and the variable of interest. From each model, copy number abundance with 95% confidence intervals, are reported for all combinations of PD group, time relative to PD and the variable of interest (Supplemental Table 12).

For analysis, the fold changes for all covariate comparisons, with 95% confidence intervals, were calculated along with *p* values for the comparisons (Tables 24-29). Table 24 shows the estimated fold changes of abundance for the covariate animal gender, modelled against the abundance of each protozoal species. When comparing the abundance of *E. gingivalis* in male to female animals, fold-change

differences in abundance are suggested at each time point during the study in both tooth progression groups (Table 24), (Fold changes of 0.20 to 0.79-fold) are seen, but none are significant ($p > 0.05$) (Table 24). When comparing the abundance of the *Trichomonas* sp. in male to female animals, greater changes in abundances are seen at time point during the study in both tooth progression groups, comparing to the *E. gingivalis* fold-changes. In both PD groups, *Trichomonas* fold changes of 0.58 to 3.00-fold are observed, but as with *E. gingivalis*, none are significant (Table 24). This covariate does not show any evidence of association with protozoa abundance with this data set.

The next covariate considered was the age of the animal at the start of trial. The data set contained animals that range from 19 to 366 weeks of age at the start of the trial (Supplemental Table 12 and [section 2.2.6](#)). The continuous variable, age (in weeks), was analysed at yearly intervals (52, 104, 156, 208, 260, 312, 364 and 416 weeks) to produced estimated levels of abundance in animals for these ages at the beginning of the study, for each tooth progression group (Supplemental Table 12). For balanced and fair, fold-change comparisons between a younger verses an older age group, only data from animals aged 156 weeks (3 years) at the start of trial were compared to data from animals aged 104 week (2 years) at the start of the study, as this provided the most comprehensive data set for analysis. Table 25 displays the data accumulated from this analysis. When comparing the abundance of *E. gingivalis* in 3 year old to 2 year old animals (age at the start of trial) small changes in abundance in both tooth progression groups are observed (Table 25). Abundance fold changes of 0.72 to 1.30-fold change are observed across both tooth progression groups, however none of the fold changes were statistically significant ($p > 0.05$) (Table 25).

When comparing the abundance of the canine *Trichomonas* sp. in 3 year old to 2 year old animals (age at the start of trial), again a small changes in abundance in both tooth progression groups are seen (fold changes of 0.81 to 1.31-fold change) (Table 25), however none are statistically significant ($p > 0.05$) and therefore these, in addition to the *E. gingivalis* fold changes, show no evidence of the covariate, age at start of trial, having any impact on protozoa abundance.

Table 24. Estimated abundance (gene copy number) fold changes for the canine oral *Trichomonas* sp. (assay TC2) and *E. gingivalis* (assay EG1) using qPCR in sample groups that progress (PD_PRESENT) or do not progress (NO_PD) to early stage periodontal disease. Abundance fold changes for male versus female dogs were compared and 95% confidence intervals were calculated along with *p* values for the comparisons. Any statistically significant fold-changes (*p* value <0.05) for each comparison are highlighted with pink shading.

(Organisms) qPCR assay	Tooth progression group	Time point during study	Comparison Sex (male vs female)	Estimated fold change	95% Confidence intervals (upper and lower)	<i>p</i> value
EG1	NO_PD	-5	M/F	0.32	(0.04, 2.4)	0.42
EG1	NO_PD	-4	M/F	0.71	(0.1, 4.95)	0.99
EG1	NO_PD	-3	M/F	0.70	(0.11, 4.69)	0.99
EG1	NO_PD	-2	M/F	0.79	(0.12, 5.23)	0.99
EG1	NO_PD	-1	M/F	0.55	(0.08, 3.71)	0.88
EG1	NO_PD	0	M/F	0.30	(0.05, 1.98)	0.32
EG1	PD_PRESENT	-5	M/F	0.41	(0.05, 3.14)	0.65
EG1	PD_PRESENT	-4	M/F	0.54	(0.08, 3.68)	0.86
EG1	PD_PRESENT	-3	M/F	0.61	(0.09, 4.02)	0.94
EG1	PD_PRESENT	-2	M/F	0.38	(0.06, 2.57)	0.52
EG1	PD_PRESENT	-1	M/F	0.47	(0.07, 3.09)	0.71
EG1	PD_PRESENT	0	M/F	0.20	(0.03, 1.36)	0.12
TC2	NO_PD	-5	M/F	1.73	(0.35, 8.52)	0.96
TC2	NO_PD	-4	M/F	0.58	(0.14, 2.48)	0.93
TC2	NO_PD	-3	M/F	1.42	(0.37, 5.51)	0.99
TC2	NO_PD	-2	M/F	1.19	(0.31, 4.51)	1.00
TC2	NO_PD	-1	M/F	0.81	(0.2, 3.26)	1.00
TC2	NO_PD	0	M/F	0.66	(0.17, 2.5)	0.98
TC2	PD_PRESENT	-5	M/F	3.00	(0.59, 15.21)	0.37
TC2	PD_PRESENT	-4	M/F	0.72	(0.18, 2.94)	0.99
TC2	PD_PRESENT	-3	M/F	1.19	(0.31, 4.53)	1.00
TC2	PD_PRESENT	-2	M/F	1.06	(0.26, 4.26)	1.00
TC2	PD_PRESENT	-1	M/F	1.15	(0.3, 4.39)	1.00
TC2	PD_PRESENT	0	M/F	0.94	(0.25, 3.61)	1.00

Tooth groups: NO_PD= non-progressing teeth, PD_PRESENT= teeth progressing to early periodontal disease. Study time points: -5, -4, -3, -2, -1, and 0 – Chronologically progressing in the study where samples were collected from subjects.

M/F: Male vs Female fold change comparison.

Table 25. Estimated abundance (gene copy number) fold changes for the canine oral *Trichomonas* sp. (assay TC2) and *E. gingivalis* (assay EG1) using qPCR in sample groups that progress (PD_PRESENT) or do not progress (NO_PD) to early stage periodontal disease. Abundance fold changes for the animal age at the start of the trial (in weeks) were compared (156 week to 104 weeks) and 95% confidence intervals were calculated along with *p* values for the comparisons. Any statistically significant fold-changes (*p* value <0.05) for each comparison are highlighted with pink shading.

(Organism) qPCR assay	Tooth progression group	Time point during study	Comparison (age at beginning of trial, weeks)	Estimated fold change	95% Confidence intervals (upper and lower)	<i>p</i> value
EG1	NO_PD	-5	156/104	0.98	(0.6, 1.61)	1.00
EG1	NO_PD	-4	156/104	1.19	(0.75, 1.89)	0.78
EG1	NO_PD	-3	156/104	1.11	(0.71, 1.75)	0.97
EG1	NO_PD	-2	156/104	0.87	(0.56, 1.37)	0.90
EG1	NO_PD	-1	156/104	1.03	(0.66, 1.61)	1.00
EG1	NO_PD	0	156/104	0.72	(0.46, 1.14)	0.23
EG1	PD_PRESENT	-5	156/104	1.05	(0.64, 1.72)	1.00
EG1	PD_PRESENT	-4	156/104	1.25	(0.79, 1.97)	0.55
EG1	PD_PRESENT	-3	156/104	1.30	(0.83, 2.04)	0.39
EG1	PD_PRESENT	-2	156/104	0.87	(0.55, 1.36)	0.88
EG1	PD_PRESENT	-1	156/104	1.11	(0.71, 1.74)	0.97
EG1	PD_PRESENT	0	156/104	0.97	(0.62, 1.53)	1.00
TC2	NO_PD	-5	156/104	1.26	(0.83, 1.91)	0.62
TC2	NO_PD	-4	156/104	1.31	(0.92, 1.86)	0.24
TC2	NO_PD	-3	156/104	0.81	(0.58, 1.13)	0.46
TC2	NO_PD	-2	156/104	1.01	(0.73, 1.41)	1.00
TC2	NO_PD	-1	156/104	1.01	(0.73, 1.4)	1.00
TC2	NO_PD	0	156/104	0.89	(0.64, 1.24)	0.95
TC2	PD_PRESENT	-5	156/104	0.92	(0.61, 1.4)	0.99
TC2	PD_PRESENT	-4	156/104	1.08	(0.78, 1.51)	0.99
TC2	PD_PRESENT	-3	156/104	1.01	(0.73, 1.39)	1.00
TC2	PD_PRESENT	-2	156/104	1.25	(0.89, 1.74)	0.39
TC2	PD_PRESENT	-1	156/104	1.07	(0.77, 1.47)	0.99
TC2	PD_PRESENT	0	156/104	0.94	(0.67, 1.31)	0.99

Tooth groups: NO_PD= non-progressing teeth, PD_PRESENT= teeth progressing to early periodontal disease. Study time points: -5, -4, -3, -2, -1, and 0 – Chronologically progressing in the study where samples were collected from subjects.

156/104: 156 week to 104 weeks at start of trial age comparison.

The next two covariates assessed, analyse if specific parts of the mouth exhibit a greater abundance of protozoa at the study collection time points (-5 to 0). The first analysis looked at the abundance of either organism in the left or right side of the dog mouth, in each tooth progression group, at time points prior to the onset of early periodontal disease.

Table 26 shows the organism abundance fold changes for each protozoal species in teeth collected from the left side of the mouth, upper and lower jaws, compared to samples collected from right side of the mouth, upper and lower jaws. Estimated fold changes for *E. gingivalis* were seen to range from 0.49 to 2.68, across both tooth progression groups (Table 26). One of these was a statistically significant increase ($p= 0.03$), a 2.68 fold-change, seen in the -2 time point, of teeth that did not progress to periodontal disease (NO_PD) (Table 26). No other significant changes ($p >0.05$) were seen with *E. gingivalis*, and as such there is no clear connection of *E. gingivalis* abundance with the left or right side of the dog mouth. Estimated fold changes for the *Trichomonas* sp. were seen to range from 0.43 to 1.99 fold-change, across both tooth progression groups (Table 26). None were statistically significant and therefore both analyses show no evidence of the covariate left or right side of mouth having any influence on protozoa abundance.

The second spatial analysis looked at the abundance of each organism in the maxilla (upper jaw) verses the mandible (lower jaw) of the dog mouth, in each tooth progression group, at time points during the study (Table 27). Estimated abundance fold changes for *E. gingivalis* were in the range 0.47 to 3.42 fold, across both tooth progression groups and study collection time points (Table 27). One of these was a statistically significant increase ($p= 0.04$), a 3.42 fold-change, seen in the -5 time point of teeth that progressed to periodontal disease (PD_PRESENT) (Table 27). No other significant changes were seen with *E. gingivalis*, and as such there is no clear connection with *E. gingivalis* abundance and an association to the maxilla or mandible jaws of the dog. Estimated fold changes, when comparing the abundance in the maxilla and mandible for the canine *Trichomonas* sp. ranged from 0.49 to 6.94 fold increases, across both tooth progression groups and the study collection time points (Table 27).

Table 26. Estimated abundance (gene copy number) fold changes for the canine oral *Trichomonas* sp. (assay TC2) and *E. gingivalis* (assay EG1) using qPCR in sample groups that progress (PD_PRESENT) or do not progress (NO_PD) to early stage periodontal disease. Abundance fold changes for each organism in either the left or right side of the mouth (upper and lower jaws) were compared, and 95% confidence intervals were calculated along with *p* values for the comparisons. Any statistically significant fold-changes (*p* value <0.05) for each comparison are highlighted with pink shading.

(Organism) qPCR assay	Tooth progression group	Time point during study	Comparison Side of mouth	Estimated fold change	95% Confidence intervals (upper and lower)	<i>p</i> value
EG1	NO_PD	-5	Right/Left	1.95	(0.59, 6.47)	0.72
EG1	NO_PD	-4	Right/Left	0.80	(0.27, 2.4)	0.99
EG1	NO_PD	-3	Right/Left	2.59	(0.98, 6.79)	0.05
EG1	NO_PD	-2	Right/Left	2.68	(1.05, 6.85)	0.03
EG1	NO_PD	-1	Right/Left	1.00	(0.36, 2.76)	1.00
EG1	NO_PD	0	Right/Left	2.48	(0.96, 6.42)	0.07
EG1	PD_PRESENT	-5	Right/Left	1.04	(0.29, 3.73)	1.00
EG1	PD_PRESENT	-4	Right/Left	0.57	(0.2, 1.64)	0.77
EG1	PD_PRESENT	-3	Right/Left	0.49	(0.18, 1.32)	0.36
EG1	PD_PRESENT	-2	Right/Left	0.80	(0.29, 2.19)	0.99
EG1	PD_PRESENT	-1	Right/Left	1.71	(0.63, 4.6)	0.75
EG1	PD_PRESENT	0	Right/Left	0.73	(0.27, 1.97)	0.99
TC2	NO_PD	-5	Right/Left	0.84	(0.21, 3.31)	1.00
TC2	NO_PD	-4	Right/Left	0.87	(0.25, 3.04)	1.00
TC2	NO_PD	-3	Right/Left	0.75	(0.25, 2.25)	0.99
TC2	NO_PD	-2	Right/Left	0.75	(0.26, 2.19)	0.99
TC2	NO_PD	-1	Right/Left	0.43	(0.14, 1.37)	0.34
TC2	NO_PD	0	Right/Left	1.91	(0.65, 5.63)	0.63
TC2	PD_PRESENT	-5	Right/Left	1.73	(0.4, 7.45)	0.97
TC2	PD_PRESENT	-4	Right/Left	1.19	(0.36, 3.96)	1.00
TC2	PD_PRESENT	-3	Right/Left	1.15	(0.37, 3.54)	1.00
TC2	PD_PRESENT	-2	Right/Left	1.99	(0.63, 6.26)	0.63
TC2	PD_PRESENT	-1	Right/Left	1.40	(0.45, 4.34)	0.99
TC2	PD_PRESENT	0	Right/Left	0.80	(0.26, 2.48)	0.99

Tooth groups: NO_PD= non-progressing teeth, PD_PRESENT= teeth progressing to early periodontal disease. Study time points: -5, -4, -3, -2, -1, and 0 – Chronologically progressing in the study where samples were collected from subjects.

Right/Left: Right vs Left side of mouth comparison.

Table 27. Estimated abundance (gene copy number) fold changes for the canine oral *Trichomonas* sp. (assay TC2) and *E. gingivalis* (assay EG1) using qPCR in sample groups that progress (PD_PRESENT) or do not progress (NO_PD) to early stage periodontal disease. Abundance fold changes for each organism in either the Maxilla or Mandible jaws were compared, and 95% confidence intervals were calculated along with *p* values for the comparisons. Any statistically significant fold-changes (*p* value <0.05) for each comparison are highlighted with pink shading

(Organism) qPCR assay	Tooth progression group	Time point during study	Comparison	Estimated fold change	95% Confidence intervals (upper and lower)	<i>p</i> value
EG1	NO_PD	-5	Maxilla/Mandible	0.91	(0.28, 2.9)	1.00
EG1	NO_PD	-4	Maxilla/Mandible	0.47	(0.17, 1.34)	0.38
EG1	NO_PD	-3	Maxilla/Mandible	1.74	(0.68, 4.42)	0.67
EG1	NO_PD	-2	Maxilla/Mandible	2.33	(0.94, 5.79)	0.08
EG1	NO_PD	-1	Maxilla/Mandible	1.27	(0.45, 3.56)	0.99
EG1	NO_PD	0	Maxilla/Mandible	1.08	(0.42, 2.74)	1.00
EG1	PD_PRESENT	-5	Maxilla/Mandible	3.42	(1.02, 11.45)	0.04
EG1	PD_PRESENT	-4	Maxilla/Mandible	1.08	(0.41, 2.83)	1.00
EG1	PD_PRESENT	-3	Maxilla/Mandible	1.04	(0.43, 2.52)	1.00
EG1	PD_PRESENT	-2	Maxilla/Mandible	0.80	(0.31, 2.06)	0.99
EG1	PD_PRESENT	-1	Maxilla/Mandible	1.95	(0.8, 4.73)	0.32
EG1	PD_PRESENT	0	Maxilla/Mandible	2.16	(0.89, 5.27)	0.14
TC2	NO_PD	-5	Maxilla/Mandible	0.82	(0.22, 3.03)	1.00
TC2	NO_PD	-4	Maxilla/Mandible	1.73	(0.54, 5.59)	0.90
TC2	NO_PD	-3	Maxilla/Mandible	6.94	(2.43, 19.81)	0.00001
TC2	NO_PD	-2	Maxilla/Mandible	1.81	(0.65, 5.03)	0.69
TC2	NO_PD	-1	Maxilla/Mandible	0.70	(0.22, 2.22)	0.99
TC2	NO_PD	0	Maxilla/Mandible	1.08	(0.38, 3.1)	1.00
TC2	PD_PRESENT	-5	Maxilla/Mandible	0.49	(0.12, 1.89)	0.80
TC2	PD_PRESENT	-4	Maxilla/Mandible	1.98	(0.67, 5.88)	0.58
TC2	PD_PRESENT	-3	Maxilla/Mandible	1.90	(0.7, 5.12)	0.54
TC2	PD_PRESENT	-2	Maxilla/Mandible	0.60	(0.21, 1.74)	0.88
TC2	PD_PRESENT	-1	Maxilla/Mandible	0.69	(0.25, 1.87)	0.98
TC2	PD_PRESENT	0	Maxilla/Mandible	4.79	(1.75, 13.08)	0.0001

Tooth groups: NO_PD= non-progressing teeth, PD_PRESENT= teeth progressing to early periodontal disease. Study time points: -5, -4, -3, -2, -1, and 0 – Chronologically progressing in the study where samples were collected from subjects.

Maxilla/Mandible: Maxilla vs Mandible jaws of mouth comparison.

Two of these changes were increases in abundance and were statistically significant, seen at the -3 time point (6.94-fold increase, $p= 0.00001$) of teeth that did not progress to periodontal disease (NO_PD), and the 0 time point (a 4.70-fold increase, $p= 0.0001$) of teeth that did progress to periodontal disease (PD_PRESENT) (Table 27). Although two significant increases were seen in the data set, they are not connected by time point or tooth progression group and cannot be used to conclude an association of the maxilla or mandible with *Trichomonas* sp. abundance.

The final covariate analysis was of the abundance of both protozoan species at all study time points and both tooth progression groups, and searched for any association with the tooth types. The abundance of each species was estimated in the incisor, canine, molar, and premolar teeth of all animals in the data set. Every tooth abundance estimate was compared to each other, and calculated any fold changes and statistical differences across all comparisons (Tables 28 and 29). In teeth that did not progress to periodontal disease (NO_PD), the fold change in abundance of *E. gingivalis* across all study time points, ranged from 0.31 to 10.20-fold in the incisor/canine comparison, 0.78 to 5.55-fold in the molar/canine comparison, 0.35 to 3.94-fold in the molar/incisor comparison, 0.75 to 4.33-fold in the premolar/canine comparison, 0.24 to 3.08-fold in the premolar/incisor comparison, and 0.62 to 1.37-fold in the premolar to molar comparison (Table 28, assay EG1 data). No statistically significant fold changes were observed for *E. gingivalis*. However, the general trend seen was fold changes increasing as the study collection time points were closer to early periodontal disease (time point 0). This trend was especially evident where molar and premolar teeth were involved in the comparisons (Table 28, assay EG1 data and Supplemental Table 12).

In teeth that did not progress to periodontal disease (NO_PD), the fold changes in abundance for *Trichomonas* sp. across all study collection time points ranged from; 0.19 to 7.12-fold in the incisor/canine comparison, 6.13 to 29.84-fold in the molar/canine comparison, 1.95 to 55.20-fold in the molar/incisor comparison, 4.30 to 20.62-fold in the premolar/canine comparison, 2.90 to 62.06-fold in the premolar/incisor comparison, and 0.50 to 1.34-fold in the premolar to molar comparison (Table 28, assay TC2 data).

Table 28. Estimated abundance (gene copy number) fold changes for the canine oral *Trichomonas* sp. (assay TC2) and *E. gingivalis* (assay EG1) using qPCR in a sample group that did not progress (NO_PD) to early stage periodontal disease. Abundance fold changes for each organism in tooth types within the mouth were compared, and 95% confidence intervals were calculated along with *p* values for the comparisons. Any statistically significant fold-changes (*p* value <0.05) for each comparison are highlighted with pink shading.

(Organism) qPCR assay	Tooth progression group	Time point during study	Comparison	Estimated fold change	95% Confidence intervals (upper and lower)	<i>p</i> value
EG1	NO_PD	-5	Incisor/Canine	0.31	(0.01, 8.76)	0.99
EG1	NO_PD	-4	Incisor/Canine	2.08	(0.09, 46.96)	1.00
EG1	NO_PD	-3	Incisor/Canine	10.20	(0.54, 191.18)	0.32
EG1	NO_PD	-2	Incisor/Canine	1.06	(0.06, 19.18)	1.00
EG1	NO_PD	-1	Incisor/Canine	0.52	(0.02, 12.79)	1.00
EG1	NO_PD	0	Incisor/Canine	1.41	(0.08, 25.01)	1.00
EG1	NO_PD	-5	Molar/Canine	0.78	(0.05, 11.92)	1.00
EG1	NO_PD	-4	Molar/Canine	2.88	(0.27, 31.32)	0.99
EG1	NO_PD	-3	Molar/Canine	3.57	(0.34, 37.62)	0.92
EG1	NO_PD	-2	Molar/Canine	1.69	(0.17, 16.84)	1.00
EG1	NO_PD	-1	Molar/Canine	1.11	(0.13, 9.37)	1.00
EG1	NO_PD	0	Molar/Canine	5.55	(0.74, 41.68)	0.20
EG1	NO_PD	-5	Molar/Incisor	2.52	(0.23, 28.14)	0.99
EG1	NO_PD	-4	Molar/Incisor	1.39	(0.13, 14.62)	1.00
EG1	NO_PD	-3	Molar/Incisor	0.35	(0.04, 2.84)	0.96
EG1	NO_PD	-2	Molar/Incisor	1.59	(0.2, 12.9)	1.00
EG1	NO_PD	-1	Molar/Incisor	2.13	(0.15, 30.32)	1.00
EG1	NO_PD	0	Molar/Incisor	3.94	(0.39, 40.12)	0.84
EG1	NO_PD	-5	Premolar/Canine	0.75	(0.04, 13.2)	1.00
EG1	NO_PD	-4	Premolar/Canine	1.78	(0.14, 23.38)	1.00
EG1	NO_PD	-3	Premolar/Canine	2.44	(0.19, 31.08)	0.99
EG1	NO_PD	-2	Premolar/Canine	1.57	(0.13, 18.85)	1.00
EG1	NO_PD	-1	Premolar/Canine	1.51	(0.15, 15.3)	1.00
EG1	NO_PD	0	Premolar/Canine	4.33	(0.47, 39.96)	0.67
EG1	NO_PD	-5	Premolar/Incisor	2.43	(0.18, 32.71)	0.99
EG1	NO_PD	-4	Premolar/Incisor	0.86	(0.06, 11.28)	1.00
EG1	NO_PD	-3	Premolar/Incisor	0.24	(0.02, 2.46)	0.79
EG1	NO_PD	-2	Premolar/Incisor	1.48	(0.15, 14.98)	1.00
EG1	NO_PD	-1	Premolar/Incisor	2.91	(0.17, 48.87)	0.99
EG1	NO_PD	0	Premolar/Incisor	3.08	(0.24, 38.64)	0.99
EG1	NO_PD	-5	Premolar/Molar	0.96	(0.18, 5.05)	1.00
EG1	NO_PD	-4	Premolar/Molar	0.62	(0.13, 2.86)	1.00
EG1	NO_PD	-3	Premolar/Molar	0.68	(0.16, 2.84)	1.00
EG1	NO_PD	-2	Premolar/Molar	0.93	(0.23, 3.75)	1.00
EG1	NO_PD	-1	Premolar/Molar	1.37	(0.32, 5.75)	1.00
EG1	NO_PD	0	Premolar/Molar	0.78	(0.19, 3.17)	1.00
TC2	NO_PD	-5	Incisor/Canine	0.58	(0.01, 24.44)	1.00
TC2	NO_PD	-4	Incisor/Canine	0.67	(0.02, 20.88)	1.00
TC2	NO_PD	-3	Incisor/Canine	7.12	(0.28, 182.38)	0.83
TC2	NO_PD	-2	Incisor/Canine	1.28	(0.05, 32.72)	1.00
TC2	NO_PD	-1	Incisor/Canine	0.82	(0.02, 29.48)	1.00
TC2	NO_PD	0	Incisor/Canine	0.19	(0.01, 4.47)	0.95
TC2	NO_PD	-5	Molar/Canine	6.13	(0.29, 128.08)	0.85
TC2	NO_PD	-4	Molar/Canine	9.76	(0.74, 128.98)	0.15
TC2	NO_PD	-3	Molar/Canine	13.90	(1.09, 176.59)	0.03
TC2	NO_PD	-2	Molar/Canine	5.98	(0.48, 75.26)	0.56
TC2	NO_PD	-1	Molar/Canine	29.84	(2.91, 305.89)	0.0001
TC2	NO_PD	0	Molar/Canine	10.44	(1.21, 90.26)	0.01
TC2	NO_PD	-5	Molar/Incisor	10.50	(0.67, 163.42)	0.20
TC2	NO_PD	-4	Molar/Incisor	14.48	(1, 209)	0.04
TC2	NO_PD	-3	Molar/Incisor	1.95	(0.18, 21.23)	1.00
TC2	NO_PD	-2	Molar/Incisor	4.67	(0.43, 50.57)	0.73
TC2	NO_PD	-1	Molar/Incisor	36.20	(1.74, 751.11)	0.005
TC2	NO_PD	0	Molar/Incisor	55.20	(3.98, 766.13)	0.00001
TC2	NO_PD	-5	Premolar/Canine	8.21	(0.35, 191.78)	0.67
TC2	NO_PD	-4	Premolar/Canine	6.10	(0.39, 95.82)	0.70
TC2	NO_PD	-3	Premolar/Canine	20.62	(1.38, 309.17)	0.01
TC2	NO_PD	-2	Premolar/Canine	4.30	(0.29, 63.09)	0.93
TC2	NO_PD	-1	Premolar/Canine	14.98	(1.27, 176.18)	0.01
TC2	NO_PD	0	Premolar/Canine	11.74	(1.14, 120.58)	0.02
TC2	NO_PD	-5	Premolar/Incisor	14.06	(0.79, 250.47)	0.11
TC2	NO_PD	-4	Premolar/Incisor	9.05	(0.52, 156.28)	0.37
TC2	NO_PD	-3	Premolar/Incisor	2.90	(0.22, 37.95)	0.99
TC2	NO_PD	-2	Premolar/Incisor	3.36	(0.26, 43.13)	0.98
TC2	NO_PD	-1	Premolar/Incisor	18.18	(0.78, 422.79)	0.11
TC2	NO_PD	0	Premolar/Incisor	62.06	(3.83, 1004.72)	0.0001
TC2	NO_PD	-5	Premolar/Molar	1.34	(0.21, 8.68)	1.00
TC2	NO_PD	-4	Premolar/Molar	0.63	(0.11, 3.44)	1.00
TC2	NO_PD	-3	Premolar/Molar	1.48	(0.31, 7.08)	1.00
TC2	NO_PD	-2	Premolar/Molar	0.72	(0.16, 3.3)	1.00
TC2	NO_PD	-1	Premolar/Molar	0.50	(0.1, 2.41)	0.99
TC2	NO_PD	0	Premolar/Molar	1.12	(0.24, 5.2)	1.00

Many of these fold change increases were statistically significant, see Molar/Canine, Molar/Incisor, Premolar/Canine, and Premolar/Incisor comparisons (Table 28, TC2 data, pink shading), and these statistically significant values are more prominent in time points closer to early periodontal disease (time point 0) and in molar and premolar teeth comparisons (Table 28 TC2 data and Supplemental Table 12).

In teeth that progressed to early periodontal disease (PD_PRESENT), the fold changes in abundance of *E. gingivalis*, across all study time points, ranged from 0.59 to 41.13-fold in the incisor/canine comparison, 0.80 to 138.30-fold in the molar/canine comparison, 0.35 to 5.90-fold in the molar/incisor comparison, 0.28 to 78.66-fold in the premolar/canine comparison, 0.12 to 27.78-fold in the premolar/incisor comparison, and 0.34 to 4.71-fold in the premolar to molar comparison (Table 29). Many of these fold change increases were statistically significant, see Molar/Canine, Premolar/Canine, Premolar/Incisor and Premolar/Molar comparisons (Table 29, EG1 data, pink shading), and are again more prominent in time points closer to early periodontal disease (time point 0), and in molar and premolar teeth comparisons (Table 29 EG1 data and Supplemental Table 12). Also in teeth that progress to periodontal disease (PD_PRESENT), fold changes in the abundance of *Trichomonas* sp. across all study time points, ranged from; 0.68 to 16.43-fold in the incisor/canine comparison, 3.78 to 45.07-fold in the molar/canine comparison, 0.78 to 10.34-fold in the molar/incisor comparison, 5.55 to 81.11-fold in the premolar/canine comparison, 1.11 to 25.71-fold in the premolar/incisor comparison, and 0.24 to 3.56-fold in the premolar to molar comparison (Table 29). Many of these fold changes were statistically significant, see Molar/Canine, Premolar/Canine, and Premolar/Incisor comparisons (Table 29, TC2 data, pink shading), and as with data seen in the above tooth comparisons, are more prominent in time points closer to early periodontal disease (time point 0), and in molar and premolar teeth comparisons (Table 29 TC2 data and Supplemental Table 12).

Statistically significant differences are clearly evident in many of the tooth abundance comparisons seen above. This tooth comparison data convey the collective message that both *E. gingivalis* and the canine *Trichomonas* sp. are more abundant in molar and premolar teeth of dogs and their numbers are more likely to

increase as the tooth progresses towards early periodontal disease (Tables 28 and 29 and Supplemental Table 12). This is less evident with *E. gingivalis* in this data set, maybe due to the abundance of *E. gingivalis* being lower in pre-periodontal disease samples ([section 3.5](#), and (Patel et al., 2017)). The reasons for the increased numbers of protozoa in molar and premolar teeth is currently unknown. However it has been seen that molars and premolar teeth in dogs have higher rates of periodontal disease incidence and also progress more quickly from a healthy state to disease (Marshall et al., 2014). The data collected here contributes to answering the question, do canine oral protozoa contribute to the onset of periodontal disease or are they opportunistically taking advantage of the changed environment? More work is required to answer this question, such as the analysis of canine samples that progress further into the later irreversible stages of periodontal disease.

Table 29. Estimated abundance (gene copy number) fold changes for the canine oral *Trichomonas* sp. (assay TC2) and *E. gingivalis* (assay EG1) using qPCR in a sample group that progressed (PD_SEEN) to early stage periodontal disease. Abundance fold changes for each organism in tooth types within the mouth were compared, and 95% confidence intervals were calculated along with *p* values for the comparisons. Any statistically significant fold-changes (*p* value <0.05) for each comparison are highlighted with pink shading.

(Organism) qPCR assay	Tooth progression group	Time point during study	Comparison	Estimated fold change	95% Confidence intervals (upper and lower)	<i>p</i> value
EG1	PD_SEEN	-5	Incisor/Canine	41.13	(0.6, 2819.8)	0.16
EG1	PD_SEEN	-4	Incisor/Canine	0.71	(0.04, 12.59)	1.00
EG1	PD_SEEN	-3	Incisor/Canine	2.29	(0.13, 41.82)	1.00
EG1	PD_SEEN	-2	Incisor/Canine	2.98	(0.15, 58.14)	0.99
EG1	PD_SEEN	-1	Incisor/Canine	12.73	(0.67, 241.71)	0.18
EG1	PD_SEEN	0	Incisor/Canine	0.59	(0.03, 12.05)	1.00
EG1	PD_SEEN	-5	Molar/Canine	138.30	(4.03, 4745.82)	0.0002
EG1	PD_SEEN	-4	Molar/Canine	1.51	(0.19, 11.78)	1.00
EG1	PD_SEEN	-3	Molar/Canine	0.80	(0.09, 6.83)	1.00
EG1	PD_SEEN	-2	Molar/Canine	5.99	(0.69, 52.25)	0.24
EG1	PD_SEEN	-1	Molar/Canine	14.81	(1.8, 121.92)	0.001
EG1	PD_SEEN	0	Molar/Canine	3.47	(0.35, 34.68)	0.92
EG1	PD_SEEN	-5	Molar/Incisor	3.36	(0.22, 50.83)	0.99
EG1	PD_SEEN	-4	Molar/Incisor	2.13	(0.2, 22.34)	1.00
EG1	PD_SEEN	-3	Molar/Incisor	0.35	(0.04, 3.39)	0.98
EG1	PD_SEEN	-2	Molar/Incisor	2.01	(0.19, 20.75)	1.00
EG1	PD_SEEN	-1	Molar/Incisor	1.16	(0.11, 11.86)	1.00
EG1	PD_SEEN	0	Molar/Incisor	5.90	(0.61, 57.33)	0.34
EG1	PD_SEEN	-5	Premolar/Canine	78.66	(2.04, 3030.53)	0.004
EG1	PD_SEEN	-4	Premolar/Canine	0.89	(0.09, 8.35)	1.00
EG1	PD_SEEN	-3	Premolar/Canine	0.28	(0.03, 2.9)	0.91
EG1	PD_SEEN	-2	Premolar/Canine	6.92	(0.64, 74.4)	0.27
EG1	PD_SEEN	-1	Premolar/Canine	34.70	(3.46, 348)	0.00001
EG1	PD_SEEN	0	Premolar/Canine	16.33	(1.38, 193.48)	0.01
EG1	PD_SEEN	-5	Premolar/Incisor	1.91	(0.11, 34.23)	1.00
EG1	PD_SEEN	-4	Premolar/Incisor	1.25	(0.1, 15.98)	1.00
EG1	PD_SEEN	-3	Premolar/Incisor	0.12	(0.01, 1.44)	0.20
EG1	PD_SEEN	-2	Premolar/Incisor	2.32	(0.18, 30.05)	1.00
EG1	PD_SEEN	-1	Premolar/Incisor	2.73	(0.22, 34.14)	0.99
EG1	PD_SEEN	0	Premolar/Incisor	27.78	(2.37, 324.9)	0.0005
EG1	PD_SEEN	-5	Premolar/Molar	0.57	(0.11, 2.98)	0.99
EG1	PD_SEEN	-4	Premolar/Molar	0.59	(0.13, 2.56)	0.99
EG1	PD_SEEN	-3	Premolar/Molar	0.34	(0.08, 1.4)	0.39
EG1	PD_SEEN	-2	Premolar/Molar	1.15	(0.26, 5.08)	1.00
EG1	PD_SEEN	-1	Premolar/Molar	2.34	(0.58, 9.47)	0.80
EG1	PD_SEEN	0	Premolar/Molar	4.71	(1.19, 18.64)	0.01
TC2	PD_SEEN	-5	Incisor/Canine	8.79	(0.08, 1024.97)	0.99
TC2	PD_SEEN	-4	Incisor/Canine	1.10	(0.05, 25.85)	1.00
TC2	PD_SEEN	-3	Incisor/Canine	16.43	(0.64, 418.99)	0.18
TC2	PD_SEEN	-2	Incisor/Canine	2.57	(0.1, 67.5)	1.00
TC2	PD_SEEN	-1	Incisor/Canine	0.68	(0.03, 17.85)	1.00
TC2	PD_SEEN	0	Incisor/Canine	4.36	(0.14, 131.18)	0.99
TC2	PD_SEEN	-5	Molar/Canine	6.87	(0.13, 363.97)	0.98
TC2	PD_SEEN	-4	Molar/Canine	7.91	(0.87, 71.63)	0.09
TC2	PD_SEEN	-3	Molar/Canine	17.22	(1.73, 171.64)	0.002
TC2	PD_SEEN	-2	Molar/Canine	22.84	(2.23, 234.35)	0.0006
TC2	PD_SEEN	-1	Molar/Canine	3.78	(0.38, 37.83)	0.89
TC2	PD_SEEN	0	Molar/Canine	45.07	(3.57, 569.67)	0.00001
TC2	PD_SEEN	-5	Molar/Incisor	0.78	(0.03, 17.55)	1.00
TC2	PD_SEEN	-4	Molar/Incisor	7.22	(0.5, 104.06)	0.46
TC2	PD_SEEN	-3	Molar/Incisor	1.05	(0.08, 14.09)	1.00
TC2	PD_SEEN	-2	Molar/Incisor	8.88	(0.63, 125.22)	0.25
TC2	PD_SEEN	-1	Molar/Incisor	5.54	(0.4, 76.86)	0.72
TC2	PD_SEEN	0	Molar/Incisor	10.34	(0.76, 140.18)	0.14
TC2	PD_SEEN	-5	Premolar/Canine	9.79	(0.17, 566.41)	0.91
TC2	PD_SEEN	-4	Premolar/Canine	28.16	(2.68, 295.92)	0.0002
TC2	PD_SEEN	-3	Premolar/Canine	42.75	(3.54, 516.02)	0.00001
TC2	PD_SEEN	-2	Premolar/Canine	5.55	(0.45, 68.56)	0.63
TC2	PD_SEEN	-1	Premolar/Canine	11.45	(0.97, 135.09)	0.05
TC2	PD_SEEN	0	Premolar/Canine	81.11	(5.62, 1170.99)	0.00001
TC2	PD_SEEN	-5	Premolar/Incisor	1.11	(0.04, 28.21)	1.00
TC2	PD_SEEN	-4	Premolar/Incisor	25.71	(1.56, 424.4)	0.007
TC2	PD_SEEN	-3	Premolar/Incisor	2.60	(0.16, 41.78)	1.00
TC2	PD_SEEN	-2	Premolar/Incisor	2.16	(0.13, 36.29)	1.00
TC2	PD_SEEN	-1	Premolar/Incisor	16.78	(1.04, 271.79)	0.04
TC2	PD_SEEN	0	Premolar/Incisor	18.61	(1.2, 289.03)	0.02
TC2	PD_SEEN	-5	Premolar/Molar	1.43	(0.22, 9.24)	1.00
TC2	PD_SEEN	-4	Premolar/Molar	3.56	(0.7, 18.09)	0.36
TC2	PD_SEEN	-3	Premolar/Molar	2.48	(0.53, 11.67)	0.87
TC2	PD_SEEN	-2	Premolar/Molar	0.24	(0.05, 1.24)	0.18
TC2	PD_SEEN	-1	Premolar/Molar	3.03	(0.66, 14.01)	0.51
TC2	PD_SEEN	0	Premolar/Molar	1.80	(0.4, 8.09)	0.99

CHAPTER 5: IDENTIFICATION OF ORAL PROTISTS IN CANINE TOTAL RNA ISOLATED FROM PLAQUE

Introduction

Oral protists have been identified in canine plaque and reported in [chapter 3](#), using methods which rely on complementary oligonucleotide hybridisations to target sequences (PCR). Existing nucleotide sequences were used to design these PCR primers, which bind to their targets and allow the amplification of DNA for identification purposes. The nucleotide sequences used for primer design were obtained from sequence databases that contain known organisms (Benson et al., 2014). The reliance on existing sequences for primer design introduces a significant weakness for the design process, because the primers can only be targeted towards these known sequences. Any target sequences present in samples that are not considered during the primer design process, due to a lack of candidate sequence availability, may be missed by the amplification protocol, especially if its target regions are significantly different to the sequences used for the primer design. The potential to miss unknown, present organisms in the sample has been demonstrated before (Klindworth et al., 2013, Poretsky et al., 2014).

The primary aim of this thesis is to identify the protozoa present in the canine mouth and to assess their relationship to canine periodontal disease. To date, very few published reports are available on this topic, so the protozoa anticipated in the canine mouth were predicted based on literature describing protozoa present in other mammalian mouths, such as *Trichomonas tenax* (Marty et al., 2017a) or *Entamoeba gingivalis* (Yazar et al., 2016). Although basing the PCR primer design on existing protozoan sequences yielded the identification of two previously unknown occupants of the canine mouth, there is still a good chance that other protozoa not considered during the primer design steps, or completely novel species, are present in the canine mouth and are not detected by the PCR protocol. PCR primers may also show a priming bias towards particular sequences and may overestimate or underestimate abundance (Tremblay et al., 2015, Kennedy et al., 2014). To address these weaknesses with PCR-based methods, a protozoa identification technique not based on the use of pre-existing sequence information and PCR was devised. This method was based on the sequencing of ribosomal RNA (rRNA) extracted from plaque samples. All eukaryotic microorganisms (and

prokaryotes) contain genes coding for RNA molecules that contribute to the structure and function of protein synthesising cellular ribosomes (Adl et al., 2012). Sequencing of these rRNA molecules can aid in the identification of all organism (prokaryotes and eukaryotes) within the sample, as all produce these RNAs for normal cellular function (Wilson and Doudna Cate, 2012). As this is a blind sequencing approach, all organisms present should be detected, as opposed to the primer based methods that use pre-existing sequences for the design of priming oligonucleotides.

This rRNA based identification method was used here to survey canine plaque samples obtained from animals with a healthy oral state and comparing to samples obtained from animals with severe canine periodontal disease (> periodontal disease stage 2). For sequencing of extracted RNA, a portable, commercially available benchtop real-time sequencer, a MinION device (Jain et al., 2016), was employed. The device is manufactured by Oxford Nanopore Technologies and is currently the only sequencing device capable of producing long-read, real-time, RNA sequence reads on the benchtop (Jain et al., 2016).

Results and discussion

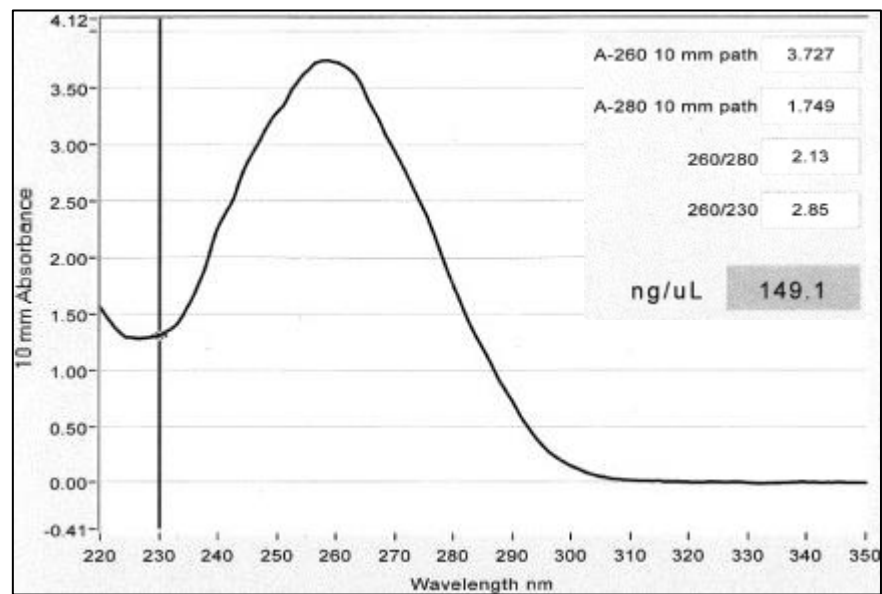
5.1. Canine plaque collection from WALTHAM (Health) and client owned (Disease) dogs and total RNA extractions

Canine plaque samples were collected from animals with a healthy oral state ([section 2.3.1](#)) and from those having a diseased oral state ([section 2.3.2](#)). The healthy samples were collected from 26 animals residing at the WALTHAM® Centre for Pet Nutrition over a four week period. Animals housed at WALTHAM, of good oral health as assessed through regular dental screening, were used for the plaque collections (Table 7). 15 of these samples were identified, pooled and underwent extraction of total RNA ([section 2.3.1](#)). Samples were also collected from animals with moderate to severe periodontal disease (PD2 or above) for comparison. These samples were collected from client owned animals visiting external veterinary practitioners for a variety of procedures or ailments, related and unrelated to periodontal disease ([section 2.3.2](#)). Both 15-dog pooled plaque samples, after a further purification step ([section 2.3.3](#)), produced high quality total RNA samples of sufficient concentration for sequencing (Figure 16).

5.2. Bacterial ribosomal RNA depletion

Total RNA extractions contain not only ribosomal RNAs, but also mRNAs, tRNAs, and a range of other small and less well understood RNA species (Vickers et al., 2015). The largest portion of a total RNA sample consists of ribosomal RNA, and from plaque samples this will be comprised mainly of bacterial large and small subunit RNA. This bacterial RNA can overwhelm and conceal other organism sequences, because only a limited number of sequence reads per sample can be achieved. To help enrich for protozoan sequences, a method was devised to help eliminate the bacterial ribosomal RNA and therefore increase the proportion of other RNA species for sequencing. The MICROBExpress™ Bacterial mRNA Enrichment Kit (ThermoFisher Scientific, UK) was employed to remove these unwanted RNAs.

(a) Health sample



(b) Disease sample

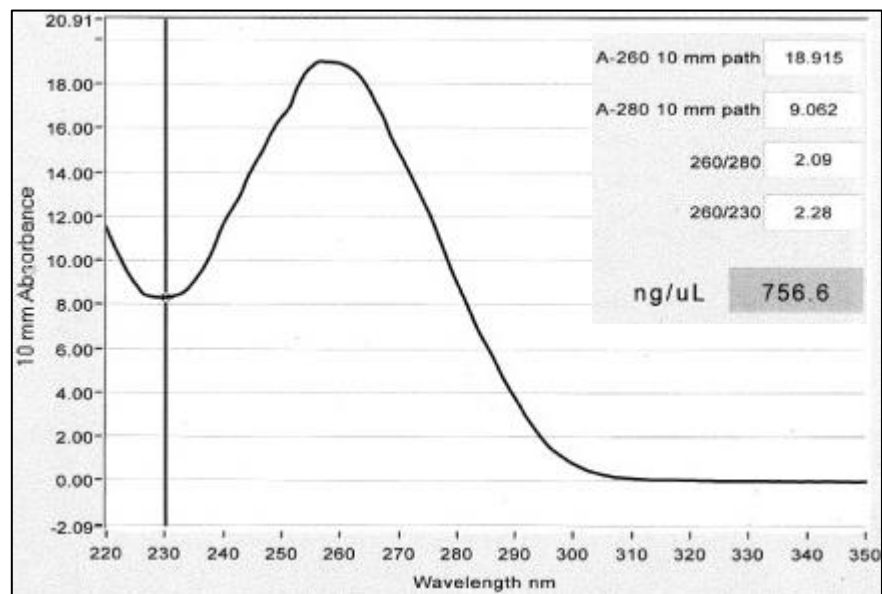


Figure 16. Total RNA extracted from 15-dog pooled canine plaque samples from **(a)** animals with a good oral health state, and **(b)** animals with moderate to severe periodontal disease ($> PD2$). Analysis with a Nanodrop spectrophotometer show clear 260 nm RNA peak is visible in both traces and low 230 peaks (contaminants) are also indicative of the purity of the extractions. Both extractions produced, high quality RNA, of sufficient concentration for sequencing.

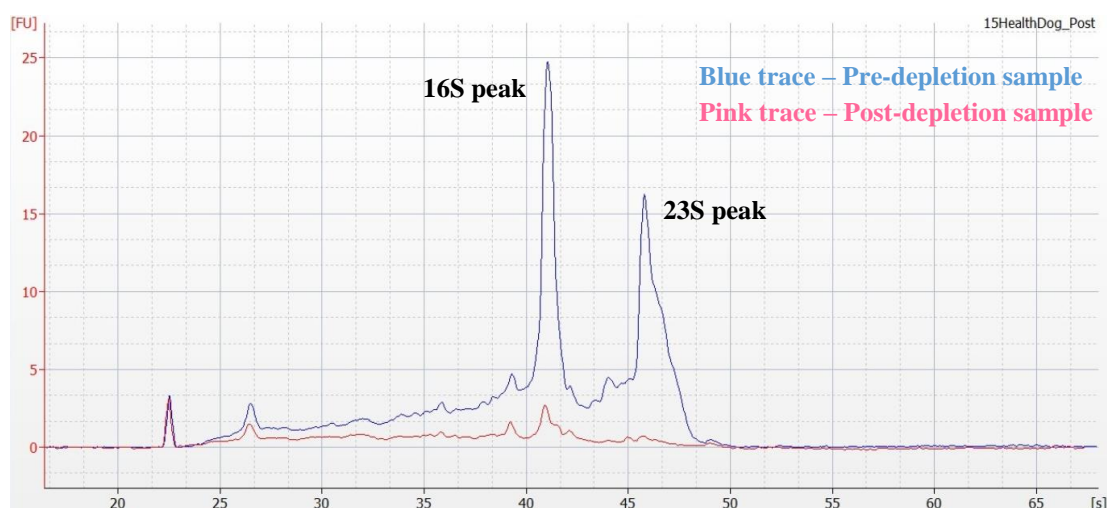
The system is more commonly used to enrich for mRNA sequences from bacterial total RNA by using proprietary bead-bound oligonucleotides, complementary to bacterial large (23S) and small (16S) subunit RNA sequences, to bind to and remove these bacterial ribosomal RNAs (Peano et al., 2013).

For the plaque total RNA samples, the enrichment kit was used with a modified protocol to remove the bacteria 16S and 23S ribosomal sequences that would mask the sequencing, potentially concealing lower proportion eukaryotic sequences ([section 2.3.5](#)). Figure 17 displays bioanalyser traces for pre- and post-depleted total RNA samples from both the Health and Disease plaque pools. Typical prominent (23S) and small-subunit (16S) RNA species peaks are seen in the pre-depleted samples (Figure 17 a and b - blue traces), and these peaks are reduced to closer to baseline levels in the post-depleted samples (Figure 17 a and b - pink traces). The remaining peaks in the post-depleted traces (Figure 17 a and b - pink traces) smaller bacterial ribosomal sequences, bacterial and eukaryotic mRNA, eukaryotic ribosomal RNA and other small RNAs. This reduced bacterial ribosomal load improved the sample for sequencing of protozoan RNA, which may have been missed in a complete total RNA sample.

5.3. MinION™ sequencing of 16S/23S depleted total rRNA using barcoded 2D cDNA sequencing

For sequencing of 16S/23S depleted RNA samples, the Oxford Nanopore Technologies 2D cDNA sequencing protocol for the SQK-NSK007 reagent kit and barcoding EXP-NDB002 protocol was used. Each depleted RNA samples (Health and Disease) was subjected to a step-wise, modified protocol which initially required the samples to undergo reverse transcription to cDNA. For this type of MinION™ sequence processing and protocol, reverse transcription greatly increase sequencing throughput and accuracy (Garalde et al., 2018). Post reverse transcription, to enable sequencing of both samples on the same sequencing flow cell, the sample sequences were individually barcoded using the EXP-NDB002 and protocol. In addition to the two depleted samples, the 16S/23S sequences depleted from each ([section 2.3.5](#)), were also barcoded and sequenced on the flow cell run.

(a) Health sample



(b) Disease sample

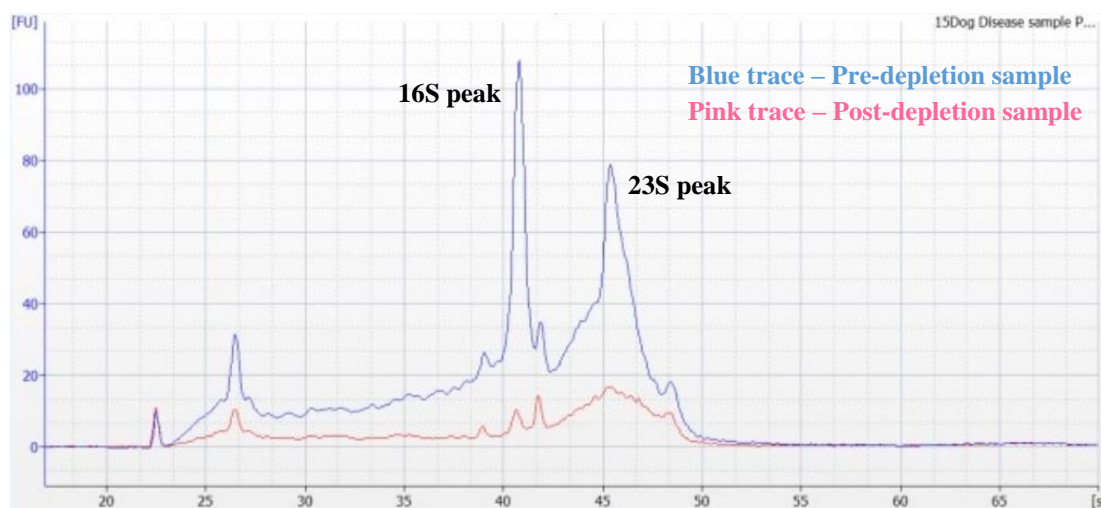


Figure 17. Bioanalyser electropherograms showing the depletion of bacterial 16S and 23S RNA. Depletion of samples was undertaken using the MICROBExpress™ Bacterial mRNA Enrichment Kit (ThermoFisher Scientific, UK), from pooled canine plaque total RNA extractions. In both **(a)** Health and **(b)** Disease samples, bacterial 16S and 23S RNA species peaks of pre-depleted total RNA (blue traces) are reduced to near baseline levels in post-depleted samples (pink traces).

To obtain these additional samples, the captured depleted sequences were eluted from their complementary oligonucleotide probes/magnetic beads (used to remove the 16S/23S sequences from the total RNA). These additional samples were sequenced for another study, and are not further discussed here. However, the presence of these samples in the sequencing run reduce the sequencing throughput and read numbers, and therefore are mentioned at this point.

The samples were processed for sequencing using a MinION™ SQK007 reagent kit and loaded onto a FLO-MIN105 flow cell. Sequences identified by the MinION™ run were analysed using Metrichor analysis website using the 2D Basecalling plus Barcoding for FLO-MIN105 250bps work flow (123683), Rev 1.125.

142473 reads were generated by the sequencing run, producing a total yield of approximately 162 million bases (Table 30). This is the total number of sequences identified by the workflow and consist of both template and complement reads (1D reads) from the sequencing run (Benitez-Paez et al., 2016). These reduced quality 1D reads (Benitez-Paez et al., 2016) had an average quality score of 5.8, an average read length of 1140 bases, and a longest read of 151.62 thousand bases (Table 30). These extremely long reads are likely to be either genomic DNA contaminants or ligations of multiple reads produced in error during the sample processing (Benitez-Paez et al., 2016).

Table 30. Statistics for MinION™ cDNA sequencing run (1D reads) of 16S/23S depleted total rRNA samples. Reads were transferred to the Metrichor automated analysis pipeline and processed using the 1D Basecalling plus Barcoding for FLO-MIN105 250bps work flow (123683), Rev 1.125.

Statistic	Count
Read Count	142473
Total Yield	162.47 M Bases
Sequence Length - Average	1.14 K bases
Sequence Length - Median	523 bases
Sequence Length - Mode	784 bases
Longest Read	151.62 K bases
QScore - Average	5.8
QScore - Median	5.9
QScore - Mode	3.6

Sequences that had both a template and complement read (separated by the hairpin adaptor – [section 2.3.6](#)) were then further aligned and processed by the analysis workflow to produce high quality 2D reads. These reads had a lower error rate and underwent mismatch correction by aligning both template and complement reads. The automated Metrichor analysis identified 90411 high quality 2D sequences. These higher quality 2D reads produced a total yield of approximately 26 million bases and had an average quality score of 10.5, an average read length of 593 bases, and a longest read of 89.93 thousand bases (Table 31). Although the average read length of the 2D reads was lower than the 1D reads, their average quality scores are nearly double. This increased read quality made the 2D reads more accurate for taxonomic assignment of reads.

Table 31. Statistics for MinION™ cDNA sequencing run (2D reads) of 16S/23S depleted total rRNA samples. Reads were transferred to the Metrichor automated analysis pipeline and processed using the 2D Basecalling plus Barcoding for FLO-MIN105 250bps work flow (123683), Rev 1.125.

Statistic	Count
Read Count	90411
Total Yield	26.38 M Bases
Sequence Length - Average	593 bases
Sequence Length - Median	330 bases
Sequence Length - Mode	275 bases
Longest Read	83.93 K bases
QScore - Average	10.5
QScore - Median	10.5
QScore - Mode	11.4

Of the higher quality 2D reads, 32938 reads were identified as containing an identifiable sequencing barcode. The barcodes were applied to each sample during the sample processing steps. For the two samples of interest, 11422 sequences were found to contain the Health sample barcode, NB01, and 5143 sequences were found with the Disease sample barcode, NB03 (Table 32). Both sets of sequences were analysed using BLAST+ analysis against the SILVA 128 SSURef sequence database (Quast et al., 2013) ([section 2.3.8](#)). From this analysis, two distinct protist

genera were identified in the two sample types. Protozoan sequences belonging to the genus *Entamoeba* made up 1.71 % of the Health RNA (cDNA) sample and 4.61 % of the Disease RNA (cDNA) sample (Table 32). Protozoan sequences belonging to the genus *Trichomonas* made up 2.03 % of the Health RNA (cDNA) sample and 1.52 % of the Disease RNA (cDNA) sample (Table 32).

Table 32. Total numbers of MinION cDNA sequencing reads and percentages for *Trichomonas* sp. and *Entamoeba* sp. Sequences were identified to taxonomic groups from pooled Health or Disease, 16S/23S depleted, RNA samples using a MinION cDNA sequencing protocol and BLAST+ assignment of sequence taxonomy against the SILVA 128 SSURef sequences.

Sample	Total number of reads in sample	<i>Trichomonas</i> sp.		<i>Entamoeba</i> sp.	
		Number of reads	Percentage of total reads (%)	Number of reads	Percentage of total reads (%)
Health sample (NB01)	11422	232	2.03	195	1.71
Disease sample (NB03)	5143	78	1.52	237	4.61

Statistical analysis of the sequence numbers was undertaken using two-sample binomial tests with a normal approximation ([section 2.3.9](#)). The proportion of sequences for each protozoan identified for each health state and the difference in proportions between the two groups, along with 95% confidence intervals, were calculated (Table 33 and Figure 18).

The proportion of *Trichomonas* sequences were found to reduce between the two samples, whereas the proportion of *Entamoeba* sequences increased, with both changes found to be significantly different (Table 33).

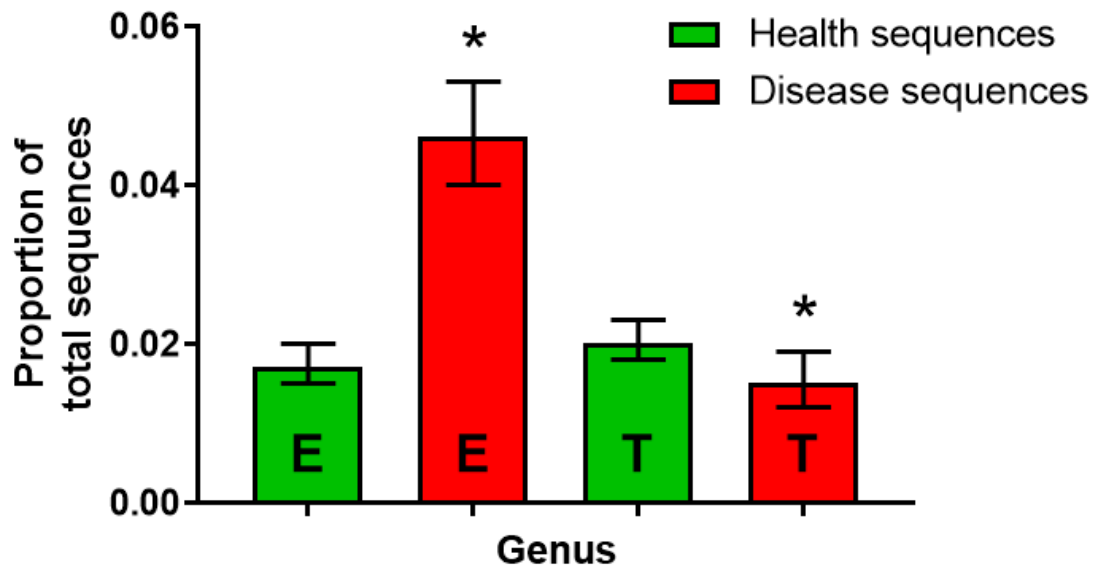


Figure 18. Proportion of *Trichomonas* sp. (T) and *Entamoeba* sp. (E) sequences found in pooled Health or Disease, 16S/23S depleted, RNA samples using a MinION cDNA sequencing protocol and BLAST+ assignment of sequence taxonomy against the SILVA 128 SSURef database. The chart displays the proportion of positively identified sequences from the total number of sequences for each sample. Asterisks indicate significantly different samples. Black bars indicate the upper and lower confidence intervals for the proportions.

Table 33. Total sequences proportions (a) and odds ratios (b), with confidence intervals (C.I) for *Trichomonas* sp. and *Entamoeba* sp. sequences found in pooled Health or Disease 16S/23S depleted RNA samples. Binomial statistical analysis was conducted to analyse the proportion of trichomonads and Entamoebae in the Health sample sequences compared to the proportion of sequences found in the Disease sample. C.I's and *p* values were calculated for each odds comparison using the test. Pink shading indicates a statistically significant difference observed.

(a)

Species	Sample	Proportion of sequences found	95% C.I Lower	95% C.I Upper
<i>Trichomonas</i> sp.	Disease	0.015	0.012	0.019
<i>Trichomonas</i> sp.	Health	0.02	0.018	0.023
<i>Entamoeba</i> sp.	Disease	0.046	0.04	0.053
<i>Entamoeba</i> sp.	Health	0.017	0.015	0.02

(b)

Species	Odds Ratio for sequence proportions	Odds 95% C.I Lower	Odds 95% C.I Upper	Standard Error of mean	<i>p</i> -value
<i>Trichomonas</i> sp.	0.743	0.573	0.962	0.132	0.024
<i>Entamoeba</i> sp.	2.781	2.294	3.372	0.098	<0.001

5.4. Direct MinION™ sequencing of total RNA extracted from canine plaque for the identification of protozoa

To directly sequence total RNA samples taken from canine plaque, the Oxford Nanopore Technologies Direct RNA Sequencing protocol, with reagent kit SQK-RNA001, was used. The current methodology involves initially adding Poly (A) tails to sequences from total RNA extractions and then reverse transcribing complementary strands of the poly (A) tailed sequences (Garalde et al., 2018). This reverse transcription process improved the sequencing throughput and efficiency and is currently recommended for effective RNA sequencing (Garalde et al., 2018). After reverse transcription, sequencing adapters were added to enable tethering of sequences to the sequencing nanopores of the flow cells. In contrast to the MinION™ cDNA sequencing ([section 2.3.6](#) and [section 5.3](#)), the direct RNA sequencing of each sample was undertaken on separate flow cells, without the use of barcoding. Barcoding and pooling of RNA samples for running on the same flow cell is currently unavailable. The samples were processed for sequencing using a MinION SQK-RNA001 reagent kit and loaded onto a FLO-MIN106 (R9.4 version) flow cell. Sequences produced by from MinION were analysed using the MinKNOW software (Oxford Nanopore Technologies, UK) using the NC_48H_sequencing_FLO-MIN106_SQK-RNA001_plus_Basecaller script, and live base calling feature.

841,687 and 682,578 RNA reads for the Health and Disease samples, respectfully, were generated by the sequencing runs, producing a total yield of approximately 496 million bases for the Health sample, and 229 million bases for the disease sample (Table 34 and Table 35). As with all next-generation sequencing technologies, the raw data set produced by the sequencer contained sequences of varying quality {Mardis, 2008 #1260. The post-nanopore sequencing processing software Nanofilt (Decoster, 2018) was used to perform this task on these datasets. Prior to Nanofilt processing, the median, mean and N50 (minimum length of the top 50% of reads) read length of the Health sample read dataset was found to be 335, 589 and 1,083 base pairs, respectfully (Table 34 and Figure 19a).

Table 34. Summary statistics of sequences obtained from Direct MinION™ RNA sequencing of total RNA obtained from a canine Health pooled plaque sample. Pre- and Post-NanoFilt software (Decoster, 2018) processing statistics indicate the success of NanoFilt at concentrating high quality reads for downstream analysis.

(a) Pre- and Post-NanoFilt sequence statistics		
	Pre-NanoFilt processing	Post NanoFilt processing
Number of reads:	841,687	367,895
Total bases:	495,847,190	372,749,479
Median read length:	335	976
Mean read length:	589	1,013
Read length N50:	1,083	1,146

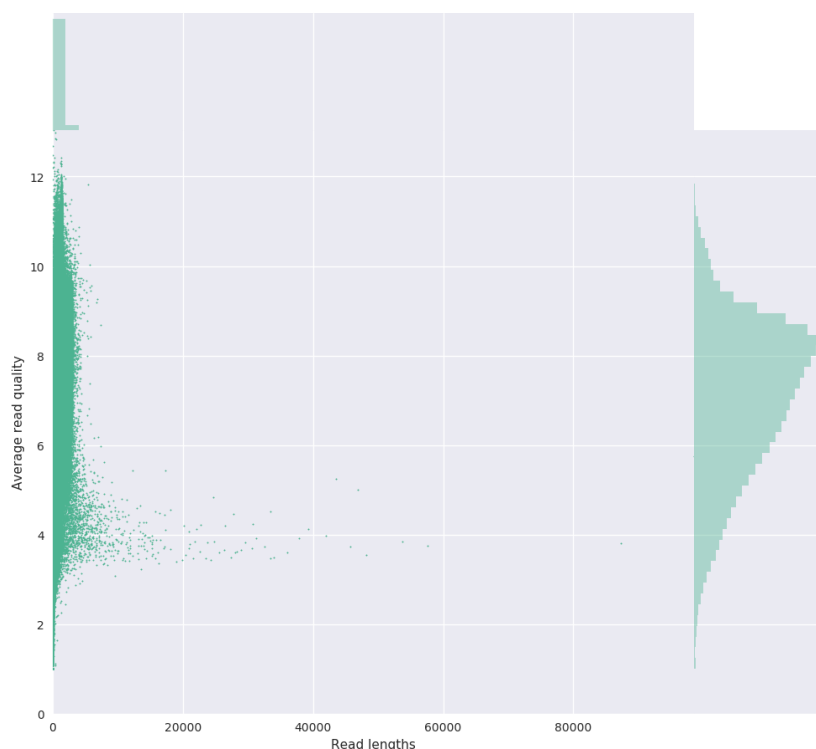
(b) Top 5 longest reads and their mean base call quality score		
	Pre-NanoFilt processing	Post-NanoFilt processing
1	98,582 (5.75)	2,499 (8.97)
2	87,292 (3.81)	2,499 (7.26)
3	57,660 (3.75)	2,499 (7.74)
4	53,698 (3.85)	2,499 (8.66)
5	48,175 (3.54)	2,499 (9.03)

(c) Top 5 highest mean base call quality scores and their read lengths		
	Pre-NanoFilt processing	Post-NanoFilt processing
1	112 (13.04)	516 (12.82)
2	387 (12.99)	1,306 (12.42)
3	367 (12.85)	1,284 (12.34)
4	516 (12.82)	1,100 (12.31)
5	5 (12.68)	1,327 (12.29)

NanoFilt was then used to process the dataset, to concentrate the dataset for reads greater than 400 base pairs and of a sequence quality score of greater than 4. Post-Nanofilt processing, the Health sample dataset quality scores were improved to a median, mean and N50 read length of 976, 1,013 and 1,146 base pairs, respectfully (Table 34 and Figure 19b). This improved dataset then consisted of 367,895 reads and a total yield of approximately 373 million bases.

The same Nanofilt processing was also applied to the Disease sample dataset.

(a) Health sample pre-NanoFilt Read lengths vs Average read quality



(b) Health sample post-NanoFilt Read lengths vs Average read quality

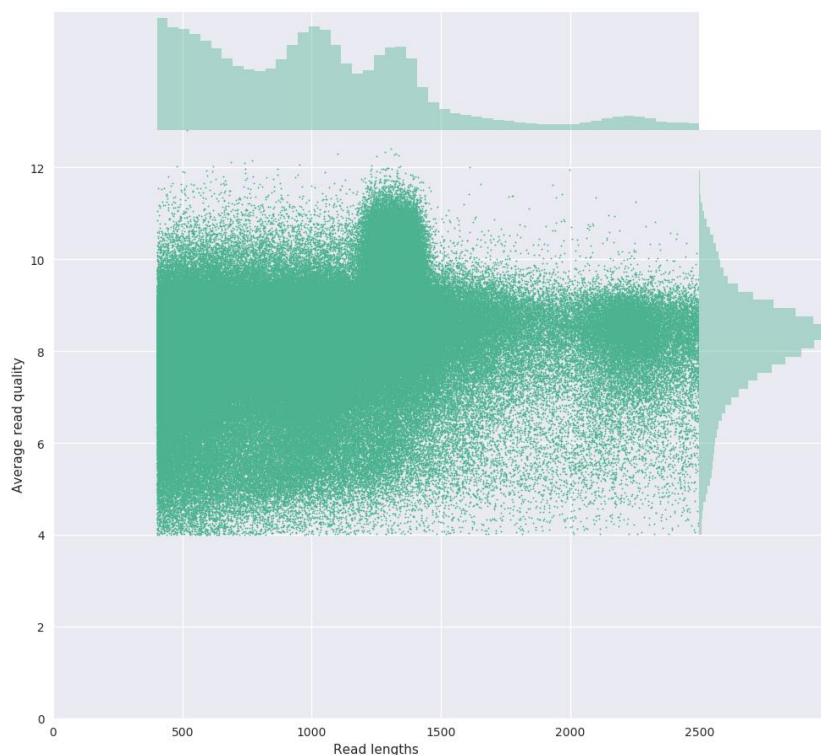


Figure 19. Dot plots of Pre- and Post-NanoFilt software (Decoster, 2018) processed Direct MinION™ RNA sequencing reads obtained from total RNA of a canine Health pooled plaque sample. **(a)** Pre-NanoFilt, the dataset comprised of reads that span quality scores from 2 to 12, a mean read length of 589, and a read length N50 of 1,083 base pairs. **(b)** Nanofilt processing improved the median, mean and N50 read lengths of the dataset. Post-Nanofilt the dataset comprised of reads that span quality scores from 4 to 12, a mean read length of 1,013, and a read length N50 of 1,146 base pairs.

Prior to Nanofilt processing, the median, mean and N50 (minimum length of the top 50% of reads) read length of the Disease sample dataset was 164, 335 and 692 base pairs, respectfully (Table 35 and Figure 20a). Post-Nanofilt processing, the disease sample dataset quality scores were improved to a median, mean and N50 read length of 804, 898 and 1,071 base pairs, respectively (Table 35 and Figure 20b). This improved dataset then consisted of 148,900 reads and a total yield of approximately 134 million bases.

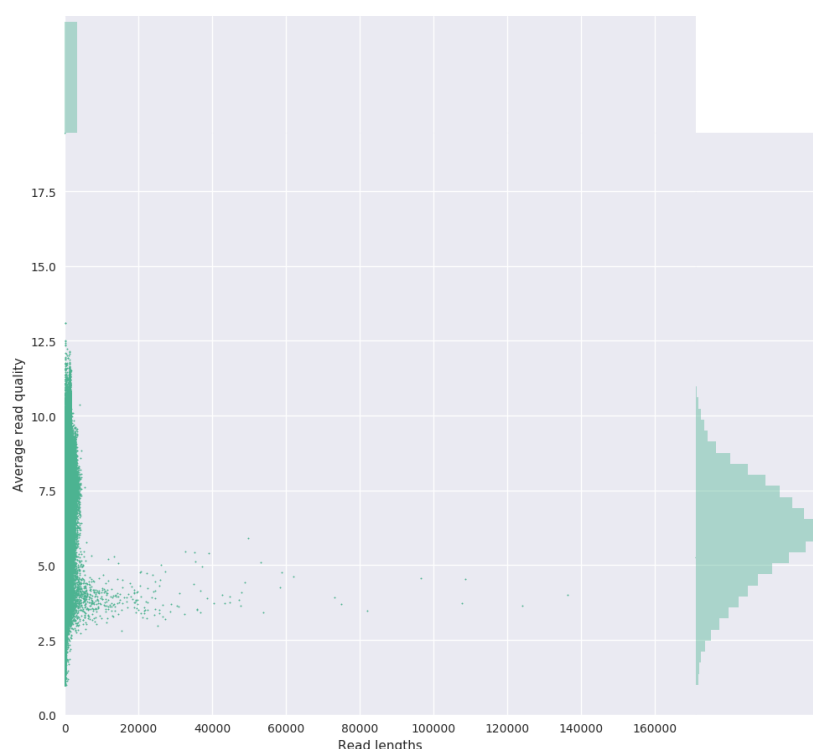
Table 35. Summary statistics of sequences obtained from Direct MinION™ RNA sequencing of total RNA obtained from a canine Disease pooled plaque sample. Pre- and Post-NanoFilt software (Decoster, 2018) processing statistics indicate the success of NanoFilt at concentrating high quality reads for downstream analysis.

(a) Pre- and Post-NanoFilt sequence statistics		
	Pre-NanoFilt processing	Post NanoFilt processing
Number of reads:	682,578	148,900
Total bases:	228,677,349	133,749,037
Median read length:	164	804
Mean read length:	335	898
Read length N50:	692	1,071

(b) Top 5 longest reads and their mean base call quality score		
	Pre-NanoFilt processing	Post-NanoFilt processing
1	170,959 (5.26)	2,499 (7.73)
2	136,339 (4.02)	2,498 (8.04)
3	123,981 (3.63)	2,498 (5.07)
4	108,523 (4.55)	2,498 (6.70)
5	107,706 (3.72)	2,498 (6.98)

(c) Top 5 highest mean base call quality scores and their read lengths		
	Pre-NanoFilt processing	Post-NanoFilt processing
1	6 (19.46)	723 (12.23)
2	74 (13.09)	1,329 (12.16)
3	84 (13.09)	1,365 (12.11)
4	70 (12.50)	1,321 (12.06)
5	72 (12.49)	731 (12.02)

(a) Disease sample pre-NanoFilt Read lengths vs Average read quality



(b) Disease sample post-NanoFilt Read lengths vs Average read quality



Figure 20. Dot plots of Pre- and Post-NanoFilt software (Decoster, 2018) processed Direct MinION™ RNA sequencing reads obtained from total RNA of a canine Disease pooled plaque sample. **(a)** Pre-NanoFilt, the dataset comprised of reads that span quality scores from 1 to 12, a mean read length of 335, and a read length N50 of 692 base pairs. **(b)** Nanofilt processing improved the median, mean and N50 read lengths of the dataset. Post-Nanofilt the dataset comprised of reads that span quality scores from 4 to 12, a mean read length of 898, and a read length N50 of 1,071 base pairs.

Both sequence datasets, improved by Nanofilt post-processing, were analysed using BLAST+ analysis against the SILVA 132 SSURef sequence database (Quast et al., 2013) ([section 2.3.8](#)). From this analysis, and as with the MinION™ cDNA sequencing, two distinct protist genera were identified in both two sample types. From the Health dataset, 293,151 sequences were identified to genus/species level using the BLAST+ analysis. From the Disease dataset, 119,190 sequences were identified to genus/species level. Protozoan sequences belonging to the genus *Entamoeba* made up 0.18 % of the Health RNA sample and 0.31 % of the Disease RNA sample (Table 36). Protozoan sequences belonging to the genus *Trichomonas* made up 0.17 % of the Health RNA sample and 0.18 % of the Disease RNA sample (Table 36).

Table 36. Total numbers of Direct MinION™ RNA sequencing reads and percentages for *Trichomonas* sp. and *Entamoeba* sp. Sequences were identified to taxonomic groups from pooled Health or Disease total RNA samples using a Direct MinION™ RNA sequencing protocol and BLAST+ assignment of sequence taxonomy against the SILVA 132 SSURef sequences.

Sample	Total number of reads in sample	<i>Trichomonas</i> sp.		<i>Entamoeba</i> sp.	
		Number of reads	Percentage of total reads (%)	Number of reads	Percentage of total reads (%)
Health sample	293,151	493	0.17	526	0.18
Disease sample	119,190	211	0.18	367	0.31

Statistical analysis of the sequence numbers was undertaken using two-sample binomial tests with a normal approximation ([section 2.3.9](#)). The proportion of sequences for each protist identified for each health state and the difference in abundance between the two groups, along with 95% confidence intervals were calculated (Table 37 and Figure 21).

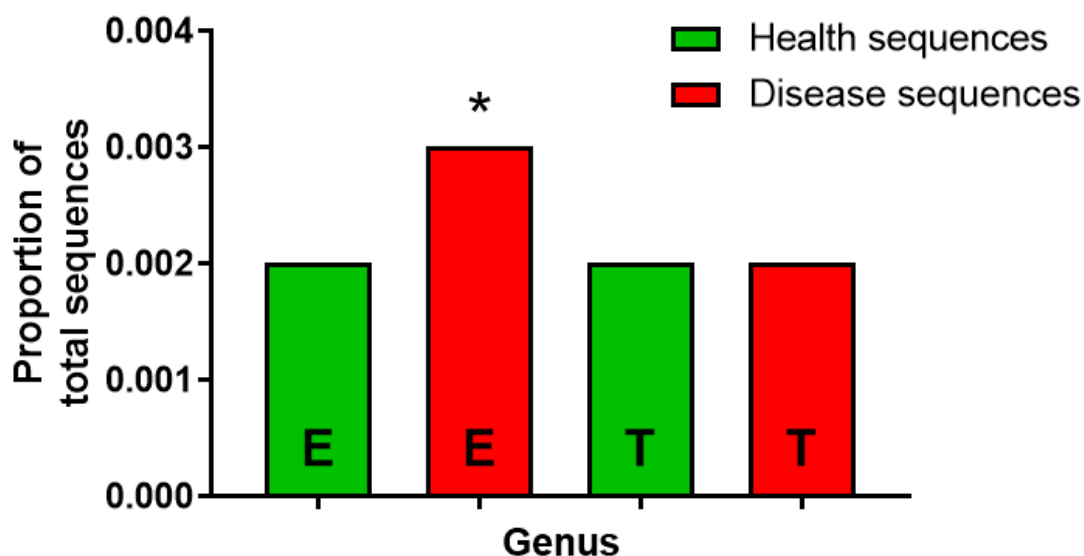


Figure 21. Proportion of *Trichomonas* sp. (T) and *Entamoeba* sp. (E) sequences found in pooled Health or Disease total RNA samples using a Direct MinION™ RNA sequencing protocol and BLAST+ assignment of sequence taxonomy against the SILVA 132 SSURef database. The chart displays the proportion of positively identified sequences from the total number of sequences for each sample type. Asterisks indicate significantly different samples. Black bars indicate the upper and lower confidence intervals for the proportions.

Table 37. Total sequences proportions (a) and odds ratios (b), with confidence intervals (C.I) for *Trichomonas* sp. and *Entamoeba* sp. sequences found in pooled Health or Disease total RNA samples. Binomial statistical analysis was conducted to analyse the proportion of trichomonads and Entamoebae in the Health sample sequences compared to the proportion of sequences found in the Disease sample. C.I's and *p* values were calculated for each odds comparison using the binomial test. Pink shading indicates a statistically significant difference observed.

(a)

Species	Sample	Proportion of sequences found	95% C.I Lower	95% C.I Upper
<i>Trichomonas</i> sp.	Disease	0.002	0.002	0.002
<i>Trichomonas</i> sp.	Health	0.002	0.002	0.002
<i>Entamoeba</i> sp.	Disease	0.003	0.003	0.003
<i>Entamoeba</i> sp.	Health	0.002	0.002	0.002

(b)

Species	Odds Ratio for sequence proportions	Odds 95% C.I Lower	Odds 95% C.I Upper	Standard Error of mean	<i>p</i> value
<i>Trichomonas</i> sp.	1.053	0.896	1.237	0.082	0.532
<i>Entamoeba</i> sp.	1.718	1.504	1.964	0.068	<0.001

The proportion of *Trichomonas* sequences found in each dataset were found to remain the same using Direct MinION™ RNA sequencing, whereas the proportion of *Entamoeba* sequences increased (Table 37 and Figure 21). When these proportions were compared between samples, the two-sample binomial test analysis found a significant difference between the *Entamoeba* sp. proportions in each sample type but no clear difference with the *Trichomonas* sp. sequences (Table 37 b).

5.5. Comparison of total RNA sequencing techniques

High throughput sequencing technologies have evolved considerably over the past few years. After the withdrawal of Roche's 454 sequencing technology in 2008 (Heather and Chain, 2016), a single market leader emerged, allowing cost effective sequencing of short amplicons. Illumina's next generation sequencing platform is now the "go-to" technology for short read, high-throughput sequencing. Although Illumina sequencing protocols, more specifically their MiSeq platform, are relatively cost effective, the sequence read lengths produced still remain short, marketed as 2 X 300 base pairs per read, but in reality are closer to 2 X 150 base pair reads, on average. For metagenomic sequencing purposes however, read length and accuracy can be crucial for successful identification of organisms to species level (Burke and Darling, 2016).

Oxford Nanopore Technologies' MinION™ platform provides a rapid, laboratory and field based sequencing platform, and is capable of ultra-long (hundreds of kilobases), accurate read lengths, all produced in real-time (Mikheyev and Tin, 2014). The company have developed several DNA sequencing protocols over that last few years and now market techniques for whole genome sequencing and shorter read sequencing such as 16S amplicons. These shorter read sequencing protocols require PCR steps which can introduce biases into the dataset (Aird et al., 2011). To combat this, they have recently released direct RNA protocols and reagents that allow the sequencing of ribonucleic acids without introducing PCR amplification bias and also enable the elucidation of epigenetic topology. These protocols are still a work in progress, but are of certain to be useful techniques that will no doubt soon rival the current leading high-throughput sequencing providers.

For this part of the project, two Oxford Nanopore Technologies protocols were tested for the purposes of identifying protozoa in canine plaque samples, with minimal or no bias introduced by the technique. The first method tested, MinION™ cDNA sequencing was used to sequence total RNA samples that were fully reverse transcribed to cDNA. A bacterial ribosomal depletion step was also added before the reverse transcription to maximise sequencing throughput for the target sequences of interest. This depletion step was successful at removing a large proportion of 16S/23S sequences (Figure 17), however the bacterial sequences remaining were sufficient to sequester a large proportion of the sequencing capacity. The sequences were also barcoded to enable higher throughput of samples though a single flow cell, allowing a significant cost saving. However, this barcoding step was found to be inefficient, with only 32,938 barcoded reads found from a total 142,473 reads obtained from the MinION™ sequencer (Tables 30-32).

The bacterial depletion and barcoding steps require further optimisation to improve the protocol. Despite these issues, protozoan sequences were detected at sufficient number for analysis (Figure 18). As seen previously in this thesis, both *Trichomonas* and *Entamoeba* were found to be the only protozoa present in samples. The proportion of *Trichomonas* sequences decreased in the disease sample in comparison to the Health sample, whereas the proportion of *Entamoeba* sequences increased. When these proportions were compared between samples using statistical methods ([section 2.3.9](#)), significant differences between both samples were found (Table 33).

The second method tested, Direct MinION™ RNA sequencing, involved the direct sequencing of RNA molecules in samples, with little pre-processing and therefore minimal processing biases. Although a first strand cDNA synthesis was undertaken during sample processing for increased efficiency and throughput reasons, the RNA strand is sequenced by the MinION™. The sequencing of the cDNA strand is used to improve accuracy of the reads obtained. The Direct MinION™ RNA sequencing technique resulted in hundreds of thousands of reads and total sequencing yields in the hundreds of megabases (Table 34 and Table 35). The raw reads contained a mixed dataset of varying read lengths and quality. To concentrate for reads of the correct length (18S reads) and of high quality, NanoFilt software was used to process the samples ([section 2.3.7](#)). NanoFilt was successfully used to significantly

improve the dataset read lengths and quality scores (Tables 34-35 and Figures 19-20).

The resultant Health and Disease sample sequences were BLAST+ analysed ([section 2.3.8](#)) and seen with the cDNA sequencing previously, both *Trichomonas* and *Entamoeba* were found to be the only protozoa present in the samples (Table 36). The proportion of *Trichomonas* sequences was not greater in the Disease sample, compared to the Health sample, however the proportion of *Entamoeba* was significantly greater in the Disease sample (Table 37 and Figure 21). Both MinION™ RNA sequencing protocols, developed here, show potential as techniques capable of identifying organisms in samples. The cDNA sequencing do have the potential hurdles of bacterial depletion and barcoding, which both require further optimisation. However, the direct RNA sequencing shows particular promise. It does not have any discernible points where bias towards a particular species is introduced, and thus shows great potential as an effective protocol for the identification of microorganisms. The MinION™ RNA sequencing technology is still in early stages of development, and with future efficiency and accuracy improvements, it should become an excellent, bias-free, method to identify microorganisms in all sample types.

The protozoa identified with both MinION™ sequencing protocols concur with the results of previous screening tools ([section 2.1](#) and [chapter 3](#)) designed in this thesis. The canine oral plaque samples consistently were shown to contain *Trichomonas* and *Entamoeba*. No other genus have been seen, even with the primer independent methods developed in this chapter. Both *Entamoeba* and *Trichomonas* have been shown to be associated with disease samples (Chapters 3 to 5). Further analysis using the MinION™ Direct RNA sequencing protocols tested here with more varied disease sample types, and possibly longitudinal samples, is required to clarify if these protozoa are a cause or consequence of disease.

CHAPTER 6: FUNCTIONAL AND POTENTIAL VIRULENCE ATTRIBUTES OF *TRICHOMONAS CANISTOMAE BRIXI* AND CONTRIBUTION TO PERIODONTAL DISEASE

Introduction

In human periodontal research, two protozoa have been shown to be present in the mouth and correlate to periodontal disease, *Entamoeba gingivalis* (Dao et al., 1983, Decarneri and Giannone, 1964, Dudko and Kurnatowska, 2007, Linke et al., 1989) and *Trichomonas tenax* (Athari et al., 2007, Dao et al., 1983, Decarneri and Giannone, 1964, Dudko and Kurnatowska, 2007, Kurnatowska et al., 2004, Linke et al., 1989). Recent studies have also indicated the potential for these organisms to influence the initiation and progression of the disease (Marty et al., 2017a, Kelleroova and Tachezy, 2017, Yazar et al., 2016, Ribeiro et al., 2015, Dimasuay and Rivera, 2014, Ghabanchi et al., 2010). In the work for this thesis, two canine protozoa have been identified and found to be associated with several stages of canine periodontal disease (Chapters 3 to 5). At the time of writing, there are no other reported studies of oral protozoa and their association with periodontal disease in dogs. The lack of knowledge in this area may contribute to the inability to combat periodontal disease in dogs and therefore more work is required to study these, and other relevant organisms, further and investigate their roles in the disease. The isolation, culture and further study of both *E. gingivalis* and the novel canine oral *Trichomonas*, are important to help identify them conclusively, and to enable study of their biology and functional attributes. Further studies may lead to intervention strategies to alleviate the progression of disease or even reverse the disease process. Several attempts have been made during the course of this project to culture clinical canine oral isolates and also to propagate commercially available cultures (a human isolate of *E. gingivalis* is available to purchase from the ATCC) of *E. gingivalis*, unfortunately with no success. Without clinical isolates, and the unsuccessful propagation of commercially available isolates, little more could be done to study *E. gingivalis* further. The remainder of this chapter and report concentrates on the isolation, identification, and potential impact on the disease of the novel canine oral *Trichomonas* of dogs. Isolates of the trichomonad were cultivated, and identified further through phylogenetic analyses.

6.1. Isolation and molecular identification of a novel canine oral

Trichomonas.

Chapters 3 to 5 of this report describe the discovery of oral trichomonads in the plaque of dogs in the United Kingdom. Using conventional PCR and Roche 454™ sequencing, an identification of these organisms at the genus level was achieved (Chapter 3). Further analyses using qPCR and restriction digestion (Chapter 4), and analysis and sequencing of ribosomal RNA sequences (Chapter 5), enabled the finding that at least two *Trichomonas* species are present in canine plaque. The first species, *T. tenax*, is commonly found in the human mouth and has been associated with poor oral health and periodontal disease previously (Marty et al., 2017a, Kelleroova and Tachezy, 2017, Yazar et al., 2016, Szczepaniak et al., 2016, Ribeiro et al., 2015, Mehr et al., 2015). Functional activities relevant to the disease process, such as their interaction and disruption of gingival epithelia, have also been investigated (Ribeiro et al., 2015). The second species in this report, has been referred to as an unidentified/novel canine oral trichomonad. The analyses reported in this thesis so far have been unable to identify the species conclusively, but so far the conclusion is that it is a novel, unreported trichomonad.

To better classify this unidentified trichomonad, 10 separate *Trichomonas* isolates from individual Labrador retrievers, Miniature schnauzers, and Cocker spaniels ([section 2.4.3](#)), were cultured using a modified version of the commonly used TYI-S-33 medium ([section 2.4.1](#)). Table 9 details the animal data of each isolation host. In an initial attempt to identify the species present, and to confirm the purity, DNA was extracted from each isolate sample using the 18S protozoa targeted PCR ([section 2.1.2](#)). An approximately 950bp region of the 18S rRNA gene was amplified and sequenced using conventional Sanger sequencing (sections [2.4.6](#) and [2.4.9](#)). All isolated sequences were found to contain a single sequence. Forward and reverse high quality amplicon sequences were aligned to produce full length sequence and each was then analysed through the Basic Local Alignment Search Tool (BLAST) (Coordinators, 2017, Altschul et al., 1990). Sequences were submitted to the BLAST service and compared against the NCBI nucleotide database ([section 2.4.9](#)). The top 10 sequence BLAST matches and associated sequence information were analysed, recorded and detailed in Supplemental Table 13. No clear sequence match was evident for any of the isolated trichomonads. 99 % hit matches (approximate) were seen against sequences annotated as

Trichomonas sp., *Trichomonas gallinae*, and *Trichomonas tenax* (Supplemental Table 13). This suggests all 10 isolated trichomonads, from different dogs, are novel, with 18S sequences currently not submitted to the database. An interesting point to note is that none of the 10 isolates were identified as *T. tenax*, even though qPCR and restriction digest analyses seen previously ([section 4.4](#)) indicated the presence *T. tenax* ([section 4.4](#)). An explanation for *T. tenax* not being isolated maybe that the isolation method used ([section 2.4.3](#)) enriched for the unidentified canine oral *Trichomonas* or does not support the growth of *T. tenax*.

As a definitive species level identification could not be made by comparing the partial 18S sequences against existing database sequences, phylogenetic analyses were undertaken to examine the relatedness of the unidentified isolates to similar trichomonads ([section 2.4.8](#) and [2.4.10](#)). Full length 18S and ITS-5.8S-ITS2 sequences were amplified from each of the 10 isolates and phylogenetically compared to sequences representing species found in the taxonomic genus *Trichomonas* ([section 2.4.10](#)). For each alignment, neighbour joining, maximum likelihood, minimum evolution and UPGMA phylogenetic trees were produced (Figures 22 and 23, and Supplemental Figures 18 and 19).

Figures 22 and 23 display phylogenetic trees inferred using the neighbour joining method (Saitou and Nei, 1987). Exactly the same, or highly similar, phylogenetic clades were seen using maximum likelihood, minimum evolution and UPGMA methods (Supplemental Figures 18 and 19). Consequently, the phylogeny of the 10 trichomonad isolates will be described here using the neighbour joining trees (Figures 22 and 23).

When examining the phylogenetic position of the 10 isolates using the eukaryotic ribosomal 18S gene (ssRNA) (Figure 22), the isolates were found to cluster together in a clade (Figure 22, red and maroon squares), distinct from other *Trichomonas* species already present in the tree, namely *T. tenax*, *T. gallinae*, *T. vaginalis* and *Trichomonas* sp.. Sequence AY24770 *Trichomonas equibuccalis* (Figure 22, black triangle), also clusters with the 10 dog trichomonads, however not as a 100 % matching sequence.

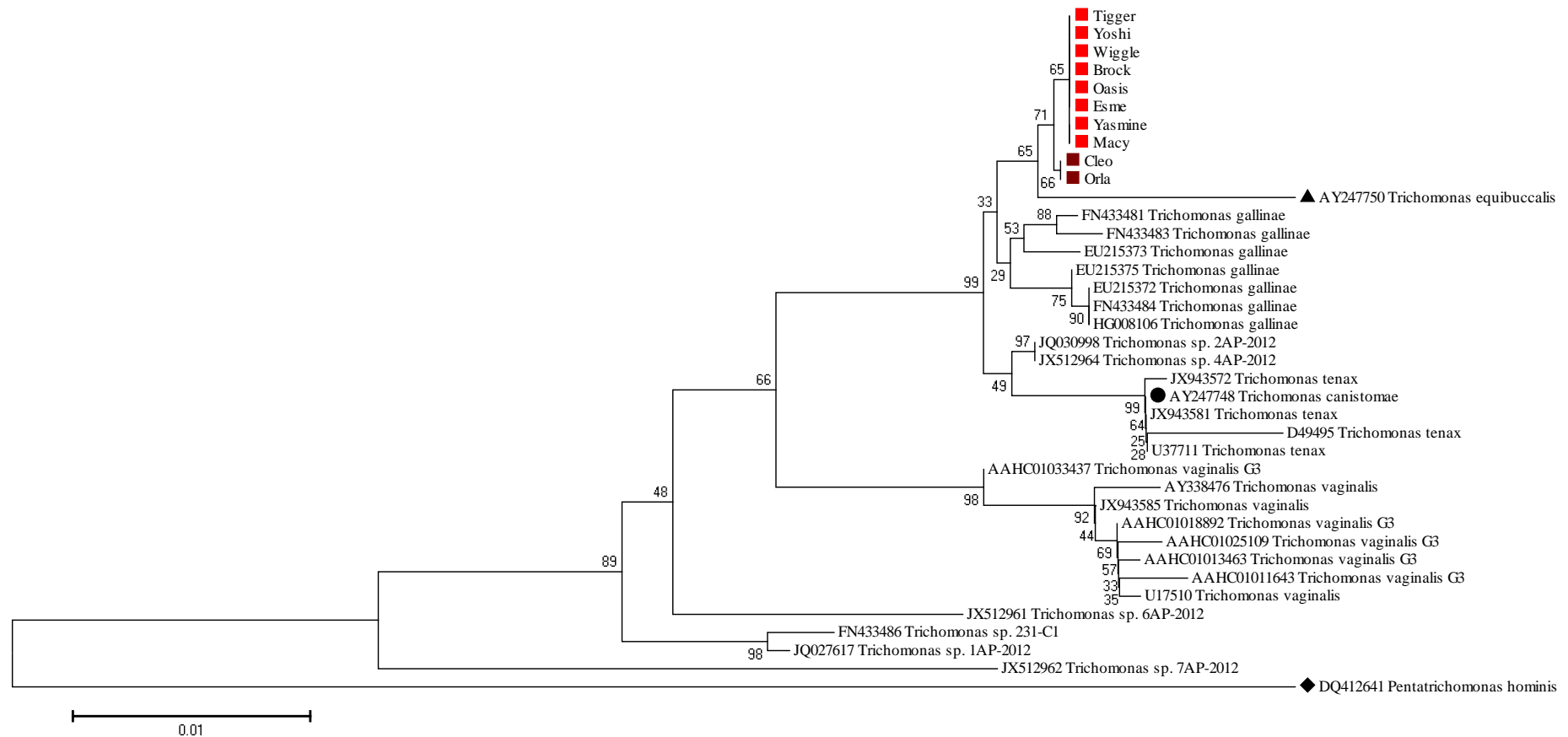


Figure 22. Phylogenetic relationships between 10 unidentified canine oral *Trichomonas* isolates (red and maroon squares) and the trichomonad genus group based on the full length eukaryotic ribosomal 18S gene. The 10 isolates (red and maroon squares) are indicated by the animal name they were isolated from. Other sequences of interest, *T. equibuccalis* (black triangle) and *T. canistomae* (black circle) are discussed further in the main text. Evolutionary history was inferred using the Neighbor-Joining method (Saitou and Nei, 1987). The optimal tree with the sum of branch length = 0.20268408 is shown. The percentage of replicate trees in which the associated taxa clustered together in the bootstrap test (1000 replicates) are shown next to the branches (Felsenstein, 1985). The tree is drawn to scale, with branch lengths in the same units as those of the evolutionary distances used to infer the phylogenetic tree. The evolutionary distances were computed using the Kimura 2-parameter method (Kimura, 1980) and are in the units of the number of base substitutions per site. The rate variation among sites was modelled with a gamma distribution (shape parameter = 1). The analysis involved 38 nucleotide sequences. All positions with less than 95% site coverage were eliminated. That is, fewer than 5% alignment gaps, missing data, and ambiguous bases were allowed at any position. There were a total of 1077 positions in the final dataset. Out group is *Pentatrichomonas hominis* (black diamond). Evolutionary analyses were conducted in MEGA6 (Tamura et al., 2013).

Sequence AY247750 had been deposited into the database by the Department of Parasitology, Charles University Faculty of Science, Prague. However, there is no associated publication or further information about the sequence. The sequence name suggests it was isolated from the mouth of *Equus caballus*, the domestic horse, and indicates that a horse *Trichomonas*, similar in ssRNA sequence to the dog oral *Trichomonas* may exist. This phylogenetic analysis also revealed some additional points of interest. Firstly, two of the 10 isolates, from samples Cleo and Orla (Figure 22, maroon squares), have a 1 base pair substitution in the ssRNA sequence analysed, thymine to cytosine, in comparison to the other 8 sequences. This may indicate a sub-species group with an altered phenotype, but extensive further functional analyses is required to determine any differences.

The second point to note is that sequence AY247748 *Trichomonas canistomae* (Figure 22, black circle), is present in the alignment, but crucially does not cluster with the 10 oral canine isolates described here. *T. canistomae* has been described as an oral *Trichomonas* isolated from dogs (Hegner and Ratcliffe, 1927). The AY247748 *Trichomonas canistomae* also was deposited in the database by the Department of Parasitology, Charles University Faculty of Science, Prague, however their sequence in these analyses clusters with *T. tenax*, the human oral trichomonad, indicating their original identification was incorrect.

Figure 23 displays the phylogenetic position of the 10 isolates using the ITS1-5.8S-ITS2 gene as the comparative sequence. As with the ssRNA neighbour joining tree, we also see in the ITS1-5.8S-ITS2 analyses (Figure 23, and Supplemental Figure 19) that the 10 canine oral *Trichomonas* isolates cluster together in a separate, distinct clade (Figure 23, red squares), away from other similar *Trichomonas* species found in the tree. Also, the sequences cluster with an earlier deposited sequence, AY244652 *Trichomonas canistomae* strain BRIXI (Figure 23, black circle).

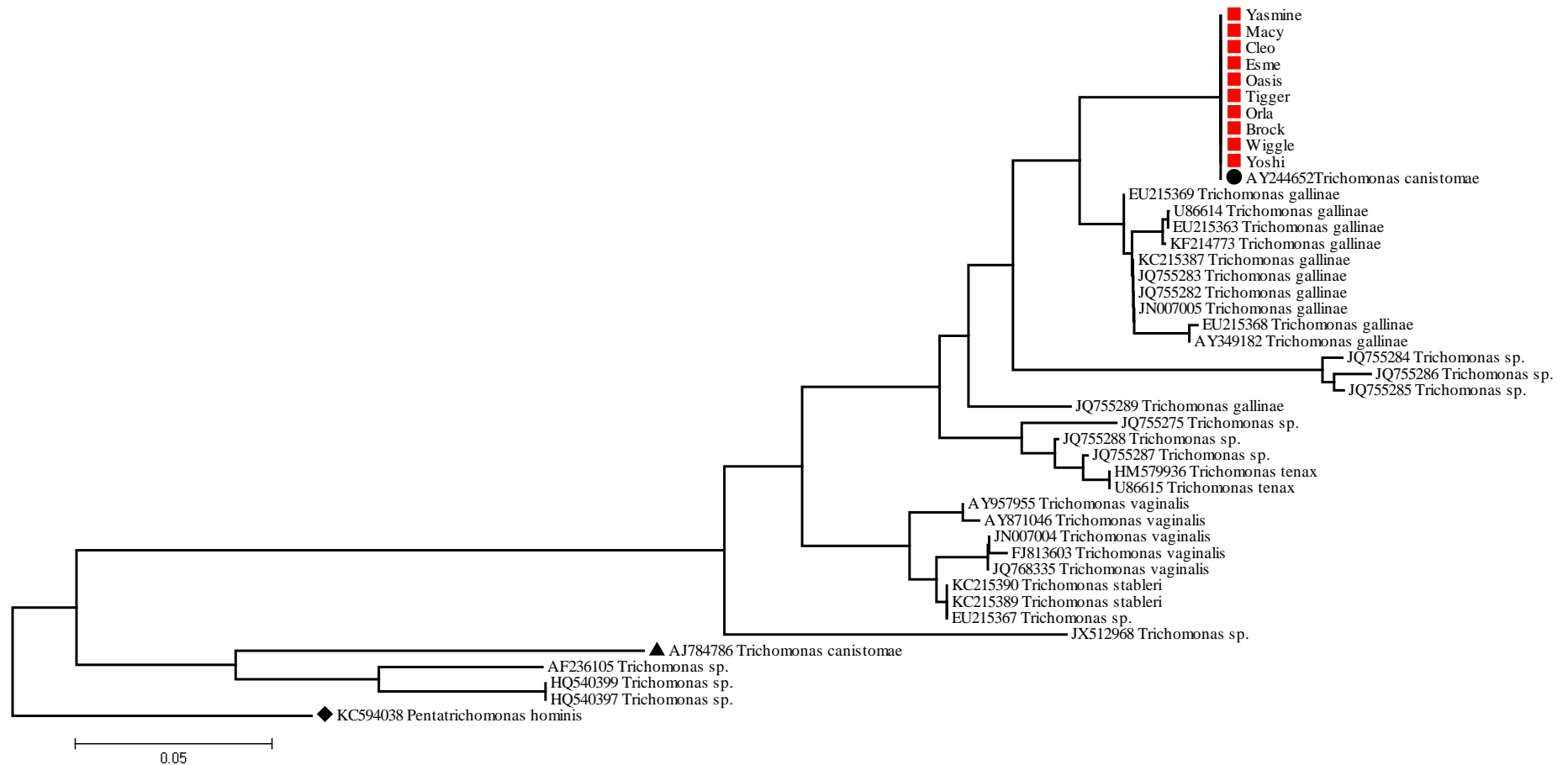


Figure 23. Phylogenetic relationships between 10 unidentified canine oral *Trichomonas* isolates (red squares) and the trichomonad genus group based on the ITS1–5.8SrRNA-ITS2 gene. The 10 isolates (red squares) are indicated by the animal name they were isolated from. Other sequences of interest, *T. canistomae* (black circle and black triangle) are discussed further in the main text. The evolutionary history was inferred using the Neighbor-Joining method (Saitou and Nei, 1987). The optimal tree with the sum of branch length = 1.03365986 is shown. The percentage of replicate trees in which the associated taxa clustered together in the bootstrap test (1000 replicates) are shown next to the branches (Felsenstein, 1985). The tree is drawn to scale, with branch lengths in the same units as those of the evolutionary distances used to infer the phylogenetic tree. The evolutionary distances were computed using the Tamura 3-parameter method (Tamura, 1992) and are in the units of the number of base substitutions per site. The rate variation among sites was modelled with a gamma distribution (shape parameter = 1). The analysis involved 44 nucleotide sequences. All positions with less than 95% site coverage were eliminated. That is, fewer than 5% alignment gaps, missing data, and ambiguous bases were allowed at any position. There were a total of 261 positions in the final dataset. Out group is *Pentatrichomonas hominis* (black diamond). Evolutionary analyses were conducted in MEGA6 (Tamura et al., 2013).

This sequence exhibits a 100 % match with the 10 sequences analysed and its co-clustering indicates that all belong to the same species of *Trichomonas*. Sequence AY244652, as seen previously, was submitted to the database by the Department of Parasitology, Charles University Faculty of Science, Prague. The sequence was submitted as part of a research paper titled “Tetratrichomonads from the oral cavity and respiratory tract of humans” (Kutisova et al., 2005), and describes the sequence as a trichomonad from the mouth of a dog. No other information was provided as to the origin or source of the sequence. Confusingly, a second ITS1-5.8S-ITS2 *T. canistomae* sequence is also present in the sequence databases and analyses, AJ784786 *Trichomonas canistomae* (Figure 23, black triangle). This sequence clusters within a *Trichomonas* sp. clade, distinct from all 10 isolate sequences and the AY244652 *Trichomonas canistomae* strain BRIXI sequence. Again, this is likely to be a misidentified isolate and sequence, and not a true *T. canistomae*.

From the sequence comparisons and phylogenetic analyses described above, it is concluded that the 10 unidentified canine oral isolates are all the same sub-species of *Trichomonas*. The phylogenetic trees (Figures 22 and 23, and Supplemental Figures 18 and 19) show that they all cluster into a distinct, previously unidentified clade. They are not members of any of the other similar *Trichomonas* species found in the group, *T. tenax*, *T. gallinae*, *T. vaginalis* and *Trichomonas* sp., and therefore, are proposed as being a novel species of *Trichomonas*. The sequence databases indicate it may have been seen and isolated previously, but itself and other similar species have been incorrectly identified or positioned phylogenetically in clades and sub groups not suitable or accurate. The analyses here clarifies the trichomonads isolated here as novel *Trichomonas* species. At the time of preparing this thesis, a research group in Prague, published the isolation and identification of what appears to be the same sub-species of trichomonads (Kellerova and Tachezy, 2017). The paper of Kellerova and Tachezy, provides evidence of oral *Trichomonas* isolates from Czech cats and dogs. They also confirm the conclusions in this thesis of the discovery of a previously unidentified canine oral *Trichomonas* species, which has been designated as *Trichomonas brixii* n. sp. (Kellerova and Tachezy, 2017).

6.2. Culture, structure and morphology of *Trichomonas brix*.

6.2.1. Culture and propagation of canine oral Trichomonads.

Molecular and phylogenetic studies in this report (chapters 4, 5 and 6) have identified a novel species of *Trichomonas*, simultaneously designated *Trichomonas brix* by (Kellerova and Tachezy, 2017), and hence forth is referred to as such. *T. brix*, can be cultured in modified TYI-S-33 medium ([section 2.4.1](#)), altered initially by Gannon and Linke, (1991) and also here modified by the removal of mucin from the recipe. The mucin was found to cloud the medium after autoclaving, which resulted in difficulty in viewing the organism and assessing structure and growth. Removal of the mucin was found not to affect the growth rate or propagation of *T. brix*, as assessed by cell counts. For *Trichomonas* isolation from canine plaque, samples were initially cultured in 50 % (v/v) modified TYI-S-33 medium/50 % (v/v) sterile filtered canine pooled saliva, because this was found to significantly increase the likelihood of the trichomonads surviving, compared to the use of modified TYI-S-33 medium alone ([section 2.4.3](#)). Desirable growth factors must be present in canine saliva.

The bacteria within canine plaque were also co-cultured with the protozoa. Attempts were made to culture the trichomonads without the accompanying bacteria (axenic culture), through the addition of a variety of antibiotics and/or separation techniques. However, attempts at axenic culture always resulted in the death of all protozoa, either due to adverse effects from the antibiotics, or maybe because of a lack of essential food/nutrient source that the bacteria provide. The accompanying bacteria were cultured and identified using 16S DNA sequencing ([section 2.4.11](#)). Two species were found to be present, the aerobic bacterium, *Pseudomonas aeruginosa*, and an anaerobic bacterium, *Bacteroides denticanoris*. Currently in xenic *Trichomonas* cultures, both bacterial strains are required for the isolation, growth and propagation of *T. brix* isolates from the dog mouth.

6.2.2. *T. brix* structure

To enable the study of the general and fine structure of *T. brix*, cultures were propagated and processed using a variety of immunostaining, silver staining and high resolution electron microscopy imaging techniques ([section 2.4.12](#) to [2.4.16](#)).

These techniques revealed identifiable characteristics for comparison to existing descriptions of other trichomonad species (Benchimol, 2004, Tasca and De Carli, 2003, de Andrade Rosa et al., 2013, Honigberg, 1990).

Using light microscopy, *T. bixi* have the general morphological characteristics of the genus *Trichomonas*, of the family trichomonadidae (Honigberg, 1990). *T. bixi* cells were fixed using Bouin's solution and stained with fluorescently labelled anti- β -tubulin antibody ([section 2.4.12](#)) to reveal the numbers of flagella, or using the protargol staining technique to reveal the fine structure (Cole and Day, 1940). The general cellular dimensions and characteristics of the cell were recorded ([section 2.4.14](#)) of 100 individual cells of a *T. bixi* isolate (strain isolate CLEO), each individually analysed and cellular metrics recorded (Supplemental Table 14). The average cell length and width were 12.77 ± 1.90 (range 8.65-17.95) μm and 6.41 ± 0.96 (range 4.46-8.79) μm , respectively (n=100). The cells exhibited four unequal length flagella from the anterior end of the cell, emerging from a peritrichous canal (Figure 24, 25 and 26).

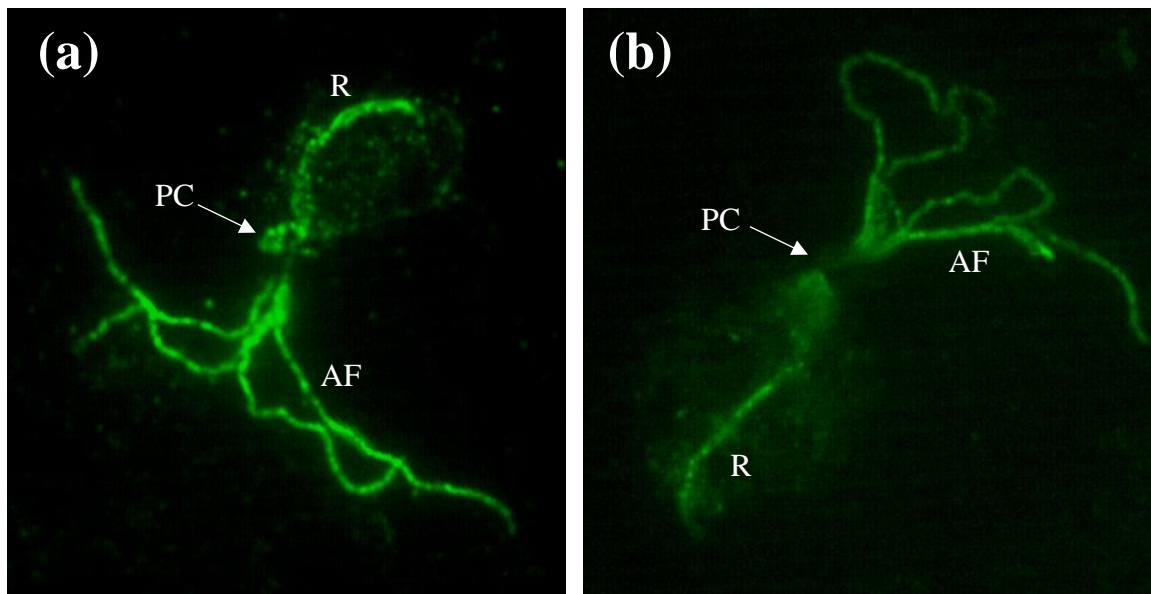


Figure 24. (a) and (b). *Trichomonas bixi* cells fixed in Bouin's solution and stained with anti- β -tubulin antibody to reveal flagella ([section 2.4.12](#)). Four β -tubulin stained anterior flagella (AF) are observed, emerging from peritrichous canal (PC) at the anterior end of the cell. Also emerging from the PC, is the recurrent flagella (R), running for approximately 2/3 of the length of cell surface (associated with the undulating membrane, not stained) towards the posterior of the cell.

Protargol stained cells ([section 2.4.14](#)), and the measurement of 200 individual random flagella, revealed the mean length of a flagellum to be, 12.84 ± 2.37 (range 6.61-18.79) μm , $n=200$ (Supplemental Table 15), and confirm their unequal length appearance under light microscopy. Transmission electron microscopy of *T. brixii* cells revealed that the anterior flagella exhibit the typical eukaryotic (and trichomonad) structure of the flagella axoneme, a 9 + 2 arrangement of microtubules (Figure 28). Also emerging from the periflagellar canal, at an approximate right angle to the emerging anterior flagella is a single recurrent flagellum (Figure 26(b) and 28(b)).

The recurrent flagellum is attached to the cell surface and runs towards the posterior end of the cell in rolling waves that associate with the undulating membrane (Figure 26(b)). This undulating structure, generally extends for about two-thirds of the cell length towards the posterior end. Protargol stained cells ([section 2.4.14](#)), and the measurements taken from 100 individual cells, reveal the length of this undulating membrane/recurrent flagellum structure, on average, to be 13.59 ± 2.69 (range 6.87-21.05) μm , $n=100$ (Supplemental Table 14), similar to the length of the anterior flagella. The recurrent flagellum runs along the margin of the undulating membrane and does not extend beyond the posterior end of the membrane (Figure 26(b)), analogous to the undulating membranes of all other members of the *Trichomonas* genus (Honigberg, 1990). The *T. brixii* recurrent flagellum also exhibits the characteristic, eukaryotic 9 + 2 arrangement of microtubules (Figure 29(a)).

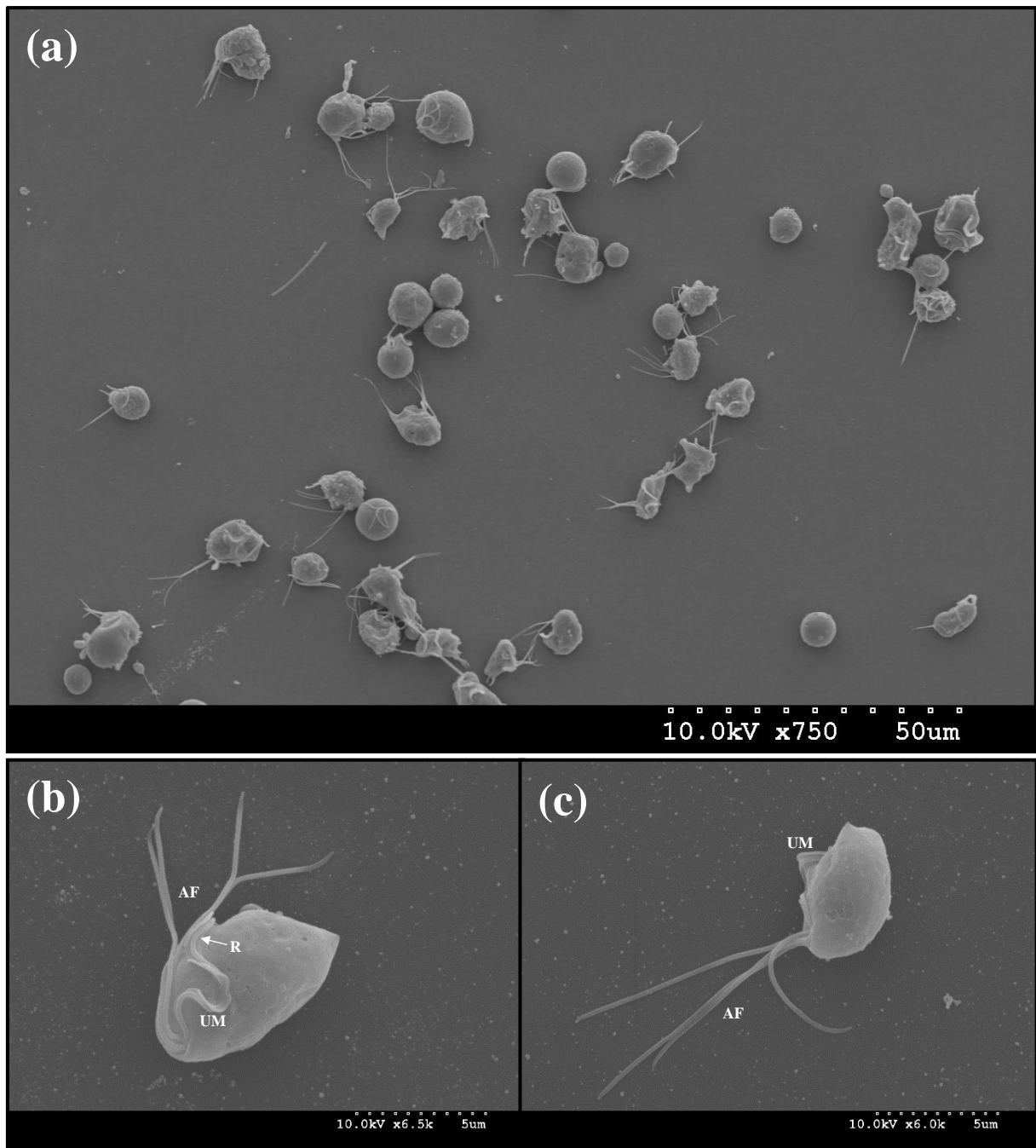


Figure 25. (a), (b), and (c). Scanning electron micrographs of *T. brixii* cells fixed with 2.5 % (v/v) glutaraldehyde and post stained with 0.5 % (v/v) Osmium Tetroxide. (a). 750 times magnification of numerous cells exhibiting their ellipsoidal or ovoid shape and four anterior flagella. (b). 6500 times magnification and (c) 6000 times magnified images displaying the fine detail of the anterior of a cell. Four unequal anterior flagella (AF) are observed and the undulating membrane (UM) with its associated recurrent flagellum (R).

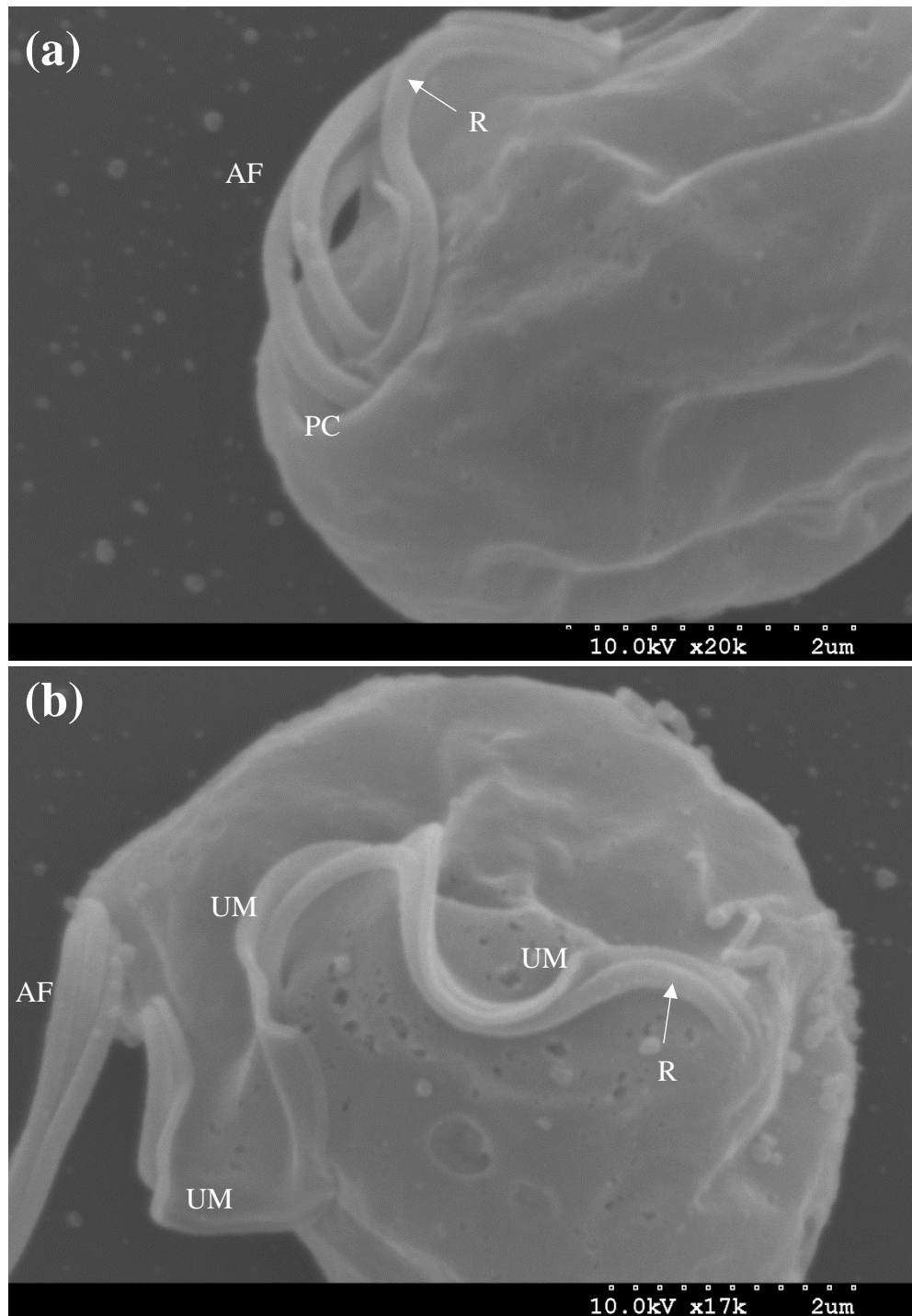


Figure 26. (a) and (b). High magnification scanning electron micrographs of *T. brixii* cells fixed with 2.5 % (v/v) glutaraldehyde and post stained with 0.5 % (v/v) Osmium tetroxide. (a). A single cell magnified 20000 times, displaying the anterior end. The periflagellar canal (PC) is seen with the anterior flagella (AF) emerging from the canal. The recurrent flagella (R) also emerges from the PC at an approximate right angle to the AF. (b). A single cell magnified 17000 times, detailing the fine structure of the undulating membrane (UM) along with its associated recurrent flagellum (R). The undulating membrane runs from the PC for approximately 2/3 of the length of the cell in a wave like manner. Note, the recurrent flagellum does not extend beyond the posterior end of the UM.

The cytoskeleton of trichomonads is poorly understood (Benchimol, 2004), nevertheless the strain examined here exhibits the highly similar cytoskeletal structures seen in other trichomonads. The pelta-axostylar complex of *T. bixi* consists of the pelta, a crescent shaped structure of microtubules that surround the periflagellar canal, reinforcing the canal wall and the flagella base (Figure 27 and 29(b)). The axostyle (Figure 27), also composed of microtubules, longitudinally aligned, surround the anteriorly located nucleus as the axostylar capitulum. The axostylar capitulum is a concave structure that partially encloses the nucleus, providing protection (Honigberg, 1990). Its posterior end wraps upon itself into a tube-like structure to form the axostyle trunk, which narrows towards the posterior, providing axial support for the cell. The narrowed axostyle trunk extends out beyond the posterior surface of the cell, still surrounded by the cell membrane, as a pointed projection (Figure 27). Protargol stained cells ([section 2.4.14](#)), and the measurement taken from 100 individual cells, reveal the length of this axostyle trunk projection from the tip of the cell, on average, to be 10.47 ± 2.30 (range 6.36-17.23) μm (Supplemental Table 14). The axostyle in *T. bixi* appears to be a distinguishing feature of the species, as other closely related, and morphologically similar species, such as *T. vaginalis* and *T. tenax*, have shorter length axostyle projections ((Honigberg, 1990)).

Another cytoskeletal structure of trichomonads (Benchimol, 2004), the costa, is also seen in *T. bixi* (Figure 30). The costa, a major rootlet filament with a periodic pattern, originates near the basal body region, close to basal body 2 (Figure 30). It extends to the posterior closely located beneath the undulating membrane, but without any direct contact. It is believed to provide support to the undulating membrane (Benchimol, 2004). The basal body structures are also a constituent of the trichomonad mastigont (Benchimol, 2004). As in other trichomonads, *T. bixi* possess five basal bodies, four forming the base of the anterior flagella and one for the recurrent flagellum (Figure 30). They also have hook-shaped filaments (F1 – F3) emanating from the basal bodies, bending in a clockwise motion (Figure 30).

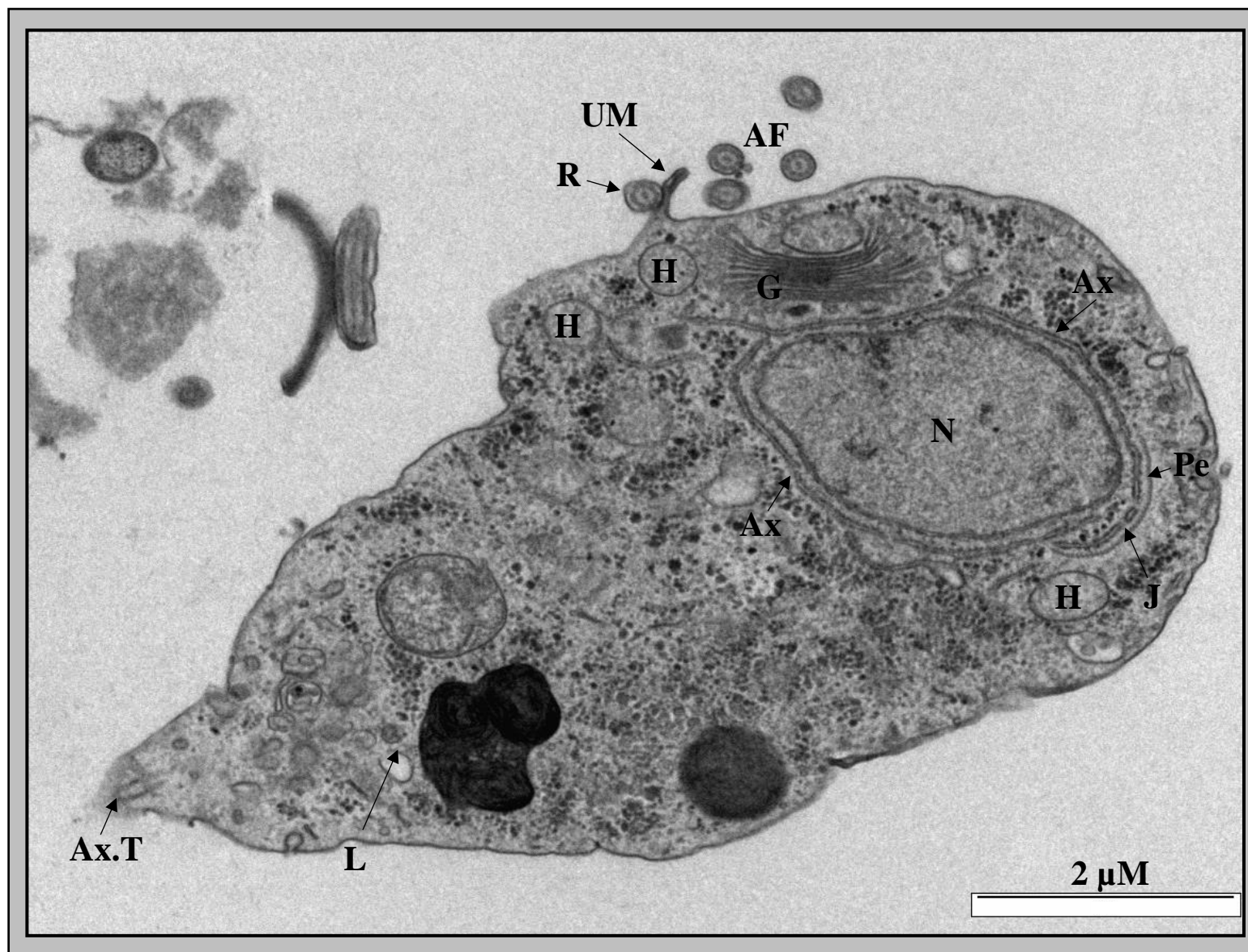


Figure 27. Transmission electron micrograph of *T. brixii* cells fixed with 2.5 % (v/v) glutaraldehyde and post stained with 1 % (v/v) Osmium Tetroxide. The species exhibits an ellipsoidal or ovoid shape and typical trichomonad cellular structures are apparent. The nucleus (N) is located anteriorly, displays chromatin masses and is encompassed by the axostylar capitulum (Ax). The axostylar capitulum narrows towards the posterior of the cell (not seen) and projects beyond the cell as the axostylar trunk (Ax.T), still surrounded by the cell membrane. The pelta (Pe) overlaps the axostyle at the pelta-axostyle junction (J). Transverse sections though the four anterior flagella (AF) are present in the image, as is the recurrent flagellum (R) and its associated undulating membrane (UM). Other typical cell organelles visible are the hydrogenosomes (H), Golgi cisternae cellular lysosomes (L) and vacuoles.

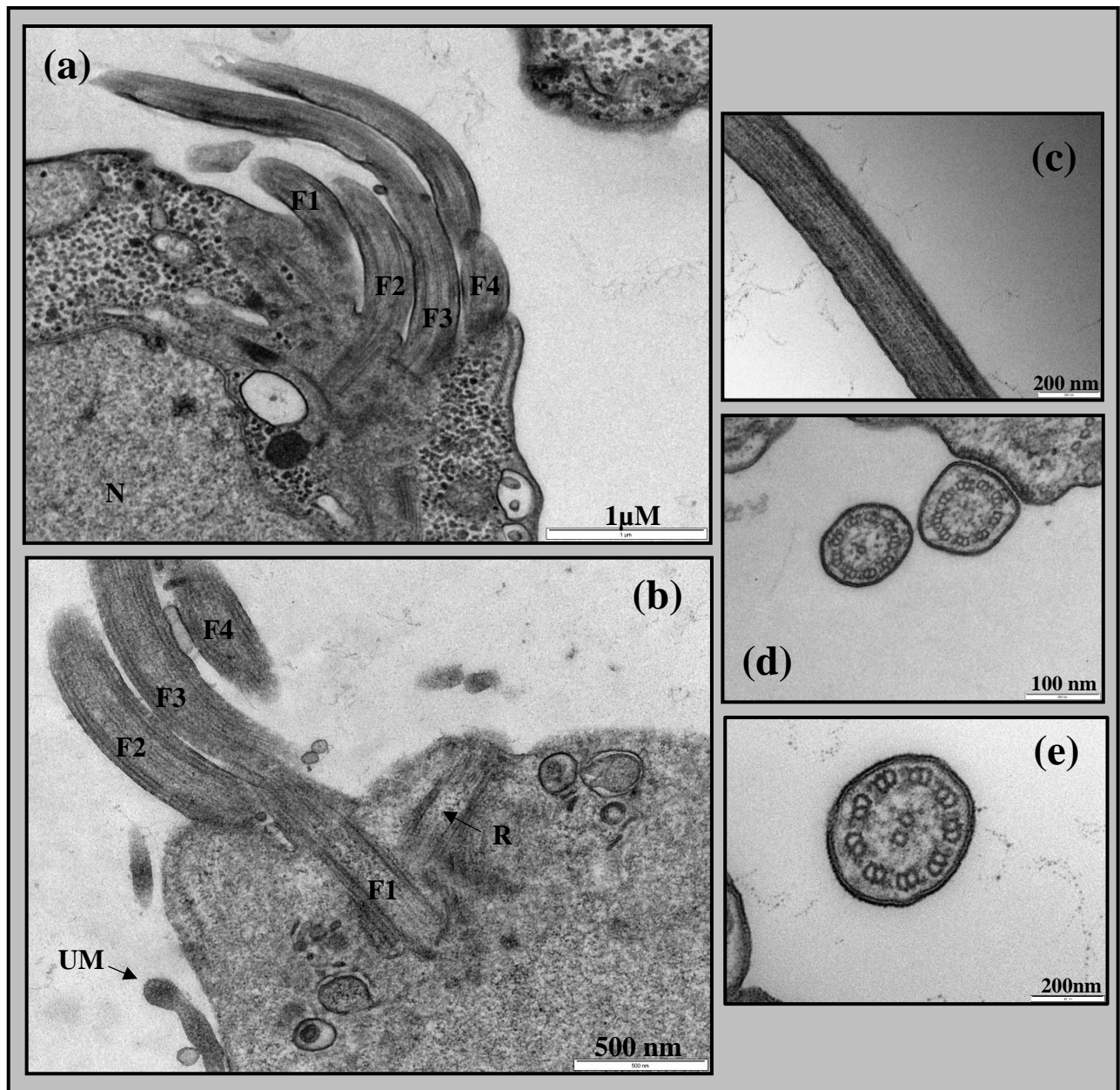


Figure 28. Transmission electron micrograph of *T. brixii* cells fixed with 2.5 % (v/v) glutaraldehyde and post stained with 1 % (v/v) Osmium Tetroxide, displaying details of the anterior flagella. (a) and (b). Four anterior flagella (F1 – F4) are visible, emerging from the periflagellar canal and their respective basal bodies (not visible). In (b), note the recurrent flagellum (R) emerging from the cell and its basal body, at a right angle to the anterior flagella. (c), (d) and (e). Longitudinal and transverse sections of the flagella showing the typical eukaryotic 9 + 2 microtubule arrangement of the axoneme.

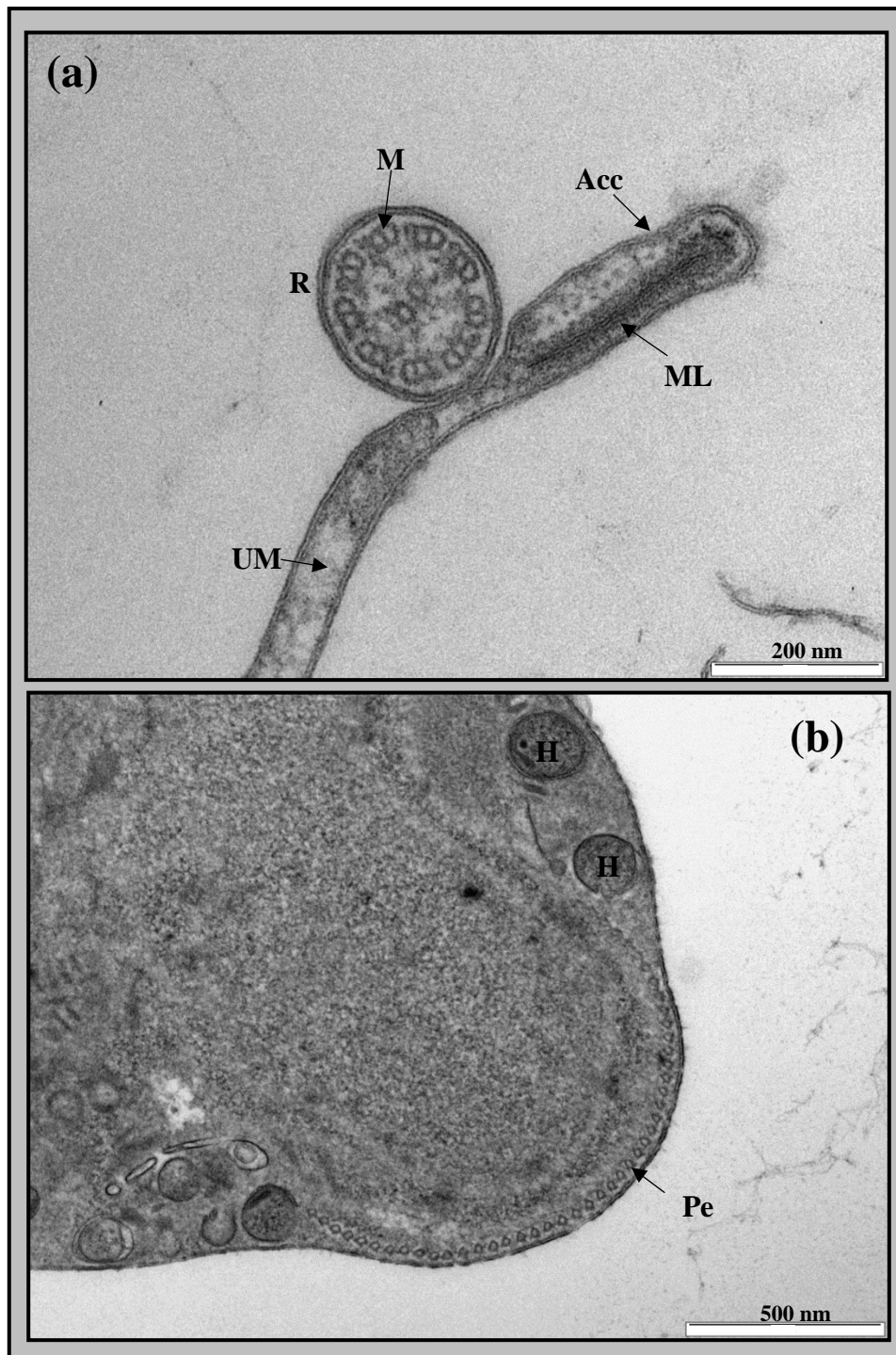


Figure 29. Transmission electron micrograph of *T. brixii* cells fixed with 2.5 % (v/v) glutaraldehyde and post stained with 1 % (v/v) Osmium Tetroxide. (a). Transverse section through the undulating membrane (UM) and recurrent flagellum (R) showing the internal structures of each. The undulating membrane is composed of the striated marginal lamella (ML) and forms into the accessory filament (Acc). The recurrent flagellum (R), as with the anterior flagella, exhibits the typical eukaryotic 9 + 2 microtubule (M) arrangement of its axoneme microtubules. (b) The microtubule structure of the pelta (Pe) is seen at the anterior end of a cell, reinforcing the periflagellar canal and the basal body region.

Two parabasal filaments (PF1 and PF2) also originate from the basal body complex, and are thought to support the Golgi complex (Figure 30). Other distinctive trichomonad fibrillar structures, such as the sigmoidal filament connecting BB2 to the pelta, and the X-fiber (X) connecting the BB2 to F1, are also visible using TEM (Figure 30). Most of these structures are thought to have supportive roles or participate in cellular division, or have unknown functions (Benchimol, 2004, Honigberg, 1990).

A variety of other characteristic trichomonad cellular organelles are present in *T. brixii* and visible using TEM. In non-dividing cells, a single nucleus is anteriorly located in the cell, within the concave portion of the axostylar capitulum, which provides support and protection (Figure 27). In *T. brixii*, the nucleus length and width, as measured in protargol stained cells, is 4.24 ± 0.80 (range 1.65-5.97) μm , $n=100$ and 2.78 ± 0.54 (range 1.30-4.427) μm , $n=100$, respectively (Supplemental Table 14).

Other typical cell organelles visible through TEM are the Golgi cisternae, cellular lysosomes and vacuoles (Figure 27). An organelle, found in other eukaryotic cells, but absent in all trichomonads, is the mitochondrion. In its place, all Trichomonads have organelles called Hydrogenosomes (Lindmark and Muller, 1973), and *T. brixii* is no different, as can be seen in Figures 27 and 29(b). Hydrogenosomes are enclosed organelles containing a variety of enzymes that participate in pyruvate metabolism to provide a source of cellular hydrogen for energy generation in trichomonads (Hrdy et al., 2004). They are found in all parts of the cell but are commonly seen in close proximity and parallel to the costa or axostyle trunk (Benchimol, 2004, Honigberg, 1990).

T. brixii (Kellerova and Tachezy, 2017), and the UK canine oral *Trichomonas* identified in this thesis, bear all the characteristics of true representative of the genus *Trichomonas*, of the family trichomonadidae. Canine oral trichomonads have been isolated previously (Hegner and Ratcliffe, 1927), however their description in the literature indicate the (Hegner and Ratcliffe, 1927) isolates were not true trichomonads, and were indeed later reclassified as *Tritrichomonas* sp. (Kellerova and Tachezy, 2017, Cepicka et al., 2010).

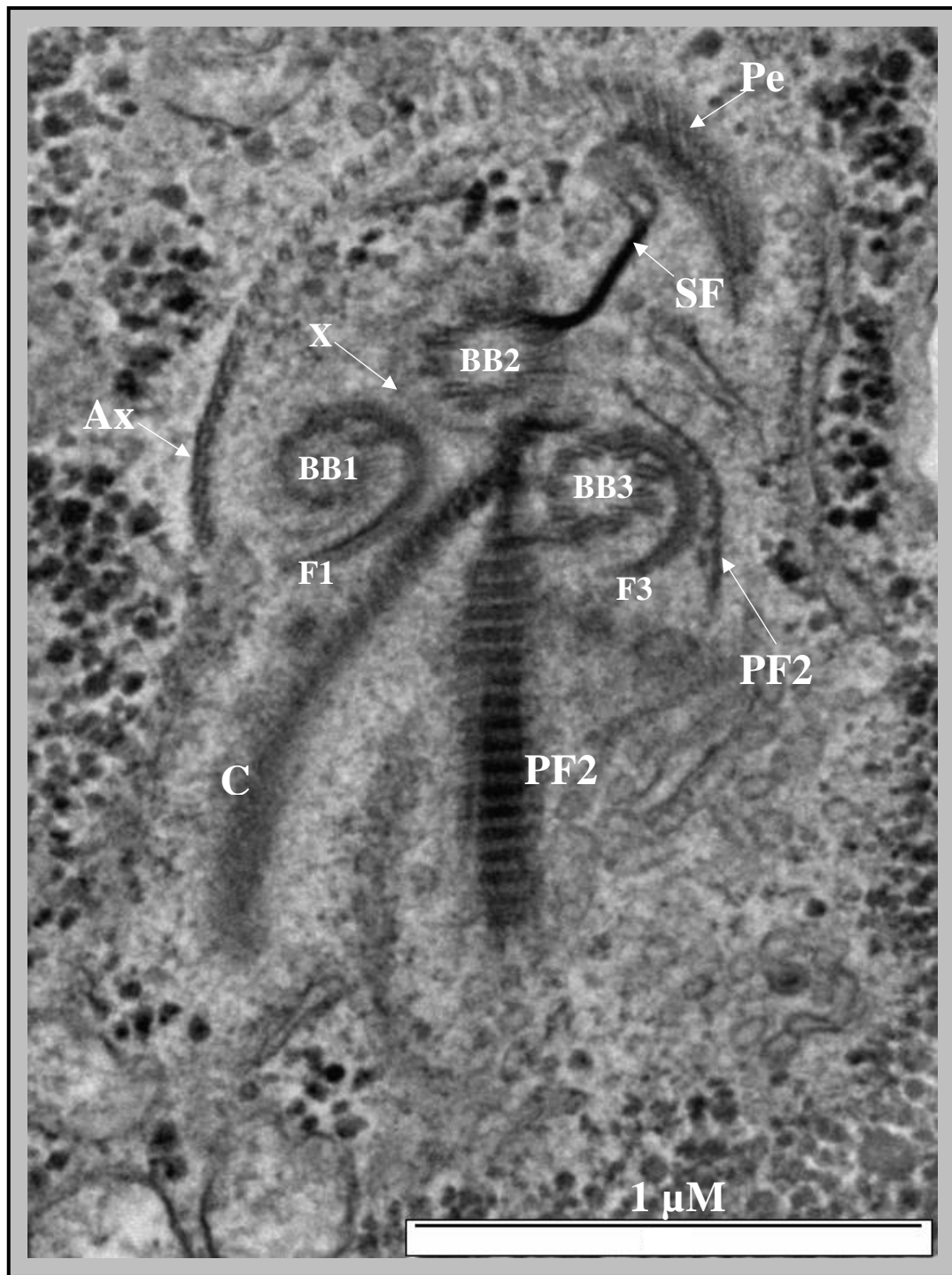


Figure 30. Transmission electron micrograph of *T. brixii* cells fixed with 2.5 % (v/v) glutaraldehyde and post stained with 1 % (v/v) Osmium Tetroxide, displaying the pelta (Pe) and axostyle (Ax) microtubules, and the basal body complexes. Three basal bodies (BB) are visible (the forth is not visible in this image), forming bases for the four anterior flagella. They also have hook-shaped filaments emanating (F1 and F3) that bend clockwise. Originating from BB2, the costa (C) is thought to support the undulating membrane. Two parabasal filaments (PF) also originate from the basal body complex, and are thought to support the Golgi complex. Other fibrillar structures, such as the sigmoidal filament (SF) connecting BB2 to the pelta, and the X-fiber (X) connecting the BB2 to F1, are also visible.

The morphological characteristics identified in trichomonads from the UK (Patel et al., 2017) and [section 6.2.2](#)) and from mainland European canine oral isolates (Kellerova and Tachezy, 2017), both have features of the genus *Trichomonas* and are a previously undescribed *Trichomonas*. The species has been given the name, *Trichomonas bixi* (Kellerova and Tachezy, 2017). The cellular length and width measurements recorded in this study do not seamlessly match those measured from isolates derived from dogs in the Czech Republic (Kellerova and Tachezy, 2017). These differences may be due to varying protocols in the protargol slide preparations and/or variations in the fixation of the cells prior to staining. Both isolates do however match at the genetic level ([section 2.4.10](#) and [6.1](#)) and possess all the characteristics of the genus *Trichomonas* and therefore are concluded to be the same strain. More research is required to determine if this strain is present globally in the mouth of dogs, or is a Europe only strain.

6.3. Functional activity of *T. bixi* and its potential contribution to canine periodontal disease

T. bixi, has been shown to be a new member of the *Trichomonas* genus. It has morphological characteristics ([section 6.2](#)) highly similar to other species in the genus, but molecular analysis has shown them to be novel ([section 6.1](#)). Several members of the *Trichomonas* genus are important pathogens and causes of disease in man and animals. In humans, *T. vaginalis* is highly prevalent and is the aetiological cause of trichomoniasis, a sexually transmitted disease of the male and female sexual organs (Soper, 2004). Also in humans, *T. tenax* is commonly observed in the mouth, in particular the dental regions, and has until very recently been associated with oral disease, but generally it is regarded as a commensal (Athari et al., 2007, Honigberg and Lee, 1959, Ribeiro et al., 2015). However, in recent years a growing number of researchers have further investigated oral diseases and have challenged the views about *T. tenax* and oral disease (Marty et al., 2017a, Kellerova and Tachezy, 2017, Yazar et al., 2016, Ribeiro et al., 2015, Mehr et al., 2015, Dimasuay and Rivera, 2014). Both *T. vaginalis* and *T. tenax* and a several others from the *Trichomonas* genus are capable of causing or contributing to disease. Because the new species described in the thesis, *T. bixi*, has been shown

to be associated with canine periodontal disease (sections 3-5), it is important to investigate if it is capable of causing or contributing to disease.

There are no published studies that have investigated the pathogenic potential of *T. brixii* or other canine oral trichomonads. Other Trichomonads implicated in human disease, *T. vaginalis* and *T. tenax*, secrete a variety of substances that contribute to disease (Kucknoor et al., 2007, Stafkova et al., 2018, Segovic et al., 1998, Nagao et al., 2000) or interact with host cells to bring about damage (Arroyo et al., 1992, Lustig et al., 2013, Ribeiro et al., 2015). To begin investigations with *T. brixii*, the approach adopted was to identify cell associated or secreted factors that have potential to contribute to canine periodontal disease.

6.3.1. API® ZYM® semi-quantitative enzymatic activity strips

A semi-quantitative method was employed to survey the species for enzyme activity. *T. brixii* cultures were incubated for 4 hours in API® ZYM® semi-quantitative enzymatic activity strips ([section 2.4.17](#)). These strips detect a variety of enzyme activities and give the first indication of potential pathogenic attributes of *T. brixii*. Table 38 displays the results obtained from the API® ZYM® strip enzyme assays and the semi-quantitative scores assigned for the production of reaction products from each enzyme assay. These were between 0 and 5, 0 being no reaction and 5 indicating a maximum reaction. Six of the assays were seen to produce a notable score, of 2 or greater (Table 38).

Two assays of these six, esterase and esterase lipase were given scores of 2 and 3 respectively. Esterase enzymes hydrolyse ester bonds. Knowledge about their biological function is currently limited (Williams, 1985). This extensive group of enzymes have been previously implicated in disease (Dumoulin et al., 2015, Feng et al., 2011, Williams, 1985), and also could play a role in periodontal disease (Bimstein et al., 2004, Roberts et al., 2003), but very little is known and extensive research is required in to importance.

The next highest reaction scores were from the alkaline phosphatase and α -glucosidase assays, both scoring 4 (Table 38). Alkaline phosphatases are endogenous enzymes expressed in the intestines by epithelial cells, contributing towards maintaining gut homeostasis and modulating bacterial populations (Fawley and Gourlay, 2016). Increased levels of alkaline phosphatase in the mouth from

host and microbial sources is also associated with increased inflammation and has been proposed as a potential marker of periodontal disease (Malhotra et al., 2010, Grover et al., 2016)). It is possible that trichomonads may secrete these enzyme also alter bacterial populations in plaque to either promote favourable bacteria as a food source or to modulate the disease process, however further research is required to provide evidence for this.

Table 38. API® ZYM® semi-quantitative enzymatic activity strip results for *T. brixii*. The results are semi-quantitative reaction scores assigned to each enzyme test. Enzymes present in the *T. brixii* pellet were allowed to react with the indicated substrates. The resultant reaction was scored between 0 and 5, 0 being no reaction and 5 being a maximum intensity reaction. The shaded result scores indicate the assays from which a greater than moderate reaction was observed with *T. brixii*.

Enzyme assay	Substrate	Reaction score [Score 0-5 (0 is no reaction, 5 is maximum reaction)]
Alkaline phosphatase	2-naphthyl phosphate	4
Esterase (C 4)	2-naphthyl butyrate	2
Esterase Lipase (C 8)	2-naphthyl caprylate	3
Lipase (C 14)	2-naphthyl myristate	0
Leucine arylamidase	L-leucyl-2-naphthylamide	5
Valine arylamidase	L-valyl-2-naphthylamide	1
Cystine arylamidase	L-cystyl-2-naphthylamide	1
Trypsin	N-benzoyl-DL-arginine-2-naphthylamide	0
α -chymotrypsin	N-glutaryl-phenylalanine-2-naphthylamide	0
Acid phosphatase	2-naphthyl phosphate	5
Naphthol-AS-BI-phosphohydrolase	Naphthol-AS-Bi-phosphate	1
α -galactosidase	6-Br-2-naphthyl- α D-galactopyranoside	0
β -galactosidase	2-naphthyl- β D-galactopyranoside	0
β -glucuronidase	Naphthol-AS-BI- β D-glucuronide	0
α -glucosidase	2-naphthyl- α D-glucopyranoside	4
β -glucosidase	6-Br-2-naphthyl- β D-glucopyranoside	1
N-acetyl- β -glucosaminidase	1-naphthyl-N-acetyl- β D-glucosaminide	1
α -mannosidase	6-Br-2-naphthyl- α D-mannopyranoside	0
α -fucosidase	2-naphthyl- α L-fucopyranoside	0

α -glucosidase activity was also scored as 4 in the API® ZYM® strip assay. α -glucosidases and other glycosidase enzyme activities are also found to increase in mouths where periodontal disease is present (Beighton et al., 1992). The function, if any, of α -glucosidases in periodontal disease is far from clear. However they could be used by *T. brixii* to cleave oligosaccharides from host derived glycoproteins to be used as a nutrient source (Ter Steeg et al., 1988, Beighton et al., 1988) or render the host glycoproteins more prone to proteolytic activity (Beighton et al., 1992).

The final two enzyme assays gave a maximum reaction, a score of 5 (Table 38). The first, Leucine arylamidase is a member of the metallo-peptidase group of enzymes. Metallo- peptidases have been extensively studied in relation to periodontal disease and some are implicated in alveolar bone loss during the disease process (Cochran, 2008, Schwartz et al., 1997). However, little published material is available on the role of Leucine arylamidases in disease, and therefore more work is required to identify if they have a role in periodontal disease, and more specifically leucine arylamidase produced by trichomonads.

The second enzyme scoring a maximum 5 was Acid phosphatase. As seen with several of the enzymes discussed above, Acid phosphatases are found at increased levels in oral fluids where periodontitis is evident (Pushparani, 2015, Dabra and Singh, 2012). Acid phosphatases catalyse a variety of reactions (Bull et al., 2002) and have been implicated in the destruction of host cells by protozoa (Aguirre-Garcia et al., 2003, de Jesus et al., 2002). Both leucine arylamidase and acid phosphatase production by *T. brixii* is significant (Table 38) and their ability to produce them at substantial levels may have implications for canine periodontal disease.

6.3.2. Non-specific protease detection

The detection of non-specific protease produced by *T. brixii* was undertaken using milk agar to observe zones of clearance in the agar caused by exported protease ([section 2.4.18](#)). Zones of clearance (ZOC) were measured and recorded (Table 39). A control organism known to produce non-specific proteases, *Bacillus subtilis* (Yang et al., 2000), was used within the experiment and found to produce an average ZOC of 29.72 mm (\pm 0.12) and 21.16 mm (\pm 0.445) under CO₂ and

anaerobic conditions, respectively, n=2 (Table 39). The *T. bixi* cultures however did not produce any ZOC's either under CO₂ or anaerobic conditions (Table 39). This negative result was a surprise as other trichomonad species are known to produce secreted extracellular proteases (Sibley, 2013, Rosenthal, 1999, Kummer et al., 2008, Sommer et al., 2005, Draper et al., 1998{Garber, 1994 #804, Segovic et al., 1998, Bozner and Demes, 1991a, Garber and Lemchuk-Favel, 1994). It was apparent that *T. bixi* do have the ability to produce proteases, e.g. leucine arylamidase, detected using the API® ZYM® strips (section [2.4.17](#) and [6.3.1](#)). Milk agar is used as a general protease detection system, however it specifically tests for the ability of the organism to hydrolyse casein as a substrate. It is possible that *T. bixi* does not have this non-specific protease cleavage or is only available or upregulated under the influence of an external stimulus.

Table 39. Non-specific protease detection. *T. bixi* and *B. subtilis* (ATCC 6051) cultures were incubated in 5 mm holes bored into Milk agar. Agar plates were incubated under (a) **carbon dioxide** or (b) **Anerobic** conditions for 18 hours at 38 °C, after which any visible zone of clearance in the agar was measured (mm).

(a) <u>Carbon dioxide</u>		Diameter of clearance zone (mm)		
Culture tested	Replicate 1	Replicate 2	Average of replicates	
<i>B. subtilis</i>	29.85	29.60	29.72	
<i>T. bixi</i>	0	0	0	

(b) <u>Anaerobic</u>		Diameter of clearance zone (mm)		
Culture tested	Replicate 1	Replicate 2	Average of replicates	
<i>B. subtilis</i>	20.71	21.60	21.16	
<i>T. bixi</i>	0	0	0	

6.3.3. Serine protease activity of *T. brixii*

As the non-specific protease assay detection protocol did not produce the expected results ([section 6.3.2](#)), detection of more specific protease was employed. Oral bacterial pathogens such as *Porphyromonas gingivalis* and *Bacteroides forsythus*, as well as pathogenic trichomonad species use cysteine and serine proteases to contribute to disease processes (Kesavalu et al., 1996, Curtis et al., 1993, Grenier, 1995, Draper et al., 1998, Hernandez-Romano et al., 2010). The benzoylarginine p-nitroanilide (BAPNA) assay (Hayakawa et al., 1980) was undertaken to detect the production of serine proteases, e.g. trypsin, by *T. brixii* ([section 2.4.19](#)). Cell pellets and medium supernatant from *T. brixii* cultures were tested, as well as cell pellets and medium supernatant from *T. brixii*/canine gingival fibroblast co-culture experiments ([section 2.4.23](#)). Also, a canine oral bacterial culture, *Porphyromonas gulae* II (Davis et al., 2013), was also used in the assay as a trypsin producing control organism (Fournier et al., 2001). Figure 31 displays the relative levels of trypsin detected in each of the samples.

The ability to hydrolyse a Na-Benzoyl-DL-arginine 4-nitroanilide hydrochloride, a chromogenic trypsin substrate, releasing the chromophore p-nitroaniline, was monitored by measuring the absorption of the sample at 405 nm. The *T. brixii* cell pellet and supernatant samples produced mean absorption values of 1.12 (SD. 0.17) and 0.46 (SD. 0.04), respectively (Figure 31 and Supplemental Table 16a). When the samples were compared to the DMEM control using ordinary one-way ANOVA analysis, the *T. brixii* cell pellet was confirmed as being significantly different but not the cell supernatant (Figure 31 and Supplemental Table 16b). This indicates *T. brixii* has a cell associated trypsin activity.

Interesting results were also seen, when *T. brixii* was co-cultured with canine fibroblasts for 48 hours ([section 2.4.19](#)). The cell pellet and supernatant of the co-culture was tested with the BAPNA assay and found to produce mean absorption values of 2.17 (SD. 0.33) and 0.75 (SD. 0.33), respectively (Figure 31 and Supplemental Table 16a). Both samples when compared to the DMEM control using ordinary one-way ANOVA analysis were significantly different to the control (Figure 31 and Supplemental Table 16b). Both co-culture pellet and supernatant show a greater level of trypsin from *T. brixii* cells, indicating that the trichomonad may upregulate trypsin production in the presence of canine gingival cells, helping to lyse host cells.

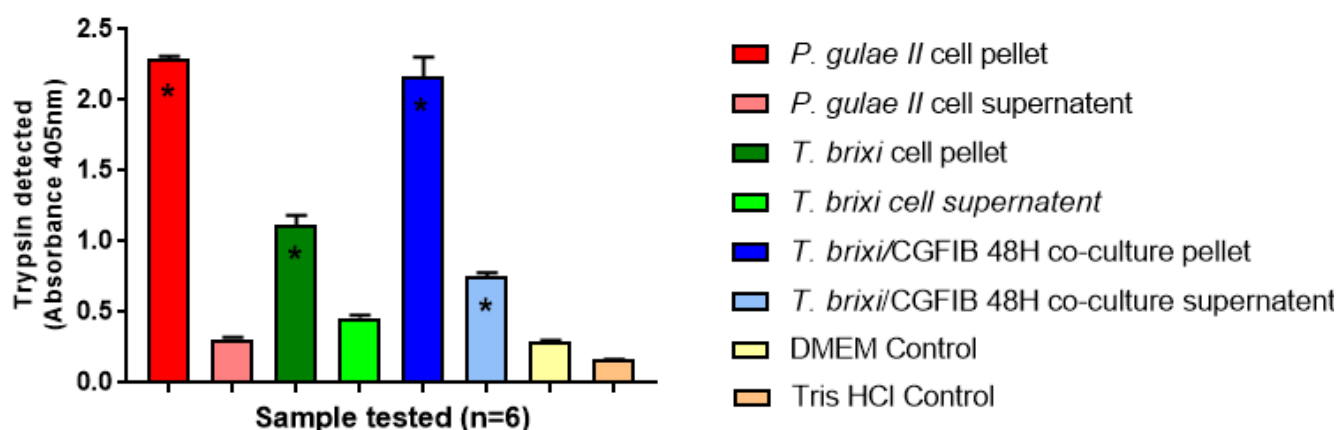


Figure 31. Mean trypsin detected in *T. bixi* cell pellets (n=6) and supernatants, and *T. bixi*/canine gingival fibroblast co-culture cell pellet and supernatants. A bacterial strain, *P. gulae II*, known to exhibit trypsin-like activity was a positive control. DMEM and Tris-HCl were the buffer negative controls. Samples were tested in sextuplet. Black bars indicate the standard error of the mean. Asterisks indicate significantly different ($p < 0.05$) values when compared to the DMEM media control using one-way ANOVA analysis. *P. gulae II*, and *T. bixi* cell pellets both exhibit significantly increased levels of trypsin production compared to the DMEM medium control. Both *T. bixi*/canine gingival fibroblast co-culture cell pellet and supernatants also exhibit significantly increased levels of trypsin production compared to the DMEM media control.

The *P. gulae II* pellet control sample produced the greatest level of the chromophore p-nitroaniline, with mean absorption value of 2.29 (SD. 0.04), at 405 nm (Figure 31 and Supplemental Table 16a), whereas the *P. gulae II* supernatant was substantially lower, at 0.31 (SD. 0.03). This indicates that *P. gulae II* has a significant cell associated trypsin activity, as seen previously (Fournier et al., 2001). All samples were quantified for the amounts of trypsin present using a non-linear fit Allosteric sigmoidal model trypsin standard curve and interpolating trypsin values for each sample mean (Table 40 and Supplemental Figure 20). The highest level of trypsin was seen in the *P. gulae II* cell pellet sample, an interpolated value of 33.75 ng/mL (Table 40). The *T. bixi* cell pellet and supernatant samples gave a reading of 14.71 and 4.57 ng/mL, respectively (Table 40). Although not at the same levels as the *P. gulae* control sample, the *T. bixi*-only cell pellet sample produced a significant specific trypsin activity ($p=0.0001$). However, in the presence of canine gingival cells, the *T. bixi* specific activity was nearly as much the control *P. gulae* sample,

a value of 31.63 ng/mL of trypsin for the co-culture cell pellets and 9.08 ng/mL for the co-culture supernatant (Table 40).

Table 40. Mean absorbance values at 405 nm (n=6) for *T. bixi* cell pellets and supernatants, *T. bixi*/canine gingival fibroblast co-culture cell pellets and supernatants and *P. gulae II* cell pellets and supernatants. A trypsin standard curve was plotted using a non-linear fit Allosteric sigmoidal model (Supplemental Figure 20). Each test value was interpolated into absolute trypsin concentrations (nanograms of trypsin per millilitre of sample) using the standard curve and the equation $Y = \text{Bottom} + (\text{Top} - \text{Bottom}) / (1 + 10^{-(\text{LogEC50} - X) * \text{HillSlope}})$ in Prism software (GraphPad software, Inc, USA). BDR=Below detectable range.

Sample	Mean Absorbance 405nm	Interpolated value (ng/mL)
<i>P. gulae II</i> cell pellet	2.29	33.75
<i>P. gulae II</i> cell supernatant	0.30	2.21
<i>T. bixi</i> cell pellet	1.11	14.71
<i>T. bixi</i> cell supernatant	0.46	4.57
<i>T. bixi</i> /CGFIB 48H co-culture pellet	2.16	31.63
<i>T. bixi</i> /CGFIB 48H co-culture supernatant	0.75	9.08
DMEM Control	0.29	2.01
Tris HCL Control	0.164	BDR

The data produced by this experiment show that the specific trypsin activity of *T. bixi* is similar to that of *P. gulae*, and this trypsin activity may increase in the presence of gingival cells. For many years the focus of periodontal disease research has been to investigate the biology and pathology of the disease with research mainly concentrating on the bacterial populations and their activities. Oral protists, such as trichomonads, have been considered commensal with respect to the aetiology of the disease, and given little attention. It has been assumed that they do not contribute to the disease but merely take advantage of the change in the oral environment (Athari et al., 2007, Honigberg and Lee, 1959, Ribeiro et al., 2015). The results here indicate that oral trichomonads have the ability to contribute to cell destruction and thus to the disease process.

6.3.4. Haemolytic activity of *T. brixii*

Section 6.3.3 provides evidence for the capability of *T. brixii* to produce cell associated and secreted serine proteases. However, other oral contributors to periodontal disease produce a variety of cell surface or secreted biomolecules that progress or add to disease (Imamura, 2003, Dashper et al., 2011). One of these important virulence factors are haemolysins (Hillman et al., 1993, Socransky and Haffajee, 1992, Grenier, 1991). A simple haemolysis assay was devised, adapting from (Dailey et al., 1990) to assess the ability of *T. brixii* to lyse red blood cells ([section 2.4.20](#)). Cell pellets and supernatants from *T. brixii* cultures were applied to the assay, as well as medium supernatant from a *T. brixii*/canine gingival fibroblast co-culture experiment ([section 2.4.23](#)). Also, a canine oral bacterial culture, *P. gulae* II (Davis et al., 2013), was also used in the assay as a control organism, with high haemolytic activity (Fournier et al., 2001).

Figure 32 displays the relative levels of haemolytic activity of each of the samples tested. Samples were incubated with either canine (Figure 32a and Supplemental Table 17a) or horse (Figure 32b and Supplemental Table 17b) red blood cells and lysis of cells was monitored by absorbance at 405 nm. The percentage lysis was calculated by dividing the absorbance reading of samples by the average of the A405 nm readings of the 100 % lysis control replicates (Triton X-100), and expressing the values as percentages. With horse red blood cells, *T. brixii* cell pellet and supernatant samples exhibit a mean percentage haemolysis value of 14.75 % (SD. 1.93 %) and 7.49 % (SD. 0.52 %), respectively (Figure 32b and Supplemental Table 17b). One-way ANOVA analysis confirms that the *T. brixii* cell pellet sample produce a significantly increased level ($p=0.0012$) of haemolysis in horse cells compared to the DMEM control (Figure 32b and Supplemental Table 18b). When the same samples are tested with canine blood cells, a further increase in the level of haemolysis is observed. Mean percentage haemolysis value for the *T. brixii* cell pellet and supernatant samples were 27.16 % (SD. 5.31 %) and 7.75 % (SD. 0.36 %), respectively (Figure 32a and Supplemental Table 17a). One-way ANOVA analysis confirms that the *T. brixii* cell pellet sample gives a significantly increased level of haemolysis ($p=0.001$) in canine cells compared to the DMEM control (Figure 32a and Supplemental Table 18a).

With horse red blood cells, the *T. brixii*/canine gingival fibroblast co-culture supernatant sample exhibited a mean percentage haemolysis value of 9.86 % (SD.

0.50 %) (Figure 32b and Supplemental Table 17b), not significantly different ($p>0.05$) from the DMEM control (Figure 32b and Supplemental Table 18b). However with canine blood cells there was an increase in haemolysis with this sample.

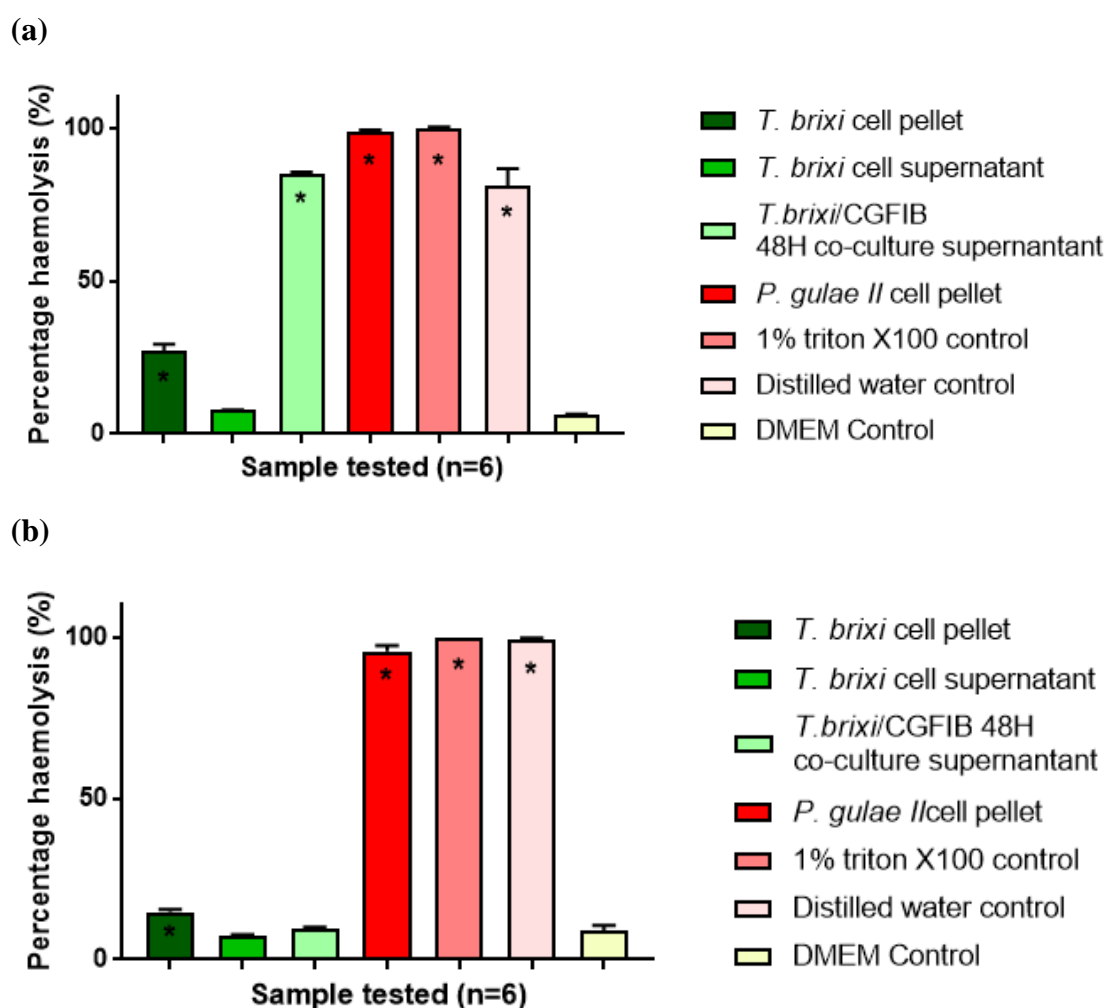


Figure 32. Mean percentage haemolysis values (n=6) of (a) canine red blood cells and (b) equine blood cells, exhibited by *T. brixii* cell pellets and supernatants, and *T. brixii*/canine gingival fibroblast co-culture supernatant. 1 % triton X-100 and distilled water are 100% lysis controls. A known haemolytic bacterial strain, *P. gulae II*, was a positive control and DMEM the buffer negative control. Samples were tested in sextuplet. Black bars indicate the standard error of the mean. Asterisks indicate significantly different ($p < 0.05$) values when compared to the DMEM medium control. The *T. brixii* cell pellets exhibit 14-27% haemolysis of both canine and horse blood cells. *T. brixii* cell supernatants do not enable haemolysis. The *T. brixii*/canine gingival fibroblast co-culture supernatant produced 85% haemolysis of canine blood cells but not in horse blood cells.

A mean haemolytic value of 84.91 % (SD. 1.64 %) was seen with the *T. brixii*/canine gingival fibroblast co-culture supernatant sample and canine blood (Figure 32a and Supplemental Table 17a), significantly different ($p=0.0001$) to the DMEM control (Figure 32a and Supplemental Table 18a). The positive control sample, a *P. gulae* *II* bacterial cell pellet, showed as expected haemolytic activity with both canine and horse blood. Haemolysis mean values of 98.81 % (SD. 1.32 %) and 95.66 % (SD. 4.30 %) were seen, with canine and horse blood cell respectively (Figure 32a and b and Supplemental Tables 17a and b), both values being significantly different ($p=0.0001$) to the DMEM control (Figure 32a and b and Supplemental Tables 18a and b).

The results of this experiment reveal the capability of *T. brixii* to haemolyse red blood cells. Noticeably greater haemolysis was seen with canine blood cells compared to equine cells. The haemolytic activity of *T. brixii* was found to be cell associated only. *T. brixii* in the presence of canine gingival fibroblast cells show a dramatic increase in secreted haemolytic activity, possibly due to upregulated expression of haemolytic factor (s). This change is probably a result of the trichomonads sensing the host cell in their environment.

There is no evidence in the literature of innate cellular haemolytic activity from mammalian host cells, however to confirm that the haemolytic activity seen with the co-culture supernatant came from *T. brixii*, and not from the host cells, the experiment was repeated with lysed host gingival cells (Figure 33 and Supplemental Table 19a and b). Mean haemolysis values of canine gingival fibroblast cell pellets and supernatants were found to be only 5.94 % (SD. 0.57 %) and 7.69 % (SD. 1.27 %) with canine blood cells, respectively (Figure 33a and Supplemental Table 19a), and only 4.66 % (SD. 0.24 %) and 5.20 % (SD. 0.82 %) with horse blood cells, respectively (Figure 33b and Supplemental Table 19b). All haemolysis values for these gingival cell fibroblasts only samples were not significantly different ($p>0.05$) to the DMEM control using one-way ANOVA analysis (Figure 33 and Supplemental Table 20). The absence of this difference from the DMEM control samples confirm there was no haemolytic activity in canine gingival fibroblasts. Therefore, the haemolytic activity observed with the co-culture experiments must come from *T. brixii*. A variety of oral microorganisms exhibit haemolytic activity (Falkler et al., 1983, Grenier, 1991, Socransky and Haffajee, 1992, Sela, 2001, Okamoto et al., 1999) and are thought to contribute to this complex disease using

these abilities. Bacteria such as *Fusobacterium* sp. (Falkler et al., 1983), *Trepenema* sp. (Grenier, 1991), and *Prevotella* sp. (Okamoto et al., 1999) were shown to agglutinate and lyse human red blood cells, using these abilities as part of virulence mechanisms that contribute to periodontal disease (Socransky and Haffajee, 1992).

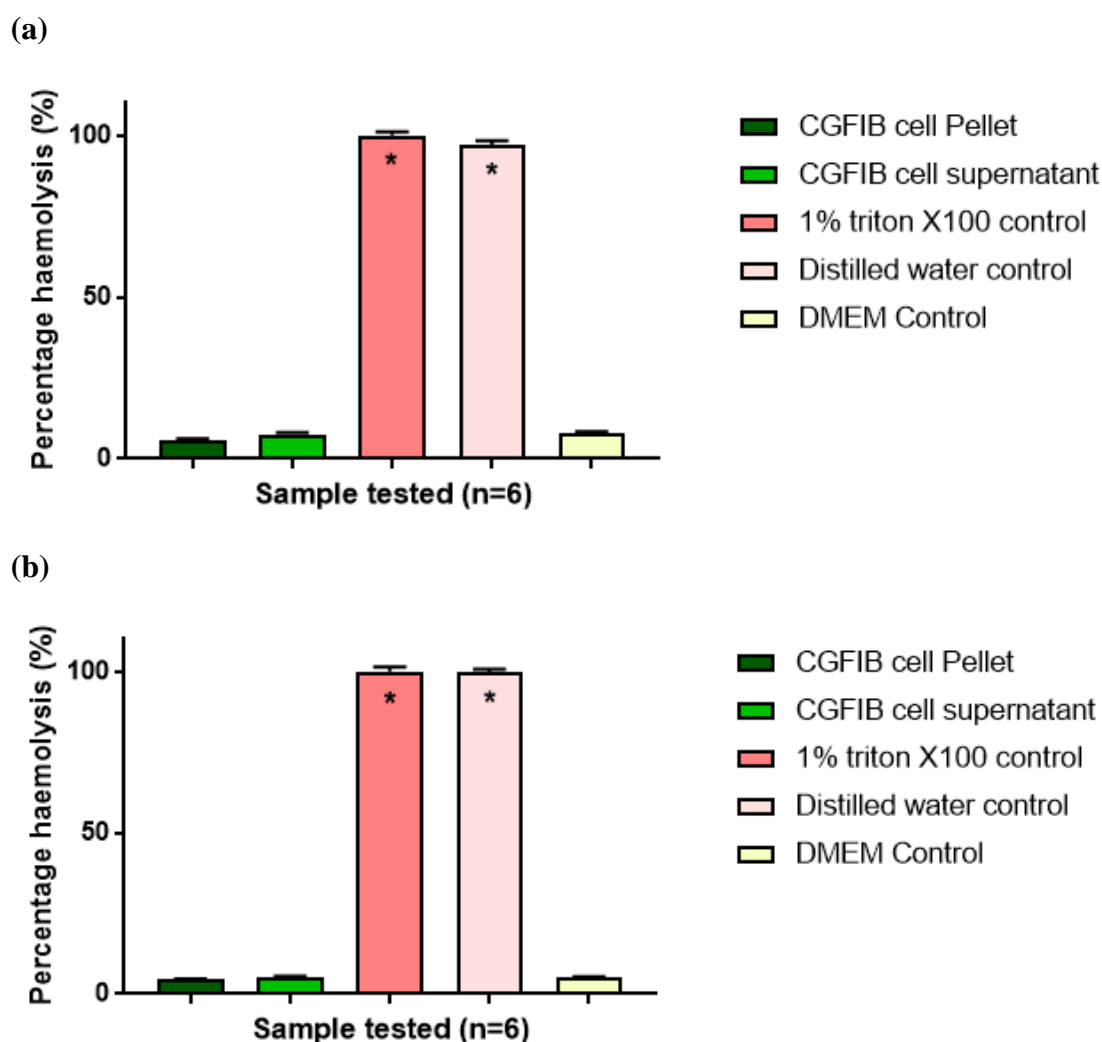


Figure 33. Mean percentage haemolysis values (n=6) of (a) canine red blood cells and (b) equine blood cells, exhibited by canine gingival fibroblast (CGFIB) cell pellets and cell supernatant. 1 % triton X-100 and distilled water are 100% lysis controls. DMEM was the buffer negative control. Samples were tested in sextuplet. Black bars indicate the standard error of the mean. Asterisks indicate significantly different ($p < 0.05$) values when compared to the DMEM medium control. CGFIB cell pellets or supernatant did not induced red blood cell haemolysis in either canine or horse blood.

The same mechanisms and potential to damage blood cells is also seen in protozoa such as *Entamoeba* sp. (Lopez-Revilla and Said-Fernandez, 1980) and *Trichomonas vaginalis* (Krieger et al., 1983). The data collected here indicates *T. bixi* as an organism that may contribute to disease through haemolysis.

6.3.5. Elastase activity of *T. bixi*

Elastins in the gingiva are a components that make up the microtubules of the periodontal ligament (Tsuruga et al., 2002). The breakdown of these ligaments is a key part of the disease process and leads to eventual tooth loss (Irfan et al., 2001). Their destruction is mediated by the enzyme elastase and levels of elastase are an indicator of periodontal disease progression (Palcanis et al., 1992, Chen et al., 2000). A variety of microorganisms have the potential to produce elastases (Werb et al., 1982) or bring about the release of elastases from polymorphonuclear leukocytes (Ding et al., 1997). To assess if *T. bixi* produce elastase, an assay was devised to measure elastase activity in cell culture pellets and supernatants ([section 2.4.21](#)). Cell pellets and medium supernatant from *T. bixi* cultures were applied to the assay, as were cell pellets and medium supernatant from *T. bixi*/canine gingival fibroblast co-culture experiments ([section 2.4.23](#)).

Six technical replicates of each sample was added to the assay substrate, N-Succinyl-Ala-Ala-Ala-p-nitroanilide, and breakdown of this substrate by elastases were monitored by measuring the absorbance at 405 nm. Figure 34 shows the results of the experiment. None of the test samples produced any detectable signs of elastase. The assay was found to be viable as a strong increasing signal from the chromophore p-nitroanilide breakdown product of the assay substrate, was produced by the enzyme control sample, 0.4 U of porcine elastase (Figure 34).

In periodontal pockets, increased levels of elastase is linked with periodontal disease samples (Palcanis et al., 1992, Chen et al., 2000). The periodontal pathogens, *Fusobacterium nucleatum* and *Treponema denticola*, do not produce elastases themselves, but bring about their release from polymorphonuclear leukocytes (Ding et al., 1997, Ding et al., 1996). If *T. bixi* do influence the levels of elastase at the site of periodontitis, this interaction with leukocytes is potentially a method by which they may bring this about. More work and experiments are

required to determine whether interaction with host immune cells results in elastase release.

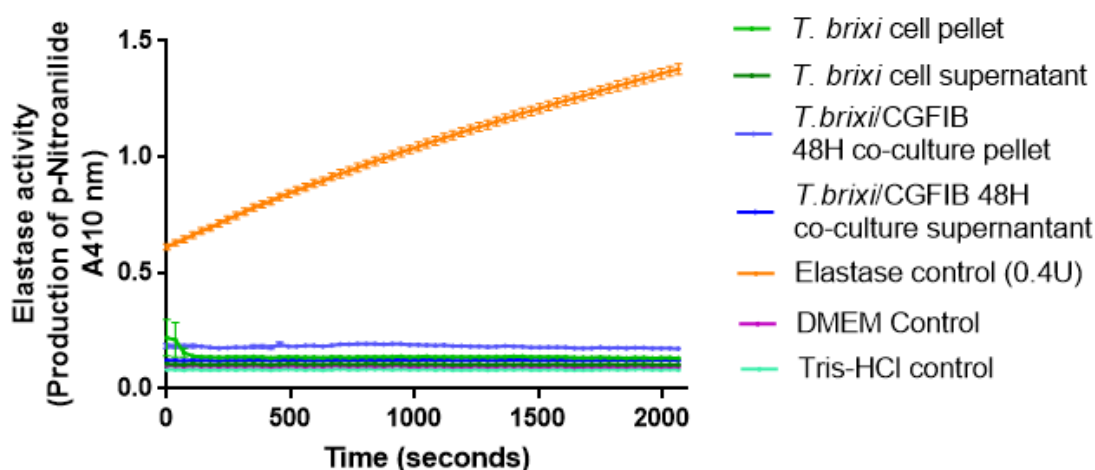


Figure 34. Elastase enzyme activity of *T. brixii* cell pellets and supernatants (n=6), *T. brixii*/canine gingival fibroblast co-culture cell pellet and supernatants (n=6), and *P. gulae II* cell pellets and supernatants (n=6). DMEM and Tris-HCl were the buffer negative controls. A 0.4U elastase enzyme control was used as a positive control for the assay. Elastase activity was assessed by monitoring the enzymatic breakdown of the assay substrate N-Succinyl-Ala-Ala-Ala-p-nitroanilide, to N-Succinyl-Ala-Ala-Ala and p-Nitroanilide. p-Nitroanilide formation was detected by measuring absorbance at 410nm. None of the test samples showed increased absorbance at 410nm during the experiment, indicating no inherent elastase activity in each.

6.3.6. *T. brixii* cytopathic effect on canine gingival fibroblasts

Sections 6.3.1 to 6.3.5 of this chapter reported that the canine oral protozoan, *T. brixii*, can produce a variety of biomolecules and these may influence and contribute to periodontal disease and other oral disorders. Canine periodontal disease, as in humans and other mammals, is an inflammatory mediated, tissue destroying disease that eventually leads to alveolar bone retraction and eventual loss of teeth (Harvey, 1998). To monitor the effects of *T. brixii* on tissue cells *in vitro*, a previously immortalised canine gingival fibroblast cell line, initially isolated as a primary cell line from a 6 year old Great Dane ([section 2.4.22](#)), was used in a co-culture experiment ([section 2.4.23](#)). The gingival cells were seeded into wells at

approximately 10000 cells per well and approximately 5000 *T. brixii* cells were added to each well. The two cell types were co-incubated for 48 hours and the number of gingival cells present was monitored at regular time points throughout the experiment, by measuring cell viability, using a metabolic indicator, and counting cell nuclei ([section 2.4.23](#)).

Figure 35 and Supplemental Table 21 display the results of cell viability measurements during the experiment. The cell viability assays is determined from cell metabolic activity using the alamarBlue® indicator dye, a cell permeable, non-fluorescent resazurin compound, which is reduced by active cells to a fluorescent compound, resorufin (Nakayama et al., 1997). The amount of resorufin product formed is directly proportional to the number of live cells present.

During the first 24 hours of co-culture, the number of metabolically active canine gingival fibroblasts cells remain stable, and not significantly different ($p=>0.05$), in both fibroblast only wells and the co-culture wells (Figure 35 and Supplemental Tables 21 and 22). At 24 hours the mean metabolic activity recorded from the gingival fibroblast wells gave a value of 95924 (SD. 15314) fluorescence units, and the co-culture wells gave a value of 93888 (SD. 2318) fluorescence units. But after 48 hours, the gingival fibroblast wells still gave a reading of 82005 (SD. 3546) fluorescence units, however the co-culture only gave a significantly reduced metabolic activity reading ($p=<0.0001$) of 6950 (SD. 1070) fluorescence units (Figure 35 and Supplemental Tables 21 and 22). In these co-culture wells, after 48 hours incubation, the metabolic activity of canine gingival fibroblasts had reduced by approximately 92 %. By contrast, the metabolic activity of canine gingival fibroblasts in the control wells (no *T. brixii* added) had reduced by 14 %.

To confirm if these changes, the cell nuclei of gingival cells were counted in each well of the experiment. The cells remaining in each well were fixed in position using 2 % (w/v) paraformaldehyde, and the nuclei of remaining cells were stained with the DNA intercalating dye DAPI (4',6-diamidino-2-phenylindole). Six fields of view images of each well were taken using a DAPI image filter and the cells (nuclei) remaining in each well enumerated using an ImageXpress Micro XLS Widefield High-Content Analysis System ([section 2.4.23](#)).

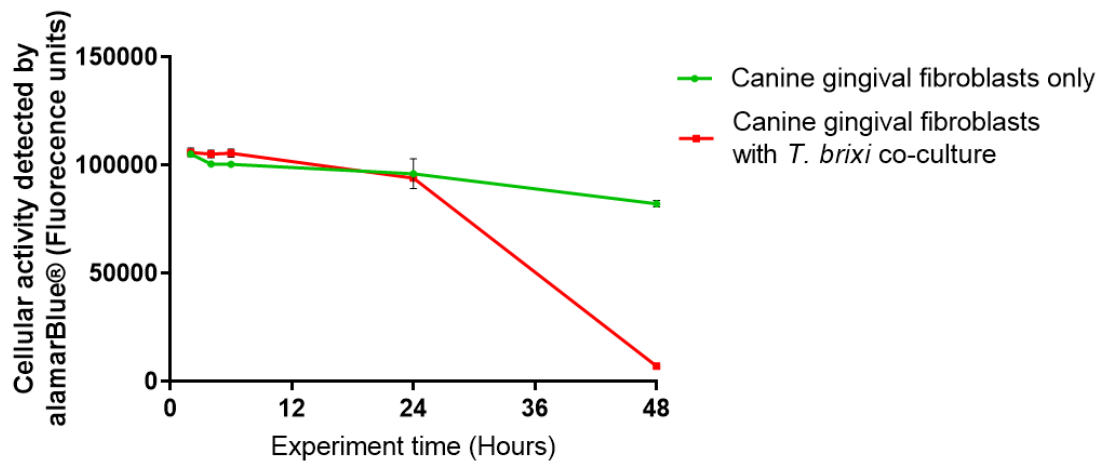


Figure 35. Mean values (n=6) of cellular activity from canine gingival fibroblasts co-cultured with, and without, the canine oral trichomonad, *T. brixii*. Cellular activity was monitored at time points covering a 48 hour period using the cell health indicator fluorescent dye alamarBlue®. Fibroblasts co-cultured with *T. brixii* were seen to become less metabolically active after 24 hours of co-incubation, and virtually no cellular activity was seen at 48 hours, with a significantly reduced reading (see Supplemental Table 22). Black bars indicate the standard error of the mean for each sample.

The numbers of cells, identified by their nuclei in each sample are displayed in Figure 36 and Supplemental Table 23. As seen with the cell metabolic activity data, the number of canine gingival fibroblasts cells present in wells up to the first 24 hours of the experiment, remain fairly stable in both the fibroblast only wells and the co-culture wells (Figure 36 and Supplemental Table 23). The exception was time point 4 hours, where a significantly reduced mean cell nuclei count ($p=0.0043$) was observed in the co-culture well, compared to the gingival fibroblast only wells (Supplemental Table 24). At 6 hours the mean number of cells identified in the gingival fibroblast only wells was 1453 cells (SD. 267) per view analysed, and the co-culture wells was 1543 cells (SD. 109) per view analysed. However by 24 hours, the mean number of cells identified in the gingival fibroblast only wells had increased slightly to 2442 cells (SD. 122) per view analysed, and the co-culture wells had reduced significantly to 290 cells (SD. 38) per view analysed $p<0.0001$ (Figure 36 and Supplemental Table 23 and 24). At the final time point, 48 hours, the mean number of cells identified in the gingival fibroblast only wells was 2327 cells (SD. 152) per view analysed, and the co-culture wells had reduced significantly further, to 67 cells (SD. 10) per view analysed, $p<0.0001$ (Figure 36 and Supplemental Table 23 and 24).

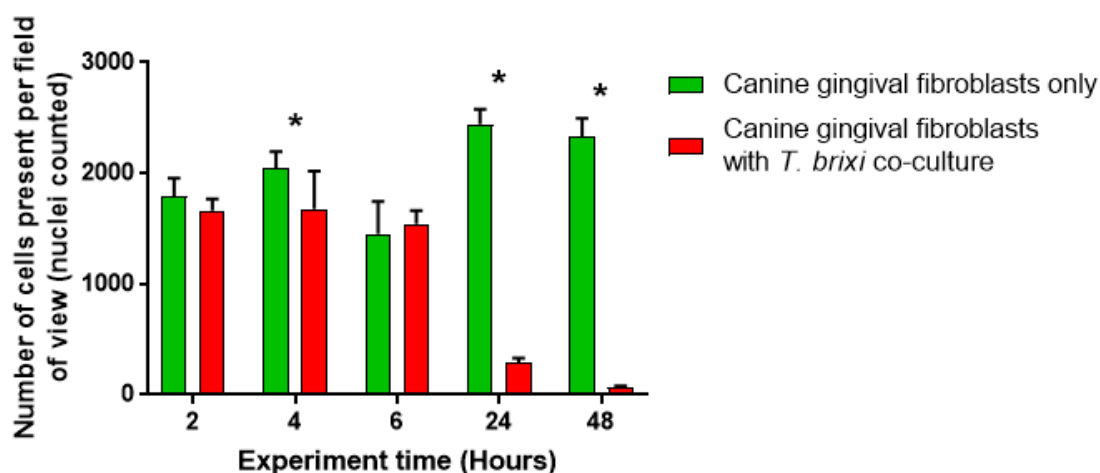


Figure 36. Mean values for cell numbers of canine gingival fibroblasts co-cultured with, and without, the canine oral trichomonad, *T. bixi*. Cell counts were conducted by counting stained nuclei over a 48 hour period using an ImageXpress Micro XLS Widefield High-Content Analysis System and MetaXpress software V5.3 (Molecular Devices, UK). Fibroblast cell destruction was seen in samples co-cultured with *T. bixi*. Cell numbers steadily decrease at 24 hours of co-incubation, and virtually no cells are present at 48 hours. Asterisks indicate significantly different values between time point counts (see Supplemental Table 24). Black bars indicate the standard error of the mean for each sample.

In the co-culture wells, after 48 hours incubation, the number of canine gingival fibroblasts had reduced by 96 %. By contrast, the numbers of canine gingival fibroblasts in the control wells (no *T. bixi* added) has increased by 29 %.

The data in these series of experiments show that culturing *T. bixi* with canine gingival fibroblasts results in a loss of metabolic activity in the fibroblasts (approximately a reduction of 92 %), presumably reflecting cell death through cytotoxic effects, as seen by a reduction of approximately 96 % in cell numbers. *T. vaginalis* and *T. tenax* also are capable of causing cell death through cytopathic effects in a variety of cell types (Gonzalez-Robles et al., 1995, Gilbert et al., 2000, Salvador-Membreve et al., 2014, Ribeiro et al., 2015). These species are thought to induce cytotoxicity through cell interactions (Arroyo et al., 1992, Lustig et al., 2013, Ribeiro et al., 2015), or via a *Trichomonas* led phagocytosis mechanism (Pereira-Neves and Benchimol, 2007, Midlej and Benchimol, 2010). As with *T. vaginalis* and *T. tenax*, *T. bixi* may also interact with canine gingival host cells in a similar way, however more work is required to elucidate this mechanism(s). The

data provided here add more weight to argument that *T. brixii* is contributor to canine periodontal disease, rather than an organism that takes advantage of the favourable environment. However more work, such as further *in vitro* assays and animal models are required to decide this conclusively.

General Conclusions and Discussion

CHAPTER 7: GENERAL CONCLUSIONS AND DISCUSSION

7.1. Detection of protozoa

Canine periodontal disease is a widespread oral disorder of dogs (Kyllar and Witter, 2005). The population prevalence is estimated to range from 44-64% of all individuals (V. Butković et al., 2001, Hamp et al., 1984). Plaque is the main cause of periodontal disease and for several decades researchers have focused on examining the bacterial communities present in plaque, however other organisms are known to exist in plaque. Understanding periodontal disease at all stages of its progression still requires extensive research and more studies are needed to assess the impact of other microorganisms in plaque.

The primary aim of this thesis was to determine if protozoa are present in the canine mouth and, if so, to evaluate if they have an impact on the canine periodontal disease process. To screen for the presence of protozoa a tool was required that would identify protozoa within samples, in a simple, cost and time efficient manner. Although some detection methods for protozoa are available, they rely on species specific modes of identification which use time and labour intensive microscopy protocols (CDC_protocol, 2013, Bogoch et al., 2006, Gonzalez-Ruiz et al., 1994, Utzinger et al., 2010) or use costly antigen detection systems (Badaro et al., 1986, Davison et al., 1999, Kehl et al., 1995, Moody, 2002, Ota-Sullivan and Blecker-Shelly, 2013, Singh et al., 2009, Zimmerman and Needham, 1995). These labour intensive and costly methods were deemed unsuitable for the purpose of this study, so molecular methods of identification were investigated. Molecular based detection methods have been developed to identify some protozoa and have proven to be highly sensitive, but are inclined to be species specific in their detection (Becker et al., 2004, Bharti et al., 2007, Birkenheuer et al., 2003, Huston et al., 1999, Madico et al., 1998, Qvarnstrom et al., 2006, Verweij, 2014, Verweij and Stensvold, 2014) or require multiplex PCR techniques to identify a limited group of organisms within samples (Bruijnesteijn van Coppenraet et al., 2009, Maas et al., 2014, Orlandi and Lampel, 2000, Verweij et al., 2004).

At the time, it was unknown which protozoa were present in canine plaque, if any, so a broad spectrum molecular detection method, targeted towards the identification of all protozoa was required. No published sets of targeted primers were available

to amplify DNA from a broad range of protozoan organisms. Thus, the first section of the thesis was dedicated to the development of this method.

The aim was to develop a targeted, molecular based method for the identification of protozoa in microbial, complex samples. A PCR based method was devised that enabled the rapid, multiplexed identification of protozoa in multi-species clinical samples ([Chapter 3](#)). The protocol enables the amplification of an approximately 900 to 1500bp amplicon (depending on the organism) of the eukaryotic 18S rRNA gene containing variable regions 4 to 8 (Van de Peer and De Wachter, 1997). This amplicon allowed the identification of the protozoan organisms in sample based on the PCR product size ([section 3.1](#)). The PCR was seen to be highly sensitive with detection limits found to be as low as 3.2 picograms of protozoan DNA per PCR. All organisms tested were detected with as little as 10 ng of DNA per PCR reaction, or at 200 cells and lower per PCR reaction under spiked sample conditions ([section 3.3](#)). A disadvantage of the new PCR protocol was that it did not detect organisms from the eukaryotic classification group Fornicata. Although *in silico*, the PCR is predicted to amplify DNA from these organisms ([section 2.1.1](#)), it is evident that an amplicon was not produced from the test species, *G. intestinalis* ([section 3.4](#)). As the 18S PCR developed in this thesis is directed at identifying prominent protist species within clinical samples, the lack of *Giardia* spp. detection and other members of the Fornicata family is a noteworthy deficiency of the protocol. To combat this deficiency, the protocol was enhanced by the addition of supplementary primers to detect faecal protozoa. It was found to exhibit a marked improvement in protozoa detection compared to common microscopy-based and antigen detection-based diagnostic methods ([section 3.4](#)). This amendment to the protocol widened the detection abilities of the method. In comparison to the commercial wet-mount microscopy and antigen detection methods, the 18S-*giardia gdh* PCR protocol identified more positive samples and more protozoan species present in the samples. This exhibits a discernible improvement in protozoa detection in clinical (faecal) samples and provides a more effective tool for researchers, clinicians and healthcare professionals.

The evaluation experiments of the PCR protocol conclude that it is fit for purpose, providing a targeted and sensitive protocol to screen for the presence of protozoa in complex samples. It has the capability to identify protozoa in a variety of sample

types and could prove highly useful for researchers and clinicians as a fast, efficient and cost effective diagnostic tool. Ideally, a single set of primers that would identify all protozoa present in the sample is preferred as this would make the protocol simpler and easier to conduct. If further time was available more work could be carried out to investigate other regions of the 18S gene or indeed other eukaryotic genes that could provide a target for primer that bind to all species.

Using the developed PCR tool, two distinct protists were identified as being present in a collection of canine plaque, consisting of 92 samples. *Trichomonas* sp. was observed in 20% of healthy dogs, 61% of dogs with gingivitis, 73% of dogs with periodontal disease stage 1, and 67% of dogs with severe periodontal disease ([section 3.5](#)). *Entamoeba* sp was identified in 22% of severe disease samples but was not seen in any of the other sample types ([section 3.5](#)). The overall prevalence of trichomonads and Entamoebae detected in the total sample population was 56.52 % (52/92) and 4.34 % (4/92) respectively. Upon analysing the 18S sequence abundance for each organism using Roche 454™ GS FLX+ sequencing, *Entamoeba* made up 0.01 % of a 'Health' pool sample, 0.01 % of a 'Gingivitis' pool sample, 0.80 % of a 'PD1' pool and 7.91 % of a 'Severe Disease' pool sample ([section 3.5](#)). 18S protozoan sequences belonging to the genus *Trichomonas* were 3.51 % of the 'Health' pool sample, 2.84 % of the 'Gingivitis' pool sample, 6.07 % of the 'PD1' pool and 35.04 % of the 'Severe Disease' pool ([section 3.5](#)).

Both techniques reveal for the first time the presence of trichomonads and Entamoebae in the dental plaque of dogs. Statistical analysis of the data sets also concluded both genera were more likely to be present in the later stage periodontal disease samples ([section 3.5](#)). The findings also give an initial indication of a role for canine oral protists in the periodontal disease process. It is thought that the disease results as a consequence of the complex interaction between bacterial species and the host immune system (Genco and Slots, 1984), however these finding indicate that protists could also be involved in this process and require greater consideration.

The presence and potential impact on human periodontal disease of both trichomonads (Athari et al., 2007, Cuevas et al., 2008, Dudko and Kurnatowska, 2007) and Entamoebae (Bonner et al., 2014, Decarneri and Giannone, 1964, Trim

et al., 2011) have been described. In humans, both have been shown to have the potential of contributing to disease and also damage host cells (El Sibaei et al., 2012, Ribeiro et al., 2015, Yamamoto et al., 2000). These pathogenic capabilities should be investigated further to conclude if they are indeed relevant to the disease process. Canine oral protozoa have been described during this thesis, and as such, more research should now be undertaken to decipher if these canine strains are similar to the human strains, and if they can contribute to canine periodontal disease.

7.2. Temporal dynamics

To investigate the prevalence of both *Entamoeba* and *Trichomonas* in canine plaque samples further, and in more localised samples, two qPCR assays, targeting the two canine oral protozoa identified, were developed ([chapter 4](#)). These assays enabled the detection and quantification of these organisms localised to teeth, within a longitudinal data set, giving further insights into their associations with periodontal disease. Both assays were developed as part of this thesis as no published qPCR assays were available for the detection of the two species of interest.

The sensitivity and robustness of each assay was evaluated using standard quantitative PCR techniques (Bustin et al., 2009). Both displayed excellent reaction efficiencies ([section 4.2](#)), well within the accepted range of 90-105% efficiency, and R^2 values greater than 0.980 (Bustin et al., 2009). Each assay was also tested to ascertain its limit of detection ([section 4.2](#)). It was possible to detect protozoa DNA using both assays at very low levels. The limits of detection were determined to be 30.63 C_t units (467 gene copies) and 31.16 C_t units (666 gene copies) for the *E. gingivalis* EG1 and *Trichomonas* spp. TC2 assays, respectively ([section 4.2](#)). Genomes for both species are not available so an accurate estimate of how many actual cells of an organisms these copy number detection limits equate to is difficult to decipher without cultured isolates. However, a measured estimate would be below 100 cells for both assay, considering the eukaryotic gene is commonly repeated in tandem arrays in most eukaryotic species (Malone, 2015).

The Assay EG1 did not show cross-reactivity with any of the microorganisms tested and was shown to be completely specific ([section 4.3](#)). The Assay TC2 showed cross-reactivity with only one of the microorganisms tested ([section 4.3](#)), an

unexpected positive reaction with *T. tenax*. No other positive reactions were seen for the other samples tested. Although this limited the species-specific quantification abilities of the assay, a further modification to the overall protocol was introduced to distinguish the precise species of *Trichomonas* that were present in each sample. Digestion of the qPCR amplicon formed during the assay allowed the identification of the species present in the sample ([section 4.4](#)). If a single species is present in samples then the TC2 qPCR assay can be used without modification. However, recent publications using culture and molecular-based methods have indicated the possibility of several *Trichomonas* species being present in canine mouths (Kellerova and Tachezy, 2017, Kutisova et al., 2005). In this mixed sample type, the TC2 assay offers a more efficient method of oral *Trichomonas* identification and quantification due to its duplex identification technique. Without this method a separate, species-specific, assay for each trichomonad present in the samples would need to be designed, validated and carried out for all samples, adding significant cost and time.

The additional digestion step required to distinguish between the Trichomonad species is an obvious disadvantage of the protocol. Future work would involve redeveloping the assay possibly targeting another sequence region of gene to provide a specific assay for the detection of the canine oral Trichomonad, as is the assay targeting *E. gingivalis*. This said, the developed assay still enables the rapid identification of the oral trichomonad in low concentration samples.

The optimised qPCR assays were used to survey an exceptional set of samples collected from the individual teeth of 30 dogs over a period of 60 weeks after cessation of tooth brushing ([section 4.5](#)). Sample collections took place every six weeks and the health state of teeth was monitored and only allowed to progress until early stage periodontal disease (<25% attachment loss). These samples provided an excellent opportunity to study the disease progression in samples rarely collected in these numbers or sample detail. A subset of samples, 444 from the 30 dogs were identified for analysis. The abundance of both protists was analysed with the newly developed qPCR assays.

The sample set consisted of 47 teeth that progressed to early periodontitis (<25% attachment loss), designated as “Progressing” and a separate set of 47 matched teeth that did not progress beyond mild gingivitis during the 60 week study, designated as “Non Progressing” ([section 4.5](#)). The metadata collected during the study was

extensive and provided the opportunity to analyse a variety of dynamics from the dataset.

The first factor investigated was the protozoa abundance at each time point during the study as the samples progressed towards early periodontal disease ([section 4.5.1](#)). The estimated collective abundance (estimated by gene copy number) of both organisms at each time point during the study (-5 to 0) was analysed. No significant differences in abundance of the canine oral *Trichomonas* sp. or *E. gingivalis* were seen when comparing teeth that progress into early periodontal disease to teeth that did not progress ([section 4.5.1](#)). However, for both organisms, significant increases in protozoa abundance were seen in the latest study time points (time point 0) compared to the earliest time points (time point -5) ([section 4.5.1](#)). In conclusion, the primary analyses of the data set suggests that the abundance of *E. gingivalis* and the canine oral *Trichomonas* sp. is not associated with the progression of canine teeth into early stage periodontal disease. However, statistically significant increases in the numbers of both protozoa (abundance) were seen as time progressed, in both groups of teeth.

The disease “Progressing” data set was comprised only of teeth that progressed to early stage periodontal disease (<25 % attachment loss). At this early stage, the disease is still reversible and can be returned to healthy through dental treatment (Harvey, 1998, Socransky and Haffajee, 1992). The data set is therefore not a set that progresses to the final stages of periodontal disease (PD2-4). It is still unclear if either organism contributes to the disease or merely takes advantage of the more favourable conditions. More studies are required with sample types that progress further into the more advanced stages of the disease, to test this hypothesis.

The data set was also examined to investigate the probability of detecting the two protists during the study timeline ([section 4.5.2](#)) and also to investigate if a particular species of *Trichomonas* is more associated with disease progression ([section 4.5.3](#)), however neither analyses showed any statistical correlations to the disease samples or disease progression.

The data set was analysed further to identify if any of the metadata recorded for each animal sample, age at the start of trial, sex, tooth type, tooth location (side of the mouth) and tooth area (of the mouth), have a relationship with the abundance of either organism. Most of these data covariates produced no or very weak associations with organism abundance, however the tooth type covariate showed

more interesting and convincing evidence of correlation. Both *E. gingivalis* and the canine *Trichomonas* sp. were clearly more abundant in the molar and premolar teeth of dogs and their numbers are more likely to increase as the tooth progresses towards early periodontal disease ([section 4.5.4](#)). This is less evident with *E. gingivalis* in this data set, maybe due to the abundance of *E. gingivalis* being lower in pre-periodontal disease samples ([section 3.5](#), and (Patel et al., 2017)). The reasons for the increased numbers of protozoa in molar and premolar teeth is currently unknown. However it has been seen that molars and premolar teeth in Miniature Schnauzer dogs have higher rates of periodontal disease incidence and also progress more quickly from a healthy state to disease (Marshall et al., 2014), but a link between these facts and oral protozoa has not been tested.

These qPCR data analyses provide interesting results. The abundance of both protozoa are clearly correlated to more diseased samples and to particular teeth (molars and premolars) within the mouth. The reasons for these correlations are unknown and further work is required to explore this more. Unfortunately we were unable to collect samples that progressed further towards the later stages of periodontal disease, due to ethical limits. However, if these samples are possible to obtain using alternative sources, for example from dogs that progress to a later disease stage seen in veterinary practice, they could conclusively evaluate the association of these organisms with periodontal disease. Any future work using these assay that investigate canine periodontal disease should consider these later disease stage samples.

7.3. Primer independent tools

Using traditional molecular-based techniques, the early part of this thesis has identified oral protists in canine plaque. These methods use existing nucleotide sequences for the purposes of PCR primer design, which bind to their targets and allow the amplification of DNA for identification purposes. The reliance on existing sequences for primer design introduces a significant weakness for the design process. Target sequences within samples that are not considered during the primer design process, due to a lack of candidate sequence availability, may be neglected by the amplification protocol, especially if its target regions are significantly different to the sequences used for the primer design (Klindworth et al., 2013,

Poretsky et al., 2014). Although two distinct protozoa were identified using the PCR based methods, there was the potential that unknown or untargeted protozoa present in samples were not detected. PCR primers may also show a priming bias towards particular sequences and may overestimate or underestimate abundance (Tremblay et al., 2015, Kennedy et al., 2014). To address these weaknesses with PCR-based methods, a protozoa identification technique not based on the use of pre-existing sequence information and PCR was devised ([Chapter 5](#)). The methods developed were based on the direct sequencing of ribosomal RNA (rRNA) extracted from plaque samples, which all eukaryotic microorganisms (and prokaryotes) encode genes for (Adl et al., 2012).

Two separate methods were developed and used to determine the protozoa present in canine plaque samples. The methods employed the use of the Oxford Nanopore Technologies' MinION™ platform, a sequencing device capable of producing long-read, real-time, RNA sequence reads on the benchtop (Jain et al., 2016). The first method was successfully used to sequence RNA samples that were fully reverse transcribed to cDNA. A bacterial ribosomal depletion step was added before the reverse transcription to maximise sequencing throughput for the target sequences of interest ([section 5.2](#)). This depletion step was successful at removing a large proportion of 16S/23S sequences, however the bacterial sequences remaining were persistent enough to sequester a large proportion of the sequencing capacity ([section 5.3](#)). The method also suffered from inefficient barcoding of samples, where only 32,938 barcoded reads were found from a total 142,473 reads obtained from the MinION™ sequencer ([section 5.3](#)). As this initial methodology was found to possess several weaknesses a second it was not explored further and an alternative, but similar method was developed and tested.

The second method, direct MinION™ RNA sequencing, involved the direct sequencing of RNA molecules in samples, with little pre-processing and therefore minimal processing biases ([section 5.4](#)). This alternate method to sequence RNA molecules produced hundreds of thousands of reads and total sequencing yields in the hundreds of megabases ([section 5.4](#)). Although a second strand synthesis reaction is involved in this alternate method, the second strand does not introduce any bias to the sequencing as it is only used to improve flowthrough of the sequencing technology and used to proofread and thus improve the overall read quality. This affords a sizable advantage over the cDNA sequencing method. In

addition, the sequencing of RNA molecules present in samples gives an indication of microorganism activity as the number of ribosomes present are proportional to organism metabolic activity.

The protozoa identified with both MinION™ sequencing protocols developed in this thesis concur with the results of previous PCR screening tools designed in this thesis ([chapter 3](#)). The plaque samples tested, were consistently shown to contain *Trichomonas* and *Entamoeba* only. No other protozoan genus have been detected, even with these primer independent methods. These results conclude that these two organisms are the only protozoa genera likely to be present in canine plaque, however multiple species from within each genus could be found in the canine mouth (Kellerova and Tachezy, 2017, Kutisova et al., 2005). Also, a point to note is that the sequences are identified by comparison against existing 18S sequences (Altschul et al., 1990, Quast et al., 2013). Therefore, if unknown protist sequences are present, they will not be identified. Methods similar to the operational taxonomic unit-based cluster identification techniques would in theory allow the discovery of these sequences (Schloss and Westcott, 2011, Schloss et al., 2009, Rideout et al., 2014), however these techniques are still not without their drawbacks (Edgar, 2018).

Both MinION™ RNA sequencing protocols, developed here, show excellent potential as techniques capable of identifying microorganisms in mixed species samples. The cDNA sequencing protocol does have the potential hurdles of bacterial depletion and barcoding, which both require further optimisation. However, the direct RNA sequencing shows particular promise. It does not have any discernible points where bias towards a particular species is introduced, and thus shows great potential as an effective protocol for the identification of microorganisms. The MinION™ RNA sequencing technology is still in early stages of development, and with future efficiency and accuracy improvements, it should become an excellent, bias-free, method to identify microorganisms in all sample types. Researchers with an interest in the bacterial populations present in mixed multispecies samples should pay particular attention to the direct RNA sequencing methodology. The current method of choice for bacterial identification uses the MiSeq Illumina Sequencing Platform (Kozich et al., 2013), however this type of short-read analyses can suffer from sequencing biases, variation introduced by the gene region sequenced, and though the use of different bioinformatics processing

methods (Kennedy et al., 2014, Klindworth et al., 2013, Kozich et al., 2013, Schloss, 2010).

Both *Entamoeba* and *Trichomonas* have been shown to be associated with disease samples (Chapters 3 to 5). Further analysis using the MinION™ Direct RNA sequencing protocols tested here with more varied disease sample types, and possibly longitudinal samples, is required to clarify the role these protozoa play in periodontal disease. The samples tested above pooled multiple plaque samples so as to allow sufficient amounts of total RNA extraction for the protocol. Further experimentation would also prove useful to conclude the minimal amounts of plaque required to obtain sufficient sample for sequencing. If the method is sensitive enough to detect RNA isolated from individual animals or better still, individual teeth, it would prove an excellent method to investigate the links between periodontal teeth and oral protozoa.

7.4. Virulence

Chapters 3-5 describe, for the first time, the identification of two protozoa found in the mouth of dogs, and their association to canine periodontal disease. At the time of writing, there are no other reported studies of oral protozoa and their association with periodontal disease in dogs.

The first of these organisms, *E. gingivalis*, is a species commonly found in the human mouth and is occasionally found in saliva and on the tonsils (Brumpt, 1913, Gros, 1849). It has until now, not been reported in the canine mouth. For further study of their biology and functional attributes, the isolation and culture of *E. gingivalis* from the canine mouth was attempted, as was the propagation of commercially available human isolates. Unfortunately, all attempts were unsuccessful and as such, further studies were not possible with this organism. As described in chapters 3, 4 and 5, *E. gingivalis* was consistently seen in, and associated with, the disease stages of canine periodontal disease, indicating they could be important in the disease process. It is therefore important that more studies are conducted with canine *E. gingivalis* isolates. Future work should concentrate on successful isolation and propagation of the strain for further biological studies.

The second organism identified as present in the canine mouth was *Trichomonas* spp. The molecular screens used to detect the organism and to investigate their

association with canine periodontal disease (chapters 3-5) were not able to conclude their species but qPCR analyses carried out in [section 4.4](#) indicated that more than one species of *Trichomonas* could be present (*T. bixi* and *T. tenax*). To enable further studies and to conclude the identity of the trichomonads present, 10 separate *Trichomonas* isolates from individual Labrador retrievers, miniature Schnauzers, and Cocker spaniels were cultured. Their molecular phylogeny was analysed to determine their species ([section 6.2.1](#)). All 10 isolates were determined to be the same species, but phylogenetically distinct from other *Trichomonas* species, therefore not previously described or published. Simultaneously, the strain was designated as *Trichomonas bixi* by a separate research group (Kellerova and Tachezy, 2017).

The structure and morphology of the strain was analysed through techniques such as antibody and silver proteinate staining, light microscopy, and scanning and transmission electron microscopy. These techniques revealed identifiable characteristics, comparable to existing descriptions common to most other trichomonad species (Benchimol, 2004, Tasca and De Carli, 2003, de Andrade Rosa et al., 2013, Honigberg, 1990). Both structural and molecular identification studies carried out in this thesis (section 6.1-6.2) indicate that isolates identified here in UK dogs resemble and are genetically the same as those in the Czech republic (Kellerova and Tachezy, 2017). Potential collaboration with researchers around the globe is a potential to compare strains. More research is required to determine if this strain is present globally in the mouth of dogs, or is a European-only strain.

As the strain identified here is unique, there are no published studies that have investigated the pathogenic potential of *T. bixi*. Human trichomonads, implicated in disease, such as *T. vaginalis* and *T. tenax*, secrete a variety of substances that contribute to disease (Kucknoor et al., 2007, Stafkova et al., 2018, Segovic et al., 1998, Nagao et al., 2000) or interact with host cells to bring about damage (Arroyo et al., 1992, Lustig et al., 2013, Ribeiro et al., 2015). Initial investigations with *T. bixi*, were conducted here to identify cell-associated or secreted factors that have potential to contribute to canine periodontal disease. *T. bixi* was found to produce significant levels of both leucine arylamidase and acid phosphatase, as well as moderate levels of α -glucosidase ([section 6.3.1](#)). The ability to produce them at generous levels may have implications for canine periodontal disease but further work to determine the exact levels produced, and if these may indeed impact in

animal or *in vitro* models, is required. *T. brixii* were shown to produce specific serine protease, similar in levels to the periodontal bacterial pathogen, *P. gulae* ([section 6.3.2](#)), and this trypsin-like activity may increase in the presence of gingival cells, again indicating a contributory factor to periodontal disease. A similar response in the presence of canine cells is also seen from *T. brixii* with regards to haemolytic activity ([section 6.3.4](#)). They were shown to exhibit haemolytic activity, which was intensified against canine blood cells in comparison to equine cells. This type of damage to blood cells is also seen in protozoa such as *Entamoeba* sp. (Lopez-Revilla and Said-Fernandez, 1980) and *T. vaginalis* (Krieger et al., 1983). In periodontal disease, the production of haemolysins is a known contributor to periodontal disease (Hillman et al., 1993, Socransky and Haffajee, 1992, Grenier, 1991).

These basic studies provide an initial indication of the potential of *T. brixii* to produce substances that may play a role in periodontal disease. Many more more sophisticated studies should be now conducted to elucidate this link further.

T. brixii is also capable of direct damage to host cells ([section 6.3.6](#)). Experiments conducted here show that culturing *T. brixii* with canine gingival fibroblasts results in a loss of metabolic activity in the fibroblasts (approximately a reduction of 92 %), reflecting cell death through cytotoxic effects, seen by a reduction of approximately 96 % in cell numbers. This direct contact damage is also seen with disease causing trichomonads such as *T. vaginalis* and *T. tenax*, which are capable of causing cell death through cytopathic effects in a variety of cell types (Gonzalez-Robles et al., 1995, Gilbert et al., 2000, Salvador-Membreve et al., 2014, Ribeiro et al., 2015).

The experiments conducted here, investigating the potential for *T. brixii* to contribute to canine periodontal disease, are the beginning of many studies that are required to investigate the role this organism may have in disease. The early indications are that they do indeed possess a variety of cellular mechanisms that may cause or contribute to periodontal disease under the correct circumstances. They are certainly associated with the various disease stages of periodontal disease ([chapter 3](#) and [chapter 5](#)), but were not concluded as paramount for the progression a healthy mouth to an early disease state ([chapter 4](#)). Many more studies are required to elucidate the role that this organism may play.

7.5. Final conclusions

The aims and objectives of this thesis have by the large part been met. The aim of identifying if oral protozoa are present in the canine mouth has been fulfilled by the discovery of the *E. gingivalis* and *T. bixi* in canine plaque samples using targeted molecular screening tools. Until the studies carried out here this information was not available. The studies conducted here also have concluded that both organisms are associated with canine periodontal disease samples and therefore may be either involved in the periodontal disease process or proliferate in the more favourable disease environment.

The second aim of the study was to examine the temporal abundance of protozoa in canine plaque during the progression of the disease, and to assess any associations of the protozoa with the progression of disease. This was conducted using two novel qPCR assays that allowed the sensitive specific quantification of the organisms found. The abundance of species in samples was quantified in longitudinally collected plaque samples from animals that progressed into early stage periodontal disease, however no association with this progression to early disease was evident.

The third aim of the project was to develop a primer-independent method using cutting edge third generation-based sequencing technologies to identify the protozoa present in canine plaque samples. MinION™ sequencing technology was successfully employed to develop a direct RNA sequencing protocol with no primer or amplification biases. The methodology was used to screen pooled health and disease plaque samples and confirmed the presence of only *E. gingivalis* and *Trichomonas* spp. and also the associations with periodontal disease seen with the PCR based protocols.

The fourth and final aim of the project was to isolate and culture canine oral protozoa, to describe their classification and morphology and to assess their potential contribution to canine periodontal disease. Although a canine *E. gingivalis* isolate was not cultured, ten individual *T. bixi* isolates were cultured and their phylogeny and molecular ancestry was characterised. Using commonly used techniques the fine structure and morphology of *T. bixi* was also described. Finally, initial investigation were also conducted, to assess the potential of *T. bixi* to contribute to canine periodontal disease. Experiments found the trichomonad isolated was capable of secreting an assortment of functionally active substances,

all of which may actively contribute to periodontal disease. They were also seen to directly destroy host cells.

Researchers of periodontal disease and those attempting to reduce the diseases burden on dogs and on humans, should focus much more attention to both oral Entamoebae and trichomonads. Both are currently neglected organisms, and for years have been dismissed as irrelevant or not important to disease. The research focus has always been targeted towards the bacterial species found in the canine mouth and their interaction with the host. The research outcomes demonstrated by this thesis go a long way in concluding that oral protozoa are present in canine mouths, associated with periodontal disease samples and are more than capable of contributing to the canine periodontal disease process.

Bibliography

- ADL, S. M., SIMPSON, A. G., FARMER, M. A., ANDERSEN, R. A., ANDERSON, O. R., BARTA, J. R., BOWSER, S. S., BRUGEROLLE, G., FENSOME, R. A., FREDERICQ, S., JAMES, T. Y., KARPOV, S., KUGRENS, P., KRUG, J., LANE, C. E., LEWIS, L. A., LODGE, J., LYNN, D. H., MANN, D. G., MCCOURT, R. M., MENDOZA, L., MOESTRUP, O., MOZLEY-STANDRIDGE, S. E., NERAD, T. A., SHEARER, C. A., SMIRNOV, A. V., SPIEGEL, F. W. & TAYLOR, M. F. 2005. The new higher level classification of eukaryotes with emphasis on the taxonomy of protists. *J Eukaryot Microbiol*, 52, 399-451.
- ADL, S. M., SIMPSON, A. G., LANE, C. E., LUKES, J., BASS, D., BOWSER, S. S., BROWN, M. W., BURKI, F., DUNTHORN, M., HAMPL, V., HEISS, A., HOPPENRATH, M., LARA, E., LE GALL, L., LYNN, D. H., MCMANUS, H., MITCHELL, E. A., MOZLEY-STANRIDGE, S. E., PARFREY, L. W., PAWLOWSKI, J., RUECKERT, S., SHADWICK, L., SCHOCH, C. L., SMIRNOV, A. & SPIEGEL, F. W. 2012. The revised classification of eukaryotes. *J Eukaryot Microbiol*, 59, 429-93.
- AGUIRRE-GARCIA, M. M., ANAYA-RUIZ, M. & TALAMAS-ROHANA, P. 2003. Membrane-bound acid phosphatase (MAP) from *Entamoeba histolytica* has phosphotyrosine phosphatase activity and disrupts the actin cytoskeleton of host cells. *Parasitology*, 126, 195-202.
- AHO, A. V., KERNIGHAN, B. W. & WEINBERGER, P. J. 1978. *Awk -- A Pattern Scanning and Processing Language (Second Edition)*.
- AIRD, D., ROSS, M. G., CHEN, W. S., DANIELSSON, M., FENNELL, T., RUSS, C., JAFFE, D. B., NUSBAUM, C. & GNIRKE, A. 2011. Analyzing and minimizing PCR amplification bias in Illumina sequencing libraries. *Genome Biol*, 12, R18.
- AL-SAEED, W. 2003. Pathogenic effect of *Entamoeba gingivalis* on gingival tissues of rats. *Al-Rafidain Dent Journal*, 3, 70-73.
- ALTSCHUL, S. F., GISH, W., MILLER, W., MYERS, E. W. & LIPMAN, D. J. 1990. Basic local alignment search tool. *J Mol Biol*, 215, 403-10.
- ARROYO, R., ENGBRING, J. & ALDERETE, J. F. 1992. Molecular basis of host epithelial cell recognition by *Trichomonas vaginalis*. *Mol Microbiol*, 6, 853-62.
- ATHARI, A., SOGHANDI, L., HAGHIGHI, A. & KAZEM, B. 2007. Prevalence of Oral Trichomoniasis in Patients with Periodontitis and Gingivitis Using PCR and Direct Smear. *Iranian Journal of Public Health*, 36, 33-37.
- BABAEI, Z., OORMAZDI, H., REZAEI, S., REZAEIAN, M. & RAZMJOU, E. 2011. Giardia intestinalis: DNA extraction approaches to improve PCR results. *Exp Parasitol*, 128, 159-62.
- BADARO, R., JONES, T. C., CARVALHO, E. M., SAMPAIO, D., REED, S. G., BARRAL, A., TEIXEIRA, R. & JOHNSON, W. D., JR. 1986. New perspectives on a subclinical form of visceral leishmaniasis. *J Infect Dis*, 154, 1003-11.
- BANETH, G., KOUTINAS, A. F., SOLANO-GALLEGO, L., BOURDEAU, P. & FERRER, L. 2008. Canine leishmaniosis - new concepts and insights on an expanding zoonosis: part one. *Trends Parasitol*, 24, 324-30.
- BATES, D., MÄCHLER, M., BOLKER, B. & WALKER, S. 2015. Fitting Linear Mixed-Effects Models Using lme4. 2015, 67, 48.
- BECKER, S., FRANCO, J. R., SIMARRO, P. P., STICH, A., ABEL, P. M. & STEVERDING, D. 2004. Real-time PCR for detection of *Trypanosoma brucei* in human blood samples. *Diagn Microbiol Infect Dis*, 50, 193-9.
- BEIGHTON, D., RADFORD, J. R. & NAYLOR, M. N. 1992. Glycosidase activities in gingival crevicular fluid in subjects with adult periodontitis or gingivitis. *Arch Oral Biol*, 37, 343-8.
- BEIGHTON, D., SMITH, K., GLENISTER, D. A., SALAMON, K. & KEEVIL, C. W. 1988. Increased Degradative Enzyme Production by Dental Plaque Bacteria in Mucin-limited Continuous Culture. *Microbial Ecology in Health and Disease*, 1, 85-94.

- BENCHIMOL, M. 2004. Trichomonads under Microscopy. *Microsc Microanal*, 10, 528-50.
- BENITEZ-PAEZ, A., PORTUNE, K. J. & SANZ, Y. 2016. Species-level resolution of 16S rRNA gene amplicons sequenced through the MinION portable nanopore sequencer. *Gigascience*, 5, 4.
- BENSON, D. A., CLARK, K., KARSCH-MIZRACHI, I., LIPMAN, D. J., OSTELL, J. & SAYERS, E. W. 2014. GenBank. *Nucleic Acids Res*, 42, D32-7.
- BENSON, D. A., CLARK, K., KARSCH-MIZRACHI, I., LIPMAN, D. J., OSTELL, J. & SAYERS, E. W. 2015. GenBank. *Nucleic Acids Res*, 43, D30-5.
- BERGQUIST, R. 2009. Parasitic infections affecting the oral cavity. *Periodontol 2000*, 49, 96-105.
- BHARTI, A. R., PATRA, K. P., CHUQUIYAURI, R., KOSEK, M., GILMAN, R. H., LLANOS-CUENTAS, A. & VINETZ, J. M. 2007. Polymerase chain reaction detection of Plasmodium vivax and Plasmodium falciparum DNA from stored serum samples: implications for retrospective diagnosis of malaria. *Am J Trop Med Hyg*, 77, 444-6.
- BIETH, J., SPIESS, B. & WERMUTH, C. G. 1974. The synthesis and analytical use of a highly sensitive and convenient substrate of elastase. *Biochem Med*, 11, 350-7.
- BIMSTEIN, E., SMALL, P. A., JR. & MAGNUSSON, I. 2004. Leukocyte esterase and protein levels in saliva, as indicators of gingival and periodontal diseases in children. *Pediatr Dent*, 26, 310-5.
- BIRKENHEUER, A. J., LEVY, M. G. & BREITSCHWERDT, E. B. 2003. Development and evaluation of a seminested PCR for detection and differentiation of Babesia gibsoni (Asian genotype) and B. canis DNA in canine blood samples. *J Clin Microbiol*, 41, 4172-7.
- BOGOCH, II, RASO, G., N'GORAN, E. K., MARTI, H. P. & UTZINGER, J. 2006. Differences in microscopic diagnosis of helminths and intestinal protozoa among diagnostic centres. *Eur J Clin Microbiol Infect Dis*, 25, 344-7.
- BONNER, M., AMARD, V., BAR-PINATEL, C., CHARPENTIER, F., CHATARD, J. M., DESMUYCK, Y., IHLER, S., ROCHET, J. P., ROUX DE LA TRIBOUILLE, V., SALADIN, L., VERDY, M., GIRONES, N., FRESNO, M. & SANTI-ROCCA, J. 2014. Detection of the amoeba Entamoeba gingivalis in periodontal pockets. *Parasite*, 21, 30.
- BOZNER, P. & DEMES, P. 1991a. Cell-associated and extracellular proteolytic activity of an oral flagellate, Trichomonas tenax. *Arch Oral Biol*, 36, 77-83.
- BOZNER, P. & DEMES, P. 1991b. Degradation of collagen types I, III, IV and V by extracellular proteinases of an oral flagellate Trichomonas tenax. *Arch Oral Biol*, 36, 765-70.
- BRODY, J. R. & KERN, S. E. 2004. Sodium boric acid: a Tris-free, cooler conductive medium for DNA electrophoresis. *Biotechniques*, 36, 214-6.
- BRUIJNESTEIJN VAN COPPENRAET, L. E., WALLINGA, J. A., RUIJS, G. J., BRUINS, M. J. & VERWEIJ, J. J. 2009. Parasitological diagnosis combining an internally controlled real-time PCR assay for the detection of four protozoa in stool samples with a testing algorithm for microscopy. *Clin Microbiol Infect*, 15, 869-74.
- BRUMPT, E. 1913. *Précis de Parasitologie*, Paris.
- BULL, H., MURRAY, P. G., THOMAS, D., FRASER, A. M. & NELSON, P. N. 2002. Acid phosphatases. *Mol Pathol*, 55, 65-72.
- BURKE, C. M. & DARLING, A. E. 2016. A method for high precision sequencing of near full-length 16S rRNA genes on an Illumina MiSeq. *PeerJ*, 4, e2492.
- BUSTIN, S. A., BENES, V., GARSON, J. A., HELLEMANS, J., HUGGETT, J., KUBISTA, M., MUELLER, R., NOLAN, T., PFAFFL, M. W., SHIPLEY, G. L., VANDESOMPELE, J. & WITTEWER, C. T. 2009. The MIQE guidelines: minimum information for publication of quantitative real-time PCR experiments. *Clin Chem*, 55, 611-22.
- CAPORASO, J. G., KUCZYNSKI, J., STOMBAUGH, J., BITTINGER, K., BUSHMAN, F. D., COSTELLO, E. K., FIERER, N., PENA, A. G., GOODRICH, J. K., GORDON, J. I., HUTTLEY,

- G. A., KELLEY, S. T., KNIGHTS, D., KOENIG, J. E., LEY, R. E., LOZUPONE, C. A., MCDONALD, D., MUEGGE, B. D., PIRRUNG, M., REEDER, J., SEVINSKY, J. R., TURNBAUGH, P. J., WALTERS, W. A., WIDMANN, J., YATSUNENKO, T., ZANEVELD, J. & KNIGHT, R. 2010. QIIME allows analysis of high-throughput community sequencing data. *Nat Methods*, 7, 335-6.
- CDC_PROTOCOL. 2013. *Centers for Disease Control and Prevention (CDC) - DPDx - Laboratory Identification of Parasitic Diseases of Public Health Concern* [Online]. Available: <http://www.cdc.gov/dpdx> [Accessed 30 Oct 2014].
- CEPICKA, I., HAMPL, V. & KULDA, J. 2010. Critical taxonomic revision of Parabasalids with description of one new genus and three new species. *Protist*, 161, 400-33.
- CHEN, H. Y., COX, S. W., ELEY, B. M., MANTYLA, P., RONKA, H. & SORSA, T. 2000. Matrix metalloproteinase-8 levels and elastase activities in gingival crevicular fluid from chronic adult periodontitis patients. *J Clin Periodontol*, 27, 366-9.
- CIELECKA, D., BORSUK, P., GRYTNER-ZIECINA, B. & TURKOWICZ, M. 2000. First detection of trichomonas tenax in dog and cat by PCR-RFLP. *Acta Parasitol*, 350-352.
- CLARK, C. G. & DIAMOND, L. S. 2002. Methods for cultivation of luminal parasitic protists of clinical importance. *Clin Microbiol Rev*, 15, 329-41.
- COCHRAN, D. L. 2008. Inflammation and bone loss in periodontal disease. *J Periodontol*, 79, 1569-76.
- COLE, R. M. & DAY, M. F. 1940. The use of silver albumose (Protargol) in protozoological technique. Abstract 47. *Journal of Parasitology*, 26, 30-31.
- COLLABORATORS, G. M. A. C. O. D. 2015. Global, regional, and national age-sex specific all-cause and cause-specific mortality for 240 causes of death, 1990-2013: a systematic analysis for the Global Burden of Disease Study 2013. *Lancet*, 385, 117-71.
- COORDINATORS, N. R. 2017. Database Resources of the National Center for Biotechnology Information. *Nucleic Acids Res*, 45, D12-D17.
- CROUCH, M. L. & ALDERETE, J. F. 1999. Trichomonas vaginalis interactions with fibronectin and laminin. *Microbiology*, 145 (Pt 10), 2835-43.
- CUEVAS, R. F., BARQUERA RAMOS, M. A. S., CONTRERAS, C. C. & HERNÁNDEZ-SIERRA, F. 2008. Prevalencia y asociación epidemiológica de los protozoarios orales Entamoeba gingivalis y Trichomonas tenax en niños mexicanos. *Rev. ADM*, 65, 259-262.
- CURTIS, M. A., SLANEY, J. M., CARMAN, R. J. & PEMBERTON, P. A. 1993. Interaction of a trypsin-like enzyme of Porphyromonas gingivalis W83 with antithrombin III. *FEMS Microbiol Lett*, 108, 169-74.
- DABRA, S. & SINGH, P. 2012. Evaluating the levels of salivary alkaline and acid phosphatase activities as biochemical markers for periodontal disease: A case series. *Dent Res J (Isfahan)*, 9, 41-5.
- DAILEY, D. C., CHANG, T. H. & ALDERETE, J. F. 1990. Characterization of Trichomonas vaginalis haemolysis. *Parasitology*, 101 Pt 2, 171-5.
- DAO, A. H., ROBINSON, D. P. & WONG, S. W. 1983. Frequency of Entamoeba gingivalis in human gingival scrapings. *Am J Clin Pathol*, 80, 380-3.
- DARVEAU, R. P. 2010. Periodontitis: a polymicrobial disruption of host homeostasis. *Nat Rev Microbiol*, 8, 481-90.
- DASHPER, S. G., SEERS, C. A., TAN, K. H. & REYNOLDS, E. C. 2011. Virulence factors of the oral spirochete Treponema denticola. *J Dent Res*, 90, 691-703.
- DAVIS, I. J., WALLIS, C., DEUSCH, O., COLYER, A., MILELLA, L., LOMAN, N. & HARRIS, S. 2013. A cross-sectional survey of bacterial species in plaque from client owned dogs with healthy gingiva, gingivitis or mild periodontitis. *PLoS One*, 8, e83158.
- DAVISON, H. C., THRUSFIELD, M. V., MUHARSINI, S., HUSEIN, A., PARTOUTOMO, S., RAE, P. F., MASAKE, R. & LUCKINS, A. G. 1999. Evaluation of antigen detection and antibody

- detection tests for *Trypanosoma evansi* infections of buffaloes in Indonesia. *Epidemiol Infect*, 123, 149-55.
- DE ANDRADE ROSA, I., DE SOUZA, W. & BENCHIMOL, M. 2013. High-resolution scanning electron microscopy of the cytoskeleton of *Tritrichomonas foetus*. *J Struct Biol*, 183, 412-418.
- DE JESUS, J. B., PODLYSKA, T. M., HAMPSHIRE, A., LOPES, C. S., VANNIER-SANTOS, M. A. & MEYER-FERNANDES, J. R. 2002. Characterization of an ecto-phosphatase activity in the human parasite *Trichomonas vaginalis*. *Parasitol Res*, 88, 991-7.
- DECARNERI, I. & GIANNONE, R. 1964. Frequency of *Trichomonas Vaginalis*, *Trichomonas Tenax* and *Entamoeba Gingivalis* Infections and Absence of Correlation between Oral and Vaginal Protozooses in Italian Women. *Am J Trop Med Hyg*, 13, 261-4.
- DECOSTER, W. 2018. *NanoFilt - Filtering and trimming of long read sequencing data* [Online]. <http://github.com>. Available: <https://github.com/wdecoster/nanofilt> [Accessed 2018].
- DEWHIRST, F. E., KLEIN, E. A., THOMPSON, E. C., BLANTON, J. M., CHEN, T., MILELLA, L., BUCKLEY, C. M., DAVIS, I. J., BENNETT, M. L. & MARSHALL-JONES, Z. V. 2012. The canine oral microbiome. *PLoS One*, 7, e36067.
- DIMASUAY, K. G. & RIVERA, W. L. 2013. Molecular characterization of trichomonads isolated from animal hosts in the Philippines. *Vet Parasitol*, 196, 289-95.
- DIMASUAY, K. G. & RIVERA, W. L. 2014. First report of *Trichomonas tenax* infections in the Philippines. *Parasitol Int*, 63, 400-2.
- DING, Y., HAAPASALO, M., KEROSUO, E., LOUNATMAA, K., KOTIRANTA, A. & SORSA, T. 1997. Release and activation of human neutrophil matrix metallo- and serine proteinases during phagocytosis of *Fusobacterium nucleatum*, *Porphyromonas gingivalis* and *Treponema denticola*. *J Clin Periodontol*, 24, 237-48.
- DING, Y., UITTO, V. J., HAAPASALO, M., LOUNATMAA, K., KONTTINEN, Y. T., SALO, T., GRENIER, D. & SORSA, T. 1996. Membrane components of *Treponema denticola* trigger proteinase release from human polymorphonuclear leukocytes. *J Dent Res*, 75, 1986-93.
- DRAPER, D., DONOHOE, W., MORTIMER, L. & HEINE, R. P. 1998. Cysteine proteases of *Trichomonas vaginalis* degrade secretory leukocyte protease inhibitor. *J Infect Dis*, 178, 815-9.
- DUDKO, A. & KURNATOWSKA, A. J. 2007. [Occurrence of fungi in oral cavity of patients with periodontitis]. *Wiad Parazytol*, 53, 295-300.
- DUMOULIN, E. N., VAN BIERVLIET, S., DE VOS, M., HIMPE, J., SPEECKAERT, M. M. & DELANGHE, J. R. 2015. Faecal leukocyte esterase activity is an alternative biomarker in inflammatory bowel disease. *Clin Chem Lab Med*, 53, 2003-8.
- EDGAR, R. C. 2018. Updating the 97% identity threshold for 16S ribosomal RNA OTUs. *Bioinformatics*.
- EL SIBAEI, M. M., ABDEL-FATTAH, N. S., AHMED, S. A. & ABOU-SERI, H. M. 2012. Growth kinetics, antigen profiling, and proteinase activity of Egyptian *Trichomonas tenax* isolates derived from patients having oral infections. *Exp Parasitol*, 130, 416-22.
- ELLIOTT, D. R., WILSON, M., BUCKLEY, C. M. & SPRATT, D. A. 2005. Cultivable oral microbiota of domestic dogs. *J Clin Microbiol*, 43, 5470-6.
- FALKLER, W. A., JR., CLAYMAN, E. B. & SHAEFER, D. F. 1983. Haemolysis of human erythrocytes by the *Fusobacterium nucleatum* associated with periodontal disease. *Arch Oral Biol*, 28, 735-9.
- FARELL, E. M. & ALEXANDRE, G. 2012. Bovine serum albumin further enhances the effects of organic solvents on increased yield of polymerase chain reaction of GC-rich templates. *BMC Res Notes*, 5, 257.

- FAWLEY, J. & GOURLAY, D. M. 2016. Intestinal alkaline phosphatase: a summary of its role in clinical disease. *J Surg Res*, 202, 225-34.
- FEINSTEIN, G., KUPFER, A. & SOKOLOVSKY, M. 1973. N-acetyl-(L-Ala) 3 -p-nitroanilide as a new chromogenic substrate for elastase. *Biochem Biophys Res Commun*, 50, 1020-6.
- FELLEISEN, R. S. 1997. Comparative sequence analysis of 5.8S rRNA genes and internal transcribed spacer (ITS) regions of trichomonadid protozoa. *Parasitology*, 115 (Pt 2), 111-9.
- FELSENSTEIN, J. 1985. Confidence Limits on Phylogenies: An Approach Using the Bootstrap. *Evolution*, 39, 783-791.
- FENG, J., WANG, F., HUGHES, G. R., KAMINSKYJ, S. & WEI, Y. 2011. An important role for secreted esterase in disease establishment of the wheat powdery mildew fungus *Blumeria graminis* f. sp. *tritici*. *Can J Microbiol*, 57, 211-6.
- FOURNIER, D., MOUTON, C., LAPIERRE, P., KATO, T., OKUDA, K. & MENARD, C. 2001. *Porphyromonas gulae* sp. nov., an anaerobic, gram-negative coccobacillus from the gingival sulcus of various animal hosts. *Int J Syst Evol Microbiol*, 51, 1179-89.
- GANNON, J. T. & LINKE, H. A. 1991. An antibiotic-free medium for the xenic cultivation of *Entamoeba gingivalis*. *Int J Parasitol*, 21, 403-7.
- GARALDE, D. R., SNELL, E. A., JACHIMOWICZ, D., SIPOS, B., LLOYD, J. H., BRUCE, M., PANTIC, N., ADMASSU, T., JAMES, P., WARLAND, A., JORDAN, M., CICCONE, J., SERRA, S., KEENAN, J., MARTIN, S., MCNEILL, L., WALLACE, E. J., JAYASINGHE, L., WRIGHT, C., BLASCO, J., YOUNG, S., BROCKLEBANK, D., JUUL, S., CLARKE, J., HERON, A. J. & TURNER, D. J. 2018. Highly parallel direct RNA sequencing on an array of nanopores. *Nat Methods*, 15, 201-206.
- GARBER, G. E. & LEMCHUK-FAVEL, L. T. 1994. Analysis of the extracellular proteases of *Trichomonas vaginalis*. *Parasitol Res*, 80, 361-5.
- GARCIA, G., RAMOS, F., MALDONADO, J., FERNANDEZ, A., YANEZ, J., HERNANDEZ, L. & GAYTAN, P. 2018a. Prevalence of two *Entamoeba gingivalis* ST1 and ST2-kamaktli subtypes in the human oral cavity under various conditions. *Parasitol Res*, 117, 2941-2948.
- GARCIA, G., RAMOS, F., MARTINEZ-HERNANDEZ, F., HERNANDEZ, L., YANEZ, J. & GAYTAN, P. 2018b. A new subtype of *Entamoeba gingivalis*: "E. gingivalis ST2, kamaktli variant". *Parasitol Res*, 117, 1277-1284.
- GENCO, R. J. 1994. Assessment of risk of periodontal disease. *Compend Suppl*, S678-83; quiz S714-7.
- GENCO, R. J. & SLOTS, J. 1984. Host responses in periodontal diseases. *J Dent Res*, 63, 441-51.
- GHABANCHI, J., ZIBAEI, M., AFKAR, M. D. & SARBAZIE, A. H. 2010. Prevalence of oral *Entamoeba gingivalis* and *Trichomonas tenax* in patients with periodontal disease and healthy population in Shiraz, southern Iran. *Indian J Dent Res*, 21, 89-91.
- GHARAVI M. J., HEKMAT S., EBRAHIMI A. & M., J. 2006. Buccal cavity protozoa in patients referred to the faculty of dentistry in Tehran, Iran. . *Iranian Journal of Parasitology* 1, 43-46.
- GHOSH, P. K., CASTELLANOS-BARBA, C. & ORTIZ-ORTIZ, L. 1995. Intestinal amebiasis: cyclic suppression of the immune response. *Parasitol Res*, 81, 475-80.
- GILBERT, R. O., ELIA, G., BEACH, D. H., KLAESSIG, S. & SINGH, B. N. 2000. Cytopathogenic effect of *Trichomonas vaginalis* on human vaginal epithelial cells cultured in vitro. *Infect Immun*, 68, 4200-6.
- GONZALEZ-ROBLES, A., LAZARO-HALLER, A., ESPINOSA-CANTELLANO, M., ANAYA-VELAZQUEZ, F. & MARTINEZ-PALOMO, A. 1995. *Trichomonas vaginalis*: ultrastructural bases of the cytopathic effect. *J Eukaryot Microbiol*, 42, 641-51.

- GONZALEZ-RUIZ, A., HAQUE, R., AGUIRRE, A., CASTANON, G., HALL, A., GUHL, F., RUIZ-PALACIOS, G., MILES, M. A. & WARHURST, D. C. 1994. Value of microscopy in the diagnosis of dysentery associated with invasive *Entamoeba histolytica*. *J Clin Pathol*, 47, 236-9.
- GOTTLIEB, D. S. & MILLER, L. H. 1971. *Entamoeba gingivalis* in periodontal disease. *J Periodontol*, 42, 412-5.
- GRENIER, D. 1991. Characteristics of hemolytic and hemagglutinating activities of *Treponema denticola*. *Oral Microbiol Immunol*, 6, 246-9.
- GRENIER, D. 1995. Characterization of the trypsin-like activity of *Bacteroides forsythus*. *Microbiology*, 141, 921-926.
- GROS, G. 1849. Fragments d'helminthologie et de physiologie microscopique. *Bulletin de la Société Impériale des Naturalistes de Moscou*, 22, 549-573.
- GROSSI, S. G., GENCO, R. J., MACHTEI, E. E., HO, A. W., KOCH, G., DUNFORD, R., ZAMBON, J. J. & HAUSMANN, E. 1995. Assessment of risk for periodontal disease. II. Risk indicators for alveolar bone loss. *J Periodontol*, 66, 23-9.
- GROSSI, S. G., ZAMBON, J. J., HO, A. W., KOCH, G., DUNFORD, R. G., MACHTEI, E. E., NORDERYD, O. M. & GENCO, R. J. 1994. Assessment of risk for periodontal disease. I. Risk indicators for attachment loss. *J Periodontol*, 65, 260-7.
- GROVER, V., MALHOTRA, R., KAPOOR, A., BITHER, R. & SACHDEVA, S. 2016. Correlation of alkaline phosphatase activity to clinical parameters of inflammation in smokers suffering from chronic periodontitis. *J Indian Soc Periodontol*, 20, 254-9.
- HADZIAVDIC, K., LEKANG, K., LANZEN, A., JONASSEN, I., THOMPSON, E. M. & TROEDSSON, C. 2014. Characterization of the 18S rRNA gene for designing universal eukaryote specific primers. *PLoS One*, 9, e87624.
- HAJISHENGALLIS, G., LIANG, S., PAYNE, M. A., HASHIM, A., JOTWANI, R., ESKAN, M. A., MCINTOSH, M. L., ALSAM, A., KIRKWOOD, K. L., LAMBRIS, J. D., DARVEAU, R. P. & CURTIS, M. A. 2011. Low-abundance biofilm species orchestrates inflammatory periodontal disease through the commensal microbiota and complement. *Cell Host Microbe*, 10, 497-506.
- HAMP, S. E., OLSSON, S. E., FARSE-MADSEN, K., VIKLANDS, P. & FORNELL, J. 1984. A MACROSCOPIC AND RADIOLOGIC INVESTIGATION OF DENTAL DISEASES OF THE DOG. *Veterinary Radiology*, 25, 86-92.
- HARVEY, C. E. 1998. Periodontal disease in dogs. Etiopathogenesis, prevalence, and significance. *Vet Clin North Am Small Anim Pract*, 28, 1111-28, vi.
- HAYAKAWA, T., KONDO, T., YAMAZAKI, Y., IINUMA, Y. & MIZUNO, R. 1980. A simple and specific determination of trypsin in human duodenal juice. *Gastroenterol Jpn*, 15, 135-9.
- HEATHER, J. M. & CHAIN, B. 2016. The sequence of sequencers: The history of sequencing DNA. *Genomics*, 107, 1-8.
- HEGNER, R. & RATCLIFFE, H. 1927. Trichomonads from the Mouth of the Dog. *The Journal of Parasitology*, 14, 51-53.
- HERNANDEZ-ROMANO, P., HERNANDEZ, R., ARROYO, R., ALDERETE, J. F. & LOPEZ-VILLASENOR, I. 2010. Identification and characterization of a surface-associated, subtilisin-like serine protease in *Trichomonas vaginalis*. *Parasitology*, 137, 1621-35.
- HILLMAN, J. D., MAIDEN, M. F., PFALLER, S. P., MARTIN, L., DUNCAN, M. J. & SOCRANSKY, S. S. 1993. Characterization of hemolytic bacteria in subgingival plaque. *J Periodontal Res*, 28, 173-9.
- HOLCOMBE, L. J., PATEL, N., COLYER, A., DEUSCH, O., O'FLYNN, C. & HARRIS, S. 2014. Early canine plaque biofilms: characterization of key bacterial interactions involved in initial colonization of enamel. *PLoS One*, 9, e113744.

- HONIGBERG, B. M. 1990. *Trichomonads Parasitic in Humans*, New York, Springer-Verlag New York.
- HONIGBERG, B. M. & LEE, J. J. 1959. Structure and division of *Trichomonas tenax* (O.F. Muller). *Am J Hyg*, 69, 177-201.
- HOTHORN, T., BRETZ, F. & WESTFALL, P. 2008. Simultaneous inference in general parametric models. *Biom J*, 50, 346-63.
- HRDY, I., HIRT, R. P., DOLEZAL, P., BARDONOVA, L., FOSTER, P. G., TACHEZY, J. & EMBLEY, T. M. 2004. *Trichomonas* hydrogenosomes contain the NADH dehydrogenase module of mitochondrial complex I. *Nature*, 432, 618-22.
- HUSTON, C. D., HAQUE, R. & PETRI, W. A., JR. 1999. Molecular-based diagnosis of *Entamoeba histolytica* infection. *Expert Rev Mol Med*, 1999, 1-11.
- IMAMURA, T. 2003. The role of gingipains in the pathogenesis of periodontal disease. *J Periodontol*, 74, 111-8.
- IOVINO, A., MILLER, D., LONNEN, J., KILVINGTON, S. & ALFONSO, E. C. 2011. Extraction of *Acanthamoeba* DNA by use of Chelex resin. *J Clin Microbiol*, 49, 476-7.
- ISHAQ, S. L. & WRIGHT, A. D. 2014. Design and validation of four new primers for next-generation sequencing to target the 18S rRNA genes of gastrointestinal ciliate protozoa. *Appl Environ Microbiol*, 80, 5515-21.
- JAIN, M., OLSEN, H. E., PATEN, B. & AKESON, M. 2016. The Oxford Nanopore MinION: delivery of nanopore sequencing to the genomics community. *Genome Biol*, 17, 239.
- JAKUBOVICS, N. S. & PALMER JR., R. J. 2013. *Oral Microbial Ecology: Current Research and New Perspectives*, Caister Academic Press.
- JASKOSKI, B. J. 1963. Incidence of Oral Protozoa. 82, 420.
- JIAN, B., KOLANSKY, A. S., BALOACH, Z. W. & GUPTA, P. K. 2008. *Entamoeba gingivalis* pulmonary abscess - diagnosed by fine needle aspiration. *Cytojournal*, 5, 12.
- KAMATA, N., FUJIMOTO, R., TOMONARI, M., TAKI, M., NAGAYAMA, M. & YASUMOTO, S. 2004. Immortalization of human dental papilla, dental pulp, periodontal ligament cells and gingival fibroblasts by telomerase reverse transcriptase. *J Oral Pathol Med*, 33, 417-23.
- KEDJARUNE, U., PONGPRERACHOK, S., ARPORNMAEKLONG, P. & UNGKUSONMONGKHON, K. 2001. Culturing primary human gingival epithelial cells: comparison of two isolation techniques. *J Craniomaxillofac Surg*, 29, 224-31.
- KEHL, K. S., CICIRELLO, H. & HAVENS, P. L. 1995. Comparison of four different methods for detection of *Cryptosporidium* species. *J Clin Microbiol*, 33, 416-8.
- KELLEROVA, P. & TACHEZY, J. 2017. Zoonotic *Trichomonas tenax* and a new trichomonad species, *Trichomonas bixi* n. sp., from the oral cavities of dogs and cats. *Int J Parasitol*, 47, 247-255.
- KENNEDY, K., HALL, M. W., LYNCH, M. D., MORENO-HAGELSIEB, G. & NEUFELD, J. D. 2014. Evaluating bias of illumina-based bacterial 16S rRNA gene profiles. *Appl Environ Microbiol*, 80, 5717-22.
- KESAVALU, L., HOLT, S. C. & EBERSOLE, J. L. 1996. Trypsin-like protease activity of *Porphyromonas gingivalis* as a potential virulence factor in a murine lesion model. *Microb Pathog*, 20, 1-10.
- KIMURA, M. 1980. A simple method for estimating evolutionary rates of base substitutions through comparative studies of nucleotide sequences. *J Mol Evol*, 16, 111-20.
- KLINDWORTH, A., PRUESSE, E., SCHWEER, T., PEPLIES, J., QUAIST, C., HORN, M. & GLOCKNER, F. O. 2013. Evaluation of general 16S ribosomal RNA gene PCR primers for classical and next-generation sequencing-based diversity studies. *Nucleic Acids Res*, 41, e1.

- KOLENBRANDER, P. E. & LONDON, J. 1993. Adhere today, here tomorrow: oral bacterial adherence. *J Bacteriol*, 175, 3247-52.
- KORESSAAR, T. & REMM, M. 2007. Enhancements and modifications of primer design program Primer3. *Bioinformatics*, 23, 1289-91.
- KOZICH, J. J., WESTCOTT, S. L., BAXTER, N. T., HIGHLANDER, S. K. & SCHLOSS, P. D. 2013. Development of a dual-index sequencing strategy and curation pipeline for analyzing amplicon sequence data on the MiSeq Illumina sequencing platform. *Appl Environ Microbiol*, 79, 5112-20.
- KRIEGER, J. N., POISSON, M. A. & REIN, M. F. 1983. Beta-hemolytic activity of *Trichomonas vaginalis* correlates with virulence. *Infect Immun*, 41, 1291-5.
- KUCKNOOR, A. S., MUNDODI, V. & ALDERETE, J. 2009. Genetic identity and differential gene expression between *Trichomonas vaginalis* and *Trichomonas tenax*. *BMC Microbiol*, 9, 58.
- KUCKNOOR, A. S., MUNDODI, V. & ALDERETE, J. F. 2007. The proteins secreted by *Trichomonas vaginalis* and vaginal epithelial cell response to secreted and episomally expressed AP65. *Cell Microbiol*, 9, 2586-97.
- KUMMER, S., HAYES, G. R., GILBERT, R. O., BEACH, D. H., LUCAS, J. J. & SINGH, B. N. 2008. Induction of human host cell apoptosis by *Trichomonas vaginalis* cysteine proteases is modulated by parasite exposure to iron. *Microb Pathog*, 44, 197-203.
- KURNATOWSKA, A. J., DUDKO, A. & KURNATOWSKI, P. 2004. [Invasion of *Trichomonas tenax* in patients with periodontal diseases]. *Wiad Parazytol*, 50, 397-403.
- KUTISOVA, K., KULDA, J., CEPICKA, I., FLEGR, J., KOUDELA, B., TERAS, J. & TACHEZY, J. 2005. Tetratrichomonads from the oral cavity and respiratory tract of humans. *Parasitology*, 131, 309-19.
- KYLLAR, M. & WITTER, K. 2005. Prevalence of dental disorders in pet dogs. *Veterinarni Medicina*, 50, 496-505.
- LENG, J., ZHONG, X., ZHU, R. J., YANG, S. L., GOU, X. & MAO, H. M. 2011. Assessment of protozoa in Yunnan Yellow cattle rumen based on the 18S rRNA sequences. *Mol Biol Rep*, 38, 577-85.
- LI, J., HELMERHORST, E. J., LEONE, C. W., TROXLER, R. F., YASKELL, T., HAFFAJEE, A. D., SOCRANSKY, S. S. & OPPENHEIM, F. G. 2004. Identification of early microbial colonizers in human dental biofilm. *J Appl Microbiol*, 97, 1311-8.
- LINDMARK, D. G. & MULLER, M. 1973. Hydrogenosome, a cytoplasmic organelle of the anaerobic flagellate *Tritrichomonas foetus*, and its role in pyruvate metabolism. *J Biol Chem*, 248, 7724-8.
- LINKE, H. A., GANNON, J. T. & OBIN, J. N. 1989. Clinical survey of *Entamoeba gingivalis* by multiple sampling in patients with advanced periodontal disease. *Int J Parasitol*, 19, 803-8.
- LOPEZ-REVILLA, R. & SAID-FERNANDEZ, S. 1980. Cytopathogenicity of *Entamoeba histolytica*: hemolytic activity of trophozoite homogenates. *Am J Trop Med Hyg*, 29, 209-12.
- LOVEGROVE, J. M. 2004. Dental plaque revisited: bacteria associated with periodontal disease. *J N Z Soc Periodontol*, 7-21.
- LUCHT, E., EVENGARD, B., SKOTT, J., PEHRSON, P. & NORD, C. E. 1998. *Entamoeba gingivalis* in human immunodeficiency virus type 1-infected patients with periodontal disease. *Clin Infect Dis*, 27, 471-3.
- LUSTIG, G., RYAN, C. M., SECOR, W. E. & JOHNSON, P. J. 2013. *Trichomonas vaginalis* contact-dependent cytolysis of epithelial cells. *Infect Immun*, 81, 1411-9.
- LYONS, T., SCHOLTEN, T., PALMER, J. C. & STANFIELD, E. 1983. Oral amoebiasis: the role of *Entamoeba gingivalis* in periodontal disease. *Quintessence Int Dent Dig*, 14, 1245-8.

- LYONS, T. & STANFIELD, E. 1989. *Introduction to protozoa and fungi in periodontal infections : a manual of microbiological diagnosis and nonsurgical treatment*, Ottawa, Ontario, Canada : T. Lyons, 1989.
- MAAS, L., DORIGO-ZETSMA, J. W., DE GROOT, C. J., BOUTER, S., PLOTZ, F. B. & VAN EWIIK, B. E. 2014. Detection of intestinal protozoa in paediatric patients with gastrointestinal symptoms by multiplex real-time PCR. *Clin Microbiol Infect*, 20, 545-50.
- MACHIDA, R. J. & KNOWLTON, N. 2012. PCR primers for metazoan nuclear 18S and 28S ribosomal DNA sequences. *PLoS One*, 7, e46180.
- MADICO, G., QUINN, T. C., ROMPALO, A., MCKEE, K. T., JR. & GAYDOS, C. A. 1998. Diagnosis of *Trichomonas vaginalis* infection by PCR using vaginal swab samples. *J Clin Microbiol*, 36, 3205-10.
- MALHOTRA, R., GROVER, V., KAPOOR, A. & KAPUR, R. 2010. Alkaline phosphatase as a periodontal disease marker. *Indian J Dent Res*, 21, 531-6.
- MALONE, J. H. 2015. Balancing copy number in ribosomal DNA. *Proc Natl Acad Sci U S A*, 112, 2635-6.
- MARSHALL-JONES, Z., BAILLON, M.-L., BUCKLEY, C. & DEWHIRST, F. 2007. *Methods and kits for dog plaque disease*. WO patent application WO2008137506A2.
- MARSHALL, M. D., WALLIS, C. V., MILELLA, L., COLYER, A., TWEEDIE, A. D. & HARRIS, S. 2014. A longitudinal assessment of periodontal disease in 52 Miniature Schnauzers. *BMC Vet Res*, 10, 166.
- MARTY, M., LEMAITRE, M., KEMOUN, P., MORRIER, J. J. & MONSARRAT, P. 2017a. *Trichomonas tenax* and periodontal diseases: a concise review. *Parasitology*, 1-9.
- MARTY, M., LEMAITRE, M., KEMOUN, P., MORRIER, J. J. & MONSARRAT, P. 2017b. *Trichomonas tenax* and periodontal diseases: a concise review. *Parasitology*, 144, 1417-1425.
- MCALLISTER-SISTILLI, C. G., CAGGIULA, A. R., KNOPE, S., ROSE, C. A., MILLER, A. L. & DONNY, E. C. 1998. The effects of nicotine on the immune system. *Psychoneuroendocrinology*, 23, 175-87.
- MEHR, A. K., ZARANDI, A. & ANUSH, K. 2015. Prevalence of Oral *Trichomonas tenax* in Periodontal Lesions of Down Syndrome in Tabriz, Iran. *J Clin Diagn Res*, 9, ZC88-90.
- MIDDLEJ, V. & BENCHIMOL, M. 2010. *Trichomonas vaginalis* kills and eats--evidence for phagocytic activity as a cytopathic effect. *Parasitology*, 137, 65-76.
- MIKHEYEV, A. S. & TIN, M. M. 2014. A first look at the Oxford Nanopore MinION sequencer. *Mol Ecol Resour*, 14, 1097-102.
- MOODY, A. 2002. Rapid diagnostic tests for malaria parasites. *Clin Microbiol Rev*, 15, 66-78.
- NAGAO, E., YAMAMOTO, A., IGARASHI, T., GOTO, N. & SASA, R. 2000. Two distinct hemolysins in *Trichomonas tenax* ATCC 30207. *Oral Microbiol Immunol*, 15, 355-9.
- NAKAYAMA, G. R., CATON, M. C., NOVA, M. P. & PARANDOOSH, Z. 1997. Assessment of the Alamar Blue assay for cellular growth and viability in vitro. *J Immunol Methods*, 204, 205-8.
- NIE, D. 1950. Morphology and taxonomy of the intestinal protozoa of the guinea-pig, *Cavia porcella*. *J Morphol*, 86, 381-494.
- NIEMIEC, B. A. 2008. Periodontal disease. *Top Companion Anim Med*, 23, 72-80.
- OHIRA, T. & NOGUUCHI, H. 1917. The Cultivation of *Trichomonas* of the Human Mouth (*Tetratrichomonas Hominis*). *J Exp Med*, 25, 341-7.
- OKAMOTO, M., MAEDA, N., KONDO, K. & LEUNG, K. P. 1999. Hemolytic and hemagglutinating activities of *Prevotella intermedia* and *Prevotella nigrescens*. *FEMS Microbiol Lett*, 178, 299-304.

- ORLANDI, P. A. & LAMPEL, K. A. 2000. Extraction-free, filter-based template preparation for rapid and sensitive PCR detection of pathogenic parasitic protozoa. *J Clin Microbiol*, 38, 2271-7.
- ORTEGA, Y. R. & ADAM, R. D. 1997. Giardia: overview and update. *Clin Infect Dis*, 25, 545-9; quiz 550.
- OTA-SULLIVAN, K. & BLECKER-SHELLY, D. L. 2013. Use of the rapid BinaxNOW malaria test in a 24-hour laboratory associated with accurate detection and decreased malaria testing turnaround times in a pediatric setting where malaria is not endemic. *J Clin Microbiol*, 51, 1567-9.
- PAGE, R. C. & SCHROEDER, H. E. 1976. Pathogenesis of inflammatory periodontal disease. A summary of current work. *Lab Invest*, 34, 235-49.
- PALCANIS, K. G., LARIAVA, I. K., WELLS, B. R., SUGGS, K. A., LANDIS, J. R., CHADWICK, D. E. & JEFFCOAT, M. K. 1992. Elastase as an Indicator of Periodontal Disease Progression. *Journal of Periodontology*, 63, 237-242.
- PAN, X., BOURLAND, W. A. & SONG, W. 2013. Protargol synthesis: an in-house protocol. *J Eukaryot Microbiol*, 60, 609-14.
- PATEL, N., COLYER, A., HARRIS, S., HOLCOMBE, L. & ANDREW, P. 2017. The Prevalence of Canine Oral Protozoa and Their Association with Periodontal Disease. *J Eukaryot Microbiol*, 64, 286-292.
- PEANO, C., PIETRELLI, A., CONSOLANDI, C., ROSSI, E., PETITI, L., TAGLIABUE, L., DE BELLIS, G. & LANDINI, P. 2013. An efficient rRNA removal method for RNA sequencing in GC-rich bacteria. *Microb Inform Exp*, 3, 1.
- PEREIRA-NEVES, A. & BENCHIMOL, M. 2007. Phagocytosis by *Trichomonas vaginalis*: new insights. *Biol Cell*, 99, 87-101.
- POPOVA, C., DOSSEVA-PANOVA, V. & PANOV, V. 2013. Microbiology of Periodontal Diseases. A Review. *Biotechnology & Biotechnological Equipment*, 27, 3754-3759.
- PORETSKY, R., RODRIGUEZ, R. L., LUO, C., TSEMENTZI, D. & KONSTANTINIDIS, K. T. 2014. Strengths and limitations of 16S rRNA gene amplicon sequencing in revealing temporal microbial community dynamics. *PLoS One*, 9, e93827.
- PUSHPARANI, D. S. 2015. High acid phosphatase level in the gingival tissues of periodontitis subjects. *J Basic Clin Pharm*, 6, 59-63.
- QUAST, C., PRUESSE, E., YILMAZ, P., GERKEN, J., SCHWEER, T., YARZA, P., PEPLIES, J. & GLOCKNER, F. O. 2013. The SILVA ribosomal RNA gene database project: improved data processing and web-based tools. *Nucleic Acids Res*, 41, D590-6.
- QUE, X. & REED, S. L. 1997. The role of extracellular cysteine proteinases in pathogenesis of *Entamoeba histolytica* invasion. *Parasitol Today*, 13, 190-4.
- QVARNSTROM, Y., VISVESVARA, G. S., SRIRAM, R. & DA SILVA, A. J. 2006. Multiplex real-time PCR assay for simultaneous detection of *Acanthamoeba* spp., *Balamuthia mandrillaris*, and *Naegleria fowleri*. *J Clin Microbiol*, 44, 3589-95.
- RAMFJORD, S. P., KNOWLES, J. W., NISSE, R. R., SHICK, R. A. & BURGETT, F. G. 1973. Longitudinal study of periodontal therapy. 44, 77.
- READ, C. M., MONIS, P. T. & THOMPSON, R. C. 2004. Discrimination of all genotypes of *Giardia duodenalis* at the glutamate dehydrogenase locus using PCR-RFLP. *Infect Genet Evol*, 4, 125-30.
- REICHEL, R. 2007. *Scanning Electron Microscopy*, New York, Springer.
- REYNOLDS, J. J., HEMBRY, R. M. & MEIKLE, M. C. 1994. Connective tissue degradation in health and periodontal disease and the roles of matrix metalloproteinases and their natural inhibitors. *Adv Dent Res*, 8, 312-9.
- RIBAUX, C. L., MAGLOIRE, H., JOFFRE, A. & MORRIER, J. J. 1983. Immunohistochemical localization of fibronectin-like protein on the cell surface of the oral flagellate *Trichomonas tenax*. *J Biol Buccale*, 11, 41-51.

- RIBEIRO, L. C., SANTOS, C. & BENCHIMOL, M. 2015. Is *Trichomonas tenax* a Parasite or a Commensal? *Protist*, 166, 196-210.
- RICKARD, A. H., GILBERT, P., HIGH, N. J., KOLENBRANDER, P. E. & HANDLEY, P. S. 2003. Bacterial coaggregation: an integral process in the development of multi-species biofilms. *Trends Microbiol*, 11, 94-100.
- RIDEOUT, J. R., HE, Y., NAVAS-MOLINA, J. A., WALTERS, W. A., URSELL, L. K., GIBBONS, S. M., CHASE, J., MCDONALD, D., GONZALEZ, A., ROBBINS-PIANKA, A., CLEMENTE, J. C., GILBERT, J. A., HUSE, S. M., ZHOU, H. W., KNIGHT, R. & CAPORASO, J. G. 2014. Subsampled open-reference clustering creates consistent, comprehensive OTU definitions and scales to billions of sequences. *PeerJ*, 2, e545.
- RIVERA, F., MEDINA, F., RAMIREZ, P., ALCOCER, J., VILACLARA, G. & ROBLES, E. 1984. Pathogenic and free-living protozoa cultured from the nasopharyngeal and oral regions of dental patients. *Environ Res*, 33, 428-40.
- RIVERA, F., ROSAS, I., CASTILLO, M., CHAVEZ, M., GOMEZ, R., CHIO, R. E. & ISLAS, J. 1986. Pathogenic and free-living protozoa cultured from the nasopharyngeal and oral regions of dental patients: II. *Environ Res*, 39, 364-71.
- ROBERTS, A., SHAH, M. & CHAPPLE, I. L. 2003. C-1 esterase inhibitor dysfunction localised to the periodontal tissues: clues to the role of stress in the pathogenesis of chronic periodontitis? *J Clin Periodontol*, 30, 271-7.
- ROSENTHAL, P. J. 1999. Proteases of protozoan parasites. *Adv Parasitol*, 43, 105-59.
- ROUSSET, J. J., LAISSUS, B. & MICHEL, C. 1970. [Preliminary data on canine enzootics due to *Trichomonas canistomae* and *Entamoeba gingivalis* in Parisian dogs]. *C R Seances Soc Biol Fil*, 164, 2468-9.
- SAITOU, N. & NEI, M. 1987. The neighbor-joining method: a new method for reconstructing phylogenetic trees. *Mol Biol Evol*, 4, 406-25.
- SAKAMOTO, M., SUZUKI, M., UMEDA, M., ISHIKAWA, I. & BENNO, Y. 2002. Reclassification of *Bacteroides forsythus* (Tanner et al. 1986) as *Tannerella forsythensis* corrig., gen. nov., comb. nov. *Int J Syst Evol Microbiol*, 52, 841-9.
- SALVADOR-MEMBREVE, D. M., JACINTO, S. D. & RIVERA, W. L. 2014. *Trichomonas vaginalis* induces cytopathic effect on human lung alveolar basal carcinoma epithelial cell line A549. *Exp Parasitol*, 147, 33-40.
- SANGER, F. & COULSON, A. R. 1975. A rapid method for determining sequences in DNA by primed synthesis with DNA polymerase. *J Mol Biol*, 94, 441-8.
- SCHLOSS, P. D. 2010. The effects of alignment quality, distance calculation method, sequence filtering, and region on the analysis of 16S rRNA gene-based studies. *PLoS Comput Biol*, 6, e1000844.
- SCHLOSS, P. D. & WESTCOTT, S. L. 2011. Assessing and improving methods used in operational taxonomic unit-based approaches for 16S rRNA gene sequence analysis. *Appl Environ Microbiol*, 77, 3219-26.
- SCHLOSS, P. D., WESTCOTT, S. L., RYABIN, T., HALL, J. R., HARTMANN, M., HOLLISTER, E. B., LESNIEWSKI, R. A., OAKLEY, B. B., PARKS, D. H., ROBINSON, C. J., SAHL, J. W., STRES, B., THALLINGER, G. G., VAN HORN, D. J. & WEBER, C. F. 2009. Introducing mothur: open-source, platform-independent, community-supported software for describing and comparing microbial communities. *Appl Environ Microbiol*, 75, 7537-41.
- SCHRADER, C., SCHIELKE, A., ELLERBROEK, L. & JOHNE, R. 2012. PCR inhibitors - occurrence, properties and removal. *J Appl Microbiol*, 113, 1014-26.
- SCHWARTZ, Z., GOULTSCHIN, J., DEAN, D. D. & BOYAN, B. D. 1997. Mechanisms of alveolar bone destruction in periodontitis. *Periodontol 2000*, 14, 158-72.
- SEGOVIC, S., BUNTAK-KOBLER, D., GALIC, N. & KATUNARIC, M. 1998. *Trichomonas tenax* proteolytic activity. *Coll Antropol*, 22 Suppl, 45-9.

- SELA, M. N. 2001. Role of *Treponema denticola* in periodontal diseases. *Crit Rev Oral Biol Med*, 12, 399-413.
- SHIN, E. C., CHO, K. M., LIM, W. J., HONG, S. Y., AN, C. L., KIM, E. J., KIM, Y. K., CHOI, B. R., AN, J. M., KANG, J. M., KIM, H. & YUN, H. D. 2004. Phylogenetic analysis of protozoa in the rumen contents of cow based on the 18S rDNA sequences. *J Appl Microbiol*, 97, 378-83.
- SIBLEY, L. D. 2013. The roles of intramembrane proteases in protozoan parasites. *Biochim Biophys Acta*, 1828, 2908-15.
- SIMITCH, T. 1938. Sur une amibe buccale du chien *Entamoeba canibuccalis* n. sp. *Ann. Parasitol. Hum. Comp.*, 16, 251-253.
- SINGH, A., HOUP, E. & PETRI, W. A. 2009. Rapid Diagnosis of Intestinal Parasitic Protozoa, with a Focus on *Entamoeba histolytica*. *Interdiscip Perspect Infect Dis*, 2009, 547090.
- SMITH, L. M., SANDERS, J. Z., KAISER, R. J., HUGHES, P., DODD, C., CONNELL, C. R., HEINER, C., KENT, S. B. & HOOD, L. E. 1986. Fluorescence detection in automated DNA sequence analysis. *Nature*, 321, 674-9.
- SOCRANSKY, S. S. & HAFFAJEE, A. D. 1992. The bacterial etiology of destructive periodontal disease: current concepts. *J Periodontol*, 63, 322-31.
- SOCRANSKY, S. S., HAFFAJEE, A. D., CUGINI, M. A., SMITH, C. & KENT, R. L., JR. 1998. Microbial complexes in subgingival plaque. *J Clin Periodontol*, 25, 134-44.
- SOMMER, U., COSTELLO, C. E., HAYES, G. R., BEACH, D. H., GILBERT, R. O., LUCAS, J. J. & SINGH, B. N. 2005. Identification of *Trichomonas vaginalis* cysteine proteases that induce apoptosis in human vaginal epithelial cells. *J Biol Chem*, 280, 23853-60.
- SOPER, D. 2004. Trichomoniasis: under control or undercontrolled? *Am J Obstet Gynecol*, 190, 281-90.
- STAFKOVA, J., RADA, P., MELONI, D., ZARSKY, V., SMUTNA, T., ZIMMANN, N., HARANT, K., POMPACH, P., HRDY, I. & TACHEZY, J. 2018. Dynamic secretome of *Trichomonas vaginalis*: Case study of beta-amylases. *Mol Cell Proteomics*, 17, 304-320.
- STAROSCIK, A. 2004. *URI Genomics & Sequencing Center - Calculator for determining the number of copies of a template* [Online]. Available: <http://cels.uri.edu/gsc/cndna.html> [Accessed].
- STOTHARD, P. 2000. The sequence manipulation suite: JavaScript programs for analyzing and formatting protein and DNA sequences. *Biotechniques*, 28, 1102, 1104.
- SZABO, G., KLENK, G., VEER, A. & NEMETH, Z. 1999. Correlation of the combination of alcoholism and smoking with the occurrence of cancer in the oral cavity. A screening study in an endangered population. *Mund Kiefer Gesichtschir*, 3, 119-22.
- SZCZEPANIAK, K., LOJSZCZYK-SZCZEPANIAK, A., TOMCZUK, K., SKRZYPEK, T., LISIAK, B. & ABD-AL-HAMMZA ABBASS, Z. 2016. Canine *Trichomonas tenax* mandibular gland infestation. *Acta Vet Scand*, 58, 15.
- TAMURA, K. 1992. Estimation of the number of nucleotide substitutions when there are strong transition-transversion and G+C-content biases. *Mol Biol Evol*, 9, 678-87.
- TAMURA, K., STECHER, G., PETERSON, D., FILIPSKI, A. & KUMAR, S. 2013. MEGA6: Molecular Evolutionary Genetics Analysis version 6.0. *Mol Biol Evol*, 30, 2725-9.
- TASCA, T. & DE CARLI, G. A. 2003. Scanning electron microscopy study of *Trichomonas gallinae*. *Vet Parasitol*, 118, 37-42.
- TATAKIS, D. N. & KUMAR, P. S. 2005. Etiology and pathogenesis of periodontal diseases. 49, 516.
- TAYLOR, M. 2000. Protozoal disease in cattle and sheep. *In Practice*, 22, 604-617.
- TER STEEG, P. F., VAN DER HOEVEN, J. S., DE JONG, M. H., VAN MUNSTER, P. J. J. & JANSEN, M. J. H. 1988. Modelling the Gingival Pocket by Enrichment of Subgingival

- Microflora in Human Serum in Chemostats. *Microbial Ecology in Health and Disease*, 1, 73-84.
- THOMPSON, J. D., GIBSON, T. J. & HIGGINS, D. G. 2002. Multiple sequence alignment using ClustalW and ClustalX. *Curr Protoc Bioinformatics*, Chapter 2, Unit 2 3.
- TILLACK, M., BILLER, L., IRMER, H., FREITAS, M., GOMES, M. A., TANNICH, E. & BRUCHHAUS, I. 2007. The *Entamoeba histolytica* genome: primary structure and expression of proteolytic enzymes. *BMC Genomics*, 8, 170.
- TREMBLAY, J., SINGH, K., FERN, A., KIRTON, E. S., HE, S., WOYKE, T., LEE, J., CHEN, F., DANGL, J. L. & TRINGE, S. G. 2015. Primer and platform effects on 16S rRNA tag sequencing. *Front Microbiol*, 6, 771.
- TRIM, R. D., SKINNER, M. A., FARONE, M. B., DUBOIS, J. D. & NEWSOME, A. L. 2011. Use of PCR to detect *Entamoeba gingivalis* in diseased gingival pockets and demonstrate its absence in healthy gingival sites. *Parasitol Res*, 109, 857-64.
- TSURUGA, E., IRIE, K., SAKAKURA, Y. & YAJIMA, T. 2002. Expression of fibrillins and tropoelastin by human gingival and periodontal ligament fibroblasts in vitro. *J Periodontal Res*, 37, 23-8.
- UNTERGASSER, A., CUTCUTACHE, I., KORESSAAR, T., YE, J., FAIRCLOTH, B. C., REMM, M. & ROZEN, S. G. 2012. Primer3--new capabilities and interfaces. *Nucleic Acids Res*, 40, e115.
- UTZINGER, J., BOTERO-KLEIVEN, S., CASTELLI, F., CHIODINI, P. L., EDWARDS, H., KOHLER, N., GULLETTA, M., LEBBAD, M., MANSER, M., MATTHYS, B., N'GORAN, E. K., TANNICH, E., VOUNATSOU, P. & MARTI, H. 2010. Microscopic diagnosis of sodium acetate-acetic acid-formalin-fixed stool samples for helminths and intestinal protozoa: a comparison among European reference laboratories. *Clin Microbiol Infect*, 16, 267-73.
- V. BUTKOVIĆ, M. ŠEHIČ, D. STANIN, M. ŠIMPRAGA, D. CAPAK & KOS, J. 2001. Dental Diseases in Dogs: A Retrospective Study of Radiological Data. *Acta Vet. Brno*, 70, 203-208.
- VALSTER, R. M., WULLINGS, B. A., BAKKER, G., SMIDT, H. & VAN DER KOOIJ, D. 2009. Free-living protozoa in two unchlorinated drinking water supplies, identified by phylogenetic analysis of 18S rRNA gene sequences. *Appl Environ Microbiol*, 75, 4736-46.
- VAN DE PEER, Y. & DE WACHTER, R. 1997. Evolutionary relationships among the eukaryotic crown taxa taking into account site-to-site rate variation in 18S rRNA. *J Mol Evol*, 45, 619-30.
- VERWEIJ, J. J. 2014. Application of PCR-based methods for diagnosis of intestinal parasitic infections in the clinical laboratory. *Parasitology*, 141, 1863-72.
- VERWEIJ, J. J., BLANGE, R. A., TEMPLETON, K., SCHINKEL, J., BRIENEN, E. A., VAN ROOYEN, M. A., VAN LIESHOUT, L. & POLDERMAN, A. M. 2004. Simultaneous detection of *Entamoeba histolytica*, *Giardia lamblia*, and *Cryptosporidium parvum* in fecal samples by using multiplex real-time PCR. *J Clin Microbiol*, 42, 1220-3.
- VERWEIJ, J. J. & STENSVOLD, C. R. 2014. Molecular testing for clinical diagnosis and epidemiological investigations of intestinal parasitic infections. *Clin Microbiol Rev*, 27, 371-418.
- VICKERS, K. C., ROTETA, L. A., HUCHESON-DILKS, H., HAN, L. & GUO, Y. 2015. Mining diverse small RNA species in the deep transcriptome. *Trends Biochem Sci*, 40, 4-7.
- VISVESVARA, G. S., MOURA, H. & SCHUSTER, F. L. 2007. Pathogenic and opportunistic free-living amoebae: *Acanthamoeba* spp., *Balamuthia mandrillaris*, *Naegleria fowleri*, and *Sappinia diploidea*. *FEMS Immunol Med Microbiol*, 50, 1-26.

- VRABLIC, J., TOMOVA, S., CATAR, G., RANDOVA, L. & SUTTOVA, S. 1991. [Morphology and diagnosis of *Entamoeba gingivalis* and *Trichomonas tenax* and their occurrence in children and adolescents]. *Bratisl Lek Listy*, 92, 241-6.
- W.H.O. 1997. Weekly Epidemiological Record No. 17.
- WAGNER, Y., NOACK, B., HOFFMANN, T., JACOBS, E. & CHRISTIAN LUCK, P. 2006. Periodontopathogenic bacteria multiply in the environmental amoeba *Acanthamoeba castellanii*. *Int J Hyg Environ Health*, 209, 535-9.
- WALLIS, C., MARSHALL, M., COLYER, A., O'FLYNN, C., DEUSCH, O. & HARRIS, S. 2015. A longitudinal assessment of changes in bacterial community composition associated with the development of periodontal disease in dogs. *Vet Microbiol*, 181, 271-82.
- WANG, W. & CHADEE, K. 1995. *Entamoeba histolytica* suppresses gamma interferon-induced macrophage class II major histocompatibility complex Ia molecule and I-A beta mRNA expression by a prostaglandin E2-dependent mechanism. *Infect Immun*, 63, 1089-94.
- WANTLAND, W. W. & WANTLAND, E. M. 1960. Incidence, ecology, and reproduction of oral protozoa. *J Dent Res*, 39, 863.
- WERB, Z., BANDA, M. J., MCKERROW, J. H. & SANDHAUS, R. A. 1982. Elastases and elastin degradation. *J Invest Dermatol*, 79 Suppl 1, 154s-159s.
- WICKHAM, H. 2009. *ggplot2: elegant graphics for data analysis*, Springer-Verlag New York.
- WIGGS, R. B. & LOBPRISE, H. B. 1997. Periodontology. In: *Veterinary Dentistry, Principles and Practice*. 231.
- WILLIAMS, D. B. & CARTER, C. B. 2009. *Transmission Electron Microscopy*, Springer US.
- WILLIAMS, F. M. 1985. Clinical significance of esterases in man. *Clin Pharmacokinet*, 10, 392-403.
- WILSON, D. N. & DOUDNA CATE, J. H. 2012. The structure and function of the eukaryotic ribosome. *Cold Spring Harb Perspect Biol*, 4.
- YAMAMOTO, A., ASAGA, E., NAGAO, E., IGARASHI, T. & GOTO, N. 2000. Characterization of the cathepsin B-like proteinases of *Trichomonas tenax* ATCC 30207. *Oral Microbiol Immunol*, 15, 360-4.
- YANG, J., SHIH, I. I., TZENG, Y. & WANG, S. 2000. Production and purification of protease from a *Bacillus subtilis* that can deproteinize crustacean wastes*. *Enzyme Microb Technol*, 26, 406-413.
- YAZAR, S., CETINKAYA, U., HAMAMCI, B., ALKAN, A., SISMAN, Y., ESEN, C. & KOLAY, M. 2016. Investigation of *Entamoeba gingivalis* and *Trichomonas tenax* in Periodontitis or Gingivitis Patients in Kayseri. *Turkiye Parazitol Derg*, 40, 17-21.
- YE, J., COULOURIS, G., ZARETSKAYA, I., CUTCUTACHE, I., ROZEN, S. & MADDEN, T. L. 2012. Primer-BLAST: a tool to design target-specific primers for polymerase chain reaction. *BMC Bioinformatics*, 13, 134.
- YILMAZ, P., PARFREY, L. W., YARZA, P., GERKEN, J., PRUESSE, E., QUAST, C., SCHWEER, T., PEPLIES, J., LUDWIG, W. & GLOCKNER, F. O. 2014. The SILVA and "All-species Living Tree Project (LTP)" taxonomic frameworks. *Nucleic Acids Res*, 42, D643-8.
- ZHANG, Z., KERMEKCHIEV, M. B. & BARNES, W. M. 2010. Direct DNA amplification from crude clinical samples using a PCR enhancer cocktail and novel mutants of Taq. *J Mol Diagn*, 12, 152-61.
- ZIMMERMAN, S. K. & NEEDHAM, C. A. 1995. Comparison of conventional stool concentration and preserved-smear methods with Merifluor Cryptosporidium/Giardia Direct Immunofluorescence Assay and ProSpecT Giardia EZ Microplate Assay for detection of *Giardia lamblia*. *J Clin Microbiol*, 33, 1942-3.

Appendices

Supplemental Tables

Supplemental Table 1. 18S rRNA gene amplicon sizes produced from protozoa and other eukaryotic organisms using the 18S PCR developed. PCR product sizes observed are stated in base pairs.

Organism	Approximate 18S PCR product size (base pairs)
<i>Plasmodium falciparum</i> (isolate 3D7)	1400
<i>Leishmania donovani</i> (MHOM/IN/80/DD8)	1500
<i>Trypanosoma b. brucei</i> (strain 427)	1450
<i>Toxoplasma gondii</i> (ATCC 50174D)	1050
<i>Hartmannella</i> sp.(environmental isolate)	1150
<i>Acanthamoeba polyphaga</i> (CCAP 1501/3G)	1500
<i>Giardia intestinalis</i> (ATCC 50581)	0
<i>Entamoeba moshkovskii</i> (Laredo strain)	1250
<i>Trichomonas tenax</i> (ATCC 30207)	950
<i>Vahlkampfia</i> sp. (environmental isolate)	1400
<i>Tetramitus</i> sp. (environmental isolate)	1450
<i>Naegleria</i> sp. (environmental isolate)	1300
<i>Saccharomyces cerevisiae</i> gDNA	1100
Canine gDNA	1100
<i>Fusarium solani</i> (ATCC 36031)	1100
<i>Aspergillus niger</i> (DSM 737)	1100
<i>E.coli</i> DH5 α (ATCC 53868)	0

Supplemental Table 2. Standard curve data obtained for qPCR assay EG1 targeting *E. gingivalis*. Data was recorded by 7900HT Fast Real-Time PCR System (Applied Biosystems, UK) and analysed with Applied Biosystems SDS V2.4 software.

PlateID

Assay Type Absolute Quantification

Run DateTin 14/01/2016 13:39

Operator

ThermalCycleParams

Sample Information

Well	Sample Name	Detector Name	Reporter	Task	Ct	Tm Value	Tm Type	Quantity	Ct Type	Baseline Type	Threshold Type	Threshold
1	EG1 -4	18S Gene	SYBR	Standard	13.31806	74.5	Auto Tm	1.00E-04	Manual Ct	Automatic	Manual	0.04902255
2	EG1 -4	18S Gene	SYBR	Standard	13.323428	74.8	Auto Tm	1.00E-04	Manual Ct	Automatic	Manual	0.04902255
3	EG1 -4	18S Gene	SYBR	Standard	13.28929	74.8	Auto Tm	1.00E-04	Manual Ct	Automatic	Manual	0.04902255
49	EG1 -5	18S Gene	SYBR	Standard	16.604126	74.8	Auto Tm	1.00E-05	Manual Ct	Automatic	Manual	0.04902255
50	EG1 -5	18S Gene	SYBR	Standard	16.387987	74.8	Auto Tm	1.00E-05	Manual Ct	Automatic	Manual	0.04902255
51	EG1 -5	18S Gene	SYBR	Standard	16.568815	75	Auto Tm	1.00E-05	Manual Ct	Automatic	Manual	0.04902255
97	EG1 -6	18S Gene	SYBR	Standard	20.110332	75.1	Auto Tm	1.00E-06	Manual Ct	Automatic	Manual	0.04902255
99	EG1 -6	18S Gene	SYBR	Standard	20.223154	75	Auto Tm	1.00E-06	Manual Ct	Automatic	Manual	0.04902255
145	EG1 -7	18S Gene	SYBR	Standard	23.830114	75.1	Auto Tm	1.00E-07	Manual Ct	Automatic	Manual	0.04902255
146	EG1 -7	18S Gene	SYBR	Standard	23.737244	75.3	Auto Tm	1.00E-07	Manual Ct	Automatic	Manual	0.04902255
147	EG1 -7	18S Gene	SYBR	Standard	23.602745	75.3	Auto Tm	1.00E-07	Manual Ct	Automatic	Manual	0.04902255
193	EG1 -8	18S Gene	SYBR	Standard	27.183512	75.1	Auto Tm	1.00E-08	Manual Ct	Automatic	Manual	0.04902255
194	EG1 -8	18S Gene	SYBR	Standard	27.406921	75.3	Auto Tm	1.00E-08	Manual Ct	Automatic	Manual	0.04902255
195	EG1 -8	18S Gene	SYBR	Standard	27.486143	75.3	Auto Tm	1.00E-08	Manual Ct	Automatic	Manual	0.04902255
242	EG1 5e-9	18S Gene	SYBR	Standard	28.857298	75.1	Auto Tm	5.00E-09	Manual Ct	Automatic	Manual	0.04902255
243	EG1 5e-9	18S Gene	SYBR	Standard	28.556726	75.3	Auto Tm	5.00E-09	Manual Ct	Automatic	Manual	0.04902255
289	EG1 2.5e-9	18S Gene	SYBR	Standard	29.517157	74.8	Auto Tm	2.50E-09	Manual Ct	Automatic	Manual	0.04902255
291	EG1 2.5e-9	18S Gene	SYBR	Standard	29.229643	75	Auto Tm	2.50E-09	Manual Ct	Automatic	Manual	0.04902255
337	EG1 1.25e-9	18S Gene	SYBR	Standard	30.050064	74.5	Auto Tm	1.25E-09	Manual Ct	Automatic	Manual	0.04902255
338	EG1 1.25e-9	18S Gene	SYBR	Standard	30.00158	74.8	Auto Tm	1.25E-09	Manual Ct	Automatic	Manual	0.04902255
339	EG1 1.25e-9	18S Gene	SYBR	Standard	30.305773	74.8	Auto Tm	1.25E-09	Manual Ct	Automatic	Manual	0.04902255
6	EG1 6.25e-10	18S Gene	SYBR	Standard	30.71459	75.6	Auto Tm	6.25E-10	Manual Ct	Automatic	Manual	0.04902255
7	EG1 6.25e-10	18S Gene	SYBR	Standard	30.552015	75.5	Auto Tm	6.25E-10	Manual Ct	Automatic	Manual	0.04902255
101	EG1 NTC	18S Gene	SYBR	NTC	Undetermined	62.2	Auto Tm	0	Manual Ct	Automatic	Manual	0.04902255
102	EG1 NTC	18S Gene	SYBR	NTC	Undetermined	62.2	Auto Tm	0	Manual Ct	Automatic	Manual	0.04902255
103	EG1 NTC	18S Gene	SYBR	NTC	Undetermined	62.2	Auto Tm	0	Manual Ct	Automatic	Manual	0.04902255

Slope -3.4627023 cycles/log decade

Y-Intercept -0.5782391

R^2 0.9975501

Supplemental Table 3. Standard curve data obtained for qPCR assay EG2 targeting *E. gingivalis*. Data was recorded by 7900HT Fast Real-Time PCR System (Applied Biosystems, UK) and analysed with Applied Biosystems SDS V2.4 software.

PlateID

Assay Type Absolute Quantification

Run DateTin 14/01/2016 13:39

Operator

ThermalCycleParams

Sample Information

Well	Sample Name	Detector Name	Reporter	Task	Ct	Tm Value	Tm Type	Quantity	Ct Type	Baseline Type	Threshold Type	Threshold
9	EG2 -4	18s Gene 2	SYBR	Standard	14.01742	76.3	Auto Tm	1.00E-04	Manual Ct	Automatic	Manual	0.10077301
10	EG2 -4	18s Gene 2	SYBR	Standard	13.913392	76.3	Auto Tm	1.00E-04	Manual Ct	Automatic	Manual	0.10077301
11	EG2 -4	18s Gene 2	SYBR	Standard	13.979651	76.3	Auto Tm	1.00E-04	Manual Ct	Automatic	Manual	0.10077301
57	EG2 -5	18s Gene 2	SYBR	Standard	17.241747	76.3	Auto Tm	1.00E-05	Manual Ct	Automatic	Manual	0.10077301
58	EG2 -5	18s Gene 2	SYBR	Standard	17.237368	76.3	Auto Tm	1.00E-05	Manual Ct	Automatic	Manual	0.10077301
59	EG2 -5	18s Gene 2	SYBR	Standard	17.373432	76.3	Auto Tm	1.00E-05	Manual Ct	Automatic	Manual	0.10077301
105	EG2 -6	18s Gene 2	SYBR	Standard	20.882778	76.3	Auto Tm	1.00E-06	Manual Ct	Automatic	Manual	0.10077301
106	EG2 -6	18s Gene 2	SYBR	Standard	20.934942	76.6	Auto Tm	1.00E-06	Manual Ct	Automatic	Manual	0.10077301
107	EG2 -6	18s Gene 2	SYBR	Standard	20.969763	76.6	Auto Tm	1.00E-06	Manual Ct	Automatic	Manual	0.10077301
153	EG2 -7	18s Gene 2	SYBR	Standard	24.517483	76.3	Auto Tm	1.00E-07	Manual Ct	Automatic	Manual	0.10077301
154	EG2 -7	18s Gene 2	SYBR	Standard	24.757711	76.6	Auto Tm	1.00E-07	Manual Ct	Automatic	Manual	0.10077301
155	EG2 -7	18s Gene 2	SYBR	Standard	24.754862	76.6	Auto Tm	1.00E-07	Manual Ct	Automatic	Manual	0.10077301
202	EG2 -8	18s Gene 2	SYBR	Standard	28.210491	76.6	Auto Tm	1.00E-08	Manual Ct	Automatic	Manual	0.10077301
203	EG2 -8	18s Gene 2	SYBR	Standard	28.468287	76.6	Auto Tm	1.00E-08	Manual Ct	Automatic	Manual	0.10077301
249	EG2 5e-9	18s Gene 2	SYBR	Standard	28.952864	76.3	Auto Tm	5.00E-09	Manual Ct	Automatic	Manual	0.10077301
250	EG2 5e-9	18s Gene 2	SYBR	Standard	29.132307	76.6	Auto Tm	5.00E-09	Manual Ct	Automatic	Manual	0.10077301
297	EG2 2.5e-9	18s Gene 2	SYBR	Standard	30.273445	76.3	Auto Tm	2.50E-09	Manual Ct	Automatic	Manual	0.10077301
299	EG2 2.5e-9	18s Gene 2	SYBR	Standard	30.005142	76.6	Auto Tm	2.50E-09	Manual Ct	Automatic	Manual	0.10077301
109	EG2 NTC	18s Gene 2	SYBR	NTC	Undetermined	62.1	Auto Tm	0	Manual Ct	Automatic	Manual	0.10077301
110	EG2 NTC	18s Gene 2	SYBR	NTC	Undetermined	62.1	Auto Tm	0	Manual Ct	Automatic	Manual	0.10077301
111	EG2 NTC	18s Gene 2	SYBR	NTC	39.64261	72.6	Auto Tm	5.72E-12	Manual Ct	Automatic	Manual	0.10077301

Slope -3.557752 cycles/log decade

Y-Intercept -0.35480922

R^2 0.9992102

Supplemental Table 4. Standard curve data obtained for qPCR assay TC1 targeting the a canine oral *Trichomonas* sp.. Data was recorded by 7900HT Fast Real-Time PCR System (Applied Biosystems, UK) and analysed with Applied Biosystems SDS V2.4 software.

PlateID

Assay Type Absolute Quantification

Run DateTime 14/01/2016 13:39

Operator

ThermalCycleParams

Sample Information

Well	Sample Name	Detector Name	Reporter	Task	Ct	Tm Value	Tm Type	Quantity	Ct Type	Baseline Type	Threshold Type	Threshold
17	TC1 -5	ITS1-5.8S-ITS2	SYBR	Standard	14.969554	74.4	Auto Tm	1.00E-05	Manual Ct	Automatic	Manual	0.051020127
18	TC1 -5	ITS1-5.8S-ITS2	SYBR	Standard	14.879811	74.4	Auto Tm	1.00E-05	Manual Ct	Automatic	Manual	0.051020127
19	TC1 -5	ITS1-5.8S-ITS2	SYBR	Standard	14.872597	74.1	Auto Tm	1.00E-05	Manual Ct	Automatic	Manual	0.051020127
65	TC1 -6	ITS1-5.8S-ITS2	SYBR	Standard	18.436237	74.4	Auto Tm	1.00E-06	Manual Ct	Automatic	Manual	0.051020127
67	TC1 -6	ITS1-5.8S-ITS2	SYBR	Standard	18.348812	74.4	Auto Tm	1.00E-06	Manual Ct	Automatic	Manual	0.051020127
113	TC1 -7	ITS1-5.8S-ITS2	SYBR	Standard	22.009611	74.7	Auto Tm	1.00E-07	Manual Ct	Automatic	Manual	0.051020127
114	TC1 -7	ITS1-5.8S-ITS2	SYBR	Standard	21.928171	74.7	Auto Tm	1.00E-07	Manual Ct	Automatic	Manual	0.051020127
115	TC1 -7	ITS1-5.8S-ITS2	SYBR	Standard	21.975224	74.4	Auto Tm	1.00E-07	Manual Ct	Automatic	Manual	0.051020127
161	TC1 -8	ITS1-5.8S-ITS2	SYBR	Standard	25.48453	74.7	Auto Tm	1.00E-08	Manual Ct	Automatic	Manual	0.051020127
162	TC1 -8	ITS1-5.8S-ITS2	SYBR	Standard	25.208143	74.7	Auto Tm	1.00E-08	Manual Ct	Automatic	Manual	0.051020127
209	TC1 -9	ITS1-5.8S-ITS2	SYBR	Standard	28.544527	74.7	Auto Tm	1.00E-09	Manual Ct	Automatic	Manual	0.051020127
211	TC1 -9	ITS1-5.8S-ITS2	SYBR	Standard	28.31776	74.6	Auto Tm	1.00E-09	Manual Ct	Automatic	Manual	0.051020127
116	TC1 NTC	ITS1-5.8S-ITS2	SYBR	NTC	37.48392	76	Auto Tm	2.54E-12	Manual Ct	Automatic	Manual	0.051020127
117	TC1 NTC	ITS1-5.8S-ITS2	SYBR	NTC	35.910007	76.2	Auto Tm	7.34E-12	Manual Ct	Automatic	Manual	0.051020127
118	TC1 NTC	ITS1-5.8S-ITS2	SYBR	NTC	Undetermined	74.6	Auto Tm	0	Manual Ct	Automatic	Manual	0.051020127
Slope	-3.4091868	cycles/log decade										
Y-Intercept	-2.048195											
R^2	0.99896234											

Supplemental Table 5. Standard curve data obtained for qPCR assay TC2 targeting the a canine oral *Trichomonas* sp. Data was recorded by 7900HT Fast Real-Time PCR System (Applied Biosystems, UK) and analysed with Applied Biosystems SDS V2.4 software.

PlateID

Assay Type Absolute Quantification

Run DateTime 14/01/2016 13:39

Operator

ThermalCycleParams

Sample Information

Well	Sample Name	Detector Name	Reporter	Task	Ct	Tm Value	Tm Type	Quantity	Ct Type	Baseline Type	Threshold Type	Threshold
4	TC2 -5	ITS1-5.8S-ITS2 - B	SYBR	Standard	15.839625	80.3	Auto Tm	1.00E-05	Manual Ct	Automatic	Manual	0.076093294
8	TC2 -5	ITS1-5.8S-ITS2 - B	SYBR	Standard	15.752181	80.8	Auto Tm	1.00E-05	Manual Ct	Automatic	Manual	0.076093294
12	TC2 -5	ITS1-5.8S-ITS2 - B	SYBR	Standard	15.901018	80.8	Auto Tm	1.00E-05	Manual Ct	Automatic	Manual	0.076093294
52	TC2 -6	ITS1-5.8S-ITS2 - B	SYBR	Standard	19.026726	80.3	Auto Tm	1.00E-06	Manual Ct	Automatic	Manual	0.076093294
56	TC2 -6	ITS1-5.8S-ITS2 - B	SYBR	Standard	19.042278	80.8	Auto Tm	1.00E-06	Manual Ct	Automatic	Manual	0.076093294
100	TC2 -7	ITS1-5.8S-ITS2 - B	SYBR	Standard	23.095171	80.6	Auto Tm	1.00E-07	Manual Ct	Automatic	Manual	0.076093294
104	TC2 -7	ITS1-5.8S-ITS2 - B	SYBR	Standard	23.1597	80.8	Auto Tm	1.00E-07	Manual Ct	Automatic	Manual	0.076093294
108	TC2 -7	ITS1-5.8S-ITS2 - B	SYBR	Standard	23.382345	80.8	Auto Tm	1.00E-07	Manual Ct	Automatic	Manual	0.076093294
148	TC2 -8	ITS1-5.8S-ITS2 - B	SYBR	Standard	26.205809	80.6	Auto Tm	1.00E-08	Manual Ct	Automatic	Manual	0.076093294
152	TC2 -8	ITS1-5.8S-ITS2 - B	SYBR	Standard	26.168283	80.8	Auto Tm	1.00E-08	Manual Ct	Automatic	Manual	0.076093294
200	TC2 -9	ITS1-5.8S-ITS2 - B	SYBR	Standard	29.97628	80.8	Auto Tm	1.00E-09	Manual Ct	Automatic	Manual	0.076093294
204	TC2 -9	ITS1-5.8S-ITS2 - B	SYBR	Standard	29.746859	81.1	Auto Tm	1.00E-09	Manual Ct	Automatic	Manual	0.076093294
244	TC2 5e-10	ITS1-5.8S-ITS2 - B	SYBR	Standard	30.797123	80.3	Auto Tm	5.00E-10	Manual Ct	Automatic	Manual	0.076093294
248	TC2 5e-10	ITS1-5.8S-ITS2 - B	SYBR	Standard	30.637384	80.8	Auto Tm	5.00E-10	Manual Ct	Automatic	Manual	0.076093294
252	TC2 5e-10	ITS1-5.8S-ITS2 - B	SYBR	Standard	30.51245	80.8	Auto Tm	5.00E-10	Manual Ct	Automatic	Manual	0.076093294
292	TC2 2.5e-10	ITS1-5.8S-ITS2 - B	SYBR	Standard	31.349417	80.3	Auto Tm	2.50E-10	Manual Ct	Automatic	Manual	0.076093294
296	TC2 2.5e-10	ITS1-5.8S-ITS2 - B	SYBR	Standard	31.060194	80.6	Auto Tm	2.50E-10	Manual Ct	Automatic	Manual	0.076093294
300	TC2 2.5e-10	ITS1-5.8S-ITS2 - B	SYBR	Standard	31.079418	80.8	Auto Tm	2.50E-10	Manual Ct	Automatic	Manual	0.076093294
112	TC2 NTC	ITS1-5.8S-ITS2 - B	SYBR	NTC	38.327297	75.2	Auto Tm	2.59E-12	Manual Ct	Automatic	Manual	0.076093294
119	TC2 NTC	ITS1-5.8S-ITS2 - B	SYBR	NTC	36.36606	75.4	Auto Tm	9.81E-12	Manual Ct	Automatic	Manual	0.076093294
120	TC2 NTC	ITS1-5.8S-ITS2 - B	SYBR	NTC	39.046684	74.9	Auto Tm	1.59E-12	Manual Ct	Automatic	Manual	0.076093294
Slope		-3.3957865 cycles/log decade										
Y-Intercept		-1.0163795										
R^2		0.9968978										

Supplemental Table 6. Cycle data obtained for qPCR assay EG1 tested against a range of protozoan, mammalian, fungal, bacterial and clinical samples. Data exhibiting a positive qPCR reaction, within the assay limits of detection, are displayed. Data that fell outside the assay cut-offs and limits of detection are not included in the table. Data was recorded by 7900HT Fast Real-Time PCR System (Applied Biosystems, UK) and analysed with Applied Biosystems SDS V2.4 software.

SDS 2.4	AQ Results	1
Filename	27.01.16	
PlateID		
Assay Type	Absolute Quantification	
Run DateTime	27/01/2016 10:40	
Operator		
ThermalCycleParams		

Sample Information

Well	Sample Name	Detector Name	Reporter	Ct	Tm Value	Tm Type	Ct Median	Ct Mean	Ct StdDev	Ct Type	Baseline Type	Threshold Type	Threshold
149	18P	18S Gene	SYBR	22.354435	76.3	Auto Tm	22.289171	22.31076	0.03782457	Manual Ct	Automatic	Manual	0.05720534
150	18P	18S Gene	SYBR	22.288673	76.3	Auto Tm	22.289171	22.31076	0.03782457	Manual Ct	Automatic	Manual	0.05720534
151	18P	18S Gene	SYBR	22.289171	76.3	Auto Tm	22.289171	22.31076	0.03782457	Manual Ct	Automatic	Manual	0.05720534
245	E. gingivalis 18S amplicon 10E-7	18S Gene	SYBR	23.958368	76.1	Auto Tm	24.04839	24.062332	0.11159243	Manual Ct	Automatic	Manual	0.05720534
246	E. gingivalis 18S amplicon 10E-7	18S Gene	SYBR	24.180243	76.3	Auto Tm	24.04839	24.062332	0.11159243	Manual Ct	Automatic	Manual	0.05720534
247	E. gingivalis 18S amplicon 10E-7	18S Gene	SYBR	24.04839	76.3	Auto Tm	24.04839	24.062332	0.11159243	Manual Ct	Automatic	Manual	0.05720534
101	SD pool	18S Gene	SYBR	28.328415	76.3	Auto Tm	28.497835	28.497835	0.2395964	Manual Ct	Automatic	Manual	0.05720534
103	SD pool	18S Gene	SYBR	28.667255	76.6	Auto Tm	28.497835	28.497835	0.2395964	Manual Ct	Automatic	Manual	0.05720534

Supplemental Table 7. Cycle data obtained for qPCR assay TC2 tested against a range of protozoan, mammalian, fungal, bacterial and clinical samples. Data exhibiting a positive qPCR reaction, within the assay limits of detection, are displayed. Data that fell outside the assay cut-offs and limits of detection are not included in the table. Data was recorded by 7900HT Fast Real-Time PCR System (Applied Biosystems, UK) and analysed with Applied Biosystems SDS V2.4 software.

SDS 2.4 AQ Results 1
 Filename 27.01.16
 PlateID
 Assay Type Absolute Quantification
 Run DateTime 27/01/2016 10:40
 Operator
 ThermalCycleParams

Sample Information

Well	Sample Name	Detector Name	Reporter	Ct	Tm Value	Tm Type	Ct Median	Ct Mean	Ct StdDev	Ct Type	Baseline Type	Threshold Type	Threshold
61	Unidentified <i>Trichomonas</i> (CLEO) genomic	ITS1-5.8S-ITS2	SYBR	13.370423	80.8	Auto Tm	13.370423	13.336178	0.074753	Manual Ct	Automatic	Manual	0.0386495
62	Unidentified <i>Trichomonas</i> (CLEO) genomic	ITS1-5.8S-ITS2	SYBR	13.250438	80.8	Auto Tm	13.370423	13.336178	0.074753	Manual Ct	Automatic	Manual	0.0386495
63	Unidentified <i>Trichomonas</i> (CLEO) genomic	ITS1-5.8S-ITS2	SYBR	13.387674	80.8	Auto Tm	13.370423	13.336178	0.074753	Manual Ct	Automatic	Manual	0.0386495
205	Unidentified <i>Trichomonas</i> 5.8S amplicon	ITS1-5.8S-ITS2	SYBR	22.525858	80.8	Auto Tm	22.525858	22.59777	0.1890393	Manual Ct	Automatic	Manual	0.0386495
206	Unidentified <i>Trichomonas</i> 5.8S amplicon	ITS1-5.8S-ITS2	SYBR	22.812214	80.8	Auto Tm	22.525858	22.59777	0.1890393	Manual Ct	Automatic	Manual	0.0386495
207	Unidentified <i>Trichomonas</i> 5.8S amplicon	ITS1-5.8S-ITS2	SYBR	22.455242	80.8	Auto Tm	22.525858	22.59777	0.1890393	Manual Ct	Automatic	Manual	0.0386495
153	<i>T. tenax</i> genomic DNA	ITS1-5.8S-ITS2	SYBR	13.388168	79.7	Auto Tm	13.335233	13.351692	0.0316393	Manual Ct	Automatic	Manual	0.0386495
154	<i>T. tenax</i> genomic DNA	ITS1-5.8S-ITS2	SYBR	13.335233	80	Auto Tm	13.335233	13.351692	0.0316393	Manual Ct	Automatic	Manual	0.0386495
155	<i>T. tenax</i> genomic DNA	ITS1-5.8S-ITS2	SYBR	13.331676	80	Auto Tm	13.335233	13.351692	0.0316393	Manual Ct	Automatic	Manual	0.0386495

Supplemental Table 8. Coded canine plaque samples qPCR sample 384-well plates. 444 samples from 30 dogs were chosen for qPCR analysis using the qPCR **EG1** assay. Each assay sample set contains 444 randomised triplicate samples (OHLPQ), an *E. gingivalis* DNA positive control (EG), a *Trichomonas* sp. DNA negative control (TC), a no template control (NT). An *E. gingivalis* DNA standard curve is also present in each sample set (EG Std Curve).

	1	2	3	4	5	6	7	8	9	10	11	12	13	14	15	16	17	18	19	20	21	22	23	24
A	OHLP006308	OHLP006308	OHLP006308	OHLP006317	OHLP006317	OHLP006317	OHLP006328	OHLP006328	OHLP006328	OHLP006348	OHLP006348	OHLP006348	OHLP006352	OHLP006352	OHLP006352	OHLP006375	OHLP006375	OHLP006375	Blank	Blank	Blank	OHLP001047	OHLP001047	OHLP001047
B	OHLP006309	OHLP006309	OHLP006309	OHLP006336	OHLP006336	OHLP006336	OHLP006340	OHLP006340	OHLP006340	OHLP006341	OHLP006341	OHLP006341	OHLP006383	OHLP006383	OHLP006383	OHLP006463	OHLP006463	OHLP006463	OHLP001052	OHLP001052	OHLP001052	TC control (-7) P1	TC control (-7) P1	TC control (-7) P1
C	OHLP006455	OHLP006455	OHLP006455	OHLP006506	OHLP006506	OHLP006506	OHLP006502	OHLP006502	OHLP006502	OHLP006522	OHLP006522	OHLP006522	OHLP000552	OHLP000552	OHLP000552	OHLP000583	OHLP000583	OHLP000583	OHLP001604	OHLP001604	OHLP001604	OHLP001629	OHLP001629	OHLP001629
D	OHLP006498	OHLP006498	OHLP006498	OHLP006550	OHLP006550	OHLP006550	OHLP006554	OHLP006554	OHLP006554	OHLP000560	OHLP000560	OHLP000560	OHLP000591	OHLP000591	OHLP000591	OHLP005745	OHLP005745	OHLP005745	OHLP001607	OHLP001607	OHLP001607	EG control (-7) P1	EG control (-7) P1	EG control (-7) P1
E	OHLP005753	OHLP005753	OHLP005753	OHLP005892	OHLP005892	OHLP005892	OHLP005893	OHLP005893	OHLP005893	OHLP005888	OHLP005888	OHLP005888	OHLP005943	OHLP005943	OHLP005943	OHLP005911	OHLP005911	OHLP005911	OHLP000225	OHLP000225	OHLP000225	OHLP002561	OHLP002561	OHLP002561
F	OHLP000837	OHLP000837	OHLP000837	OHLP005903	OHLP005903	OHLP005903	OHLP005901	OHLP005901	OHLP005901	OHLP005951	OHLP005951	OHLP005951	OHLP005908	OHLP005908	OHLP005908	OHLP006161	OHLP006161	OHLP006161	OHLP000226	OHLP000226	OHLP000226	NT control P1	NT control P1	NT control P1
G	OHLP006169	OHLP006169	OHLP006169	OHLP006176	OHLP006176	OHLP006176	OHLP006056	OHLP006056	OHLP006056	OHLP006052	OHLP006052	OHLP006052	OHLP000756	OHLP000756	OHLP000756	OHLP000781	OHLP000781	OHLP000781	OHLP003484	OHLP003484	OHLP003484	OHLP003537	OHLP003537	OHLP003537
H	OHLP006175	OHLP006175	OHLP006175	OHLP006168	OHLP006168	OHLP006168	OHLP000644	OHLP000644	OHLP000644	OHLP000777	OHLP000777	OHLP000777	OHLP000759	OHLP000759	OHLP000759	OHLP000776	OHLP000776	OHLP000776	OHLP003497	OHLP003497	OHLP003497	Blank	Blank	Blank
I	OHLP000800	OHLP000801	OHLP000800	OHLP000873	OHLP000873	OHLP000873	OHLP000899	OHLP000899	OHLP000899	OHLP000956	OHLP000956	OHLP000956	OHLP000969	OHLP000969	OHLP000969	OHLP000144	OHLP000144	OHLP000144	OHLP001242	OHLP001242	OHLP001242	OHLP002122	OHLP002122	OHLP002122
J	OHLP000845	OHLP000845	OHLP000845	OHLP000981	OHLP000981	OHLP000981	OHLP000948	OHLP000948	OHLP000948	OHLP000961	OHLP000961	OHLP000961	OHLP000143	OHLP000143	OHLP000143	OHLP000181	OHLP000181	OHLP000181	OHLP002079	OHLP002079	OHLP002079	Blank	Blank	Blank
K	OHLP000182	OHLP000182	OHLP000182	OHLP001736	OHLP001736	OHLP001736	OHLP002592	OHLP002592	OHLP002592	OHLP002721	OHLP002721	OHLP002721	OHLP002736	OHLP002736	OHLP002736	OHLP002748	OHLP002748	OHLP002748	OHLP002972	OHLP002972	OHLP002972	OHLP002954	OHLP002954	OHLP002954
L	OHLP001744	OHLP001744	OHLP001744	OHLP002028	OHLP002028	OHLP002028	OHLP002584	OHLP002584	OHLP002584	OHLP002734	OHLP002734	OHLP002734	OHLP002728	OHLP002728	OHLP002728	OHLP002743	OHLP002743	OHLP002743	OHLP002953	OHLP002953	OHLP002953	Blank	Blank	Blank
M	OHLP002769	OHLP002769	OHLP002769	OHLP005009	OHLP005009	OHLP005009	OHLP005023	OHLP005023	OHLP005023	OHLP005024	OHLP005024	OHLP005024	OHLP005024	OHLP005024	OHLP005024	OHLP005023	OHLP005023	OHLP005023	OHLP005023	OHLP005023	OHLP005023	OHLP001408	OHLP001408	OHLP001408
N	OHLP002777	OHLP002777	OHLP002777	OHLP005017	OHLP005017	OHLP005017	OHLP005051	OHLP005051	OHLP005051	OHLP005051	OHLP005051	OHLP005051	OHLP005051	OHLP005051	OHLP005051	OHLP005052	OHLP005052	OHLP005052	OHLP005052	OHLP005052	OHLP005052	OHLP001311	OHLP001311	OHLP001311
O	OHLP005263	OHLP005263	OHLP005263	OHLP005253	OHLP005253	OHLP005253	OHLP005253	OHLP005248	OHLP005248	OHLP005248	OHLP005220	OHLP005220	OHLP005220	OHLP005232	OHLP005232	OHLP005232	OHLP000888	OHLP000888	OHLP000888	OHLP002176	OHLP002176	OHLP002176	Blank	Blank
P	OHLP005255	OHLP005255	OHLP005255	OHLP005261	OHLP005261	OHLP005261	OHLP005240	OHLP005240	OHLP005240	OHLP005240	OHLP005221	OHLP005221	OHLP005221	OHLP000896	OHLP000896	OHLP000896	OHLP001030	OHLP001030	OHLP001030	OHLP002137	OHLP002137	OHLP002137	Blank	Blank

qPCR EGI Plate 2																									
	1	2	3	4	5	6	7	8	9	10	11	12	13	14	15	16	17	18	19	20	21	22	23	24	
A	OHLPO01073	OHLPO01073	OHLPO01073	OHLPO00077	OHLPO00077	OHLPO00077	OHLPO00089	OHLPO00089	OHLPO00089	OHLPO00097	OHLPO00097	OHLPO00097	OHLPO01163	OHLPO01163	OHLPO01163	OHLPO03082	OHLPO03082	OHLPO03082	OHLPO03068	OHLPO03068	OHLPO03068	OHLPO03172	OHLPO03172	OHLPO03172	OHLPO03172
B	OHLPO01081	OHLPO01081	OHLPO01081	OHLPO00078	OHLPO00078	OHLPO00078	OHLPO00090	OHLPO00090	OHLPO00090	OHLPO00098	OHLPO00098	OHLPO00098	TC control (-7) P2	TC control (-7) P2	TC control (-7) P2	OHLPO03067	OHLPO03067	OHLPO03067	OHLPO03164	OHLPO03164	OHLPO03164	OHLPO03180	OHLPO03180	OHLPO03180	OHLPO03180
C	OHLPO01624	OHLPO01624	OHLPO01624	OHLPO01829	OHLPO01829	OHLPO01829	OHLPO01796	OHLPO01796	OHLPO01796	OHLPO01809	OHLPO01809	OHLPO01809	OHLPO00204	OHLPO00204	OHLPO00204	OHLPO03325	OHLPO03325	OHLPO03325	OHLPO03365	OHLPO03365	OHLPO03365	OHLPO03580	OHLPO03580	OHLPO03580	OHLPO03580
D	OHLPO01721	OHLPO01721	OHLPO01721	OHLPO01837	OHLPO01837	OHLPO01837	OHLPO01804	OHLPO01804	OHLPO01804	OHLPO00202	OHLPO00202	OHLPO00202	EG control (-7) P2	EG control (-7) P2	EG control (-7) P2	OHLPO03328	OHLPO03328	OHLPO03328	OHLPO03373	OHLPO03373	OHLPO03373	OHLPO03575	OHLPO03575	OHLPO03575	OHLPO03575
E	OHLPO02569	OHLPO02569	OHLPO02569	OHLPO02685	OHLPO02685	OHLPO02685	OHLPO02652	OHLPO02652	OHLPO02652	OHLPO03377	OHLPO03377	OHLPO03377	OHLPO03469	OHLPO03469	OHLPO03469	OHLPO01886	OHLPO01886	OHLPO01886	OHLPO02335	OHLPO02335	OHLPO02335	OHLPO02348	OHLPO02348	OHLPO02348	OHLPO02348
F	OHLPO02677	OHLPO02677	OHLPO02677	OHLPO02644	OHLPO02644	OHLPO02644	OHLPO02665	OHLPO02665	OHLPO02665	OHLPO03461	OHLPO03461	OHLPO03461	NT control P2	NT control P2	NT control P2	OHLPO02332	OHLPO02332	OHLPO02332	OHLPO02340	OHLPO02340	OHLPO02340	OHLPO02533	OHLPO02533	OHLPO02533	OHLPO02533
G	OHLPO03545	OHLPO03545	OHLPO03545	OHLPO03543	OHLPO03543	OHLPO03543	OHLPO02654	OHLPO02654	OHLPO02654	OHLPO01214	OHLPO01214	OHLPO01214	OHLPO01258	OHLPO01258	OHLPO01258	OHLPO02866	OHLPO02866	OHLPO02866	OHLPO02876	OHLPO02876	OHLPO02876	OHLPO02876	OHLPO03370	OHLPO03370	OHLPO03370
H	OHLPO03551	OHLPO03551	OHLPO03551	OHLPO03544	OHLPO03544	OHLPO03544	OHLPO01215	OHLPO01215	OHLPO01215	OHLPO01260	OHLPO01260	OHLPO01260	Blank	Blank	Blank	OHLPO02875	OHLPO02875	OHLPO02875	OHLPO03758	OHLPO03758	OHLPO03758	OHLPO03772	OHLPO03772	OHLPO03772	OHLPO03772
I	OHLPO02124	OHLPO02124	OHLPO02124	OHLPO02106	OHLPO02106	OHLPO02106	OHLPO01685	OHLPO01685	OHLPO01685	OHLPO02926	OHLPO02926	OHLPO02926	OHLPO02970	OHLPO02970	OHLPO02970	OHLPO03933	OHLPO03933	OHLPO03933	OHLPO04141	OHLPO04141	OHLPO04141	OHLPO04845	OHLPO04845	OHLPO04845	OHLPO04845
J	OHLPO02105	OHLPO02105	OHLPO02105	OHLPO01648	OHLPO01648	OHLPO01648	OHLPO01693	OHLPO01693	OHLPO01693	OHLPO02927	OHLPO02927	OHLPO02927	Blank	Blank	Blank	OHLPO03934	OHLPO03934	OHLPO03934	OHLPO04136	OHLPO04136	OHLPO04136	OHLPO04840	OHLPO04840	OHLPO04840	OHLPO04840
K	OHLPO02937	OHLPO02937	OHLPO02937	OHLPO03104	OHLPO03104	OHLPO03104	OHLPO03122	OHLPO03122	OHLPO03122	OHLPO03126	OHLPO03126	OHLPO03126	OHLPO03127	OHLPO03127	OHLPO03127	OHLPO03881	OHLPO03881	OHLPO03881	OHLPO03915	OHLPO03915	OHLPO03915	OHLPO03936	OHLPO03936	OHLPO03936	OHLPO03936
L	OHLPO02938	OHLPO02938	OHLPO02938	OHLPO03096	OHLPO03096	OHLPO03096	OHLPO03134	OHLPO03134	OHLPO03134	OHLPO03135	OHLPO03135	OHLPO03135	Blank	Blank	Blank	OHLPO03882	OHLPO03882	OHLPO03882	OHLPO03916	OHLPO03916	OHLPO03916	OHLPO03928	OHLPO03928	OHLPO03928	OHLPO03928
M	OHLPO04000	OHLPO04000	OHLPO04000	OHLPO04031	OHLPO04031	OHLPO04031	OHLPO04092	OHLPO04092	OHLPO04092	OHLPO0557	OHLPO0557	OHLPO0557	OHLPO02175	OHLPO02175	OHLPO02175	OHLPO03988	OHLPO03988	OHLPO03988	OHLPO04010	OHLPO04010	OHLPO04010	OHLPO04063	OHLPO04063	OHLPO04063	OHLPO04063
N	OHLPO04139	OHLPO04139	OHLPO04139	OHLPO04187	OHLPO04187	OHLPO04187	OHLPO0500	OHLPO0500	OHLPO0500	OHLPO0560	OHLPO0560	OHLPO0560	Blank	Blank	Blank	OHLPO03996	OHLPO03996	OHLPO03996	OHLPO04002	OHLPO04002	OHLPO04002	OHLPO04064	OHLPO04064	OHLPO04064	OHLPO04064
O	OHLPO02250	OHLPO02250	OHLPO02250	OHLPO02303	OHLPO02303	OHLPO02303	OHLPO03023	OHLPO03023	OHLPO03023	OHLPO02985	OHLPO02985	OHLPO02985	OHLPO03081	OHLPO03081	OHLPO03081	OHLPO05311	OHLPO05311	OHLPO05311	OHLPO05268	OHLPO05268	OHLPO05268	OHLPO05359	OHLPO05359	OHLPO05359	OHLPO05359
P	OHLPO02264	OHLPO02264	OHLPO02264	OHLPO02295	OHLPO02295	OHLPO02295	OHLPO03024	OHLPO03024	OHLPO03024	OHLPO02988	OHLPO02988	OHLPO02988	Blank	Blank	Blank	OHLPO05303	OHLPO05303	OHLPO05303	OHLPO05271	OHLPO05271	OHLPO05271	OHLPO05351	OHLPO05351	OHLPO05351	OHLPO05351

Supplemental Table 8 continued.

qPCR EG1 Plate 3																								
	1	2	3	4	5	6	7	8	9	10	11	12	13	14	15	16	17	18	19	20	21	22	23	24
A	OHLPO03284	OHLPO03284	OHLPO03284	OHLPO03245	OHLPO03245	OHLPO03245	OHLPO03309	OHLPO03309	OHLPO03309	OHLPO05673	OHLPO05673	OHLPO05673	OHLPO05680	OHLPO05680	OHLPO05680	OHLPO06050	OHLPO06050	OHLPO06050	OHLPO06054	OHLPO06054	OHLPO06054	OHLPO06074	OHLPO06074	OHLPO06074
B	OHLPO03287	OHLPO03287	OHLPO03287	OHLPO03240	OHLPO03240	OHLPO03240	OHLPO03304	OHLPO03304	OHLPO03304	OHLPO05671	OHLPO05671	OHLPO05671	OHLPO05672	OHLPO05672	OHLPO05672	OHLPO06058	OHLPO06058	OHLPO06058	OHLPO06066	OHLPO06066	OHLPO06066	TC control (-7) P3	TC control (-7) P3	TC control (-7) P3
C	OHLPO03593	OHLPO03593	OHLPO03593	OHLPO03624	OHLPO03624	OHLPO03624	OHLPO03724	OHLPO03724	OHLPO03724	OHLPO07005	OHLPO07005	OHLPO07005	OHLPO06692	OHLPO06692	OHLPO06692	OHLPO06693	OHLPO06693	OHLPO06693	OHLPO06720	OHLPO06720	OHLPO06720	OHLPO06725	OHLPO06725	OHLPO06725
D	OHLPO03632	OHLPO03632	OHLPO03632	OHLPO03723	OHLPO03723	OHLPO03723	OHLPO0385	OHLPO0385	OHLPO0385	OHLPO07013	OHLPO07013	OHLPO07013	OHLPO06703	OHLPO06703	OHLPO06703	OHLPO06701	OHLPO06701	OHLPO06701	OHLPO06712	OHLPO06712	OHLPO06712	EG control (-7) P3	EG control (-7) P3	EG control (-7) P3
E	OHLPO02413	OHLPO02413	OHLPO02413	OHLPO02455	OHLPO02455	OHLPO02455	OHLPO02493	OHLPO02493	OHLPO02493	OHLPO04293	OHLPO04293	OHLPO04293	OHLPO04308	OHLPO04308	OHLPO04308	OHLPO04400	OHLPO04400	OHLPO04400	OHLPO04369	OHLPO04369	OHLPO04369	OHLPO04384	OHLPO04384	OHLPO04384
F	OHLPO02452	OHLPO02452	OHLPO02452	OHLPO02477	OHLPO02477	OHLPO02477	OHLPO02496	OHLPO02496	OHLPO02496	OHLPO04301	OHLPO04301	OHLPO04301	OHLPO04316	OHLPO04316	OHLPO04316	OHLPO04392	OHLPO04392	OHLPO04392	OHLPO04377	OHLPO04377	OHLPO04377	NT control P3	NT control P3	NT control P3
G	OHLPO03785	OHLPO03785	OHLPO03785	OHLPO03791	OHLPO03791	OHLPO03791	OHLPO03801	OHLPO03801	OHLPO03801	OHLPO04527	OHLPO04527	OHLPO04527	OHLPO04557	OHLPO04557	OHLPO04557	OHLPO04564	OHLPO04564	OHLPO04564	OHLPO04567	OHLPO04567	OHLPO04567	OHLPO04573	OHLPO04573	OHLPO04573
H	OHLPO03786	OHLPO03786	OHLPO03786	OHLPO03792	OHLPO03792	OHLPO03792	OHLPO03802	OHLPO03802	OHLPO03802	OHLPO04519	OHLPO04519	OHLPO04519	OHLPO04560	OHLPO04560	OHLPO04560	OHLPO04575	OHLPO04575	OHLPO04575	OHLPO04565	OHLPO04565	OHLPO04565	Blank	Blank	Blank
I	OHLPO03819	OHLPO03819	OHLPO03819	OHLPO03823	OHLPO03823	OHLPO03823	OHLPO03849	OHLPO03849	OHLPO03849	OHLPO04595	OHLPO04595	OHLPO04595	OHLPO04592	OHLPO04592	OHLPO04592	OHLPO05861	OHLPO05861	OHLPO05861	OHLPO04604	OHLPO04604	OHLPO04604	OHLPO04608	OHLPO04608	OHLPO04608
J	OHLPO03820	OHLPO03820	OHLPO03820	OHLPO03824	OHLPO03824	OHLPO03824	OHLPO03852	OHLPO03852	OHLPO03852	OHLPO04592	OHLPO04592	OHLPO04592	OHLPO05860	OHLPO05860	OHLPO05860	OHLPO05872	OHLPO05872	OHLPO05872	OHLPO04597	OHLPO04597	OHLPO04597	Blank	Blank	Blank
K	OHLPO03954	OHLPO03954	OHLPO03954	OHLPO03966	OHLPO03966	OHLPO03966	OHLPO03967	OHLPO03967	OHLPO03967	OHLPO04647	OHLPO04647	OHLPO04647	OHLPO04711	OHLPO04711	OHLPO04711	OHLPO04762	OHLPO04762	OHLPO04762	OHLPO04758	OHLPO04758	OHLPO04758	OHLPO04778	OHLPO04778	OHLPO04778
L	OHLPO03962	OHLPO03962	OHLPO03962	OHLPO03958	OHLPO03958	OHLPO03958	OHLPO03959	OHLPO03959	OHLPO03959	OHLPO04719	OHLPO04719	OHLPO04719	OHLPO04754	OHLPO04754	OHLPO04754	OHLPO04766	OHLPO04766	OHLPO04766	OHLPO04770	OHLPO04770	OHLPO04770	Blank	Blank	Blank
M	OHLPO05169	OHLPO05169	OHLPO05169	OHLPO05183	OHLPO05183	OHLPO05183	OHLPO0537	OHLPO0537	OHLPO0537	OHLPO06060	OHLPO06060	OHLPO06060	OHLPO02356	OHLPO02356	OHLPO02356	OHLPO04036	OHLPO04036	OHLPO04036	OHLPO0516	OHLPO0516	OHLPO0516	OHLPO03196	OHLPO03196	OHLPO03196
N	OHLPO05177	OHLPO05177	OHLPO05177	OHLPO05175	OHLPO05175	OHLPO05175	OHLPO0538	OHLPO0538	OHLPO0538	OHLPO0508	OHLPO0508	OHLPO0508	OHLPO03188	OHLPO03188	OHLPO03188	OHLPO0668	OHLPO0668	OHLPO0668	OHLPO02364	OHLPO02364	OHLPO02364	Blank	Blank	Blank
O	OHLPO05410	OHLPO05410	OHLPO05410	OHLPO05422	OHLPO05422	OHLPO05422	OHLPO05434	OHLPO05434	OHLPO05434	OHLPO0715	OHLPO0715	OHLPO0715	OHLPO03379	OHLPO03379	OHLPO03379	OHLPO00058	OHLPO00058	OHLPO00058	OHLPO0724	OHLPO0724	OHLPO0724	OHLPO03388	OHLPO03388	OHLPO03388
P	OHLPO05418	OHLPO05418	OHLPO05418	OHLPO05414	OHLPO05414	OHLPO05414	OHLPO05665	OHLPO05665	OHLPO05665	OHLPO02563	OHLPO02563	OHLPO02563	OHLPO04211	OHLPO04211	OHLPO04211	OHLPO00876	OHLPO00876	OHLPO00876	OHLPO02572	OHLPO02572	OHLPO02572	Blank	Blank	Blank

qPCR EG1 Plate 4																								
	1	2	3	4	5	6	7	8	9	10	11	12	13	14	15	16	17	18	19	20	21	22	23	24
A	OHLPO06996	OHLPO06996	OHLPO06996	OHLPO06997	OHLPO06997	OHLPO06997	OHLPO02707	OHLPO02707	OHLPO02707	OHLPO02459	OHLPO02459	OHLPO02459	OHLPO02535	OHLPO02535	OHLPO02535	OHLPO02319	OHLPO02319	OHLPO02319	OHLPO01860	OHLPO01860	OHLPO01860	OHLPO01887	OHLPO01887	OHLPO01887
B	OHLPO07007	OHLPO07007	OHLPO07007	TC control (-7) P4	TC control (-7) P4	TC control (-7) P4	OHLPO02708	OHLPO02708	OHLPO02708	OHLPO02463	OHLPO02463	OHLPO02463	OHLPO02315	OHLPO02315	OHLPO02315	OHLPO01859	OHLPO01859	OHLPO01859	OHLPO01891	OHLPO01891	OHLPO01891	OHLPO02072	OHLPO02072	OHLPO02072
C	OHLPO06751	OHLPO06751	OHLPO06751	OHLPO06874	OHLPO06874	OHLPO06874	OHLPO02075	OHLPO02075	OHLPO02075	OHLPO01543	OHLPO01543	OHLPO01543	OHLPO01387	OHLPO01387	OHLPO01387	OHLPO00839	OHLPO00839	OHLPO00839	OHLPO00535	OHLPO00535	OHLPO00535	OHLPO01208	OHLPO01208	OHLPO01208
D	OHLPO06743	OHLPO06743	OHLPO06743	EG control (-7) P4	EG control (-7) P4	EG control (-7) P4	OHLPO01547	OHLPO01547	OHLPO01547	OHLPO01383	OHLPO01383	OHLPO01383	OHLPO00843	OHLPO00843	OHLPO00843	OHLPO005435	OHLPO005435	OHLPO005435	OHLPO00539	OHLPO00539	OHLPO00539	OHLPO01211	OHLPO01211	OHLPO01211
E	OHLPO04417	OHLPO04417	OHLPO04417	OHLPO04513	OHLPO04513	OHLPO04513	OHLPO03223	OHLPO03223	OHLPO03223	OHLPO03367	OHLPO03367	OHLPO03367	OHLPO01012	OHLPO01012	OHLPO01012	OHLPO00767	OHLPO00767	OHLPO00767	OHLPO04192	OHLPO04192	OHLPO04192	OHLPO02251	OHLPO02251	OHLPO02251
F	OHLPO04425	OHLPO04425	OHLPO04425	NT control P4	NT control P4	NT control P4	OHLPO03371	OHLPO03371	OHLPO03371	OHLPO03347	OHLPO03347	OHLPO03347	OHLPO00763	OHLPO00763	OHLPO00763	OHLPO04189	OHLPO04189	OHLPO04189	OHLPO02247	OHLPO02247	OHLPO02247	OHLPO02395	OHLPO02395	OHLPO02395
G	OHLPO04592	OHLPO04592	OHLPO04592	OHLPO01900	OHLPO01900	OHLPO01900	OHLPO02391	OHLPO02391	OHLPO02391	OHLPO05211	OHLPO05211	OHLPO05211	OHLPO03291	OHLPO03291	OHLPO03291	OHLPO02920	OHLPO02920	OHLPO02920	OHLPO03079	OHLPO03079	OHLPO03079	OHLPO00699	OHLPO00699	OHLPO00699
H	OHLPO00050	OHLPO00050	OHLPO00050	Blank	Blank	Blank	OHLPO01611	OHLPO01611	OHLPO01611	OHLPO05215	OHLPO05215	OHLPO05215	OHLPO03295	OHLPO03295	OHLPO03295	OHLPO02923	OHLPO02923	OHLPO02923	OHLPO03083	OHLPO03083	OHLPO03083	OHLPO00695	OHLPO00695	OHLPO00695
I	OHLPO04623	OHLPO04623	OHLPO04623	OHLPO04644	OHLPO04644	OHLPO04644	OHLPO06075	OHLPO06075	OHLPO06075	OHLPO00119	OHLPO00119	OHLPO00119	OHLPO00059	OHLPO00059	OHLPO00059	OHLPO03755	OHLPO03755	OHLPO03755	OHLPO04559	OHLPO04559	OHLPO04559	OHLPO04783	OHLPO04783	OHLPO04783
J	OHLPO04615	OHLPO04615	OHLPO04615	Blank	Blank	Blank	OHLPO06079	OHLPO06079	OHLPO06079	OHLPO00121	OHLPO00121	OHLPO00121	OHLPO03752	OHLPO03752	OHLPO03752	OHLPO04555	OHLPO04555	OHLPO04555	OHLPO04779	OHLPO04779	OHLPO04779	OHLPO04197	OHLPO04197	OHLPO04197
K	OHLPO05999	OHLPO05999	OHLPO05999	OHLPO06551	OHLPO06551	OHLPO06551	OHLPO04205	OHLPO04205	OHLPO04205	EG Std Curve 10-4	EG Std Curve 10-4	EG Std Curve 10-4	EG Std Curve 10-10	EG Std Curve 10-10	EG Std Curve 10-10	Blank	Blank	Blank	Blank	Blank	Blank	Blank	Blank	Blank
L	OHLPO06559	OHLPO06559	OHLPO06559	Blank	Blank	Blank	Blank	Blank	Blank	Blank	Blank	Blank	Blank	Blank	Blank	Blank	Blank	Blank	Blank	Blank	Blank	Blank	Blank	Blank
M	OHLPO04044	OHLPO04044	OHLPO04044	OHLPO00867	OHLPO00867	OHLPO00867	Blank	Blank	Blank	EG Std Curve 10-6	EG Std Curve 10-6	EG Std Curve 10-6	Blank	Blank	Blank	Blank	Blank	Blank	Blank	Blank	Blank	Blank	Blank	Blank
N	OHLPO00055	OHLPO00055	OHLPO00055	Blank	Blank	Blank	Blank	Blank	Blank	EG Std Curve 10-7	EG Std Curve 10-7	EG Std Curve 10-7	Blank	Blank	Blank	Blank	Blank	Blank	Blank	Blank	Blank	Blank	Blank	Blank
O	OHLPO00059	OHLPO00059	OHLPO00059	OHLPO04071	OHLPO04071	OHLPO04071	Blank	Blank	Blank	EG Std Curve 10-8	EG Std Curve 10-8	EG Std Curve 10-8	Blank	Blank	Blank	Blank	Blank	Blank	Blank	Blank	Blank	Blank	Blank	Blank
P	OHLPO04075	OHLPO04075	OHLPO04075	Blank	Blank	Blank	Blank	Blank	Blank	EG Std Curve 10-9	EG Std Curve 10-9	EG Std Curve 10-9	Blank	Blank	Blank	Blank	Blank	Blank	Blank	Blank	Blank	Blank	Blank	Blank

Supplemental Table 9. Coded canine plaque samples qPCR sample 384-well plates. 444 samples from 30 dogs were chosen for qPCR analysis using the qPCR **TC2** assay. Each assay sample set contains 444 randomised triplicate samples (OHL PQ), an *E. gingivalis* DNA positive control (EG), a *Trichomonas* sp. DNA negative control (TC), a no template control (NT). A *Trichomonas* sp. DNA standard curve is also present in each sample set (TC Std Curve).

qPCR TC2 Plate 1																								
	1	2	3	4	5	6	7	8	9	10	11	12	13	14	15	16	17	18	19	20	21	22	23	24
A	OHLPQ06308	OHLPQ06308	OHLPQ06308	OHLPQ06317	OHLPQ06317	OHLPQ06317	OHLPQ06328	OHLPQ06328	OHLPQ06328	OHLPQ06348	OHLPQ06348	OHLPQ06348	OHLPQ06352	OHLPQ06352	OHLPQ06352	OHLPQ06375	OHLPQ06375	OHLPQ06375	Blank	Blank	Blank	OHLPQ01047	OHLPQ01047	OHLPQ01047
B	OHLPQ06309	OHLPQ06309	OHLPQ06309	OHLPQ06336	OHLPQ06336	OHLPQ06336	OHLPQ06340	OHLPQ06340	OHLPQ06340	OHLPQ06341	OHLPQ06341	OHLPQ06341	OHLPQ06383	OHLPQ06383	OHLPQ06383	OHLPQ06463	OHLPQ06463	OHLPQ06463	OHLPQ01052	OHLPQ01052	OHLPQ01052	TC control (-7) P1	TC control (-7) P1	TC control (-7) P1
C	OHLPQ06455	OHLPQ06455	OHLPQ06455	OHLPQ06506	OHLPQ06506	OHLPQ06506	OHLPQ06502	OHLPQ06502	OHLPQ06502	OHLPQ06522	OHLPQ06522	OHLPQ06522	OHLPQ00552	OHLPQ00552	OHLPQ00552	OHLPQ00583	OHLPQ00583	OHLPQ00583	OHLPQ01604	OHLPQ01604	OHLPQ01604	OHLPQ01629	OHLPQ01629	OHLPQ01629
D	OHLPQ06498	OHLPQ06498	OHLPQ06498	OHLPQ06510	OHLPQ06510	OHLPQ06510	OHLPQ06514	OHLPQ06514	OHLPQ06514	OHLPQ00560	OHLPQ00560	OHLPQ00560	OHLPQ00591	OHLPQ00591	OHLPQ00591	OHLPQ005745	OHLPQ005745	OHLPQ005745	OHLPQ01607	OHLPQ01607	OHLPQ01607	EG control (-7) P1	EG control (-7) P1	EG control (-7) P1
E	OHLPQ05753	OHLPQ05753	OHLPQ05753	OHLPQ05892	OHLPQ05892	OHLPQ05892	OHLPQ05893	OHLPQ05893	OHLPQ05893	OHLPQ05888	OHLPQ05888	OHLPQ05888	OHLPQ05943	OHLPQ05943	OHLPQ05943	OHLPQ05911	OHLPQ05911	OHLPQ05911	OHLPQ00225	OHLPQ00225	OHLPQ00225	OHLPQ02561	OHLPQ02561	OHLPQ02561
F	OHLPQ00837	OHLPQ00837	OHLPQ00837	OHLPQ05903	OHLPQ05903	OHLPQ05903	OHLPQ05901	OHLPQ05901	OHLPQ05901	OHLPQ05951	OHLPQ05951	OHLPQ05951	OHLPQ05908	OHLPQ05908	OHLPQ05908	OHLPQ06161	OHLPQ06161	OHLPQ06161	OHLPQ00226	OHLPQ00226	OHLPQ00226	NT control P1	NT control P1	NT control P1
G	OHLPQ06169	OHLPQ06169	OHLPQ06169	OHLPQ06176	OHLPQ06176	OHLPQ06176	OHLPQ0636	OHLPQ0636	OHLPQ0636	OHLPQ0652	OHLPQ0652	OHLPQ0652	OHLPQ00756	OHLPQ00756	OHLPQ00756	OHLPQ00781	OHLPQ00781	OHLPQ00781	OHLPQ03484	OHLPQ03484	OHLPQ03484	OHLPQ03537	OHLPQ03537	OHLPQ03537
H	OHLPQ06175	OHLPQ06175	OHLPQ06175	OHLPQ06168	OHLPQ06168	OHLPQ06168	OHLPQ00644	OHLPQ00644	OHLPQ00644	OHLPQ00717	OHLPQ00717	OHLPQ00717	OHLPQ00759	OHLPQ00759	OHLPQ00759	OHLPQ00776	OHLPQ00776	OHLPQ00776	OHLPQ03497	OHLPQ03497	OHLPQ03497	Blank	Blank	Blank
I	OHLPQ00800	OHLPQ00801	OHLPQ00800	OHLPQ00873	OHLPQ00873	OHLPQ00873	OHLPQ00989	OHLPQ00989	OHLPQ00989	OHLPQ00956	OHLPQ00956	OHLPQ00956	OHLPQ00969	OHLPQ00969	OHLPQ00969	OHLPQ00144	OHLPQ00144	OHLPQ00144	OHLPQ01242	OHLPQ01242	OHLPQ01242	OHLPQ02122	OHLPQ02122	OHLPQ02122
J	OHLPQ00845	OHLPQ00845	OHLPQ00845	OHLPQ00981	OHLPQ00981	OHLPQ00981	OHLPQ00948	OHLPQ00948	OHLPQ00948	OHLPQ00961	OHLPQ00961	OHLPQ00961	OHLPQ00143	OHLPQ00143	OHLPQ00143	OHLPQ00161	OHLPQ00161	OHLPQ00161	OHLPQ02079	OHLPQ02079	OHLPQ02079	Blank	Blank	Blank
K	OHLPQ00182	OHLPQ00182	OHLPQ00182	OHLPQ01736	OHLPQ01736	OHLPQ01736	OHLPQ02292	OHLPQ02292	OHLPQ02292	OHLPQ02721	OHLPQ02721	OHLPQ02721	OHLPQ02736	OHLPQ02736	OHLPQ02736	OHLPQ02748	OHLPQ02748	OHLPQ02748	OHLPQ02972	OHLPQ02972	OHLPQ02972	OHLPQ02954	OHLPQ02954	OHLPQ02954
L	OHLPQ01744	OHLPQ01744	OHLPQ01744	OHLPQ02028	OHLPQ02028	OHLPQ02028	OHLPQ02584	OHLPQ02584	OHLPQ02584	OHLPQ02734	OHLPQ02734	OHLPQ02734	OHLPQ02728	OHLPQ02728	OHLPQ02728	OHLPQ02743	OHLPQ02743	OHLPQ02743	OHLPQ02953	OHLPQ02953	OHLPQ02953	Blank	Blank	Blank
M	OHLPQ02769	OHLPQ02769	OHLPQ02769	OHLPQ05009	OHLPQ05009	OHLPQ05009	OHLPQ05023	OHLPQ05023	OHLPQ05023	OHLPQ05024	OHLPQ05024	OHLPQ05024	OHLPQ05024	OHLPQ05024	OHLPQ05024	OHLPQ05213	OHLPQ05213	OHLPQ05213	OHLPQ05252	OHLPQ05252	OHLPQ05252	OHLPQ01311	OHLPQ01311	OHLPQ01311
N	OHLPQ02777	OHLPQ02777	OHLPQ02777	OHLPQ05017	OHLPQ05017	OHLPQ05017	OHLPQ05015	OHLPQ05015	OHLPQ05015	OHLPQ05016	OHLPQ05016	OHLPQ05016	OHLPQ05016	OHLPQ05016	OHLPQ05016	OHLPQ05216	OHLPQ05216	OHLPQ05216	OHLPQ05260	OHLPQ05260	OHLPQ05260	OHLPQ01312	OHLPQ01312	OHLPQ01312
O	OHLPQ05263	OHLPQ05263	OHLPQ05263	OHLPQ05253	OHLPQ05253	OHLPQ05253	OHLPQ05248	OHLPQ05248	OHLPQ05248	OHLPQ05220	OHLPQ05220	OHLPQ05220	OHLPQ05232	OHLPQ05232	OHLPQ05232	OHLPQ00888	OHLPQ00888	OHLPQ00888	OHLPQ02176	OHLPQ02176	OHLPQ02176	OHLPQ02249	OHLPQ02249	OHLPQ02249
P	OHLPQ05255	OHLPQ05255	OHLPQ05255	OHLPQ05261	OHLPQ05261	OHLPQ05261	OHLPQ05240	OHLPQ05240	OHLPQ05240	OHLPQ05221	OHLPQ05221	OHLPQ05221	OHLPQ00896	OHLPQ00896	OHLPQ00896	OHLPQ01030	OHLPQ01030	OHLPQ01030	OHLPQ02137	OHLPQ02137	OHLPQ02137	Blank	Blank	Blank

qPCR TC2 Plate 2																								
	1	2	3	4	5	6	7	8	9	10	11	12	13	14	15	16	17	18	19	20	21	22	23	24
A	OHLPQ01073	OHLPQ01073	OHLPQ01073	OHLPQ00077	OHLPQ00077	OHLPQ00077	OHLPQ00089	OHLPQ00089	OHLPQ00089	OHLPQ00097	OHLPQ00097	OHLPQ00097	OHLPQ01163	OHLPQ01163	OHLPQ01163	OHLPQ03082	OHLPQ03082	OHLPQ03082	OHLPQ03068	OHLPQ03068	OHLPQ03068	OHLPQ03172	OHLPQ03172	OHLPQ03172
B	OHLPQ01081	OHLPQ01081	OHLPQ01081	OHLPQ00078	OHLPQ00078	OHLPQ00078	OHLPQ00090	OHLPQ00090	OHLPQ00090	OHLPQ00098	OHLPQ00098	OHLPQ00098	TC control (-7) P2	TC control (-7) P2	TC control (-7) P2	OHLPQ03067	OHLPQ03067	OHLPQ03067	OHLPQ03164	OHLPQ03164	OHLPQ03164	OHLPQ03180	OHLPQ03180	OHLPQ03180
C	OHLPQ01624	OHLPQ01624	OHLPQ01624	OHLPQ01829	OHLPQ01829	OHLPQ01829	OHLPQ01796	OHLPQ01796	OHLPQ01796	OHLPQ01809	OHLPQ01809	OHLPQ01809	OHLPQ00204	OHLPQ00204	OHLPQ00204	OHLPQ03325	OHLPQ03325	OHLPQ03325	OHLPQ03365	OHLPQ03365	OHLPQ03365	OHLPQ03580	OHLPQ03580	OHLPQ03580
D	OHLPQ01721	OHLPQ01721	OHLPQ01721	OHLPQ01837	OHLPQ01837	OHLPQ01837	OHLPQ01804	OHLPQ01804	OHLPQ01804	OHLPQ00202	OHLPQ00202	OHLPQ00202	EG control (-7) P2	EG control (-7) P2	EG control (-7) P2	OHLPQ03328	OHLPQ03328	OHLPQ03328	OHLPQ03373	OHLPQ03373	OHLPQ03373	OHLPQ03575	OHLPQ03575	OHLPQ03575
E	OHLPQ02569	OHLPQ02569	OHLPQ02569	OHLPQ02685	OHLPQ02685	OHLPQ02685	OHLPQ02652	OHLPQ02652	OHLPQ02652	OHLPQ03377	OHLPQ03377	OHLPQ03377	OHLPQ03469	OHLPQ03469	OHLPQ03469	OHLPQ01386	OHLPQ01386	OHLPQ01386	OHLPQ02335	OHLPQ02335	OHLPQ02335	OHLPQ02348	OHLPQ02348	OHLPQ02348
F	OHLPQ02677	OHLPQ02677	OHLPQ02677	OHLPQ02644	OHLPQ02644	OHLPQ02644	OHLPQ02665	OHLPQ02665	OHLPQ02665	OHLPQ03461	OHLPQ03461	OHLPQ03461	NT control P2	NT control P2	NT control P2	OHLPQ02332	OHLPQ02332	OHLPQ02332	OHLPQ02340	OHLPQ02340	OHLPQ02340	OHLPQ02533	OHLPQ02533	OHLPQ02533
G	OHLPQ03545	OHLPQ03545	OHLPQ03545	OHLPQ03543	OHLPQ03543	OHLPQ03543	OHLPQ01214	OHLPQ01214	OHLPQ01214	OHLPQ01258	OHLPQ01258	OHLPQ01258	OHLPQ01241	OHLPQ01241	OHLPQ01241	OHLPQ02866	OHLPQ02866	OHLPQ02866	OHLPQ02876	OHLPQ02876	OHLPQ02876	OHLPQ03770	OHLPQ03770	OHLPQ03770
H	OHLPQ03551	OHLPQ03551	OHLPQ03551	OHLPQ03544	OHLPQ03544	OHLPQ03544	OHLPQ01215	OHLPQ01215	OHLPQ01215	OHLPQ01260	OHLPQ01260	OHLPQ01260	Blank	Blank	Blank	OHLPQ02875	OHLPQ02875	OHLPQ02875	OHLPQ03758	OHLPQ03758	OHLPQ03758	OHLPQ03772	OHLPQ03772	OHLPQ03772
I	OHLPQ02124	OHLPQ02124	OHLPQ02124	OHLPQ02106	OHLPQ02106	OHLPQ02106	OHLPQ01685	OHLPQ01685	OHLPQ01685	OHLPQ02926	OHLPQ02926	OHLPQ02926	OHLPQ02970	OHLPQ02970	OHLPQ02970	OHLPQ03393	OHLPQ03393	OHLPQ03393	OHLPQ04141	OHLPQ04141	OHLPQ04141	OHLPQ04845	OHLPQ04845	OHLPQ04845
J	OHLPQ02105	OHLPQ02105	OHLPQ02105	OHLPQ01648	OHLPQ01648	OHLPQ01648	OHLPQ01693	OHLPQ01693	OHLPQ01693	OHLPQ02927	OHLPQ02927	OHLPQ02927	Blank	Blank	Blank	OHLPQ00394	OHLPQ00394	OHLPQ00394	OHLPQ04136	OHLPQ04136	OHLPQ04136	OHLPQ04840	OHLPQ04840	OHLPQ04840
K	OHLPQ02937	OHLPQ02937	OHLPQ02937	OHLPQ03104	OHLPQ03104	OHLPQ03104	OHLPQ03122	OHLPQ03122	OHLPQ03122	OHLPQ03126	OHLPQ03126	OHLPQ03126	OHLPQ03127	OHLPQ03127	OHLPQ03127	OHLPQ03881	OHLPQ03881	OHLPQ03881	OHLPQ03915	OHLPQ03915	OHLPQ03915	OHLPQ03936	OHLPQ03936	OHLPQ03936
L	OHLPQ02938	OHLPQ02938	OHLPQ02938	OHLPQ03096	OHLPQ03096	OHLPQ03096	OHLPQ03134	OHLPQ03134	OHLPQ03134	OHLPQ03135	OHLPQ03135	OHLPQ03135	Blank	Blank	Blank	OHLPQ03882	OHLPQ03882	OHLPQ03882	OHLPQ03916	OHLPQ03916	OHLPQ03916	OHLPQ03928	OHLPQ03928	OHLPQ03928
M	OHLPQ01400	OHLPQ01400	OHLPQ01400	OHLPQ01431	OHLPQ01431	OHLPQ01431	OHLPQ01492	OHLPQ01492	OHLPQ01492	OHLPQ01557	OHLPQ01557	OHLPQ01557	OHLPQ02175	OHLPQ02175	OHLPQ02175	OHLPQ03988	OHLPQ03988	OHLPQ03988	OHLPQ04010	OHLPQ04010	OHLPQ04010	OHLPQ00463	OHLPQ00463	OHLPQ00463
N	OHLPQ01439	OHLPQ01439	OHLPQ01439	OHLPQ01487	OHLPQ01487	OHLPQ01487	OHLPQ01500	OHLPQ01500	OHLPQ01500	OHLPQ01560	OHLPQ01560	OHLPQ01560	Blank	Blank	Blank	OHLPQ03996	OHLPQ03996	OHLPQ03996	OHLPQ04002	OHLPQ04002	OHLPQ04002	OHLPQ00464	OHLPQ00464	OHLPQ00464
O	OHLPQ02250	OHLPQ02250	OHLPQ02250	OHLPQ02303	OHLPQ02303	OHLPQ02303	OHLPQ03023	OHLPQ03023	OHLPQ03023	OHLPQ02985	OHLPQ02985	OHLPQ02985	OHLPQ03081	OHLPQ03081	OHLPQ03081	OHLPQ05311	OHLPQ05311	OHLPQ05311	OHLPQ05268	OHLPQ05268	OHLPQ05268	OHLPQ05359	OHLPQ05359	OHLPQ05359
P	OHLPQ02264	OHLPQ02264	OHLPQ02264	OHLPQ02295	OHLPQ02295	OHLPQ02295	OHLPQ03024	OHLPQ03024	OHLPQ03024	OHLPQ02988	OHLPQ02988	OHLPQ02988	Blank	Blank	Blank	OHLPQ05303	OHLPQ05303	OHLPQ05303	OHLPQ05271	OHLPQ05271	OHLPQ05271	OHLPQ05351	OHLPQ05351	OHLPQ05351

Supplemental Table 9 continued.

qPCR TC2 Plate 3																									
	1	2	3	4	5	6	7	8	9	10	11	12	13	14	15	16	17	18	19	20	21	22	23	24	
A	OHLPO03284	OHLPO03284	OHLPO03284	OHLPO03245	OHLPO03245	OHLPO03245	OHLPO03309	OHLPO03309	OHLPO03309	OHLPO05673	OHLPO05673	OHLPO05673	OHLPO05680	OHLPO05680	OHLPO05680	OHLPO06050	OHLPO06050	OHLPO06050	OHLPO06054	OHLPO06054	OHLPO06054	OHLPO06074	OHLPO06074	OHLPO06074	
B	OHLPO03287	OHLPO03287	OHLPO03287	OHLPO03240	OHLPO03240	OHLPO03240	OHLPO03304	OHLPO03304	OHLPO03304	OHLPO05671	OHLPO05671	OHLPO05671	OHLPO05672	OHLPO05672	OHLPO05672	OHLPO06058	OHLPO06058	OHLPO06058	OHLPO06066	OHLPO06066	OHLPO06066	TC control (-7) P3	TC control (-7) P3	TC control (-7) P3	
C	OHLPO03593	OHLPO03593	OHLPO03593	OHLPO03624	OHLPO03624	OHLPO03624	OHLPO03724	OHLPO03724	OHLPO03724	OHLPO07005	OHLPO07005	OHLPO07005	OHLPO06692	OHLPO06692	OHLPO06692	OHLPO06693	OHLPO06693	OHLPO06693	OHLPO06720	OHLPO06720	OHLPO06720	OHLPO06725	OHLPO06725	OHLPO06725	
D	OHLPO03632	OHLPO03632	OHLPO03632	OHLPO03723	OHLPO03723	OHLPO03723	OHLPO0385	OHLPO0385	OHLPO0385	OHLPO07013	OHLPO07013	OHLPO07013	OHLPO06703	OHLPO06703	OHLPO06703	OHLPO06701	OHLPO06701	OHLPO06701	OHLPO06712	OHLPO06712	OHLPO06712	EG control (-7) P3	EG control (-7) P3	EG control (-7) P3	
E	OHLPO02413	OHLPO02413	OHLPO02413	OHLPO02455	OHLPO02455	OHLPO02455	OHLPO02493	OHLPO02493	OHLPO02493	OHLPO04293	OHLPO04293	OHLPO04293	OHLPO04308	OHLPO04308	OHLPO04308	OHLPO04400	OHLPO04400	OHLPO04400	OHLPO04369	OHLPO04369	OHLPO04369	OHLPO04384	OHLPO04384	OHLPO04384	
F	OHLPO02452	OHLPO02452	OHLPO02452	OHLPO02477	OHLPO02477	OHLPO02477	OHLPO02496	OHLPO02496	OHLPO02496	OHLPO04301	OHLPO04301	OHLPO04301	OHLPO04316	OHLPO04316	OHLPO04316	OHLPO04392	OHLPO04392	OHLPO04392	OHLPO04377	OHLPO04377	OHLPO04377	NT control P3	NT control P3	NT control P3	
G	OHLPO03785	OHLPO03785	OHLPO03785	OHLPO03791	OHLPO03791	OHLPO03791	OHLPO03801	OHLPO03801	OHLPO03801	OHLPO04527	OHLPO04527	OHLPO04527	OHLPO04557	OHLPO04557	OHLPO04557	OHLPO04564	OHLPO04564	OHLPO04564	OHLPO04567	OHLPO04567	OHLPO04567	OHLPO04573	OHLPO04573	OHLPO04573	
H	OHLPO03786	OHLPO03786	OHLPO03786	OHLPO03792	OHLPO03792	OHLPO03792	OHLPO03802	OHLPO03802	OHLPO03802	OHLPO04519	OHLPO04519	OHLPO04519	OHLPO04560	OHLPO04560	OHLPO04560	OHLPO04575	OHLPO04575	OHLPO04575	OHLPO04575	OHLPO04565	OHLPO04565	OHLPO04565	Blank	Blank	Blank
I	OHLPO03819	OHLPO03819	OHLPO03819	OHLPO03823	OHLPO03823	OHLPO03823	OHLPO03849	OHLPO03849	OHLPO03849	OHLPO0895	OHLPO0895	OHLPO0895	OHLPO0929	OHLPO0929	OHLPO0929	OHLPO05861	OHLPO05861	OHLPO05861	OHLPO04604	OHLPO04604	OHLPO04604	OHLPO04608	OHLPO04608	OHLPO04608	
J	OHLPO03820	OHLPO03820	OHLPO03820	OHLPO03824	OHLPO03824	OHLPO03824	OHLPO03852	OHLPO03852	OHLPO03852	OHLPO0921	OHLPO0921	OHLPO0921	OHLPO05860	OHLPO05860	OHLPO05860	OHLPO05872	OHLPO05872	OHLPO05872	OHLPO04597	OHLPO04597	OHLPO04597	Blank	Blank	Blank	
K	OHLPO03954	OHLPO03954	OHLPO03954	OHLPO03966	OHLPO03966	OHLPO03966	OHLPO03967	OHLPO03967	OHLPO03967	OHLPO04647	OHLPO04647	OHLPO04647	OHLPO04711	OHLPO04711	OHLPO04711	OHLPO04762	OHLPO04762	OHLPO04762	OHLPO04758	OHLPO04758	OHLPO04758	OHLPO04778	OHLPO04778	OHLPO04778	
L	OHLPO03962	OHLPO03962	OHLPO03962	OHLPO03958	OHLPO03958	OHLPO03958	OHLPO03959	OHLPO03959	OHLPO03959	OHLPO04719	OHLPO04719	OHLPO04719	OHLPO04754	OHLPO04754	OHLPO04754	OHLPO04766	OHLPO04766	OHLPO04766	OHLPO04770	OHLPO04770	OHLPO04770	Blank	Blank	Blank	
M	OHLPO05169	OHLPO05169	OHLPO05169	OHLPO05183	OHLPO05183	OHLPO05183	OHLPO05537	OHLPO05537	OHLPO05537	OHLPO06660	OHLPO06660	OHLPO06660	OHLPO02356	OHLPO02356	OHLPO02356	OHLPO04036	OHLPO04036	OHLPO04036	OHLPO04036	OHLPO04036	OHLPO04036	OHLPO04036	OHLPO04036	OHLPO04036	
N	OHLPO05177	OHLPO05177	OHLPO05177	OHLPO05175	OHLPO05175	OHLPO05175	OHLPO05538	OHLPO05538	OHLPO05538	OHLPO05508	OHLPO05508	OHLPO05508	OHLPO03188	OHLPO03188	OHLPO03188	OHLPO00668	OHLPO00668	OHLPO00668	OHLPO02364	OHLPO02364	OHLPO02364	Blank	Blank	Blank	
O	OHLPO05410	OHLPO05410	OHLPO05410	OHLPO05422	OHLPO05422	OHLPO05422	OHLPO05434	OHLPO05434	OHLPO05434	OHLPO0715	OHLPO0715	OHLPO0715	OHLPO03379	OHLPO03379	OHLPO03379	OHLPO00058	OHLPO00058	OHLPO00058	OHLPO0724	OHLPO0724	OHLPO0724	OHLPO03388	OHLPO03388	OHLPO03388	
P	OHLPO05418	OHLPO05418	OHLPO05418	OHLPO05414	OHLPO05414	OHLPO05414	OHLPO05665	OHLPO05665	OHLPO05665	OHLPO02563	OHLPO02563	OHLPO02563	OHLPO04211	OHLPO04211	OHLPO04211	OHLPO0876	OHLPO0876	OHLPO0876	OHLPO02572	OHLPO02572	OHLPO02572	Blank	Blank	Blank	

qPCR TC2 Plate 4																									
	1	2	3	4	5	6	7	8	9	10	11	12	13	14	15	16	17	18	19	20	21	22	23	24	
A	OHLPO06996	OHLPO06996	OHLPO06996	OHLPO06997	OHLPO06997	OHLPO06997	OHLPO02707	OHLPO02707	OHLPO02707	OHLPO02459	OHLPO02459	OHLPO02459	OHLPO02535	OHLPO02535	OHLPO02535	OHLPO02319	OHLPO02319	OHLPO02319	OHLPO02319	OHLPO0860	OHLPO0860	OHLPO0860	OHLPO0867	OHLPO0867	OHLPO0867
B	OHLPO07007	OHLPO07007	OHLPO07007	TC control (-7) P4	TC control (-7) P4	TC control (-7) P4	OHLPO02708	OHLPO02708	OHLPO02708	OHLPO02463	OHLPO02463	OHLPO02463	OHLPO02315	OHLPO02315	OHLPO02315	OHLPO0859	OHLPO0859	OHLPO0859	OHLPO0859	OHLPO0861	OHLPO0861	OHLPO0861	OHLPO02072	OHLPO02072	OHLPO02072
C	OHLPO06751	OHLPO06751	OHLPO06751	OHLPO06874	OHLPO06874	OHLPO06874	OHLPO02075	OHLPO02075	OHLPO02075	OHLPO0543	OHLPO0543	OHLPO0543	OHLPO0387	OHLPO0387	OHLPO0387	OHLPO00839	OHLPO00839	OHLPO00839	OHLPO00839	OHLPO00535	OHLPO00535	OHLPO00535	OHLPO0208	OHLPO0208	OHLPO0208
D	OHLPO06743	OHLPO06743	OHLPO06743	EG control (-7) P4	EG control (-7) P4	EG control (-7) P4	OHLPO01547	OHLPO01547	OHLPO01547	OHLPO0383	OHLPO0383	OHLPO0383	OHLPO00843	OHLPO00843	OHLPO00843	OHLPO05435	OHLPO05435	OHLPO05435	OHLPO05435	OHLPO00539	OHLPO00539	OHLPO00539	OHLPO01211	OHLPO01211	OHLPO01211
E	OHLPO04417	OHLPO04417	OHLPO04417	OHLPO04453	OHLPO04453	OHLPO04453	OHLPO03223	OHLPO03223	OHLPO03223	OHLPO03367	OHLPO03367	OHLPO03367	OHLPO01012	OHLPO01012	OHLPO01012	OHLPO00767	OHLPO00767	OHLPO00767	OHLPO00767	OHLPO04192	OHLPO04192	OHLPO04192	OHLPO02251	OHLPO02251	OHLPO02251
F	OHLPO04425	OHLPO04425	OHLPO04425	NT control P4	NT control P4	NT control P4	OHLPO03371	OHLPO03371	OHLPO03371	OHLPO03147	OHLPO03147	OHLPO03147	OHLPO00763	OHLPO00763	OHLPO00763	OHLPO04189	OHLPO04189	OHLPO04189	OHLPO04189	OHLPO02247	OHLPO02247	OHLPO02247	OHLPO02395	OHLPO02395	OHLPO02395
G	OHLPO04592	OHLPO04592	OHLPO04592	OHLPO0900	OHLPO0900	OHLPO0900	OHLPO02391	OHLPO02391	OHLPO02391	OHLPO05211	OHLPO05211	OHLPO05211	OHLPO03291	OHLPO03291	OHLPO03291	OHLPO02920	OHLPO02920	OHLPO02920	OHLPO02920	OHLPO03079	OHLPO03079	OHLPO03079	OHLPO00699	OHLPO00699	OHLPO00699
H	OHLPO00050	OHLPO00050	OHLPO00050				OHLPO01611	OHLPO01611	OHLPO01611	OHLPO05215	OHLPO05215	OHLPO05215	OHLPO03295	OHLPO03295	OHLPO03295	OHLPO02923	OHLPO02923	OHLPO02923	OHLPO02923	OHLPO03083	OHLPO03083	OHLPO03083	OHLPO00695	OHLPO00695	OHLPO00695
I	OHLPO04623	OHLPO04623	OHLPO04623	OHLPO04644	OHLPO04644	OHLPO04644	OHLPO06075	OHLPO06075	OHLPO06075	OHLPO00119	OHLPO00119	OHLPO00119	OHLPO00059	OHLPO00059	OHLPO00059	OHLPO03755	OHLPO03755	OHLPO03755	OHLPO03755	OHLPO04559	OHLPO04559	OHLPO04559	OHLPO04783	OHLPO04783	OHLPO04783
J	OHLPO04615	OHLPO04615	OHLPO04615				OHLPO06079	OHLPO06079	OHLPO06079	OHLPO00121	OHLPO00121	OHLPO00121	OHLPO03752	OHLPO03752	OHLPO03752	OHLPO04555	OHLPO04555	OHLPO04555	OHLPO04555	OHLPO04779	OHLPO04779	OHLPO04779	OHLPO04197	OHLPO04197	OHLPO04197
K	OHLPO05999	OHLPO05999	OHLPO05999	OHLPO06551	OHLPO06551	OHLPO06551	OHLPO04205	OHLPO04205	OHLPO04205							TC Std Curve 10-5	TC Std Curve 10-5	TC Std Curve 10-5	TC Std Curve 10-5						
L	OHLPO06559	OHLPO06559	OHLPO06559													TC Std Curve 10-6	TC Std Curve 10-6	TC Std Curve 10-6	TC Std Curve 10-6						
M	OHLPO04044	OHLPO04044	OHLPO04044	OHLPO00867	OHLPO00867	OHLPO00867										TC Std Curve 10-7	TC Std Curve 10-7	TC Std Curve 10-7	TC Std Curve 10-7						
N	OHLPO00055	OHLPO00055	OHLPO00055													TC Std Curve 10-8	TC Std Curve 10-8	TC Std Curve 10-8	TC Std Curve 10-8						
O	OHLPO00059	OHLPO00059	OHLPO00059	OHLPO04071	OHLPO04071	OHLPO04071										TC Std Curve 10-9	TC Std Curve 10-9	TC Std Curve 10-9	TC Std Curve 10-9						
P	OHLPO04075	OHLPO04075	OHLPO04075													TC Std Curve 10-10	TC Std Curve 10-10	TC Std Curve 10-10	TC Std Curve 10-10						

Supplemental Table 10. qPCR cycle threshold (C_t) values of data obtained from qPCR assays targeting *E. gingivalis* (EG1) and a canine oral *Trichomonas* sp. (TC2) in 444 coded canine plaque samples from 30 dogs. qPCR data was recorded by 7900HT Fast Real-Time PCR System (Applied Biosystems, UK) and analysed with Applied Biosystems SDS V2.4 software. The data set contains 444 randomised triplicate qPCR samples (OHL PQ*****) each with their associated animal metadata, collection time points, normalised C_t values, converted absolute gene copy numbers for the target species, and qPCR assay detected or quantifiable values (1 = positive, 0 = negative).

Animal ID	Gender	Date of birth	Animal name	Tooth number	Side	Area	Tooth type	PD	Pairing	Time point	Sample barcode	C_t EG1	EG1 absolute copy number	C_t TC2	TC2 absolute copy number	Rep	Age at start of trial	EG1 Detected	EG1 Quantifiable	TC2 Detected	TC2 Quantifiable
MS04561	M	23/06/2004	Arnie	203	Left	Maxilla	Incisor	PD_SEEN	2	-4	OHL PQ00050	23.061	1186.1	33.485	1.040	1	355	1	1	1	0
MS04561	M	23/06/2004	Arnie	203	Left	Maxilla	Incisor	PD_SEEN	2	-4	OHL PQ00050	22.857	1350.9	34.131	0.682	2	355	1	1	1	0
MS04561	M	23/06/2004	Arnie	203	Left	Maxilla	Incisor	PD_SEEN	2	-4	OHL PQ00050	23.071	1178.1	31.703	3.327	3	355	1	1	1	0
MS04561	M	23/06/2004	Arnie	107	Right	Maxilla	Premolar	PD_SEEN	40	-5	OHL PQ00055	24.518	467.3	29.646	12.743	1	355	1	1	1	1
MS04561	M	23/06/2004	Arnie	107	Right	Maxilla	Premolar	PD_SEEN	40	-5	OHL PQ00055	24.519	466.8	28.624	24.827	2	355	1	1	1	1
MS04561	M	23/06/2004	Arnie	107	Right	Maxilla	Premolar	PD_SEEN	40	-5	OHL PQ00055	24.785	393.7	28.890	20.868	3	355	1	1	1	1
MS04561	M	23/06/2004	Arnie	208	Left	Maxilla	Premolar	NO_PD	40	-5	OHL PQ00058	26.259	153.5	27.879	40.360	1	355	1	1	1	1
MS04561	M	23/06/2004	Arnie	208	Left	Maxilla	Premolar	NO_PD	40	-5	OHL PQ00058	28.188	44.7	27.086	67.728	2	355	1	1	1	1
MS04561	M	23/06/2004	Arnie	208	Left	Maxilla	Premolar	NO_PD	40	-5	OHL PQ00058	26.040	176.5	27.856	40.969	3	355	1	1	1	1
MS05108	F	08/02/2009	Whoopee	109	Right	Maxilla	Molar	NO_PD	21	-5	OHL PQ00077		1.0	32.016	2.712	1	114	0	0	1	0
MS05108	F	08/02/2009	Whoopee	109	Right	Maxilla	Molar	NO_PD	21	-5	OHL PQ00077	35.094	0.5	30.583	6.910	2	114	1	0	1	1
MS05108	F	08/02/2009	Whoopee	109	Right	Maxilla	Molar	NO_PD	21	-5	OHL PQ00077	33.986	1.1	34.189	0.657	3	114	1	0	1	0
MS05108	F	08/02/2009	Whoopee	209	Left	Maxilla	Molar	PD_SEEN	21	-5	OHL PQ00078	31.339	6.0	30.948	5.444	1	114	1	1	1	1
MS05108	F	08/02/2009	Whoopee	209	Left	Maxilla	Molar	PD_SEEN	21	-5	OHL PQ00078		1.0		1.000	2	114	0	0	0	0
MS05108	F	08/02/2009	Whoopee	209	Left	Maxilla	Molar	PD_SEEN	21	-5	OHL PQ00078		1.0		1.000	3	114	0	0	0	0
MS05116	M	08/05/2009	Yankee	108	Right	Maxilla	Premolar	PD_SEEN	26	-5	OHL PQ00089		1.0	27.569	49.417	1	101	0	0	1	1
MS05116	M	08/05/2009	Yankee	108	Right	Maxilla	Premolar	PD_SEEN	26	-5	OHL PQ00089	33.876	1.2	26.893	76.852	2	101	1	0	1	1
MS05116	M	08/05/2009	Yankee	108	Right	Maxilla	Premolar	PD_SEEN	26	-5	OHL PQ00089	36.188	0.3	26.933	74.848	3	101	1	0	1	1
MS05116	M	08/05/2009	Yankee	208	Left	Maxilla	Premolar	NO_PD	26	-5	OHL PQ00090	37.064	0.2	27.742	44.140	1	101	1	0	1	1
MS05116	M	08/05/2009	Yankee	208	Left	Maxilla	Premolar	NO_PD	26	-5	OHL PQ00090	36.932	0.2	26.573	94.698	2	101	1	0	1	1
MS05116	M	08/05/2009	Yankee	208	Left	Maxilla	Premolar	NO_PD	26	-5	OHL PQ00090	37.451	0.1	26.852	78.935	3	101	1	0	1	1
MS05120	F	08/05/2009	Yetti	103	Right	Maxilla	Incisor	PD_SEEN	28	-4	OHL PQ00097	35.904	0.3	32.360	2.167	1	101	1	0	1	0
MS05120	F	08/05/2009	Yetti	103	Right	Maxilla	Incisor	PD_SEEN	28	-4	OHL PQ00097	31.883	4.2	34.664	0.482	2	101	1	1	1	0
MS05120	F	08/05/2009	Yetti	103	Right	Maxilla	Incisor	PD_SEEN	28	-4	OHL PQ00097		1.0	32.896	1.527	3	101	0	0	1	0
MS05120	F	08/05/2009	Yetti	203	Left	Maxilla	Incisor	NO_PD	28	-4	OHL PQ00098	26.857	104.7	34.757	0.453	1	101	1	1	1	0
MS05120	F	08/05/2009	Yetti	203	Left	Maxilla	Incisor	NO_PD	28	-4	OHL PQ00098	26.271	152.3	32.642	1.803	2	101	1	1	1	0
MS05120	F	08/05/2009	Yetti	203	Left	Maxilla	Incisor	NO_PD	28	-4	OHL PQ00098	25.674	223.1		1.000	3	101	1	1	0	0
MS04712	M	10/05/2006	Elton	107	Right	Maxilla	Premolar	NO_PD	51	-3	OHL PQ00119	26.833	106.3	28.424	28.278	1	257	1	1	1	1
MS04712	M	10/05/2006	Elton	107	Right	Maxilla	Premolar	NO_PD	51	-3	OHL PQ00119	29.182	23.7	30.295	8.341	2	257	1	1	1	1
MS04712	M	10/05/2006	Elton	107	Right	Maxilla	Premolar	NO_PD	51	-3	OHL PQ00119	28.956	27.4	29.378	15.172	3	257	1	1	1	1
MS04712	M	10/05/2006	Elton	108	Right	Maxilla	Premolar	PD_SEEN	51	-3	OHL PQ00121	25.083	325.6	25.506	189.926	1	257	1	1	1	1
MS04712	M	10/05/2006	Elton	108	Right	Maxilla	Premolar	PD_SEEN	51	-3	OHL PQ00121	25.066	329.1	24.720	317.305	2	257	1	1	1	1
MS04712	M	10/05/2006	Elton	108	Right	Maxilla	Premolar	PD_SEEN	51	-3	OHL PQ00121	25.137	314.4	24.192	447.783	3	257	1	1	1	1
MS04559	F	23/06/2004	Halle	309	Left	Manible	Molar	NO_PD	1	-5	OHL PQ00143	31.653	4.9	33.229	1.229	1	355	1	1	1	0
MS04559	F	23/06/2004	Halle	309	Left	Manible	Molar	NO_PD	1	-5	OHL PQ00143		1.0	30.085	9.569	2	355	0	0	1	1
MS04559	F	23/06/2004	Halle	309	Left	Manible	Molar	NO_PD	1	-5	OHL PQ00143	30.050	13.6	29.159	17.505	3	355	1	1	1	1
MS04559	F	23/06/2004	Halle	409	Right	Manible	Molar	PD_SEEN	1	-5	OHL PQ00144		1.0	28.206	32.611	1	355	0	0	1	1
MS04559	F	23/06/2004	Halle	409	Right	Manible	Molar	PD_SEEN	1	-5	OHL PQ00144		1.0	29.328	15.676	2	355	0	0	1	1
MS04559	F	23/06/2004	Halle	409	Right	Manible	Molar	PD_SEEN	1	-5	OHL PQ00144	31.605	5.0	29.786	11.626	3	355	1	1	1	1
MS04929	M	05/01/2008	Norris	304	Left	Manible	Canine	PD_SEEN	12	-3	OHL PQ00181	32.667	2.6		1.000	1	171	1	0	0	0

MS04929	M	05/01/2008	Norris	304	Left	Manible	Canine	PD_SEEN	12	-3	OHLPQ00181	30.095	13.2	29.613	13.014	2	171	1	1	1	1
MS04929	M	05/01/2008	Norris	304	Left	Manible	Canine	PD_SEEN	12	-3	OHLPQ00181	35.113	0.5		1.000	3	171	1	0	0	0
MS04929	M	05/01/2008	Norris	404	Right	Manible	Canine	NO_PD	12	-3	OHLPQ00182		1.0	31.817	3.088	1	171	0	0	1	0
MS04929	M	05/01/2008	Norris	404	Right	Manible	Canine	NO_PD	12	-3	OHLPQ00182	32.215	3.4		1.000	2	171	1	0	0	0
MS04929	M	05/01/2008	Norris	404	Right	Manible	Canine	NO_PD	12	-3	OHLPQ00182		1.0	35.828	0.225	3	171	0	0	1	0
MS05107	F	08/02/2009	Willow	208	Left	Maxilla	Premolar	PD_SEEN	61	-4	OHLPQ00202	25.711	217.9	25.602	178.472	1	114	1	1	1	1
MS05107	F	08/02/2009	Willow	208	Left	Maxilla	Premolar	PD_SEEN	61	-4	OHLPQ00202	25.898	193.4	26.103	128.668	2	114	1	1	1	1
MS05107	F	08/02/2009	Willow	208	Left	Maxilla	Premolar	PD_SEEN	61	-4	OHLPQ00202	25.729	215.4	26.368	108.212	3	114	1	1	1	1
MS05107	F	08/02/2009	Willow	408	Right	Manible	Premolar	NO_PD	61	-4	OHLPQ00204	27.786	57.8	22.519	1335.150	1	114	1	1	1	1
MS05107	F	08/02/2009	Willow	408	Right	Manible	Premolar	NO_PD	61	-4	OHLPQ00204	27.083	90.6	22.852	1074.178	2	114	1	1	1	1
MS05107	F	08/02/2009	Willow	408	Right	Manible	Premolar	NO_PD	61	-4	OHLPQ00204	27.215	83.3	22.626	1245.166	3	114	1	1	1	1
MS05115	F	08/05/2009	Yoyo	103	Right	Maxilla	Incisor	NO_PD	25	-5	OHLPQ00225	24.896	366.9	34.502	0.535	1	101	1	1	1	0
MS05115	F	08/05/2009	Yoyo	103	Right	Maxilla	Incisor	NO_PD	25	-5	OHLPQ00225	25.586	236.0	34.404	0.571	2	101	1	1	1	0
MS05115	F	08/05/2009	Yoyo	103	Right	Maxilla	Incisor	NO_PD	25	-5	OHLPQ00225	25.152	311.4		1.000	3	101	1	1	0	0
MS05115	F	08/05/2009	Yoyo	203	Left	Maxilla	Incisor	PD_SEEN	25	-5	OHLPQ00226	32.439	3.0	34.122	0.686	1	101	1	0	1	0
MS05115	F	08/05/2009	Yoyo	203	Left	Maxilla	Incisor	PD_SEEN	25	-5	OHLPQ00226		1.0	32.325	2.217	2	101	0	0	1	0
MS05115	F	08/05/2009	Yoyo	203	Left	Maxilla	Incisor	PD_SEEN	25	-5	OHLPQ00226	33.186	1.8	32.278	2.285	3	101	1	0	1	0
MS05152	M	03/12/2010	Bentley	108	Right	Maxilla	Premolar	NO_PD	33	-4	OHLPQ00393	33.758	1.3	30.136	9.251	1	19	1	0	1	1
MS05152	M	03/12/2010	Bentley	108	Right	Maxilla	Premolar	NO_PD	33	-4	OHLPQ00393	35.449	0.4	30.455	7.511	2	19	1	0	1	1
MS05152	M	03/12/2010	Bentley	108	Right	Maxilla	Premolar	NO_PD	33	-4	OHLPQ00393	31.809	4.4	33.727	0.888	3	19	1	1	1	0
MS05152	M	03/12/2010	Bentley	208	Left	Maxilla	Premolar	PD_SEEN	33	-4	OHLPQ00394		1.0	31.427	3.983	1	19	0	0	1	0
MS05152	M	03/12/2010	Bentley	208	Left	Maxilla	Premolar	PD_SEEN	33	-4	OHLPQ00394		1.0	33.913	0.786	2	19	0	0	1	0
MS05152	M	03/12/2010	Bentley	208	Left	Maxilla	Premolar	PD_SEEN	33	-4	OHLPQ00394	31.517	5.3	34.799	0.441	3	19	1	1	1	0
MS05158	F	15/01/2010	Connie	309	Left	Manible	Molar	PD_SEEN	37	-4	OHLPQ00463		1.0	28.368	29.336	1	65	0	0	1	1
MS05158	F	15/01/2010	Connie	309	Left	Manible	Molar	PD_SEEN	37	-4	OHLPQ00463		1.0	28.874	21.080	2	65	0	0	1	1
MS05158	F	15/01/2010	Connie	309	Left	Manible	Molar	PD_SEEN	37	-4	OHLPQ00463		1.0	34.913	0.409	3	65	0	0	1	0
MS05158	F	15/01/2010	Connie	409	Right	Manible	Molar	NO_PD	37	-4	OHLPQ00464		1.0	31.470	3.874	1	65	0	0	1	0
MS05158	F	15/01/2010	Connie	409	Right	Manible	Molar	NO_PD	37	-4	OHLPQ00464		1.0	32.902	1.522	2	65	0	0	1	0
MS05158	F	15/01/2010	Connie	409	Right	Manible	Molar	NO_PD	37	-4	OHLPQ00464		1.0	30.944	5.460	3	65	0	0	1	1
MS04923	F	05/01/2008	Nettie	107	Right	Maxilla	Premolar	NO_PD	59	-3	OHLPQ00535	25.468	254.5	32.291	2.266	1	171	1	1	1	0
MS04923	F	05/01/2008	Nettie	107	Right	Maxilla	Premolar	NO_PD	59	-3	OHLPQ00535	25.179	306.1	32.059	2.637	2	171	1	1	1	0
MS04923	F	05/01/2008	Nettie	107	Right	Maxilla	Premolar	NO_PD	59	-3	OHLPQ00535	25.475	253.3	33.075	1.358	3	171	1	1	1	0
MS04923	F	05/01/2008	Nettie	108	Right	Maxilla	Premolar	NO_PD	9	-4	OHLPQ00537	24.164	585.9	29.251	16.490	1	171	1	1	1	1
MS04923	F	05/01/2008	Nettie	108	Right	Maxilla	Premolar	NO_PD	9	-4	OHLPQ00537	24.239	558.4		1.000	2	171	1	1	0	0
MS04923	F	05/01/2008	Nettie	108	Right	Maxilla	Premolar	NO_PD	9	-4	OHLPQ00537	24.580	448.9	30.214	8.795	3	171	1	1	1	1
MS04923	F	05/01/2008	Nettie	208	Left	Maxilla	Premolar	PD_SEEN	9	-4	OHLPQ00538	24.685	419.8	27.344	57.231	1	171	1	1	1	1
MS04923	F	05/01/2008	Nettie	208	Left	Maxilla	Premolar	PD_SEEN	9	-4	OHLPQ00538	24.663	425.8	27.162	64.460	2	171	1	1	1	1
MS04923	F	05/01/2008	Nettie	208	Left	Maxilla	Premolar	PD_SEEN	9	-4	OHLPQ00538	24.981	347.5	27.339	57.422	3	171	1	1	1	1
MS04923	F	05/01/2008	Nettie	308	Left	Manible	Premolar	PD_SEEN	59	-3	OHLPQ00539	23.781	748.3	24.346	405.013	1	171	1	1	1	1
MS04923	F	05/01/2008	Nettie	308	Left	Manible	Premolar	PD_SEEN	59	-3	OHLPQ00539	23.798	740.4	25.241	225.834	2	171	1	1	1	1
MS04923	F	05/01/2008	Nettie	308	Left	Manible	Premolar	PD_SEEN	59	-3	OHLPQ00539	23.566	858.5	24.982	267.396	3	171	1	1	1	1
MS05109	M	08/02/2009	Wellington	409	Right	Manible	Molar	NO_PD	22	-4	OHLPQ00552		1.0	29.602	13.111	1	114	0	0	1	1
MS05109	M	08/02/2009	Wellington	409	Right	Manible	Molar	NO_PD	22	-4	OHLPQ00552		1.0	34.430	0.561	2	114	0	0	1	0
MS05109	M	08/02/2009	Wellington	409	Right	Manible	Molar	NO_PD	22	-4	OHLPQ00552		1.0		1.000	3	114	0	0	0	0
MS05109	M	08/02/2009	Wellington	309	Left	Manible	Molar	PD_SEEN	22	-4	OHLPQ00560		1.0	29.087	18.347	1	114	0	0	1	1
MS05109	M	08/02/2009	Wellington	309	Left	Manible	Molar	PD_SEEN	22	-4	OHLPQ00560		1.0	29.586	13.247	2	114	0	0	1	1
MS05109	M	08/02/2009	Wellington	309	Left	Manible	Molar	PD_SEEN	22	-4	OHLPQ00560	34.894	0.6	29.470	14.288	3	114	1	0	1	1
MS05118	M	08/05/2009	Yoshi	408	Right	Manible	Premolar	NO_PD	27	-4	OHLPQ00583		1.0	27.188	63.382	1	101	0	0	1	1
MS05118	M	08/05/2009	Yoshi	408	Right	Manible	Premolar	NO_PD	27	-4	OHLPQ00583	35.711	0.4	28.676	23.997	2	101	1	0	1	1
MS05118	M	08/05/2009	Yoshi	408	Right	Manible	Premolar	NO_PD	27	-4	OHLPQ00583	32.801	2.3	27.792	42.714	3	101	1	0	1	1
MS05118	M	08/05/2009	Yoshi	308	Left	Manible	Premolar	PD_SEEN	27	-4	OHLPQ00591	31.600	5.0	31.972	2.791	1	101	1	1	1	0
MS05118	M	08/05/2009	Yoshi	308	Left	Manible	Premolar	PD_SEEN	27	-4	OHLPQ00591	29.832	15.6	31.601	3.556	2	101	1	1	1	0
MS05118	M	08/05/2009	Yoshi	308	Left	Manible	Premolar	PD_SEEN	27	-4	OHLPQ00591	36.527	0.2	34.330	0.599	3	101	1	0	1	0
MS04563	F	23/06/2004	China	208	Left	Maxilla	Premolar	PD_SEEN	42	-3	OHLPQ00636	24.024	640.7	28.488	27.125	1	355	1	1	1	1

MS04563	F	23/06/2004	China	208	Left	Maxilla	Premolar	PD_SEEN	42	-3	OHL PQ00636	23.847	717.6	30.570	6.971	2	355	1	1	1	1
MS04563	F	23/06/2004	China	208	Left	Maxilla	Premolar	PD_SEEN	42	-3	OHL PQ00636	24.444	489.9	31.609	3.537	3	355	1	1	1	0
MS04599	M	09/04/2004	Rooney	108	Right	Maxilla	Premolar	PD_SEEN	6	-4	OHL PQ00644	34.617	0.7	32.373	2.148	1	366	1	0	1	0
MS04599	M	09/04/2004	Rooney	108	Right	Maxilla	Premolar	PD_SEEN	6	-4	OHL PQ00644		1.0	32.464	2.024	2	366	0	0	1	0
MS04599	M	09/04/2004	Rooney	108	Right	Maxilla	Premolar	PD_SEEN	6	-4	OHL PQ00644	33.780	1.3	31.601	3.557	3	366	1	0	1	0
MS04599	M	09/04/2004	Rooney	208	Left	Maxilla	Premolar	NO_PD	6	-4	OHL PQ00652	33.132	1.9	33.685	0.912	1	366	1	0	1	0
MS04599	M	09/04/2004	Rooney	208	Left	Maxilla	Premolar	NO_PD	6	-4	OHL PQ00652	32.820	2.3	34.214	0.646	2	366	1	0	1	0
MS04599	M	09/04/2004	Rooney	208	Left	Maxilla	Premolar	NO_PD	6	-4	OHL PQ00652	33.182	1.8	33.940	0.773	3	366	1	0	1	0
MS04595	M	09/04/2004	Dallas	108	Right	Maxilla	Premolar	NO_PD	5	-4	OHL PQ00660		1.0	26.012	136.557	1	366	0	0	1	1
MS04595	M	09/04/2004	Dallas	108	Right	Maxilla	Premolar	NO_PD	5	-4	OHL PQ00660		1.0	24.560	352.339	2	366	0	0	1	1
MS04595	M	09/04/2004	Dallas	108	Right	Maxilla	Premolar	NO_PD	5	-4	OHL PQ00660		1.0	24.991	265.830	3	366	0	0	1	1
MS04595	M	09/04/2004	Dallas	208	Left	Maxilla	Premolar	PD_SEEN	5	-4	OHL PQ00668	35.867	0.3	26.934	74.781	1	366	1	0	1	1
MS04595	M	09/04/2004	Dallas	208	Left	Maxilla	Premolar	PD_SEEN	5	-4	OHL PQ00668	32.756	2.4	27.338	57.453	2	366	1	0	1	1
MS04595	M	09/04/2004	Dallas	208	Left	Maxilla	Premolar	PD_SEEN	5	-4	OHL PQ00668		1.0	27.666	46.392	3	366	0	0	1	1
MS04648	M	10/12/2005	Winston	408	Right	Manible	Premolar	PD_SEEN	48	-4	OHL PQ00695	34.972	0.6	27.728	44.548	1	279	1	0	1	1
MS04648	M	10/12/2005	Winston	408	Right	Manible	Premolar	PD_SEEN	48	-4	OHL PQ00695	27.112	89.0	27.634	47.383	2	279	1	1	1	1
MS04648	M	10/12/2005	Winston	408	Right	Manible	Premolar	PD_SEEN	48	-4	OHL PQ00695		1.0	29.374	15.215	3	279	0	0	1	1
MS04648	M	10/12/2005	Winston	207	Left	Maxilla	Premolar	NO_PD	48	-4	OHL PQ00699	33.354	1.6	26.058	132.491	1	279	1	0	1	1
MS04648	M	10/12/2005	Winston	207	Left	Maxilla	Premolar	NO_PD	48	-4	OHL PQ00699	33.083	2.0	26.454	102.318	2	279	1	0	1	1
MS04648	M	10/12/2005	Winston	207	Left	Maxilla	Premolar	NO_PD	48	-4	OHL PQ00699	36.340	0.2	26.244	117.322	3	279	1	0	1	1
MS04645	F	10/12/2005	Mimi	209	Left	Maxilla	Molar	NO_PD	47	-3	OHL PQ00717		1.0	28.033	36.508	1	279	0	0	1	1
MS04645	F	10/12/2005	Mimi	209	Left	Maxilla	Molar	NO_PD	47	-3	OHL PQ00717	33.184	1.8	27.651	46.854	2	279	1	0	1	1
MS04645	F	10/12/2005	Mimi	209	Left	Maxilla	Molar	NO_PD	47	-3	OHL PQ00717	32.649	2.6	29.174	17.336	3	279	1	0	1	1
MS04643	F	10/12/2005	Faith	108	Right	Maxilla	Premolar	NO_PD	46	-3	OHL PQ00756		1.0	26.793	82.003	1	279	0	0	1	1
MS04643	F	10/12/2005	Faith	108	Right	Maxilla	Premolar	NO_PD	46	-3	OHL PQ00756	33.000	2.1	25.701	167.250	2	279	1	0	1	1
MS04643	F	10/12/2005	Faith	108	Right	Maxilla	Premolar	NO_PD	46	-3	OHL PQ00756	31.257	6.3	25.461	195.630	3	279	1	1	1	1
MS04643	F	10/12/2005	Faith	408	Right	Manible	Premolar	PD_SEEN	46	-3	OHL PQ00759	30.993	7.4	31.690	3.356	1	279	1	1	1	0
MS04643	F	10/12/2005	Faith	408	Right	Manible	Premolar	PD_SEEN	46	-3	OHL PQ00759	33.471	1.5		1.000	2	279	1	0	0	0
MS04643	F	10/12/2005	Faith	408	Right	Manible	Premolar	PD_SEEN	46	-3	OHL PQ00759		1.0	29.616	12.988	3	279	0	0	1	1
MS04643	F	10/12/2005	Faith	207	Left	Maxilla	Premolar	NO_PD	45	-3	OHL PQ00763	30.264	11.9	29.060	18.679	1	279	1	1	1	1
MS04643	F	10/12/2005	Faith	207	Left	Maxilla	Premolar	NO_PD	45	-3	OHL PQ00763		1.0	28.342	29.848	2	279	0	0	1	1
MS04643	F	10/12/2005	Faith	207	Left	Maxilla	Premolar	NO_PD	45	-3	OHL PQ00763	29.154	24.1	33.274	1.193	3	279	1	1	1	0
MS04643	F	10/12/2005	Faith	308	Left	Manible	Premolar	PD_SEEN	45	-3	OHL PQ00767	29.271	22.4	26.460	101.950	1	279	1	1	1	1
MS04643	F	10/12/2005	Faith	308	Left	Manible	Premolar	PD_SEEN	45	-3	OHL PQ00767	26.561	126.6	27.036	70.004	2	279	1	1	1	1
MS04643	F	10/12/2005	Faith	308	Left	Manible	Premolar	PD_SEEN	45	-3	OHL PQ00767	28.580	34.8	26.853	78.856	3	279	1	1	1	1
MS04714	M	10/05/2006	Eddie	409	Right	Manible	Molar	PD_SEEN	55	-5	OHL PQ00776	33.656	1.4	30.099	9.479	1	257	1	0	1	1
MS04714	M	10/05/2006	Eddie	409	Right	Manible	Molar	PD_SEEN	55	-5	OHL PQ00776		1.0	31.771	3.183	2	257	0	0	1	0
MS04714	M	10/05/2006	Eddie	409	Right	Manible	Molar	PD_SEEN	55	-5	OHL PQ00776		1.0	31.469	3.876	3	257	0	0	1	0
MS04714	M	10/05/2006	Eddie	209	Left	Maxilla	Molar	NO_PD	55	-5	OHL PQ00781		1.0	25.905	146.466	1	257	0	0	1	1
MS04714	M	10/05/2006	Eddie	209	Left	Maxilla	Molar	NO_PD	55	-5	OHL PQ00781	34.255	0.9	26.937	74.660	2	257	1	0	1	1
MS04714	M	10/05/2006	Eddie	209	Left	Maxilla	Molar	NO_PD	55	-5	OHL PQ00781		1.0	27.395	55.382	3	257	0	0	1	1
MS04715	F	10/05/2006	Edna	309	Left	Manible	Molar	PD_SEEN	56	-4	OHL PQ00800	25.529	244.8	29.001	19.405	1	257	1	1	1	1
MS04715	F	10/05/2006	Edna	309	Left	Manible	Molar	PD_SEEN	56	-4	OHL PQ00800	26.269	152.5	28.479	27.286	2	257	1	1	1	1
MS04715	F	10/05/2006	Edna	309	Left	Manible	Molar	PD_SEEN	56	-4	OHL PQ00800	26.804	108.3	30.812	5.951	3	257	1	1	1	1
MS04846	M	13/09/2007	Jigsaw	109	Right	Maxilla	Molar	NO_PD	8	-4	OHL PQ00837		1.0	29.163	17.466	1	187	0	0	1	1
MS04846	M	13/09/2007	Jigsaw	109	Right	Maxilla	Molar	NO_PD	8	-4	OHL PQ00837	28.576	34.9		1.000	2	187	1	1	0	0
MS04846	M	13/09/2007	Jigsaw	109	Right	Maxilla	Molar	NO_PD	8	-4	OHL PQ00837	30.466	10.4	29.814	11.418	3	187	1	1	1	1
MS04846	M	13/09/2007	Jigsaw	408	Right	Manible	Premolar	PD_SEEN	58	-3	OHL PQ00839	32.321	3.2	31.378	4.113	1	187	1	0	1	1
MS04846	M	13/09/2007	Jigsaw	408	Right	Manible	Premolar	PD_SEEN	58	-3	OHL PQ00839	31.587	5.1		1.000	2	187	1	1	0	0
MS04846	M	13/09/2007	Jigsaw	408	Right	Manible	Premolar	PD_SEEN	58	-3	OHL PQ00839		1.0	31.490	3.824	3	187	0	0	1	0
MS04846	M	13/09/2007	Jigsaw	207	Left	Maxilla	Premolar	NO_PD	58	-3	OHL PQ00843		1.0		1.000	1	187	0	0	0	0
MS04846	M	13/09/2007	Jigsaw	207	Left	Maxilla	Premolar	NO_PD	58	-3	OHL PQ00843	34.984	0.6	33.316	1.161	2	187	1	0	1	0
MS04846	M	13/09/2007	Jigsaw	207	Left	Maxilla	Premolar	NO_PD	58	-3	OHL PQ00843	33.321	1.7	30.950	5.438	3	187	1	0	1	1
MS04846	M	13/09/2007	Jigsaw	209	Left	Maxilla	Molar	PD_SEEN	8	-4	OHL PQ00845	34.315	0.9	26.131	126.369	1	187	1	0	1	1

MS04846	M	13/09/2007	Jigsaw	209	Left	Maxilla	Molar	PD_SEEN	8	-4	OHL PQ00845	1.0	27.459	53.088	2	187	0	0	1	
MS04846	M	13/09/2007	Jigsaw	209	Left	Maxilla	Molar	PD_SEEN	8	-4	OHL PQ00845	1.0	28.166	33.474	3	187	0	0	1	
MS04561	M	23/06/2004	Arnie	107	Right	Maxilla	Premolar	PD_SEEN	40	-4	OHL PQ00867	23.751	762.7	27.274	59.922	1	355	1	1	1
MS04561	M	23/06/2004	Arnie	107	Right	Maxilla	Premolar	PD_SEEN	40	-4	OHL PQ00867	23.698	789.2	26.988	72.192	2	355	1	1	1
MS04561	M	23/06/2004	Arnie	107	Right	Maxilla	Premolar	PD_SEEN	40	-4	OHL PQ00867	24.117	603.5	27.078	68.085	3	355	1	1	1
MS04561	M	23/06/2004	Arnie	203	Left	Maxilla	Incisor	PD_SEEN	2	-3	OHL PQ00873	23.729	773.9	33.034	1.396	1	355	1	1	0
MS04561	M	23/06/2004	Arnie	203	Left	Maxilla	Incisor	PD_SEEN	2	-3	OHL PQ00873	23.429	937.5	35.283	0.321	2	355	1	1	0
MS04561	M	23/06/2004	Arnie	203	Left	Maxilla	Incisor	PD_SEEN	2	-3	OHL PQ00873	23.536	875.3	31.824	3.074	3	355	1	1	0
MS04561	M	23/06/2004	Arnie	208	Left	Maxilla	Premolar	NO_PD	40	-4	OHL PQ00876	19.848	9247.1	29.847	11.175	1	355	1	1	1
MS04561	M	23/06/2004	Arnie	208	Left	Maxilla	Premolar	NO_PD	40	-4	OHL PQ00876	20.182	7471.1	33.525	1.013	2	355	1	1	1
MS04561	M	23/06/2004	Arnie	208	Left	Maxilla	Premolar	NO_PD	40	-4	OHL PQ00876	20.301	6923.0	27.893	39.990	3	355	1	1	1
MS04559	F	23/06/2004	Halle	409	Right	Manible	Molar	PD_SEEN	1	-4	OHL PQ00888	1.0	34.520	0.529	1	355	0	0	1	0
MS04559	F	23/06/2004	Halle	409	Right	Manible	Molar	PD_SEEN	1	-4	OHL PQ00888	33.911	1.2	29.509	13.934	2	355	1	0	1
MS04559	F	23/06/2004	Halle	409	Right	Manible	Molar	PD_SEEN	1	-4	OHL PQ00888	34.234	0.9	32.744	1.686	3	355	1	0	1
MS04559	F	23/06/2004	Halle	309	Left	Manible	Molar	NO_PD	1	-4	OHL PQ00896	1.0	24.407	389.313	1	355	0	0	1	1
MS04559	F	23/06/2004	Halle	309	Left	Manible	Molar	NO_PD	1	-4	OHL PQ00896	1.0	24.730	315.190	2	355	0	0	1	1
MS04559	F	23/06/2004	Halle	309	Left	Manible	Molar	NO_PD	1	-4	OHL PQ00896	1.0	24.096	476.753	3	355	0	0	1	1
MS05116	M	08/05/2009	Yankee	108	Right	Maxilla	Premolar	PD_SEEN	26	-4	OHL PQ00948	31.768	4.5	30.660	6.574	1	101	1	1	1
MS05116	M	08/05/2009	Yankee	108	Right	Maxilla	Premolar	PD_SEEN	26	-4	OHL PQ00948	1.0	30.394	7.818	2	101	0	0	1	1
MS05116	M	08/05/2009	Yankee	108	Right	Maxilla	Premolar	PD_SEEN	26	-4	OHL PQ00948	1.0	33.048	1.383	3	101	0	0	1	0
MS05116	M	08/05/2009	Yankee	208	Left	Maxilla	Premolar	NO_PD	26	-4	OHL PQ00956	34.537	0.8	27.008	71.261	1	101	1	0	1
MS05116	M	08/05/2009	Yankee	208	Left	Maxilla	Premolar	NO_PD	26	-4	OHL PQ00956	1.0	27.404	55.044	2	101	0	0	1	1
MS05116	M	08/05/2009	Yankee	208	Left	Maxilla	Premolar	NO_PD	26	-4	OHL PQ00956	1.0	27.554	49.898	3	101	0	0	1	1
MS05120	F	08/05/2009	Yetti	103	Right	Maxilla	Incisor	PD_SEEN	28	-3	OHL PQ00961	1.0	34.301	0.610	1	101	0	0	1	0
MS05120	F	08/05/2009	Yetti	103	Right	Maxilla	Incisor	PD_SEEN	28	-3	OHL PQ00961	29.702	17.0	1.000	2	101	1	1	0	0
MS05120	F	08/05/2009	Yetti	103	Right	Maxilla	Incisor	PD_SEEN	28	-3	OHL PQ00961	35.525	0.4	34.780	0.446	3	101	1	0	1
MS05120	F	08/05/2009	Yetti	203	Left	Maxilla	Incisor	NO_PD	28	-3	OHL PQ00969	33.706	1.3	32.614	1.836	1	101	1	0	1
MS05120	F	08/05/2009	Yetti	203	Left	Maxilla	Incisor	NO_PD	28	-3	OHL PQ00969	1.0	32.712	1.722	2	101	0	0	1	0
MS05120	F	08/05/2009	Yetti	203	Left	Maxilla	Incisor	NO_PD	28	-3	OHL PQ00969	36.139	0.3	34.108	0.692	3	101	1	0	1
MS05108	F	08/02/2009	Whoopee	109	Right	Maxilla	Molar	NO_PD	21	-4	OHL PQ00981	33.328	1.7	31.537	3.708	1	114	1	0	1
MS05108	F	08/02/2009	Whoopee	109	Right	Maxilla	Molar	NO_PD	21	-4	OHL PQ00981	1.0	30.312	8.248	2	114	0	0	1	1
MS05108	F	08/02/2009	Whoopee	109	Right	Maxilla	Molar	NO_PD	21	-4	OHL PQ00981	35.677	0.4	31.903	2.921	3	114	1	0	1
MS05108	F	08/02/2009	Whoopee	209	Left	Maxilla	Molar	PD_SEEN	21	-4	OHL PQ00989	1.0	29.148	17.628	1	114	0	0	1	1
MS05108	F	08/02/2009	Whoopee	209	Left	Maxilla	Molar	PD_SEEN	21	-4	OHL PQ00989	1.0	33.319	1.159	2	114	0	0	1	0
MS05108	F	08/02/2009	Whoopee	209	Left	Maxilla	Molar	PD_SEEN	21	-4	OHL PQ00989	33.805	1.2	29.297	16.000	3	114	1	0	1
MS04712	M	10/05/2006	Elton	108	Right	Maxilla	Premolar	PD_SEEN	51	-2	OHL PQ01012	27.664	62.5	25.523	187.835	1	257	1	1	1
MS04712	M	10/05/2006	Elton	108	Right	Maxilla	Premolar	PD_SEEN	51	-2	OHL PQ01012	26.934	99.7	25.651	172.811	2	257	1	1	1
MS04712	M	10/05/2006	Elton	108	Right	Maxilla	Premolar	PD_SEEN	51	-2	OHL PQ01012	27.053	92.4	26.545	96.415	3	257	1	1	1
MS04929	M	05/01/2008	Norris	404	Right	Manible	Canine	NO_PD	12	-2	OHL PQ01030	34.425	0.8	33.598	0.966	1	171	1	0	1
MS04929	M	05/01/2008	Norris	404	Right	Manible	Canine	NO_PD	12	-2	OHL PQ01030	1.0	35.400	0.298	2	171	0	0	1	0
MS04929	M	05/01/2008	Norris	404	Right	Manible	Canine	NO_PD	12	-2	OHL PQ01030	35.443	0.4	35.035	0.378	3	171	1	0	1
MS05107	F	08/02/2009	Willow	408	Right	Manible	Premolar	NO_PD	61	-3	OHL PQ01047	28.518	36.2	27.025	70.493	1	114	1	1	1
MS05107	F	08/02/2009	Willow	408	Right	Manible	Premolar	NO_PD	61	-3	OHL PQ01047	29.150	24.2	27.494	51.904	2	114	1	1	1
MS05107	F	08/02/2009	Willow	408	Right	Manible	Premolar	NO_PD	61	-3	OHL PQ01047	28.662	33.0	28.623	24.836	3	114	1	1	1
MS05107	F	08/02/2009	Willow	208	Left	Maxilla	Premolar	PD_SEEN	61	-3	OHL PQ01052	28.185	44.8	31.498	3.803	1	114	1	1	0
MS05107	F	08/02/2009	Willow	208	Left	Maxilla	Premolar	PD_SEEN	61	-3	OHL PQ01052	28.363	40.0	29.179	17.277	2	114	1	1	1
MS05107	F	08/02/2009	Willow	208	Left	Maxilla	Premolar	PD_SEEN	61	-3	OHL PQ01052	28.324	41.0	30.688	6.453	3	114	1	1	1
MS05115	F	08/05/2009	Yoyo	103	Right	Maxilla	Incisor	NO_PD	25	-4	OHL PQ01073	34.695	0.7	1.000	1	101	1	0	0	0
MS05115	F	08/05/2009	Yoyo	103	Right	Maxilla	Incisor	NO_PD	25	-4	OHL PQ01073	35.918	0.3	33.353	1.133	2	101	1	0	1
MS05115	F	08/05/2009	Yoyo	103	Right	Maxilla	Incisor	NO_PD	25	-4	OHL PQ01073	36.043	0.3	31.920	2.888	3	101	1	0	1
MS05115	F	08/05/2009	Yoyo	203	Left	Maxilla	Incisor	PD_SEEN	25	-4	OHL PQ01081	25.801	205.8	1.000	1	101	1	1	0	0
MS05115	F	08/05/2009	Yoyo	203	Left	Maxilla	Incisor	PD_SEEN	25	-4	OHL PQ01081	26.018	179.0	1.000	2	101	1	1	0	0
MS05115	F	08/05/2009	Yoyo	203	Left	Maxilla	Incisor	PD_SEEN	25	-4	OHL PQ01081	25.527	245.0	33.536	1.006	3	101	1	1	1
MS05031	F	26/01/2009	Violet	308	Left	Manible	Premolar	PD_SEEN	18	-5	OHL PQ01163	33.176	1.8	26.616	92.036	1	116	1	0	1

MS05031	F	26/01/2009	Violet	308	Left	Manible	Premolar	PD_SEEN	18	-5	OHL PQ01163	36.241	0.3	27.474	52.579	2	116	1	0	1	1
MS05031	F	26/01/2009	Violet	308	Left	Manible	Premolar	PD_SEEN	18	-5	OHL PQ01163	34.031	1.1	27.599	48.463	3	116	1	0	1	1
MS05114	F	08/05/2009	Yasmine	207	Left	Maxilla	Premolar	NO_PD	63	-5	OHL PQ01208	32.712	2.5	29.571	13.377	1	101	1	0	1	1
MS05114	F	08/05/2009	Yasmine	207	Left	Maxilla	Premolar	NO_PD	63	-5	OHL PQ01208		1.0	29.763	11.804	2	101	0	0	1	1
MS05114	F	08/05/2009	Yasmine	207	Left	Maxilla	Premolar	NO_PD	63	-5	OHL PQ01208	34.288	0.9	28.685	23.858	3	101	1	0	1	1
MS05114	F	08/05/2009	Yasmine	308	Left	Manible	Premolar	PD_SEEN	63	-5	OHL PQ01211	33.456	1.5	30.824	5.906	1	101	1	0	1	1
MS05114	F	08/05/2009	Yasmine	308	Left	Manible	Premolar	PD_SEEN	63	-5	OHL PQ01211	31.323	6.0	27.775	43.209	2	101	1	1	1	1
MS05114	F	08/05/2009	Yasmine	308	Left	Manible	Premolar	PD_SEEN	63	-5	OHL PQ01211		1.0	29.709	12.225	3	101	0	0	1	1
MS05114	F	08/05/2009	Yasmine	209	Left	Maxilla	Molar	NO_PD	64	-5	OHL PQ01214		1.0	29.819	11.377	1	101	0	0	1	1
MS05114	F	08/05/2009	Yasmine	209	Left	Maxilla	Molar	NO_PD	64	-5	OHL PQ01214	34.244	0.9	34.643	0.488	2	101	1	0	1	0
MS05114	F	08/05/2009	Yasmine	209	Left	Maxilla	Molar	NO_PD	64	-5	OHL PQ01214	31.495	5.4	29.719	12.146	3	101	1	1	1	1
MS05114	F	08/05/2009	Yasmine	309	Left	Manible	Molar	PD_SEEN	64	-5	OHL PQ01215		1.0		1.000	1	101	0	0	0	0
MS05114	F	08/05/2009	Yasmine	309	Left	Manible	Molar	PD_SEEN	64	-5	OHL PQ01215	26.933	99.7	34.127	0.684	2	101	1	1	1	0
MS05114	F	08/05/2009	Yasmine	309	Left	Manible	Molar	PD_SEEN	64	-5	OHL PQ01215	34.518	0.8	32.505	1.971	3	101	1	0	1	0
MS05152	M	03/12/2010	Bentley	108	Right	Maxilla	Premolar	NO_PD	33	-3	OHL PQ01241	33.379	1.6	28.434	28.092	1	19	1	0	1	1
MS05152	M	03/12/2010	Bentley	108	Right	Maxilla	Premolar	NO_PD	33	-3	OHL PQ01241		1.0	29.815	11.412	2	19	0	0	1	1
MS05152	M	03/12/2010	Bentley	108	Right	Maxilla	Premolar	NO_PD	33	-3	OHL PQ01241		1.0	27.446	53.570	3	19	0	0	1	1
MS05152	M	03/12/2010	Bentley	208	Left	Maxilla	Premolar	PD_SEEN	33	-3	OHL PQ01242		1.0	29.310	15.860	1	19	0	0	1	1
MS05152	M	03/12/2010	Bentley	208	Left	Maxilla	Premolar	PD_SEEN	33	-3	OHL PQ01242	35.353	0.5	29.394	15.013	2	19	1	0	1	1
MS05152	M	03/12/2010	Bentley	208	Left	Maxilla	Premolar	PD_SEEN	33	-3	OHL PQ01242		1.0	27.908	39.621	3	19	0	0	1	1
MS05151	F	03/12/2010	Bramble	208	Left	Maxilla	Premolar	NO_PD	69	-5	OHL PQ01258		1.0	28.706	23.536	1	19	0	0	1	1
MS05151	F	03/12/2010	Bramble	208	Left	Maxilla	Premolar	NO_PD	69	-5	OHL PQ01258	31.161	6.7	29.711	12.212	2	19	1	1	1	1
MS05151	F	03/12/2010	Bramble	208	Left	Maxilla	Premolar	NO_PD	69	-5	OHL PQ01258		1.0	28.072	35.599	3	19	0	0	1	1
MS05151	F	03/12/2010	Bramble	408	Right	Manible	Premolar	PD_SEEN	69	-5	OHL PQ01260	29.476	19.6	33.886	0.800	1	19	1	1	1	0
MS05151	F	03/12/2010	Bramble	408	Right	Manible	Premolar	PD_SEEN	69	-5	OHL PQ01260	28.216	43.9	29.798	11.535	2	19	1	1	1	1
MS05151	F	03/12/2010	Bramble	408	Right	Manible	Premolar	PD_SEEN	69	-5	OHL PQ01260	30.660	9.2	29.651	12.698	3	19	1	1	1	1
MS05158	F	15/01/2010	Connie	309	Left	Manible	Molar	PD_SEEN	37	-3	OHL PQ01311		1.0	28.168	33.426	1	65	0	0	1	1
MS05158	F	15/01/2010	Connie	309	Left	Manible	Molar	PD_SEEN	37	-3	OHL PQ01311		1.0	26.870	78.016	2	65	0	0	1	1
MS05158	F	15/01/2010	Connie	309	Left	Manible	Molar	PD_SEEN	37	-3	OHL PQ01311		1.0	28.330	30.069	3	65	0	0	1	1
MS05158	F	15/01/2010	Connie	409	Right	Manible	Molar	NO_PD	37	-3	OHL PQ01312	33.595	1.4	25.258	223.380	1	65	1	0	1	1
MS05158	F	15/01/2010	Connie	409	Right	Manible	Molar	NO_PD	37	-3	OHL PQ01312	31.511	5.3	25.747	162.327	2	65	1	1	1	1
MS05158	F	15/01/2010	Connie	409	Right	Manible	Molar	NO_PD	37	-3	OHL PQ01312		1.0	24.714	318.527	3	65	0	0	1	1
MS04923	F	05/01/2008	Nettie	107	Right	Maxilla	Premolar	NO_PD	59	-2	OHL PQ01383	23.886	699.5		1.000	1	171	1	1	0	0
MS04923	F	05/01/2008	Nettie	107	Right	Maxilla	Premolar	NO_PD	59	-2	OHL PQ01383	23.545	870.0		1.000	2	171	1	1	0	0
MS04923	F	05/01/2008	Nettie	107	Right	Maxilla	Premolar	NO_PD	59	-2	OHL PQ01383	23.762	757.5		1.000	3	171	1	1	0	0
MS04923	F	05/01/2008	Nettie	108	Right	Maxilla	Premolar	NO_PD	9	-3	OHL PQ01385	23.934	678.7	34.440	0.557	1	171	1	1	1	0
MS04923	F	05/01/2008	Nettie	108	Right	Maxilla	Premolar	NO_PD	9	-3	OHL PQ01385	24.044	632.7	30.180	8.993	2	171	1	1	1	1
MS04923	F	05/01/2008	Nettie	108	Right	Maxilla	Premolar	NO_PD	9	-3	OHL PQ01385	23.939	676.3		1.000	3	171	1	1	0	0
MS04923	F	05/01/2008	Nettie	208	Left	Maxilla	Premolar	PD_SEEN	9	-3	OHL PQ01386	25.789	207.2	34.420	0.565	1	171	1	1	1	0
MS04923	F	05/01/2008	Nettie	208	Left	Maxilla	Premolar	PD_SEEN	9	-3	OHL PQ01386	25.914	191.4	33.594	0.968	2	171	1	1	1	0
MS04923	F	05/01/2008	Nettie	208	Left	Maxilla	Premolar	PD_SEEN	9	-3	OHL PQ01386	25.667	224.0	32.625	1.823	3	171	1	1	1	0
MS04923	F	05/01/2008	Nettie	308	Left	Manible	Premolar	PD_SEEN	59	-2	OHL PQ01387	25.003	342.5	25.843	152.448	1	171	1	1	1	1
MS04923	F	05/01/2008	Nettie	308	Left	Manible	Premolar	PD_SEEN	59	-2	OHL PQ01387	24.616	438.8	25.777	159.135	2	171	1	1	1	1
MS04923	F	05/01/2008	Nettie	308	Left	Manible	Premolar	PD_SEEN	59	-2	OHL PQ01387	25.316	280.5	25.428	199.877	3	171	1	1	1	1
MS05109	M	08/02/2009	Wellington	409	Right	Manible	Molar	NO_PD	22	-3	OHL PQ01400		1.0	29.194	17.114	1	114	0	0	1	1
MS05109	M	08/02/2009	Wellington	409	Right	Manible	Molar	NO_PD	22	-3	OHL PQ01400		1.0	29.416	14.805	2	114	0	0	1	1
MS05109	M	08/02/2009	Wellington	409	Right	Manible	Molar	NO_PD	22	-3	OHL PQ01400		1.0	30.186	8.953	3	114	0	0	1	1
MS05109	M	08/02/2009	Wellington	309	Left	Manible	Molar	PD_SEEN	22	-3	OHL PQ01408	31.065	7.1	27.401	55.167	1	114	1	1	1	1
MS05109	M	08/02/2009	Wellington	309	Left	Manible	Molar	PD_SEEN	22	-3	OHL PQ01408	31.756	4.6	27.470	52.720	2	114	1	1	1	1
MS05109	M	08/02/2009	Wellington	309	Left	Manible	Molar	PD_SEEN	22	-3	OHL PQ01408	34.560	0.8	28.860	21.286	3	114	1	0	1	1
MS05118	M	08/05/2009	Yoshi	408	Right	Manible	Premolar	NO_PD	27	-3	OHL PQ01431	24.009	647.0	29.040	18.925	1	101	1	1	1	1
MS05118	M	08/05/2009	Yoshi	408	Right	Manible	Premolar	NO_PD	27	-3	OHL PQ01431	23.958	668.3	28.876	21.062	2	101	1	1	1	1
MS05118	M	08/05/2009	Yoshi	408	Right	Manible	Premolar	NO_PD	27	-3	OHL PQ01431	29.257	22.6	26.735	85.174	3	101	1	1	1	1
MS05118	M	08/05/2009	Yoshi	308	Left	Manible	Premolar	PD_SEEN	27	-3	OHL PQ01439	23.871	706.5	28.888	20.889	1	101	1	1	1	1

MS05118	M	08/05/2009	Yoshi	308	Left	Manible	Premolar	PD_SEEN	27	-3	OHLPQ01439	24.926	359.9	28.067	35.700	2	101	1	1	1	1
MS05118	M	08/05/2009	Yoshi	308	Left	Manible	Premolar	PD_SEEN	27	-3	OHLPQ01439	24.144	593.3	28.943	20.154	3	101	1	1	1	1
MS04563	F	23/06/2004	China	308	Left	Manible	Premolar	NO_PD	42	-2	OHLPQ01487	28.306	41.5	29.701	12.292	1	355	1	1	1	1
MS04563	F	23/06/2004	China	308	Left	Manible	Premolar	NO_PD	42	-2	OHLPQ01487	28.901	28.3	28.861	21.268	2	355	1	1	1	1
MS04563	F	23/06/2004	China	308	Left	Manible	Premolar	NO_PD	42	-2	OHLPQ01487	23.583	849.0	29.435	14.618	3	355	1	1	1	1
MS04599	M	09/04/2004	Rooney	108	Right	Maxilla	Premolar	PD_SEEN	6	-3	OHLPQ01492	30.198	12.4	27.263	60.364	1	366	1	1	1	1
MS04599	M	09/04/2004	Rooney	108	Right	Maxilla	Premolar	PD_SEEN	6	-3	OHLPQ01492	28.174	45.1		1.000	2	366	1	1	0	0
MS04599	M	09/04/2004	Rooney	108	Right	Maxilla	Premolar	PD_SEEN	6	-3	OHLPQ01492		1.0	32.612	1.838	3	366	0	0	1	0
MS04599	M	09/04/2004	Rooney	208	Left	Maxilla	Premolar	NO_PD	6	-3	OHLPQ01500	33.344	1.7		1.000	1	366	1	0	0	0
MS04599	M	09/04/2004	Rooney	208	Left	Maxilla	Premolar	NO_PD	6	-3	OHLPQ01500	34.663	0.7	33.891	0.797	2	366	1	0	1	0
MS04599	M	09/04/2004	Rooney	208	Left	Maxilla	Premolar	NO_PD	6	-3	OHLPQ01500	34.259	0.9	33.579	0.978	3	366	1	0	1	0
MS04595	M	09/04/2004	Dallas	108	Right	Maxilla	Premolar	NO_PD	5	-3	OHLPQ01508	34.036	1.1	22.914	1031.198	1	366	1	0	1	1
MS04595	M	09/04/2004	Dallas	108	Right	Maxilla	Premolar	NO_PD	5	-3	OHLPQ01508		1.0	22.919	1028.017	2	366	0	0	1	1
MS04595	M	09/04/2004	Dallas	108	Right	Maxilla	Premolar	NO_PD	5	-3	OHLPQ01508	28.748	31.3	22.731	1162.545	3	366	1	1	1	1
MS04595	M	09/04/2004	Dallas	208	Left	Maxilla	Premolar	PD_SEEN	5	-3	OHLPQ01516	35.972	0.3	25.385	205.630	1	366	1	0	1	1
MS04595	M	09/04/2004	Dallas	208	Left	Maxilla	Premolar	PD_SEEN	5	-3	OHLPQ01516	35.548	0.4	25.381	206.129	2	366	1	0	1	1
MS04595	M	09/04/2004	Dallas	208	Left	Maxilla	Premolar	PD_SEEN	5	-3	OHLPQ01516	32.756	2.4	26.463	101.721	3	366	1	0	1	1
MS04648	M	10/12/2005	Winston	408	Right	Manible	Premolar	PD_SEEN	48	-3	OHLPQ01543	31.108	6.9	23.907	539.450	1	279	1	1	1	1
MS04648	M	10/12/2005	Winston	408	Right	Manible	Premolar	PD_SEEN	48	-3	OHLPQ01543	33.048	2.0	23.635	644.308	2	279	1	0	1	1
MS04648	M	10/12/2005	Winston	408	Right	Manible	Premolar	PD_SEEN	48	-3	OHLPQ01543		1.0	23.532	689.078	3	279	0	0	1	1
MS04648	M	10/12/2005	Winston	207	Left	Maxilla	Premolar	NO_PD	48	-3	OHLPQ01547	31.770	4.5		1.000	1	279	1	1	0	0
MS04648	M	10/12/2005	Winston	207	Left	Maxilla	Premolar	NO_PD	48	-3	OHLPQ01547	33.796	1.2	31.653	3.436	2	279	1	0	1	0
MS04648	M	10/12/2005	Winston	207	Left	Maxilla	Premolar	NO_PD	48	-3	OHLPQ01547	34.533	0.8		1.000	3	279	1	0	0	0
MS04645	F	10/12/2005	Mimi	209	Left	Maxilla	Molar	NO_PD	47	-2	OHLPQ01557	35.575	0.4	28.689	23.786	1	279	1	0	1	1
MS04645	F	10/12/2005	Mimi	209	Left	Maxilla	Molar	NO_PD	47	-2	OHLPQ01557	32.490	2.9	29.539	13.664	2	279	1	0	1	1
MS04645	F	10/12/2005	Mimi	209	Left	Maxilla	Molar	NO_PD	47	-2	OHLPQ01557	34.637	0.7	30.227	8.720	3	279	1	0	1	1
MS04645	F	10/12/2005	Mimi	409	Right	Manible	Molar	PD_SEEN	47	-2	OHLPQ01560	30.670	9.1	26.838	79.846	1	279	1	1	1	1
MS04645	F	10/12/2005	Mimi	409	Right	Manible	Molar	PD_SEEN	47	-2	OHLPQ01560	31.379	5.8	29.142	17.701	2	279	1	1	1	1
MS04645	F	10/12/2005	Mimi	409	Right	Manible	Molar	PD_SEEN	47	-2	OHLPQ01560	30.744	8.7	30.190	8.932	3	279	1	1	1	1
MS04643	F	10/12/2005	Faith	108	Right	Maxilla	Premolar	NO_PD	46	-2	OHLPQ01604	33.925	1.1	27.663	46.473	1	279	1	0	1	1
MS04643	F	10/12/2005	Faith	108	Right	Maxilla	Premolar	NO_PD	46	-2	OHLPQ01604	35.672	0.4	29.129	17.853	2	279	1	0	1	1
MS04643	F	10/12/2005	Faith	108	Right	Maxilla	Premolar	NO_PD	46	-2	OHLPQ01604		1.0	27.992	37.492	3	279	0	0	1	1
MS04643	F	10/12/2005	Faith	408	Right	Manible	Premolar	PD_SEEN	46	-2	OHLPQ01607	31.607	5.0	25.441	198.155	1	279	1	1	1	1
MS04643	F	10/12/2005	Faith	408	Right	Manible	Premolar	PD_SEEN	46	-2	OHLPQ01607		1.0	26.263	115.900	2	279	0	0	1	1
MS04643	F	10/12/2005	Faith	408	Right	Manible	Premolar	PD_SEEN	46	-2	OHLPQ01607	30.648	9.3	26.482	100.485	3	279	1	1	1	1
MS04643	F	10/12/2005	Faith	207	Left	Maxilla	Premolar	NO_PD	45	-2	OHLPQ01611		1.0	30.941	5.470	1	279	0	0	1	1
MS04643	F	10/12/2005	Faith	207	Left	Maxilla	Premolar	NO_PD	45	-2	OHLPQ01611		1.0	32.644	1.800	2	279	0	0	1	0
MS04643	F	10/12/2005	Faith	207	Left	Maxilla	Premolar	NO_PD	45	-2	OHLPQ01611		1.0	33.755	0.872	3	279	0	0	1	0
MS04714	M	10/05/2006	Eddie	409	Right	Manible	Molar	PD_SEEN	55	-4	OHLPQ01624	31.864	4.3	25.745	162.497	1	257	1	1	1	1
MS04714	M	10/05/2006	Eddie	409	Right	Manible	Molar	PD_SEEN	55	-4	OHLPQ01624	31.946	4.0	25.947	142.437	2	257	1	1	1	1
MS04714	M	10/05/2006	Eddie	409	Right	Manible	Molar	PD_SEEN	55	-4	OHLPQ01624		1.0	25.861	150.679	3	257	0	0	1	1
MS04714	M	10/05/2006	Eddie	209	Left	Maxilla	Molar	NO_PD	55	-4	OHLPQ01629	34.287	0.9	25.917	145.269	1	257	1	0	1	1
MS04714	M	10/05/2006	Eddie	209	Left	Maxilla	Molar	NO_PD	55	-4	OHLPQ01629	33.909	1.2	26.274	115.050	2	257	1	0	1	1
MS04714	M	10/05/2006	Eddie	209	Left	Maxilla	Molar	NO_PD	55	-4	OHLPQ01629		1.0	26.324	111.395	3	257	0	0	1	1
MS04715	F	10/05/2006	Edna	309	Left	Manible	Molar	PD_SEEN	56	-3	OHLPQ01648	28.655	33.2	25.709	166.428	1	257	1	1	1	1
MS04715	F	10/05/2006	Edna	309	Left	Manible	Molar	PD_SEEN	56	-3	OHLPQ01648	27.799	57.3	26.292	113.708	2	257	1	1	1	1
MS04715	F	10/05/2006	Edna	309	Left	Manible	Molar	PD_SEEN	56	-3	OHLPQ01648	33.245	1.8	25.941	143.011	3	257	1	0	1	1
MS04846	M	13/09/2007	Jigsaw	109	Right	Maxilla	Molar	NO_PD	8	-3	OHLPQ01685	32.468	2.9	27.363	56.533	1	187	1	0	1	1
MS04846	M	13/09/2007	Jigsaw	109	Right	Maxilla	Molar	NO_PD	8	-3	OHLPQ01685		1.0	28.740	23.007	2	187	0	0	1	1
MS04846	M	13/09/2007	Jigsaw	109	Right	Maxilla	Molar	NO_PD	8	-3	OHLPQ01685		1.0	27.926	39.160	3	187	0	0	1	1
MS04846	M	13/09/2007	Jigsaw	408	Right	Manible	Premolar	PD_SEEN	58	-2	OHLPQ01687		1.0	28.355	29.583	1	187	0	0	1	1
MS04846	M	13/09/2007	Jigsaw	408	Right	Manible	Premolar	PD_SEEN	58	-2	OHLPQ01687	34.539	0.8	27.412	54.755	2	187	1	0	1	1
MS04846	M	13/09/2007	Jigsaw	408	Right	Manible	Premolar	PD_SEEN	58	-2	OHLPQ01687		1.0	27.436	53.920	3	187	0	0	1	1
MS04846	M	13/09/2007	Jigsaw	207	Left	Maxilla	Premolar	NO_PD	58	-2	OHLPQ01691		1.0		1.000	1	187	0	0	0	0

MS04846	M	13/09/2007	Jigsaw	207	Left	Maxilla	Premolar	NO_PD	58	-2	OHLPQ01691	30.140	12.8	1.000	2	187	1	1	0	
MS04846	M	13/09/2007	Jigsaw	207	Left	Maxilla	Premolar	NO_PD	58	-2	OHLPQ01691	30.399	10.9	30.394	7.818	3	187	1	1	1
MS04846	M	13/09/2007	Jigsaw	209	Left	Maxilla	Molar	PD_SEEN	8	-3	OHLPQ01693		1.0	25.403	203.232	1	187	0	0	1
MS04846	M	13/09/2007	Jigsaw	209	Left	Maxilla	Molar	PD_SEEN	8	-3	OHLPQ01693	35.246	0.5	25.305	216.566	2	187	1	0	1
MS04846	M	13/09/2007	Jigsaw	209	Left	Maxilla	Molar	PD_SEEN	8	-3	OHLPQ01693		1.0	25.656	172.260	3	187	0	0	1
MS04561	M	23/06/2004	Arnie	107	Right	Maxilla	Premolar	PD_SEEN	40	-3	OHLPQ01715	25.847	199.7	30.079	9.605	1	355	1	1	1
MS04561	M	23/06/2004	Arnie	107	Right	Maxilla	Premolar	PD_SEEN	40	-3	OHLPQ01715	25.950	187.0		1.000	2	355	1	1	0
MS04561	M	23/06/2004	Arnie	107	Right	Maxilla	Premolar	PD_SEEN	40	-3	OHLPQ01715	25.777	208.8	32.226	2.364	3	355	1	1	1
MS04561	M	23/06/2004	Arnie	203	Left	Maxilla	Incisor	PD_SEEN	2	-2	OHLPQ01721		1.0	33.161	1.284	1	355	0	0	1
MS04561	M	23/06/2004	Arnie	203	Left	Maxilla	Incisor	PD_SEEN	2	-2	OHLPQ01721	33.663	1.3		1.000	2	355	1	0	0
MS04561	M	23/06/2004	Arnie	203	Left	Maxilla	Incisor	PD_SEEN	2	-2	OHLPQ01721	34.296	0.9	31.996	2.748	3	355	1	0	1
MS04561	M	23/06/2004	Arnie	208	Left	Maxilla	Premolar	NO_PD	40	-3	OHLPQ01724	24.880	370.6	30.650	6.613	1	355	1	1	1
MS04561	M	23/06/2004	Arnie	208	Left	Maxilla	Premolar	NO_PD	40	-3	OHLPQ01724	24.783	394.4	29.763	11.800	2	355	1	1	1
MS04561	M	23/06/2004	Arnie	208	Left	Maxilla	Premolar	NO_PD	40	-3	OHLPQ01724	25.249	292.7	33.524	1.014	3	355	1	1	0
MS04559	F	23/06/2004	Halle	409	Right	Manible	Molar	PD_SEEN	1	-3	OHLPQ01736		1.0	26.751	84.306	1	355	0	0	1
MS04559	F	23/06/2004	Halle	409	Right	Manible	Molar	PD_SEEN	1	-3	OHLPQ01736		1.0	27.338	57.480	2	355	0	0	1
MS04559	F	23/06/2004	Halle	409	Right	Manible	Molar	PD_SEEN	1	-3	OHLPQ01736	32.380	3.1	26.709	86.636	3	355	1	0	1
MS04559	F	23/06/2004	Halle	309	Left	Manible	Molar	NO_PD	1	-3	OHLPQ01744	35.304	0.5	28.420	28.352	1	355	1	0	1
MS04559	F	23/06/2004	Halle	309	Left	Manible	Molar	NO_PD	1	-3	OHLPQ01744		1.0	27.018	70.823	2	355	0	0	1
MS04559	F	23/06/2004	Halle	309	Left	Manible	Molar	NO_PD	1	-3	OHLPQ01744		1.0	27.118	66.349	3	355	0	0	1
MS05116	M	08/05/2009	Yankee	108	Right	Maxilla	Premolar	PD_SEEN	26	-3	OHLPQ01796		1.0	30.821	5.916	1	101	0	0	1
MS05116	M	08/05/2009	Yankee	108	Right	Maxilla	Premolar	PD_SEEN	26	-3	OHLPQ01796	34.241	0.9		1.000	2	101	1	0	0
MS05116	M	08/05/2009	Yankee	108	Right	Maxilla	Premolar	PD_SEEN	26	-3	OHLPQ01796		1.0		1.000	3	101	0	0	0
MS05116	M	08/05/2009	Yankee	208	Left	Maxilla	Premolar	NO_PD	26	-3	OHLPQ01804		1.0	29.023	19.131	1	101	0	0	1
MS05116	M	08/05/2009	Yankee	208	Left	Maxilla	Premolar	NO_PD	26	-3	OHLPQ01804	37.366	0.1	27.432	54.046	2	101	1	0	1
MS05116	M	08/05/2009	Yankee	208	Left	Maxilla	Premolar	NO_PD	26	-3	OHLPQ01804		1.0	28.774	22.511	3	101	0	0	1
MS05120	F	08/05/2009	Yetti	103	Right	Maxilla	Incisor	PD_SEEN	28	-2	OHLPQ01809	33.335	1.7	30.350	8.046	1	101	1	0	1
MS05120	F	08/05/2009	Yetti	103	Right	Maxilla	Incisor	PD_SEEN	28	-2	OHLPQ01809		1.0	30.919	5.551	2	101	0	0	1
MS05120	F	08/05/2009	Yetti	103	Right	Maxilla	Incisor	PD_SEEN	28	-2	OHLPQ01809		1.0		1.000	3	101	0	0	0
MS05108	F	08/02/2009	Whoopee	109	Right	Maxilla	Molar	NO_PD	21	-3	OHLPQ01829	32.636	2.6	29.856	11.109	1	114	1	0	1
MS05108	F	08/02/2009	Whoopee	109	Right	Maxilla	Molar	NO_PD	21	-3	OHLPQ01829	35.013	0.6	29.449	14.484	2	114	1	0	1
MS05108	F	08/02/2009	Whoopee	109	Right	Maxilla	Molar	NO_PD	21	-3	OHLPQ01829	34.629	0.7	34.627	0.493	3	114	1	0	0
MS05108	F	08/02/2009	Whoopee	209	Left	Maxilla	Molar	PD_SEEN	21	-3	OHLPQ01837		1.0	32.252	2.325	1	114	0	0	1
MS05108	F	08/02/2009	Whoopee	209	Left	Maxilla	Molar	PD_SEEN	21	-3	OHLPQ01837	35.120	0.5	28.050	36.104	2	114	1	0	1
MS05108	F	08/02/2009	Whoopee	209	Left	Maxilla	Molar	PD_SEEN	21	-3	OHLPQ01837		1.0	29.514	13.885	3	114	0	0	1
MS04712	M	10/05/2006	Elton	107	Right	Maxilla	Premolar	NO_PD	51	-1	OHLPQ01859	28.342	40.5	31.838	3.047	1	257	1	1	0
MS04712	M	10/05/2006	Elton	107	Right	Maxilla	Premolar	NO_PD	51	-1	OHLPQ01859	27.517	68.7		1.000	2	257	1	1	0
MS04712	M	10/05/2006	Elton	107	Right	Maxilla	Premolar	NO_PD	51	-1	OHLPQ01859	29.217	23.2	32.918	1.505	3	257	1	1	0
MS04712	M	10/05/2006	Elton	108	Right	Maxilla	Premolar	PD_SEEN	51	-1	OHLPQ01860	24.928	359.5	26.252	116.760	1	257	1	1	1
MS04712	M	10/05/2006	Elton	108	Right	Maxilla	Premolar	PD_SEEN	51	-1	OHLPQ01860	24.994	344.6	26.573	94.684	2	257	1	1	1
MS04712	M	10/05/2006	Elton	108	Right	Maxilla	Premolar	PD_SEEN	51	-1	OHLPQ01860	24.193	575.0	26.333	110.711	3	257	1	1	1
MS05107	F	08/02/2009	Willow	408	Right	Manible	Premolar	NO_PD	61	-2	OHLPQ01895	22.728	1466.8	24.823	296.655	1	114	1	1	1
MS05107	F	08/02/2009	Willow	408	Right	Manible	Premolar	NO_PD	61	-2	OHLPQ01895	23.275	1033.9	24.777	305.797	2	114	1	1	1
MS05107	F	08/02/2009	Willow	408	Right	Manible	Premolar	NO_PD	61	-2	OHLPQ01895	22.571	1622.5	25.884	148.485	3	114	1	1	1
MS05107	F	08/02/2009	Willow	208	Left	Maxilla	Premolar	PD_SEEN	61	-2	OHLPQ01900	24.496	473.9	25.504	190.287	1	114	1	1	1
MS05107	F	08/02/2009	Willow	208	Left	Maxilla	Premolar	PD_SEEN	61	-2	OHLPQ01900	24.883	369.9	26.290	113.870	2	114	1	1	1
MS05107	F	08/02/2009	Willow	208	Left	Maxilla	Premolar	PD_SEEN	61	-2	OHLPQ01900	24.695	417.1	25.608	177.712	3	114	1	1	1
MS05115	F	08/05/2009	Yoyo	103	Right	Maxilla	Incisor	NO_PD	25	-3	OHLPQ01921	26.893	102.4		1.000	1	101	1	1	0
MS05115	F	08/05/2009	Yoyo	103	Right	Maxilla	Incisor	NO_PD	25	-3	OHLPQ01921	25.555	240.7	32.533	1.935	2	101	1	1	0
MS05115	F	08/05/2009	Yoyo	103	Right	Maxilla	Incisor	NO_PD	25	-3	OHLPQ01921	25.838	200.9	31.487	3.831	3	101	1	1	0
MS05115	F	08/05/2009	Yoyo	203	Left	Maxilla	Incisor	PD_SEEN	25	-3	OHLPQ01929	21.598	3021.5	32.559	1.903	1	101	1	1	0
MS05115	F	08/05/2009	Yoyo	203	Left	Maxilla	Incisor	PD_SEEN	25	-3	OHLPQ01929	22.035	2285.5	31.351	4.188	2	101	1	1	1
MS05115	F	08/05/2009	Yoyo	203	Left	Maxilla	Incisor	PD_SEEN	25	-3	OHLPQ01929	21.870	2538.6	32.890	1.533	3	101	1	1	1
MS05031	F	26/01/2009	Violet	408	Right	Manible	Premolar	NO_PD	18	-4	OHLPQ02028		1.0	28.942	20.174	1	116	0	0	1

MS05031	F	26/01/2009	Violet	408	Right	Manible	Premolar	NO_PD	18	-4	OHL PQ02028		1.0	29.750	11.905	2	116	0	0	1	1
MS05031	F	26/01/2009	Violet	408	Right	Manible	Premolar	NO_PD	18	-4	OHL PQ02028	36.039	0.3	29.320	15.758	3	116	1	0	1	1
MS05114	F	08/05/2009	Yasmine	207	Left	Maxilla	Premolar	NO_PD	63	-4	OHL PQ02072	34.272	0.9	28.466	27.520	1	101	1	0	1	1
MS05114	F	08/05/2009	Yasmine	207	Left	Maxilla	Premolar	NO_PD	63	-4	OHL PQ02072	34.045	1.1	29.113	18.039	2	101	1	0	1	1
MS05114	F	08/05/2009	Yasmine	207	Left	Maxilla	Premolar	NO_PD	63	-4	OHL PQ02072	29.902	14.9	27.313	58.420	3	101	1	1	1	1
MS05114	F	08/05/2009	Yasmine	308	Left	Manible	Premolar	PD_SEEN	63	-4	OHL PQ02075		1.0	1.000	1	101	0	0	0	0	0
MS05114	F	08/05/2009	Yasmine	308	Left	Manible	Premolar	PD_SEEN	63	-4	OHL PQ02075	36.067	0.3	1.000	2	101	1	0	0	0	0
MS05114	F	08/05/2009	Yasmine	308	Left	Manible	Premolar	PD_SEEN	63	-4	OHL PQ02075	27.240	81.9	1.000	3	101	1	1	0	0	0
MS05114	F	08/05/2009	Yasmine	309	Left	Manible	Molar	PD_SEEN	64	-4	OHL PQ02079	34.613	0.7	25.664	171.366	1	101	1	0	1	1
MS05114	F	08/05/2009	Yasmine	309	Left	Manible	Molar	PD_SEEN	64	-4	OHL PQ02079		1.0	26.167	123.441	2	101	0	0	1	1
MS05114	F	08/05/2009	Yasmine	309	Left	Manible	Molar	PD_SEEN	64	-4	OHL PQ02079	36.332	0.2	25.473	194.145	3	101	1	0	1	1
MS05152	M	03/12/2010	Bentley	108	Right	Maxilla	Premolar	NO_PD	33	-2	OHL PQ02105	29.687	17.2	29.383	15.125	1	19	1	1	1	1
MS05152	M	03/12/2010	Bentley	108	Right	Maxilla	Premolar	NO_PD	33	-2	OHL PQ02105		1.0	1.000	2	19	0	0	0	0	0
MS05152	M	03/12/2010	Bentley	108	Right	Maxilla	Premolar	NO_PD	33	-2	OHL PQ02105		1.0	31.242	4.495	3	19	0	0	1	1
MS05152	M	03/12/2010	Bentley	208	Left	Maxilla	Premolar	PD_SEEN	33	-2	OHL PQ02106		1.0	30.778	6.086	1	19	0	0	1	1
MS05152	M	03/12/2010	Bentley	208	Left	Maxilla	Premolar	PD_SEEN	33	-2	OHL PQ02106		1.0	31.696	3.341	2	19	0	0	1	0
MS05152	M	03/12/2010	Bentley	208	Left	Maxilla	Premolar	PD_SEEN	33	-2	OHL PQ02106	28.984	26.9	31.733	3.262	3	19	1	1	1	0
MS05151	F	03/12/2010	Bramble	208	Left	Maxilla	Premolar	NO_PD	69	-4	OHL PQ02122	34.257	0.9	27.963	38.216	1	19	1	0	1	1
MS05151	F	03/12/2010	Bramble	208	Left	Maxilla	Premolar	NO_PD	69	-4	OHL PQ02122		1.0	27.304	58.749	2	19	0	0	1	1
MS05151	F	03/12/2010	Bramble	208	Left	Maxilla	Premolar	NO_PD	69	-4	OHL PQ02122	32.085	3.7	28.851	21.406	3	19	1	1	1	1
MS05151	F	03/12/2010	Bramble	408	Right	Manible	Premolar	PD_SEEN	69	-4	OHL PQ02124	32.571	2.7	26.464	101.639	1	19	1	0	1	1
MS05151	F	03/12/2010	Bramble	408	Right	Manible	Premolar	PD_SEEN	69	-4	OHL PQ02124	30.209	12.3	29.084	18.382	2	19	1	1	1	1
MS05151	F	03/12/2010	Bramble	408	Right	Manible	Premolar	PD_SEEN	69	-4	OHL PQ02124		1.0	28.462	27.595	3	19	0	0	1	1
MS05163	M	15/01/2010	Chesney	108	Right	Maxilla	Premolar	NO_PD	71	-5	OHL PQ02137	25.968	184.9	27.548	50.112	1	65	1	1	1	1
MS05163	M	15/01/2010	Chesney	108	Right	Maxilla	Premolar	NO_PD	71	-5	OHL PQ02137	25.843	200.3	29.376	15.196	2	65	1	1	1	1
MS05163	M	15/01/2010	Chesney	108	Right	Maxilla	Premolar	NO_PD	71	-5	OHL PQ02137	25.695	220.2	28.382	29.070	3	65	1	1	1	1
MS05158	F	15/01/2010	Connie	309	Left	Manible	Molar	PD_SEEN	37	-2	OHL PQ02175		1.0	33.728	0.887	1	65	0	0	1	0
MS05158	F	15/01/2010	Connie	309	Left	Manible	Molar	PD_SEEN	37	-2	OHL PQ02175	31.239	6.4	31.229	4.533	2	65	1	1	1	1
MS05158	F	15/01/2010	Connie	309	Left	Manible	Molar	PD_SEEN	37	-2	OHL PQ02175	35.121	0.5	33.993	0.746	3	65	1	0	1	0
MS05158	F	15/01/2010	Connie	409	Right	Manible	Molar	NO_PD	37	-2	OHL PQ02176	29.492	19.4	27.967	68.594	1	65	1	1	1	1
MS05158	F	15/01/2010	Connie	409	Right	Manible	Molar	NO_PD	37	-2	OHL PQ02176	34.082	1.0	25.445	197.665	2	65	1	0	1	1
MS05158	F	15/01/2010	Connie	409	Right	Manible	Molar	NO_PD	37	-2	OHL PQ02176		1.0	26.601	92.962	3	65	0	0	1	1
MS04923	F	05/01/2008	Nettie	107	Right	Maxilla	Premolar	NO_PD	59	-1	OHL PQ02247	27.792	57.6	34.225	0.641	1	171	1	1	1	0
MS04923	F	05/01/2008	Nettie	107	Right	Maxilla	Premolar	NO_PD	59	-1	OHL PQ02247	29.343	21.4	34.319	0.603	2	171	1	1	1	0
MS04923	F	05/01/2008	Nettie	107	Right	Maxilla	Premolar	NO_PD	59	-1	OHL PQ02247	29.541	18.8	34.337	0.596	3	171	1	1	1	0
MS04923	F	05/01/2008	Nettie	108	Right	Maxilla	Premolar	NO_PD	9	-2	OHL PQ02249	31.235	6.4	31.580	3.605	1	171	1	1	1	0
MS04923	F	05/01/2008	Nettie	108	Right	Maxilla	Premolar	NO_PD	9	-2	OHL PQ02249	28.677	32.7	32.338	2.198	2	171	1	1	1	0
MS04923	F	05/01/2008	Nettie	108	Right	Maxilla	Premolar	NO_PD	9	-2	OHL PQ02249	29.266	22.4	35.074	0.368	3	171	1	1	1	0
MS04923	F	05/01/2008	Nettie	208	Left	Maxilla	Premolar	PD_SEEN	9	-2	OHL PQ02250	25.823	202.9	26.211	119.878	1	171	1	1	1	1
MS04923	F	05/01/2008	Nettie	208	Left	Maxilla	Premolar	PD_SEEN	9	-2	OHL PQ02250	25.798	206.0	28.093	35.095	2	171	1	1	1	1
MS04923	F	05/01/2008	Nettie	208	Left	Maxilla	Premolar	PD_SEEN	9	-2	OHL PQ02250	25.262	290.4	27.718	44.849	3	171	1	1	1	1
MS04923	F	05/01/2008	Nettie	308	Left	Manible	Premolar	PD_SEEN	59	-1	OHL PQ02251	24.871	372.9	32.041	2.669	1	171	1	1	1	0
MS04923	F	05/01/2008	Nettie	308	Left	Manible	Premolar	PD_SEEN	59	-1	OHL PQ02251	24.739	405.6	29.094	18.268	2	171	1	1	1	1
MS04923	F	05/01/2008	Nettie	308	Left	Manible	Premolar	PD_SEEN	59	-1	OHL PQ02251	24.930	358.9	33.311	1.165	3	171	1	1	1	0
MS05109	M	08/02/2009	Wellington	409	Right	Manible	Molar	NO_PD	22	-2	OHL PQ02264		1.0	1.000	1	114	0	0	0	0	0
MS05109	M	08/02/2009	Wellington	409	Right	Manible	Molar	NO_PD	22	-2	OHL PQ02264		1.0	1.000	2	114	0	0	0	0	0
MS05109	M	08/02/2009	Wellington	409	Right	Manible	Molar	NO_PD	22	-2	OHL PQ02264		1.0	1.000	3	114	0	0	0	0	0
MS05118	M	08/05/2009	Yoshi	408	Right	Manible	Premolar	NO_PD	27	-2	OHL PQ02295	25.527	245.1	30.094	9.508	1	101	1	1	1	1
MS05118	M	08/05/2009	Yoshi	408	Right	Manible	Premolar	NO_PD	27	-2	OHL PQ02295	25.167	308.6	30.092	9.520	2	101	1	1	1	1
MS05118	M	08/05/2009	Yoshi	408	Right	Manible	Premolar	NO_PD	27	-2	OHL PQ02295	27.783	57.9	29.094	18.267	3	101	1	1	1	1
MS05118	M	08/05/2009	Yoshi	308	Left	Manible	Premolar	PD_SEEN	27	-2	OHL PQ02303	27.297	79.0	33.863	0.812	1	101	1	1	1	0
MS05118	M	08/05/2009	Yoshi	308	Left	Manible	Premolar	PD_SEEN	27	-2	OHL PQ02303	27.201	84.0	32.132	2.515	2	101	1	1	1	0
MS05118	M	08/05/2009	Yoshi	308	Left	Manible	Premolar	PD_SEEN	27	-2	OHL PQ02303	25.171	307.7	1.000	3	101	1	1	0	0	0
MS05164	M	15/01/2010	Colin	207	Left	Maxilla	Premolar	PD_SEEN	72	-5	OHL PQ02315	33.108	1.9	31.063	5.051	1	65	1	0	1	1

MS05164	M	15/01/2010	Colin	207	Left	Maxilla	Premolar	PD_SEEN	72	-5	OHLPQ02315	34.736	0.7	31.909	2.908	2	65	1	0	1	0
MS05164	M	15/01/2010	Colin	207	Left	Maxilla	Premolar	PD_SEEN	72	-5	OHLPQ02315		1.0	30.803	5.988	3	65	0	0	1	0
MS05164	M	15/01/2010	Colin	308	Left	Manible	Premolar	NO_PD	72	-5	OHLPQ02319		1.0		1.000	1	65	0	0	0	1
MS05164	M	15/01/2010	Colin	308	Left	Manible	Premolar	NO_PD	72	-5	OHLPQ02319		1.0		1.000	2	65	0	0	0	0
MS05164	M	15/01/2010	Colin	308	Left	Manible	Premolar	NO_PD	72	-5	OHLPQ02319		1.0	32.668	1.772	3	65	0	0	1	0
MS04563	F	23/06/2004	China	208	Left	Maxilla	Premolar	PD_SEEN	42	-1	OHLPQ02332	26.920	100.6	32.607	1.845	1	355	1	1	1	0
MS04563	F	23/06/2004	China	208	Left	Maxilla	Premolar	PD_SEEN	42	-1	OHLPQ02332	26.888	102.7	33.119	1.320	2	355	1	1	1	0
MS04563	F	23/06/2004	China	208	Left	Maxilla	Premolar	PD_SEEN	42	-1	OHLPQ02332	26.525	129.5	31.098	4.939	3	355	1	1	1	1
MS04563	F	23/06/2004	China	308	Left	Manible	Premolar	NO_PD	42	-1	OHLPQ02335	29.653	17.5	31.603	3.551	1	355	1	1	1	0
MS04563	F	23/06/2004	China	308	Left	Manible	Premolar	NO_PD	42	-1	OHLPQ02335	29.382	20.8	32.104	2.561	2	355	1	1	1	1
MS04563	F	23/06/2004	China	308	Left	Manible	Premolar	NO_PD	42	-1	OHLPQ02335	35.327	0.5	31.369	4.137	3	355	1	0	1	1
MS04599	M	09/04/2004	Rooney	108	Right	Maxilla	Premolar	PD_SEEN	6	-2	OHLPQ02340		1.0	1.000	1	366	0	0	0	0	0
MS04599	M	09/04/2004	Rooney	108	Right	Maxilla	Premolar	PD_SEEN	6	-2	OHLPQ02340	33.060	2.0	1.000	2	366	1	0	0	0	0
MS04599	M	09/04/2004	Rooney	108	Right	Maxilla	Premolar	PD_SEEN	6	-2	OHLPQ02340	32.834	2.3	1.000	3	366	1	0	0	0	0
MS04599	M	09/04/2004	Rooney	208	Left	Maxilla	Premolar	NO_PD	6	-2	OHLPQ02348		1.0	31.381	4.105	1	366	0	0	1	1
MS04599	M	09/04/2004	Rooney	208	Left	Maxilla	Premolar	NO_PD	6	-2	OHLPQ02348		1.0	29.015	19.231	2	366	0	0	1	1
MS04599	M	09/04/2004	Rooney	208	Left	Maxilla	Premolar	NO_PD	6	-2	OHLPQ02348		1.0		1.000	3	366	0	0	0	0
MS04595	M	09/04/2004	Dallas	108	Right	Maxilla	Premolar	NO_PD	5	-2	OHLPQ02356	30.589	9.6	22.796	1113.813	1	366	1	1	1	1
MS04595	M	09/04/2004	Dallas	108	Right	Maxilla	Premolar	NO_PD	5	-2	OHLPQ02356	35.124	0.5	22.726	1166.122	2	366	1	0	1	1
MS04595	M	09/04/2004	Dallas	108	Right	Maxilla	Premolar	NO_PD	5	-2	OHLPQ02356	35.986	0.3	23.292	806.136	3	366	1	0	1	1
MS04595	M	09/04/2004	Dallas	208	Left	Maxilla	Premolar	PD_SEEN	5	-2	OHLPQ02364		1.0	24.895	283.079	1	366	0	0	1	1
MS04595	M	09/04/2004	Dallas	208	Left	Maxilla	Premolar	PD_SEEN	5	-2	OHLPQ02364	34.195	1.0	25.383	205.829	2	366	1	0	1	1
MS04595	M	09/04/2004	Dallas	208	Left	Maxilla	Premolar	PD_SEEN	5	-2	OHLPQ02364		1.0	25.562	183.208	3	366	0	0	1	1
MS04648	M	10/12/2005	Winston	408	Right	Manible	Premolar	PD_SEEN	48	-2	OHLPQ02391		1.0	23.210	850.089	1	279	0	0	1	1
MS04648	M	10/12/2005	Winston	408	Right	Manible	Premolar	PD_SEEN	48	-2	OHLPQ02391	32.866	2.2	22.851	1074.704	2	279	1	0	1	1
MS04648	M	10/12/2005	Winston	408	Right	Manible	Premolar	PD_SEEN	48	-2	OHLPQ02391	30.098	13.2	23.095	916.585	3	279	1	1	1	1
MS04648	M	10/12/2005	Winston	207	Left	Maxilla	Premolar	NO_PD	48	-2	OHLPQ02395		1.0	29.091	18.305	1	279	0	0	1	1
MS04648	M	10/12/2005	Winston	207	Left	Maxilla	Premolar	NO_PD	48	-2	OHLPQ02395	32.845	2.3	29.192	17.130	2	279	1	0	1	1
MS04648	M	10/12/2005	Winston	207	Left	Maxilla	Premolar	NO_PD	48	-2	OHLPQ02395		1.0	28.015	36.945	3	279	0	0	1	1
MS04645	F	10/12/2005	Mimi	209	Left	Maxilla	Molar	NO_PD	47	-1	OHLPQ02413	30.557	9.8	27.829	41.700	1	279	1	1	1	1
MS04645	F	10/12/2005	Mimi	209	Left	Maxilla	Molar	NO_PD	47	-1	OHLPQ02413		1.0	26.708	86.714	2	279	0	0	1	1
MS04645	F	10/12/2005	Mimi	209	Left	Maxilla	Molar	NO_PD	47	-1	OHLPQ02413	33.114	1.9	26.895	76.727	3	279	1	0	1	1
MS04643	F	10/12/2005	Faith	108	Right	Maxilla	Premolar	NO_PD	46	-1	OHLPQ02452	34.523	0.8	27.074	68.279	1	279	1	0	1	1
MS04643	F	10/12/2005	Faith	108	Right	Maxilla	Premolar	NO_PD	46	-1	OHLPQ02452		1.0	27.209	62.503	2	279	0	0	1	1
MS04643	F	10/12/2005	Faith	108	Right	Maxilla	Premolar	NO_PD	46	-1	OHLPQ02452	33.521	1.5	26.998	71.741	3	279	1	0	1	1
MS04643	F	10/12/2005	Faith	408	Right	Manible	Premolar	PD_SEEN	46	-1	OHLPQ02455		1.0	26.429	103.980	1	279	0	0	1	1
MS04643	F	10/12/2005	Faith	408	Right	Manible	Premolar	PD_SEEN	46	-1	OHLPQ02455		1.0	26.883	77.312	2	279	0	0	1	1
MS04643	F	10/12/2005	Faith	408	Right	Manible	Premolar	PD_SEEN	46	-1	OHLPQ02455		1.0	26.000	137.586	3	279	0	0	1	1
MS04643	F	10/12/2005	Faith	207	Left	Maxilla	Premolar	NO_PD	45	-1	OHLPQ02459	32.916	2.2	24.492	368.207	1	279	1	0	1	1
MS04643	F	10/12/2005	Faith	207	Left	Maxilla	Premolar	NO_PD	45	-1	OHLPQ02459	34.266	0.9	24.430	383.422	2	279	1	0	1	1
MS04643	F	10/12/2005	Faith	207	Left	Maxilla	Premolar	NO_PD	45	-1	OHLPQ02459	33.775	1.3	24.193	447.600	3	279	1	0	1	1
MS04643	F	10/12/2005	Faith	308	Left	Manible	Premolar	PD_SEEN	45	-1	OHLPQ02463	31.708	4.7	25.006	263.320	1	279	1	1	1	1
MS04643	F	10/12/2005	Faith	308	Left	Manible	Premolar	PD_SEEN	45	-1	OHLPQ02463	30.543	9.9	25.192	233.218	2	279	1	1	1	1
MS04643	F	10/12/2005	Faith	308	Left	Manible	Premolar	PD_SEEN	45	-1	OHLPQ02463	32.737	2.4	26.171	123.073	3	279	1	0	1	1
MS04714	M	10/05/2006	Eddie	209	Left	Maxilla	Molar	NO_PD	55	-3	OHLPQ02477	30.779	8.5	30.698	6.410	1	257	1	1	1	1
MS04714	M	10/05/2006	Eddie	209	Left	Maxilla	Molar	NO_PD	55	-3	OHLPQ02477	30.986	7.5	29.488	14.125	2	257	1	1	1	1
MS04714	M	10/05/2006	Eddie	209	Left	Maxilla	Molar	NO_PD	55	-3	OHLPQ02477	30.727	8.8	31.367	4.142	3	257	1	1	1	1
MS04715	F	10/05/2006	Edna	209	Left	Maxilla	Molar	NO_PD	56	-2	OHLPQ02493		1.0	29.612	13.027	1	257	0	0	1	1
MS04715	F	10/05/2006	Edna	209	Left	Maxilla	Molar	NO_PD	56	-2	OHLPQ02493	32.695	2.5	29.409	14.867	2	257	1	0	1	1
MS04715	F	10/05/2006	Edna	209	Left	Maxilla	Molar	NO_PD	56	-2	OHLPQ02493		1.0	34.388	0.577	3	257	0	0	1	0
MS04715	F	10/05/2006	Edna	309	Left	Manible	Molar	PD_SEEN	56	-2	OHLPQ02496	32.991	2.1	1.000	1	257	1	0	0	0	0
MS04715	F	10/05/2006	Edna	309	Left	Manible	Molar	PD_SEEN	56	-2	OHLPQ02496		1.0	32.733	1.699	2	257	0	0	1	0
MS04715	F	10/05/2006	Edna	309	Left	Manible	Molar	PD_SEEN	56	-2	OHLPQ02496		1.0		1.000	3	257	0	0	0	0
MS04846	M	13/09/2007	Jigsaw	109	Right	Maxilla	Molar	NO_PD	8	-2	OHLPQ02533		1.0	32.267	2.302	1	187	0	0	1	0

MS04846	M	13/09/2007	Jigsaw	109	Right	Maxilla	Molar	NO_PD	8	-2	OHL PQ02533		1.0	30.689	6.448	2	187	0	0	1	1
MS04846	M	13/09/2007	Jigsaw	109	Right	Maxilla	Molar	NO_PD	8	-2	OHL PQ02533	31.566	5.2	29.916	10.682	3	187	1	1	1	1
MS04846	M	13/09/2007	Jigsaw	408	Right	Manible	Premolar	PD_SEEN	58	-1	OHL PQ02535		1.0	31.874	2.975	1	187	0	0	1	0
MS04846	M	13/09/2007	Jigsaw	408	Right	Manible	Premolar	PD_SEEN	58	-1	OHL PQ02535		1.0	35.538	0.272	2	187	0	0	1	0
MS04846	M	13/09/2007	Jigsaw	408	Right	Manible	Premolar	PD_SEEN	58	-1	OHL PQ02535	32.528	2.8	30.369	7.945	3	187	1	0	1	1
MS04561	M	23/06/2004	Arnie	103	Right	Maxilla	Incisor	NO_PD	2	-1	OHL PQ02561	29.019	26.3	32.595	1.859	1	355	1	1	1	0
MS04561	M	23/06/2004	Arnie	103	Right	Maxilla	Incisor	NO_PD	2	-1	OHL PQ02561	28.384	39.4	32.942	1.482	2	355	1	1	1	0
MS04561	M	23/06/2004	Arnie	103	Right	Maxilla	Incisor	NO_PD	2	-1	OHL PQ02561	29.028	26.1		1.000	3	355	1	1	0	0
MS04561	M	23/06/2004	Arnie	107	Right	Maxilla	Premolar	PD_SEEN	40	-2	OHL PQ02563	25.913	191.5	29.145	17.668	1	355	1	1	1	1
MS04561	M	23/06/2004	Arnie	107	Right	Maxilla	Premolar	PD_SEEN	40	-2	OHL PQ02563	26.203	159.1	28.310	30.467	2	355	1	1	1	1
MS04561	M	23/06/2004	Arnie	107	Right	Maxilla	Premolar	PD_SEEN	40	-2	OHL PQ02563	25.981	183.4	28.054	36.010	3	355	1	1	1	1
MS04561	M	23/06/2004	Arnie	203	Left	Maxilla	Incisor	PD_SEEN	2	-1	OHL PQ02569		1.0	33.691	0.909	1	355	0	0	1	0
MS04561	M	23/06/2004	Arnie	203	Left	Maxilla	Incisor	PD_SEEN	2	-1	OHL PQ02569	34.956	0.6		1.000	2	355	1	0	0	0
MS04561	M	23/06/2004	Arnie	203	Left	Maxilla	Incisor	PD_SEEN	2	-1	OHL PQ02569		1.0	31.670	3.400	3	355	0	0	1	0
MS04561	M	23/06/2004	Arnie	208	Left	Maxilla	Premolar	NO_PD	40	-2	OHL PQ02572	25.785	207.8	26.078	130.814	1	355	1	1	1	1
MS04561	M	23/06/2004	Arnie	208	Left	Maxilla	Premolar	NO_PD	40	-2	OHL PQ02572	25.901	192.9	27.154	64.797	2	355	1	1	1	1
MS04561	M	23/06/2004	Arnie	208	Left	Maxilla	Premolar	NO_PD	40	-2	OHL PQ02572	25.412	263.7	26.341	110.142	3	355	1	1	1	1
MS04559	F	23/06/2004	Halle	409	Right	Manible	Molar	PD_SEEN	1	-2	OHL PQ02584	30.274	11.8	33.219	1.236	1	355	1	1	1	0
MS04559	F	23/06/2004	Halle	409	Right	Manible	Molar	PD_SEEN	1	-2	OHL PQ02584	30.759	8.6	30.457	7.503	2	355	1	1	1	1
MS04559	F	23/06/2004	Halle	409	Right	Manible	Molar	PD_SEEN	1	-2	OHL PQ02584	31.728	4.7	34.402	0.571	3	355	1	1	1	0
MS04559	F	23/06/2004	Halle	309	Left	Manible	Molar	NO_PD	1	-2	OHL PQ02592	35.418	0.4	27.622	47.734	1	355	1	0	1	1
MS04559	F	23/06/2004	Halle	309	Left	Manible	Molar	NO_PD	1	-2	OHL PQ02592		1.0	28.032	36.541	2	355	0	0	1	1
MS04559	F	23/06/2004	Halle	309	Left	Manible	Molar	NO_PD	1	-2	OHL PQ02592	33.535	1.5	27.777	43.135	3	355	1	0	1	1
MS05116	M	08/05/2009	Yankee	108	Right	Maxilla	Premolar	PD_SEEN	26	-2	OHL PQ02644		1.0	28.891	20.856	1	101	0	0	1	1
MS05116	M	08/05/2009	Yankee	108	Right	Maxilla	Premolar	PD_SEEN	26	-2	OHL PQ02644	34.088	1.0	27.866	40.720	2	101	1	0	1	1
MS05116	M	08/05/2009	Yankee	108	Right	Maxilla	Premolar	PD_SEEN	26	-2	OHL PQ02644	25.468	254.5	27.937	13.675	3	101	1	1	1	1
MS05116	M	08/05/2009	Yankee	208	Left	Maxilla	Premolar	NO_PD	26	-2	OHL PQ02652		1.0	26.699	87.232	1	101	0	0	1	1
MS05116	M	08/05/2009	Yankee	208	Left	Maxilla	Premolar	NO_PD	26	-2	OHL PQ02652	30.464	10.4	26.913	75.846	2	101	1	1	1	1
MS05116	M	08/05/2009	Yankee	208	Left	Maxilla	Premolar	NO_PD	26	-2	OHL PQ02652		1.0	26.013	136.495	3	101	0	0	1	1
MS05120	F	08/05/2009	Yetti	203	Left	Maxilla	Incisor	NO_PD	28	-1	OHL PQ02665	29.158	24.0	1.000		1	101	1	1	0	0
MS05120	F	08/05/2009	Yetti	203	Left	Maxilla	Incisor	NO_PD	28	-1	OHL PQ02665	30.726	8.8	33.372	1.119	2	101	1	1	1	0
MS05120	F	08/05/2009	Yetti	203	Left	Maxilla	Incisor	NO_PD	28	-1	OHL PQ02665	28.924	27.9	32.768	1.660	3	101	1	1	1	0
MS05108	F	08/02/2009	Whoopee	109	Right	Maxilla	Molar	NO_PD	21	-2	OHL PQ02677	28.130	46.4	31.147	4.783	1	114	1	1	1	1
MS05108	F	08/02/2009	Whoopee	109	Right	Maxilla	Molar	NO_PD	21	-2	OHL PQ02677	28.888	28.6	28.335	29.976	2	114	1	1	1	1
MS05108	F	08/02/2009	Whoopee	109	Right	Maxilla	Molar	NO_PD	21	-2	OHL PQ02677	29.627	17.8	31.524	3.740	3	114	1	1	1	0
MS05108	F	08/02/2009	Whoopee	209	Left	Maxilla	Molar	PD_SEEN	21	-2	OHL PQ02685	25.388	267.8	30.038	9.863	1	114	1	1	1	1
MS05108	F	08/02/2009	Whoopee	209	Left	Maxilla	Molar	PD_SEEN	21	-2	OHL PQ02685	25.326	278.7	27.439	53.795	2	114	1	1	1	1
MS05108	F	08/02/2009	Whoopee	209	Left	Maxilla	Molar	PD_SEEN	21	-2	OHL PQ02685		1.0	33.878	0.804	3	114	0	0	1	0
MS04712	M	10/05/2006	Elton	107	Right	Maxilla	Premolar	NO_PD	51	0	OHL PQ02707	28.670	32.9	27.963	38.214	1	257	1	1	1	1
MS04712	M	10/05/2006	Elton	107	Right	Maxilla	Premolar	NO_PD	51	0	OHL PQ02707	28.253	42.9	29.721	12.131	2	257	1	1	1	1
MS04712	M	10/05/2006	Elton	107	Right	Maxilla	Premolar	NO_PD	51	0	OHL PQ02707	28.848	29.3	29.908	10.735	3	257	1	1	1	1
MS04712	M	10/05/2006	Elton	108	Right	Maxilla	Premolar	PD_SEEN	51	0	OHL PQ02708	29.976	14.3	28.825	21.774	1	257	1	1	1	1
MS04712	M	10/05/2006	Elton	108	Right	Maxilla	Premolar	PD_SEEN	51	0	OHL PQ02708		1.0	28.915	20.535	2	257	0	0	1	1
MS04712	M	10/05/2006	Elton	108	Right	Maxilla	Premolar	PD_SEEN	51	0	OHL PQ02708	34.567	0.8	28.073	35.571	3	257	1	0	1	1
MS04929	M	05/01/2008	Norris	103	Right	Maxilla	Incisor	NO_PD	10	-5	OHL PQ02721		1.0	29.448	14.494	1	171	0	0	1	1
MS04929	M	05/01/2008	Norris	103	Right	Maxilla	Incisor	NO_PD	10	-5	OHL PQ02721		1.0	27.982	37.744	2	171	0	0	1	1
MS04929	M	05/01/2008	Norris	103	Right	Maxilla	Incisor	NO_PD	10	-5	OHL PQ02721		1.0	27.923	39.238	3	171	0	0	1	1
MS04929	M	05/01/2008	Norris	409	Right	Manible	Molar	NO_PD	14	-5	OHL PQ02728	31.897	4.2	24.654	331.258	1	171	1	1	1	1
MS04929	M	05/01/2008	Norris	409	Right	Manible	Molar	NO_PD	14	-5	OHL PQ02728		1.0	24.633	335.861	2	171	0	0	1	1
MS04929	M	05/01/2008	Norris	409	Right	Manible	Molar	NO_PD	14	-5	OHL PQ02728	33.495	1.5	24.807	299.827	3	171	1	0	1	1
MS04929	M	05/01/2008	Norris	304	Left	Manible	Canine	PD_SEEN	12	0	OHL PQ02734		1.0	26.513	98.475	1	171	0	0	1	1
MS04929	M	05/01/2008	Norris	304	Left	Manible	Canine	PD_SEEN	12	0	OHL PQ02734		1.0	26.380	107.408	2	171	0	0	1	1
MS04929	M	05/01/2008	Norris	304	Left	Manible	Canine	PD_SEEN	12	0	OHL PQ02734		1.0	28.816	21.893	3	171	0	0	1	1
MS04929	M	05/01/2008	Norris	309	Left	Manible	Molar	PD_SEEN	14	-5	OHL PQ02736	34.314	0.9	24.121	469.238	1	171	1	0	1	1

MS04929	M	05/01/2008	Norris	309	Left	Manible	Molar	PD_SEEN	14	-5	OHL PQ02736	33.651	1.4	23.599	659.749	2	171	1	0	1	1
MS04929	M	05/01/2008	Norris	309	Left	Manible	Molar	PD_SEEN	14	-5	OHL PQ02736	32.243	3.3	23.284	810.291	3	171	1	0	1	1
MS05107	F	08/02/2009	Willow	408	Right	Manible	Premolar	NO_PD	61	-1	OHL PQ02743	27.468	70.9	28.897	20.772	1	114	1	1	1	1
MS05107	F	08/02/2009	Willow	408	Right	Manible	Premolar	NO_PD	61	-1	OHL PQ02743	28.638	33.5	29.491	14.100	2	114	1	1	1	1
MS05107	F	08/02/2009	Willow	408	Right	Manible	Premolar	NO_PD	61	-1	OHL PQ02743	31.700	4.7	33.627	0.948	3	114	1	1	1	0
MS05107	F	08/02/2009	Willow	208	Left	Maxilla	Premolar	PD_SEEN	61	-1	OHL PQ02748	28.915	28.1	29.841	11.214	1	114	1	1	1	1
MS05107	F	08/02/2009	Willow	208	Left	Maxilla	Premolar	PD_SEEN	61	-1	OHL PQ02748	28.726	31.7	29.109	18.085	2	114	1	1	1	1
MS05107	F	08/02/2009	Willow	208	Left	Maxilla	Premolar	PD_SEEN	61	-1	OHL PQ02748	28.146	45.9	30.731	6.274	3	114	1	1	1	1
MS05115	F	08/05/2009	Yoyo	103	Right	Maxilla	Incisor	NO_PD	25	-2	OHL PQ02769	26.242	155.1	33.431	1.077	1	101	1	1	1	0
MS05115	F	08/05/2009	Yoyo	103	Right	Maxilla	Incisor	NO_PD	25	-2	OHL PQ02769	25.415	263.3	30.066	9.684	2	101	1	1	1	1
MS05115	F	08/05/2009	Yoyo	103	Right	Maxilla	Incisor	NO_PD	25	-2	OHL PQ02769	25.591	235.2	34.459	0.550	3	101	1	1	1	0
MS05115	F	08/05/2009	Yoyo	203	Left	Maxilla	Incisor	PD_SEEN	25	-2	OHL PQ02777	22.957	1267.4	34.183	0.659	1	101	1	1	1	0
MS05115	F	08/05/2009	Yoyo	203	Left	Maxilla	Incisor	PD_SEEN	25	-2	OHL PQ02777	22.602	1590.0	34.194	0.654	2	101	1	1	1	0
MS05115	F	08/05/2009	Yoyo	203	Left	Maxilla	Incisor	PD_SEEN	25	-2	OHL PQ02777	22.855	1352.4		1.000	3	101	1	1	0	0
MS05031	F	26/01/2009	Violet	203	Left	Maxilla	Incisor	PD_SEEN	17	-4	OHL PQ02866	36.200	0.3		1.000	1	116	1	0	0	0
MS05031	F	26/01/2009	Violet	203	Left	Maxilla	Incisor	PD_SEEN	17	-4	OHL PQ02866	35.582	0.4	32.651	1.792	2	116	1	0	1	0
MS05031	F	26/01/2009	Violet	203	Left	Maxilla	Incisor	PD_SEEN	17	-4	OHL PQ02866		1.0	33.769	0.864	3	116	0	0	1	0
MS05031	F	26/01/2009	Violet	308	Left	Manible	Premolar	PD_SEEN	18	-3	OHL PQ02875	30.113	13.1	29.394	15.018	1	116	1	1	1	1
MS05031	F	26/01/2009	Violet	308	Left	Manible	Premolar	PD_SEEN	18	-3	OHL PQ02875	30.785	8.5	30.243	8.629	2	116	1	1	1	1
MS05031	F	26/01/2009	Violet	308	Left	Manible	Premolar	PD_SEEN	18	-3	OHL PQ02875	34.422	0.8	31.399	4.057	3	116	1	0	1	1
MS05031	F	26/01/2009	Violet	408	Right	Manible	Premolar	NO_PD	18	-3	OHL PQ02876	35.218	0.5	29.915	10.685	1	116	1	0	1	1
MS05031	F	26/01/2009	Violet	408	Right	Manible	Premolar	NO_PD	18	-3	OHL PQ02876	33.080	2.0	28.850	21.424	2	116	1	0	1	1
MS05031	F	26/01/2009	Violet	408	Right	Manible	Premolar	NO_PD	18	-3	OHL PQ02876	36.240	0.3	29.852	11.136	3	116	1	0	1	1
MS05114	F	08/05/2009	Yasmine	207	Left	Maxilla	Premolar	NO_PD	63	-3	OHL PQ02920	34.202	1.0	33.151	1.293	1	101	1	0	1	0
MS05114	F	08/05/2009	Yasmine	207	Left	Maxilla	Premolar	NO_PD	63	-3	OHL PQ02920	35.086	0.5		1.000	2	101	1	0	0	0
MS05114	F	08/05/2009	Yasmine	207	Left	Maxilla	Premolar	NO_PD	63	-3	OHL PQ02920		1.0	31.275	4.398	3	101	0	0	1	1
MS05114	F	08/05/2009	Yasmine	308	Left	Manible	Premolar	PD_SEEN	63	-3	OHL PQ02923	31.603	5.0	27.578	49.122	1	101	1	1	1	1
MS05114	F	08/05/2009	Yasmine	308	Left	Manible	Premolar	PD_SEEN	63	-3	OHL PQ02923	30.065	13.5	27.630	47.478	2	101	1	1	1	1
MS05114	F	08/05/2009	Yasmine	308	Left	Manible	Premolar	PD_SEEN	63	-3	OHL PQ02923	33.325	1.7	28.077	35.474	3	101	1	0	1	1
MS05114	F	08/05/2009	Yasmine	209	Left	Maxilla	Molar	NO_PD	64	-3	OHL PQ02926	35.201	0.5	31.323	4.264	1	101	1	0	1	1
MS05114	F	08/05/2009	Yasmine	209	Left	Maxilla	Molar	NO_PD	64	-3	OHL PQ02926		1.0		1.000	2	101	0	0	0	0
MS05114	F	08/05/2009	Yasmine	209	Left	Maxilla	Molar	NO_PD	64	-3	OHL PQ02926		1.0	30.531	7.147	3	101	0	0	1	1
MS05114	F	08/05/2009	Yasmine	309	Left	Manible	Molar	PD_SEEN	64	-3	OHL PQ02927		1.0	32.437	2.060	1	101	0	0	1	0
MS05114	F	08/05/2009	Yasmine	309	Left	Manible	Molar	PD_SEEN	64	-3	OHL PQ02927		1.0	33.128	1.313	2	101	0	0	1	0
MS05114	F	08/05/2009	Yasmine	309	Left	Manible	Molar	PD_SEEN	64	-3	OHL PQ02927	34.253	0.9	34.931	0.405	3	101	1	0	1	0
MS05156	M	03/12/2010	Brock	108	Right	Maxilla	Premolar	NO_PD	35	-5	OHL PQ02937	31.504	5.4	31.794	3.135	1	19	1	1	1	0
MS05156	M	03/12/2010	Brock	108	Right	Maxilla	Premolar	NO_PD	35	-5	OHL PQ02937		1.0	31.291	4.354	2	19	0	0	1	1
MS05156	M	03/12/2010	Brock	108	Right	Maxilla	Premolar	NO_PD	35	-5	OHL PQ02937	34.097	1.0	31.330	4.245	3	19	1	0	1	1
MS05156	M	03/12/2010	Brock	208	Left	Maxilla	Premolar	PD_SEEN	35	-5	OHL PQ02938		1.0	26.750	84.348	1	19	0	0	1	1
MS05156	M	03/12/2010	Brock	208	Left	Maxilla	Premolar	PD_SEEN	35	-5	OHL PQ02938		1.0	26.724	85.817	2	19	0	0	1	1
MS05156	M	03/12/2010	Brock	208	Left	Maxilla	Premolar	PD_SEEN	35	-5	OHL PQ02938	33.350	1.6	27.205	62.679	3	19	1	0	1	1
MS05152	M	03/12/2010	Bentley	108	Right	Maxilla	Premolar	NO_PD	33	-1	OHL PQ02953	34.996	0.6	27.797	42.595	1	19	1	0	1	1
MS05152	M	03/12/2010	Bentley	108	Right	Maxilla	Premolar	NO_PD	33	-1	OHL PQ02953	34.799	0.7	27.270	60.064	2	19	1	0	1	1
MS05152	M	03/12/2010	Bentley	108	Right	Maxilla	Premolar	NO_PD	33	-1	OHL PQ02953	34.348	0.9	27.768	43.410	3	19	1	0	1	1
MS05152	M	03/12/2010	Bentley	208	Left	Maxilla	Premolar	PD_SEEN	33	-1	OHL PQ02954	35.192	0.5	26.354	109.227	1	19	1	0	1	1
MS05152	M	03/12/2010	Bentley	208	Left	Maxilla	Premolar	PD_SEEN	33	-1	OHL PQ02954	30.369	11.1	26.443	103.064	2	19	1	1	1	1
MS05152	M	03/12/2010	Bentley	208	Left	Maxilla	Premolar	PD_SEEN	33	-1	OHL PQ02954	35.343	0.5	26.737	85.081	3	19	1	0	1	1
MS05151	F	03/12/2010	Bramble	208	Left	Maxilla	Premolar	NO_PD	69	-3	OHL PQ02970		1.0	26.881	77.449	1	19	0	0	1	1
MS05151	F	03/12/2010	Bramble	208	Left	Maxilla	Premolar	NO_PD	69	-3	OHL PQ02970		1.0	27.889	40.106	2	19	0	0	1	1
MS05151	F	03/12/2010	Bramble	208	Left	Maxilla	Premolar	NO_PD	69	-3	OHL PQ02970		1.0	27.867	40.674	3	19	0	0	1	1
MS05151	F	03/12/2010	Bramble	408	Right	Manible	Premolar	PD_SEEN	69	-3	OHL PQ02972	34.791	0.7	29.321	15.752	1	19	1	0	1	1
MS05151	F	03/12/2010	Bramble	408	Right	Manible	Premolar	PD_SEEN	69	-3	OHL PQ02972		1.0	28.034	36.486	2	19	0	0	1	1
MS05151	F	03/12/2010	Bramble	408	Right	Manible	Premolar	PD_SEEN	69	-3	OHL PQ02972	36.045	0.3	26.523	97.817	3	19	1	0	1	1
MS05163	M	15/01/2010	Chesney	108	Right	Maxilla	Premolar	NO_PD	71	-4	OHL PQ02985	25.019	339.0	24.836	294.268	1	65	1	1	1	1

MS05163	M	15/01/2010	Chesney	108	Right	Maxilla	Premolar	NO_PD	71	-4	OHL PQ02985	25.789	207.3	25.039	257.728	2	65	1	1	1	1
MS05163	M	15/01/2010	Chesney	108	Right	Maxilla	Premolar	NO_PD	71	-4	OHL PQ02985	25.450	257.4	25.179	235.246	3	65	1	1	1	1
MS05163	M	15/01/2010	Chesney	408	Right	Manible	Premolar	PD_SEEN	71	-4	OHL PQ02988	25.277	287.6	27.784	42.940	1	65	1	1	1	1
MS05163	M	15/01/2010	Chesney	408	Right	Manible	Premolar	PD_SEEN	71	-4	OHL PQ02988	24.762	399.7	27.336	57.555	2	65	1	1	1	1
MS05163	M	15/01/2010	Chesney	408	Right	Manible	Premolar	PD_SEEN	71	-4	OHL PQ02988	25.020	338.9	27.149	64.994	3	65	1	1	1	1
MS05158	F	15/01/2010	Connie	309	Left	Manible	Molar	PD_SEEN	37	-1	OHL PQ03023	30.897	7.9	29.093	18.282	1	65	1	1	1	1
MS05158	F	15/01/2010	Connie	309	Left	Manible	Molar	PD_SEEN	37	-1	OHL PQ03023		1.0		12.985	2	65	0	0	1	1
MS05158	F	15/01/2010	Connie	309	Left	Manible	Molar	PD_SEEN	37	-1	OHL PQ03023		1.0		1.000	3	65	0	0	0	0
MS05158	F	15/01/2010	Connie	409	Right	Manible	Molar	NO_PD	37	-1	OHL PQ03024	32.472	2.9	31.533	3.718	1	65	1	0	1	0
MS05158	F	15/01/2010	Connie	409	Right	Manible	Molar	NO_PD	37	-1	OHL PQ03024		1.0	28.051	36.089	2	65	0	0	1	1
MS05158	F	15/01/2010	Connie	409	Right	Manible	Molar	NO_PD	37	-1	OHL PQ03024	30.849	8.2	28.371	29.275	3	65	1	1	1	1
MS04930	F	05/01/2008	Niamh	308	Left	Manible	Premolar	PD_SEEN	15	-5	OHL PQ03067	26.845	105.5	31.797	3.129	1	171	1	1	1	0
MS04930	F	05/01/2008	Niamh	308	Left	Manible	Premolar	PD_SEEN	15	-5	OHL PQ03067	27.133	87.8	28.296	30.757	2	171	1	1	1	1
MS04930	F	05/01/2008	Niamh	308	Left	Manible	Premolar	PD_SEEN	15	-5	OHL PQ03067	26.696	116.1	30.379	7.894	3	171	1	1	1	1
MS04930	F	05/01/2008	Niamh	408	Right	Manible	Premolar	NO_PD	15	-5	OHL PQ03068	28.882	28.7	26.564	95.261	1	171	1	1	1	1
MS04930	F	05/01/2008	Niamh	408	Right	Manible	Premolar	NO_PD	15	-5	OHL PQ03068	29.138	24.4	26.384	107.095	2	171	1	1	1	1
MS04930	F	05/01/2008	Niamh	408	Right	Manible	Premolar	NO_PD	15	-5	OHL PQ03068	28.426	38.4	26.730	85.456	3	171	1	1	1	1
MS04923	F	05/01/2008	Nettie	107	Right	Maxilla	Premolar	NO_PD	59	0	OHL PQ03079	25.731	215.1	25.049	256.073	1	171	1	1	1	1
MS04923	F	05/01/2008	Nettie	107	Right	Maxilla	Premolar	NO_PD	59	0	OHL PQ03079	25.767	210.3	24.930	276.750	2	171	1	1	1	1
MS04923	F	05/01/2008	Nettie	107	Right	Maxilla	Premolar	NO_PD	59	0	OHL PQ03079	25.506	248.5	24.896	282.823	3	171	1	1	1	1
MS04923	F	05/01/2008	Nettie	108	Right	Maxilla	Premolar	NO_PD	9	-1	OHL PQ03081	27.176	85.4	24.760	309.243	1	171	1	1	1	1
MS04923	F	05/01/2008	Nettie	108	Right	Maxilla	Premolar	NO_PD	9	-1	OHL PQ03081	27.515	68.8	24.477	371.809	2	171	1	1	1	1
MS04923	F	05/01/2008	Nettie	108	Right	Maxilla	Premolar	NO_PD	9	-1	OHL PQ03081	28.396	39.2	24.994	265.453	3	171	1	1	1	1
MS04923	F	05/01/2008	Nettie	208	Left	Maxilla	Premolar	PD_SEEN	9	-1	OHL PQ03082	26.764	111.1	28.190	32.962	1	171	1	1	1	1
MS04923	F	05/01/2008	Nettie	208	Left	Maxilla	Premolar	PD_SEEN	9	-1	OHL PQ03082	26.362	143.7	27.754	43.789	2	171	1	1	1	1
MS04923	F	05/01/2008	Nettie	208	Left	Maxilla	Premolar	PD_SEEN	9	-1	OHL PQ03082	26.611	122.6	29.039	18.928	3	171	1	1	1	1
MS04923	F	05/01/2008	Nettie	308	Left	Manible	Premolar	PD_SEEN	59	0	OHL PQ03083	23.942	675.1	27.558	49.788	1	171	1	1	1	1
MS04923	F	05/01/2008	Nettie	308	Left	Manible	Premolar	PD_SEEN	59	0	OHL PQ03083	24.366	514.7	26.686	87.933	2	171	1	1	1	1
MS04923	F	05/01/2008	Nettie	308	Left	Manible	Premolar	PD_SEEN	59	0	OHL PQ03083	23.855	713.8	28.451	27.786	3	171	1	1	1	1
MS05109	M	08/02/2009	Wellington	409	Right	Manible	Molar	NO_PD	22	-1	OHL PQ03096		1.0		1.000	1	114	0	0	0	0
MS05109	M	08/02/2009	Wellington	409	Right	Manible	Molar	NO_PD	22	-1	OHL PQ03096		1.0	34.651	0.486	2	114	0	0	1	0
MS05109	M	08/02/2009	Wellington	409	Right	Manible	Molar	NO_PD	22	-1	OHL PQ03096		1.0	33.624	0.949	3	114	0	0	1	0
MS05109	M	08/02/2009	Wellington	309	Left	Manible	Molar	PD_SEEN	22	-1	OHL PQ03104		1.0	28.569	25.736	1	114	0	0	1	1
MS05109	M	08/02/2009	Wellington	309	Left	Manible	Molar	PD_SEEN	22	-1	OHL PQ03104		1.0	27.833	41.593	2	114	0	0	1	1
MS05109	M	08/02/2009	Wellington	309	Left	Manible	Molar	PD_SEEN	22	-1	OHL PQ03104	36.455	0.2	27.829	41.710	3	114	1	0	1	1
MS05118	M	08/05/2009	Yoshi	104	Right	Maxilla	Canine	PD_SEEN	66	-5	OHL PQ03122	29.248	22.7		1.000	1	101	1	1	0	0
MS05118	M	08/05/2009	Yoshi	104	Right	Maxilla	Canine	PD_SEEN	66	-5	OHL PQ03122	30.744	8.7		1.000	2	101	1	1	0	0
MS05118	M	08/05/2009	Yoshi	104	Right	Maxilla	Canine	PD_SEEN	66	-5	OHL PQ03122	30.209	12.3		1.000	3	101	1	1	0	0
MS05118	M	08/05/2009	Yoshi	404	Right	Manible	Canine	NO_PD	67	-5	OHL PQ03126		1.0	33.568	0.985	1	101	0	0	1	0
MS05118	M	08/05/2009	Yoshi	404	Right	Manible	Canine	NO_PD	67	-5	OHL PQ03126		1.0	31.262	4.437	2	101	0	0	1	1
MS05118	M	08/05/2009	Yoshi	404	Right	Manible	Canine	NO_PD	67	-5	OHL PQ03126	33.253	1.8	29.053	18.766	3	101	1	0	1	1
MS05118	M	08/05/2009	Yoshi	408	Right	Manible	Premolar	NO_PD	27	-1	OHL PQ03127	23.584	849.0	26.142	125.423	1	101	1	1	1	1
MS05118	M	08/05/2009	Yoshi	408	Right	Manible	Premolar	NO_PD	27	-1	OHL PQ03127	24.620	437.7	26.691	87.642	2	101	1	1	1	1
MS05118	M	08/05/2009	Yoshi	408	Right	Manible	Premolar	NO_PD	27	-1	OHL PQ03127	24.399	503.9	27.262	60.381	3	101	1	1	1	1
MS05118	M	08/05/2009	Yoshi	304	Left	Manible	Canine	NO_PD	66	-5	OHL PQ03134	28.904	28.3	35.275	0.323	1	101	1	1	1	0
MS05118	M	08/05/2009	Yoshi	304	Left	Manible	Canine	NO_PD	66	-5	OHL PQ03134	27.546	67.4	33.450	1.063	2	101	1	1	1	0
MS05118	M	08/05/2009	Yoshi	304	Left	Manible	Canine	NO_PD	66	-5	OHL PQ03134	27.323	77.7		1.000	3	101	1	1	0	0
MS05118	M	08/05/2009	Yoshi	308	Left	Manible	Premolar	PD_SEEN	27	-1	OHL PQ03135	27.391	74.4	29.279	16.192	1	101	1	1	1	1
MS05118	M	08/05/2009	Yoshi	308	Left	Manible	Premolar	PD_SEEN	27	-1	OHL PQ03135	26.824	106.9	29.740	11.980	2	101	1	1	1	1
MS05118	M	08/05/2009	Yoshi	308	Left	Manible	Premolar	PD_SEEN	27	-1	OHL PQ03135	26.872	103.7	29.118	17.979	3	101	1	1	1	1
MS05164	M	15/01/2010	Colin	207	Left	Maxilla	Premolar	PD_SEEN	72	-4	OHL PQ03147		1.0	33.335	1.146	1	65	0	0	1	0
MS05164	M	15/01/2010	Colin	207	Left	Maxilla	Premolar	PD_SEEN	72	-4	OHL PQ03147	32.006	3.9		1.000	2	65	1	1	0	0
MS05164	M	15/01/2010	Colin	207	Left	Maxilla	Premolar	PD_SEEN	72	-4	OHL PQ03147		1.0	34.276	0.620	3	65	0	0	1	0
MS04563	F	23/06/2004	China	208	Left	Maxilla	Premolar	PD_SEEN	42	0	OHL PQ03164	28.650	33.3	28.714	23.408	1	355	1	1	1	1

MS04563	F	23/06/2004	China	208	Left	Maxilla	Premolar	PD_SEEN	42	0	OHL PQ03164	30.682	9.1	29.103	18.163	2	355	1	1	1	1
MS04563	F	23/06/2004	China	208	Left	Maxilla	Premolar	PD_SEEN	42	0	OHL PQ03164	28.914	28.1	30.723	6.306	3	355	1	1	1	1
MS04599	M	09/04/2004	Rooney	108	Right	Maxilla	Premolar	PD_SEEN	6	-1	OHL PQ03172		1.0	26.969	73.111	1	366	0	0	1	1
MS04599	M	09/04/2004	Rooney	108	Right	Maxilla	Premolar	PD_SEEN	6	-1	OHL PQ03172	33.306	1.7	26.875	77.747	2	366	1	0	1	1
MS04599	M	09/04/2004	Rooney	108	Right	Maxilla	Premolar	PD_SEEN	6	-1	OHL PQ03172		1.0	28.003	37.229	3	366	0	0	1	1
MS04599	M	09/04/2004	Rooney	208	Left	Maxilla	Premolar	NO_PD	6	-1	OHL PQ03180	31.956	4.0	28.775	22.496	1	366	1	1	1	1
MS04599	M	09/04/2004	Rooney	208	Left	Maxilla	Premolar	NO_PD	6	-1	OHL PQ03180	33.579	1.4	27.940	38.804	2	366	1	0	1	1
MS04599	M	09/04/2004	Rooney	208	Left	Maxilla	Premolar	NO_PD	6	-1	OHL PQ03180		1.0	29.293	16.036	3	366	0	0	1	1
MS04595	M	09/04/2004	Dallas	108	Right	Maxilla	Premolar	NO_PD	5	-1	OHL PQ03188	33.911	1.2	25.944	142.785	1	366	1	0	1	1
MS04595	M	09/04/2004	Dallas	108	Right	Maxilla	Premolar	NO_PD	5	-1	OHL PQ03188	35.739	0.4	25.982	139.283	2	366	1	0	1	1
MS04595	M	09/04/2004	Dallas	108	Right	Maxilla	Premolar	NO_PD	5	-1	OHL PQ03188	35.118	0.5	25.724	164.839	3	366	1	0	1	1
MS04595	M	09/04/2004	Dallas	208	Left	Maxilla	Premolar	PD_SEEN	5	-1	OHL PQ03196	32.452	2.9	24.683	325.027	1	366	1	0	1	1
MS04595	M	09/04/2004	Dallas	208	Left	Maxilla	Premolar	PD_SEEN	5	-1	OHL PQ03196	34.221	0.9	25.340	211.705	2	366	1	0	1	1
MS04595	M	09/04/2004	Dallas	208	Left	Maxilla	Premolar	PD_SEEN	5	-1	OHL PQ03196	31.913	4.1	25.742	162.898	3	366	1	1	1	1
MS04648	M	10/12/2005	Winston	408	Right	Manible	Premolar	PD_SEEN	48	-1	OHL PQ03223		1.0	26.799	81.711	1	279	0	0	1	1
MS04648	M	10/12/2005	Winston	408	Right	Manible	Premolar	PD_SEEN	48	-1	OHL PQ03223	30.545	9.9	26.529	97.422	2	279	1	1	1	1
MS04648	M	10/12/2005	Winston	408	Right	Manible	Premolar	PD_SEEN	48	-1	OHL PQ03223	29.707	16.9	26.212	119.798	3	279	1	1	1	1
MS04645	F	10/12/2005	Mimi	409	Right	Manible	Molar	PD_SEEN	47	0	OHL PQ03240	35.553	0.4	26.260	116.108	1	279	1	0	1	1
MS04645	F	10/12/2005	Mimi	409	Right	Manible	Molar	PD_SEEN	47	0	OHL PQ03240	31.926	4.1	27.058	68.993	2	279	1	1	1	1
MS04645	F	10/12/2005	Mimi	409	Right	Manible	Molar	PD_SEEN	47	0	OHL PQ03240		1.0	26.257	116.376	3	279	0	0	1	1
MS04645	F	10/12/2005	Mimi	209	Left	Maxilla	Molar	NO_PD	47	0	OHL PQ03245		1.0	27.959	38.303	1	279	0	0	1	1
MS04645	F	10/12/2005	Mimi	209	Left	Maxilla	Molar	NO_PD	47	0	OHL PQ03245	34.720	0.7	26.868	78.110	2	279	1	0	1	1
MS04645	F	10/12/2005	Mimi	209	Left	Maxilla	Molar	NO_PD	47	0	OHL PQ03245	31.348	5.9	27.481	52.355	3	279	1	1	1	1
MS04643	F	10/12/2005	Faith	108	Right	Maxilla	Premolar	NO_PD	46	0	OHL PQ03284	32.841	2.3	25.865	150.264	1	279	1	0	1	1
MS04643	F	10/12/2005	Faith	108	Right	Maxilla	Premolar	NO_PD	46	0	OHL PQ03284		1.0	25.403	203.211	2	279	0	0	1	1
MS04643	F	10/12/2005	Faith	108	Right	Maxilla	Premolar	NO_PD	46	0	OHL PQ03284		1.0	26.630	91.226	3	279	0	0	1	1
MS04643	F	10/12/2005	Faith	408	Right	Manible	Premolar	PD_SEEN	46	0	OHL PQ03287	30.162	12.7	24.948	273.482	1	279	1	1	1	1
MS04643	F	10/12/2005	Faith	408	Right	Manible	Premolar	PD_SEEN	46	0	OHL PQ03287		1.0	25.070	252.601	2	279	0	0	1	1
MS04643	F	10/12/2005	Faith	408	Right	Manible	Premolar	PD_SEEN	46	0	OHL PQ03287		1.0	24.408	389.138	3	279	0	0	1	1
MS04643	F	10/12/2005	Faith	207	Left	Maxilla	Premolar	NO_PD	45	0	OHL PQ03291		1.0	23.343	779.809	1	279	0	0	1	1
MS04643	F	10/12/2005	Faith	207	Left	Maxilla	Premolar	NO_PD	45	0	OHL PQ03291	33.743	1.3	23.316	793.440	2	279	1	0	1	1
MS04643	F	10/12/2005	Faith	207	Left	Maxilla	Premolar	NO_PD	45	0	OHL PQ03291	34.612	0.7	22.792	1116.810	3	279	1	0	1	1
MS04643	F	10/12/2005	Faith	308	Left	Manible	Premolar	PD_SEEN	45	0	OHL PQ03295	34.353	0.9	27.175	63.923	1	279	1	0	1	1
MS04643	F	10/12/2005	Faith	308	Left	Manible	Premolar	PD_SEEN	45	0	OHL PQ03295		1.0	27.424	54.339	2	279	0	0	1	1
MS04643	F	10/12/2005	Faith	308	Left	Manible	Premolar	PD_SEEN	45	0	OHL PQ03295	31.662	4.9	27.238	61.344	3	279	1	1	1	1
MS04714	M	10/05/2006	Eddie	409	Right	Manible	Molar	PD_SEEN	55	-2	OHL PQ03304	33.057	2.0	28.057	35.952	1	257	1	0	1	1
MS04714	M	10/05/2006	Eddie	409	Right	Manible	Molar	PD_SEEN	55	-2	OHL PQ03304	31.891	4.2		1.000	2	257	1	1	0	0
MS04714	M	10/05/2006	Eddie	409	Right	Manible	Molar	PD_SEEN	55	-2	OHL PQ03304	34.767	0.7	30.097	9.488	3	257	1	0	1	1
MS04714	M	10/05/2006	Eddie	209	Left	Maxilla	Molar	NO_PD	55	-2	OHL PQ03309	35.065	0.6	30.718	6.330	1	257	1	0	1	1
MS04714	M	10/05/2006	Eddie	209	Left	Maxilla	Molar	NO_PD	55	-2	OHL PQ03309	31.523	5.3	29.620	12.957	2	257	1	1	1	1
MS04714	M	10/05/2006	Eddie	209	Left	Maxilla	Molar	NO_PD	55	-2	OHL PQ03309		1.0	29.221	16.808	3	257	0	0	1	1
MS04715	F	10/05/2006	Edna	209	Left	Maxilla	Molar	NO_PD	56	-1	OHL PQ03325	29.500	19.3	25.678	169.772	1	257	1	1	1	1
MS04715	F	10/05/2006	Edna	209	Left	Maxilla	Molar	NO_PD	56	-1	OHL PQ03325	30.251	12.0	24.432	382.902	2	257	1	1	1	1
MS04715	F	10/05/2006	Edna	209	Left	Maxilla	Molar	NO_PD	56	-1	OHL PQ03325	29.131	24.5	25.311	215.722	3	257	1	1	1	1
MS04715	F	10/05/2006	Edna	309	Left	Manible	Molar	PD_SEEN	56	-1	OHL PQ03328	25.462	255.5	24.416	386.955	1	257	1	1	1	1
MS04715	F	10/05/2006	Edna	309	Left	Manible	Molar	PD_SEEN	56	-1	OHL PQ03328	25.255	291.6	23.869	553.030	2	257	1	1	1	1
MS04715	F	10/05/2006	Edna	309	Left	Manible	Molar	PD_SEEN	56	-1	OHL PQ03328	24.968	350.3	24.411	388.311	3	257	1	1	1	1
MS04846	M	13/09/2007	Jigsaw	109	Right	Maxilla	Molar	NO_PD	8	-1	OHL PQ03365		1.0	32.889	1.535	1	187	0	0	1	0
MS04846	M	13/09/2007	Jigsaw	109	Right	Maxilla	Molar	NO_PD	8	-1	OHL PQ03365		1.0	32.050	2.653	2	187	0	0	1	0
MS04846	M	13/09/2007	Jigsaw	109	Right	Maxilla	Molar	NO_PD	8	-1	OHL PQ03365		1.0	33.845	0.822	3	187	0	0	1	0
MS04846	M	13/09/2007	Jigsaw	408	Right	Manible	Premolar	PD_SEEN	58	0	OHL PQ03367	31.419	5.7	19.948	7147.069	1	187	1	1	1	1
MS04846	M	13/09/2007	Jigsaw	408	Right	Manible	Premolar	PD_SEEN	58	0	OHL PQ03367		1.0	19.941	7180.993	2	187	0	0	1	1
MS04846	M	13/09/2007	Jigsaw	408	Right	Manible	Premolar	PD_SEEN	58	0	OHL PQ03367		1.0	20.058	6653.412	3	187	0	0	1	1
MS04846	M	13/09/2007	Jigsaw	207	Left	Maxilla	Premolar	NO_PD	58	0	OHL PQ03371	30.090	13.3	26.604	92.755	1	187	1	1	1	1

MS04846	M	13/09/2007	Jigsaw	207	Left	Maxilla	Premolar	NO_PD	58	0	OHL PQ03371	34.447	0.8	25.756	161.339	2	187	1	0	1	1
MS04846	M	13/09/2007	Jigsaw	207	Left	Maxilla	Premolar	NO_PD	58	0	OHL PQ03371	29.029	26.1	25.249	224.728	3	187	1	1	1	1
MS04846	M	13/09/2007	Jigsaw	209	Left	Maxilla	Molar	PD_SEEN	8	-1	OHL PQ03373	31.024	7.3	24.992	265.789	1	187	1	1	1	1
MS04846	M	13/09/2007	Jigsaw	209	Left	Maxilla	Molar	PD_SEEN	8	-1	OHL PQ03373	34.156	1.0	24.920	278.430	2	187	1	0	1	1
MS04846	M	13/09/2007	Jigsaw	209	Left	Maxilla	Molar	PD_SEEN	8	-1	OHL PQ03373		1.0	25.051	255.599	3	187	0	0	1	1
MS04561	M	23/06/2004	Arnie	103	Right	Maxilla	Incisor	NO_PD	2	0	OHL PQ03377	31.240	6.4	34.365	0.586	1	355	1	1	1	0
MS04561	M	23/06/2004	Arnie	103	Right	Maxilla	Incisor	NO_PD	2	0	OHL PQ03377		1.0	33.966	0.760	2	355	0	0	1	0
MS04561	M	23/06/2004	Arnie	103	Right	Maxilla	Incisor	NO_PD	2	0	OHL PQ03377	31.261	6.3		1.000	3	355	1	1	0	0
MS04561	M	23/06/2004	Arnie	107	Right	Maxilla	Premolar	PD_SEEN	40	-1	OHL PQ03379	22.523	1673.0	32.910	1.513	1	355	1	1	1	0
MS04561	M	23/06/2004	Arnie	107	Right	Maxilla	Premolar	PD_SEEN	40	-1	OHL PQ03379	22.657	1535.7		1.000	2	355	1	1	0	0
MS04561	M	23/06/2004	Arnie	107	Right	Maxilla	Premolar	PD_SEEN	40	-1	OHL PQ03379	22.710	1483.9	31.932	2.865	3	355	1	1	1	0
MS04561	M	23/06/2004	Arnie	208	Left	Maxilla	Premolar	NO_PD	40	-1	OHL PQ03388	23.828	726.0	24.877	286.435	1	355	1	1	1	1
MS04561	M	23/06/2004	Arnie	208	Left	Maxilla	Premolar	NO_PD	40	-1	OHL PQ03388	23.634	822.3	25.340	211.783	2	355	1	1	1	1
MS04561	M	23/06/2004	Arnie	208	Left	Maxilla	Premolar	NO_PD	40	-1	OHL PQ03388	23.527	880.4	25.251	224.460	3	355	1	1	1	1
MS05108	F	08/02/2009	Whoopee	109	Right	Maxilla	Molar	NO_PD	21	-1	OHL PQ03461	29.440	20.1	31.809	3.105	1	114	1	1	1	0
MS05108	F	08/02/2009	Whoopee	109	Right	Maxilla	Molar	NO_PD	21	-1	OHL PQ03461	35.289	0.5	29.358	15.375	2	114	1	0	1	1
MS05108	F	08/02/2009	Whoopee	109	Right	Maxilla	Molar	NO_PD	21	-1	OHL PQ03461	29.721	16.8	31.671	3.397	3	114	1	1	1	0
MS05108	F	08/02/2009	Whoopee	209	Left	Maxilla	Molar	PD_SEEN	21	-1	OHL PQ03469	33.031	2.0		1.000	1	114	1	0	0	0
MS05108	F	08/02/2009	Whoopee	209	Left	Maxilla	Molar	PD_SEEN	21	-1	OHL PQ03469		1.0		1.000	2	114	0	0	0	0
MS05108	F	08/02/2009	Whoopee	209	Left	Maxilla	Molar	PD_SEEN	21	-1	OHL PQ03469	29.682	17.2		1.000	3	114	1	1	0	0
MS05116	M	08/05/2009	Yankee	208	Left	Maxilla	Premolar	NO_PD	26	-1	OHL PQ03484	32.058	3.8	27.016	70.904	1	101	1	1	1	1
MS05116	M	08/05/2009	Yankee	208	Left	Maxilla	Premolar	NO_PD	26	-1	OHL PQ03484	32.286	3.3	26.916	75.672	2	101	1	0	1	1
MS05116	M	08/05/2009	Yankee	208	Left	Maxilla	Premolar	NO_PD	26	-1	OHL PQ03484	31.679	4.8	26.387	106.906	3	101	1	1	1	1
MS05120	F	08/05/2009	Yetti	203	Left	Maxilla	Incisor	NO_PD	28	0	OHL PQ03497	30.963	7.6	31.928	2.873	1	101	1	1	1	0
MS05120	F	08/05/2009	Yetti	203	Left	Maxilla	Incisor	NO_PD	28	0	OHL PQ03497	30.050	13.6	31.704	3.325	2	101	1	1	1	0
MS05120	F	08/05/2009	Yetti	203	Left	Maxilla	Incisor	NO_PD	28	0	OHL PQ03497		1.0	32.112	2.547	3	101	0	0	1	0
MS04929	M	05/01/2008	Norris	103	Right	Maxilla	Incisor	NO_PD	10	-4	OHL PQ03537	30.442	10.6	27.960	38.292	1	171	1	1	1	1
MS04929	M	05/01/2008	Norris	103	Right	Maxilla	Incisor	NO_PD	10	-4	OHL PQ03537		1.0	29.925	10.617	2	171	0	0	1	1
MS04929	M	05/01/2008	Norris	103	Right	Maxilla	Incisor	NO_PD	10	-4	OHL PQ03537		1.0	29.527	13.766	3	171	0	0	1	1
MS04929	M	05/01/2008	Norris	408	Right	Manible	Premolar	NO_PD	13	-5	OHL PQ03543	32.681	2.5	22.581	1281.837	1	171	1	0	1	1
MS04929	M	05/01/2008	Norris	408	Right	Manible	Premolar	NO_PD	13	-5	OHL PQ03543		1.0	23.678	626.304	2	171	0	0	1	1
MS04929	M	05/01/2008	Norris	408	Right	Manible	Premolar	NO_PD	13	-5	OHL PQ03543		1.0		1.000	3	171	0	0	0	0
MS04929	M	05/01/2008	Norris	409	Right	Manible	Molar	NO_PD	14	-4	OHL PQ03544		1.0	25.626	175.716	1	171	0	0	1	1
MS04929	M	05/01/2008	Norris	409	Right	Manible	Molar	NO_PD	14	-4	OHL PQ03544	36.475	0.2	25.552	184.319	2	171	1	0	1	1
MS04929	M	05/01/2008	Norris	409	Right	Manible	Molar	NO_PD	14	-4	OHL PQ03544		1.0	25.530	186.972	3	171	0	0	1	1
MS04929	M	05/01/2008	Norris	203	Left	Maxilla	Incisor	PD_SEEN	10	-4	OHL PQ03545		1.0	30.110	9.413	1	171	0	0	1	1
MS04929	M	05/01/2008	Norris	203	Left	Maxilla	Incisor	PD_SEEN	10	-4	OHL PQ03545	36.047	0.3		1.000	2	171	1	0	0	0
MS04929	M	05/01/2008	Norris	203	Left	Maxilla	Incisor	PD_SEEN	10	-4	OHL PQ03545	35.074	0.5	33.183	1.266	3	171	1	0	1	0
MS04929	M	05/01/2008	Norris	308	Left	Manible	Premolar	PD_SEEN	13	-5	OHL PQ03551	32.927	2.2	30.204	8.849	1	171	1	0	1	1
MS04929	M	05/01/2008	Norris	308	Left	Manible	Premolar	PD_SEEN	13	-5	OHL PQ03551	32.507	2.8	32.216	2.380	2	171	1	0	1	0
MS04929	M	05/01/2008	Norris	308	Left	Manible	Premolar	PD_SEEN	13	-5	OHL PQ03551	35.667	0.4	30.119	9.359	3	171	1	0	1	1
MS05107	F	08/02/2009	Willow	408	Right	Manible	Premolar	NO_PD	61	0	OHL PQ03575	26.327	147.0		1.000	1	114	1	1	0	0
MS05107	F	08/02/2009	Willow	408	Right	Manible	Premolar	NO_PD	61	0	OHL PQ03575	26.163	163.2	29.985	10.208	2	114	1	1	1	1
MS05107	F	08/02/2009	Willow	408	Right	Manible	Premolar	NO_PD	61	0	OHL PQ03575	26.226	156.8	32.350	2.181	3	114	1	1	1	0
MS05107	F	08/02/2009	Willow	208	Left	Maxilla	Premolar	PD_SEEN	61	0	OHL PQ03580	28.747	31.3	26.999	71.700	1	114	1	1	1	1
MS05107	F	08/02/2009	Willow	208	Left	Maxilla	Premolar	PD_SEEN	61	0	OHL PQ03580	27.115	88.8	27.562	49.663	2	114	1	1	1	1
MS05107	F	08/02/2009	Willow	208	Left	Maxilla	Premolar	PD_SEEN	61	0	OHL PQ03580	27.835	56.0	28.951	20.046	3	114	1	1	1	1
MS05115	F	08/05/2009	Yoyo	203	Left	Maxilla	Incisor	PD_SEEN	25	-1	OHL PQ03593		1.0		1.000	1	101	0	0	0	0
MS05115	F	08/05/2009	Yoyo	203	Left	Maxilla	Incisor	PD_SEEN	25	-1	OHL PQ03593		1.0		1.000	2	101	0	0	0	0
MS05115	F	08/05/2009	Yoyo	203	Left	Maxilla	Incisor	PD_SEEN	25	-1	OHL PQ03593	27.031	93.7	30.497	7.312	3	101	1	1	1	1
MS04559	F	23/06/2004	Halle	409	Right	Manible	Molar	PD_SEEN	1	-1	OHL PQ03624	24.826	383.8	25.006	263.363	1	355	1	1	1	1
MS04559	F	23/06/2004	Halle	409	Right	Manible	Molar	PD_SEEN	1	-1	OHL PQ03624	25.722	216.3	24.564	351.356	2	355	1	1	1	1
MS04559	F	23/06/2004	Halle	409	Right	Manible	Molar	PD_SEEN	1	-1	OHL PQ03624	25.426	261.5	25.272	221.380	3	355	1	1	1	1
MS04559	F	23/06/2004	Halle	309	Left	Manible	Molar	NO_PD	1	-1	OHL PQ03632	28.816	29.9	33.562	0.989	1	355	1	1	1	0

MS04559	F	23/06/2004	Halle	309	Left	Manible	Molar	NO_PD	1	-1	OHL PQ03632	28.395	39.2	30.433	7.621	2	355	1	1	1	1
MS04559	F	23/06/2004	Halle	309	Left	Manible	Molar	NO_PD	1	-1	OHL PQ03632	28.305	41.5		1.000	3	355	1	1	0	0
MS05031	F	26/01/2009	Violet	308	Left	Manible	Premolar	PD_SEEN	18	-2	OHL PQ03723		1.0	28.183	33.100	1	116	0	0	1	1
MS05031	F	26/01/2009	Violet	308	Left	Manible	Premolar	PD_SEEN	18	-2	OHL PQ03723		1.0	28.099	34.960	2	116	0	0	1	1
MS05031	F	26/01/2009	Violet	308	Left	Manible	Premolar	PD_SEEN	18	-2	OHL PQ03723	31.463	5.5	27.112	66.579	3	116	1	1	1	1
MS05031	F	26/01/2009	Violet	408	Right	Manible	Premolar	NO_PD	18	-2	OHL PQ03724	35.012	0.6	26.312	112.265	1	116	1	0	1	1
MS05031	F	26/01/2009	Violet	408	Right	Manible	Premolar	NO_PD	18	-2	OHL PQ03724	33.300	1.7	26.563	95.281	2	116	1	0	1	1
MS05031	F	26/01/2009	Violet	408	Right	Manible	Premolar	NO_PD	18	-2	OHL PQ03724		1.0	27.478	52.446	3	116	0	0	1	1
MS05114	F	08/05/2009	Yasmine	207	Left	Maxilla	Premolar	NO_PD	63	-2	OHL PQ03752	32.095	3.7	33.853	0.817	1	101	1	1	1	0
MS05114	F	08/05/2009	Yasmine	207	Left	Maxilla	Premolar	NO_PD	63	-2	OHL PQ03752	32.956	2.1	30.473	7.424	2	101	1	0	1	1
MS05114	F	08/05/2009	Yasmine	207	Left	Maxilla	Premolar	NO_PD	63	-2	OHL PQ03752		1.0	29.351	15.443	3	101	0	0	1	1
MS05114	F	08/05/2009	Yasmine	308	Left	Manible	Premolar	PD_SEEN	63	-2	OHL PQ03755	30.806	8.4	26.608	92.557	1	101	1	1	1	1
MS05114	F	08/05/2009	Yasmine	308	Left	Manible	Premolar	PD_SEEN	63	-2	OHL PQ03755		2.9	27.516	51.156	2	101	1	0	1	1
MS05114	F	08/05/2009	Yasmine	308	Left	Manible	Premolar	PD_SEEN	63	-2	OHL PQ03755	31.761	4.6	27.771	43.317	3	101	1	1	1	1
MS05114	F	08/05/2009	Yasmine	209	Left	Maxilla	Molar	NO_PD	64	-2	OHL PQ03758	34.863	0.6	32.985	1.441	1	101	1	0	1	0
MS05114	F	08/05/2009	Yasmine	209	Left	Maxilla	Molar	NO_PD	64	-2	OHL PQ03758		1.0	31.731	3.266	2	101	0	0	1	0
MS05114	F	08/05/2009	Yasmine	209	Left	Maxilla	Molar	NO_PD	64	-2	OHL PQ03758		1.0	33.268	1.198	3	101	0	0	1	0
MS05151	F	03/12/2010	Bramble	208	Left	Maxilla	Premolar	NO_PD	69	-2	OHL PQ03770	30.172	12.6	25.083	250.351	1	19	1	1	1	1
MS05151	F	03/12/2010	Bramble	208	Left	Maxilla	Premolar	NO_PD	69	-2	OHL PQ03770		1.0	25.982	139.272	2	19	0	0	1	1
MS05151	F	03/12/2010	Bramble	208	Left	Maxilla	Premolar	NO_PD	69	-2	OHL PQ03770		1.0	25.538	186.072	3	19	0	0	1	1
MS05151	F	03/12/2010	Bramble	408	Right	Manible	Premolar	PD_SEEN	69	-2	OHL PQ03772		1.0	34.035	0.726	1	19	0	0	1	0
MS05151	F	03/12/2010	Bramble	408	Right	Manible	Premolar	PD_SEEN	69	-2	OHL PQ03772	34.002	1.1	34.614	0.498	2	19	1	0	1	0
MS05151	F	03/12/2010	Bramble	408	Right	Manible	Premolar	PD_SEEN	69	-2	OHL PQ03772	34.401	0.8		1.000	3	19	1	0	0	0
MS05152	M	03/12/2010	Bentley	108	Right	Maxilla	Premolar	NO_PD	33	0	OHL PQ03785		1.0	25.805	156.280	1	19	0	0	1	1
MS05152	M	03/12/2010	Bentley	108	Right	Maxilla	Premolar	NO_PD	33	0	OHL PQ03785	33.818	1.2	25.075	251.712	2	19	1	0	1	1
MS05152	M	03/12/2010	Bentley	108	Right	Maxilla	Premolar	NO_PD	33	0	OHL PQ03785		1.6	24.892	283.608	3	19	1	0	1	1
MS05152	M	03/12/2010	Bentley	208	Left	Maxilla	Premolar	PD_SEEN	33	0	OHL PQ03786	33.255	1.8	28.647	24.461	1	19	1	0	1	1
MS05152	M	03/12/2010	Bentley	208	Left	Maxilla	Premolar	PD_SEEN	33	0	OHL PQ03786	34.006	1.1	30.644	6.642	2	19	1	0	1	1
MS05152	M	03/12/2010	Bentley	208	Left	Maxilla	Premolar	PD_SEEN	33	0	OHL PQ03786	34.330	0.9		1.000	3	19	1	0	0	0
MS05152	M	03/12/2010	Bentley	309	Left	Manible	Molar	PD_SEEN	34	-5	OHL PQ03791		1.0	26.790	82.148	1	19	0	0	1	1
MS05152	M	03/12/2010	Bentley	309	Left	Manible	Molar	PD_SEEN	34	-5	OHL PQ03791	34.138	1.0	26.382	107.260	2	19	1	0	1	1
MS05152	M	03/12/2010	Bentley	309	Left	Manible	Molar	PD_SEEN	34	-5	OHL PQ03791		1.0	26.974	72.867	3	19	0	0	1	1
MS05152	M	03/12/2010	Bentley	409	Right	Manible	Molar	NO_PD	34	-5	OHL PQ03792	31.101	6.9	34.363	0.586	1	19	1	1	1	0
MS05152	M	03/12/2010	Bentley	409	Right	Manible	Molar	NO_PD	34	-5	OHL PQ03792		1.0	30.365	7.969	2	19	0	0	1	1
MS05152	M	03/12/2010	Bentley	409	Right	Manible	Molar	NO_PD	34	-5	OHL PQ03792	34.305	0.9	31.198	4.626	3	19	1	0	1	1
MS05156	M	03/12/2010	Brock	108	Right	Maxilla	Premolar	NO_PD	35	-4	OHL PQ03801	31.128	6.8		1.000	1	19	1	1	0	0
MS05156	M	03/12/2010	Brock	108	Right	Maxilla	Premolar	NO_PD	35	-4	OHL PQ03801		1.0		1.000	2	19	0	0	0	0
MS05156	M	03/12/2010	Brock	108	Right	Maxilla	Premolar	NO_PD	35	-4	OHL PQ03801	30.175	12.6	32.476	2.008	3	19	1	1	1	0
MS05156	M	03/12/2010	Brock	208	Left	Maxilla	Premolar	PD_SEEN	35	-4	OHL PQ03802		1.0	32.606	1.845	1	19	0	0	1	0
MS05156	M	03/12/2010	Brock	208	Left	Maxilla	Premolar	PD_SEEN	35	-4	OHL PQ03802		1.0	30.990	5.299	2	19	0	0	1	1
MS05156	M	03/12/2010	Brock	208	Left	Maxilla	Premolar	PD_SEEN	35	-4	OHL PQ03802	32.122	3.6	35.429	0.292	3	19	1	1	1	0
MS05158	F	15/01/2010	Connie	308	Left	Manible	Premolar	PD_SEEN	36	-5	OHL PQ03819		1.0		1.000	1	65	0	0	0	0
MS05158	F	15/01/2010	Connie	308	Left	Manible	Premolar	PD_SEEN	36	-5	OHL PQ03819	34.370	0.9	31.476	3.858	2	65	1	0	1	0
MS05158	F	15/01/2010	Connie	308	Left	Manible	Premolar	PD_SEEN	36	-5	OHL PQ03819		1.0		1.000	3	65	0	0	0	0
MS05158	F	15/01/2010	Connie	408	Right	Manible	Premolar	NO_PD	36	-5	OHL PQ03820	30.019	13.9	31.090	4.964	1	65	1	1	1	1
MS05158	F	15/01/2010	Connie	408	Right	Manible	Premolar	NO_PD	36	-5	OHL PQ03820	31.087	7.0		1.000	2	65	1	1	0	0
MS05158	F	15/01/2010	Connie	408	Right	Manible	Premolar	NO_PD	36	-5	OHL PQ03820	35.455	0.4	28.873	21.104	3	65	1	0	1	1
MS05158	F	15/01/2010	Connie	309	Left	Manible	Molar	PD_SEEN	37	0	OHL PQ03823		1.0	26.209	120.099	1	65	0	0	1	1
MS05158	F	15/01/2010	Connie	309	Left	Manible	Molar	PD_SEEN	37	0	OHL PQ03823	35.885	0.3	25.266	222.192	2	65	1	0	1	1
MS05158	F	15/01/2010	Connie	309	Left	Manible	Molar	PD_SEEN	37	0	OHL PQ03823		1.0	25.405	202.909	3	65	0	0	1	1
MS05158	F	15/01/2010	Connie	409	Right	Manible	Molar	NO_PD	37	0	OHL PQ03824	30.833	8.2	25.790	157.819	1	65	1	1	1	1
MS05158	F	15/01/2010	Connie	409	Right	Manible	Molar	NO_PD	37	0	OHL PQ03824		1.0	25.980	139.449	2	65	0	0	1	1
MS05158	F	15/01/2010	Connie	409	Right	Manible	Molar	NO_PD	37	0	OHL PQ03824	30.890	7.9	26.117	127.491	3	65	1	1	1	1
MS05163	M	15/01/2010	Chesney	108	Right	Maxilla	Premolar	NO_PD	71	-3	OHL PQ03849	29.735	16.6	25.743	162.718	1	65	1	1	1	1

MS05163	M	15/01/2010	Chesney	108	Right	Maxilla	Premolar	NO_PD	71	-3	OHL PQ03849	27.813	56.8	25.875	149.334	2	65	1	1	1	1
MS05163	M	15/01/2010	Chesney	108	Right	Maxilla	Premolar	NO_PD	71	-3	OHL PQ03849	30.032	13.8	26.675	88.555	3	65	1	1	1	1
MS05163	M	15/01/2010	Chesney	408	Right	Manible	Premolar	PD_SEEN	71	-3	OHL PQ03852	26.496	131.9	25.804	156.407	1	65	1	1	1	1
MS05163	M	15/01/2010	Chesney	408	Right	Manible	Premolar	PD_SEEN	71	-3	OHL PQ03852	25.799	206.0	25.582	180.736	2	65	1	1	1	1
MS05163	M	15/01/2010	Chesney	408	Right	Manible	Premolar	PD_SEEN	71	-3	OHL PQ03852	26.199	159.4	24.870	287.778	3	65	1	1	1	1
MS04923	F	05/01/2008	Nettie	108	Right	Maxilla	Premolar	NO_PD	9	0	OHL PQ03881	26.216	157.7	30.841	5.841	1	171	1	1	1	1
MS04923	F	05/01/2008	Nettie	108	Right	Maxilla	Premolar	NO_PD	9	0	OHL PQ03881	26.535	128.7	30.718	6.327	2	171	1	1	1	1
MS04923	F	05/01/2008	Nettie	108	Right	Maxilla	Premolar	NO_PD	9	0	OHL PQ03881	26.253	154.1	27.847	41.227	3	171	1	1	1	1
MS04923	F	05/01/2008	Nettie	208	Left	Maxilla	Premolar	PD_SEEN	9	0	OHL PQ03882	25.816	203.7	31.348	4.195	1	171	1	1	1	1
MS04923	F	05/01/2008	Nettie	208	Left	Maxilla	Premolar	PD_SEEN	9	0	OHL PQ03882	26.057	174.7	30.878	5.701	2	171	1	1	1	1
MS04923	F	05/01/2008	Nettie	208	Left	Maxilla	Premolar	PD_SEEN	9	0	OHL PQ03882	26.227	156.7	29.109	18.089	3	171	1	1	1	1
MS04930	F	05/01/2008	Niamh	308	Left	Manible	Premolar	PD_SEEN	15	-4	OHL PQ03915	25.649	226.6	33.411	1.091	1	171	1	1	1	0
MS04930	F	05/01/2008	Niamh	308	Left	Manible	Premolar	PD_SEEN	15	-4	OHL PQ03915	25.935	188.9	33.288	1.183	2	171	1	1	1	0
MS04930	F	05/01/2008	Niamh	308	Left	Manible	Premolar	PD_SEEN	15	-4	OHL PQ03915	25.917	191.0	32.191	2.419	3	171	1	1	1	0
MS04930	F	05/01/2008	Niamh	408	Right	Manible	Premolar	NO_PD	15	-4	OHL PQ03916	27.430	72.6	26.154	124.499	1	171	1	1	1	1
MS04930	F	05/01/2008	Niamh	408	Right	Manible	Premolar	NO_PD	15	-4	OHL PQ03916	26.645	119.9	27.244	61.093	2	171	1	1	1	1
MS04930	F	05/01/2008	Niamh	408	Right	Manible	Premolar	NO_PD	15	-4	OHL PQ03916	26.393	140.9	26.699	87.229	3	171	1	1	1	1
MS05109	M	08/02/2009	Wellington	409	Right	Manible	Molar	NO_PD	22	0	OHL PQ03928		1.0	30.194	8.908	1	114	0	0	1	1
MS05109	M	08/02/2009	Wellington	409	Right	Manible	Molar	NO_PD	22	0	OHL PQ03928		1.0	29.206	16.973	2	114	0	0	1	1
MS05109	M	08/02/2009	Wellington	409	Right	Manible	Molar	NO_PD	22	0	OHL PQ03928	33.875	1.2	28.950	20.063	3	114	1	0	1	1
MS05109	M	08/02/2009	Wellington	309	Left	Manible	Molar	PD_SEEN	22	0	OHL PQ03936	33.872	1.2	30.270	8.476	1	114	1	0	1	1
MS05109	M	08/02/2009	Wellington	309	Left	Manible	Molar	PD_SEEN	22	0	OHL PQ03936	32.974	2.1	33.680	0.916	2	114	1	0	1	0
MS05109	M	08/02/2009	Wellington	309	Left	Manible	Molar	PD_SEEN	22	0	OHL PQ03936		1.0	29.469	14.303	3	114	0	0	1	1
MS05118	M	08/05/2009	Yoshi	104	Right	Maxilla	Canine	PD_SEEN	66	-4	OHL PQ03954	29.969	14.3	32.539	1.927	1	101	1	1	1	0
MS05118	M	08/05/2009	Yoshi	104	Right	Maxilla	Canine	PD_SEEN	66	-4	OHL PQ03954	29.181	23.7	34.445	0.556	2	101	1	1	1	0
MS05118	M	08/05/2009	Yoshi	104	Right	Maxilla	Canine	PD_SEEN	66	-4	OHL PQ03954	27.229	82.6	31.353	4.181	3	101	1	1	1	1
MS05118	M	08/05/2009	Yoshi	404	Right	Manible	Canine	NO_PD	67	-4	OHL PQ03958	28.948	27.5	33.719	0.892	1	101	1	1	1	0
MS05118	M	08/05/2009	Yoshi	404	Right	Manible	Canine	NO_PD	67	-4	OHL PQ03958	29.261	22.5	31.849	3.025	2	101	1	1	1	0
MS05118	M	08/05/2009	Yoshi	404	Right	Manible	Canine	NO_PD	67	-4	OHL PQ03958	27.527	68.2	30.354	8.027	3	101	1	1	1	1
MS05118	M	08/05/2009	Yoshi	408	Right	Manible	Premolar	NO_PD	27	0	OHL PQ03959	22.890	1322.7	24.569	350.238	1	101	1	1	1	1
MS05118	M	08/05/2009	Yoshi	408	Right	Manible	Premolar	NO_PD	27	0	OHL PQ03959	22.933	1286.8	25.503	190.338	2	101	1	1	1	1
MS05118	M	08/05/2009	Yoshi	408	Right	Manible	Premolar	NO_PD	27	0	OHL PQ03959	22.891	1322.2	24.650	332.220	3	101	1	1	1	1
MS05118	M	08/05/2009	Yoshi	204	Left	Maxilla	Canine	PD_SEEN	67	-4	OHL PQ03962	27.595	65.3	31.766	3.193	1	101	1	1	1	0
MS05118	M	08/05/2009	Yoshi	204	Left	Maxilla	Canine	PD_SEEN	67	-4	OHL PQ03962	28.351	40.3	34.498	0.537	2	101	1	1	1	0
MS05118	M	08/05/2009	Yoshi	204	Left	Maxilla	Canine	PD_SEEN	67	-4	OHL PQ03962	28.584	34.7	29.401	14.948	3	101	1	1	1	1
MS05118	M	08/05/2009	Yoshi	304	Left	Manible	Canine	NO_PD	66	-4	OHL PQ03966	27.895	53.9	29.655	12.666	1	101	1	1	1	1
MS05118	M	08/05/2009	Yoshi	304	Left	Manible	Canine	NO_PD	66	-4	OHL PQ03966	28.493	36.8	31.889	2.946	2	101	1	1	1	0
MS05118	M	08/05/2009	Yoshi	304	Left	Manible	Canine	NO_PD	66	-4	OHL PQ03966	26.218	157.5	32.865	1.558	3	101	1	1	1	0
MS05118	M	08/05/2009	Yoshi	308	Left	Manible	Premolar	PD_SEEN	27	0	OHL PQ03967	24.786	393.6	24.097	476.583	1	101	1	1	1	1
MS05118	M	08/05/2009	Yoshi	308	Left	Manible	Premolar	PD_SEEN	27	0	OHL PQ03967	25.695	220.2	24.010	504.408	2	101	1	1	1	1
MS05118	M	08/05/2009	Yoshi	308	Left	Manible	Premolar	PD_SEEN	27	0	OHL PQ03967	25.312	281.3	24.544	356.019	3	101	1	1	1	1
MS04599	M	09/04/2004	Rooney	108	Right	Maxilla	Premolar	PD_SEEN	6	0	OHL PQ03988	31.150	6.7		1.000	1	366	1	1	0	0
MS04599	M	09/04/2004	Rooney	108	Right	Maxilla	Premolar	PD_SEEN	6	0	OHL PQ03988	35.259	0.5	33.600	0.965	2	366	1	0	1	0
MS04599	M	09/04/2004	Rooney	108	Right	Maxilla	Premolar	PD_SEEN	6	0	OHL PQ03988	34.244	0.9	32.370	2.153	3	366	1	0	1	0
MS04599	M	09/04/2004	Rooney	208	Left	Maxilla	Premolar	NO_PD	6	0	OHL PQ03996	31.301	6.1	29.512	13.902	1	366	1	1	1	1
MS04599	M	09/04/2004	Rooney	208	Left	Maxilla	Premolar	NO_PD	6	0	OHL PQ03996		1.0	32.374	2.147	2	366	0	0	1	0
MS04599	M	09/04/2004	Rooney	208	Left	Maxilla	Premolar	NO_PD	6	0	OHL PQ03996	33.409	1.6	31.168	4.716	3	366	1	0	1	1
MS05164	M	15/01/2010	Colin	204	Left	Maxilla	Canine	NO_PD	38	-5	OHL PQ04002		1.0	31.205	4.606	1	65	0	0	1	1
MS05164	M	15/01/2010	Colin	204	Left	Maxilla	Canine	NO_PD	38	-5	OHL PQ04002	34.820	0.6		1.000	2	65	1	0	0	0
MS05164	M	15/01/2010	Colin	204	Left	Maxilla	Canine	NO_PD	38	-5	OHL PQ04002	30.226	12.1	27.792	42.738	3	65	1	1	1	1
MS05164	M	15/01/2010	Colin	207	Left	Maxilla	Premolar	PD_SEEN	72	-3	OHL PQ04010	32.821	2.3	34.908	0.411	1	65	1	0	1	0
MS05164	M	15/01/2010	Colin	207	Left	Maxilla	Premolar	PD_SEEN	72	-3	OHL PQ04010		1.0	35.295	0.319	2	65	0	0	1	0
MS05164	M	15/01/2010	Colin	207	Left	Maxilla	Premolar	PD_SEEN	72	-3	OHL PQ04010		1.0	35.261	0.326	3	65	0	0	1	0
MS05164	M	15/01/2010	Colin	308	Left	Manible	Premolar	NO_PD	72	-3	OHL PQ04036	33.630	1.4	21.228	3099.632	1	65	1	0	1	1

MS05164	M	15/01/2010	Colin	308	Left	Manible	Premolar	NO_PD	72	-3	OHLPQ04036	33.686	1.3	21.133	3297.599	2	65	1	0	1	1
MS05164	M	15/01/2010	Colin	308	Left	Manible	Premolar	NO_PD	72	-3	OHLPQ04036	35.566	0.4	21.468	2651.240	3	65	1	0	1	1
MS05164	M	15/01/2010	Colin	104	Right	Maxilla	Canine	PD_SEEN	38	-5	OHLPQ04044	31.460	5.5	22.969	995.099	1	65	1	1	1	1
MS05164	M	15/01/2010	Colin	104	Right	Maxilla	Canine	PD_SEEN	38	-5	OHLPQ04044	36.363	0.2	22.766	1136.140	2	65	1	0	1	1
MS05164	M	15/01/2010	Colin	104	Right	Maxilla	Canine	PD_SEEN	38	-5	OHLPQ04044		1.0	23.051	943.385	3	65	0	0	1	1
MS04595	M	09/04/2004	Dallas	108	Right	Maxilla	Premolar	NO_PD	5	0	OHLPQ04071		1.0	22.386	1455.818	1	366	0	0	1	1
MS04595	M	09/04/2004	Dallas	108	Right	Maxilla	Premolar	NO_PD	5	0	OHLPQ04071	32.655	2.6	22.526	1328.813	2	366	1	0	1	1
MS04595	M	09/04/2004	Dallas	108	Right	Maxilla	Premolar	NO_PD	5	0	OHLPQ04071	32.003	3.9	23.095	916.712	3	366	1	1	1	1
MS04648	M	10/12/2005	Winston	207	Left	Maxilla	Premolar	NO_PD	48	0	OHLPQ04075	36.347	0.2	31.516	3.760	1	279	1	0	1	0
MS04648	M	10/12/2005	Winston	207	Left	Maxilla	Premolar	NO_PD	48	0	OHLPQ04075	35.726	0.4	30.484	7.371	2	279	1	0	1	1
MS04648	M	10/12/2005	Winston	207	Left	Maxilla	Premolar	NO_PD	48	0	OHLPQ04075		1.0	30.242	8.634	3	279	0	0	1	1
MS04714	M	10/05/2006	Eddie	409	Right	Manible	Molar	PD_SEEN	55	-1	OHLPQ04136		1.0	1.000	1	257	0	0	0	0	0
MS04714	M	10/05/2006	Eddie	409	Right	Manible	Molar	PD_SEEN	55	-1	OHLPQ04136		1.0	29.986	10.203	2	257	0	0	1	1
MS04714	M	10/05/2006	Eddie	409	Right	Manible	Molar	PD_SEEN	55	-1	OHLPQ04136	33.885	1.2	1.000	3	257	1	0	0	0	0
MS04714	M	10/05/2006	Eddie	209	Left	Maxilla	Molar	NO_PD	55	-1	OHLPQ04141		1.0	31.974	2.788	1	257	0	0	1	0
MS04714	M	10/05/2006	Eddie	209	Left	Maxilla	Molar	NO_PD	55	-1	OHLPQ04141	31.176	6.6	32.091	2.583	2	257	1	1	1	0
MS04714	M	10/05/2006	Eddie	209	Left	Maxilla	Molar	NO_PD	55	-1	OHLPQ04141	35.833	0.3	29.752	11.888	3	257	1	0	1	1
MS04715	F	10/05/2006	Edna	209	Left	Maxilla	Molar	NO_PD	56	0	OHLPQ04189	34.635	0.7	1.000	1	257	1	0	0	0	0
MS04715	F	10/05/2006	Edna	209	Left	Maxilla	Molar	NO_PD	56	0	OHLPQ04189		1.0	1.000	2	257	0	0	0	0	0
MS04715	F	10/05/2006	Edna	209	Left	Maxilla	Molar	NO_PD	56	0	OHLPQ04189	34.390	0.8	33.474	1.047	3	257	1	0	1	0
MS04715	F	10/05/2006	Edna	309	Left	Manible	Molar	PD_SEEN	56	0	OHLPQ04192	23.819	730.4	24.703	320.814	1	257	1	1	1	1
MS04715	F	10/05/2006	Edna	309	Left	Manible	Molar	PD_SEEN	56	0	OHLPQ04192	23.529	879.2	25.277	220.588	2	257	1	1	1	1
MS04715	F	10/05/2006	Edna	309	Left	Manible	Molar	PD_SEEN	56	0	OHLPQ04192	23.624	827.3	24.976	268.559	3	257	1	1	1	1
MS04846	M	13/09/2007	Jigsaw	109	Right	Maxilla	Molar	NO_PD	8	0	OHLPQ04197		1.0	25.390	204.930	1	187	0	0	1	1
MS04846	M	13/09/2007	Jigsaw	109	Right	Maxilla	Molar	NO_PD	8	0	OHLPQ04197	33.458	1.5	25.061	254.012	2	187	1	0	1	1
MS04846	M	13/09/2007	Jigsaw	109	Right	Maxilla	Molar	NO_PD	8	0	OHLPQ04197	33.338	1.7	25.442	198.103	3	187	1	0	1	1
MS04846	M	13/09/2007	Jigsaw	209	Left	Maxilla	Molar	PD_SEEN	8	0	OHLPQ04205	34.863	0.6	22.267	1573.504	1	187	1	0	1	1
MS04846	M	13/09/2007	Jigsaw	209	Left	Maxilla	Molar	PD_SEEN	8	0	OHLPQ04205	34.664	0.7	22.425	1419.311	2	187	1	0	1	1
MS04846	M	13/09/2007	Jigsaw	209	Left	Maxilla	Molar	PD_SEEN	8	0	OHLPQ04205	30.096	13.2	22.458	1388.980	3	187	1	1	1	1
MS04561	M	23/06/2004	Arnie	107	Right	Maxilla	Premolar	PD_SEEN	40	0	OHLPQ04211	24.539	461.0	1.000	1	355	1	1	0	0	0
MS04561	M	23/06/2004	Arnie	107	Right	Maxilla	Premolar	PD_SEEN	40	0	OHLPQ04211	25.133	315.2	34.725	0.463	2	355	1	1	1	0
MS04561	M	23/06/2004	Arnie	107	Right	Maxilla	Premolar	PD_SEEN	40	0	OHLPQ04211	24.893	367.6	33.233	1.226	3	355	1	1	1	0
MS05108	F	08/02/2009	Whoopee	109	Right	Maxilla	Molar	NO_PD	21	0	OHLPQ04293	23.495	898.4	24.014	503.140	1	114	1	1	1	1
MS05108	F	08/02/2009	Whoopee	109	Right	Maxilla	Molar	NO_PD	21	0	OHLPQ04293	23.561	861.2	23.507	700.361	2	114	1	1	1	1
MS05108	F	08/02/2009	Whoopee	109	Right	Maxilla	Molar	NO_PD	21	0	OHLPQ04293	23.400	954.6	24.091	478.562	3	114	1	1	1	1
MS05108	F	08/02/2009	Whoopee	209	Left	Maxilla	Molar	PD_SEEN	21	0	OHLPQ04301	23.304	1015.4	26.044	133.765	1	114	1	1	1	1
MS05108	F	08/02/2009	Whoopee	209	Left	Maxilla	Molar	PD_SEEN	21	0	OHLPQ04301	23.367	975.0	25.314	215.285	2	114	1	1	1	1
MS05108	F	08/02/2009	Whoopee	209	Left	Maxilla	Molar	PD_SEEN	21	0	OHLPQ04301	23.983	657.7	25.081	250.649	3	114	1	1	1	1
MS05116	M	08/05/2009	Yankee	108	Right	Maxilla	Premolar	PD_SEEN	26	0	OHLPQ04308		1.0	28.205	32.638	1	101	0	0	1	1
MS05116	M	08/05/2009	Yankee	108	Right	Maxilla	Premolar	PD_SEEN	26	0	OHLPQ04308		1.0	27.717	44.882	2	101	0	0	1	1
MS05116	M	08/05/2009	Yankee	108	Right	Maxilla	Premolar	PD_SEEN	26	0	OHLPQ04308		1.0	27.691	45.627	3	101	0	0	1	1
MS05116	M	08/05/2009	Yankee	208	Left	Maxilla	Premolar	NO_PD	26	0	OHLPQ04316		1.0	28.737	23.054	1	101	0	0	1	1
MS05116	M	08/05/2009	Yankee	208	Left	Maxilla	Premolar	NO_PD	26	0	OHLPQ04316	33.128	1.9	1.000	2	101	1	0	0	0	0
MS05116	M	08/05/2009	Yankee	208	Left	Maxilla	Premolar	NO_PD	26	0	OHLPQ04316	30.864	8.1	1.000	3	101	1	1	0	0	0
MS04929	M	05/01/2008	Norris	103	Right	Maxilla	Incisor	NO_PD	10	-3	OHLPQ04369		1.0	34.153	0.672	1	171	0	0	1	0
MS04929	M	05/01/2008	Norris	103	Right	Maxilla	Incisor	NO_PD	10	-3	OHLPQ04369	34.832	0.6	31.049	5.100	2	171	1	0	1	1
MS04929	M	05/01/2008	Norris	103	Right	Maxilla	Incisor	NO_PD	10	-3	OHLPQ04369		1.0	33.146	1.297	3	171	0	0	1	0
MS04929	M	05/01/2008	Norris	203	Left	Maxilla	Incisor	PD_SEEN	10	-3	OHLPQ04377	35.261	0.5	1.000	1	171	1	0	0	0	0
MS04929	M	05/01/2008	Norris	203	Left	Maxilla	Incisor	PD_SEEN	10	-3	OHLPQ04377	32.058	3.8	33.641	0.939	2	171	1	1	1	0
MS04929	M	05/01/2008	Norris	203	Left	Maxilla	Incisor	PD_SEEN	10	-3	OHLPQ04377		1.0	1.000	3	171	0	0	0	0	0
MS04929	M	05/01/2008	Norris	309	Left	Manible	Molar	PD_SEEN	14	-3	OHLPQ04384	31.038	7.2	30.631	6.698	1	171	1	1	1	1
MS04929	M	05/01/2008	Norris	309	Left	Manible	Molar	PD_SEEN	14	-3	OHLPQ04384	30.560	9.8	29.183	17.230	2	171	1	1	1	1
MS04929	M	05/01/2008	Norris	309	Left	Manible	Molar	PD_SEEN	14	-3	OHLPQ04384		1.0	30.223	8.739	3	171	0	0	1	1
MS04559	F	23/06/2004	Halle	409	Right	Manible	Molar	PD_SEEN	1	0	OHLPQ04392	27.108	89.2	31.216	4.571	1	355	1	1	1	1

MS04559	F	23/06/2004	Halle	409	Right	Manible	Molar	PD_SEEN	1	0	OHLPPQ04392	28.446	37.9	29.392	15.040	2	355	1	1	1	1
MS04559	F	23/06/2004	Halle	409	Right	Manible	Molar	PD_SEEN	1	0	OHLPPQ04392	26.583	124.7	33.559	0.991	3	355	1	1	1	0
MS04559	F	23/06/2004	Halle	309	Left	Manible	Molar	NO_PD	1	0	OHLPPQ04400	31.904	4.2	29.135	17.784	1	355	1	1	1	1
MS04559	F	23/06/2004	Halle	309	Left	Manible	Molar	NO_PD	1	0	OHLPPQ04400	35.022	0.6	30.648	6.622	2	355	1	0	1	1
MS04559	F	23/06/2004	Halle	309	Left	Manible	Molar	NO_PD	1	0	OHLPPQ04400		1.0		1.000	3	355	0	0	0	0
MS05115	F	08/05/2009	Yoyo	103	Right	Maxilla	Incisor	NO_PD	25	0	OHLPPQ04417	24.046	631.7	32.591	1.863	1	101	1	1	1	0
MS05115	F	08/05/2009	Yoyo	103	Right	Maxilla	Incisor	NO_PD	25	0	OHLPPQ04417	24.250	554.5	34.826	0.433	2	101	1	1	1	0
MS05115	F	08/05/2009	Yoyo	103	Right	Maxilla	Incisor	NO_PD	25	0	OHLPPQ04417	23.581	850.6	33.451	1.063	3	101	1	1	1	0
MS05115	F	08/05/2009	Yoyo	203	Left	Maxilla	Incisor	PD_SEEN	25	0	OHLPPQ04425	27.116	88.8	33.324	1.155	1	101	1	1	1	0
MS05115	F	08/05/2009	Yoyo	203	Left	Maxilla	Incisor	PD_SEEN	25	0	OHLPPQ04425	27.166	86.0	31.578	3.611	2	101	1	1	1	0
MS05115	F	08/05/2009	Yoyo	203	Left	Maxilla	Incisor	PD_SEEN	25	0	OHLPPQ04425	27.283	79.7		1.000	3	101	1	1	0	0
MS05031	F	26/01/2009	Violet	103	Right	Maxilla	Incisor	NO_PD	17	-2	OHLPPQ04513		1.0	33.470	1.050	1	116	0	0	1	0
MS05031	F	26/01/2009	Violet	103	Right	Maxilla	Incisor	NO_PD	17	-2	OHLPPQ04513		1.0	32.727	1.705	2	116	0	0	1	0
MS05031	F	26/01/2009	Violet	103	Right	Maxilla	Incisor	NO_PD	17	-2	OHLPPQ04513		1.0	31.719	3.292	3	116	0	0	1	0
MS05031	F	26/01/2009	Violet	408	Right	Manible	Premolar	NO_PD	18	-1	OHLPPQ04519	35.033	0.6	26.252	116.782	1	116	1	0	1	1
MS05031	F	26/01/2009	Violet	408	Right	Manible	Premolar	NO_PD	18	-1	OHLPPQ04519	30.532	10.0	25.872	149.587	2	116	1	1	1	1
MS05031	F	26/01/2009	Violet	408	Right	Manible	Premolar	NO_PD	18	-1	OHLPPQ04519		1.0	25.716	165.616	3	116	0	0	1	1
MS05031	F	26/01/2009	Violet	308	Left	Manible	Premolar	PD_SEEN	18	-1	OHLPPQ04527		1.0	31.103	4.922	1	116	0	0	1	1
MS05031	F	26/01/2009	Violet	308	Left	Manible	Premolar	PD_SEEN	18	-1	OHLPPQ04527	32.484	2.9	28.878	21.036	2	116	1	0	1	1
MS05031	F	26/01/2009	Violet	308	Left	Manible	Premolar	PD_SEEN	18	-1	OHLPPQ04527		1.0	33.623	0.950	3	116	0	0	1	0
MS05114	F	08/05/2009	Yasmine	207	Left	Maxilla	Premolar	NO_PD	63	-1	OHLPPQ04555	29.683	17.2	27.441	53.730	1	101	1	1	1	1
MS05114	F	08/05/2009	Yasmine	207	Left	Maxilla	Premolar	NO_PD	63	-1	OHLPPQ04555	29.858	15.4	29.295	16.018	2	101	1	1	1	1
MS05114	F	08/05/2009	Yasmine	207	Left	Maxilla	Premolar	NO_PD	63	-1	OHLPPQ04555		1.0	28.913	20.560	3	101	0	0	1	1
MS05114	F	08/05/2009	Yasmine	209	Left	Maxilla	Molar	NO_PD	64	-1	OHLPPQ04557	34.375	0.9	28.193	32.884	1	101	1	0	1	1
MS05114	F	08/05/2009	Yasmine	209	Left	Maxilla	Molar	NO_PD	64	-1	OHLPPQ04557		1.0	29.521	13.827	2	101	0	0	1	1
MS05114	F	08/05/2009	Yasmine	209	Left	Maxilla	Molar	NO_PD	64	-1	OHLPPQ04557	31.570	5.1	28.851	21.401	3	101	1	1	1	1
MS05114	F	08/05/2009	Yasmine	308	Left	Manible	Premolar	PD_SEEN	63	-1	OHLPPQ04559	29.516	19.1	28.745	22.938	1	101	1	1	1	1
MS05114	F	08/05/2009	Yasmine	308	Left	Manible	Premolar	PD_SEEN	63	-1	OHLPPQ04559	29.870	15.3	28.495	26.999	2	101	1	1	1	1
MS05114	F	08/05/2009	Yasmine	308	Left	Manible	Premolar	PD_SEEN	63	-1	OHLPPQ04559	31.933	4.1	29.177	17.301	3	101	1	1	1	1
MS05114	F	08/05/2009	Yasmine	309	Left	Manible	Molar	PD_SEEN	64	-1	OHLPPQ04560	25.878	195.9	24.966	270.274	1	101	1	1	1	1
MS05114	F	08/05/2009	Yasmine	309	Left	Manible	Molar	PD_SEEN	64	-1	OHLPPQ04560	25.458	256.1	25.268	221.942	2	101	1	1	1	1
MS05114	F	08/05/2009	Yasmine	309	Left	Manible	Molar	PD_SEEN	64	-1	OHLPPQ04560	25.980	183.5	25.300	217.383	3	101	1	1	1	1
MS05151	F	03/12/2010	Bramble	108	Right	Maxilla	Premolar	NO_PD	68	-5	OHLPPQ04564	32.358	3.1	27.956	38.383	1	19	1	0	1	1
MS05151	F	03/12/2010	Bramble	108	Right	Maxilla	Premolar	NO_PD	68	-5	OHLPPQ04564	34.387	0.8	28.163	33.542	2	19	1	0	1	1
MS05151	F	03/12/2010	Bramble	108	Right	Maxilla	Premolar	NO_PD	68	-5	OHLPPQ04564	34.532	0.8	29.193	17.118	3	19	1	0	1	1
MS05151	F	03/12/2010	Bramble	109	Right	Maxilla	Molar	PD_SEEN	31	-5	OHLPPQ04565	33.222	1.8	24.126	467.530	1	19	1	0	1	1
MS05151	F	03/12/2010	Bramble	109	Right	Maxilla	Molar	PD_SEEN	31	-5	OHLPPQ04565	32.819	2.3	24.390	393.721	2	19	1	0	1	1
MS05151	F	03/12/2010	Bramble	109	Right	Maxilla	Molar	PD_SEEN	31	-5	OHLPPQ04565	32.957	2.1	25.055	255.001	3	19	1	0	1	1
MS05151	F	03/12/2010	Bramble	408	Right	Manible	Premolar	PD_SEEN	69	-1	OHLPPQ04567		1.0	27.168	64.222	1	19	0	0	1	1
MS05151	F	03/12/2010	Bramble	408	Right	Manible	Premolar	PD_SEEN	69	-1	OHLPPQ04567	36.189	0.3	27.757	43.721	2	19	1	0	1	1
MS05151	F	03/12/2010	Bramble	408	Right	Manible	Premolar	PD_SEEN	69	-1	OHLPPQ04567	32.453	2.9	28.960	19.929	3	19	1	0	1	1
MS05151	F	03/12/2010	Bramble	209	Left	Maxilla	Molar	NO_PD	31	-5	OHLPPQ04573	26.955	98.3	25.438	198.570	1	19	1	1	1	1
MS05151	F	03/12/2010	Bramble	209	Left	Maxilla	Molar	NO_PD	31	-5	OHLPPQ04573	35.058	0.6	25.796	157.221	2	19	1	0	1	1
MS05151	F	03/12/2010	Bramble	209	Left	Maxilla	Molar	NO_PD	31	-5	OHLPPQ04573	33.715	1.3	25.042	257.163	3	19	1	0	1	1
MS05151	F	03/12/2010	Bramble	308	Left	Manible	Premolar	PD_SEEN	68	-5	OHLPPQ04575		1.0	27.256	60.634	1	19	0	0	1	1
MS05151	F	03/12/2010	Bramble	308	Left	Manible	Premolar	PD_SEEN	68	-5	OHLPPQ04575	32.821	2.3	28.087	35.248	2	19	1	0	1	1
MS05151	F	03/12/2010	Bramble	308	Left	Manible	Premolar	PD_SEEN	68	-5	OHLPPQ04575		1.0	28.012	37.019	3	19	0	0	1	1
MS05152	M	03/12/2010	Bentley	309	Left	Manible	Molar	PD_SEEN	34	-4	OHLPPQ04592	31.097	7.0	24.819	297.536	1	19	1	1	1	1
MS05152	M	03/12/2010	Bentley	309	Left	Manible	Molar	PD_SEEN	34	-4	OHLPPQ04592	32.130	3.6	24.493	367.984	2	19	1	1	1	1
MS05152	M	03/12/2010	Bentley	309	Left	Manible	Molar	PD_SEEN	34	-4	OHLPPQ04592		1.0	24.520	361.619	3	19	0	0	1	1
MS05156	M	03/12/2010	Brock	109	Right	Maxilla	Molar	PD_SEEN	70	-5	OHLPPQ04597	36.717	0.2	28.936	20.254	1	19	1	0	1	1
MS05156	M	03/12/2010	Brock	109	Right	Maxilla	Molar	PD_SEEN	70	-5	OHLPPQ04597	33.914	1.1	29.451	14.467	2	19	1	0	1	1
MS05156	M	03/12/2010	Brock	109	Right	Maxilla	Molar	PD_SEEN	70	-5	OHLPPQ04597	32.839	2.3	28.471	27.436	3	19	1	0	1	1
MS05156	M	03/12/2010	Brock	208	Left	Maxilla	Premolar	PD_SEEN	35	-3	OHLPPQ04604		1.0	28.907	20.636	1	19	0	0	1	1

MS05156	M	03/12/2010	Brock	208	Left	Maxilla	Premolar	PD_SEEN	35	-3	OHLPQ04604	29.527	19.0	26.692	87.593	2	19	1	1	1	1
MS05156	M	03/12/2010	Brock	208	Left	Maxilla	Premolar	PD_SEEN	35	-3	OHLPQ04604		1.0	28.109	34.740	3	19	0	0	1	1
MS05156	M	03/12/2010	Brock	309	Left	Manible	Molar	NO_PD	70	-5	OHLPQ04608		1.0	24.753	310.640	1	19	0	0	1	1
MS05156	M	03/12/2010	Brock	309	Left	Manible	Molar	NO_PD	70	-5	OHLPQ04608		1.0	24.625	337.656	2	19	0	0	1	1
MS05156	M	03/12/2010	Brock	309	Left	Manible	Molar	NO_PD	70	-5	OHLPQ04608		1.0	24.383	395.309	3	19	0	0	1	1
MS05158	F	15/01/2010	Connie	408	Right	Manible	Premolar	NO_PD	36	-4	OHLPQ04615		1.0	30.032	9.904	1	65	0	0	1	1
MS05158	F	15/01/2010	Connie	408	Right	Manible	Premolar	NO_PD	36	-4	OHLPQ04615	36.386	0.2	28.538	26.250	2	65	1	0	1	1
MS05158	F	15/01/2010	Connie	408	Right	Manible	Premolar	NO_PD	36	-4	OHLPQ04615	31.462	5.5	31.342	4.212	3	65	1	1	1	1
MS05158	F	15/01/2010	Connie	308	Left	Manible	Premolar	PD_SEEN	36	-4	OHLPQ04623	30.875	8.0	21.107	3354.608	1	65	1	1	1	1
MS05158	F	15/01/2010	Connie	308	Left	Manible	Premolar	PD_SEEN	36	-4	OHLPQ04623		1.0	21.724	2243.127	2	65	0	0	1	1
MS05158	F	15/01/2010	Connie	308	Left	Manible	Premolar	PD_SEEN	36	-4	OHLPQ04623	33.504	1.5	21.605	2424.778	3	65	1	0	1	1
MS05163	M	15/01/2010	Chesney	108	Right	Maxilla	Premolar	NO_PD	71	-2	OHLPQ04644	23.979	659.2	27.390	55.539	1	65	1	1	1	1
MS05163	M	15/01/2010	Chesney	108	Right	Maxilla	Premolar	NO_PD	71	-2	OHLPQ04644	24.328	527.5	27.280	59.689	2	65	1	1	1	1
MS05163	M	15/01/2010	Chesney	108	Right	Maxilla	Premolar	NO_PD	71	-2	OHLPQ04644	24.100	610.2	26.510	98.634	3	65	1	1	1	1
MS05163	M	15/01/2010	Chesney	408	Right	Manible	Premolar	PD_SEEN	71	-2	OHLPQ04647	27.214	83.3	26.368	108.208	1	65	1	1	1	1
MS05163	M	15/01/2010	Chesney	408	Right	Manible	Premolar	PD_SEEN	71	-2	OHLPQ04647	27.701	61.0	27.430	54.103	2	65	1	1	1	1
MS05163	M	15/01/2010	Chesney	408	Right	Manible	Premolar	PD_SEEN	71	-2	OHLPQ04647	27.178	85.3		1.000	3	65	1	1	0	0
MS04930	F	05/01/2008	Niamh	408	Right	Manible	Premolar	NO_PD	15	-3	OHLPQ04711	22.264	1974.0	26.433	103.720	1	171	1	1	1	1
MS04930	F	05/01/2008	Niamh	408	Right	Manible	Premolar	NO_PD	15	-3	OHLPQ04711	22.124	2158.8	26.351	109.464	2	171	1	1	1	1
MS04930	F	05/01/2008	Niamh	408	Right	Manible	Premolar	NO_PD	15	-3	OHLPQ04711	22.429	1776.7	25.949	142.298	3	171	1	1	1	1
MS04930	F	05/01/2008	Niamh	308	Left	Manible	Premolar	PD_SEEN	15	-3	OHLPQ04719	23.721	777.4	25.668	170.940	1	171	1	1	1	1
MS04930	F	05/01/2008	Niamh	308	Left	Manible	Premolar	PD_SEEN	15	-3	OHLPQ04719	24.309	533.9	25.582	180.834	2	171	1	1	1	1
MS04930	F	05/01/2008	Niamh	308	Left	Manible	Premolar	PD_SEEN	15	-3	OHLPQ04719	23.889	698.5	25.349	210.495	3	171	1	1	1	1
MS05118	M	08/05/2009	Yoshi	104	Right	Maxilla	Canine	PD_SEEN	66	-3	OHLPQ04754	23.631	823.7	27.771	43.328	1	101	1	1	1	1
MS05118	M	08/05/2009	Yoshi	104	Right	Maxilla	Canine	PD_SEEN	66	-3	OHLPQ04754	23.166	1108.8	28.757	22.760	2	101	1	1	1	1
MS05118	M	08/05/2009	Yoshi	104	Right	Maxilla	Canine	PD_SEEN	66	-3	OHLPQ04754	23.579	851.6	27.973	37.955	3	101	1	1	1	1
MS05118	M	08/05/2009	Yoshi	404	Right	Manible	Canine	NO_PD	67	-3	OHLPQ04758	25.497	249.8	34.806	0.439	1	101	1	1	1	0
MS05118	M	08/05/2009	Yoshi	404	Right	Manible	Canine	NO_PD	67	-3	OHLPQ04758	26.317	147.9	34.120	0.687	2	101	1	1	1	0
MS05118	M	08/05/2009	Yoshi	404	Right	Manible	Canine	NO_PD	67	-3	OHLPQ04758	25.782	208.2	1.000		3	101	1	1	0	0
MS05118	M	08/05/2009	Yoshi	204	Left	Maxilla	Canine	PD_SEEN	67	-3	OHLPQ04762	24.986	346.4	26.739	84.950	1	101	1	1	1	1
MS05118	M	08/05/2009	Yoshi	204	Left	Maxilla	Canine	PD_SEEN	67	-3	OHLPQ04762	25.017	339.5	27.800	42.503	2	101	1	1	1	1
MS05118	M	08/05/2009	Yoshi	204	Left	Maxilla	Canine	PD_SEEN	67	-3	OHLPQ04762	25.591	235.2	26.203	120.535	3	101	1	1	1	1
MS05118	M	08/05/2009	Yoshi	304	Left	Manible	Canine	NO_PD	66	-3	OHLPQ04766	22.292	1939.0	20.894	3854.863	1	101	1	1	1	1
MS05118	M	08/05/2009	Yoshi	304	Left	Manible	Canine	NO_PD	66	-3	OHLPQ04766	22.447	1755.4	21.154	3254.747	2	101	1	1	1	1
MS05118	M	08/05/2009	Yoshi	304	Left	Manible	Canine	NO_PD	66	-3	OHLPQ04766	22.426	1779.6	20.990	3621.012	3	101	1	1	1	1
MS05164	M	15/01/2010	Colin	104	Right	Maxilla	Canine	PD_SEEN	38	-4	OHLPQ04770		1.0	32.715	1.718	1	65	0	0	1	0
MS05164	M	15/01/2010	Colin	104	Right	Maxilla	Canine	PD_SEEN	38	-4	OHLPQ04770	34.778	0.7	31.849	3.024	2	65	1	0	1	0
MS05164	M	15/01/2010	Colin	104	Right	Maxilla	Canine	PD_SEEN	38	-4	OHLPQ04770		1.0		1.000	3	65	0	0	0	0
MS05164	M	15/01/2010	Colin	204	Left	Maxilla	Canine	NO_PD	38	-4	OHLPQ04778	35.030	0.6		1.000	1	65	1	0	0	0
MS05164	M	15/01/2010	Colin	204	Left	Maxilla	Canine	NO_PD	38	-4	OHLPQ04778	34.288	0.9	32.931	1.492	2	65	1	0	1	0
MS05164	M	15/01/2010	Colin	204	Left	Maxilla	Canine	NO_PD	38	-4	OHLPQ04778	32.178	3.5	33.330	1.150	3	65	1	0	1	0
MS05164	M	15/01/2010	Colin	207	Left	Maxilla	Premolar	PD_SEEN	72	-2	OHLPQ04779	30.893	7.9	29.602	13.110	1	65	1	1	1	1
MS05164	M	15/01/2010	Colin	207	Left	Maxilla	Premolar	PD_SEEN	72	-2	OHLPQ04779	31.001	7.4	27.277	59.803	2	65	1	1	1	1
MS05164	M	15/01/2010	Colin	207	Left	Maxilla	Premolar	PD_SEEN	72	-2	OHLPQ04779	34.759	0.7	30.712	6.352	3	65	1	0	1	1
MS05164	M	15/01/2010	Colin	308	Left	Manible	Premolar	NO_PD	72	-2	OHLPQ04783		1.0	28.767	22.611	1	65	0	0	1	1
MS05164	M	15/01/2010	Colin	308	Left	Manible	Premolar	NO_PD	72	-2	OHLPQ04783	31.199	6.5	32.011	2.722	2	65	1	1	1	0
MS05164	M	15/01/2010	Colin	308	Left	Manible	Premolar	NO_PD	72	-2	OHLPQ04783	32.782	2.4	30.566	6.987	3	65	1	0	1	1
MS04714	M	10/05/2006	Eddie	409	Right	Manible	Molar	PD_SEEN	55	0	OHLPQ04840	35.002	0.6	24.898	282.546	1	257	1	0	1	1
MS04714	M	10/05/2006	Eddie	409	Right	Manible	Molar	PD_SEEN	55	0	OHLPQ04840	27.679	61.9	26.153	124.529	2	257	1	1	1	1
MS04714	M	10/05/2006	Eddie	409	Right	Manible	Molar	PD_SEEN	55	0	OHLPQ04840		1.0	23.336	782.938	3	257	0	0	1	1
MS04714	M	10/05/2006	Eddie	209	Left	Maxilla	Molar	NO_PD	55	0	OHLPQ04845	34.701	0.7	25.534	186.520	1	257	1	0	1	1
MS04714	M	10/05/2006	Eddie	209	Left	Maxilla	Molar	NO_PD	55	0	OHLPQ04845	34.053	1.1	26.162	123.827	2	257	1	0	1	1
MS04714	M	10/05/2006	Eddie	209	Left	Maxilla	Molar	NO_PD	55	0	OHLPQ04845		1.0	25.805	156.334	3	257	0	0	1	1
MS04929	M	05/01/2008	Norris	103	Right	Maxilla	Incisor	NO_PD	10	-2	OHLPQ05009	32.075	3.7	28.176	33.257	1	171	1	1	1	1

MS04929	M	05/01/2008	Norris	103	Right	Maxilla	Incisor	NO_PD	10	-2	OHL PQ05009	35.046	0.6	30.189	8.940	2	171	1	0	1	1
MS04929	M	05/01/2008	Norris	103	Right	Maxilla	Incisor	NO_PD	10	-2	OHL PQ05009		1.0	29.876	10.966	3	171	0	0	1	1
MS04929	M	05/01/2008	Norris	408	Right	Manible	Premolar	NO_PD	13	-3	OHL PQ05015		1.0	26.845	79.282	1	171	0	0	1	1
MS04929	M	05/01/2008	Norris	408	Right	Manible	Premolar	NO_PD	13	-3	OHL PQ05015	35.765	0.4	26.955	73.796	2	171	1	0	1	1
MS04929	M	05/01/2008	Norris	408	Right	Manible	Premolar	NO_PD	13	-3	OHL PQ05015	30.903	7.9	26.475	100.913	3	171	1	1	1	1
MS04929	M	05/01/2008	Norris	409	Right	Manible	Molar	NO_PD	14	-2	OHL PQ05016		1.0	29.858	11.095	1	171	0	0	1	1
MS04929	M	05/01/2008	Norris	409	Right	Manible	Molar	NO_PD	14	-2	OHL PQ05016	32.368	3.1	28.919	20.482	2	171	1	0	1	1
MS04929	M	05/01/2008	Norris	409	Right	Manible	Molar	NO_PD	14	-2	OHL PQ05016	30.765	8.6		1.000	3	171	1	1	0	0
MS04929	M	05/01/2008	Norris	203	Left	Maxilla	Incisor	PD_SEEN	10	-2	OHL PQ05017	35.684	0.4	34.660	0.483	1	171	1	0	1	0
MS04929	M	05/01/2008	Norris	203	Left	Maxilla	Incisor	PD_SEEN	10	-2	OHL PQ05017		1.0	34.906	0.411	2	171	0	0	1	0
MS04929	M	05/01/2008	Norris	203	Left	Maxilla	Incisor	PD_SEEN	10	-2	OHL PQ05017		1.0	34.952	0.399	3	171	0	0	1	0
MS04929	M	05/01/2008	Norris	308	Left	Manible	Premolar	PD_SEEN	13	-3	OHL PQ05023	35.212	0.5	28.723	23.266	1	171	1	0	1	1
MS04929	M	05/01/2008	Norris	308	Left	Manible	Premolar	PD_SEEN	13	-3	OHL PQ05023	33.311	1.7	29.129	17.853	2	171	1	0	1	1
MS04929	M	05/01/2008	Norris	308	Left	Manible	Premolar	PD_SEEN	13	-3	OHL PQ05023		1.0	30.442	7.575	3	171	0	0	1	1
MS04929	M	05/01/2008	Norris	309	Left	Manible	Molar	PD_SEEN	14	-2	OHL PQ05024		1.0	26.803	81.500	1	171	0	0	1	1
MS04929	M	05/01/2008	Norris	309	Left	Manible	Molar	PD_SEEN	14	-2	OHL PQ05024		1.0	27.121	66.190	2	171	0	0	1	1
MS04929	M	05/01/2008	Norris	309	Left	Manible	Molar	PD_SEEN	14	-2	OHL PQ05024	34.194	1.0	27.249	60.883	3	171	1	0	1	1
MS05031	F	26/01/2009	Violet	103	Right	Maxilla	Incisor	NO_PD	17	-1	OHL PQ05169		1.0	33.443	1.068	1	116	0	0	1	0
MS05031	F	26/01/2009	Violet	103	Right	Maxilla	Incisor	NO_PD	17	-1	OHL PQ05169		1.0	34.402	0.572	2	116	0	0	1	0
MS05031	F	26/01/2009	Violet	103	Right	Maxilla	Incisor	NO_PD	17	-1	OHL PQ05169	32.191	3.5	33.179	1.269	3	116	1	0	1	0
MS05031	F	26/01/2009	Violet	408	Right	Manible	Premolar	NO_PD	18	0	OHL PQ05175		1.0	28.255	31.574	1	116	0	0	1	1
MS05031	F	26/01/2009	Violet	408	Right	Manible	Premolar	NO_PD	18	0	OHL PQ05175	31.874	4.2	27.875	40.484	2	116	1	1	1	1
MS05031	F	26/01/2009	Violet	408	Right	Manible	Premolar	NO_PD	18	0	OHL PQ05175		1.0	29.200	17.046	3	116	0	0	1	1
MS05031	F	26/01/2009	Violet	203	Left	Maxilla	Incisor	PD_SEEN	17	-1	OHL PQ05177		1.0	33.512	1.022	1	116	0	0	1	0
MS05031	F	26/01/2009	Violet	203	Left	Maxilla	Incisor	PD_SEEN	17	-1	OHL PQ05177	34.851	0.6		1.000	2	116	1	0	0	0
MS05031	F	26/01/2009	Violet	203	Left	Maxilla	Incisor	PD_SEEN	17	-1	OHL PQ05177		1.0		1.000	3	116	0	0	0	0
MS05031	F	26/01/2009	Violet	308	Left	Manible	Premolar	PD_SEEN	18	0	OHL PQ05183		1.0	26.324	111.391	1	116	0	0	1	1
MS05031	F	26/01/2009	Violet	308	Left	Manible	Premolar	PD_SEEN	18	0	OHL PQ05183		1.0	25.856	151.167	2	116	0	0	1	1
MS05031	F	26/01/2009	Violet	308	Left	Manible	Premolar	PD_SEEN	18	0	OHL PQ05183		1.0	27.608	48.181	3	116	0	0	1	1
MS05114	F	08/05/2009	Yasmine	207	Left	Maxilla	Premolar	NO_PD	63	0	OHL PQ05211	24.625	436.3	26.997	71.804	1	101	1	1	1	1
MS05114	F	08/05/2009	Yasmine	207	Left	Maxilla	Premolar	NO_PD	63	0	OHL PQ05211	24.235	559.7	27.198	62.976	2	101	1	1	1	1
MS05114	F	08/05/2009	Yasmine	207	Left	Maxilla	Premolar	NO_PD	63	0	OHL PQ05211	24.518	467.1	27.303	58.788	3	101	1	1	1	1
MS05114	F	08/05/2009	Yasmine	209	Left	Maxilla	Molar	NO_PD	64	0	OHL PQ05213	24.863	374.7	28.054	36.013	1	101	1	1	1	1
MS05114	F	08/05/2009	Yasmine	209	Left	Maxilla	Molar	NO_PD	64	0	OHL PQ05213	24.602	442.7	26.037	134.300	2	101	1	1	1	1
MS05114	F	08/05/2009	Yasmine	209	Left	Maxilla	Molar	NO_PD	64	0	OHL PQ05213	24.852	377.2	26.226	118.727	3	101	1	1	1	1
MS05114	F	08/05/2009	Yasmine	308	Left	Manible	Premolar	PD_SEEN	63	0	OHL PQ05215	23.960	667.4	24.540	356.939	1	101	1	1	1	1
MS05114	F	08/05/2009	Yasmine	308	Left	Manible	Premolar	PD_SEEN	63	0	OHL PQ05215	23.384	964.2	24.754	310.385	2	101	1	1	1	1
MS05114	F	08/05/2009	Yasmine	308	Left	Manible	Premolar	PD_SEEN	63	0	OHL PQ05215	23.610	834.6	25.081	250.770	3	101	1	1	1	1
MS05114	F	08/05/2009	Yasmine	309	Left	Manible	Molar	PD_SEEN	64	0	OHL PQ05216	24.470	481.8	31.506	3.784	1	101	1	1	1	0
MS05114	F	08/05/2009	Yasmine	309	Left	Manible	Molar	PD_SEEN	64	0	OHL PQ05216	24.800	390.2	30.308	8.271	2	101	1	1	1	1
MS05114	F	08/05/2009	Yasmine	309	Left	Manible	Molar	PD_SEEN	64	0	OHL PQ05216	24.527	464.3	31.493	3.816	3	101	1	1	1	0
MS05156	M	03/12/2010	Brock	108	Right	Maxilla	Premolar	NO_PD	35	-2	OHL PQ05220		1.0	1.000		1	19	0	0	0	0
MS05156	M	03/12/2010	Brock	108	Right	Maxilla	Premolar	NO_PD	35	-2	OHL PQ05220	35.798	0.3	29.063	18.636	2	19	1	0	1	1
MS05156	M	03/12/2010	Brock	108	Right	Maxilla	Premolar	NO_PD	35	-2	OHL PQ05220		1.0	32.570	1.889	3	19	0	0	1	0
MS05156	M	03/12/2010	Brock	109	Right	Maxilla	Molar	PD_SEEN	70	-4	OHL PQ05221	33.204	1.8	28.124	34.400	1	19	1	0	1	1
MS05156	M	03/12/2010	Brock	109	Right	Maxilla	Molar	PD_SEEN	70	-4	OHL PQ05221		1.0	29.591	13.208	2	19	0	0	1	1
MS05156	M	03/12/2010	Brock	109	Right	Maxilla	Molar	PD_SEEN	70	-4	OHL PQ05221		1.0	29.700	12.298	3	19	0	0	1	1
MS05156	M	03/12/2010	Brock	309	Left	Manible	Molar	NO_PD	70	-4	OHL PQ05232	30.938	7.7	33.482	1.042	1	19	1	1	1	0
MS05156	M	03/12/2010	Brock	309	Left	Manible	Molar	NO_PD	70	-4	OHL PQ05232		1.0		1.000	2	19	0	0	0	0
MS05156	M	03/12/2010	Brock	309	Left	Manible	Molar	NO_PD	70	-4	OHL PQ05232	33.284	1.7	32.382	2.136	3	19	1	0	1	0
MS05152	M	03/12/2010	Bentley	409	Right	Manible	Molar	NO_PD	34	-3	OHL PQ05240	35.469	0.4	32.379	2.140	1	19	1	0	1	0
MS05152	M	03/12/2010	Bentley	409	Right	Manible	Molar	NO_PD	34	-3	OHL PQ05240	31.416	5.7	31.560	3.652	2	19	1	1	1	0
MS05152	M	03/12/2010	Bentley	409	Right	Manible	Molar	NO_PD	34	-3	OHL PQ05240	29.599	18.1	34.713	0.466	3	19	1	1	1	0
MS05152	M	03/12/2010	Bentley	309	Left	Manible	Molar	PD_SEEN	34	-3	OHL PQ05248	34.486	0.8	26.201	120.702	1	19	1	0	1	1

MS05152	M	03/12/2010	Bentley	309	Left	Manible	Molar	PD_SEEN	34	-3	OHL PQ05248	33.484	1.5	26.035	134.546	2	19	1	0	1	1
MS05152	M	03/12/2010	Bentley	309	Left	Manible	Molar	PD_SEEN	34	-3	OHL PQ05248		1.0	26.755	84.054	3	19	0	0	1	1
MS05151	F	03/12/2010	Bramble	108	Right	Maxilla	Premolar	NO_PD	68	-4	OHL PQ05252		1.0	29.597	13.154	1	19	0	0	1	1
MS05151	F	03/12/2010	Bramble	108	Right	Maxilla	Premolar	NO_PD	68	-4	OHL PQ05252	32.254	3.3	29.074	18.503	2	19	1	0	1	1
MS05151	F	03/12/2010	Bramble	108	Right	Maxilla	Premolar	NO_PD	68	-4	OHL PQ05252	35.597	0.4	29.994	10.151	3	19	1	0	1	1
MS05151	F	03/12/2010	Bramble	109	Right	Maxilla	Molar	PD_SEEN	31	-4	OHL PQ05253	36.417	0.2	26.488	100.061	1	19	1	0	1	1
MS05151	F	03/12/2010	Bramble	109	Right	Maxilla	Molar	PD_SEEN	31	-4	OHL PQ05253		1.0	26.075	131.051	2	19	0	0	1	1
MS05151	F	03/12/2010	Bramble	109	Right	Maxilla	Molar	PD_SEEN	31	-4	OHL PQ05253	33.198	1.8	26.146	125.131	3	19	1	0	1	1
MS05151	F	03/12/2010	Bramble	408	Right	Manible	Premolar	PD_SEEN	69	0	OHL PQ05255		1.0	30.131	9.280	1	19	0	0	1	1
MS05151	F	03/12/2010	Bramble	408	Right	Manible	Premolar	PD_SEEN	69	0	OHL PQ05255	31.803	4.4	27.081	67.945	2	19	1	1	1	1
MS05151	F	03/12/2010	Bramble	408	Right	Manible	Premolar	PD_SEEN	69	0	OHL PQ05255		1.0	28.156	33.687	3	19	0	0	1	1
MS05151	F	03/12/2010	Bramble	208	Left	Maxilla	Premolar	NO_PD	69	0	OHL PQ05260		1.0	24.672	327.510	1	19	0	0	1	1
MS05151	F	03/12/2010	Bramble	208	Left	Maxilla	Premolar	NO_PD	69	0	OHL PQ05260	36.042	0.3	24.596	344.148	2	19	1	0	1	1
MS05151	F	03/12/2010	Bramble	208	Left	Maxilla	Premolar	NO_PD	69	0	OHL PQ05260		1.0	24.533	358.458	3	19	0	0	1	1
MS05151	F	03/12/2010	Bramble	209	Left	Maxilla	Molar	NO_PD	31	-4	OHL PQ05261		1.0	27.664	46.436	1	19	0	0	1	1
MS05151	F	03/12/2010	Bramble	209	Left	Maxilla	Molar	NO_PD	31	-4	OHL PQ05261		1.0	27.336	57.540	2	19	0	0	1	1
MS05151	F	03/12/2010	Bramble	209	Left	Maxilla	Molar	NO_PD	31	-4	OHL PQ05261		1.0	27.726	44.617	3	19	0	0	1	1
MS05151	F	03/12/2010	Bramble	308	Left	Manible	Premolar	PD_SEEN	68	-4	OHL PQ05263	36.370	0.2	1.000	1	19	1	0	0	0	0
MS05151	F	03/12/2010	Bramble	308	Left	Manible	Premolar	PD_SEEN	68	-4	OHL PQ05263		1.0	1.000	2	19	0	0	0	0	0
MS05151	F	03/12/2010	Bramble	308	Left	Manible	Premolar	PD_SEEN	68	-4	OHL PQ05263		1.0	1.000	3	19	0	0	0	0	0
MS05163	M	15/01/2010	Chesney	108	Right	Maxilla	Premolar	NO_PD	71	-1	OHL PQ05268	24.829	382.9	26.240	117.671	1	65	1	1	1	1
MS05163	M	15/01/2010	Chesney	108	Right	Maxilla	Premolar	NO_PD	71	-1	OHL PQ05268	25.208	300.6	27.652	46.809	2	65	1	1	1	1
MS05163	M	15/01/2010	Chesney	108	Right	Maxilla	Premolar	NO_PD	71	-1	OHL PQ05268	24.708	413.6	27.402	55.122	3	65	1	1	1	1
MS05163	M	15/01/2010	Chesney	408	Right	Manible	Premolar	PD_SEEN	71	-1	OHL PQ05271	25.367	271.4	25.912	145.767	1	65	1	1	1	1
MS05163	M	15/01/2010	Chesney	408	Right	Manible	Premolar	PD_SEEN	71	-1	OHL PQ05271	24.532	463.0	28.628	24.754	2	65	1	1	1	1
MS05163	M	15/01/2010	Chesney	408	Right	Manible	Premolar	PD_SEEN	71	-1	OHL PQ05271	24.682	426.1	28.663	24.200	3	65	1	1	1	1
MS05158	F	15/01/2010	Connie	408	Right	Manible	Premolar	NO_PD	36	-3	OHL PQ05303		1.0	28.887	20.909	1	65	0	0	1	1
MS05158	F	15/01/2010	Connie	408	Right	Manible	Premolar	NO_PD	36	-3	OHL PQ05303		1.0	28.826	21.754	2	65	0	0	1	1
MS05158	F	15/01/2010	Connie	408	Right	Manible	Premolar	NO_PD	36	-3	OHL PQ05303		1.0	28.665	24.171	3	65	0	0	1	1
MS05158	F	15/01/2010	Connie	308	Left	Manible	Premolar	PD_SEEN	36	-3	OHL PQ05311	35.242	0.5	29.188	17.175	1	65	1	0	1	1
MS05158	F	15/01/2010	Connie	308	Left	Manible	Premolar	PD_SEEN	36	-3	OHL PQ05311		1.0	29.264	16.350	2	65	0	0	1	1
MS05158	F	15/01/2010	Connie	308	Left	Manible	Premolar	PD_SEEN	36	-3	OHL PQ05311		1.0	28.160	33.594	3	65	0	0	1	1
MS04930	F	05/01/2008	Niamh	408	Right	Manible	Premolar	NO_PD	15	-2	OHL PQ05351	26.021	178.7	26.888	77.071	1	171	1	1	1	1
MS04930	F	05/01/2008	Niamh	408	Right	Manible	Premolar	NO_PD	15	-2	OHL PQ05351	25.492	250.6	27.269	60.103	2	171	1	1	1	1
MS04930	F	05/01/2008	Niamh	408	Right	Manible	Premolar	NO_PD	15	-2	OHL PQ05351	25.823	202.8	28.021	36.786	3	171	1	1	1	1
MS04930	F	05/01/2008	Niamh	308	Left	Manible	Premolar	PD_SEEN	15	-2	OHL PQ05359	23.736	770.4	27.512	51.290	1	171	1	1	1	1
MS04930	F	05/01/2008	Niamh	308	Left	Manible	Premolar	PD_SEEN	15	-2	OHL PQ05359	23.046	1197.6	26.764	83.575	2	171	1	1	1	1
MS04930	F	05/01/2008	Niamh	308	Left	Manible	Premolar	PD_SEEN	15	-2	OHL PQ05359	23.165	1109.6	26.665	89.135	3	171	1	1	1	1
MS05118	M	08/05/2009	Yoshi	104	Right	Maxilla	Canine	PD_SEEN	66	-2	OHL PQ05410	28.488	36.9	26.386	106.985	1	101	1	1	1	1
MS05118	M	08/05/2009	Yoshi	104	Right	Maxilla	Canine	PD_SEEN	66	-2	OHL PQ05410	27.303	78.8	26.005	137.183	2	101	1	1	1	1
MS05118	M	08/05/2009	Yoshi	104	Right	Maxilla	Canine	PD_SEEN	66	-2	OHL PQ05410	28.138	46.2	25.607	177.807	3	101	1	1	1	1
MS05118	M	08/05/2009	Yoshi	404	Right	Manible	Canine	NO_PD	67	-2	OHL PQ05414	24.895	417.1	32.818	1.607	1	101	1	1	1	0
MS05118	M	08/05/2009	Yoshi	404	Right	Manible	Canine	NO_PD	67	-2	OHL PQ05414	24.663	425.9	28.784	22.366	2	101	1	1	1	1
MS05118	M	08/05/2009	Yoshi	404	Right	Manible	Canine	NO_PD	67	-2	OHL PQ05414	24.803	389.3	29.945	10.479	3	101	1	1	1	1
MS05118	M	08/05/2009	Yoshi	204	Left	Maxilla	Canine	PD_SEEN	67	-2	OHL PQ05418	26.649	119.6	34.140	0.678	1	101	1	1	1	0
MS05118	M	08/05/2009	Yoshi	204	Left	Maxilla	Canine	PD_SEEN	67	-2	OHL PQ05418	28.233	43.5	1.000	2	101	1	1	0	0	0
MS05118	M	08/05/2009	Yoshi	204	Left	Maxilla	Canine	PD_SEEN	67	-2	OHL PQ05418	29.074	25.4	34.666	0.481	3	101	1	1	1	0
MS05118	M	08/05/2009	Yoshi	304	Left	Manible	Canine	NO_PD	66	-2	OHL PQ05422	27.407	73.7	31.792	3.140	1	101	1	1	1	0
MS05118	M	08/05/2009	Yoshi	304	Left	Manible	Canine	NO_PD	66	-2	OHL PQ05422	33.477	1.5	33.582	0.976	2	101	1	0	1	0
MS05118	M	08/05/2009	Yoshi	304	Left	Manible	Canine	NO_PD	66	-2	OHL PQ05422	29.523	19.0	32.119	2.535	3	101	1	1	1	0
MS05164	M	15/01/2010	Colin	204	Left	Maxilla	Canine	NO_PD	38	-3	OHL PQ05434		1.0	29.579	13.312	1	65	0	0	1	1
MS05164	M	15/01/2010	Colin	204	Left	Maxilla	Canine	NO_PD	38	-3	OHL PQ05434	35.030	0.6	1.000	2	65	1	0	0	0	0
MS05164	M	15/01/2010	Colin	204	Left	Maxilla	Canine	NO_PD	38	-3	OHL PQ05434	30.566	9.8	28.649	24.419	3	65	1	1	1	1
MS05164	M	15/01/2010	Colin	207	Left	Maxilla	Premolar	PD_SEEN	72	-1	OHL PQ05435		1.0	28.622	24.856	1	65	0	0	1	1

MS05164	M	15/01/2010	Colin	207	Left	Maxilla	Premolar	PD_SEEN	72	-1	OHLPQ05435	1.0	28.362	29.452	2	65	0	0	1	1		
MS05164	M	15/01/2010	Colin	207	Left	Maxilla	Premolar	PD_SEEN	72	-1	OHLPQ05435	1.0	27.863	40.787	3	65	0	0	1	1		
MS04929	M	05/01/2008	Norris	103	Right	Maxilla	Incisor	NO_PD	10	-1	OHLPQ05665	1.0	33.683	0.913	1	171	0	0	1	0		
MS04929	M	05/01/2008	Norris	103	Right	Maxilla	Incisor	NO_PD	10	-1	OHLPQ05665	1.0	31.198	4.625	2	171	0	0	1	1		
MS04929	M	05/01/2008	Norris	103	Right	Maxilla	Incisor	NO_PD	10	-1	OHLPQ05665	35.565	0.4	31.461	3.897	3	171	1	0	1	0	
MS04929	M	05/01/2008	Norris	408	Right	Manible	Premolar	NO_PD	13	-2	OHLPQ05671	1.0	24.433	382.828	1	171	0	0	1	1		
MS04929	M	05/01/2008	Norris	408	Right	Manible	Premolar	NO_PD	13	-2	OHLPQ05671	1.0	24.283	422.185	2	171	0	0	1	1		
MS04929	M	05/01/2008	Norris	408	Right	Manible	Premolar	NO_PD	13	-2	OHLPQ05671	1.0	24.452	377.956	3	171	0	0	1	1		
MS04929	M	05/01/2008	Norris	409	Right	Manible	Molar	NO_PD	14	-1	OHLPQ05672	1.0	22.715	1174.413	1	171	0	0	1	1		
MS04929	M	05/01/2008	Norris	409	Right	Manible	Molar	NO_PD	14	-1	OHLPQ05672	1.0	23.185	864.519	2	171	0	0	1	1		
MS04929	M	05/01/2008	Norris	409	Right	Manible	Molar	NO_PD	14	-1	OHLPQ05672	33.070	2.0	22.955	1004.089	3	171	1	0	1	1	
MS04929	M	05/01/2008	Norris	203	Left	Maxilla	Incisor	PD_SEEN	10	-1	OHLPQ05673	35.277	0.5	25.034	258.595	1	171	1	0	1	1	
MS04929	M	05/01/2008	Norris	203	Left	Maxilla	Incisor	PD_SEEN	10	-1	OHLPQ05673	1.0	25.170	236.509	2	171	0	0	1	1		
MS04929	M	05/01/2008	Norris	203	Left	Maxilla	Incisor	PD_SEEN	10	-1	OHLPQ05673	30.684	9.1	24.536	357.826	3	171	1	1	1	1	
MS04929	M	05/01/2008	Norris	309	Left	Manible	Molar	PD_SEEN	14	-1	OHLPQ05680	30.239	12.1	25.143	240.816	1	171	1	1	1	1	
MS04929	M	05/01/2008	Norris	309	Left	Manible	Molar	PD_SEEN	14	-1	OHLPQ05680	31.857	4.3	27.738	44.259	2	171	1	1	1	1	
MS04929	M	05/01/2008	Norris	309	Left	Manible	Molar	PD_SEEN	14	-1	OHLPQ05680	34.392	0.8	26.686	87.935	3	171	1	0	1	1	
MS05031	F	26/01/2009	Violet	103	Right	Maxilla	Incisor	NO_PD	17	0	OHLPQ05745	1.0	29.079	18.449	1	116	0	0	1	1		
MS05031	F	26/01/2009	Violet	103	Right	Maxilla	Incisor	NO_PD	17	0	OHLPQ05745	35.763	0.4	28.051	36.071	2	116	1	0	1	1	
MS05031	F	26/01/2009	Violet	103	Right	Maxilla	Incisor	NO_PD	17	0	OHLPQ05745	35.357	0.5	27.572	49.321	3	116	1	0	1	1	
MS05031	F	26/01/2009	Violet	203	Left	Maxilla	Incisor	PD_SEEN	17	0	OHLPQ05753	1.0	1.000	1	116	0	0	0	0	0		
MS05031	F	26/01/2009	Violet	203	Left	Maxilla	Incisor	PD_SEEN	17	0	OHLPQ05753	36.199	0.3	32.784	1.643	2	116	1	0	1	0	
MS05031	F	26/01/2009	Violet	203	Left	Maxilla	Incisor	PD_SEEN	17	0	OHLPQ05753	35.768	0.4	33.558	0.991	3	116	1	0	1	0	
MS05156	M	03/12/2010	Brock	108	Right	Maxilla	Premolar	NO_PD	35	-1	OHLPQ05860	31.117	6.9	27.500	51.684	1	19	1	1	1	1	
MS05156	M	03/12/2010	Brock	108	Right	Maxilla	Premolar	NO_PD	35	-1	OHLPQ05860	33.941	1.1	26.543	96.557	2	19	1	0	1	1	
MS05156	M	03/12/2010	Brock	108	Right	Maxilla	Premolar	NO_PD	35	-1	OHLPQ05860	1.0	27.699	45.392	3	19	0	0	1	1	1	
MS05156	M	03/12/2010	Brock	109	Right	Maxilla	Molar	PD_SEEN	70	-3	OHLPQ05861	35.238	0.5	25.482	193.005	1	19	1	0	1	1	
MS05156	M	03/12/2010	Brock	109	Right	Maxilla	Molar	PD_SEEN	70	-3	OHLPQ05861	1.0	26.339	110.292	2	19	0	0	1	1	1	
MS05156	M	03/12/2010	Brock	109	Right	Maxilla	Molar	PD_SEEN	70	-3	OHLPQ05861	1.0	25.345	211.029	3	19	0	0	1	1	1	
MS05156	M	03/12/2010	Brock	309	Left	Manible	Molar	NO_PD	70	-3	OHLPQ05872	30.685	9.1	22.883	1052.667	1	19	1	1	1	1	
MS05156	M	03/12/2010	Brock	309	Left	Manible	Molar	NO_PD	70	-3	OHLPQ05872	35.367	0.5	22.856	1071.108	2	19	1	0	1	1	
MS05156	M	03/12/2010	Brock	309	Left	Manible	Molar	NO_PD	70	-3	OHLPQ05872	34.967	0.6	22.850	1075.391	3	19	1	0	1	1	
MS05152	M	03/12/2010	Bentley	309	Left	Manible	Molar	PD_SEEN	34	-2	OHLPQ05888	1.0	33.818	0.837	1	19	0	0	1	0	0	
MS05152	M	03/12/2010	Bentley	309	Left	Manible	Molar	PD_SEEN	34	-2	OHLPQ05888	31.245	6.3	35.084	0.366	2	19	1	1	1	0	
MS05152	M	03/12/2010	Bentley	309	Left	Manible	Molar	PD_SEEN	34	-2	OHLPQ05888	33.611	1.4	34.466	0.548	3	19	1	0	1	0	
MS05151	F	03/12/2010	Bramble	108	Right	Maxilla	Premolar	NO_PD	68	-3	OHLPQ05892	1.0	26.588	93.766	1	19	0	0	1	1	1	
MS05151	F	03/12/2010	Bramble	108	Right	Maxilla	Premolar	NO_PD	68	-3	OHLPQ05892	32.157	3.5	28.021	36.791	2	19	1	0	1	1	1
MS05151	F	03/12/2010	Bramble	108	Right	Maxilla	Premolar	NO_PD	68	-3	OHLPQ05892	33.526	1.5	28.829	21.716	3	19	1	0	1	1	1
MS05151	F	03/12/2010	Bramble	109	Right	Maxilla	Molar	PD_SEEN	31	-3	OHLPQ05893	30.799	8.4	26.007	136.969	1	19	1	1	1	1	1
MS05151	F	03/12/2010	Bramble	109	Right	Maxilla	Molar	PD_SEEN	31	-3	OHLPQ05893	1.0	26.330	110.980	2	19	0	0	1	1	1	1
MS05151	F	03/12/2010	Bramble	109	Right	Maxilla	Molar	PD_SEEN	31	-3	OHLPQ05893	34.617	0.7	25.419	201.025	3	19	1	0	1	1	1
MS05151	F	03/12/2010	Bramble	209	Left	Maxilla	Molar	NO_PD	31	-3	OHLPQ05901	29.925	14.7	27.530	50.691	1	19	1	1	1	1	1
MS05151	F	03/12/2010	Bramble	209	Left	Maxilla	Molar	NO_PD	31	-3	OHLPQ05901	1.0	27.752	43.856	2	19	0	0	1	1	1	1
MS05151	F	03/12/2010	Bramble	209	Left	Maxilla	Molar	NO_PD	31	-3	OHLPQ05901	1.0	26.157	124.253	3	19	0	0	1	1	1	1
MS05151	F	03/12/2010	Bramble	308	Left	Manible	Premolar	PD_SEEN	68	-3	OHLPQ05903	1.0	27.875	40.480	1	19	0	0	1	1	1	1
MS05151	F	03/12/2010	Bramble	308	Left	Manible	Premolar	PD_SEEN	68	-3	OHLPQ05903	1.0	32.055	2.645	2	19	0	0	1	0	0	0
MS05151	F	03/12/2010	Bramble	308	Left	Manible	Premolar	PD_SEEN	68	-3	OHLPQ05903	1.0	27.788	42.829	3	19	0	0	1	1	1	1
MS05163	M	15/01/2010	Chesney	108	Right	Maxilla	Premolar	NO_PD	71	0	OHLPQ05908	27.010	94.9	30.773	6.105	1	65	1	1	1	1	1
MS05163	M	15/01/2010	Chesney	108	Right	Maxilla	Premolar	NO_PD	71	0	OHLPQ05908	26.186	160.9	28.719	23.328	2	65	1	1	1	1	1
MS05163	M	15/01/2010	Chesney	108	Right	Maxilla	Premolar	NO_PD	71	0	OHLPQ05908	26.145	165.1	34.003	0.741	3	65	1	1	1	0	0
MS05163	M	15/01/2010	Chesney	408	Right	Manible	Premolar	PD_SEEN	71	0	OHLPQ05911	25.886	194.8	27.629	47.519	1	65	1	1	1	1	1
MS05163	M	15/01/2010	Chesney	408	Right	Manible	Premolar	PD_SEEN	71	0	OHLPQ05911	26.639	120.4	27.551	50.016	2	65	1	1	1	1	1
MS05163	M	15/01/2010	Chesney	408	Right	Manible	Premolar	PD_SEEN	71	0	OHLPQ05911	26.759	111.5	26.462	101.800	3	65	1	1	1	1	1
MS05158	F	15/01/2010	Connie	408	Right	Manible	Premolar	NO_PD	36	-2	OHLPQ05943	1.0	33.863	0.812	1	65	0	0	1	0	0	0

MS05158	F	15/01/2010	Connie	408	Right	Manible	Premolar	NO_PD	36	-2	OHL PQ05943		1.0	32.750	1.680	2	65	0	0	1	0
MS05158	F	15/01/2010	Connie	408	Right	Manible	Premolar	NO_PD	36	-2	OHL PQ05943	35.889	0.3	34.215	0.646	3	65	1	0	1	0
MS05158	F	15/01/2010	Connie	308	Left	Manible	Premolar	PD_SEEN	36	-2	OHL PQ05951		1.0	33.538	1.004	1	65	0	0	1	0
MS05158	F	15/01/2010	Connie	308	Left	Manible	Premolar	PD_SEEN	36	-2	OHL PQ05951	35.952	0.3	33.817	0.837	2	65	1	0	1	0
MS05158	F	15/01/2010	Connie	308	Left	Manible	Premolar	PD_SEEN	36	-2	OHL PQ05951	32.851	2.3	33.368	1.123	3	65	1	0	1	0
MS04930	F	05/01/2008	Niamh	308	Left	Manible	Premolar	PD_SEEN	15	-1	OHL PQ05999	25.524	245.6	28.374	29.227	1	171	1	1	1	1
MS04930	F	05/01/2008	Niamh	308	Left	Manible	Premolar	PD_SEEN	15	-1	OHL PQ05999	25.451		257.2	29.202	2	171	1	1	1	1
MS04930	F	05/01/2008	Niamh	308	Left	Manible	Premolar	PD_SEEN	15	-1	OHL PQ05999	25.632	229.1	28.331	30.060	3	171	1	1	1	1
MS05118	M	08/05/2009	Yoshi	104	Right	Maxilla	Canine	PD_SEEN	66	-1	OHL PQ06050	25.412	263.8	29.173	17.353	1	101	1	1	1	1
MS05118	M	08/05/2009	Yoshi	104	Right	Maxilla	Canine	PD_SEEN	66	-1	OHL PQ06050	25.583		30.337	8.116	2	101	1	1	1	1
MS05118	M	08/05/2009	Yoshi	104	Right	Maxilla	Canine	PD_SEEN	66	-1	OHL PQ06050	26.031	177.6	32.086	2.592	3	101	1	1	1	0
MS05118	M	08/05/2009	Yoshi	404	Right	Manible	Canine	NO_PD	67	-1	OHL PQ06054	27.222		82.9	33.895	1	101	1	1	1	0
MS05118	M	08/05/2009	Yoshi	404	Right	Manible	Canine	NO_PD	67	-1	OHL PQ06054	28.393		39.2	1.000	2	101	1	1	0	0
MS05118	M	08/05/2009	Yoshi	404	Right	Manible	Canine	NO_PD	67	-1	OHL PQ06054		1.0	32.621	1.828	3	101	0	0	1	0
MS05118	M	08/05/2009	Yoshi	204	Left	Maxilla	Canine	PD_SEEN	67	-1	OHL PQ06058	29.431	20.2	31.035	5.146	1	101	1	1	1	1
MS05118	M	08/05/2009	Yoshi	204	Left	Maxilla	Canine	PD_SEEN	67	-1	OHL PQ06058	28.604	34.3	29.810	11.447	2	101	1	1	1	1
MS05118	M	08/05/2009	Yoshi	204	Left	Maxilla	Canine	PD_SEEN	67	-1	OHL PQ06058	26.448	136.0	30.685	6.465	3	101	1	1	1	1
MS05164	M	15/01/2010	Colin	104	Right	Maxilla	Canine	PD_SEEN	38	-2	OHL PQ06066	31.321	6.0		1.000	1	65	1	1	0	0
MS05164	M	15/01/2010	Colin	104	Right	Maxilla	Canine	PD_SEEN	38	-2	OHL PQ06066		1.0	35.102	0.362	2	65	0	0	1	0
MS05164	M	15/01/2010	Colin	104	Right	Maxilla	Canine	PD_SEEN	38	-2	OHL PQ06066		1.0	33.589	0.971	3	65	0	0	1	0
MS05164	M	15/01/2010	Colin	204	Left	Maxilla	Canine	NO_PD	38	-2	OHL PQ06074		1.0	30.014	10.018	1	65	0	0	1	1
MS05164	M	15/01/2010	Colin	204	Left	Maxilla	Canine	NO_PD	38	-2	OHL PQ06074	34.932	0.6	26.041	134.006	2	65	1	0	1	1
MS05164	M	15/01/2010	Colin	204	Left	Maxilla	Canine	NO_PD	38	-2	OHL PQ06074		1.0	26.275	115.008	3	65	0	0	1	1
MS05164	M	15/01/2010	Colin	207	Left	Maxilla	Premolar	PD_SEEN	72	0	OHL PQ06075		1.0	29.199	17.052	1	65	0	0	1	1
MS05164	M	15/01/2010	Colin	207	Left	Maxilla	Premolar	PD_SEEN	72	0	OHL PQ06075	32.304	3.2	28.268	31.313	2	65	1	0	1	1
MS05164	M	15/01/2010	Colin	207	Left	Maxilla	Premolar	PD_SEEN	72	0	OHL PQ06075	32.121	3.6	29.214	16.887	3	65	1	1	1	1
MS05164	M	15/01/2010	Colin	308	Left	Manible	Premolar	NO_PD	72	0	OHL PQ06079		1.0	27.379	55.934	1	65	0	0	1	1
MS05164	M	15/01/2010	Colin	308	Left	Manible	Premolar	NO_PD	72	0	OHL PQ06079	31.185	6.6	27.790	42.772	2	65	1	1	1	1
MS05164	M	15/01/2010	Colin	308	Left	Manible	Premolar	NO_PD	72	0	OHL PQ06079	32.419	3.0	26.757	83.954	3	65	1	0	1	1
MS04929	M	05/01/2008	Norris	103	Right	Maxilla	Incisor	NO_PD	10	0	OHL PQ06161		1.0	28.181	33.153	1	171	0	0	1	1
MS04929	M	05/01/2008	Norris	103	Right	Maxilla	Incisor	NO_PD	10	0	OHL PQ06161		1.0	27.121	66.190	2	171	0	0	1	1
MS04929	M	05/01/2008	Norris	103	Right	Maxilla	Incisor	NO_PD	10	0	OHL PQ06161	35.197	0.5	26.972	72.950	3	171	1	0	1	1
MS04929	M	05/01/2008	Norris	409	Right	Manible	Molar	NO_PD	14	0	OHL PQ06168	33.675	1.3	27.574	49.267	1	171	1	0	1	1
MS04929	M	05/01/2008	Norris	409	Right	Manible	Molar	NO_PD	14	0	OHL PQ06168		1.0	26.824	80.348	2	171	0	0	1	1
MS04929	M	05/01/2008	Norris	409	Right	Manible	Molar	NO_PD	14	0	OHL PQ06168		1.0	27.398	55.268	3	171	0	0	1	1
MS04929	M	05/01/2008	Norris	203	Left	Maxilla	Incisor	PD_SEEN	10	0	OHL PQ06169	35.442	0.4	31.775	3.174	1	171	1	0	1	0
MS04929	M	05/01/2008	Norris	203	Left	Maxilla	Incisor	PD_SEEN	10	0	OHL PQ06169		1.0	35.156	0.349	2	171	0	0	1	0
MS04929	M	05/01/2008	Norris	203	Left	Maxilla	Incisor	PD_SEEN	10	0	OHL PQ06169		1.0	33.841	0.824	3	171	0	0	1	0
MS04929	M	05/01/2008	Norris	308	Left	Manible	Premolar	PD_SEEN	13	-1	OHL PQ06175		1.0	33.891	0.798	1	171	0	0	1	0
MS04929	M	05/01/2008	Norris	308	Left	Manible	Premolar	PD_SEEN	13	-1	OHL PQ06175		1.0	33.445	1.067	2	171	0	0	1	0
MS04929	M	05/01/2008	Norris	308	Left	Manible	Premolar	PD_SEEN	13	-1	OHL PQ06175		1.0	32.108	2.555	3	171	0	0	1	0
MS04929	M	05/01/2008	Norris	309	Left	Manible	Molar	PD_SEEN	14	0	OHL PQ06176		1.0	27.653	46.777	1	171	0	0	1	1
MS04929	M	05/01/2008	Norris	309	Left	Manible	Molar	PD_SEEN	14	0	OHL PQ06176		1.0	27.422	54.401	2	171	0	0	1	1
MS04929	M	05/01/2008	Norris	309	Left	Manible	Molar	PD_SEEN	14	0	OHL PQ06176		1.0	27.140	65.401	3	171	0	0	1	1
MS05151	F	03/12/2010	Bramble	108	Right	Maxilla	Premolar	NO_PD	68	-2	OHL PQ06308		1.0	28.333	30.010	1	19	0	0	1	1
MS05151	F	03/12/2010	Bramble	108	Right	Maxilla	Premolar	NO_PD	68	-2	OHL PQ06308	33.325	1.7	27.163	64.407	2	19	1	0	1	1
MS05151	F	03/12/2010	Bramble	108	Right	Maxilla	Premolar	NO_PD	68	-2	OHL PQ06308		1.0	28.033	36.510	3	19	0	0	1	1
MS05151	F	03/12/2010	Bramble	109	Right	Maxilla	Molar	PD_SEEN	31	-2	OHL PQ06309		1.0	26.917	75.661	1	19	0	0	1	1
MS05151	F	03/12/2010	Bramble	109	Right	Maxilla	Molar	PD_SEEN	31	-2	OHL PQ06309	35.234	0.5	28.218	32.352	2	19	1	0	1	1
MS05151	F	03/12/2010	Bramble	109	Right	Maxilla	Molar	PD_SEEN	31	-2	OHL PQ06309		1.0	29.779	11.683	3	19	0	0	1	1
MS05151	F	03/12/2010	Bramble	209	Left	Maxilla	Molar	NO_PD	31	-2	OHL PQ06317	34.100	1.0	26.747	84.533	1	19	1	0	1	1
MS05151	F	03/12/2010	Bramble	209	Left	Maxilla	Molar	NO_PD	31	-2	OHL PQ06317	35.962	0.3	26.604	92.774	2	19	1	0	1	1
MS05151	F	03/12/2010	Bramble	209	Left	Maxilla	Molar	NO_PD	31	-2	OHL PQ06317	33.728	1.3	25.899	147.021	3	19	1	0	1	1
MS05152	M	03/12/2010	Bentley	409	Right	Manible	Molar	NO_PD	34	-1	OHL PQ06328		1.0	30.806	5.976	1	19	0	0	1	1

MS05152	M	03/12/2010	Bentley	409	Right	Manible	Molar	NO_PD	34	-1	OHLPOQ06328	33.542	1.5	29.340	15.557	2	19	1	0	1	1
MS05152	M	03/12/2010	Bentley	409	Right	Manible	Molar	NO_PD	34	-1	OHLPOQ06328	36.176	0.3	30.949	5.441	3	19	1	0	1	1
MS05152	M	03/12/2010	Bentley	309	Left	Manible	Molar	PD_SEEN	34	-1	OHLPOQ06336		1.0	29.247	16.531	1	19	0	0	1	1
MS05152	M	03/12/2010	Bentley	309	Left	Manible	Molar	PD_SEEN	34	-1	OHLPOQ06336	34.572	0.8	34.074	0.708	2	19	1	0	1	0
MS05152	M	03/12/2010	Bentley	309	Left	Manible	Molar	PD_SEEN	34	-1	OHLPOQ06336	32.295	3.2	31.358	4.167	3	19	1	0	1	1
MS05156	M	03/12/2010	Brock	108	Right	Maxilla	Premolar	NO_PD	35	0	OHLPOQ06340	24.332	526.1	29.531	13.728	1	19	1	1	1	1
MS05156	M	03/12/2010	Brock	108	Right	Maxilla	Premolar	NO_PD	35	0	OHLPOQ06340	24.548	458.2	28.119	34.511	2	19	1	1	1	1
MS05156	M	03/12/2010	Brock	108	Right	Maxilla	Premolar	NO_PD	35	0	OHLPOQ06340	24.573	451.1	29.380	15.158	3	19	1	1	1	1
MS05156	M	03/12/2010	Brock	109	Right	Maxilla	Molar	PD_SEEN	70	-2	OHLPOQ06341	23.763	756.9	26.668	88.985	1	19	1	1	1	1
MS05156	M	03/12/2010	Brock	109	Right	Maxilla	Molar	PD_SEEN	70	-2	OHLPOQ06341	23.949	672.0	26.418	104.734	2	19	1	1	1	1
MS05156	M	03/12/2010	Brock	109	Right	Maxilla	Molar	PD_SEEN	70	-2	OHLPOQ06341	23.740	768.1	26.699	87.198	3	19	1	1	1	1
MS05156	M	03/12/2010	Brock	208	Left	Maxilla	Premolar	PD_SEEN	35	0	OHLPOQ06348		1.0	30.490	7.343	1	19	0	0	1	1
MS05156	M	03/12/2010	Brock	208	Left	Maxilla	Premolar	PD_SEEN	35	0	OHLPOQ06348	33.056	2.0	31.315	4.285	2	19	1	0	1	1
MS05156	M	03/12/2010	Brock	208	Left	Maxilla	Premolar	PD_SEEN	35	0	OHLPOQ06348	29.773	16.2	30.114	9.389	3	19	1	1	1	1
MS05156	M	03/12/2010	Brock	309	Left	Manible	Molar	NO_PD	70	-2	OHLPOQ06352	23.731	772.5	25.024	260.198	1	19	1	1	1	1
MS05156	M	03/12/2010	Brock	309	Left	Manible	Molar	NO_PD	70	-2	OHLPOQ06352	23.518	885.3	25.724	164.734	2	19	1	1	1	1
MS05156	M	03/12/2010	Brock	309	Left	Manible	Molar	NO_PD	70	-2	OHLPOQ06352	24.176	581.2	27.216	62.240	3	19	1	1	1	1
MS05158	F	15/01/2010	Connie	408	Right	Manible	Premolar	NO_PD	36	-1	OHLPOQ06375	34.198	1.0	30.421	7.683	1	65	1	0	1	1
MS05158	F	15/01/2010	Connie	408	Right	Manible	Premolar	NO_PD	36	-1	OHLPOQ06375		1.0	29.940	10.513	2	65	0	0	1	1
MS05158	F	15/01/2010	Connie	408	Right	Manible	Premolar	NO_PD	36	-1	OHLPOQ06375		1.0	31.790	3.143	3	65	0	0	1	0
MS05158	F	15/01/2010	Connie	308	Left	Manible	Premolar	PD_SEEN	36	-1	OHLPOQ06383	32.778	2.4	32.601	1.851	1	65	1	0	1	0
MS05158	F	15/01/2010	Connie	308	Left	Manible	Premolar	PD_SEEN	36	-1	OHLPOQ06383		1.0	27.870	40.595	2	65	0	0	1	1
MS05158	F	15/01/2010	Connie	308	Left	Manible	Premolar	PD_SEEN	36	-1	OHLPOQ06383		1.0	28.509	26.752	3	65	0	0	1	1
MS04930	F	05/01/2008	Niamh	408	Right	Manible	Premolar	NO_PD	15	0	OHLPOQ06455	23.199	1085.5	27.377	56.011	1	171	1	1	1	1
MS04930	F	05/01/2008	Niamh	408	Right	Manible	Premolar	NO_PD	15	0	OHLPOQ06455	24.704	414.8	26.174	122.817	2	171	1	1	1	1
MS04930	F	05/01/2008	Niamh	408	Right	Manible	Premolar	NO_PD	15	0	OHLPOQ06455	23.542	871.7	26.110	128.112	3	171	1	1	1	1
MS04930	F	05/01/2008	Niamh	308	Left	Manible	Premolar	PD_SEEN	15	0	OHLPOQ06463	31.032	7.3	30.304	8.294	1	171	1	1	1	1
MS04930	F	05/01/2008	Niamh	308	Left	Manible	Premolar	PD_SEEN	15	0	OHLPOQ06463	30.877	8.0	31.731	3.267	2	171	1	1	1	0
MS04930	F	05/01/2008	Niamh	308	Left	Manible	Premolar	PD_SEEN	15	0	OHLPOQ06463	32.478	2.9	31.383	4.100	3	171	1	0	1	1
MS05118	M	08/05/2009	Yoshi	104	Right	Maxilla	Canine	PD_SEEN	66	0	OHLPOQ06498	27.396	74.2	35.235	0.332	1	101	1	1	1	0
MS05118	M	08/05/2009	Yoshi	104	Right	Maxilla	Canine	PD_SEEN	66	0	OHLPOQ06498	27.399	74.1	1.000	2	101	1	1	0	0	0
MS05118	M	08/05/2009	Yoshi	104	Right	Maxilla	Canine	PD_SEEN	66	0	OHLPOQ06498	28.630	33.7	31.842	3.038	3	101	1	1	1	0
MS05118	M	08/05/2009	Yoshi	404	Right	Manible	Canine	NO_PD	67	0	OHLPOQ06502	27.383	74.8	1.000	1	101	1	1	0	0	0
MS05118	M	08/05/2009	Yoshi	404	Right	Manible	Canine	NO_PD	67	0	OHLPOQ06502	28.375	39.7	34.038	0.725	2	101	1	1	1	0
MS05118	M	08/05/2009	Yoshi	404	Right	Manible	Canine	NO_PD	67	0	OHLPOQ06502	29.359	21.1	30.740	6.237	3	101	1	1	1	1
MS05118	M	08/05/2009	Yoshi	204	Left	Maxilla	Canine	PD_SEEN	67	0	OHLPOQ06506	36.494	0.2	33.449	1.064	1	101	1	0	1	0
MS05118	M	08/05/2009	Yoshi	204	Left	Maxilla	Canine	PD_SEEN	67	0	OHLPOQ06506	32.995	2.1	31.932	2.865	2	101	1	0	1	0
MS05118	M	08/05/2009	Yoshi	204	Left	Maxilla	Canine	PD_SEEN	67	0	OHLPOQ06506		1.0	1.000	3	101	0	0	0	0	0
MS05118	M	08/05/2009	Yoshi	304	Left	Manible	Canine	NO_PD	66	0	OHLPOQ06510	27.120	88.5	32.244	2.337	1	101	1	1	1	0
MS05118	M	08/05/2009	Yoshi	304	Left	Manible	Canine	NO_PD	66	0	OHLPOQ06510	27.371	75.4	31.973	2.789	2	101	1	1	1	0
MS05118	M	08/05/2009	Yoshi	304	Left	Manible	Canine	NO_PD	66	0	OHLPOQ06510	26.726	113.8	33.741	0.879	3	101	1	1	1	0
MS05164	M	15/01/2010	Colin	104	Right	Maxilla	Canine	PD_SEEN	38	-1	OHLPOQ06514		1.0	1.000	1	65	0	0	0	0	0
MS05164	M	15/01/2010	Colin	104	Right	Maxilla	Canine	PD_SEEN	38	-1	OHLPOQ06514	33.282	1.7	31.354	4.179	2	65	1	0	1	1
MS05164	M	15/01/2010	Colin	104	Right	Maxilla	Canine	PD_SEEN	38	-1	OHLPOQ06514	31.880	4.2	31.974	2.788	3	65	1	1	1	0
MS05164	M	15/01/2010	Colin	204	Left	Maxilla	Canine	NO_PD	38	-1	OHLPOQ06522		1.0	35.563	0.268	1	65	0	0	1	0
MS05164	M	15/01/2010	Colin	204	Left	Maxilla	Canine	NO_PD	38	-1	OHLPOQ06522		1.0	30.648	6.622	2	65	0	0	1	1
MS05164	M	15/01/2010	Colin	204	Left	Maxilla	Canine	NO_PD	38	-1	OHLPOQ06522		1.0	32.195	2.414	3	65	0	0	1	0
MS04929	M	05/01/2008	Norris	408	Right	Manible	Premolar	NO_PD	13	0	OHLPOQ06551		1.0	24.042	494.089	1	171	0	0	1	1
MS04929	M	05/01/2008	Norris	408	Right	Manible	Premolar	NO_PD	13	0	OHLPOQ06551	34.937	0.6	24.020	500.994	2	171	1	0	1	1
MS04929	M	05/01/2008	Norris	408	Right	Manible	Premolar	NO_PD	13	0	OHLPOQ06551		1.0	23.963	520.083	3	171	0	0	1	1
MS04929	M	05/01/2008	Norris	308	Left	Manible	Premolar	PD_SEEN	13	0	OHLPOQ06559		1.0	24.037	495.728	1	171	0	0	1	1
MS04929	M	05/01/2008	Norris	308	Left	Manible	Premolar	PD_SEEN	13	0	OHLPOQ06559		1.0	23.806	576.181	2	171	0	0	1	1
MS04929	M	05/01/2008	Norris	308	Left	Manible	Premolar	PD_SEEN	13	0	OHLPOQ06559	28.865	29.0	23.332	785.088	3	171	1	1	1	1
MS05151	F	03/12/2010	Bramble	108	Right	Maxilla	Premolar	NO_PD	68	-1	OHLPOQ06692	32.722	2.5	26.775	82.974	1	19	1	0	1	1

MS05151	F	03/12/2010	Bramble	108	Right	Maxilla	Premolar	NO_PD	68	-1	OHLPOQ06692	33.653	1.4	26.406	105.584	2	19	1	0	1	1
MS05151	F	03/12/2010	Bramble	108	Right	Maxilla	Premolar	NO_PD	68	-1	OHLPOQ06692		1.0	25.372	207.354	3	19	0	0	1	1
MS05151	F	03/12/2010	Bramble	109	Right	Maxilla	Molar	PD_SEEN	31	-1	OHLPOQ06693		1.0	24.638	334.779	1	19	0	0	1	1
MS05151	F	03/12/2010	Bramble	109	Right	Maxilla	Molar	PD_SEEN	31	-1	OHLPOQ06693		1.0	25.262	222.843	2	19	0	0	1	1
MS05151	F	03/12/2010	Bramble	109	Right	Maxilla	Molar	PD_SEEN	31	-1	OHLPOQ06693	35.275	0.5	25.364	208.493	3	19	1	0	1	1
MS05151	F	03/12/2010	Bramble	209	Left	Maxilla	Molar	NO_PD	31	-1	OHLPOQ06701	33.083	2.0	25.105	246.773	1	19	1	0	1	1
MS05151	F	03/12/2010	Bramble	209	Left	Maxilla	Molar	NO_PD	31	-1	OHLPOQ06701		1.0	25.832	153.573	2	19	0	0	1	1
MS05151	F	03/12/2010	Bramble	209	Left	Maxilla	Molar	NO_PD	31	-1	OHLPOQ06701	31.972	4.0	25.856	151.183	3	19	1	1	1	1
MS05151	F	03/12/2010	Bramble	308	Left	Manible	Premolar	PD_SEEN	68	-1	OHLPOQ06703	34.247	0.9	27.924	39.194	1	19	1	0	1	1
MS05151	F	03/12/2010	Bramble	308	Left	Manible	Premolar	PD_SEEN	68	-1	OHLPOQ06703	31.940	4.1	30.422	7.678	2	19	1	1	1	1
MS05151	F	03/12/2010	Bramble	308	Left	Manible	Premolar	PD_SEEN	68	-1	OHLPOQ06703		1.0	28.227	32.173	3	19	0	0	1	1
MS05152	M	03/12/2010	Bentley	409	Right	Manible	Molar	NO_PD	34	0	OHLPOQ06712	29.259	22.6	27.391	55.498	1	19	1	1	1	1
MS05152	M	03/12/2010	Bentley	409	Right	Manible	Molar	NO_PD	34	0	OHLPOQ06712		1.0	26.614	92.205	2	19	0	0	1	1
MS05152	M	03/12/2010	Bentley	409	Right	Manible	Molar	NO_PD	34	0	OHLPOQ06712	34.693	0.7	25.556	183.937	3	19	1	0	1	1
MS05152	M	03/12/2010	Bentley	309	Left	Manible	Molar	PD_SEEN	34	0	OHLPOQ06720	33.962	1.1	28.264	31.391	1	19	1	0	1	1
MS05152	M	03/12/2010	Bentley	309	Left	Manible	Molar	PD_SEEN	34	0	OHLPOQ06720	34.014	1.1	26.614	92.186	2	19	1	0	1	1
MS05152	M	03/12/2010	Bentley	309	Left	Manible	Molar	PD_SEEN	34	0	OHLPOQ06720		1.0	27.546	50.156	3	19	0	0	1	1
MS05156	M	03/12/2010	Brock	109	Right	Maxilla	Molar	PD_SEEN	70	-1	OHLPOQ06725	23.869	707.6	21.946	1940.057	1	19	1	1	1	1
MS05156	M	03/12/2010	Brock	109	Right	Maxilla	Molar	PD_SEEN	70	-1	OHLPOQ06725	23.689	793.6	21.775	2168.760	2	19	1	1	1	1
MS05156	M	03/12/2010	Brock	109	Right	Maxilla	Molar	PD_SEEN	70	-1	OHLPOQ06725	23.788	745.1	22.290	1549.940	3	19	1	1	1	1
MS05158	F	15/01/2010	Connie	408	Right	Manible	Premolar	NO_PD	36	0	OHLPOQ06743		1.0	25.976	139.770	1	65	0	0	1	1
MS05158	F	15/01/2010	Connie	408	Right	Manible	Premolar	NO_PD	36	0	OHLPOQ06743	31.547	5.2	26.091	129.674	2	65	1	1	1	1
MS05158	F	15/01/2010	Connie	408	Right	Manible	Premolar	NO_PD	36	0	OHLPOQ06743		1.0	26.536	97.021	3	65	0	0	1	1
MS05158	F	15/01/2010	Connie	308	Left	Manible	Premolar	PD_SEEN	36	0	OHLPOQ06751	33.746	1.3	25.398	203.875	1	65	1	0	1	1
MS05158	F	15/01/2010	Connie	308	Left	Manible	Premolar	PD_SEEN	36	0	OHLPOQ06751	31.612	5.0	25.352	210.111	2	65	1	1	1	1
MS05158	F	15/01/2010	Connie	308	Left	Manible	Premolar	PD_SEEN	36	0	OHLPOQ06751		1.0	25.215	229.712	3	65	0	0	1	1
MS05164	M	15/01/2010	Colin	204	Left	Maxilla	Canine	NO_PD	38	0	OHLPOQ06874		1.0	32.596	1.858	1	65	0	0	1	0
MS05164	M	15/01/2010	Colin	204	Left	Maxilla	Canine	NO_PD	38	0	OHLPOQ06874	35.971	0.3	33.306	1.168	2	65	1	0	1	0
MS05164	M	15/01/2010	Colin	204	Left	Maxilla	Canine	NO_PD	38	0	OHLPOQ06874	35.618	0.4	35.417	0.295	3	65	1	0	1	0
MS05151	F	03/12/2010	Bramble	108	Right	Maxilla	Premolar	NO_PD	68	0	OHLPOQ06996	27.368	75.5	26.421	104.588	1	19	1	1	1	1
MS05151	F	03/12/2010	Bramble	108	Right	Maxilla	Premolar	NO_PD	68	0	OHLPOQ06996	30.056	13.5	25.772	159.659	2	19	1	1	1	1
MS05151	F	03/12/2010	Bramble	108	Right	Maxilla	Premolar	NO_PD	68	0	OHLPOQ06996	32.542	2.8	25.649	173.031	3	19	1	0	1	1
MS05151	F	03/12/2010	Bramble	109	Right	Maxilla	Molar	PD_SEEN	31	0	OHLPOQ06997	33.364	1.6	26.208	120.147	1	19	1	0	1	1
MS05151	F	03/12/2010	Bramble	109	Right	Maxilla	Molar	PD_SEEN	31	0	OHLPOQ06997	32.181	3.5	25.863	150.492	2	19	1	0	1	1
MS05151	F	03/12/2010	Bramble	109	Right	Maxilla	Molar	PD_SEEN	31	0	OHLPOQ06997	32.095	3.7	25.261	222.892	3	19	1	1	1	1
MS05151	F	03/12/2010	Bramble	209	Left	Maxilla	Molar	NO_PD	31	0	OHLPOQ07005	33.076	2.0	25.856	151.152	1	19	1	0	1	1
MS05151	F	03/12/2010	Bramble	209	Left	Maxilla	Molar	NO_PD	31	0	OHLPOQ07005		1.0	27.010	71.203	2	19	0	0	1	1
MS05151	F	03/12/2010	Bramble	209	Left	Maxilla	Molar	NO_PD	31	0	OHLPOQ07005		1.0	27.762	43.573	3	19	0	0	1	1
MS05151	F	03/12/2010	Bramble	308	Left	Manible	Premolar	PD_SEEN	68	0	OHLPOQ07007	30.573	9.7	26.079	130.725	1	19	1	1	1	1
MS05151	F	03/12/2010	Bramble	308	Left	Manible	Premolar	PD_SEEN	68	0	OHLPOQ07007	35.618	0.4	29.095	18.258	2	19	1	0	1	1
MS05151	F	03/12/2010	Bramble	308	Left	Manible	Premolar	PD_SEEN	68	0	OHLPOQ07007		1.0	25.774	159.523	3	19	0	0	1	1
MS05156	M	03/12/2010	Brock	109	Right	Maxilla	Molar	PD_SEEN	70	0	OHLPOQ07013	22.869	1340.7	25.094	248.659	1	19	1	1	1	1
MS05156	M	03/12/2010	Brock	109	Right	Maxilla	Molar	PD_SEEN	70	0	OHLPOQ07013	23.539	873.6	25.297	217.749	2	19	1	1	1	1
MS05156	M	03/12/2010	Brock	109	Right	Maxilla	Molar	PD_SEEN	70	0	OHLPOQ07013	23.612	833.7	24.446	379.446	3	19	1	1	1	1

Supplemental Table 11. 262 assay TC2 positive samples that have been digested with the restriction enzyme BcnI. Samples have been coded with a binary value to indicate if the restriction digest identified the species within the sample. A value of 1 equates to a positive identification and 0 equates to the species not being present in the sample. The analysis identified 179 samples containing the canine *Trichomonas* sp., and 213 containing *T. tenax*.

Sample barcode	<i>T. tenax</i> positive?	<i>Trichomonas</i> sp. positive?	Sample barcode	<i>T. tenax</i> positive?	<i>Trichomonas p.</i> positive?	Sample barcode	<i>T. tenax</i> positive?	<i>Trichomonas</i> sp. positive?
OHL PQ00055	1	1	OHL PQ02572	1	1	OHL PQ04567	1	1
OHL PQ00058	1	0	OHL PQ02592	1	1	OHL PQ04573	1	1
OHL PQ00089	1	1	OHL PQ02644	1	0	OHL PQ04575	1	1
OHL PQ00090	1	1	OHL PQ02652	1	1	OHL PQ04592	1	1
OHL PQ00119	1	0	OHL PQ02707	0	1	OHL PQ04597	1	0
OHL PQ00121	1	1	OHL PQ02708	0	1	OHL PQ04604	1	0
OHL PQ00143	0	0	OHL PQ02721	1	1	OHL PQ04608	1	1
OHL PQ00144	1	0	OHL PQ02728	1	1	OHL PQ04615	1	1
OHL PQ00202	1	1	OHL PQ02734	1	0	OHL PQ04623	0	1
OHL PQ00204	1	1	OHL PQ02736	1	1	OHL PQ04644	1	1
OHL PQ00538	0	1	OHL PQ02876	1	1	OHL PQ04647	0	1
OHL PQ00539	1	1	OHL PQ02923	1	1	OHL PQ04711	1	0
OHL PQ00560	1	0	OHL PQ02938	1	1	OHL PQ04719	1	0
OHL PQ00583	1	1	OHL PQ02953	0	1	OHL PQ04754	1	0
OHL PQ00636	1	0	OHL PQ02954	1	1	OHL PQ04762	1	0
OHL PQ00660	0	1	OHL PQ02970	1	1	OHL PQ04766	1	0
OHL PQ00668	1	1	OHL PQ02972	1	0	OHL PQ04779	1	0
OHL PQ00695	1	0	OHL PQ02985	1	1	OHL PQ04783	1	1
OHL PQ00699	1	0	OHL PQ02988	1	0	OHL PQ04840	1	1
OHL PQ00717	0	1	OHL PQ03068	1	0	OHL PQ04845	1	1
OHL PQ00756	1	1	OHL PQ03079	0	1	OHL PQ05009	1	1
OHL PQ00767	1	1	OHL PQ03081	0	1	OHL PQ05015	1	1
OHL PQ00781	0	1	OHL PQ03082	0	1	OHL PQ05023	1	0
OHL PQ00800	0	1	OHL PQ03083	1	1	OHL PQ05024	1	1
OHL PQ00845	0	1	OHL PQ03104	1	0	OHL PQ05175	1	0
OHL PQ00867	1	0	OHL PQ03126	0	0	OHL PQ05183	1	1
OHL PQ00896	0	1	OHL PQ03127	1	1	OHL PQ05211	0	1
OHL PQ00956	1	1	OHL PQ03135	1	1	OHL PQ05213	1	1
OHL PQ00981	1	0	OHL PQ03164	1	0	OHL PQ05215	1	1
OHL PQ00989	1	1	OHL PQ03172	1	0	OHL PQ05216	1	0
OHL PQ01012	1	1	OHL PQ03180	1	1	OHL PQ05221	0	1
OHL PQ01047	1	1	OHL PQ03188	1	1	OHL PQ05248	0	1
OHL PQ01052	1	0	OHL PQ03196	1	0	OHL PQ05252	0	1
OHL PQ01163	1	0	OHL PQ03223	1	0	OHL PQ05253	1	1
OHL PQ01208	1	0	OHL PQ03240	1	1	OHL PQ05255	0	1
OHL PQ01211	0	1	OHL PQ03245	1	1	OHL PQ05260	1	1
OHL PQ01241	1	0	OHL PQ03284	1	1	OHL PQ05261	1	1
OHL PQ01242	0	1	OHL PQ03287	1	1	OHL PQ05268	1	0
OHL PQ01258	1	1	OHL PQ03291	1	1	OHL PQ05271	1	1
OHL PQ01260	0	0	OHL PQ03295	1	1	OHL PQ05303	0	1
OHL PQ01311	1	0	OHL PQ03309	0	1	OHL PQ05311	0	1
OHL PQ01312	1	1	OHL PQ03325	0	1	OHL PQ05351	1	0
OHL PQ01387	1	1	OHL PQ03328	0	1	OHL PQ05359	1	0
OHL PQ01400	1	0	OHL PQ03367	0	1	OHL PQ05410	1	1
OHL PQ01408	1	0	OHL PQ03371	0	1	OHL PQ05435	1	0
OHL PQ01431	1	1	OHL PQ03373	0	1	OHL PQ05671	1	0
OHL PQ01439	1	1	OHL PQ03388	1	0	OHL PQ05672	1	1
OHL PQ01487	1	0	OHL PQ03484	1	1	OHL PQ05673	1	0
OHL PQ01508	1	1	OHL PQ03543	1	1	OHL PQ05680	1	1
OHL PQ01516	1	0	OHL PQ03544	1	1	OHL PQ05745	1	0
OHL PQ01543	1	0	OHL PQ03580	1	1	OHL PQ05860	1	0
OHL PQ01557	1	1	OHL PQ03624	1	1	OHL PQ05861	1	1
OHL PQ01560	1	1	OHL PQ03723	1	0	OHL PQ05872	1	1
OHL PQ01604	1	1	OHL PQ03724	1	0	OHL PQ05892	1	1
OHL PQ01607	1	1	OHL PQ03752	0	0	OHL PQ05893	1	1
OHL PQ01624	1	1	OHL PQ03755	1	0	OHL PQ05901	1	1
OHL PQ01629	1	1	OHL PQ03770	1	1	OHL PQ05911	1	1
OHL PQ01648	0	1	OHL PQ03785	1	1	OHL PQ05999	1	0
OHL PQ01685	1	0	OHL PQ03791	1	1	OHL PQ06075	1	0
OHL PQ01687	1	1	OHL PQ03823	1	1	OHL PQ06079	1	1
OHL PQ01693	1	1	OHL PQ03824	1	1	OHL PQ06161	0	1
OHL PQ01736	1	0	OHL PQ03849	1	0	OHL PQ06168	1	1
OHL PQ01744	1	0	OHL PQ03852	1	1	OHL PQ06176	1	1
OHL PQ01804	1	1	OHL PQ03881	1	0	OHL PQ06308	1	1
OHL PQ01860	1	1	OHL PQ03882	1	0	OHL PQ06309	0	1
OHL PQ01895	1	1	OHL PQ03916	1	1	OHL PQ06317	1	1
OHL PQ01900	1	1	OHL PQ03928	1	0	OHL PQ06340	0	1
OHL PQ02028	1	1	OHL PQ03959	1	1	OHL PQ06341	1	0
OHL PQ02072	1	0	OHL PQ03967	1	1	OHL PQ06348	1	0
OHL PQ02079	1	1	OHL PQ04036	1	0	OHL PQ06352	1	1
OHL PQ02122	1	0	OHL PQ04044	1	0	OHL PQ06455	1	0
OHL PQ02124	1	1	OHL PQ04071	1	1	OHL PQ06514	0	0
OHL PQ02137	1	0	OHL PQ04075	1	0	OHL PQ06551	1	1
OHL PQ02176	1	1	OHL PQ04192	0	1	OHL PQ06559	1	1
OHL PQ02250	0	1	OHL PQ04197	1	1	OHL PQ06692	1	1
OHL PQ02295	1	0	OHL PQ04205	1	1	OHL PQ06693	1	1
OHL PQ02356	1	1	OHL PQ04293	1	0	OHL PQ06701	1	1
OHL PQ02364	1	1	OHL PQ04301	1	1	OHL PQ06703	1	0
OHL PQ02391	1	1	OHL PQ04308	1	0	OHL PQ06712	1	1
OHL PQ02395	0	1	OHL PQ04384	1	0	OHL PQ06720	1	0
OHL PQ02413	1	1	OHL PQ04519	1	1	OHL PQ06725	0	1
OHL PQ02452	1	1	OHL PQ04555	0	1	OHL PQ06743	1	1
OHL PQ02455	1	0	OHL PQ04557	1	1	OHL PQ06751	1	1
OHL PQ02459	0	1	OHL PQ04559	1	1	OHL PQ06996	0	1
OHL PQ02463	0	1	OHL PQ04560	1	1	OHL PQ06997	1	1
OHL PQ02493	0	1	OHL PQ04564	1	1	OHL PQ07005	1	1
OHL PQ02563	1	0	OHL PQ04565	1	1	OHL PQ07007	0	1
						OHL PQ07013	1	1

Supplemental Table 12. Estimated abundance (gene copy number) of *E. gingivalis* (EG1) and the canine oral *Trichomonas* sp. (TC2) in samples progressing (PD_PRESENT) or not progressing (NO_PD) towards early canine periodontal disease at time points during the study. Five variables were investigated to assess their relationship with the abundance of either protozoan, in each tooth progression group, using a linear mixed effects model fitted for each variable, modelling the organism abundance against tooth progression group, and the time points during the study. 95% confidence intervals are reported for all abundance estimates.

qPCR assay (Organism)	Tooth progression group	Time point during study	Gender	Side	Area	ToothType	Age at start of trial (Weeks)	Estimated abundance (gene copy number)	95% Confidence intervals (upper and lower)
EG1	NO_PD	-5	F	-	-	-	-	6.62	(1.33, 32.9)
EG1	PD_SEEN	-5	F	-	-	-	-	5.42	(1.11, 26.42)
EG1	NO_PD	-4	F	-	-	-	-	5.57	(1.2, 25.88)
EG1	PD_SEEN	-4	F	-	-	-	-	7.59	(1.67, 34.5)
EG1	NO_PD	-3	F	-	-	-	-	7.46	(1.68, 33.09)
EG1	PD_SEEN	-3	F	-	-	-	-	12.11	(2.75, 53.33)
EG1	NO_PD	-2	F	-	-	-	-	7.71	(1.76, 33.76)
EG1	PD_SEEN	-2	F	-	-	-	-	14.29	(3.18, 64.25)
EG1	NO_PD	-1	F	-	-	-	-	8.25	(1.86, 36.56)
EG1	PD_SEEN	-1	F	-	-	-	-	14.35	(3.25, 63.25)
EG1	NO_PD	0	F	-	-	-	-	19.57	(4.47, 85.7)
EG1	PD_SEEN	0	F	-	-	-	-	21.20	(4.84, 92.81)
EG1	NO_PD	-5	M	-	-	-	-	2.12	(0.46, 9.84)
EG1	PD_SEEN	-5	M	-	-	-	-	2.24	(0.46, 10.88)
EG1	NO_PD	-4	M	-	-	-	-	3.96	(0.89, 17.61)
EG1	PD_SEEN	-4	M	-	-	-	-	4.10	(0.93, 18)
EG1	NO_PD	-3	M	-	-	-	-	5.25	(1.21, 22.8)
EG1	PD_SEEN	-3	M	-	-	-	-	7.36	(1.7, 31.83)
EG1	NO_PD	-2	M	-	-	-	-	6.10	(1.4, 26.54)
EG1	PD_SEEN	-2	M	-	-	-	-	5.43	(1.24, 23.83)
EG1	NO_PD	-1	M	-	-	-	-	4.53	(1.02, 20.17)
EG1	PD_SEEN	-1	M	-	-	-	-	6.69	(1.54, 29.05)
EG1	NO_PD	0	M	-	-	-	-	5.87	(1.35, 25.47)
EG1	PD_SEEN	0	M	-	-	-	-	4.34	(0.99, 18.99)
EG1	NO_PD	-5	-	Left	-	-	-	2.57	(0.73, 9.06)
EG1	PD_SEEN	-5	-	Left	-	-	-	3.34	(0.97, 11.43)
EG1	NO_PD	-4	-	Left	-	-	-	5.54	(1.59, 19.31)
EG1	PD_SEEN	-4	-	Left	-	-	-	6.93	(2.25, 21.35)
EG1	NO_PD	-3	-	Left	-	-	-	3.72	(1.15, 12.04)
EG1	PD_SEEN	-3	-	Left	-	-	-	12.33	(4.13, 36.83)
EG1	NO_PD	-2	-	Left	-	-	-	4.01	(1.26, 12.77)
EG1	PD_SEEN	-2	-	Left	-	-	-	9.61	(3.05, 30.31)
EG1	NO_PD	-1	-	Left	-	-	-	6.28	(1.86, 21.2)
EG1	PD_SEEN	-1	-	Left	-	-	-	8.38	(2.79, 25.11)
EG1	NO_PD	0	-	Left	-	-	-	6.28	(1.93, 20.44)
EG1	PD_SEEN	0	-	Left	-	-	-	10.90	(3.63, 32.71)
EG1	NO_PD	-5	-	Right	-	-	-	5.02	(1.43, 17.62)
EG1	PD_SEEN	-5	-	Right	-	-	-	3.49	(0.9, 13.46)
EG1	NO_PD	-4	-	Right	-	-	-	4.44	(1.39, 14.15)
EG1	PD_SEEN	-4	-	Right	-	-	-	3.95	(1.13, 13.73)
EG1	NO_PD	-3	-	Right	-	-	-	9.63	(3.12, 29.74)

EG1	PD_SEEN	-3	-	Right	-	-	-	6.06	(1.78, 20.63)
EG1	NO_PD	-2	-	Right	-	-	-	10.73	(3.49, 33.04)
EG1	PD_SEEN	-2	-	Right	-	-	-	7.67	(2.34, 25.09)
EG1	NO_PD	-1	-	Right	-	-	-	6.29	(2.04, 19.43)
EG1	PD_SEEN	-1	-	Right	-	-	-	14.31	(4.21, 48.69)
EG1	NO_PD	0	-	Right	-	-	-	15.57	(5.13, 47.28)
EG1	PD_SEEN	0	-	Right	-	-	-	7.98	(2.35, 27.13)
EG1	NO_PD	-5	-	-	Manible	-	-	3.85	(1.14, 13.04)
EG1	PD_SEEN	-5	-	-	Manible	-	-	1.84	(0.5, 6.77)
EG1	NO_PD	-4	-	-	Manible	-	-	6.38	(2.02, 20.15)
EG1	PD_SEEN	-4	-	-	Manible	-	-	5.41	(1.72, 17.01)
EG1	NO_PD	-3	-	-	Manible	-	-	5.26	(1.73, 16)
EG1	PD_SEEN	-3	-	-	Manible	-	-	9.47	(3.01, 29.76)
EG1	NO_PD	-2	-	-	Manible	-	-	5.07	(1.68, 15.36)
EG1	PD_SEEN	-2	-	-	Manible	-	-	9.71	(3.04, 31.05)
EG1	NO_PD	-1	-	-	Manible	-	-	5.70	(1.87, 17.34)
EG1	PD_SEEN	-1	-	-	Manible	-	-	6.98	(2.2, 22.12)
EG1	NO_PD	0	-	-	Manible	-	-	10.52	(3.51, 31.56)
EG1	PD_SEEN	0	-	-	Manible	-	-	6.40	(2, 20.46)
EG1	NO_PD	-5	-	-	Maxilla	-	-	3.49	(0.94, 12.94)
EG1	PD_SEEN	-5	-	-	Maxilla	-	-	6.27	(1.78, 22.11)
EG1	NO_PD	-4	-	-	Maxilla	-	-	3.02	(0.85, 10.68)
EG1	PD_SEEN	-4	-	-	Maxilla	-	-	5.82	(1.74, 19.45)
EG1	NO_PD	-3	-	-	Maxilla	-	-	9.14	(2.71, 30.81)
EG1	PD_SEEN	-3	-	-	Maxilla	-	-	9.89	(3.15, 31.01)
EG1	NO_PD	-2	-	-	Maxilla	-	-	11.84	(3.56, 39.37)
EG1	PD_SEEN	-2	-	-	Maxilla	-	-	7.80	(2.42, 25.17)
EG1	NO_PD	-1	-	-	Maxilla	-	-	7.23	(2, 26.17)
EG1	PD_SEEN	-1	-	-	Maxilla	-	-	13.58	(4.34, 42.52)
EG1	NO_PD	0	-	-	Maxilla	-	-	11.31	(3.31, 38.66)
EG1	PD_SEEN	0	-	-	Maxilla	-	-	13.84	(4.45, 43.08)
EG1	NO_PD	-5	-	-	-	Canine	-	5.13	(0.38, 69.96)
EG1	PD_SEEN	-5	-	-	-	Canine	-	0.04	(0, 1.31)
EG1	NO_PD	-4	-	-	-	Canine	-	2.17	(0.21, 22.61)
EG1	PD_SEEN	-4	-	-	-	Canine	-	4.74	(0.61, 36.86)
EG1	NO_PD	-3	-	-	-	Canine	-	1.99	(0.19, 20.77)
EG1	PD_SEEN	-3	-	-	-	Canine	-	14.31	(1.64, 124.93)
EG1	NO_PD	-2	-	-	-	Canine	-	4.60	(0.46, 46.3)
EG1	PD_SEEN	-2	-	-	-	Canine	-	1.79	(0.2, 15.6)
EG1	NO_PD	-1	-	-	-	Canine	-	5.28	(0.62, 44.92)
EG1	PD_SEEN	-1	-	-	-	Canine	-	0.67	(0.08, 5.71)
EG1	NO_PD	0	-	-	-	Canine	-	2.73	(0.35, 21.23)
EG1	PD_SEEN	0	-	-	-	Canine	-	2.18	(0.22, 22)
EG1	NO_PD	-5	-	-	-	Incisor	-	1.59	(0.15, 17.12)
EG1	PD_SEEN	-5	-	-	-	Incisor	-	1.85	(0.13, 26.15)
EG1	NO_PD	-4	-	-	-	Incisor	-	4.51	(0.42, 48.39)
EG1	PD_SEEN	-4	-	-	-	Incisor	-	3.36	(0.31, 36.13)
EG1	NO_PD	-3	-	-	-	Incisor	-	20.30	(2.31, 178.48)
EG1	PD_SEEN	-3	-	-	-	Incisor	-	32.76	(3.19, 336.27)
EG1	NO_PD	-2	-	-	-	Incisor	-	4.87	(0.55, 42.82)
EG1	PD_SEEN	-2	-	-	-	Incisor	-	5.33	(0.5, 57.26)
EG1	NO_PD	-1	-	-	-	Incisor	-	2.75	(0.19, 38.92)
EG1	PD_SEEN	-1	-	-	-	Incisor	-	8.56	(0.8, 91.94)
EG1	NO_PD	0	-	-	-	Incisor	-	3.85	(0.36, 41.34)

EG1	PD_SEEN	0	-	-	-	Incisor	-	1.28	(0.13, 13.18)
EG1	NO_PD	-5	-	-	-	Molar	-	4.01	(0.93, 17.34)
EG1	PD_SEEN	-5	-	-	-	Molar	-	6.21	(1.44, 26.81)
EG1	NO_PD	-4	-	-	-	Molar	-	6.24	(1.59, 24.54)
EG1	PD_SEEN	-4	-	-	-	Molar	-	7.16	(1.82, 28.17)
EG1	NO_PD	-3	-	-	-	Molar	-	7.10	(1.9, 26.63)
EG1	PD_SEEN	-3	-	-	-	Molar	-	11.48	(3.1, 42.51)
EG1	NO_PD	-2	-	-	-	Molar	-	7.76	(2.08, 28.89)
EG1	PD_SEEN	-2	-	-	-	Molar	-	10.71	(2.8, 40.99)
EG1	NO_PD	-1	-	-	-	Molar	-	5.84	(1.51, 22.58)
EG1	PD_SEEN	-1	-	-	-	Molar	-	9.96	(2.66, 37.32)
EG1	NO_PD	0	-	-	-	Molar	-	15.15	(4.04, 56.77)
EG1	PD_SEEN	0	-	-	-	Molar	-	7.57	(2.02, 28.36)
EG1	NO_PD	-5	-	-	-	Premolar	-	3.87	(0.76, 19.75)
EG1	PD_SEEN	-5	-	-	-	Premolar	-	3.53	(0.69, 18.02)
EG1	NO_PD	-4	-	-	-	Premolar	-	3.86	(0.78, 19.02)
EG1	PD_SEEN	-4	-	-	-	Premolar	-	4.21	(0.9, 19.7)
EG1	NO_PD	-3	-	-	-	Premolar	-	4.85	(1.04, 22.68)
EG1	PD_SEEN	-3	-	-	-	Premolar	-	3.95	(0.85, 18.39)
EG1	NO_PD	-2	-	-	-	Premolar	-	7.22	(1.58, 33.07)
EG1	PD_SEEN	-2	-	-	-	Premolar	-	12.37	(2.58, 59.32)
EG1	NO_PD	-1	-	-	-	Premolar	-	7.99	(1.74, 36.61)
EG1	PD_SEEN	-1	-	-	-	Premolar	-	23.34	(5.11, 106.66)
EG1	NO_PD	0	-	-	-	Premolar	-	11.84	(2.58, 54.23)
EG1	PD_SEEN	0	-	-	-	Premolar	-	35.67	(7.94, 160.31)
EG1	NO_PD	-5	-	-	-	-	52	3.74	(0.44, 31.47)
EG1	PD_SEEN	-5	-	-	-	-	52	3.10	(0.36, 26.43)
EG1	NO_PD	-4	-	-	-	-	52	3.04	(0.37, 24.63)
EG1	PD_SEEN	-4	-	-	-	-	52	3.07	(0.39, 24.36)
EG1	NO_PD	-3	-	-	-	-	52	4.60	(0.58, 36.78)
EG1	PD_SEEN	-3	-	-	-	-	52	4.29	(0.54, 33.91)
EG1	NO_PD	-2	-	-	-	-	52	10.31	(1.29, 82.1)
EG1	PD_SEEN	-2	-	-	-	-	52	13.44	(1.66, 109.05)
EG1	NO_PD	-1	-	-	-	-	52	5.57	(0.69, 45.24)
EG1	PD_SEEN	-1	-	-	-	-	52	7.04	(0.88, 56.21)
EG1	NO_PD	0	-	-	-	-	52	27.26	(3.42, 217.28)
EG1	PD_SEEN	0	-	-	-	-	52	10.34	(1.3, 82.51)
EG1	NO_PD	-5	-	-	-	-	104	3.66	(0.67, 19.88)
EG1	PD_SEEN	-5	-	-	-	-	104	3.25	(0.59, 17.84)
EG1	NO_PD	-4	-	-	-	-	104	3.61	(0.68, 19.16)
EG1	PD_SEEN	-4	-	-	-	-	104	3.84	(0.73, 20.1)
EG1	NO_PD	-3	-	-	-	-	104	5.12	(0.98, 26.89)
EG1	PD_SEEN	-3	-	-	-	-	104	5.59	(1.07, 29.19)
EG1	NO_PD	-2	-	-	-	-	104	8.99	(1.71, 47.17)
EG1	PD_SEEN	-2	-	-	-	-	104	11.66	(2.19, 62.18)
EG1	NO_PD	-1	-	-	-	-	104	5.73	(1.07, 30.65)
EG1	PD_SEEN	-1	-	-	-	-	104	7.83	(1.49, 41.25)
EG1	NO_PD	0	-	-	-	-	104	19.71	(3.76, 103.25)
EG1	PD_SEEN	0	-	-	-	-	104	10.04	(1.91, 52.61)
EG1	NO_PD	-5	-	-	-	-	156	3.59	(0.92, 13.98)
EG1	PD_SEEN	-5	-	-	-	-	156	3.41	(0.87, 13.42)
EG1	NO_PD	-4	-	-	-	-	156	4.29	(1.13, 16.27)
EG1	PD_SEEN	-4	-	-	-	-	156	4.80	(1.28, 18.03)
EG1	NO_PD	-3	-	-	-	-	156	5.70	(1.52, 21.32)

EG1	PD_SEEN	-3	-	-	-	-	156	7.28	(1.95, 27.19)
EG1	NO_PD	-2	-	-	-	-	156	7.84	(2.1, 29.33)
EG1	PD_SEEN	-2	-	-	-	-	156	10.12	(2.67, 38.39)
EG1	NO_PD	-1	-	-	-	-	156	5.89	(1.55, 22.44)
EG1	PD_SEEN	-1	-	-	-	-	156	8.71	(2.32, 32.72)
EG1	NO_PD	0	-	-	-	-	156	14.25	(3.82, 53.17)
EG1	PD_SEEN	0	-	-	-	-	156	9.74	(2.61, 36.38)
EG1	NO_PD	-5	-	-	-	-	208	3.52	(1.03, 11.98)
EG1	PD_SEEN	-5	-	-	-	-	208	3.57	(1.04, 12.31)
EG1	NO_PD	-4	-	-	-	-	208	5.09	(1.59, 16.3)
EG1	PD_SEEN	-4	-	-	-	-	208	6.00	(1.9, 18.96)
EG1	NO_PD	-3	-	-	-	-	208	6.34	(2.04, 19.77)
EG1	PD_SEEN	-3	-	-	-	-	208	9.49	(3.06, 29.46)
EG1	NO_PD	-2	-	-	-	-	208	6.84	(2.2, 21.24)
EG1	PD_SEEN	-2	-	-	-	-	208	8.78	(2.79, 27.6)
EG1	NO_PD	-1	-	-	-	-	208	6.06	(1.93, 19.07)
EG1	PD_SEEN	-1	-	-	-	-	208	9.69	(3.11, 30.15)
EG1	NO_PD	0	-	-	-	-	208	10.31	(3.32, 31.97)
EG1	PD_SEEN	0	-	-	-	-	208	9.45	(3.04, 29.41)
EG1	NO_PD	-5	-	-	-	-	260	3.45	(0.9, 13.29)
EG1	PD_SEEN	-5	-	-	-	-	260	3.75	(0.96, 14.62)
EG1	NO_PD	-4	-	-	-	-	260	6.05	(1.77, 20.66)
EG1	PD_SEEN	-4	-	-	-	-	260	7.50	(2.24, 25.08)
EG1	NO_PD	-3	-	-	-	-	260	7.06	(2.16, 23.08)
EG1	PD_SEEN	-3	-	-	-	-	260	12.37	(3.83, 39.95)
EG1	NO_PD	-2	-	-	-	-	260	5.97	(1.85, 19.3)
EG1	PD_SEEN	-2	-	-	-	-	260	7.62	(2.33, 24.92)
EG1	NO_PD	-1	-	-	-	-	260	6.24	(1.92, 20.29)
EG1	PD_SEEN	-1	-	-	-	-	260	10.78	(3.34, 34.77)
EG1	NO_PD	0	-	-	-	-	260	7.45	(2.29, 24.2)
EG1	PD_SEEN	0	-	-	-	-	260	9.17	(2.81, 29.96)
EG1	NO_PD	-5	-	-	-	-	312	3.38	(0.63, 18.05)
EG1	PD_SEEN	-5	-	-	-	-	312	3.93	(0.73, 21.25)
EG1	NO_PD	-4	-	-	-	-	312	7.18	(1.6, 32.18)
EG1	PD_SEEN	-4	-	-	-	-	312	9.37	(2.16, 40.63)
EG1	NO_PD	-3	-	-	-	-	312	7.86	(1.86, 33.18)
EG1	PD_SEEN	-3	-	-	-	-	312	16.12	(3.9, 66.58)
EG1	NO_PD	-2	-	-	-	-	312	5.21	(1.26, 21.59)
EG1	PD_SEEN	-2	-	-	-	-	312	6.61	(1.58, 27.71)
EG1	NO_PD	-1	-	-	-	-	312	6.42	(1.55, 26.58)
EG1	PD_SEEN	-1	-	-	-	-	312	11.99	(2.91, 49.33)
EG1	NO_PD	0	-	-	-	-	312	5.39	(1.29, 22.56)
EG1	PD_SEEN	0	-	-	-	-	312	8.90	(2.11, 37.58)
EG1	NO_PD	-5	-	-	-	-	364	3.32	(0.4, 27.38)
EG1	PD_SEEN	-5	-	-	-	-	364	4.12	(0.49, 34.5)
EG1	NO_PD	-4	-	-	-	-	364	8.53	(1.29, 56.44)
EG1	PD_SEEN	-4	-	-	-	-	364	11.71	(1.85, 74.17)
EG1	NO_PD	-3	-	-	-	-	364	8.74	(1.42, 53.89)
EG1	PD_SEEN	-3	-	-	-	-	364	21.00	(3.52, 125.46)
EG1	NO_PD	-2	-	-	-	-	364	4.54	(0.75, 27.31)
EG1	PD_SEEN	-2	-	-	-	-	364	5.74	(0.94, 34.92)
EG1	NO_PD	-1	-	-	-	-	364	6.60	(1.1, 39.48)
EG1	PD_SEEN	-1	-	-	-	-	364	13.33	(2.24, 79.25)
EG1	NO_PD	0	-	-	-	-	364	3.90	(0.64, 23.78)

EG1	PD_SEEN	0	-	-	-	-	364	8.64	(1.4, 53.24)
EG1	NO_PD	-5	-	-	-	-	416	3.25	(0.24, 43.89)
EG1	PD_SEEN	-5	-	-	-	-	416	4.32	(0.31, 59.23)
EG1	NO_PD	-4	-	-	-	-	416	10.13	(0.98, 105.14)
EG1	PD_SEEN	-4	-	-	-	-	416	14.64	(1.49, 143.85)
EG1	NO_PD	-3	-	-	-	-	416	9.73	(1.02, 93.1)
EG1	PD_SEEN	-3	-	-	-	-	416	27.37	(2.98, 251.64)
EG1	NO_PD	-2	-	-	-	-	416	3.96	(0.43, 36.79)
EG1	PD_SEEN	-2	-	-	-	-	416	4.98	(0.53, 46.86)
EG1	NO_PD	-1	-	-	-	-	416	6.79	(0.74, 62.55)
EG1	PD_SEEN	-1	-	-	-	-	416	14.82	(1.62, 135.62)
EG1	NO_PD	0	-	-	-	-	416	2.82	(0.3, 26.65)
EG1	PD_SEEN	0	-	-	-	-	416	8.39	(0.88, 80.21)
TC2	NO_PD	-5	F	-	-	-	-	3.19	(0.14, 72.46)
TC2	PD_SEEN	-5	F	-	-	-	-	4.53	(0.2, 104.76)
TC2	NO_PD	-4	F	-	-	-	-	12.03	(0.72, 202.14)
TC2	PD_SEEN	-4	F	-	-	-	-	18.30	(1.16, 288.02)
TC2	NO_PD	-3	F	-	-	-	-	10.83	(0.71, 166.06)
TC2	PD_SEEN	-3	F	-	-	-	-	35.67	(2.44, 521.36)
TC2	NO_PD	-2	F	-	-	-	-	3.45	(0.23, 51.17)
TC2	PD_SEEN	-2	F	-	-	-	-	4.32	(0.29, 65)
TC2	NO_PD	-1	F	-	-	-	-	6.99	(0.48, 102.46)
TC2	PD_SEEN	-1	F	-	-	-	-	16.49	(1.13, 239.83)
TC2	NO_PD	0	F	-	-	-	-	2.04	(0.13, 30.85)
TC2	PD_SEEN	0	F	-	-	-	-	8.14	(0.53, 124.78)
TC2	NO_PD	-5	M	-	-	-	-	10.44	(2.86, 38.18)
TC2	PD_SEEN	-5	M	-	-	-	-	8.39	(2.39, 29.49)
TC2	NO_PD	-4	M	-	-	-	-	18.06	(5.62, 57.99)
TC2	PD_SEEN	-4	M	-	-	-	-	12.71	(4.14, 39.04)
TC2	NO_PD	-3	M	-	-	-	-	12.94	(4.43, 37.77)
TC2	PD_SEEN	-3	M	-	-	-	-	15.89	(5.52, 45.74)
TC2	NO_PD	-2	M	-	-	-	-	10.96	(3.86, 31.13)
TC2	PD_SEEN	-2	M	-	-	-	-	10.31	(3.42, 31.06)
TC2	NO_PD	-1	M	-	-	-	-	18.50	(6.35, 53.92)
TC2	PD_SEEN	-1	M	-	-	-	-	18.48	(6.42, 53.18)
TC2	NO_PD	0	M	-	-	-	-	40.02	(14.09, 113.71)
TC2	PD_SEEN	0	M	-	-	-	-	33.47	(11.79, 95.04)
TC2	NO_PD	-5	-	Left	-	-	-	18.11	(5.79, 56.67)
TC2	PD_SEEN	-5	-	Left	-	-	-	25.18	(7.34, 86.37)
TC2	NO_PD	-4	-	Left	-	-	-	10.46	(3.63, 30.15)
TC2	PD_SEEN	-4	-	Left	-	-	-	9.18	(3.28, 25.68)
TC2	NO_PD	-3	-	Left	-	-	-	18.41	(6.75, 50.18)
TC2	PD_SEEN	-3	-	Left	-	-	-	18.91	(7.01, 50.96)
TC2	NO_PD	-2	-	Left	-	-	-	13.00	(4.77, 35.46)
TC2	PD_SEEN	-2	-	Left	-	-	-	10.92	(3.9, 30.53)
TC2	NO_PD	-1	-	Left	-	-	-	15.04	(5.22, 43.34)
TC2	PD_SEEN	-1	-	Left	-	-	-	21.18	(7.77, 57.77)
TC2	NO_PD	0	-	Left	-	-	-	26.35	(9.66, 71.86)
TC2	PD_SEEN	0	-	Left	-	-	-	31.56	(11.43, 87.11)
TC2	NO_PD	-5	-	Right	-	-	-	15.87	(5.12, 49.15)
TC2	PD_SEEN	-5	-	Right	-	-	-	11.76	(4.02, 34.44)
TC2	NO_PD	-4	-	Right	-	-	-	14.58	(4.79, 44.45)
TC2	PD_SEEN	-4	-	Right	-	-	-	10.00	(4.13, 24.17)
TC2	NO_PD	-3	-	Right	-	-	-	18.51	(6.92, 49.54)

TC2	PD_SEEN	-3	-	Right	-	-	-	16.59	(7.31, 37.69)
TC2	NO_PD	-2	-	Right	-	-	-	14.05	(5.39, 36.63)
TC2	PD_SEEN	-2	-	Right	-	-	-	7.80	(3.09, 19.69)
TC2	NO_PD	-1	-	Right	-	-	-	28.25	(9.76, 81.75)
TC2	PD_SEEN	-1	-	Right	-	-	-	17.72	(7.73, 40.58)
TC2	NO_PD	0	-	Right	-	-	-	21.77	(8.04, 58.95)
TC2	PD_SEEN	0	-	Right	-	-	-	34.87	(15.23, 79.86)
TC2	NO_PD	-5	-	-	Manible	-	-	13.32	(4.37, 40.58)
TC2	PD_SEEN	-5	-	-	Manible	-	-	20.38	(5.65, 73.49)
TC2	NO_PD	-4	-	-	Manible	-	-	12.66	(4.91, 32.62)
TC2	PD_SEEN	-4	-	-	Manible	-	-	11.88	(3.9, 36.18)
TC2	NO_PD	-3	-	-	Manible	-	-	13.87	(5.73, 33.59)
TC2	PD_SEEN	-3	-	-	Manible	-	-	19.05	(6.5, 55.85)
TC2	NO_PD	-2	-	-	Manible	-	-	10.57	(4.4, 25.39)
TC2	PD_SEEN	-2	-	-	Manible	-	-	15.49	(5.65, 42.49)
TC2	NO_PD	-1	-	-	Manible	-	-	12.17	(5.02, 29.46)
TC2	PD_SEEN	-1	-	-	Manible	-	-	24.83	(8.47, 72.77)
TC2	NO_PD	0	-	-	Manible	-	-	41.54	(17.72, 97.43)
TC2	PD_SEEN	0	-	-	Manible	-	-	27.87	(9.51, 81.66)
TC2	NO_PD	-5	-	-	Maxilla	-	-	15.80	(5.66, 44.14)
TC2	PD_SEEN	-5	-	-	Maxilla	-	-	22.06	(6.83, 71.31)
TC2	NO_PD	-4	-	-	Maxilla	-	-	10.74	(4.33, 26.65)
TC2	PD_SEEN	-4	-	-	Maxilla	-	-	7.90	(3.22, 19.4)
TC2	NO_PD	-3	-	-	Maxilla	-	-	7.78	(3.38, 17.9)
TC2	PD_SEEN	-3	-	-	Maxilla	-	-	12.72	(5.18, 31.21)
TC2	NO_PD	-2	-	-	Maxilla	-	-	9.66	(4.24, 22.02)
TC2	PD_SEEN	-2	-	-	Maxilla	-	-	13.47	(5.33, 34.08)
TC2	NO_PD	-1	-	-	Maxilla	-	-	18.26	(7.93, 42.06)
TC2	PD_SEEN	-1	-	-	Maxilla	-	-	24.26	(9.75, 60.4)
TC2	NO_PD	0	-	-	Maxilla	-	-	31.39	(14.01, 70.32)
TC2	PD_SEEN	0	-	-	Maxilla	-	-	13.95	(5.52, 35.27)
TC2	NO_PD	-5	-	-	-	Canine	-	12.89	(3.97, 41.84)
TC2	PD_SEEN	-5	-	-	-	Canine	-	10.71	(3.58, 32.03)
TC2	NO_PD	-4	-	-	-	Canine	-	18.59	(6.19, 55.86)
TC2	PD_SEEN	-4	-	-	-	Canine	-	15.64	(5.72, 42.8)
TC2	NO_PD	-3	-	-	-	Canine	-	53.99	(19.57, 148.94)
TC2	PD_SEEN	-3	-	-	-	Canine	-	24.12	(9.95, 58.47)
TC2	NO_PD	-2	-	-	-	Canine	-	17.51	(6.5, 47.21)
TC2	PD_SEEN	-2	-	-	-	Canine	-	8.11	(3.15, 20.86)
TC2	NO_PD	-1	-	-	-	Canine	-	12.71	(4.06, 39.76)
TC2	PD_SEEN	-1	-	-	-	Canine	-	16.68	(6.89, 40.39)
TC2	NO_PD	0	-	-	-	Canine	-	33.93	(11.98, 96.07)
TC2	PD_SEEN	0	-	-	-	Canine	-	66.80	(27.92, 159.81)
TC2	NO_PD	-5	-	-	-	Incisor	-	3.13	(0.2, 48.74)
TC2	PD_SEEN	-5	-	-	-	Incisor	-	2.19	(0.05, 89.63)
TC2	NO_PD	-4	-	-	-	Incisor	-	2.44	(0.24, 25.28)
TC2	PD_SEEN	-4	-	-	-	Incisor	-	1.30	(0.19, 8.99)
TC2	NO_PD	-3	-	-	-	Incisor	-	1.35	(0.13, 13.97)
TC2	PD_SEEN	-3	-	-	-	Incisor	-	1.09	(0.13, 8.82)
TC2	NO_PD	-2	-	-	-	Incisor	-	2.99	(0.29, 30.87)
TC2	PD_SEEN	-2	-	-	-	Incisor	-	1.11	(0.14, 8.98)
TC2	NO_PD	-1	-	-	-	Incisor	-	1.26	(0.16, 10.18)
TC2	PD_SEEN	-1	-	-	-	Incisor	-	5.04	(0.62, 40.71)
TC2	NO_PD	0	-	-	-	Incisor	-	5.07	(0.73, 34.95)

TC2	PD_SEEN	0	-	-	-	Incisor	-	1.01	(0.1, 10.41)
TC2	NO_PD	-5	-	-	-	Molar	-	1.83	(0.16, 21.03)
TC2	PD_SEEN	-5	-	-	-	Molar	-	19.22	(1.13, 326.49)
TC2	NO_PD	-4	-	-	-	Molar	-	1.65	(0.14, 18.94)
TC2	PD_SEEN	-4	-	-	-	Molar	-	1.43	(0.12, 16.41)
TC2	NO_PD	-3	-	-	-	Molar	-	9.62	(1.08, 85.84)
TC2	PD_SEEN	-3	-	-	-	Molar	-	17.84	(1.59, 200.2)
TC2	NO_PD	-2	-	-	-	Molar	-	3.83	(0.43, 34.18)
TC2	PD_SEEN	-2	-	-	-	Molar	-	2.85	(0.25, 32.74)
TC2	NO_PD	-1	-	-	-	Molar	-	1.04	(0.06, 17.68)
TC2	PD_SEEN	-1	-	-	-	Molar	-	3.44	(0.3, 39.5)
TC2	NO_PD	0	-	-	-	Molar	-	0.96	(0.08, 11.02)
TC2	PD_SEEN	0	-	-	-	Molar	-	4.40	(0.39, 49.34)
TC2	NO_PD	-5	-	-	-	Premolar	-	19.20	(5.86, 62.84)
TC2	PD_SEEN	-5	-	-	-	Premolar	-	15.02	(4.59, 49.18)
TC2	NO_PD	-4	-	-	-	Premolar	-	23.85	(8.75, 65.02)
TC2	PD_SEEN	-4	-	-	-	Premolar	-	10.31	(3.78, 28.1)
TC2	NO_PD	-3	-	-	-	Premolar	-	18.78	(7.62, 46.29)
TC2	PD_SEEN	-3	-	-	-	Premolar	-	18.70	(7.78, 44.94)
TC2	NO_PD	-2	-	-	-	Premolar	-	17.90	(7.36, 43.53)
TC2	PD_SEEN	-2	-	-	-	Premolar	-	25.28	(9.82, 65.09)
TC2	NO_PD	-1	-	-	-	Premolar	-	37.68	(14.38, 98.73)
TC2	PD_SEEN	-1	-	-	-	Premolar	-	19.03	(7.73, 46.85)
TC2	NO_PD	0	-	-	-	Premolar	-	52.90	(21.47, 130.36)
TC2	PD_SEEN	0	-	-	-	Premolar	-	45.46	(18.46, 111.99)
TC2	NO_PD	-5	-	-	-		52	25.71	(6.15, 107.43)
TC2	PD_SEEN	-5	-	-	-	-	52	21.42	(5.13, 89.5)
TC2	NO_PD	-4	-	-	-	-	52	14.91	(3.8, 58.54)
TC2	PD_SEEN	-4	-	-	-	-	52	36.70	(10.28, 131)
TC2	NO_PD	-3	-	-	-	-	52	27.86	(7.81, 99.38)
TC2	PD_SEEN	-3	-	-	-	-	52	46.44	(13.02, 165.68)
TC2	NO_PD	-2	-	-	-	-	52	12.88	(3.75, 44.21)
TC2	PD_SEEN	-2	-	-	-	-	52	6.14	(1.65, 22.88)
TC2	NO_PD	-1	-	-	-	-	52	18.92	(5.51, 64.97)
TC2	PD_SEEN	-1	-	-	-	-	52	57.66	(16.77, 198.18)
TC2	NO_PD	0	-	-	-	-	52	59.48	(17.32, 204.23)
TC2	PD_SEEN	0	-	-	-	-	52	81.82	(24.62, 271.9)
TC2	NO_PD	-5	-	-	-	-	104	8.57	(1.92, 38.3)
TC2	PD_SEEN	-5	-	-	-	-	104	17.27	(3.77, 79.03)
TC2	NO_PD	-4	-	-	-	-	104	6.58	(1.59, 27.11)
TC2	PD_SEEN	-4	-	-	-	-	104	8.65	(2.21, 33.84)
TC2	NO_PD	-3	-	-	-	-	104	28.70	(7.19, 114.55)
TC2	PD_SEEN	-3	-	-	-	-	104	17.20	(4.42, 66.95)
TC2	NO_PD	-2	-	-	-	-	104	11.43	(2.89, 45.21)
TC2	PD_SEEN	-2	-	-	-	-	104	5.42	(1.31, 22.37)
TC2	NO_PD	-1	-	-	-	-	104	16.22	(3.91, 67.28)
TC2	PD_SEEN	-1	-	-	-	-	104	16.34	(4.12, 64.84)
TC2	NO_PD	0	-	-	-	-	104	45.85	(11.57, 181.66)
TC2	PD_SEEN	0	-	-	-	-	104	38.66	(9.74, 153.37)
TC2	NO_PD	-5	-	-	-	-	156	10.80	(3.38, 34.48)
TC2	PD_SEEN	-5	-	-	-	-	156	15.90	(4.86, 51.99)
TC2	NO_PD	-4	-	-	-	-	156	8.61	(2.82, 26.27)
TC2	PD_SEEN	-4	-	-	-	-	156	9.37	(3.18, 27.57)
TC2	NO_PD	-3	-	-	-	-	156	23.24	(7.82, 69.03)

TC2	PD_SEEN	-3	-	-	-	-	156	17.29	(5.89, 50.74)
TC2	NO_PD	-2	-	-	-	-	156	11.60	(3.92, 34.33)
TC2	PD_SEEN	-2	-	-	-	-	156	6.75	(2.19, 20.78)
TC2	NO_PD	-1	-	-	-	-	156	16.42	(5.29, 50.97)
TC2	PD_SEEN	-1	-	-	-	-	156	17.44	(5.85, 52.03)
TC2	NO_PD	0	-	-	-	-	156	40.70	(13.78, 120.17)
TC2	PD_SEEN	0	-	-	-	-	156	36.28	(12.29, 107.15)
TC2	NO_PD	-5	-	-	-	-	208	13.60	(5.24, 35.29)
TC2	PD_SEEN	-5	-	-	-	-	208	14.64	(5.51, 38.93)
TC2	NO_PD	-4	-	-	-	-	208	11.27	(4.58, 27.73)
TC2	PD_SEEN	-4	-	-	-	-	208	10.14	(4.23, 24.32)
TC2	NO_PD	-3	-	-	-	-	208	18.82	(7.92, 44.72)
TC2	PD_SEEN	-3	-	-	-	-	208	17.39	(7.35, 41.11)
TC2	NO_PD	-2	-	-	-	-	208	11.77	(4.97, 27.9)
TC2	PD_SEEN	-2	-	-	-	-	208	8.42	(3.43, 20.67)
TC2	NO_PD	-1	-	-	-	-	208	16.63	(6.71, 41.17)
TC2	PD_SEEN	-1	-	-	-	-	208	18.61	(7.78, 44.55)
TC2	NO_PD	0	-	-	-	-	208	36.13	(15.3, 85.3)
TC2	PD_SEEN	0	-	-	-	-	208	34.06	(14.41, 80.48)
TC2	NO_PD	-5	-	-	-	-	260	17.13	(6.55, 44.78)
TC2	PD_SEEN	-5	-	-	-	-	260	13.49	(5.03, 36.12)
TC2	NO_PD	-4	-	-	-	-	260	14.75	(6.37, 34.17)
TC2	PD_SEEN	-4	-	-	-	-	260	10.98	(4.88, 24.7)
TC2	NO_PD	-3	-	-	-	-	260	15.23	(6.99, 33.22)
TC2	PD_SEEN	-3	-	-	-	-	260	17.48	(8.1, 37.74)
TC2	NO_PD	-2	-	-	-	-	260	11.94	(5.53, 25.79)
TC2	PD_SEEN	-2	-	-	-	-	260	10.49	(4.71, 23.36)
TC2	NO_PD	-1	-	-	-	-	260	16.83	(7.56, 37.51)
TC2	PD_SEEN	-1	-	-	-	-	260	19.87	(9.15, 43.12)
TC2	NO_PD	0	-	-	-	-	260	32.07	(14.85, 69.27)
TC2	PD_SEEN	0	-	-	-	-	260	31.96	(14.73, 69.38)
TC2	NO_PD	-5	-	-	-	-	312	21.58	(6.64, 70.2)
TC2	PD_SEEN	-5	-	-	-	-	312	12.42	(3.73, 41.36)
TC2	NO_PD	-4	-	-	-	-	312	19.31	(7.37, 50.63)
TC2	PD_SEEN	-4	-	-	-	-	312	11.88	(4.74, 29.77)
TC2	NO_PD	-3	-	-	-	-	312	12.33	(5.16, 29.5)
TC2	PD_SEEN	-3	-	-	-	-	312	17.58	(7.55, 40.93)
TC2	NO_PD	-2	-	-	-	-	312	12.12	(5.18, 28.33)
TC2	PD_SEEN	-2	-	-	-	-	312	13.08	(5.46, 31.34)
TC2	NO_PD	-1	-	-	-	-	312	17.04	(7.2, 40.33)
TC2	PD_SEEN	-1	-	-	-	-	312	21.20	(9.12, 49.28)
TC2	NO_PD	0	-	-	-	-	312	28.47	(12.07, 67.19)
TC2	PD_SEEN	0	-	-	-	-	312	30.00	(12.58, 71.55)
TC2	NO_PD	-5	-	-	-	-	364	27.19	(5.94, 124.4)
TC2	PD_SEEN	-5	-	-	-	-	364	11.44	(2.44, 53.61)
TC2	NO_PD	-4	-	-	-	-	364	25.29	(7.49, 85.35)
TC2	PD_SEEN	-4	-	-	-	-	364	12.86	(4.07, 40.63)
TC2	NO_PD	-3	-	-	-	-	364	9.99	(3.33, 29.95)
TC2	PD_SEEN	-3	-	-	-	-	364	17.67	(6.17, 50.61)
TC2	NO_PD	-2	-	-	-	-	364	12.30	(4.25, 35.61)
TC2	PD_SEEN	-2	-	-	-	-	364	16.31	(5.51, 48.25)
TC2	NO_PD	-1	-	-	-	-	364	17.26	(5.98, 49.78)
TC2	PD_SEEN	-1	-	-	-	-	364	22.63	(7.95, 64.4)
TC2	NO_PD	0	-	-	-	-	364	25.28	(8.57, 74.58)

TC2	PD_SEEN	0	-	-	-	-	364	28.16	(9.4, 84.37)
TC2	NO_PD	-5	-	-	-	-	416	34.25	(5.02, 233.7)
TC2	PD_SEEN	-5	-	-	-	-	416	10.53	(1.5, 73.76)
TC2	NO_PD	-4	-	-	-	-	416	33.10	(7.12, 153.81)
TC2	PD_SEEN	-4	-	-	-	-	416	13.92	(3.27, 59.22)
TC2	NO_PD	-3	-	-	-	-	416	8.09	(2, 32.64)
TC2	PD_SEEN	-3	-	-	-	-	416	17.77	(4.7, 67.21)
TC2	NO_PD	-2	-	-	-	-	416	12.48	(3.24, 48.09)
TC2	PD_SEEN	-2	-	-	-	-	416	20.33	(5.16, 80.09)
TC2	NO_PD	-1	-	-	-	-	416	17.47	(4.6, 66.41)
TC2	PD_SEEN	-1	-	-	-	-	416	24.15	(6.44, 90.61)
TC2	NO_PD	0	-	-	-	-	416	22.44	(5.67, 88.84)
TC2	PD_SEEN	0	-	-	-	-	416	26.43	(6.55, 106.67)

Supplemental Table 13. Top 10 BLAST sequence matches and associated sequence information for 10 X canine oral *Trichomonas* sp. isolated from 10 individual dogs. No clear higher sequence match is evident for any of the 10 isolated trichomonads. 99 % hit matches are seen against sequences annotated as *Trichomonas* sp., *Trichomonas gallinae*, and *Trichomonas tenax*.

BLAST Query sequence name and animal ID.	Sequence hit number	Match Identity accession and sequence strain name	Nucleotide matches and percentage match
Yasmine MS05114	1	JQ030998.1 <i>Trichomonas</i> sp.	885/888 (99%)
	2	JQ030997.1 <i>Trichomonas</i> sp.	885/888 (99%)
	3	FN433479.1 <i>Trichomonas</i> sp.	885/888 (99%)
	4	JQ030999.1 <i>Trichomonas</i> sp.	884/888 (99%)
	5	HG008106.1 <i>Trichomonas gallinae</i>	883/888 (99%)
	6	JX943581.1 <i>Trichomonas tenax</i>	883/888 (99%)
	7	JX943576.1 <i>Trichomonas tenax</i>	883/888 (99%)
	8	JX943572.1 <i>Trichomonas tenax</i>	883/888 (99%)
	9	FN433484.2 <i>Trichomonas gallinae</i>	883/888 (99%)
	10	FN433482.1 <i>Trichomonas gallinae</i>	883/888 (99%)
Macy LR05412	1	JQ030998.1 <i>Trichomonas</i> sp.	908/911 (99%)
	2	JQ030997.1 <i>Trichomonas</i> sp.	908/911 (99%)
	3	FN433479.1 <i>Trichomonas</i> sp.	908/911 (99%)
	4	JQ030999.1 <i>Trichomonas</i> sp.	907/911 (99%)
	5	HG008106.1 <i>Trichomonas gallinae</i>	906/911 (99%)
	6	JX943581.1 <i>Trichomonas tenax</i>	906/911 (99%)
	7	JX943576.1 <i>Trichomonas tenax</i>	906/911 (99%)
	8	JX943572.1 <i>Trichomonas tenax</i>	906/911 (99%)
	9	FN433484.2 <i>Trichomonas gallinae</i>	906/911 (99%)
	10	FN433482.1 <i>Trichomonas gallinae</i>	906/911 (99%)
Cleo CS04357	1	JQ030998.1 <i>Trichomonas</i> sp.	918/920 (99%)
	2	JQ030997.1 <i>Trichomonas</i> sp.	918/920 (99%)
	3	FN433479.1 <i>Trichomonas</i> sp.	918/920 (99%)
	4	JQ030999.1 <i>Trichomonas</i> sp.	917/920 (99%)
	5	FN433482.1 <i>Trichomonas gallinae</i>	916/920 (99%)
	6	FN433481.1 <i>Trichomonas gallinae</i>	916/920 (99%)
	7	FN433480.1 <i>Trichomonas gallinae</i>	916/920 (99%)
	8	EU215374.1 <i>Trichomonas gallinae</i>	916/920 (99%)
	9	EU215373.1 <i>Trichomonas gallinae</i>	916/920 (99%)
	10	HG008106.1 <i>Trichomonas gallinae</i>	914/920 (99%)
Esme LR05202	1	JQ030998.1 <i>Trichomonas</i> sp.	878/881 (99%)
	2	JQ030997.1 <i>Trichomonas</i> sp.	878/881 (99%)
	3	FN433479.1 <i>Trichomonas</i> sp.	878/881 (99%)
	4	JQ030999.1 <i>Trichomonas</i> sp.	877/881 (99%)
	5	HG008106.1 <i>Trichomonas gallinae</i>	876/881 (99%)
	6	JX943581.1 <i>Trichomonas tenax</i>	876/881 (99%)
	7	JX943576.1 <i>Trichomonas tenax</i>	876/881 (99%)
	8	JX943572.1 <i>Trichomonas tenax</i>	876/881 (99%)
	9	FN433484.2 <i>Trichomonas gallinae</i>	876/881 (99%)
	10	FN433482.1 <i>Trichomonas gallinae</i>	876/881 (99%)
Oasis LR05445	1	JQ030998.1 <i>Trichomonas</i> sp.	808/812 (99%)
	2	JQ030997.1 <i>Trichomonas</i> sp.	808/812 (99%)
	3	FN433479.1 <i>Trichomonas</i> sp.	808/812 (99%)
	4	JQ030999.1 <i>Trichomonas</i> sp.	807/812 (99%)
	5	HG008106.1 <i>Trichomonas gallinae</i>	806/812 (99%)
	6	JX943581.1 <i>Trichomonas tenax</i>	806/812 (99%)
	7	JX943576.1 <i>Trichomonas tenax</i>	806/812 (99%)
	8	JX943572.1 <i>Trichomonas tenax</i>	806/812 (99%)
	9	FN433484.2 <i>Trichomonas gallinae</i>	806/812 (99%)
	10	FN433482.1 <i>Trichomonas gallinae</i>	806/812 (99%)
Tigger LR05009	1	JQ030998.1 <i>Trichomonas</i> sp.	916/919 (99%)
	2	JQ030997.1 <i>Trichomonas</i> sp.	916/919 (99%)
	3	FN433479.1 <i>Trichomonas</i> sp.	916/919 (99%)
	4	JQ030999.1 <i>Trichomonas</i> sp.	915/919 (99%)
	5	HG008106.1 <i>Trichomonas gallinae</i>	914/919 (99%)
	6	JX943581.1 <i>Trichomonas tenax</i>	914/919 (99%)
	7	JX943576.1 <i>Trichomonas tenax</i>	914/919 (99%)
	8	JX943572.1 <i>Trichomonas tenax</i>	914/919 (99%)
	9	FN433484.2 <i>Trichomonas gallinae</i>	914/919 (99%)
	10	FN433482.1 <i>Trichomonas gallinae</i>	914/919 (99%)

Orla LR05446	1	JQ030998.1 <i>Trichomonas</i> sp.	835/836 (99%)
	2	JQ030997.1 <i>Trichomonas</i> sp.	835/836 (99%)
	3	FN433479.1 <i>Trichomonas</i> sp.	835/836 (99%)
	4	JQ030999.1 <i>Trichomonas</i> sp.	834/836 (99%)
	5	FN433482.1 <i>Trichomonas</i> gallinae	833/836 (99%)
	6	FN433481.1 <i>Trichomonas</i> gallinae	833/836 (99%)
	7	FN433480.1 <i>Trichomonas</i> gallinae	833/836 (99%)
	8	EU215374.1 <i>Trichomonas</i> gallinae	833/836 (99%)
	9	EU215373.1 <i>Trichomonas</i> gallinae	833/836 (99%)
	10	HG008106.1 <i>Trichomonas</i> gallinae	831/836 (99%)
Brock MS05156	1	JQ030998.1 <i>Trichomonas</i> sp.	917/920 (99%)
	2	JQ030997.1 <i>Trichomonas</i> sp.	917/920 (99%)
	3	FN433479.1 <i>Trichomonas</i> sp.	917/920 (99%)
	4	JQ030999.1 <i>Trichomonas</i> sp.	916/920 (99%)
	5	HG008106.1 <i>Trichomonas</i> gallinae	915/920 (99%)
	6	JX943581.1 <i>Trichomonas</i> tenax	915/920 (99%)
	7	JX943576.1 <i>Trichomonas</i> tenax	915/920 (99%)
	8	JX943572.1 <i>Trichomonas</i> tenax	915/920 (99%)
	9	FN433484.2 <i>Trichomonas</i> gallinae	915/920 (99%)
	10	FN433482.1 <i>Trichomonas</i> gallinae	915/920 (99%)
Wiggle LR05830	1	JQ030998.1 <i>Trichomonas</i> sp.	880/883 (99%)
	2	JQ030997.1 <i>Trichomonas</i> sp.	880/883 (99%)
	3	FN433479.1 <i>Trichomonas</i> sp.	880/883 (99%)
	4	JQ030999.1 <i>Trichomonas</i> sp.	879/883 (99%)
	5	HG008106.1 <i>Trichomonas</i> gallinae	878/883 (99%)
	6	JX943581.1 <i>Trichomonas</i> tenax	878/883 (99%)
	7	JX943576.1 <i>Trichomonas</i> tenax	878/883 (99%)
	8	JX943572.1 <i>Trichomonas</i> tenax	878/883 (99%)
	9	FN433484.2 <i>Trichomonas</i> gallinae	878/883 (99%)
	10	FN433482.1 <i>Trichomonas</i> gallinae	878/883 (99%)
Yoshi MS05118	1	JQ030998.1 <i>Trichomonas</i> sp.	905/908 (99%)
	2	JQ030997.1 <i>Trichomonas</i> sp.	905/908 (99%)
	3	FN433479.1 <i>Trichomonas</i> sp.	905/908 (99%)
	4	JQ030999.1 <i>Trichomonas</i> sp.	904/908 (99%)
	5	HG008106.1 <i>Trichomonas</i> gallinae	903/908 (99%)
	6	JX943581.1 <i>Trichomonas</i> tenax	903/908 (99%)
	7	JX943576.1 <i>Trichomonas</i> tenax	903/908 (99%)
	8	JX943572.1 <i>Trichomonas</i> tenax	903/908 (99%)
	9	FN433484.2 <i>Trichomonas</i> gallinae	878/883 (99%)
	10	FN433482.1 <i>Trichomonas</i> gallinae	878/883 (99%)

Supplemental Table 14. *T. brixii* cellular metrics for 100 individually measured cells. Images of each cell were captured using a 100 X oil immersion objective and a Nikon E400 brightfield upright microscope. The cellular measurements were taken in ImageJ version 1.51n, using a calibrated image of a graticule for micrometre calibration. Cell body and width, axostyle projection, undulating membrane length, and nucleus length and width, were measured and recorded. Mean values for all measurements along with standard deviation of the means were calculated using Microsoft Excel 2013.

Cell number	Cell body length (μM)	Cell body width (μM)	Axostyle projection length (μM)	Undulating membrane length (μM)	Nucleus length (μM)	Nucleus width (μM)
1	11.011	5.349	8.641	11.057	3.7	1.789
2	12.259	4.804	10.239	12.431	4.741	3.227
3	11.722	8.101	8.975	13.118	4.456	2.919
4	10.474	5.747	10.568	16.989	4	2.919
5	11.824	7.054	8.72	14.218	3.914	2.616
6	11.737	6.621	12.289	11.973	4.671	2.786
7	15.16	5.368	15.017	14.791	4.138	3.405
8	10.6	7.09	7.498	17.376	4.223	3.077
9	9.94	4.727	10.526	12.021	4.214	2.391
10	11.42	5.206	13.73	13.785	4.546	3.405
11	10.574	7.518	7.586	11.949	4.708	2.919
12	11.686	7.112	11.055	11.44	3.255	2.695
13	11.275	6.635	12.163	16.533	4.663	2.636
14	11.577	7.14	12.372	15.133	3.728	1.889
15	12.721	6.704	9.099	12.882	4.537	3.728
16	8.656	6.192	9.183	10.429	4.858	2.519
17	10.18	4.921	14.622	18.138	5.044	2.561
18	11.498	7.503	13.211	16.37	4.479	2.833
19	13.859	6.918	10.299	14.056	5.167	2.919
20	12.077	6.192	13.188	14.173	5.508	2.636
21	14.392	7.887	9.4	12.651	5.866	2.407
22	11.267	4.465	12.53	12.767	5.544	2.203
23	13.528	7.143	10.924	17.835	4.663	2.611
24	13.175	7.06	12.563	12.973	4.1	3.488
25	11.359	6.226	8.177	9.005	4.896	1.95
26	12.367	5.829	10.846	15.946	3.214	2.467
27	13.413	7.663	12.091	15.657	5.444	3.073
28	10.908	7.308	17.231	13.549	5.391	1.306
29	14.357	5.822	12.57	16.317	4.511	1.667
30	15.153	6.492	8.236	11.719	5.255	1.957
31	11.871	6.443	10.977	12.417	3.496	2.302
32	10.569	5.691	12.216	19.905	4.278	2.753
33	14.313	6.35	9.556	14.336	4.151	2.611
34	14.635	8.488	10.452	11.968	4.375	2.636
35	16.353	7.934	11.75	16.697	4.671	2.256
36	12.351	5.71	13.758	11.294	3.432	2.828
37	16.046	5.892	12.46	12.33	1.652	2.611
38	12.547	5.644	13.618	11.807	4.447	2.407
39	12.359	5.531	11.962	6.872	4.278	3.89
40	11.636	6.018	12.023	10.682	5.113	3.081
41	13.051	6.79	14.265	15.073	4.201	3.435
42	12.8	4.851	14.443	7.394	5.192	4.42
43	14.34	5.7	12.983	16.826	5.312	2.407
44	10.6	4.735	9.37	15.068	3.323	2.611
45	13.741	6.854	7.995	21.05	4.537	3.339
46	12.968	5.635	10.784	13.014	3.275	3.37
47	12.188	6.258	11.004	16.915	3.503	2.179
48	11.172	5.774	10.345	14.381	5.287	3.275
49	12.464	7.308	8.634	13.396	4.671	2.514
50	12.871	6.667	8.275	12.767	4.632	2.636
51	13.531	4.69	7.763	14.711	2.656	2.302

52	12.734	6.504	7.801	14.105	2.302	3.043
53	16.046	5.363	13.794	14.455	4.288	2.883
54	12.457	6.673	7.934	12.948	4.405	3.094
55	14.647	5.863	8.48	12.295	3.739	1.977
56	12.326	7.005	10.956	11.826	5.972	2.828
57	13.992	6.722	11.668	14.266	4.148	1.595
58	16.281	5.051	9.471	13.134	4.858	2.477
59	10.689	7.713	10.997	11.59	3.111	3.563
60	13.562	5.767	11.546	11.644	4.467	2.105
61	10.908	6.016	7.74	10.999	3.812	3.043
62	11.883	6.555	11.524	11.404	4.502	2.319
63	14.981	6.389	8.712	15.283	3.693	3.275
64	11.397	6.667	6.368	16.309	3.97	2.986
65	11.186	6.698	9.55	18.795	3.92	2.833
66	12.436	6.696	10.142	9.019	4.861	2.753
67	16.558	4.727	8.859	9.137	4.288	2.919
68	13.628	4.802	6.946	13.412	3.303	2.865
69	15.786	7.162	8.096	12.58	5.539	2.161
70	12.423	7.649	7.509	11.655	2.87	2.772
71	13.045	5.059	9.276	9.889	4.062	3.239
72	12.147	5.562	9.066	15.746	3.339	2.611
73	15.731	5.811	11.052	14.119	2.758	3.381
74	12.781	5.876	11.862	15.491	3.756	3.339
75	14.639	7.162	12.1	20.352	4.479	2.767
76	10.265	6.673	16.147	17.14	4.815	1.97
77	17.95	6.952	7.697	13.748	4.179	3.094
78	11.681	7.432	9.159	13.012	3.839	2.435
79	15.005	6.341	9.492	14.843	4.858	3.416
80	13.526	5.7	9.993	14.855	3.577	3.111
81	10.544	7.704	7.129	10.155	3.777	2.535
82	9.308	7.887	15.356	10.65	3.777	2.514
83	12.948	5.531	10.543	15.337	3.654	2.611
84	15.956	7.039	6.492	15.524	3.89	2.828
85	17.407	7.353	10.811	13.79	5.539	2.786
86	15.503	7.969	7.027	11.473	4.052	3.323
87	13.636	7.854	10.736	14.439	4.721	3.552
88	11.383	7.391	14.205	9.806	4.138	2.986
89	10.996	5.863	8.73	12.583	5.539	3.339
90	12.41	5.892	10.867	13.398	4.129	2.715
91	9.888	5.829	11.114	10.109	3.577	2.611
92	13.437	7.067	9.842	12.844	3.756	4.36
93	13.339	6.281	7.453	14.683	3.563	2.883
94	13.989	5.103	8.022	20.405	4.049	3.537
95	12.41	7.73	12.093	14.814	3.323	2.596
96	12.808	8.794	9.015	12.366	2.111	3.115
97	10.737	6.498	8.494	12.551	4.537	2.105
98	10.992	6.025	7.714	12.368	4.275	2.919
99	15.873	7.054	10.051	10.626	4.796	2.611
100	9.824	6.198	9.578	10.775	4.853	2.13
Mean	12.77	6.41	10.47	13.59	4.24	2.78
STDEV	1.90	0.96	2.30	2.69	0.80	0.54
Min length	8.656	4.465	6.368	6.872	1.652	1.306
Max length	17.95	8.794	17.231	21.05	5.972	4.42

Supplemental Table 15. *T. brixii* flagella lengths for 200 individually measured flagella. Images were captured using a 100 X oil immersion objective and a Nikon E400 brightfield upright microscope. Measurements were taken in ImageJ version 1.51n, using a calibrated image of a graticule for micrometre calibration. Mean values for all lengths along with standard deviation of the means were calculated using Microsoft Excel 2013.

Flagella number	Flagellum length μM	Flagella number	Flagellum length μM	Flagella number	Flagellum length μM	Flagella number	Flagellum length μM
1	13.918	51	11.783	101	18.031	151	16.629
2	13.797	52	13.703	102	18.578	152	14.65
3	7.954	53	10.729	103	11.183	153	13.414
4	12.086	54	9.802	104	6.991	154	13.523
5	10.807	55	12.364	105	9.096	155	14.753
6	9.679	56	15.621	106	16.184	156	11.239
7	7.717	57	14.827	107	11.297	157	12.722
8	13.239	58	17.123	108	12.766	158	11.316
9	11.601	59	13.696	109	13.299	159	9.895
10	11.579	60	9.989	110	15.577	160	14.24
11	13.677	61	12.954	111	14.644	161	13.572
12	13.024	62	14.459	112	15.801	162	11.686
13	13.907	63	13.141	113	14.107	163	10.249
14	11.362	64	17.462	114	12.343	164	12.206
15	11.506	65	14.342	115	14.042	165	12.081
16	13.147	66	16.708	116	14.503	166	7.74
17	11.87	67	16.623	117	13.589	167	9.963
18	13.33	68	14.533	118	16.257	168	10.657
19	12.884	69	15.704	119	11.211	169	12.174
20	15.48	70	16.012	120	11.844	170	12.723
21	12.347	71	13.789	121	9.67	171	12.68
22	10.285	72	13.823	122	10.409	172	12.112
23	12.965	73	16.678	123	10.453	173	12.759
24	15.736	74	14.405	124	7.753	174	8.894
25	13.633	75	15.323	125	13.771	175	7.787
26	14.04	76	15.171	126	10.718	176	11.117
27	16.957	77	14.899	127	10.991	177	10.343
28	12.496	78	15.342	128	13.818	178	12.121
29	14.121	79	12.105	129	14.269	179	13.7
30	11.893	80	12.105	130	13.51	180	10.707
31	11.108	81	12.81	131	13.125	181	11.485
32	12.534	82	13.514	132	11.149	182	12.222
33	11.507	83	16.11	133	6.617	183	10.768
34	12.817	84	11.819	134	9.375	184	8.634
35	12.469	85	13.139	135	12.851	185	11.799
36	15.105	86	13.698	136	11.598	186	9.981
37	13.853	87	13.975	137	15.637	187	7.241
38	13.131	88	15.919	138	13.689	188	8.678
39	12.864	89	15.042	139	12.303	189	12.623
40	10.615	90	14.909	140	11.63	190	14.971
41	11.434	91	12.282	141	13.28	191	15.69
42	11.818	92	14.248	142	13.228	192	14.316
43	10.887	93	12.296	143	8.433	193	13.438
44	13.362	94	13.261	144	12.84	194	8.95
45	13.361	95	13.015	145	15.751	195	11.817
46	14.55	96	12.213	146	15.1	196	8.461
47	8.745	97	14.5	147	15.281	197	13.186
48	11.394	98	16.79	148	13.196	198	18.382
49	11.148	99	15.423	149	9.537	199	18.039
50	13.5	100	15.482	150	11.612	200	18.791
Mean	12.8448						
STDEV	2.370761						
Min	6.617						
Max	18.791						

Supplemental Table 16. (a) Optical density values (n=6), indicating trypsin activity of *T. brixii* cell pellets and supernatants, *T. brixii*/canine gingival fibroblast co-culture cell pellets and supernatants and *P. gulae II* cell pellets and supernatants. Samples were tested in sextuplet. Mean values with standard deviations, standard error of the mean, and lower and upper confidence intervals were calculated in Prism 7.03 (GraphPad software, Inc, USA). **(b)** Ordinary one-way ANOVA analysis of trypsin exhibited by *T. brixii* cell pellets and supernatants, *T. brixii*/canine gingival fibroblast co-culture cell pellets and supernatants and *P. gulae II* cell pellets and supernatants. A multiple comparison (Dunnett's) was carried out, comparing each sample mean value to the DMEM control. Significant differences were inferred at the 95 % level ($P \leq 0.05$). Analyses were calculated in Prism 7.03 (GraphPad software, Inc, USA).

(a) Trypsin levels (O.D $\Delta 405\text{nm}$)

Replicate	<i>P. gulae II</i> cell pellet	<i>P. gulae II</i> cell supernatant	<i>T. brixii</i> cell pellet	<i>T. brixii</i> cell supernatant	<i>T. brixii</i> /CGFIB 48H co-culture pellet	<i>T. brixii</i> /CGFIB 48H co-culture supernatant	DMEM Control	Tris HCL Control
1	2.30	0.35	1.19	0.44	1.85	0.80	0.28	0.18
2	2.37	0.29	1.35	0.51	2.54	0.75	0.29	0.16
3	2.28	0.28	1.25	0.42	1.91	0.65	0.32	0.16
4	2.29	0.33	0.99	0.43	2.44	0.80	0.29	0.17
5	2.25	0.28	0.94	0.48	2.43	0.79	0.30	0.16
6	2.27	0.33	0.99	0.50	1.83	0.73	0.30	0.16
Mean	2.29	0.31	1.12	0.46	2.17	0.75	0.30	0.16
Std. Deviation	0.04	0.03	0.17	0.04	0.33	0.06	0.01	0.01
Std. Error of Mean	0.02	0.01	0.07	0.02	0.14	0.02	0.00	0.00
Lower 95% CI of mean	2.25	0.28	0.94	0.42	1.82	0.69	0.29	0.16
Upper 95% CI of mean	2.34	0.34	1.29	0.50	2.52	0.82	0.31	0.17

(b) One-way ANOVA analysis

Dunnett's multiple comparisons test	Mean Diff.	95.00% CI of diff.	Significant?	Adjusted P Value
DMEM Control vs. <i>P. gulae II</i> cell pellet	-1.99	-2.21 to -1.78	Yes	0.0001
DMEM Control vs. <i>P. gulae II</i> cell supernatant	-0.01	-0.22 to 0.20	No	0.9998
DMEM Control vs. <i>T. brixii</i> cell pellet	-0.81	-1.03 to -0.60	Yes	0.0001
DMEM Control vs. <i>T. brixii</i> cell supernatant	-0.16	-0.37 to 0.04	No	0.1935
DMEM Control vs. <i>T. brixii</i> /CGFIB 48H co-culture pellet	-1.87	-2.08 to -1.65	Yes	0.0001
DMEM Control vs. <i>T. brixii</i> /CGFIB 48H co-culture supernatant	-0.45	-0.67 to -0.24	Yes	0.0001
DMEM Control vs. Tris-HCL control	0.13	-0.08 to 0.34	No	0.3928

Supplemental Table 17. Percentage haemolysis values (n=6) of **(a)** canine red blood cells and **(b)** equine blood cells, exhibited by *T. brixii* cell pellets and supernatants, and *T. brixii*/canine gingival fibroblast co-culture supernatant, 1 % Triton X-100, distilled water, *P. gulae II*, and DMEM. Samples were tested in sextuplet. Mean values with standard deviations, standard error of the mean, and lower and upper confidence intervals were calculated in Prism 7.03 (GraphPad software, Inc, USA).

(a) Canine blood % Haemolysis

Sample number	<i>T. brixii</i> cell pellet	<i>T. brixii</i> cell supernatant	<i>T.brixii</i> /CGFIB 48H co-culture supernatant	<i>P. gulae</i> <i>II</i> cell pellet	1% Triton X-100 control	Distilled water control	DMEM Control
1	18.43	7.95	83.55	100.36	98.2	54.95	5.6
2	29.6	8.27	86.03	98.5	100.36	78.85	5.97
3	24.37	7.39	86.11	97.1	100.36	90.37	6.02
4	31.08	7.27	82.81	100.36	100.36	89.42	7.27
5	33.12	7.8	84.06	98.69	100.36	84.16	6.69
6	26.37	7.85	86.87	97.82	100.36	89.29	6.5
Mean	27.16	7.75	84.91	98.81	100	81.17	6.34
Std. Deviation	5.31	0.36	1.64	1.32	0.88	13.57	0.6
Std. Error of Mean	2.17	0.15	0.67	0.54	0.36	5.53	0.24
Lower 95% CI of mean	21.58	7.36	83.18	97.41	99.07	66.93	5.71
Upper 95% CI of mean	32.74	8.14	86.63	100.2	100.9	95.41	6.97

(b) Equine blood % Haemolysis

Sample number	<i>T. brixii</i> cell pellet	<i>T. brixii</i> cell supernatant	<i>T.brixii</i> /CGFIB 48H co- culture supernatant	<i>P. gulae</i> <i>II</i> cell pellet	1% Triton X-100 control	Distilled water control	DMEM Control
1	17.09	7.65	10.16	98.21	100	100	6.19
2	16.19	7.43	9.83	93.98	100	100	6.16
3	15.84	8.11	10.27	96.91	100	96.79	9.02
4	13.6	6.96	8.91	87.84	100	100	16.82
5	11.93	6.84	9.88	97.01	100	100	9.38
6	13.87	7.99	10.16	100	100	97.76	5.91
Mean	14.75	7.49	9.86	95.66	100	99.09	8.91
Std. Deviation	1.93	0.52	0.50	4.30	0	1.44	4.16
Std. Error of Mean	0.79	0.21	0.20	1.75	0	0.58	1.70
Lower 95% CI of mean	12.72	6.94	9.34	91.14	100	97.58	4.54
Upper 95% CI of mean	16.79	8.04	10.39	100.2	100	100.6	13.28

Supplemental Table 18. Ordinary one-way ANOVA analysis of haemolysis exhibited by *T. brixii* cell pellets and supernatants, and *T. brixii*/canine gingival fibroblast co-culture supernatant, 1 % Triton X-100, distilled water, *P. gulae II*, and DMEM in **(a)** canine red blood cells and **(b)** equine blood cells. A multiple comparison (Dunnett's) was carried out, comparing each sample mean value to the DMEM control. Significant differences were inferred at the 95 % level ($P < 0.05$). Analyses were calculated in Prism 7.03 (GraphPad software, Inc, USA).

(a) Canine blood

Dunnett's multiple comparisons test	Mean Diff.	95.00% CI of diff.	Significant?	Adjusted P Value
DMEM Control vs. <i>T. brixii</i> cell pellet	-20.82	-29.51 to -12.13	Yes	0.0001
DMEM Control vs. <i>T. brixii</i> cell supernatant	-1.413	-10.11 to 7.279	No	0.9951
DMEM Control vs. <i>T.brixii</i> /CGFIB 48H co-culture supernatant	-78.56	-87.26 to -69.87	Yes	0.0001
DMEM Control vs. <i>P. gulae II</i> cell pellet	-92.46	-101.2 to -83.77	Yes	0.0001
DMEM Control vs. 1% Triton X100 control	-93.66	-102.4 to -84.97	Yes	0.0001
DMEM Control vs. Distilled water control	-74.83	-83.52 to -66.14	Yes	0.0001

(b) Equine blood

Dunnett's multiple comparisons test	Mean Diff.	95.00% CI of diff.	Significant?	Adjusted P Value
DMEM Control vs. <i>T. brixii</i> cell pellet	-5.84	-9.66 to -2.01	Yes	0.0012
DMEM Control vs. <i>T. brixii</i> cell supernatant	1.41	-2.40 to 5.24	No	0.8206
DMEM Control vs. <i>T.brixii</i> /CGFIB 48H co-culture supernatant	-0.955	-4.78 to 2.87	No	0.9624
DMEM Control vs. <i>P. gulae II</i> cell pellet	-86.75	-90.57 to -82.92	Yes	0.0001
DMEM Control vs. 1% Triton X100 control	-91.09	-94.91 to -87.26	Yes	0.0001
DMEM Control vs. Distilled water control	-90.18	-94 to -86.35	Yes	0.0001

Supplemental Table 19. Percentage haemolysis values (n=6) of (a) canine red blood cells and (b) equine blood cells, exhibited by canine gingival fibroblast (CGFIB) cell pellets and cell supernatant, 1 % Triton X-100, distilled water, and DMEM. Samples were tested in sextuplet. Mean values with standard deviations, standard error of the mean, and lower and upper confidence intervals were calculated in Prism 7.03 (GraphPad software, Inc, USA).

(a) Canine blood % Haemolysis

Replicate	<i>CGFIB cell Pellet</i>	<i>CGFIB cell supernatant</i>	<i>1% Triton X100 control</i>	<i>Distilled water control</i>	DMEM Control
1	6.94	7.19	102.59	96.89	9.01
2	5.3	7.17	96.48	98.68	7.98
3	5.87	7.47	97.54	94.77	8.7
4	6.08	6.18	101.87	94.84	7.6
5	5.49	8.23	102.59	102.59	7.5
6	6.01	9.93	98.92	94.28	8
Mean	5.94	7.69	100	97.01	8.13
Std. Deviation	0.57	1.27	2.70	3.19	0.60
Std. Error of Mean	0.23	0.52	1.10	1.30	0.24
Lower 95% CI of mean	5.34	6.35	97.16	93.65	7.49
Upper 95% CI of mean	6.55	9.03	102.8	100.4	8.76

(b) Equine blood % Haemolysis

Replicate	<i>CGFIB cell Pellet</i>	<i>CGFIB cell supernatant</i>	<i>1% Triton X100 control</i>	<i>Distilled water control</i>	DMEM Control
1	5.12	5.7	102.6	102.6	6
2	4.71	6.14	102.6	102.6	5.33
3	4.45	5.91	100.3	98.38	5.37
4	4.56	4.91	96.15	99.94	5.24
5	4.51	4.27	95.76	96.44	5.12
6	4.63	4.31	102.6	97.75	5.12
Mean	4.66	5.20	100	99.62	5.36
Std. Deviation	0.24	0.82	3.26	2.56	0.32
Std. Error of Mean	0.09	0.33	1.33	1.04	0.13
Lower 95% CI of mean	4.41	4.34	96.58	96.92	5.01
Upper 95% CI of mean	4.91	6.06	103.4	102.3	5.70

Supplemental Table 20. Ordinary one-way ANOVA analysis of haemolysis exhibited by canine gingival fibroblast (CGFIB) cell pellets and cell supernatant, 1 % Triton X-100, distilled water, and DMEM in **(a)** canine red blood cells and **(b)** equine blood cells. A multiple comparison (Dunnett's) was carried out, comparing each sample mean value to the DMEM control. Significant differences were inferred at the 95 % level ($P < 0.05$). Analyses were calculated in Prism 7.03 (GraphPad software, Inc, USA).

(a) Canine blood

Dunnett's multiple comparisons test	Mean Diff.	95.00% CI of diff.	Significant?	Adjusted P Value
DMEM Control vs. CGFIB cell Pellet	2.18	-0.81 to 5.18	No	0.2033
DMEM Control vs. CGFIB cell supernatant	0.43	-2.56 to 3.43	No	0.9863
DMEM Control vs. 1% Triton X100 control	-91.87	-94.87 to -88.87	Yes	0.0001
DMEM Control vs. Distilled water control	-88.88	-91.88 to -85.88	Yes	0.0001

(b) Equine blood

Dunnett's multiple comparisons test	Mean Diff.	95.00% CI of diff.	Significant?	Adjusted P Value
DMEM Control vs. CGFIB cell Pellet	0.7	-2.16 to 3.56	No	0.9183
DMEM Control vs. CGFIB cell supernatant	0.15	-2.70 to 3.01	No	0.9997
DMEM Control vs. 1% Triton X100 control	-94.64	-97.5 to -91.78	Yes	0.0001
DMEM Control vs. Distilled water control	-94.26	-97.12 to -91.39	Yes	0.0001

Supplemental Table 21. Mean values of cellular metabolic activity from canine gingival fibroblasts co-cultured without **(a)**, and with **(b)**, the canine oral trichomonad, *T. brixii*. Cellular metabolic activity (fluorescence units) was monitored at time points 2, 4, 6, 24 and 48 hours post co-incubation using the cell health indicator fluorescent dye alamarBlue®. Samples were tested in sextuplet. Mean values (n=6) with standard deviations, and standard error of the mean were calculated and manipulated in Prism 7.03 (GraphPad software, Inc, USA).

(a) Canine gingival fibroblasts only

Time (Hours)	Replicate 1	Replicate 2	Replicate 3	Replicate 4	Replicate 5	Replicate 6	Mean	STDEV	SEM
2	102812	104739	105969	102277	105105	109736	105107	2435	994
4	99910	101502	100154	99898	101963	99437	100477	922	376
6	100953	99212	100751	98311	96545	106337	100351	3063	1251
24	82717	80312	98691	110901	82809	120110	95924	15314	6252
48	75695	80473	81477	86994	82594	84793	82005	3546	1448
Replicate values indicate alamarBlue® activity (fluorescence unit)									

(b) Canine gingival fibroblasts/*T. brixii* co-culture - fluorescence units

Time (Hours)	Replicate 1	Replicate 2	Replicate 3	Replicate 4	Replicate 5	Replicate 6	Mean	STDEV	SEM
2	100861	106511	101085	113390	103861	108972	105780	4445	1815
4	110028	98341	106513	108295	105846	101416	105073	4006	1636
6	112322	105847	107718	104188	97717	104496	105381	4374	1786
24	89479	94918	95101	93666	97000	93162	93888	2318	946
48	8357	6631	7528	7364	4880	6936	6950	1070	437
Replicate values indicate alamarBlue® activity (fluorescence unit)									

Supplemental Table 22. Two-way ANOVA analysis of mean values of cellular metabolic activity from canine gingival fibroblasts co-cultured wells without and with, the canine oral trichomonad, *T. brixii*. A Sidak's multiple comparison test was carried out, comparing each well mean value for each experiment time point. Significant differences were inferred at the 95 % level ($P < 0.05$). Analyses were calculated in Prism 7.03 (GraphPad software, Inc, USA).

Sidak's multiple comparisons test

Canine gingival fibroblasts only wells vs Canine gingival fibroblasts with <i>T. brixii</i> co-culture	Mean Diff.	95.00% CI of diff.	Significant?	Adjusted P Value
Time point 2H	-673.7	-10296 to 8949	No	>0.9999
Time point 4H	-4596	-14218 to 5027	No	0.6886
Time point 6H	-5030	-14652 to 4593	No	0.6037
Time point 24H	2036	-7587 to 11658	No	0.9861
Time point 48H	75055	65433 to 84677	Yes	<0.0001

Supplemental Table 23. Mean values for cell numbers of canine gingival fibroblasts co-cultured without **(a)**, and with **(b)**, the canine oral trichomonad, *T. brixii*. Cell counts were conducted by counting DAPI stained nuclei at time points 2, 4, 6, 24 and 48 hour post co-incubation using an ImageXpress Micro XLS Widefield High-Content Analysis System and MetaXpress software V5.3 (Molecular Devices, UK). Samples were tested in sextuplet. Mean values (n=6) with standard deviations, and standard error of the mean were calculated and manipulated in Prism 7.03 (GraphPad software, Inc, USA).

(a) Canine gingival fibroblasts only

Time (Hours)	Replicate 1	Replicate 2	Replicate 3	Replicate 4	Replicate 5	Replicate 6	Mean	STDEV	SEM
2	1564	1870	1883	1965	1859	1606	1791	150	61
4	1979	1936	2203	2266	1927	1958	2045	136	56
6	1855	1658	1058	1571	1314	1264	1453	267	109
24	2485	2387	2251	2641	2380	2507	2442	122	50
48	2380	2434	2286	2539	2053	2272	2327	152	62
Replicate values indicate number of cells identified in six random field of view									

(b) Canine gingival fibroblasts/*T. brixii* co-culture

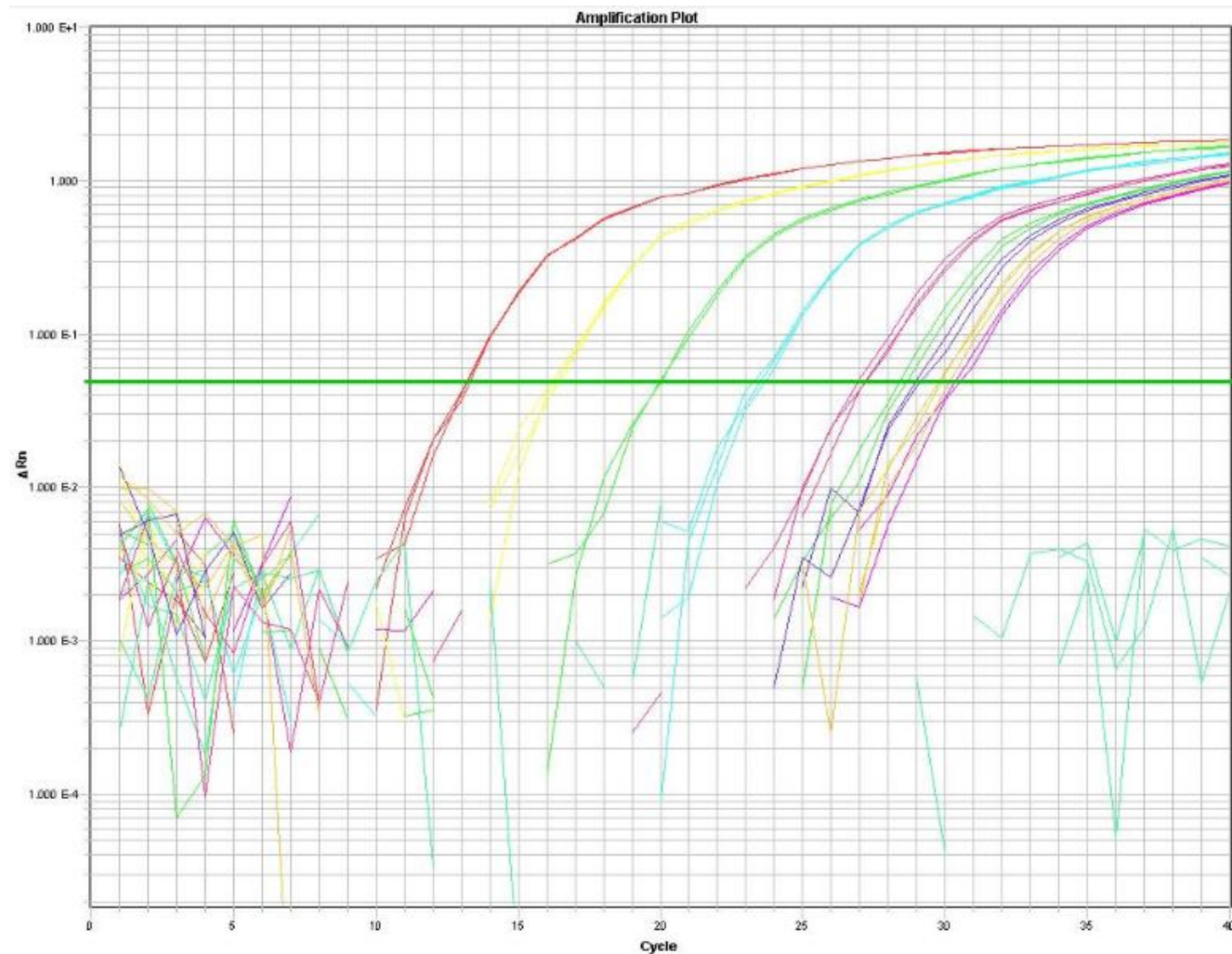
Time (Hours)	Replicate 1	Replicate 2	Replicate 3	Replicate 4	Replicate 5	Replicate 6	Mean	STDEV	SEM
2	1559	1762	1703	1766	1673	1522	1664	94	38
4	999	1921	1850	1845	1794	1641	1675	314	128
6	1457	1577	1717	1627	1482	1396	1543	109	44
24	257	250	331	255	302	343	290	38	15
48	60	68	60	86	72	57	67	10	4
Replicate values indicate number of cells identified in six random field of view									

Supplemental Table 24. Two-way ANOVA analysis of mean cell count values of canine gingival fibroblasts wells co-cultured without and with, the canine oral trichomonad, *T. brixii*. A Sidak's multiple comparison test was carried out, comparing each well mean value for each experiment time point. Significant differences were inferred at the 95 % level ($P < 0.05$). Analyses were calculated in Prism 7.03 (GraphPad software, Inc, USA).

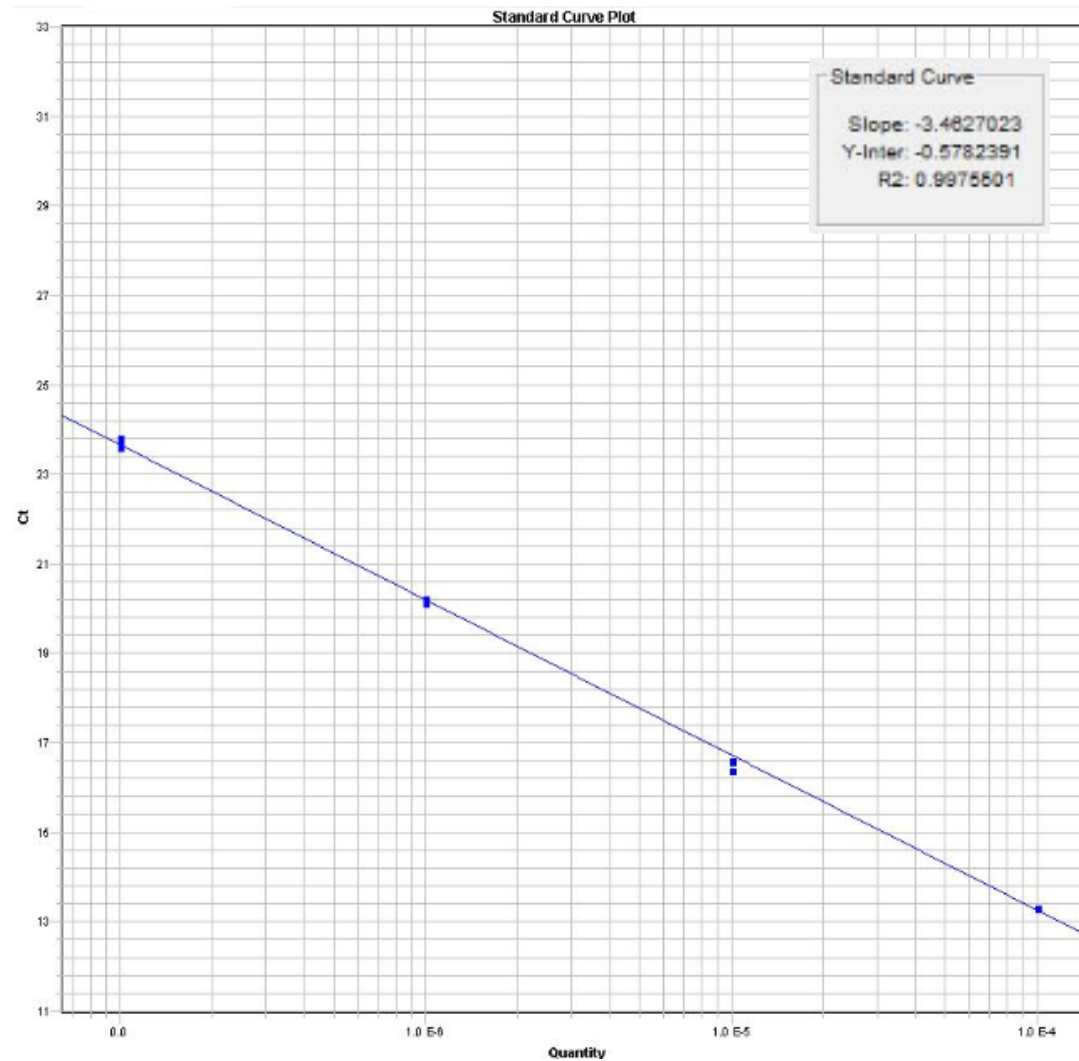
Sidak's multiple comparisons test

Canine gingival fibroblasts only wells vs Canine gingival fibroblasts with <i>T. brixii</i> co-culture	Mean Diff.	95.00% CI of diff.	Significant?	Adjusted P Value
Time point 2H	127	-151.2 to 405.2	No	0.727
Time point 4H	369.8	91.59 to 648.1	Yes	0.0043
Time point 6H	-89.33	-367.6 to 188.9	No	0.9192
Time point 24H	2152	1874 to 2430	Yes	<0.0001
Time point 48H	2260	1982 to 2538	Yes	<0.0001

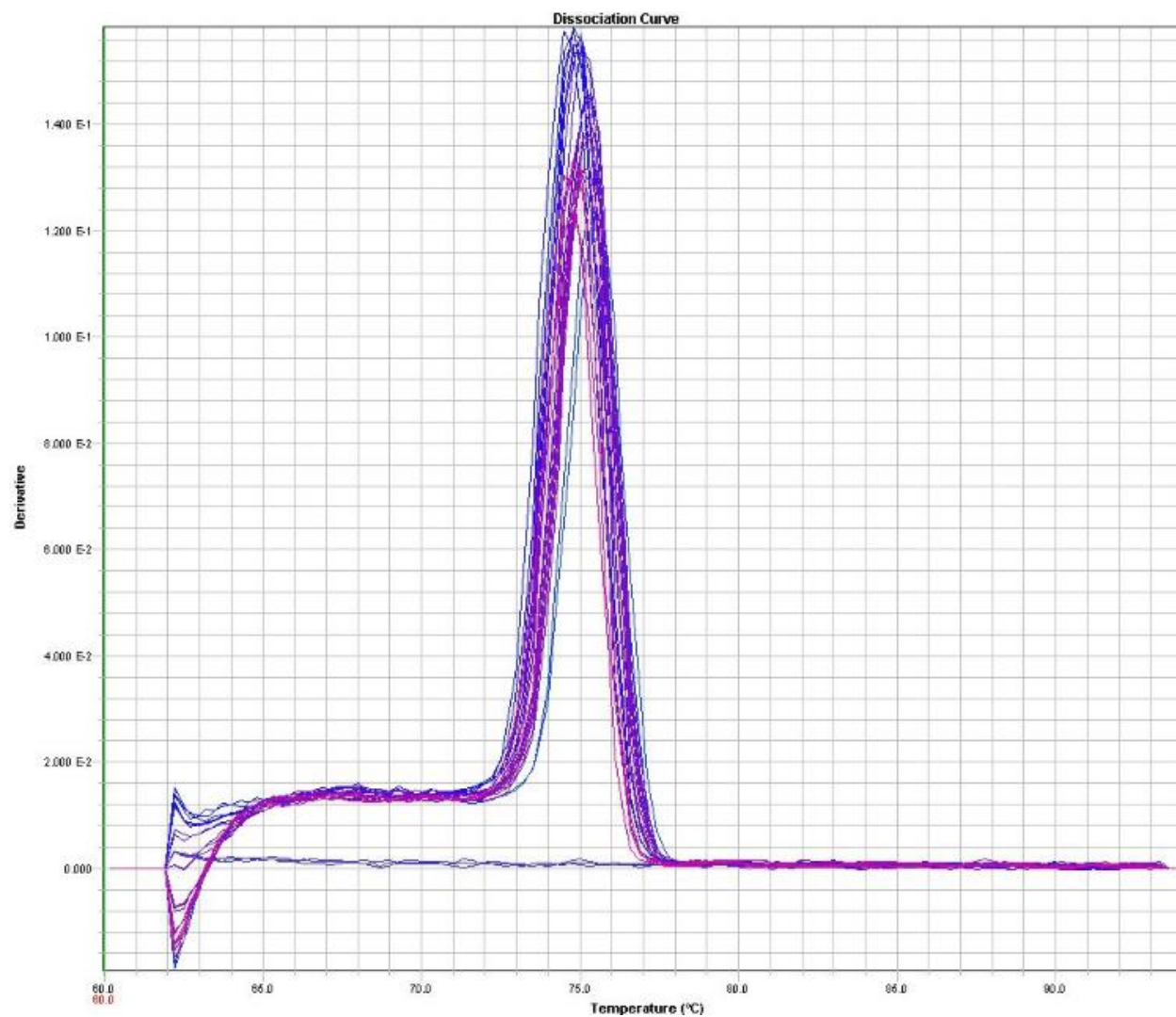
Supplemental Figures



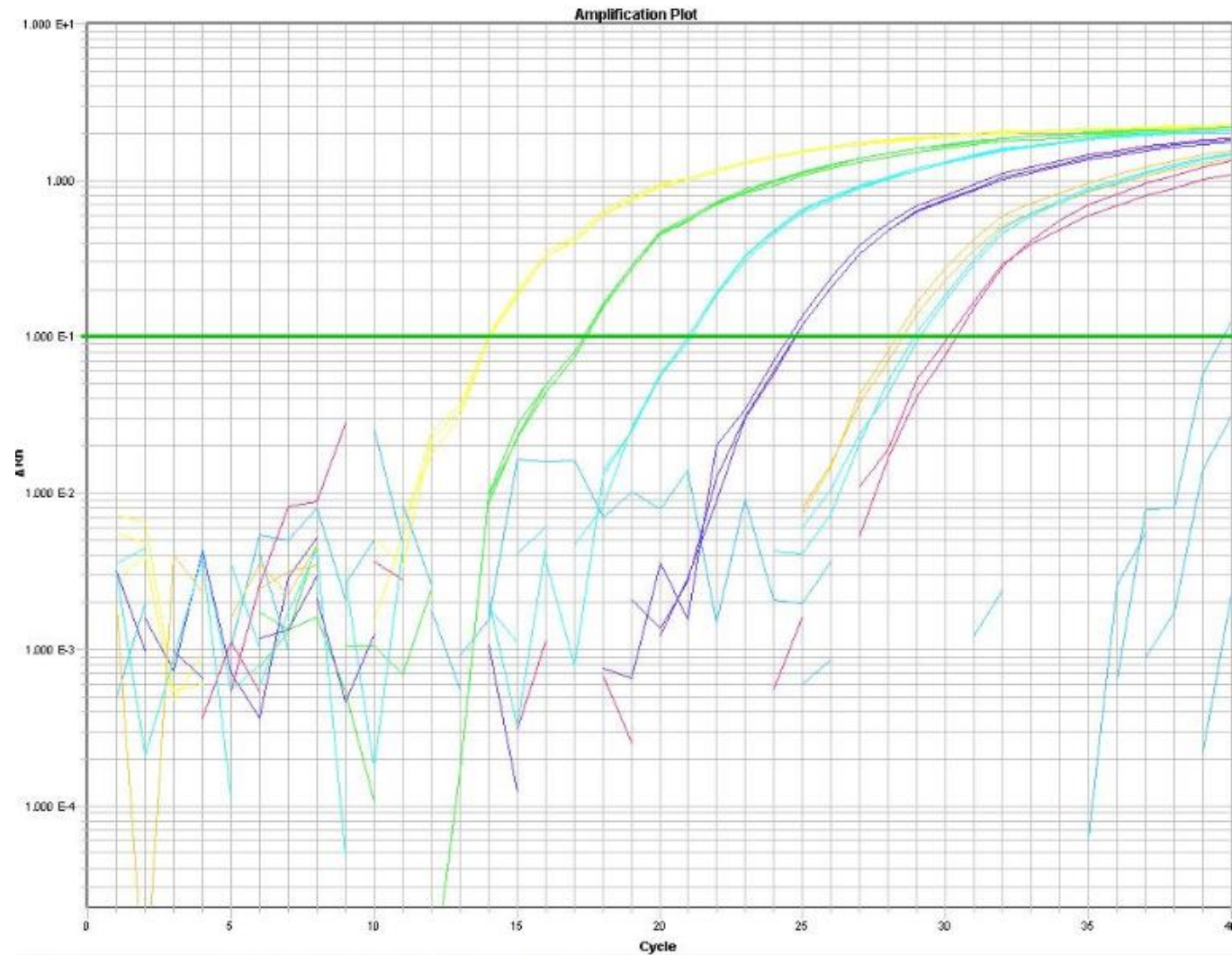
Supplemental Figure 1. Real time amplification plots of qPCR 10-fold dilution standards running left to right, for assay **EG1** targeting *E. gingivalis*. Data was recorded by 7900HT Fast Real-Time PCR System (Applied Biosystems, UK) and analysed and plotted with Applied Biosystems SDS V2.4 software.



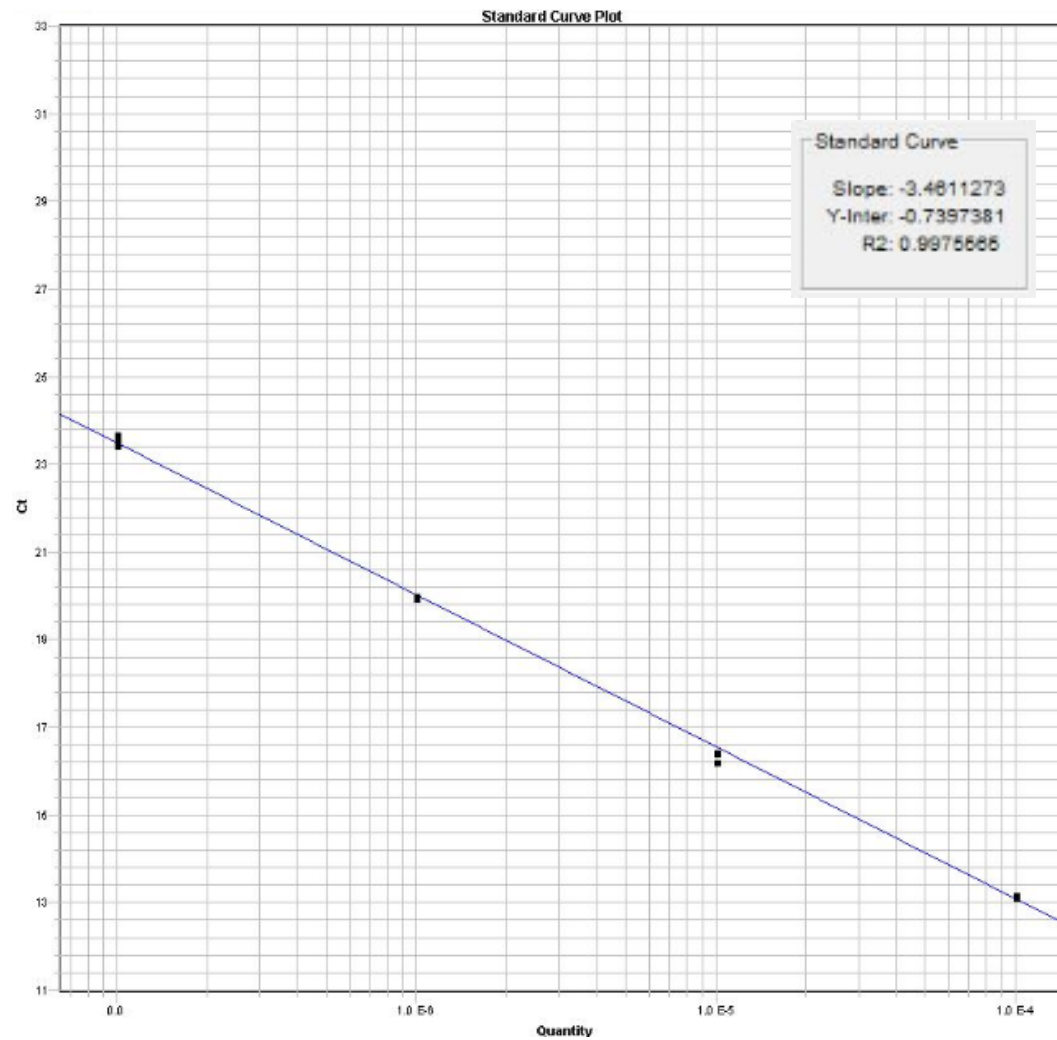
Supplemental Figure 2. Standard curve plot of 10-fold dilutions and assay efficiency values of for assay **EG1** targeting *E. gingivalis*. Data was recorded by 7900HT Fast Real-Time PCR System (Applied Biosystems, UK) and analysed and plotted with Applied Biosystems SDS V2.4 software.



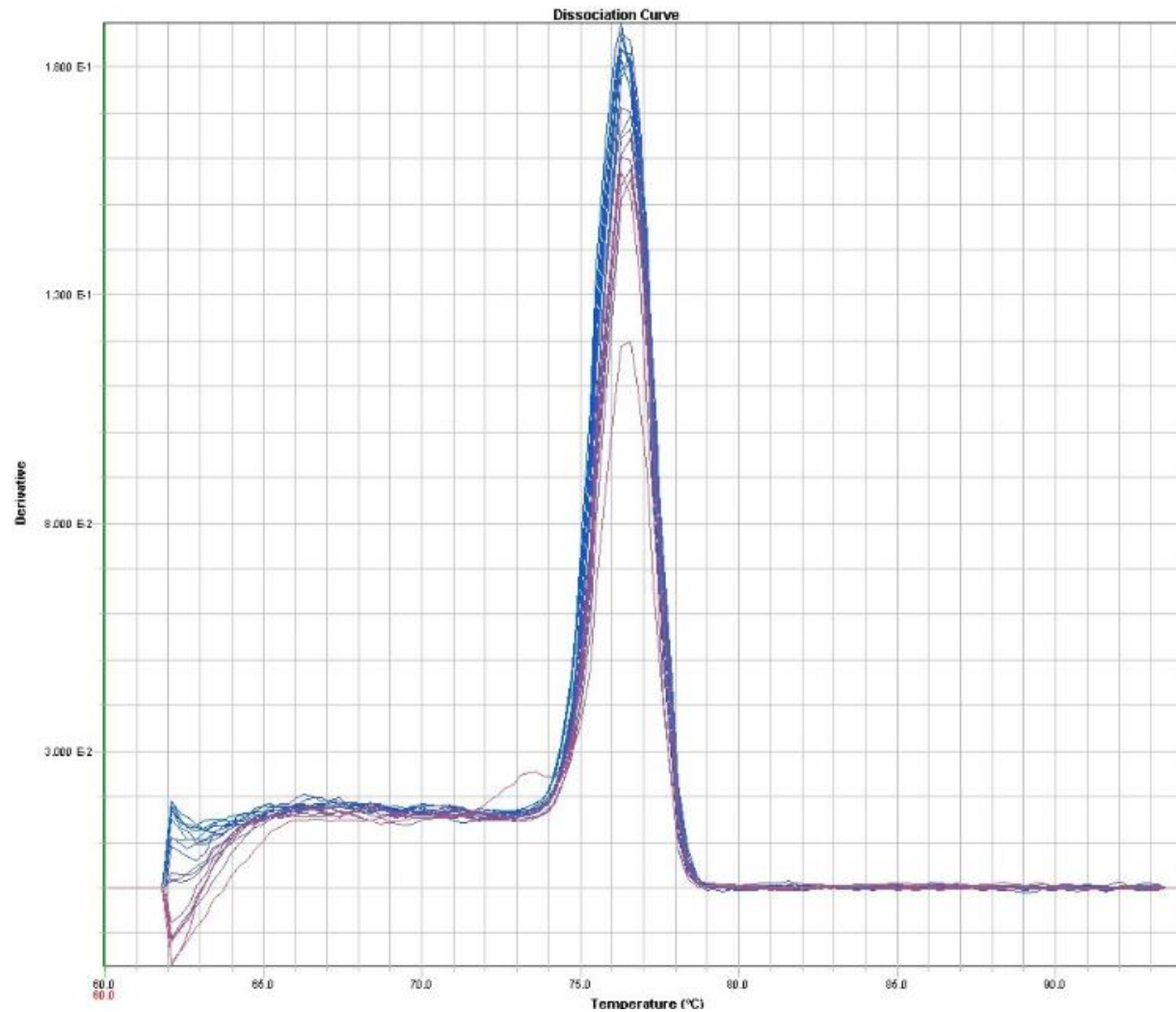
Supplemental Figure 3. Dissociation melt curve for qPCR standards amplicons run for assay **EG1** targeting *E. gingivalis*. All standards produce a single amplicon of the same length. Data was recorded by 7900HT Fast Real-Time PCR System (Applied Biosystems, UK) and analysed and plotted with Applied Biosystems SDS V2.4 software.



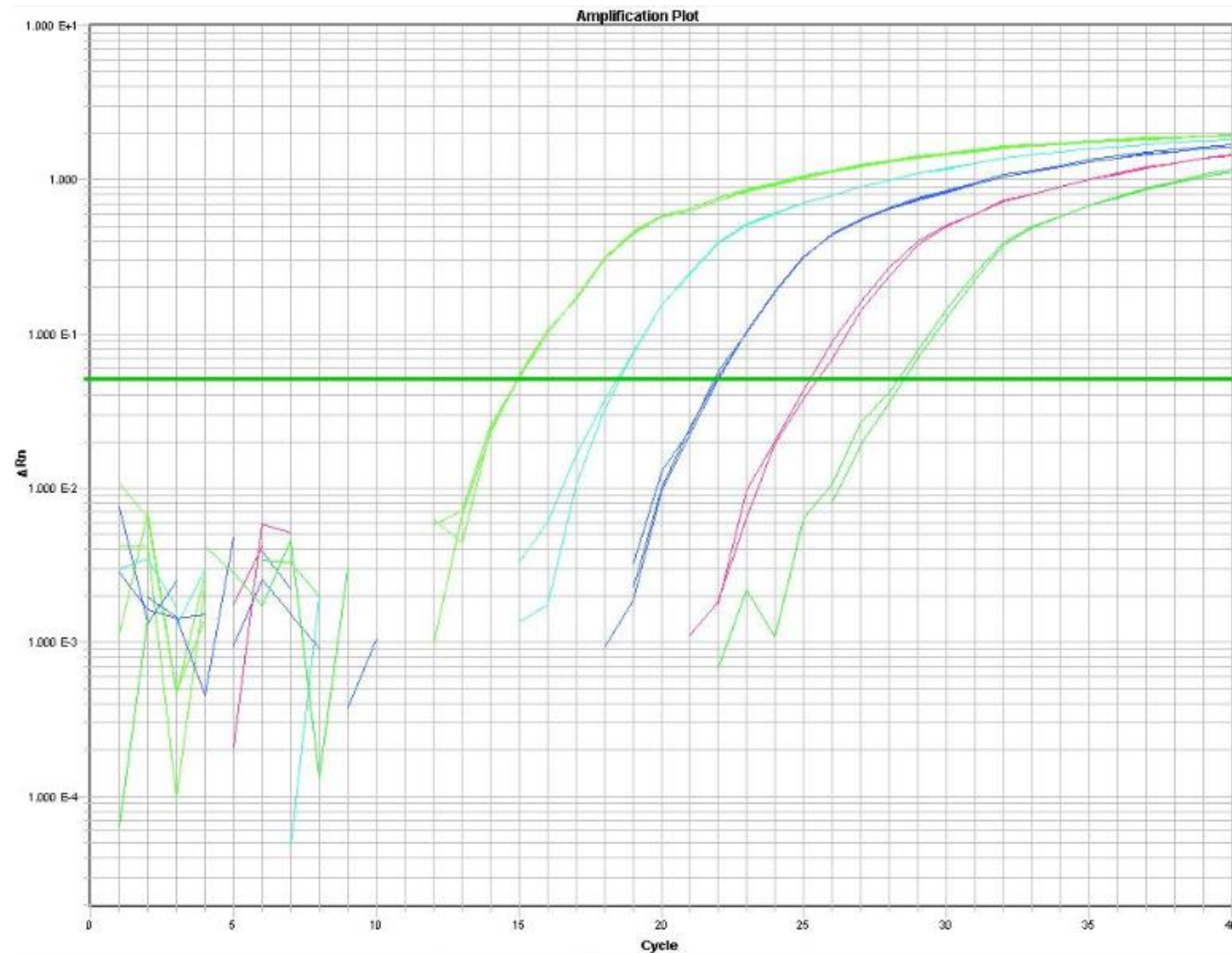
Supplemental Figure 4. Real time amplification plots of qPCR 10-fold dilution standards running left to right, for assay **EG2** targeting *E. gingivalis*. Data was recorded by 7900HT Fast Real-Time PCR System (Applied Biosystems, UK) and analysed and plotted with Applied Biosystems SDS V2.4 software



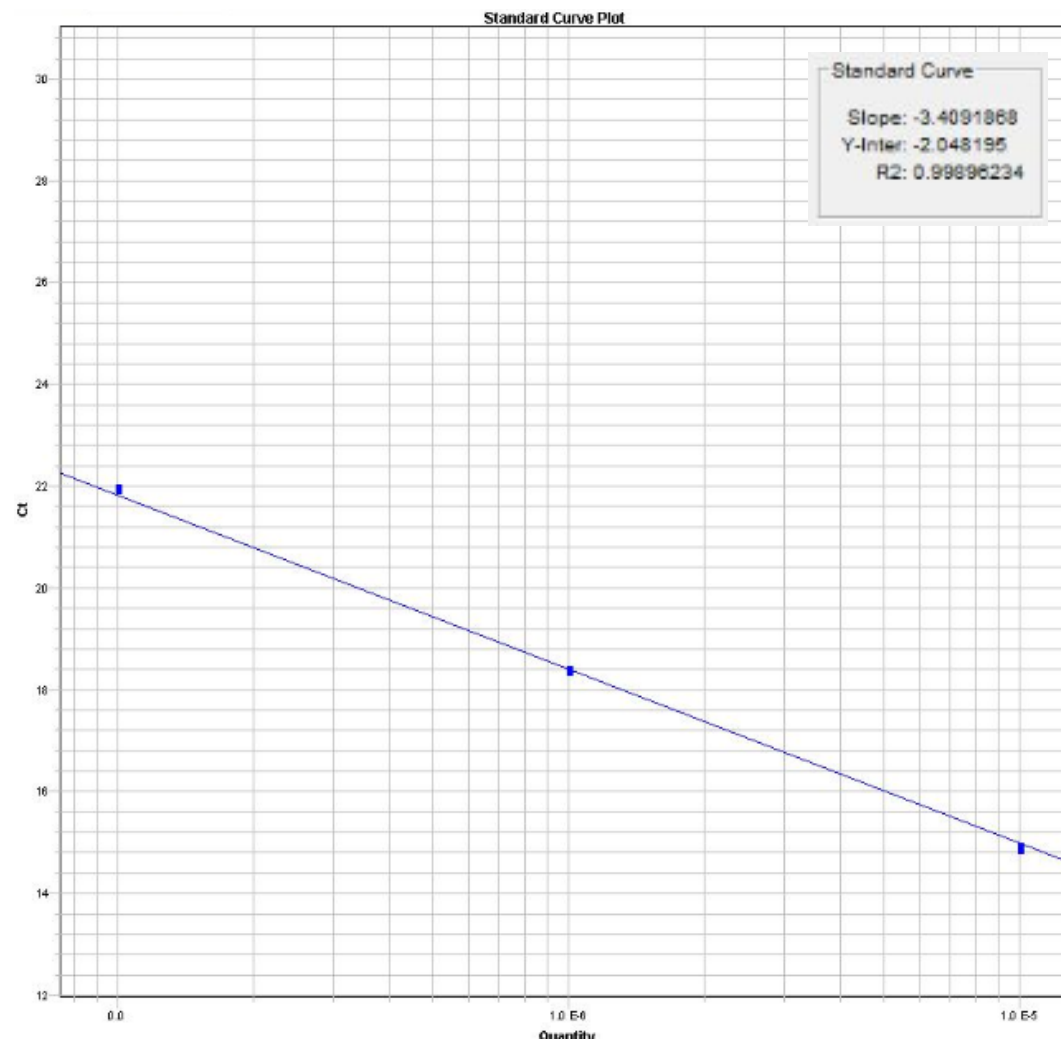
Supplemental Figure 5. Standard curve plot of 10-fold dilutions and assay efficiency values of for assay **EG2** targeting *E. gingivalis*. Data was recorded by 7900HT Fast Real-Time PCR System (Applied Biosystems, UK) and analysed and plotted with Applied Biosystems SDS V2.4 software.



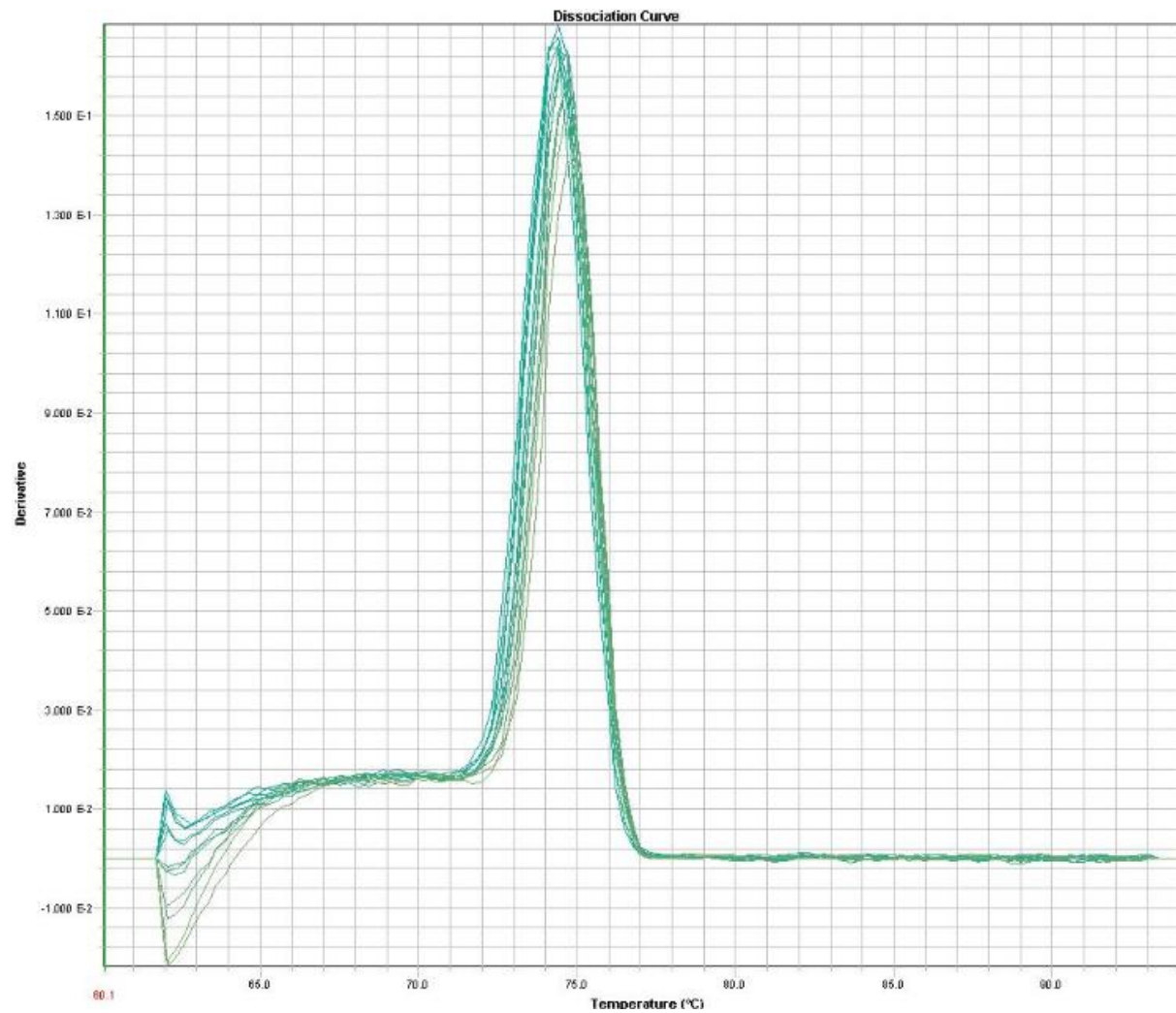
Supplemental Figure 6. Dissociation melt curve for qPCR standards amplicons run for assay **EG2** targeting *E. gingivalis*. All standards produce a single amplicon of the same length. Data was recorded by 7900HT Fast Real-Time PCR System (Applied Biosystems, UK) and analysed and plotted with Applied Biosystems SDS V2.4 software.



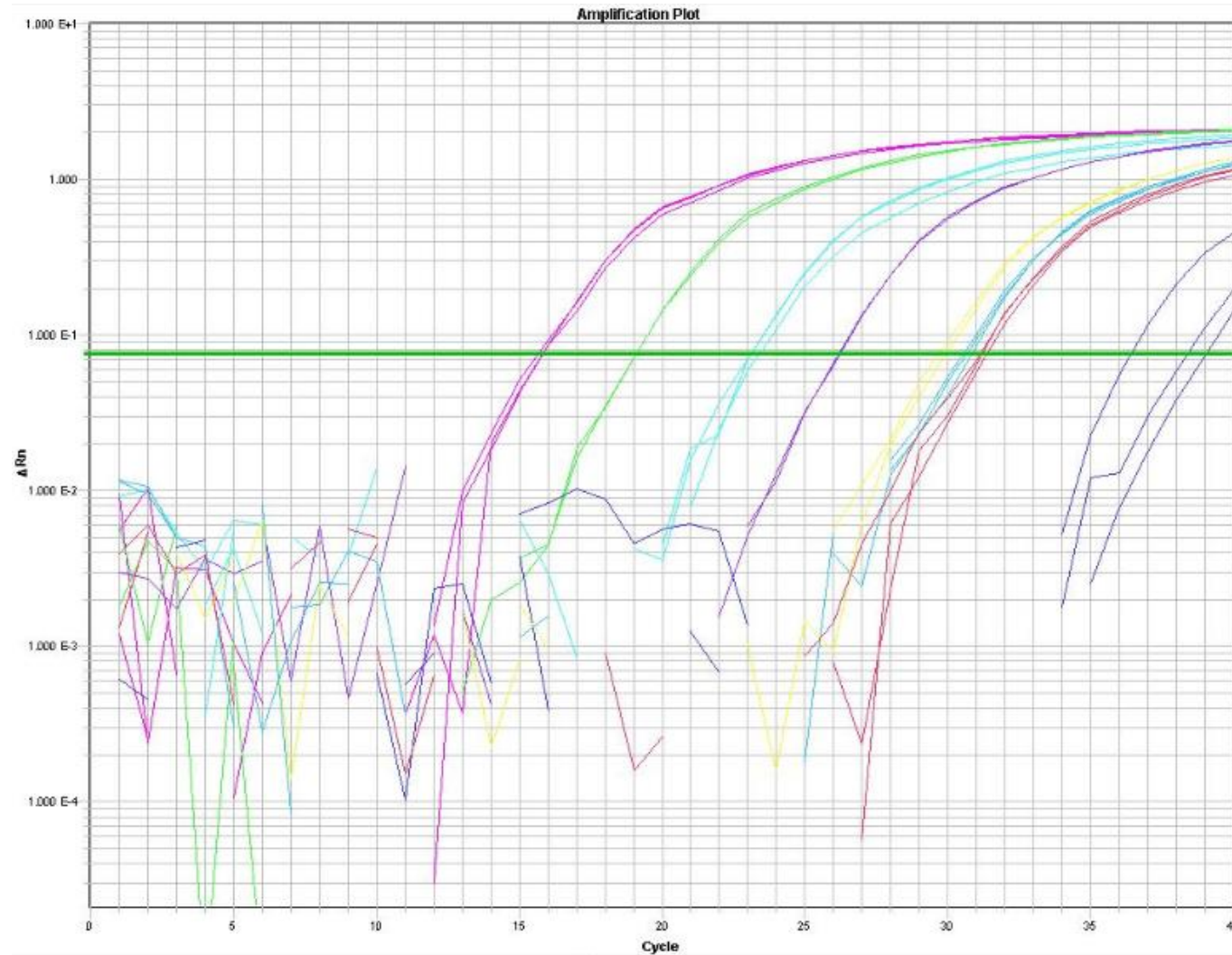
Supplemental Figure 7. Real time amplification plots of qPCR 10-fold dilution standards running left to right, for assay **TC1** targeting an unidentified *Trichomonas*. Data was recorded by 7900HT Fast Real-Time PCR System (Applied Biosystems, UK) and analysed and plotted with Applied Biosystems SDS V2.4 software.



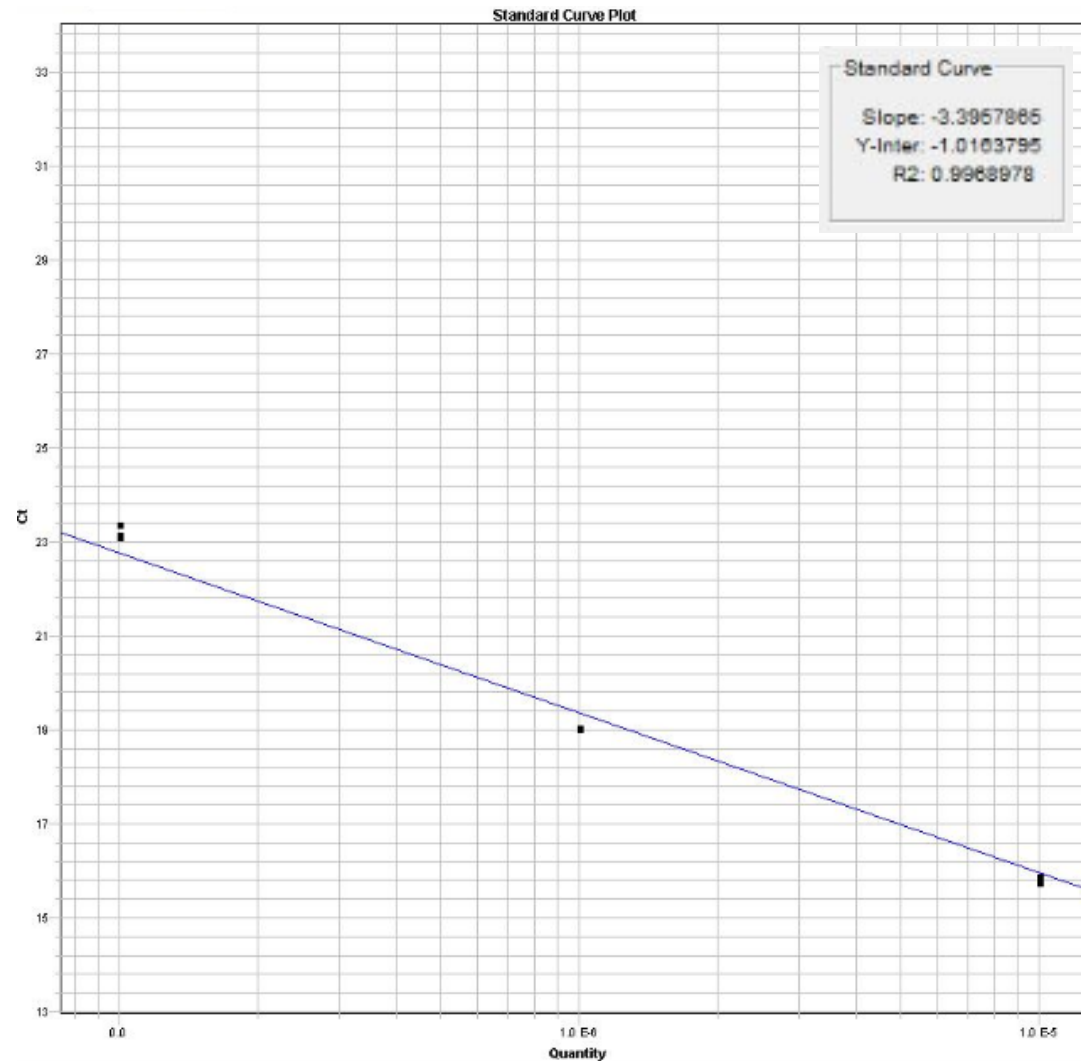
Supplemental Figure 8. Standard curve plot of 10-fold dilutions and assay efficiency values of for assay **TC1** targeting an unidentified *Trichomonas*. Data was recorded by 7900HT Fast Real-Time PCR System (Applied Biosystems, UK) and analysed and plotted with Applied Biosystems SDS V2.4 software.



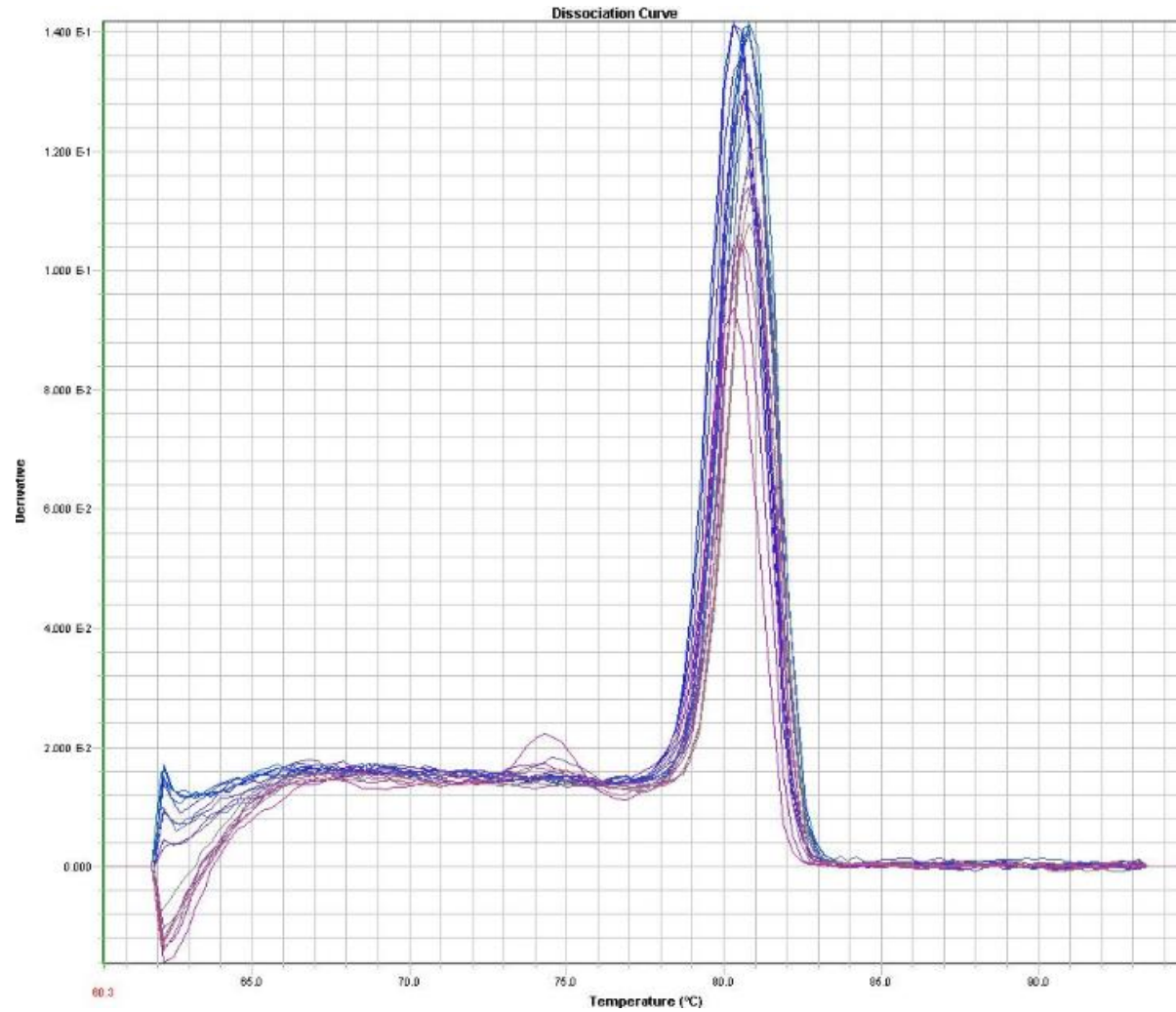
Supplemental Figure 9. Dissociation melt curve for qPCR standards amplicons run for assay **TC1** targeting an unidentified *Trichomonas*. All standards produce a single amplicon of the same length. Data was recorded by 7900HT Fast Real-Time PCR System (Applied Biosystems, UK) and analysed and plotted with Applied Biosystems SDS V2.4 software.



Supplemental Figure 10. Real time amplification plots of qPCR 10-fold dilution standards running left to right, for assay **TC2** targeting an unidentified *Trichomonas*. Data was recorded by 7900HT Fast Real-Time PCR System (Applied Biosystems, UK) and analysed and plotted with Applied Biosystems SDS V2.4 software.



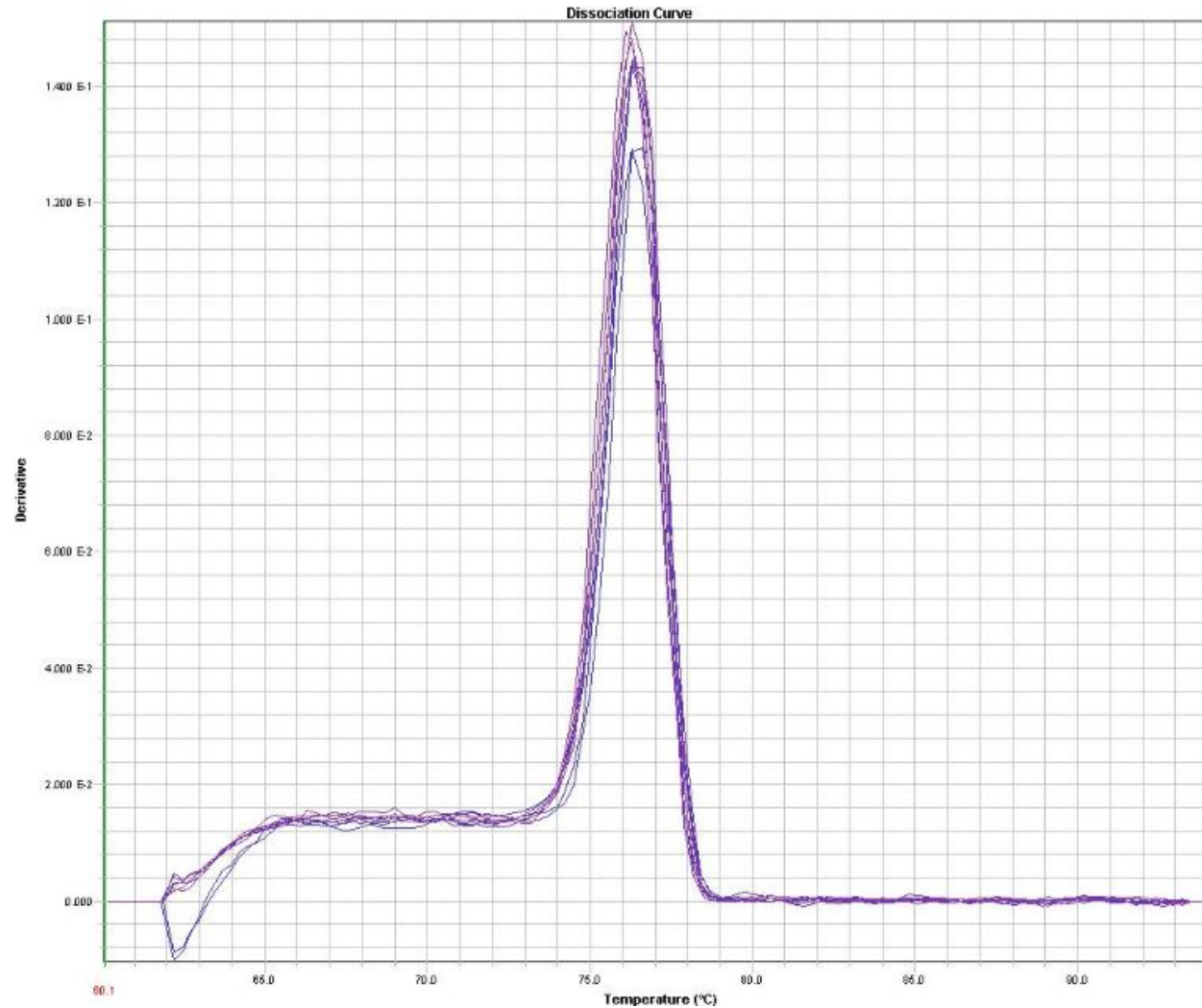
Supplemental Figure 11. Standard curve plot of 10-fold dilutions and assay efficiency values of for assay **TC2** targeting an unidentified *Trichomonas*. Data was recorded by 7900HT Fast Real-Time PCR System (Applied Biosystems, UK) and analysed and plotted with Applied Biosystems SDS V2.4 software.



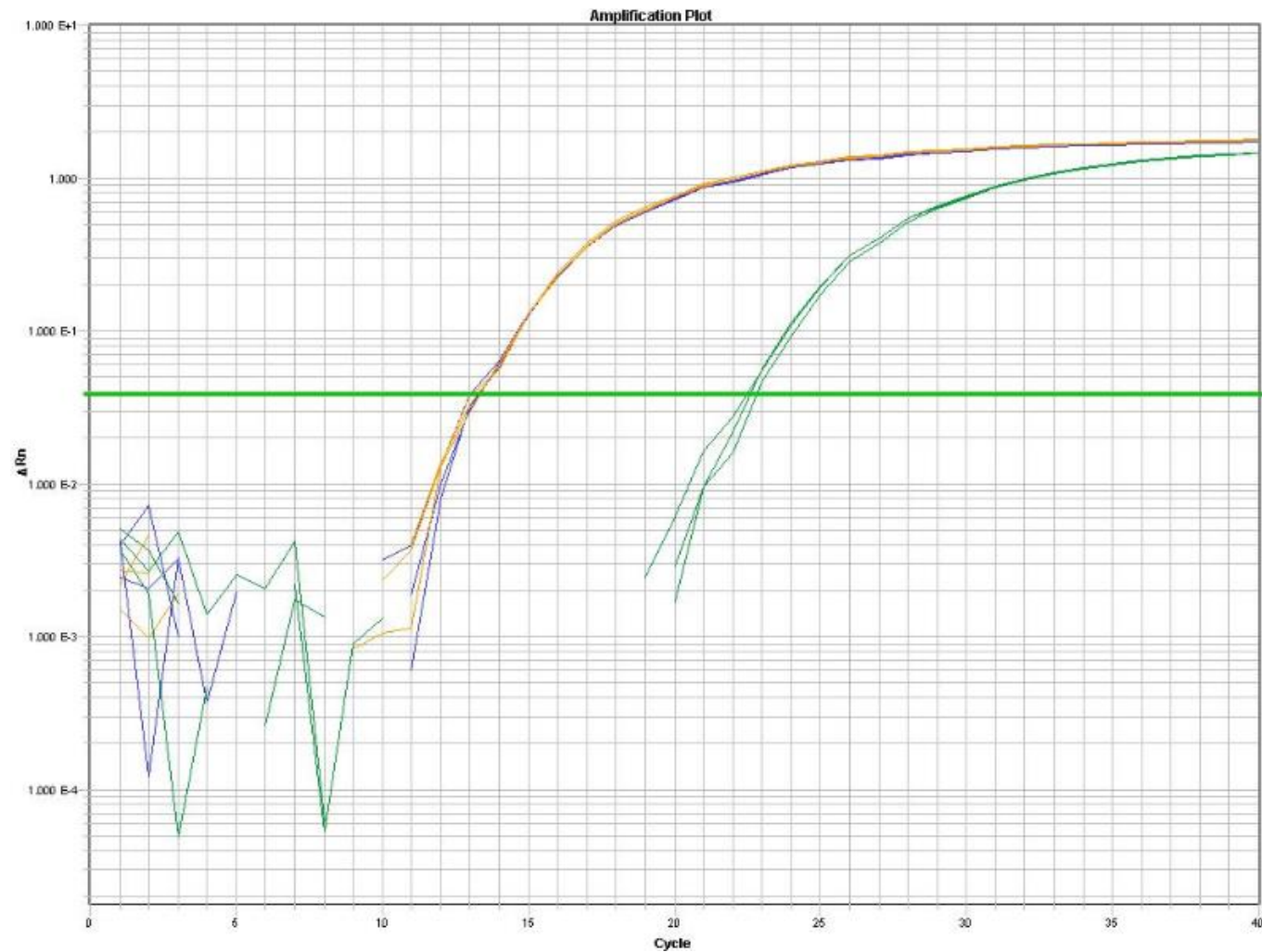
Supplemental Figure 12. Dissociation melt curve for qPCR standards amplicons run for assay **TC2** targeting an unidentified *Trichomonas*. All standards produce a single amplicon of the same length. Data was recorded by 7900HT Fast Real-Time PCR System (Applied Biosystems, UK) and analysed and plotted with Applied Biosystems SDS V2.4 software.



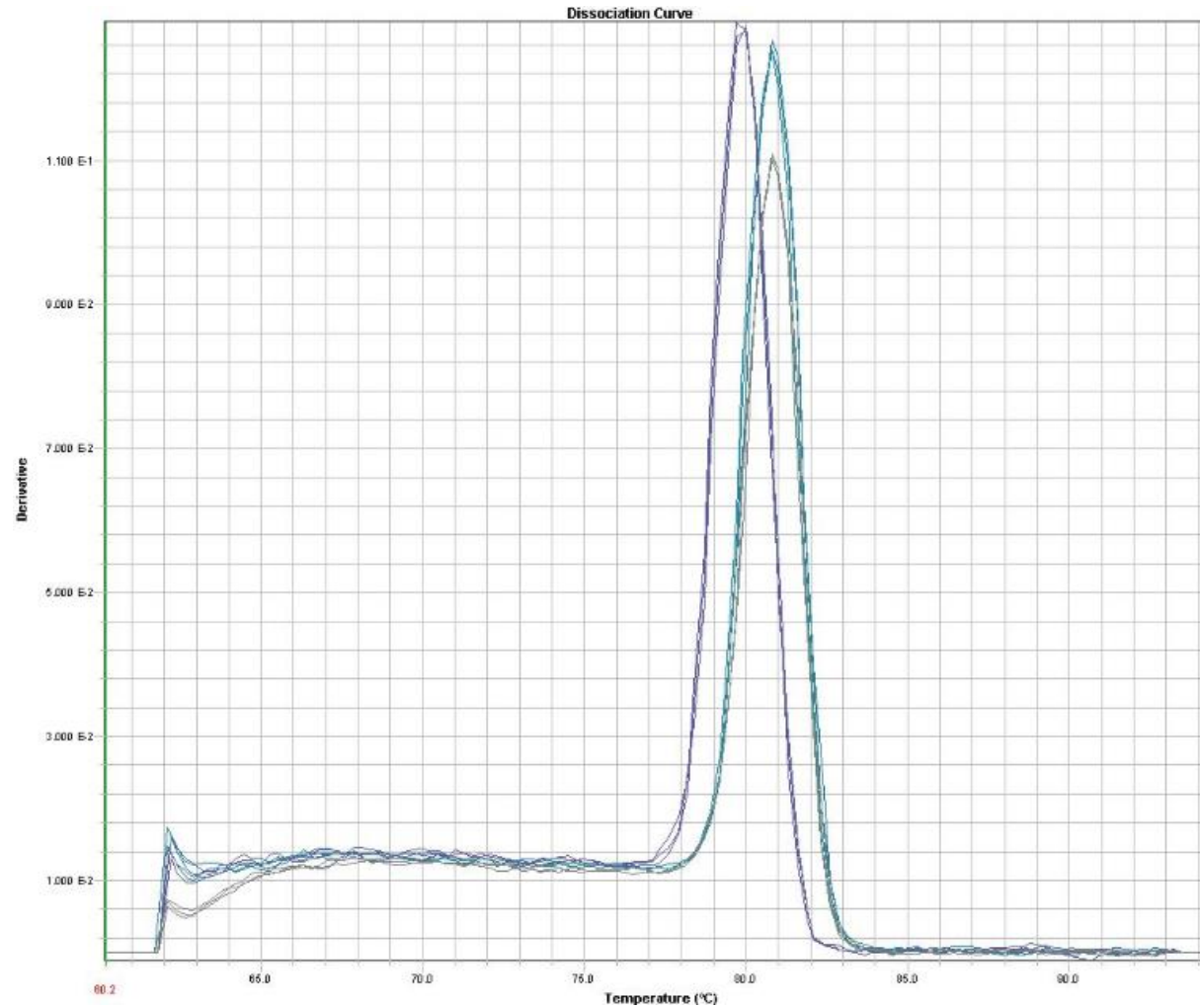
Supplemental Figure 13. Real time amplification plots for qPCR assay **EG1**, tested against a range of microorganisms and clinical samples to assess for species cross reactivity. Positive reactions are only seen with an 18S *E. gingivalis* amplicon (green lines), and two clinical samples known to contain *Entamoeba*, sample 18P (red lines) and SD pool (blue lines). No other positive reactions are seen for the other samples tested.



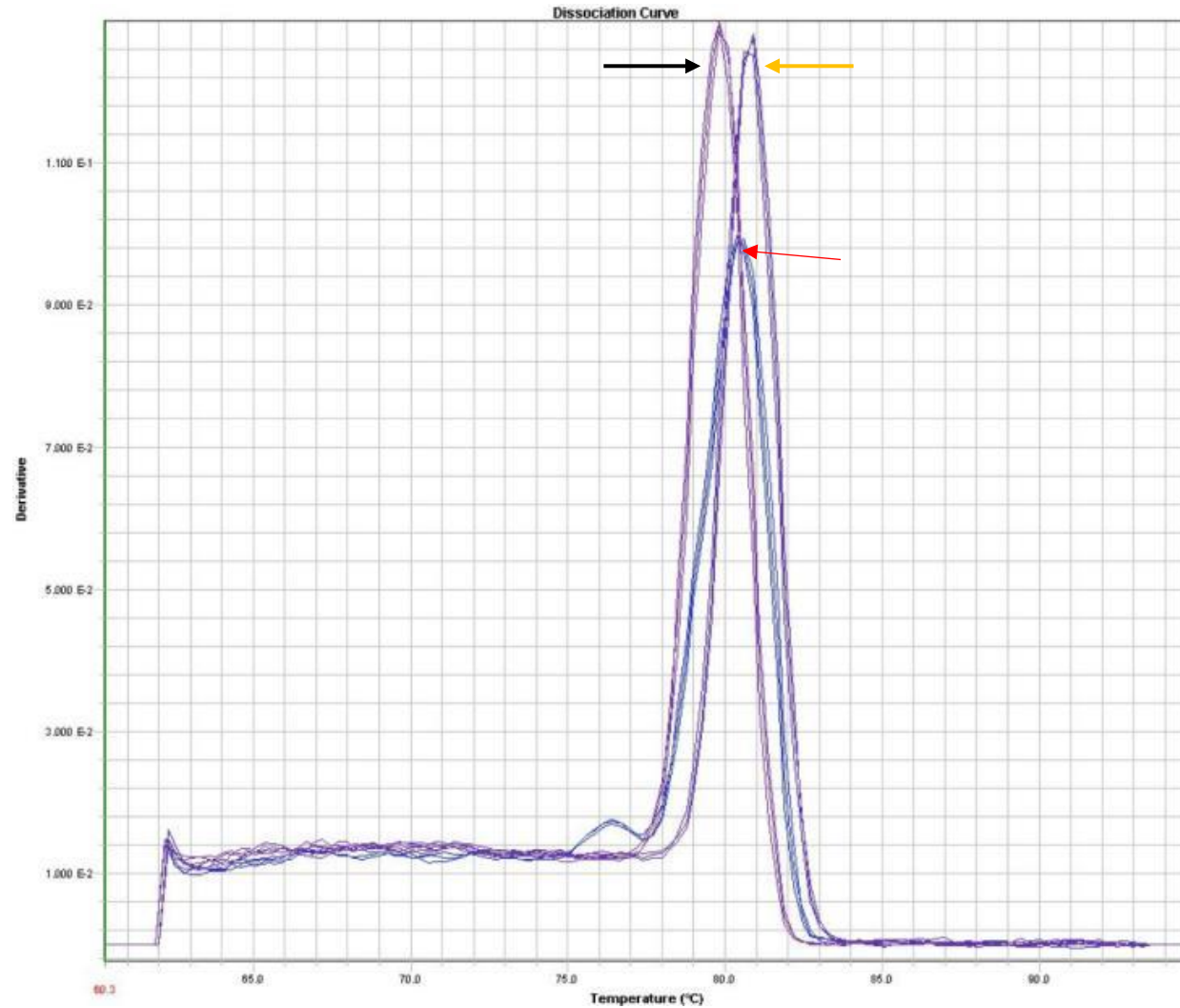
Supplemental Figure 14. Dissociation curve analysis plots for qPCR assay **EG1**, tested against a range of microorganisms and clinical samples to assess for species cross reactivity. A single qPCR product is seen across all three samples showing a positive reaction, with an average melt temperature of 76.3°C (+/- 0.3). No other positive reactions are seen for the other samples tested.



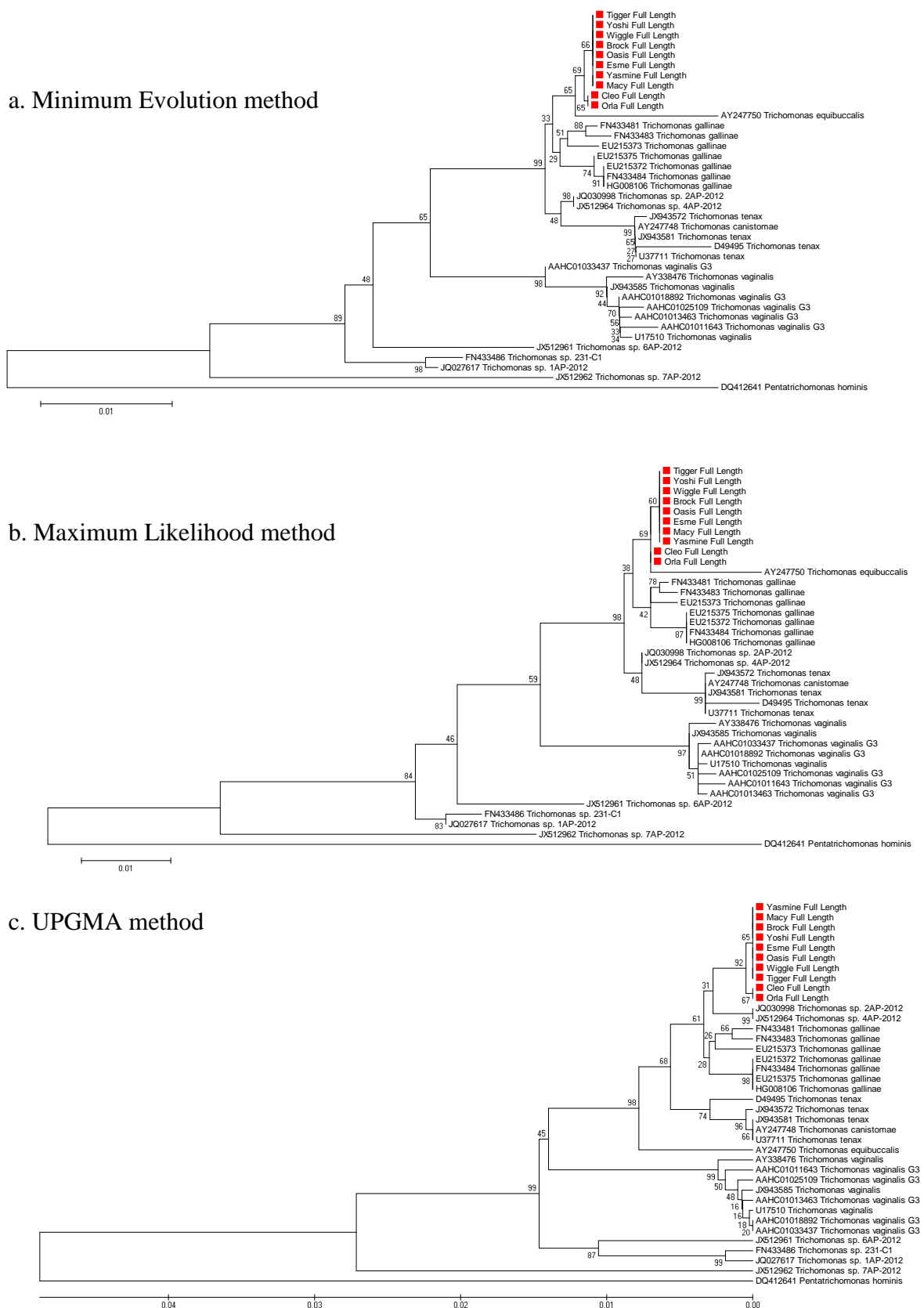
Supplemental Figure 15. Real time amplification plots for qPCR assay **TC2**, tested against a range of microorganisms and clinical samples to assess for species cross reactivity. Positive reactions are seen with the unidentified *Trichomonas* ITS1-5.8S-ITS2 amplicon sample (green lines), the unidentified *Trichomonas* (CLEO) genomic DNA sample (blue lines) and *T. tenax* genomic DNA sample (orange lines). No other positive reactions are seen for the other samples tested.



Supplemental Figure 16. Dissociation curve analysis plots for qPCR assay **TC2**, tested against a range of microorganisms and clinical samples to assess for species cross reactivity. A qPCR amplicon with an average melt temperature of 80.8°C is seen with *Trichomonas* sp. 5.8S amplicon sample and the *Trichomonas* sp. (CLEO isolate) genomic DNA sample. A qPCR amplicon with an average melt temperature of 80.0°C (+/- 0.3) is seen with the *T. tenax* genomic DNA sample. No other positive reactions are seen for the other samples tested.



Supplemental Figure 17. Dissociation curve analysis plots for qPCR assay **TC2**, tested against a sample containing *Trichomonas* sp. (CLEO isolate) genomic DNA (peak shown with black arrow), a sample containing *T. tenax* genomic DNA (peak shown with orange arrow), or a 1:1 (v/v) mix of the two DNA extractions (peak shown with red arrow).

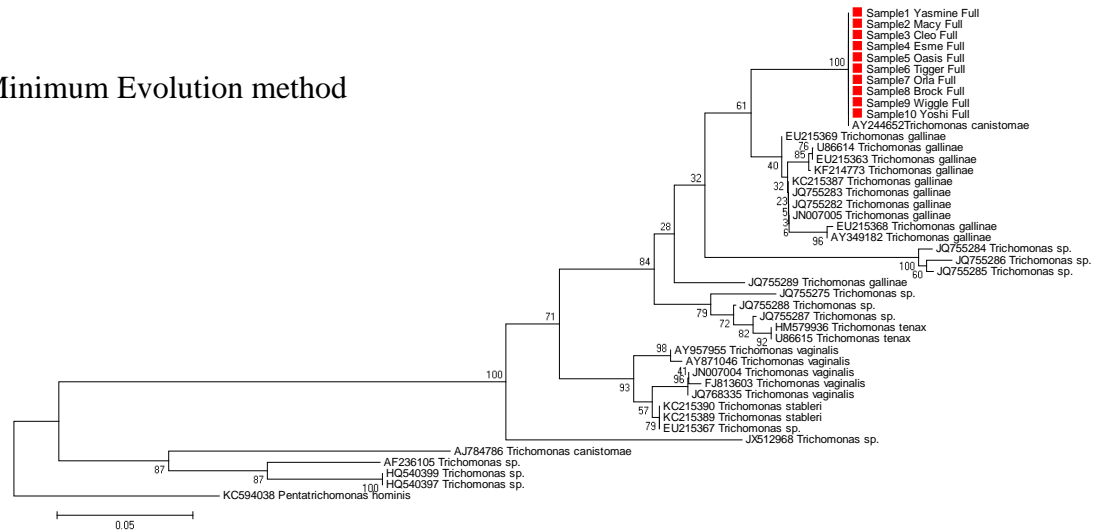


Supplemental Figure 18. Phylogenetic relationships between 10 unidentified canine oral *Trichomonas* isolates and the trichomonad genus group based on the eukaryotic ribosomal 18S gene. The evolutionary relationships were calculated using 3 different phylogenetic models. **(a).** Evolutionary history inferred using the Minimum Evolution method (Rzhetsky A. and Nei M. (1992). The optimal tree with the sum of

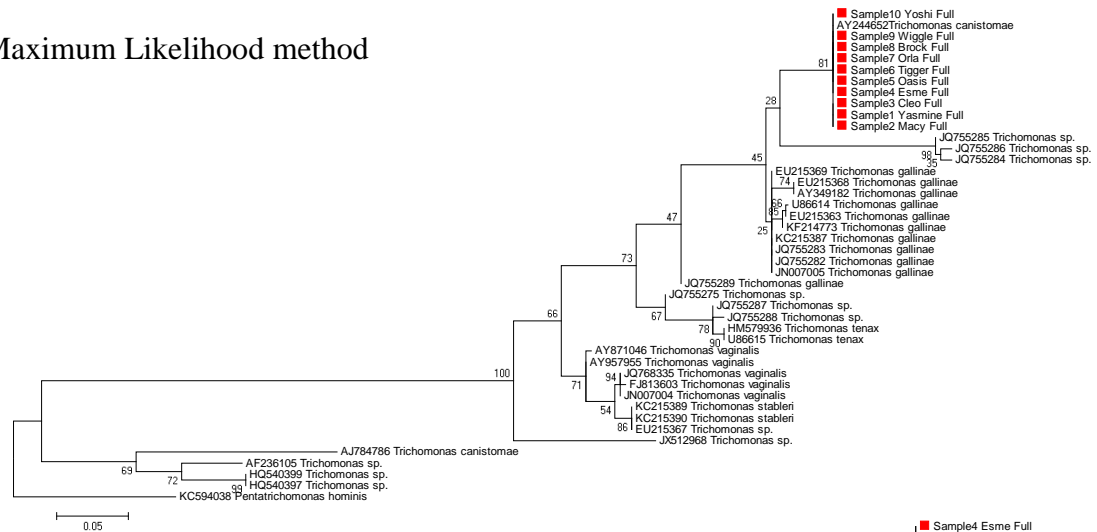
branch length = 0.20268408 is shown. The percentage of replicate trees in which the associated taxa clustered together in the bootstrap test (1000 replicates) are shown next to the branches (Felsenstein J. (1985). The tree is drawn to scale, with branch lengths in the same units as those of the evolutionary distances used to infer the phylogenetic tree. The evolutionary distances were computed using the Kimura 2-parameter method (Kimura M. (1980) and are in the units of the number of base substitutions per site. The rate variation among sites was modelled with a gamma distribution (shape parameter = 1). The ME tree was searched using the Close-Neighbor-Interchange (CNI) algorithm (Nei M. and Kumar S. (2000) at a search level of 1. **(b)**. Evolutionary history inferred by using the Maximum Likelihood method based on the Kimura 2-parameter model (Kimura M. (1980). The tree with the highest log likelihood (-2799.4796) is shown. The percentage of trees in which the associated taxa clustered together is shown next to the branches. Initial tree(s) for the heuristic search were obtained by applying the Neighbor-Joining method to a matrix of pairwise distances estimated using the Maximum Composite Likelihood (MCL) approach. A discrete Gamma distribution was used to model evolutionary rate differences among sites (5 categories (+G, parameter = 0.5271)). The tree is drawn to scale, with branch lengths measured in the number of substitutions per site. **(c)**. Evolutionary history inferred using the UPGMA method (Sneath P.H.A. and Sokal R.R. (1973). The optimal tree with the sum of branch length = 0.20305419 is shown. The percentage of replicate trees in which the associated taxa clustered together in the bootstrap test (1000 replicates) are shown next to the branches (Felsenstein J. (1985). The tree is drawn to scale, with branch lengths in the same units as those of the evolutionary distances used to infer the phylogenetic tree. The evolutionary distances were computed using the Kimura 2-parameter method (Kimura M. (1980) and are in the units of the number of base substitutions per site. The rate variation among sites was modeled with a gamma distribution (shape parameter = 1).

The Neighbor-joining algorithm (Saitou N. and Nei M. (1987) was used to generate the initial trees. The analysis involved 38 nucleotide sequences. All positions with less than 95% site coverage were eliminated. That is, fewer than 5% alignment gaps, missing data, and ambiguous bases were allowed at any position. There were a total of 1077 positions in the final dataset. Evolutionary analyses were conducted in MEGA6 (Tamura K., Stecher G., Peterson D., Filipski A., and Kumar S. (2013).

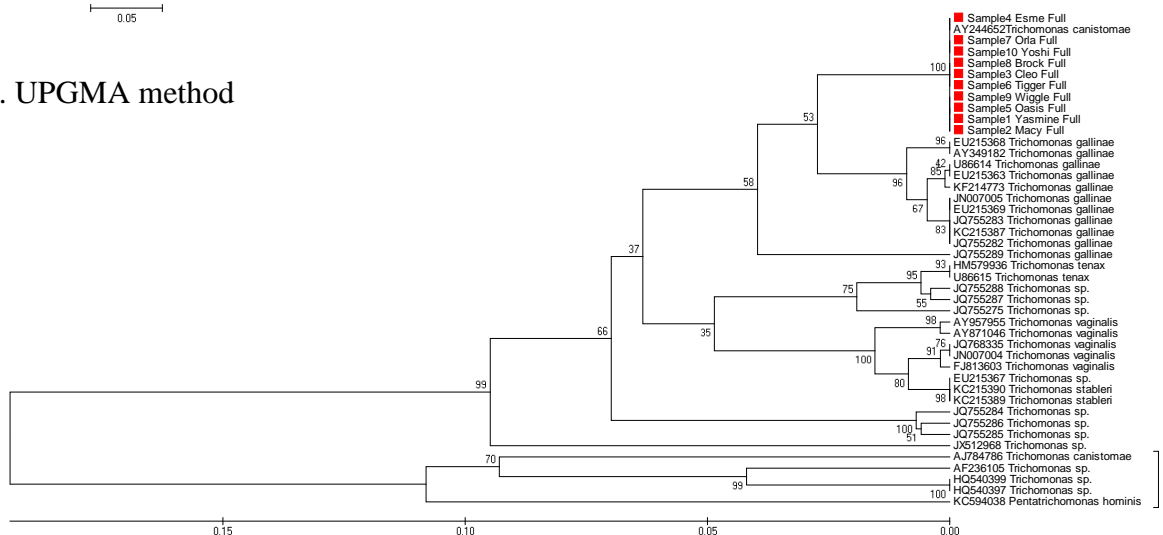
a. Minimum Evolution method



b. Maximum Likelihood method

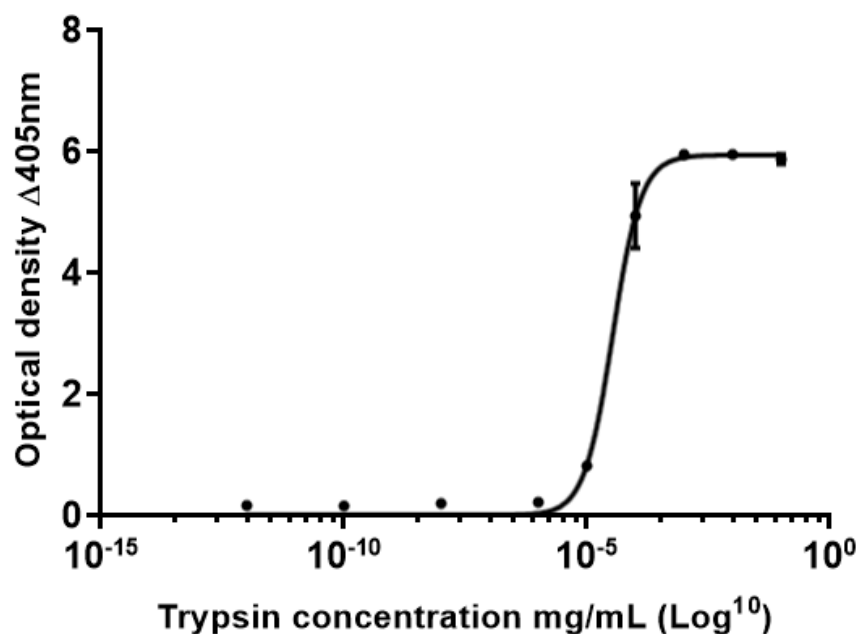


c. UPGMA method



Supplemental Figure 19. Phylogenetic relationships between 10 unidentified canine oral *Trichomonas* isolates and the trichomonad genus group based on the ITS1–5.8SrRNA-ITS2 gene. The evolutionary relationships were calculated using 3 different phylogenetic models. **(a).** Evolutionary history inferred using the Minimum Evolution method (Rzhetsky A. and Nei M. (1992)). The optimal tree with the sum of branch length = 1.03365986 is shown. The percentage of replicate trees in which the associated taxa clustered together in the bootstrap test (1000 replicates) are shown next to the branches (Felsenstein J. (1985)). The tree is drawn to scale, with branch lengths in the same units as those of the evolutionary distances used to infer the

phylogenetic tree. The evolutionary distances were computed using the Tamura 3-parameter method (Tamura K. (1992) and are in the units of the number of base substitutions per site. The rate variation among sites was modeled with a gamma distribution (shape parameter = 1). The ME tree was searched using the Close-Neighbor-Interchange (CNI) algorithm [4] at a search level of 1. **(b).** Evolutionary history inferred by using the Maximum Likelihood method based on the Tamura 3-parameter model (Tamura K. (1992). The tree with the highest log likelihood (-1489.3270) is shown. The percentage of trees in which the associated taxa clustered together is shown next to the branches. Initial tree(s) for the heuristic search were obtained by applying the Neighbor-Joining method to a matrix of pairwise distances estimated using the Maximum Composite Likelihood (MCL) approach. A discrete Gamma distribution was used to model evolutionary rate differences among sites (5 categories (+G, parameter = 0.5581)). The tree is drawn to scale, with branch lengths measured in the number of substitutions per site. **(c).** Evolutionary history was inferred using the UPGMA method (Sneath P.H.A. and Sokal R.R. (1973). The optimal tree with the sum of branch length = 1.05840930 is shown. The percentage of replicate trees in which the associated taxa clustered together in the bootstrap test (1000 replicates) are shown next to the branches (Felsenstein J. (1985). The tree is drawn to scale, with branch lengths in the same units as those of the evolutionary distances used to infer the phylogenetic tree. The evolutionary distances were computed using the Tamura 3-parameter method (Tamura K. (1992) and are in the units of the number of base substitutions per site. The rate variation among sites was modeled with a gamma distribution (shape parameter = 1). The Neighbor-joining algorithm (Saitou N. and Nei M. (1987) was used to generate the initial trees. The analysis involved 38 nucleotide sequences. All positions with less than 95% site coverage were eliminated. That is, fewer than 5% alignment gaps, missing data, and ambiguous bases were allowed at any position. There were a total of 1077 positions in the final dataset. Evolutionary analyses were conducted in MEGA6 (Tamura K., Stecher G., Peterson D., Filipski A., and Kumar S. (2013).



Supplemental Figure 20. Trypsin standard curve plotted using the Allosteric sigmoidal enzyme kinetics model (Equation 5.47, in RA Copeland, *Enzymes*, 2nd edition, Wiley, 2000). Trypsin standards were prepared from triplicate 0.1 mg per millilitre samples which were diluted 10-fold in series to 0.0001 picograms per millilitre. The optical density of each was measured at 405 nm and the resultant values plotted using Prism 7.03 (GraphPad software, Inc, USA). Black bars, where visible, indicate the standard error of the mean for each data point.